

Final Design Report

ELECTRIC COMMUTER MULTICOPTER

CALIFORNIA POLYTECHNIC STATE UNIVERSITY,

SAN LUIS OBISPO

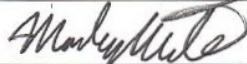
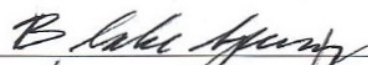
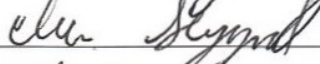

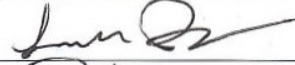
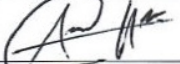
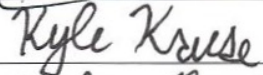
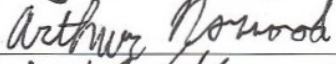
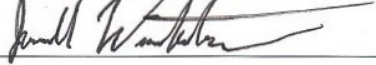
ME 430

Prepared for:

Bob Addis and Bill Bruner

June 12, 2015

Prepared by:

Marley Miller		mmille58@calpoly.edu
Blake Sperry		bsperry@calpoly.edu
Ike Sheppard		isheppar@calpoly.edu
Ollie Kunz		okunz@calpoly.edu
Samuel Juday		sjuday@calpoly.edu
Alex O'Hearn		aohearn@calpoly.edu
Kyle Kruse		kkruse@calpoly.edu
Arthur Norwood		anorwood@calpoly.edu
Jarrell Washington		jawashin@calpoly.edu

Statement of Disclaimer

Since this project is a result of a class assignment, it has been graded and accepted as fulfillment of the course requirements. Acceptance does not imply technical accuracy or reliability. Any use of information in this report is done at the risk of the user. These risks may include catastrophic failure of the device or infringement of patent or copyright laws. California Polytechnic State University at San Luis Obispo and its staff cannot be held liable for any use or misuse of the project.

TABLE OF CONTENTS

<u>Section</u>	<u>Page</u>
1 EXECUTIVE SUMMARY	1
2 INTRODUCTION	3
3 BACKGROUND	4
3.1 REGULATIONS	4
3.2 EXISTING FLIGHT PLATFORMS	5
3.2.1 E-VOLO MULTICOPTERS.....	5
3.2.2 HOVERBIKES.....	6
3.2.3 AUTOGYROS.....	8
3.2.4 JETPACKS.....	9
3.2.5 PARAMOTORS.....	10
3.2.6 BLIMPS.....	11
3.2.7 MOSQUITO ULTRALIGHT.....	11
3.2.8 FIREFLY ULTRALIGHT.....	12
3.2.9 CARTER AVIATION.....	13
3.3 PATENTS	14
3.4 SUBSYSTEM RESEARCH	17
3.4.1 FLIGHT SYSTEM DYNAMICS AND CONTROLS.....	17
3.4.2 R/C CONTROL SYSTEMS.....	18
3.4.3 ACTUATOR DISK THEORY.....	19
3.4.4 GROUND EFFECT.....	19
3.4.5 POWER SYSTEMS.....	20
3.4.6 BATTERIES.....	21
3.4.7 DUCTED FANS.....	22
3.5 CURRENT COMMUTER ISSUES	23
4 OBJECTIVES	25
5 PROJECT PLANNING	27
5.1 METHOD OF APPROACH	27
5.2 CONSTRUCTION PLAN	29
5.3 MANAGEMENT PLAN	30
6 TOP CONCEPT DESIGNS	32
6.1 DESIGN #1: MULTICOPTER (UNDER-BODY PROPS)	32
6.2 DESIGN #2: MULTICOPTER (OVERHEAD PROPS)	33
6.3 DESIGN #3: HOVERBIKE/HOVERBOARD	34
6.4 DESIGN #4: POWERED VTOL GYROCOPTER	35
6.5 DESIGN #5: MULTI-GYROCOPTER	36
7 CONCEPT DECISION PROCESS	37
8 PRELIMINARY DESIGN	41
9 INITIAL MULTICOPTER CONFIGURATION EVALUATION	46
9.1 TOOL OVERVIEW	46
9.2 FINAL OUTPUT AND ANALYSIS	51
9.3 MAJOR ASSUMPTIONS	52
10 REVISIONS TO PRELIMINARY DESIGN	53
11 FINAL MULTICOPTER DESIGN	55
11.1 STRUCTURE	55
11.1.1 LAYOUT.....	55

11.1.2 MAIN ARMS	56
11.1.3 MOTOR SPARS.....	57
11.1.4 CENTER MOUNT.....	58
11.1.5 SEAT PLATE AND SEAT	60
11.1.6 ARM MOUNTS	61
11.1.7 MOTOR MOUNTS.....	63
11.1.8 LANDING GEAR.....	66
11.2 PROPULSION	68
11.2.1 PROPELLERS.....	68
11.2.2 MOTORS.....	68
11.2.3 BATTERIES	69
11.2.4 WIRE.....	69
11.2.5 STACKED PROP CONFIGURATIONS	72
11.3 CONTROLS	72
11.3.1 MULTICOPTER DYNAMICS	72
11.3.2 USER INTERFACE	77
11.3.2.1 Saitek X52 Flight Control System	77
11.3.2.2 Xbox 360 Controller	78
11.3.2.3 Mad Catz F.L.Y. 5 Stick for PC	78
11.3.2.4 Spektrum Dx6 Transmitter	79
11.3.2.5 Decision	80
11.3.3 SYSTEM COMMUNICATIONS	80
11.3.4 MICROCONTROLLERS.....	81
11.3.4.1 Open Pilot Revolution Flight Controller	81
11.3.4.2 APM 2.6 Set Flight Controller	82
11.3.4.3 HoverflyOPEN	83
11.3.4.4 Decision	83
11.3.5 OPENPILOT GCS.....	84
11.3.6 PERIPHERAL ADD-ONS.....	84
12 COST	85
13 WEIGHT	87
14 SAFETY	89
14.1 CRITICAL DESIGN HAZARD CHECKLIST	89
14.2 STRUCTURE	89
14.3 PROPULSION	89
14.4 CONTROLS	90
15 DESIGN ANALYSIS	91
15.1 STRUCTURE	91
15.1.1 LOADING CASES AND ASSUMPTIONS	91
15.1.2 MAIN ARMS AND MOTOR SPARS.....	91
15.1.3 CENTER MOUNT ASSEMBLY	96
15.1.4 ARM MOUNT ASSEMBLY	99
15.1.5 MOTOR MOUNT ASSEMBLY	100
15.1.6 LANDING GEAR.....	101
15.2 PROPELLERS	103
15.2.1 DIMENSIONS.....	103
15.2.2 MATERIAL.....	104
15.2.3 NUMBER OF PROPELLERS.....	105
15.2.4 PROPELLER ANALYSIS	105
15.3 MOTOR	106
16 MATERIAL SELECTION	112
16.1 UNIDIRECTIONAL CARBON FIBER TUBING	112
16.2 EPOXIES AND BOND LINE CONTROLLER	113

16.3	CARBON FIBER TAPE	113
16.4	4130 CHROMOLY TUBING	114
16.5	4130 STEEL PLATE	115
16.6	6061-T6 ALUMINUM PLATE	115
16.7	WELDING FILLER METAL	115
16.8	NETTING	115
17	CONSTRUCTION PLANS	116
17.1	STRUCTURE	116
17.1.1	MAIN ARMS	116
17.1.2	MOTOR SPARS.....	116
17.1.3	CENTER MOUNT.....	116
17.1.4	CENTER MOUNT BRACKET	117
17.1.5	SEAT PLATE AND SEAT	118
17.1.6	ARM MOUNT.....	118
17.1.7	ARM MOUNT BRACKET.....	118
17.1.8	MOTOR MOUNTS.....	118
17.1.9	INNER & OUTER RING MOUNTS	119
17.1.10	PROPELLER RINGS.....	119
17.1.11	LANDING GEAR.....	119
17.1.12	CRAFT ASSEMBLY.....	120
17.2	PROPULSION	122
17.2.1	PROPELLERS.....	122
17.2.2	MOTORS.....	122
17.2.3	WIRE LAYOUT/CIRCUIT DIAGRAM.....	122
17.3	CONTROLS	124
18	EXPECTATIONS AND FUTURE PLANS	125
18.1	OPTION 1	125
18.2	OPTION 2	125
18.3	OPTION 3	126
19	ADDITIONAL DESIGN CONSIDERATIONS	127
19.1	HEXCOPTER CONFIGURATION	127
19.2	NON-TRADITIONAL QUADCOPTER CONTROL SCHEME	129
19.3	ALTERNATIVE LANDING GEAR DESIGNS	130
19.4	MULTICOPTER CONTROL INTERFACE	131
19.5	COMMUNICATION MODIFICATIONS	140
19.6	MICROCONTROLLER MODIFICATIONS	141
19.7	PILOT PROTECTIVE STRUCTURE	141
20	TEST PLAN	143
20.1	STRUCTURE	143
20.1.1	ABSTRACT.....	143
20.1.2	THREE-POINT BEAM TEST	143
20.1.2.1	Purpose	143
20.1.2.2	Equipment	144
20.1.2.3	Setup & Procedures	144
20.1.2.4	Safety Concerns & Solutions	146
20.1.2.5	Expected Results	146
20.1.2.6	Testing Results	146
20.1.2.7	Conclusion	147
20.1.3	CANTILEVER BEAM TEST.....	148
20.1.3.1	Purpose	148
20.1.3.2	Equipment	148
20.1.3.3	Setup & Procedures	149
20.1.3.4	Safety Concerns & Solutions	150

20.1.3.5	Expected Results	151
20.1.3.6	Testing Results	151
20.1.3.7	Conclusion	152
20.2	PROPULSION	152
20.2.1	ABSTRACT.....	152
20.2.2	INTRODUCTION	152
20.2.3	EXPERIMENTAL APPARATUS AND PROCEDURE	152
20.2.4	RESULTS AND DISCUSSION.....	154
20.2.5	IMPROVEMENTS FOR FUTURE TESTS	155
20.2.6	OTHER NOTES.....	156
20.2.7	CONCLUSION.....	156
20.3	CONTROLS	156
20.3.1	PURPOSE	156
20.4	MANUFACTURING	156
20.4.1	INTRODUCTION	156
20.4.2	COMPONENT SELECTION.....	157
20.4.3	MICROCONTROLLER AND CALIBRATION	158
20.4.4	FABRICATION	158
20.4.5	ASSEMBLY	158
20.5	BUDGET	160
20.6	TESTING EQUIPMENT	161
20.7	SUMMARY OF TESTS	161
20.7.1	TEST A: MOTOR DRIVE TEST.....	161
20.7.2	TEST B: PROPELLER THRUST INTERFERENCE TEST.....	161
20.7.3	TEST C: FLOATING TETHER TEST.....	162
20.7.4	TEST D: REDUNDANCY TESTING.....	162
20.7.5	TEST E: DISTURBANCE TEST.....	162
20.7.6	TEST F: USER INTERFACE TEST.....	162
20.8	SETUP AND PROCEDURE	162
20.8.1	TEST A: MOTOR DRIVE TEST.....	162
20.8.2	TEST B: PROPELLER THRUST INTERFERENCE AND MAXIMUM THRUST TEST.....	163
20.8.3	TEST C: FLOATING TETHER TEST.....	164
20.8.4	TEST D: REDUNDANCY TESTING.....	165
20.8.5	TEST E: DISTURBANCE TEST.....	166
20.8.6	TEST F: USER INTERFACE TEST.....	166
20.9	DATA ACQUISITION	166
20.9.1	TEST A: MOTOR DRIVE TEST	166
20.9.2	TEST B: PROPELLER THRUST INTERFERENCE AND MAXIMUM THRUST TEST.....	166
20.9.3	TEST C: FLOATING TETHER TEST.....	167
20.9.4	TEST D: REDUNDANCY TESTING.....	167
20.9.5	TEST E: DISTURBANCE TEST.....	167
20.9.6	TEST F: USER INTERFACE TEST.....	167
20.10	EXPECTED RESULTS	168
20.10.1	TEST A: MOTOR DRIVE TEST	168
20.10.2	TEST B: PROPELLER THRUST INTERFERENCE AND MAXIMUM THRUST TEST.....	168
20.10.3	TEST C: FLOATING TETHER TEST.....	168
20.10.4	TEST D: REDUNDANCY TESTING.....	168
20.10.5	TEST E: DISTURBANCE TEST.....	168
20.10.6	TEST F: USER INTERFACE TEST.....	168
20.11	SAFETY CONCERNS AND SOLUTIONS	169
20.11.1	TEST A: MOTOR DRIVE TEST	169
20.11.2	TEST B: PROPELLER THRUST INTERFERENCE AND MAXIMUM THRUST TEST.....	169
20.11.3	TEST C: FLOATING TETHER TEST.....	169
20.11.4	TEST D: REDUNDANCY TESTING.....	169
20.11.5	TEST E: DISTURBANCE TEST.....	169
20.11.6	TEST F: USER INTERFACE TEST.....	169

20.12 SAFETY EQUIPMENT	170
20.12.1 TEST A: MOTOR DRIVE TEST	170
20.12.2 TEST B: PROPELLER THRUST INTERFERENCE AND MAXIMUM THRUST TEST	170
20.12.3 TEST D: FLOATING TETHER TEST	170
20.12.4 TEST D: REDUNDANCY TESTING	170
20.12.5 TEST E: DISTURBANCE TEST	170
20.12.6 TEST F: USER INTERFACE TEST	170
20.13 RESULTS AND ANALYSIS	170
20.13.1 TEST A: MOTOR DRIVE TEST	170
20.13.2 TEST B: PROPELLER THRUST INTERFERENCE AND MAXIMUM THRUST TEST	171
20.13.3 TEST C: FLOATING TETHER TEST	172
20.13.4 TEST D: REDUNDANCY TESTING	172
20.13.5 TEST E: DISTURBANCE TEST	172
20.13.6 TEST F: USER INTERFACE TEST	173
20.14 CONCLUSION	173
21 RECOMMENDATIONS	174
21.1 STRUCTURES	174
21.1.1 LOADING CASES: DYNAMIC, STATIC, AND VIBRATION	174
21.1.2 DIFFERENT ADHESIVES/TORSIONAL SHEAR	174
21.1.3 DIFFERENT LAYUP SCHEDULE OF MAIN ARMS AND SPARS	175
21.1.4 CARBON FIBER/COMPOSITE MOUNTS	175
21.1.5 REDESIGN LANDING GEAR	175
21.1.6 STRESS CONCENTRATION ANALYSIS/FEA	175
21.1.7 DISASSEMBLY, POTTED INSERTS & ATTACHMENTS	175
21.1.8 MINIMIZE FOOTPRINT/COMPACT PROPELLERS	176
21.2 PROPULSION	176
21.2.1 IMPROVE THE THRUST TEST RIG	176
21.2.2 REANALYZE THE NUMBER AND SIZE OF PROPELLERS	176
21.2.3 ANALYZE THE PROPELLER PITCH	176
21.2.4 USING DIFFERENT MOTORS	177
21.2.5 MULTI-BLADE PROPELLERS AND STACKING PROPELLERS	177
21.2.6 CONSIDER THRUST LOSS DUE TO NEIGHBORING PROPELLERS	177
21.2.7 DETERMINE THE BENEFITS OF CARBON FIBER PROPELLERS	178
21.2.8 REANALYZE CONFIGURATION TOOL	178
21.2.9 CFD	178
21.3 CONTROLS	179
21.3.1 INCREASE MINI FLIGHT TIME	179
21.3.2 FIRST PERSON VIEW (FPV GOGGLES)	179
21.3.3 BATTERY CHARGING/TESTING	179
21.3.4 CALIBRATION - LONG ARM	179
21.3.5 STEPS TOWARDS OUTDOOR FLIGHT	180
21.3.6 ADDITIONAL FLIGHT CONTROLLER MODULES (GPS, ETC.)	180
21.3.7 DIFFERENT FLIGHT CONTROLLER	180
21.3.8 OTHER POWER SOURCES	181
21.3.9 CUSTOM BATTERY PACKS	181
21.3.10 ASYMMETRIC WEIGHT DISTRIBUTION TESTING	181
21.3.11 DISTURBANCE TESTING (WIND, ETC.)	181
21.3.12 HARD-WIRING CONTROLS	181
21.4 ECM TEAM (FUTURE PROJECT DIRECTION)	182
21.4.1 MULTIDISCIPLINARY PROJECT (CSE, EE, AERO, ME)	182
21.4.2 SMALLER SENIOR PROJECT	182
21.4.3 LARGER SENIOR PROJECT	182
21.4.4 ADVERTISING (OUTSIDE FINANCING)	183
21.4.5 OBJECTIVE DEFINED/CLARITY	183
21.4.6 SET STANDARDS/FORMATTING	183

21.4.7	OBJECTIVE DEFINED/ULTRALIGHT REGULATION.....	183
21.4.8	MONETARY TRANSPARENCY/OUTSIDE FINANCING.....	183
21.4.9	INCREASED SPONSOR INTERACTION.....	184
21.4.10	IMPLEMENTING GOOD DATA MANAGEMENT PRACTICES.....	184
21.5	OTHER DESIGNS.....	184
21.5.1	DESIGN PARAMETRIC STUDY FOR VARYING PAYLOADS.....	184
21.5.2	GYROCOPTER (IF VTOL IS NOT A REQUIREMENT).....	184
21.5.3	OVER-BODY VEHICLE RESEARCH.....	184
21.5.4	TRUSS STRUCTURE.....	185
21.5.5	FAIRING/ROLL CAGE.....	185
22	CONCLUSION	186
23	ACKNOWLEDGEMENTS	188
24	REFERENCES:	189

LIST OF FIGURES

Figure	Page
FIGURE 1: VC-1 ELECTRIC MULTICOPTER VEHICLE BY E-VOLO.	5
FIGURE 2: VC200 ELECTRIC MULTICOPTER BY E-VOLO, SEEN HERE WITH TWO OF THE VEHICLE’S CREATORS.	6
FIGURE 3: PROTOTYPE OF CHRIS MALLOY’S HOVERBIKE.	7
FIGURE 4: CAD MODEL OF MARK DEROCHE’S PROTOTYPE AERO-X.	8
FIGURE 5: BUTTERFLY LLC ULTRALIGHT AUTOGYRO.	9
FIGURE 6: TEST PILOT FLIES IN A MARTIN JETPACK.	10
FIGURE 7: SCOUT PARAMOTORS’ DEVICE TO COUNTER THE ANGULAR MOMENTUM OF THE PARAMOTOR.	10
FIGURE 8: PARAMOTOR ASSEMBLY WITH PROPELLER, PILOT, ENGINE, AND GLIDER.	11
FIGURE 9: MOSQUITO ULTRALIGHT WITH RIDER.	12
FIGURE 10: KOLB’S FIREFLY ULTRALIGHT IN FLIGHT.	13
FIGURE 11: CARTER AVIATION 4-PLACE PAV IN FLIGHT.	13
FIGURE 12: MULTIROTOR WITH PATENTED “FAILSAFE NETWORK”	14
FIGURE 13: PATENTS FOR ELECTRIC MULTICOPTER AIRCRAFT.	16
FIGURE 14: QUADCOPTER LAYOUT AND POSSIBLE DIRECTIONS OF MOTION: ROLL, PITCH AND YAW [32].	17
FIGURE 15: AN R/C QUADCOPTER.	18
FIGURE 16: ENERGY DENSITY OF COMMON BATTERY TYPES ($1\text{Wh/kg} = 3.6\text{KJ/kg}$) [42]	21
FIGURE 17: MODEL OF AIRFLOW AROUND A DUCTED FAN [45].	22
FIGURE 18: FORMAL DESIGN PROCESS AS SEEN FROM ULLMAN’S “THE MECHANICAL DESIGN PROCESS” [52].	27
FIGURE 19: MULTICOPTER (UNDER-BODY PROPS)	32
FIGURE 20: MULTICOPTER (OVERHEAD PROPS)	33
FIGURE 21: HOVERBIKE/HOVERBOARD	34
FIGURE 22: VTOL GYROCOPTER	35
FIGURE 23: MULTI-GYROCOPTER	36
FIGURE 24: MULTICOPTER WITH UNDERBODY PROPS.	40
FIGURE 25: GROUPING OF PROPELLERS ON EACH ARM IN PRELIMINARY DESIGN.	41
FIGURE 26: A CLOSER LOOK AT THE PROPELLER AND PROP RING ON THE END OF EACH ARM.	42
FIGURE 27: VIEW OF THE UNDERSIDE OF THE VEHICLE SHOWING LANDING GEAR AND BATTERY ARRANGEMENT.	42
FIGURE 28: A SIDE VIEW OF THE PRELIMINARY DESIGN DEMONSTRATING THE ROUGH HEIGHT OF THE DESIGN.	43
FIGURE 29: AN INITIAL LAYOUT OF THE MODEL SHOWING THE MAIN ARMS AND SMALLER ARMS.	44
FIGURE 30: OVERVIEW OF CONFIGURATION ANALYSIS TOOL	46
FIGURE 31: VEHICLE WIDTH IN FEET BASED ON CONFIGURATION	47
FIGURE 32: INDIVIDUAL MOTOR POWER FOR VARIOUS CONFIGURATIONS OF NUMBER AND PROPELLER SIZE	48
FIGURE 33: INDIVIDUAL MOTOR POWER FOR VARIOUS CONFIGURATIONS	49
FIGURE 34: MOTOR WEIGHT VS POWER DATA AND TREND LINE USED TO MODEL RELATIONSHIP	50
FIGURE 35: ESTIMATED FLIGHT TIME IN MINUTES BASED ON CONFIGURATION	51
FIGURE 36: FULL MULTICOPTER DESIGN	55
FIGURE 37: MAIN CARBON FIBER SPAR	56
FIGURE 38: AUXILIARY CARBON FIBER SPARS	57
FIGURE 39: BOTTOM VIEW OF CENTER MOUNT ASSEMBLY	58
FIGURE 40: STEEL CENTER MOUNT	59
FIGURE 41: CENTER MOUNT WALLS	59
FIGURE 42: CENTER MOUNT LANDING GEAR PLATE	60
FIGURE 43: SEAT MOUNTING PLATE	61
FIGURE 44: SUMMIT LIGHTWEIGHT SEAT	61
FIGURE 45: ARM MOUNT ASSEMBLY	61
FIGURE 46: ARM MOUNT WALLS	62
FIGURE 47: MOTOR MOUNT ASSEMBLY	63
FIGURE 48: CLOSE-UP OF MOTOR MOUNT	64
FIGURE 49: PROPELLER SHROUD SPAR	64
FIGURE 50: INNER PROP RING BRACKET	65
FIGURE 51: PROPELLER RINGS	66
FIGURE 52: UNDERSIDE VIEW OF THE LANDING GEAR	66
FIGURE 53: EXPLODED VIEW OF THE LANDING GEAR ASSEMBLY	67
FIGURE 54: DIAGRAMS FOR THE 12 (LEFT) AND 16 (RIGHT) CLUSTERED QUADROTOR CONFIGURATIONS	73

FIGURE 55: DIAGRAM FOR THE 16 ROTOR CONFIGURATION OF THE “INDEPENDENT VEHICLE” CONTROL SCHEME	74
FIGURE 56: DIAGRAM FOR THE 12 ROTOR CONFIGURATION OF THE “INDEPENDENT VEHICLE” CONTROL SCHEME	75
FIGURE 57: THE SAITEK X52 FLIGHT CONTROL SYSTEM	77
FIGURE 58: MICROSOFT’S XBOX 360 CONSOLE CONTROLLER	78
FIGURE 59: THE MAD CATZ F.L.Y 5 STICK FOR PC AND PS3	79
FIGURE 60: SPEKTRUM DX6 TRANSMITTER	79
FIGURE 61: COMPUFLY USB TO PPM CONVERTER	80
FIGURE 62: SCHERRER LRS Tx7000 LITE TRANSMITTER AND RECEIVER SET	81
FIGURE 63: OPEN PILOT REVOLUTION HARDWARE BUNDLE	82
FIGURE 64: 3D ROBOTIC’S APM 206 SET FLIGHT CONTROLLER	82
FIGURE 65: HOVERFLYOPEN FLIGHT CONTROLLER	83
FIGURE 66: SCREENSHOT OF FLIGHT DATA TAB FOR THE OPENPILOT GCS SOFTWARE	84
FIGURE 67: FINITE ELEMENT ANALYSIS OF LANDING GEAR PLATE UNDER MAXIMUM LOADING CONDITIONS	103
FIGURE 68: MOUNTED WOODEN PROPELLER ON JOBY JM1S MOTOR	107
FIGURE 69: ACTUATOR DISK THEORY CONTOUR PLOTS GENERATE IN MATLAB PROGRAM, SHOWING POWER IN TERMS OF BLADE RADIUS AND PROPELLER NUMBER	108
FIGURE 70: RPM AT HOVER HEIGHT, SHOWING CONTOURS OF RPM OVER A RANGE OF THRUST AND VELOCITY (NORMALIZED). THIS HELPS VALIDATE MATHEMATICALLY THE EXPERIMENTAL RESULTS PRESENTED BY JOBY	109
FIGURE 71: GENERALIZED JOBY MOTOR MODEL WITH AN EFFICIENCY AT 89%, TORQUE OF 9.5 FT-LB, AND RPM OF 6134. THE “K” FACTORS ARE DETERMINED BASED OFF OF MOTOR MAX RPM AND TORQUE	110
FIGURE 72: RPM AT HOVER HEIGHT, SHOWING CONTOURS OF RPM OVER A RANGE OF THRUST AND VELOCITY (NORMALIZED) FOR THE 3D ROBOTIC’S IRIS+ MULTICOPTER. THE RESULTS ARE COMPARABLE TO THE DATA PROVIDED BY 3D ROBOTICS AND VALIDATES THE PROGRAM	111
FIGURE 73: TOP VIEW OF HEXCOPTER CONCEPT	127
FIGURE 74: HEXCOPTER CONCEPT	128
FIGURE 75: NON-TRADITIONAL QUADCOPTER CONTROL SCHEME	129
FIGURE 76: LANDING GEAR PRELIMINARY DESIGN 1	130
FIGURE 77: LANDING GEAR PRELIMINARY DESIGN 2	131
FIGURE 78: FULL CONTROLS INTERFACE ASSEMBLY PLACED ON FULL SCALE VEHICLE.	132
FIGURE 79: SOLID MODEL OF THE REVISED SEAT PLATE STRUCTURE, EXTENDED TO ALLOW ROOM FOR THE THROTTLE STAND, FOOT PEGS, AND JOYSTICK STAND.	133
FIGURE 80: UNDERSIDE VIEW SHOWING THE ADDITIONAL PLATE TO SPAR SUPPORT BRACES.	134
FIGURE 81: VIEW OF THE RIDER LEG SUPPORT TUBE AS WELL AS ADJUSTABLE FOOT PEGS.	135
FIGURE 82: SOLID MODEL OF THE JOYSTICK FORK, WHICH ALLOWS THE USER TO ROTATE THE JOYSTICK PLATE AWAY FROM THE USER DURING ENTRY AND RE-ENTRY.	136
FIGURE 83: JOYSTICK STAND USED TO LOCK DOWN THE JOYSTICK FORK FOR OPERATIONAL USE	138
FIGURE 84: VIEW OF THE VEHICLE’S THROTTLE STAND POSITIONED OVER ITS SLOT FOR EASY ADJUSTABILITY.	139
FIGURE 85: NEEWER 3DR TELEMETRY KIT INCLUDING BOTH MODULES, TWO ANTENNA, AND THE TELEMETRY PORT CONNECTOR.	141
FIGURE 86: ONE POSSIBLE ROLL CAGE DESIGN CONSTRUCTED FROM CARBON FIBER ADDED TO THE FINAL MULTICOPTER STRUCTURE.	142
FIGURE 87: EXPERIMENTAL APPARATUS FOR THE THREE-POINT BEND TEST. NOTE THE PAIR OF DIAL INDICATORS ON EITHER SIDE OF THE LOAD.	145
FIGURE 88: STRESS-STRAIN CURVE FOR THE CARBON FIBER MAIN ARM DURING THREE POINT BEND TESTING.	146
FIGURE 89: STRESS-STRAIN PLOT FOR THE TUBE DURING THE THREE POINT BEND TEST UTILIZING STRAIN GAUGES.	147
FIGURE 90: STEEL CENTER MOUNT TEST PIECE.	149
FIGURE 91: CANTILEVER BEAM TEST JIG	150
FIGURE 92: CANTILEVER BEAM TEST ASSEMBLY ILLUSTRATING ONE QUADRANT OF THE ELECTRIC COMMUTER MULTICOPTER WITH A 52” CARBON FIBER TUBE, CENTER MOUNT AND TEST FIXTURE.	150
FIGURE 93: MOTOR TEST SCHEMATIC.	153
FIGURE 94: MOTOR TEST SETUP	153
FIGURE 95: THRUST VS. TIME FOR THE THREE THROTTLE UPS	154
FIGURE 96: eCALC XCOPTERCALC HYPOTHETICAL PERFORMANCE CHARACTERISTICS.	157
FIGURE 97: SOLIDWORKS ASSEMBLY SOLID MODEL OF THE STRUCTURAL COMPONENTS OF THE MINI MULTICOPTER INCLUDING MOTORS AND PROPELLERS FOR PROP SPACING.	158
FIGURE 98: FINAL FULLY ASSEMBLED MINI MULTICOPTER WITH ELECTRONICS FULLY INSTALLED.	159

FIGURE 99: SIMPLIFIED CIRCUIT DIAGRAM OF THE MINI DRONE.	160
FIGURE 100: SCHEMATIC OF 1,6, AND 12 MOTOR DRIVE TESTS	163
FIGURE 101: SCHEMATIC OF THE FIXED ARM CLUSTER TEST WITH 1 AND 3 MOTORS.	164
FIGURE 102: FLOATING TETHER TEST FLIGHT PATTERNS.	165
FIGURE 103: REDUNDANCY TEST SCHEMATIC SHOWING KILL-FUSE.	166
FIGURE 104: EFFECT OF PROP INTERFERENCE ON THRUST PER MOTOR.	171

LIST OF TABLES

<u>Table</u>	<u>Page</u>
TABLE 1: BATTERY DATA	21
TABLE 2: ANNUAL AND DAILY MILES TRAVELED BY VARIOUS AGE GROUPS IN THE UNITED STATES.	23
TABLE 3: EFFICIENCY COMPARISON OF SEVERAL GROUND VEHICLES AND AIRCRAFT.	24
TABLE 4: TARGET ENGINEERING SPECIFICATIONS.	26
TABLE 5: NEC TABLE 310.16 FOR COVERED WIRES	70
TABLE 6: NEC TABLE 310.17 FOR WIRES IN FREE AIR	71
TABLE 7: COST BREAKDOWN BY SECTION	85
TABLE 8: COST ANALYSIS	86
TABLE 9: WEIGHT ANALYSIS	88
TABLE 10: EFFECT OF PITCH ON POWER CONSUMPTION	104
TABLE 11: COMPARISON OF 12 AND 16 PROPELLER POWER CONSUMPTION AND WEIGHT	105
TABLE 12: MOTOR PERFORMANCE REQUIREMENTS ESTIMATES	106
TABLE 13: APPROXIMATE WEIGHT THE CONTROL COMPONENTS ADD TO THE MULTICOPTERS TOTAL WEIGHT.	140
TABLE 14: COST ESTIMATE FOR THE THREE POINT BEND TEST.	144
TABLE 15: COST ANALYSIS OF THE TEST FIXTURE FOR	148
TABLE 16: MOTOR PERFORMANCE AT RATED MAX CONDITIONS	155
TABLE 17: SUMMARY OF COMPONENT SELECTION AND COST FOR THE MINI	161
TABLE 18: SUMMARY OF MINI MULTICOPTER MEASURED AND EXPECTED FLIGHT CHARACTERISTICS.	165
TABLE 19: RESULT OF GO / NO GO TEST FOR 1, 6, AND 12 MOTORS	171
TABLE 20: RECORDED VOLTAGES AT EACH MOTOR CONFIGURATION TEST	171
TABLE 21: FLIGHT TIME AND FLIGHT OPERATIONS RESULTS	172

1 EXECUTIVE SUMMARY

This document describes the design, analysis, and overall goals of the Electric Commuter Multicopter (ECM) Senior Project. It was presented by Bob Addis and Bill Burner to the senior mechanical engineering class of 2015 at Cal Poly, San Luis Obispo. The progress and development of the project are described in detail and to an extent that an individual or group with similar aspirations can construct their own multicopter or expand upon this one. The goal of this project was to create an Ultralight, as defined by FAA Part 103, commuter multicopter vehicle capable of transporting an individual to and from home, work, or school with the potential of becoming a safe, reliable, and efficient alternative to automobiles.

The text contains a background of the project and description of the specific design criteria used to define the function and applicability of the aircraft. Available options of flight, such as planes, autogyros, and helicopters are identified as well as particular components that would be beneficial in ECM's design. Additionally, the main competitor and reference for the multicopter's success is the Evolo VC1 because it is currently the sole ultralight manned multicopter. The document moves through the steps used to develop a final theoretical model of the craft. These steps range from preliminary research to detailed analysis and part drawings.

The design of ECM is a 12-propeller aerial vehicle with a traditional quadcopter layout encompassing 4, 3-propeller clusters in a 12' x 12' square area. All 3 propellers in a cluster operate synchronously, acting as one. Each carbon fiber propeller is mounted to a JM1S in-runner motor manufactured by Joby Motors, which has a continuous power of 8.2 kW and a constant efficiency of 85%. These motors are powered by 14s LiPo battery packs, and the number of batteries per motor depends on the end-vehicle-weight, so the number of batteries and flight time is tentative.

The aerial vehicle's structural materials comprises of carbon fiber and 4130 Chromoly steel. There are three components made of carbon fiber: the main arms, motor spars, and propeller rings. The 52" main arms and 22" motor spars are made of unidirectional carbon fiber with a layup schedule of three 0° plies and two 45° plies, surrounding an additional 0° ply in the center. The 52" main arms extend outward from the center mount to the arm mounts. The motor spars extend outward from the arm mounts to the motor mounts, which hold the motor and propeller assembly. The propeller rings are made from a biaxially braided carbon fiber tape with fibers arranged in a +/- 25° configuration. For building the propeller rings, West System's 105 Resin with their 206 hardener will be used.

The center mount, arm mounts, motor mounts, rings mounts, all brackets and plates are made out of 4130 Chromoly steel. This is based off the premises that the vehicle will experience a significant number of cycles and that steel is a highly reliable material. In addition, lighter metals, such as aluminum, cannot handle the loads for the desired application. Each mount is of circular geometry and fits concentrically into the carbon fiber arms. These steel to carbon fits will be rigidly attached by epoxying the overlapping surface area with 3M Scotch-Weld 2216 2-part epoxy.

The control system of ECM comprises of a Saitek control interface with a Scherrer transmitter, linked via a CompuFly cable. The selected microcontroller is an OpenPilot GCS because it allows for 12 inputs, one input for each motor, and enables an engineer to configure the propeller layout with the built-in software.

Along with the craft's development, the structure of the team is outlined, providing insight for how tasks are delegated. Task delegation involves assigning individual and team roles with respect to management and finances, as well as approaches for accomplishing more technical tasks within the three main project subgroups: structure, propulsion, and controls.

Additional attention is given to the financial limitations placed on this project. To account for the possibility of not reaching the funding goal for a full-scale prototype, two other options are presented. Results of any of the 3 options will be used to validate the feasibility of this project. However, the disadvantages and advantages of each option are outlined for the reader to realize their value.

To conclude, the theoretical results for a twelve rotor, battery powered, manned multicopter indicate a total expected flight time approaching ten minutes. As such, it will not be until the energy density and weight of small-scale power supplies improve significantly that a vehicle capable of replacing the automobile will be possible. However, this is the first iteration of ECM, and the team believes this project can move forward with great momentum if a full scale prototype is built.

2 INTRODUCTION

Today's society depends on convenient modes of transportation in order to function productively.

The automobile significantly enhanced our way of living, which few other inventions can claim. Since 1885, gasoline-powered ground vehicles have served as our primary means of convenient transportation. However, this mode of transportation is beginning to show an inconvenience in our daily lives. With millions of automobiles utilizing public roadways we witness an increase in traffic congestion, a significant amount of incidents per year, and a large mortality rate. Now is the time to investigate alternative methods of convenient transportation. But where does one begin? We believe that the best way to start is by looking *up*.

We are a team of nine Mechanical Engineering students who have undertaken the Electric Commuter Multicopter Senior Project. This project was submitted to Cal Poly by Bob Addis and Bill Bruner from Vertical Enterprise in coordination with Lawrence Livermore National Laboratory. The purpose of this project was to create a small, single-seat aircraft which complies with FAR Part 103 of the US Federal Aviation Administration. This vehicle should be capable of sustained flight, which can be operated by an uncertified pilot in both manned and unmanned configurations.

Our main goal was to provide stakeholders with a design, and the accompanying engineering analysis, for a full-scale aerial vehicle. We believe future design iterations and improvements should continue thereafter, which will pave a path for the commercialization of the aerial commuter vehicle. The project is primarily based on the amount of funding the team has access to. If there was an abundance of funding to proceed with construction, the team would extend its goals to include the building and testing of a full-scale prototype. With a smaller amount of funding the team would modify project goals to include scale model vehicle tests, a feasibility study, or both.

3 BACKGROUND

The background research encompasses various ultralight aircrafts including multicopters, fixed-wing, and personal helicopters as well as potential methods for powering and controlling these vehicles. One of the first items the team researched is the US Federal Aviation Regulations (FAR) and how they pertain to this project.

3.1 Regulations

Complying with Federal Aviation Administration FAR Part 103 is one of the more imperative requirements this project will meet. FAR Part 103 [1] establishes what constitutes as an ultralight aircraft and the governing rules of ultralight aircraft operation in the United States. The main benefit of FAR Part 103 is that "operators of ultralight vehicles are not required to meet any aeronautical knowledge, age, or experience requirements to operate those vehicles or to have airman or medical certificates" [2]. In essence, no pilot's license or training is required to purchase and operate these vehicles, making their operation far more convenient and accessible than that of a regular aircraft.

In order for an aircraft to meet FAR Part 103 requirements, it must be 155 lbs or less if unpowered or have an empty weight under 254 lbs if powered. The empty weight of a powered aircraft does not include safety devices which are deployed in case of a catastrophic situation. A powered ultralight can have a maximum of five gallons (U.S.) of fuel capacity; fuel weight is not applied to the empty weight of the aircraft. However, in response to a letter sent from the team's sponsor to the FAA, the FAA mandated the use of batteries for an electric ultralight would be included in the empty weight of the aircraft. In addition, ultralight vehicles must not be able to travel faster than 55 knots in full-power level flight. Lastly, the vehicle is intended for a single occupant, and the vehicle is flown only for recreational purposes.

While FAR Part 103 is restricting with regards to weight limit and the purpose of flight, the regulations also provide many freedoms. Normal non-ultralight aircraft have heavy restrictions on where, how far, and how high they can fly based on aircraft size, flight purpose, flight conditions, and caliber of the pilot's license. Ultralights are not subject to the majority of these restrictions. FAR Part 103-compliant aircraft can fly everywhere except within airport airspace, over congested areas, and above 18,000ft MSL (mean sea level) [1] [3]. Ultralight aircraft must fly in Visual Flight Rules (VFR) conditions and within the sunlight hours of the day. There are no restrictions on flight time or distance traveled for ultralights in the United States.

In the United States, ultralights do not have to be registered in comparison to Canada, under similar ultralight regulations, the ultralights do have to be registered. In October 2010 ultralights made up 19% of the total registered civilian aircraft in Canada [4]. Most, if not all of these aircraft, except for the Mosquito Ultralight, do not have vertical takeoff and landing (VTOL) capabilities. The majority of ultralights are fixed-wing or powered paragliders, which require a runway or sudden change in altitude, such as a cliff, for takeoff. With civilians oftentimes building ultralights from kits and using their home garage as a hangar, finding and transporting an ultralight to a legal runway can be inconvenient for the recreational ultralight pilot. With that in mind, VTOL capabilities in an ultralight aircraft could be very desirable to many potential and current ultralight pilots, as it would allow them to operate in more places that would otherwise be restrictive for normal aircraft.

It is imperative to understand that even if this project fulfills all customer requirements and meets its engineering specifications, the prototype wouldn't legally be allowed to operate as a commuter vehicle in the United States. Not until federal regulations are altered to allow for operating an aerial vehicle in congested areas (where one could conceivably benefit from flying instead of driving to a location) will

commercialization become feasible. This would mark a drastic change in policy, as currently there is no policy which covers the widespread use of personal aircraft for commuting purposes in congested areas. The Team's prototype would then act as a proof of concept, demonstrating that there are vehicles ready to challenge the existing state of aviation regulations.

3.2 Existing Flight Platforms

3.2.1 E-volo Multicopters

The closest existing vehicle to an electric commuter multicopter came from E-volo, an independent German company. They are notable for pioneering manned flight with electrically powered multicopters, capable of vertical takeoff and landing. In 2011, they successfully launched the first manned flight with one of their prototype vehicles, the E-Volo VC1 [5]. The E-volo VC1 can be seen below in Figure 1.



Figure 1: VC-1 electric multicopter vehicle by E-volo.

The E-volo VC1 was quite unlike anything else built before it. This proof-of-concept vehicle has 4 arms like a standard quadrotor, but has 4 sets of electric motors and open propellers on each arm rather than 1. The vehicle spans 17' by 17' yet weighs only 176 lbs due to its aluminum construction [6]. Built into the bottom of the craft is an exercise ball, presumably to interface with the ground and to help absorb any impact the craft may take if it makes a sudden landing. According to its creators, the VC1 was designed with redundant motors so that it can potentially make a safe landing in the event of a motor failure. With its onboard batteries (distributed throughout the craft along the arms), the VC1 can manage 20 minutes of sustained flight, although it is not clear if this figure accounts for elevation changes and lateral movement or only hovering.

The VC1 appears to meet many of the customer requirements and engineering technical specifications for the Electric Commuter Multicopter project. It is a single-passenger, VTOL aircraft made mostly from commercially available parts. Because it weighs less than the 254 lb weight limit and most likely cannot fly faster than 55 nautical miles per hour, it most likely meets FAR Part 103. It is flown by an operator using a remote control, indicating that the vehicle is probably simple to operate and capable of both unmanned and manned flight. However, there is much room for improvement with the design of the VC1. Critically,

the design lacks propeller guards and other safety equipment. It also could benefit from composite construction and increased battery capacity. In addition, the components of the vehicle are all completely exposed, making it unlikely that the vehicle electronics are well insulated.

Today, E-volo's current electric multicopter vehicle project is known as the VC200. The successor to the experimental VC1, the VC200 should be a significant step up both in form and function over E-volo's first craft. The VC200 design is a two-seater multicopter (the first of its kind) and will have 18 sets of electric motors and propellers, giving it a maximum takeoff weight of 450 kg [7]. E-volo hopes to reach an altitude of 6500 feet, cruise at 54 nautical miles per hour, and fly for at least one hour. The current design of the aircraft is sleek and attractive, looking very much like a commercially viable and marketable product, despite only being a prototype. The VC200 will be a serial hybrid electric vehicle with a range extender, meaning that it will have an onboard generator to recharge the vehicle's batteries and power the motor when necessary, hopefully extending the range of the vehicle significantly [8]. The E-volo VC200 can be seen below in Figure 2.



Figure 2: VC200 electric multicopter by E-volo, seen here with two of the vehicle's creators.

While the VC200 prototype may be impressive, it is not a viable option for the Electric Commuter Multicopter project. Most notably, it does not fulfill FAR Part 103 due to its weight, passenger capacity, and speed capabilities, meaning that it would require a pilot's license for operation within the United States. Also, its hybrid drive system necessitates a greater amount of complexity and weight than a simpler all-electric drive system.

3.2.2 Hoverbikes

The team also investigated the advantages and disadvantages of the hoverbike, a relatively new type of aircraft. Several of these vehicles are in the development stage but ECM focused on two in particular: one by Chris Malloy and his Hoverbike and another by Mark DeRoche and his Aero-X. Neither of these are on the market yet but both are due to be released in the next couple of years. The Hoverbike uses a 4-stroke 1170 cc engine that burns 30 liters of fuel per hour. It has a 105 kg dry weight (231 lbs), maximum range of 148 km (92 mi) at 80 knots and a maximum static hover height of 9800 ft [9]. Although this vehicle is under the 254 lb FAR part 103 weight limit, its speed of 80 knots surpasses the maximum allowable

speed of 55 knots and a fuel capacity larger than five gallons, which is not allowed. This product is expected to sell for \$50,000. However, in accordance with the customers' specifications of the aircraft, its 1.3 meter by 3.0 meter dimensions means that it will comfortably fit into a parking space. The prototype for the Hoverbike is shown below in Figure 3.



Figure 3: Prototype of Chris Malloy's Hoverbike.

The Aero-X can also fit into a parking space and can take off and land vertically; however, it has a dry weight of 785 lbs, disqualifying it as an ultralight, but because it is surface-effect vehicle, the Aero-X is classified as an off-highway vehicle or boat, therefore, no pilot's license is required. Like the Hoverbike, this vehicle was designed with many industries in mind as potential customers, such as entertainment, agriculture, ranching, military, and search and rescue operations. However, the Aero-X is planned to sell for \$80,000, greatly restricting access to middle and lower-class individuals [10]. A CAD depiction of the Aero-X is shown below in Figure 4.

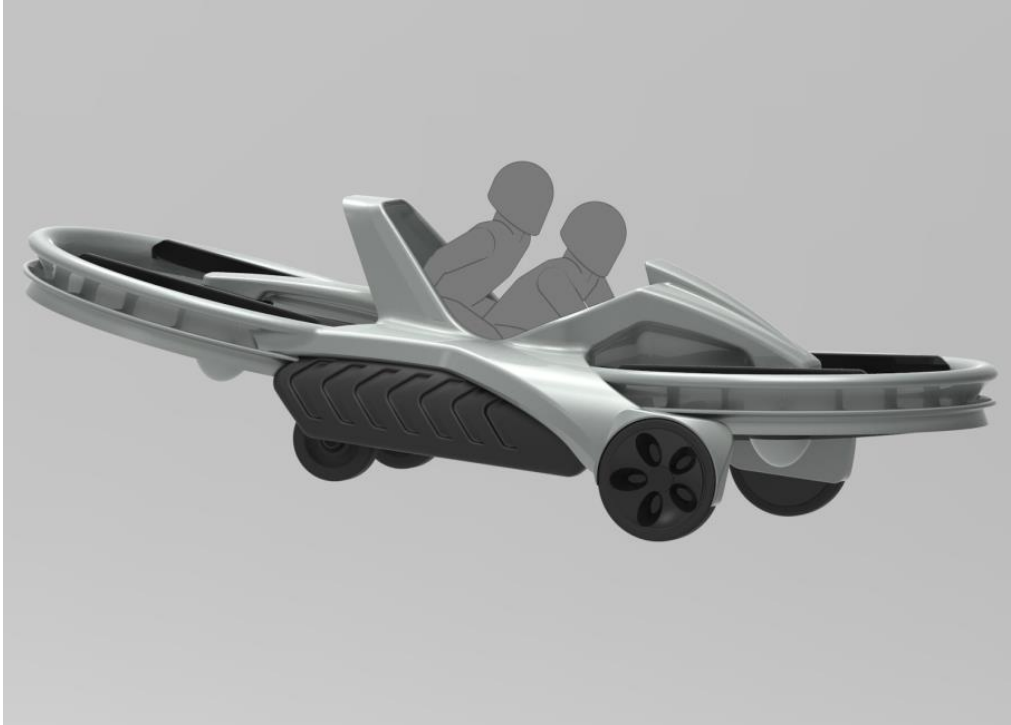


Figure 4: CAD model of Mark DeRoche's prototype Aero-X.

3.2.3 Autogyros

Autogyros, also known as gyrocopters, are a hybrid between helicopters and fixed wing aircraft which give it advantageous inflight characteristics. As a rotary wing aircraft, autogyros use an unpowered rotor by utilizing air passing by the blades to force the rotation. The rotors of the autogyro are pitched back in flight and as the relative wind passes underneath the blades, the rotors spin and provide lift. For forward propulsion autogyros usually have a propeller, as in an airplane. Autogyros have particular advantages over fixed wing aircraft, for one they are able to perform short takeoff and landings, around 15 to 50 feet of runway space because of the quick lift provided by the rotor. These aircraft are also able to fly at considerably lower speeds than a conventional plane due to autorotation of the rotors. Since the rotors are spinning due to the airflow, the lift of the vehicle is dependent on the speed of the rotors not the aircraft speed. So autogyros can achieve low speeds of 15 miles per hour without losing lift. This characteristic also gives the aircraft the inability to stall at these low speeds. When flying at speeds less than the required speed of autorotation the rotors slow down to steady state, and since the rotors are still spinning, they still provide lift. So as autogyros lose power they descend relatively gently. Unfortunately autogyros have a much larger drag profile than fixed wing aircraft in comparable size, so they can't reach high speeds and long range flight. Autogyros do have top speeds higher than helicopters due to the fact that helicopter rotors must maintain lift and thrust, as opposed to autogyro rotors which just create lift. These vehicles are also less complicated than helicopters, which lowers weight, cost and required maintenance [11]. Helicopters can hover, unlike autogyros, which is an important advantage for an aircraft. Normal autogyros are about 500 lbs and cost around \$10,000 for a kit in the United States. They can reach speeds of 45 to 60 mph and have a ceiling of around 3,000 ft. When researching autogyros for viability the team looked at its advantages in lift capabilities, cost, safety, weight, and complexity. Autogyros can come in an ultralight variety such as the Butterfly LLC manufactured by Aerial Surveillance LLC [12]. However, the inability to hover is a considerable disadvantage which ECM values as a requirement of the commuter vehicle design [13]. The ultralight Butterfly LLC can be seen in Figure 5.



Figure 5: Butterfly LLC ultralight autogyro.

3.2.4 Jetpacks

A more compelling prototype vehicle out today is the Martin Jetpack created by the Martin Aircraft Company based out of New Zealand. It is a ducted-fan, personal aircraft purposely designed as the first responder vehicle and a heavy lift unmanned vehicle. The Martin Jetpack is a VTOL aircraft with composite materials and a custom built V4 two stroke engine. The jetpack can provide a zero airspeed hover when there is no pilot control input. In 2011 the jetpack was able to reach 5,000 feet above sea level which is an incredible feat. Martin Aircrafts hopes to sell this vehicle in the \$150,000 to \$250,000 range in the United States, which is similar to the price of a sports car [14]. The aircraft can provide a flight time of 30 minutes at 74 km/h (46 mph). Unlike the team's design this jetpack falls under New Zealand's class 1: microlight, which gives them more wiggle room than the USA FAR part 103. With an unmanned weight of 180 kg (397 lbs) this vehicle exceeds FAR 103's maximum requirement for weight. The Martin Jetpack can be seen below in Figure 6.



Figure 6: Test pilot flies in a Martin Jetpack.

3.2.5 Paramotors

Another vehicle considered was the Paramotor, a paraglider configuration powered by a motor or engine. These vehicles take full advantage of their glider capability, making them very lightweight, generally around 50 lbs [16]. This allows quick response to pilot input and extends flight time to around three hours, or 60 miles on a four gallon tank of gas [17]. Once a reasonable altitude is attained, the motor can be shut off, allowing the pilot to glide on wind currents. This adds a significant amount of safety to the device because in the event of engine failure the pilot can land almost as easily and safely as they could with the engine. Like the Mosquito, the paramotor experiences problems with the angular momentum associated with its propeller, which forces the rider either to break or weight shift to the opposite side [18] to compensate. One company has developed a technology that essentially counters this angular momentum by implementing a fan-shape into the frame of the paramotor. Figure 7 below shows the counter measurement for the angular momentum problem faced by paramotorists.



Figure 7: Scout Paramotors' device to counter the angular momentum of the paramotor.

Paramotors are reasonably simple machines; a new pilot can learn to fly comfortably in a couple of days [19]. Additionally, they are compact, which makes transporting them by car relatively easy, and one can take off within the length of a football field and land in a mid-sized backyard [20]. They are reasonably

priced, generally falling within the \$4000-\$7000 range. The paramotor has numerous attributes that make it an appealing aircraft, but it cannot vertically takeoff and land. Figure 8 below shows a classic paramotor design, with a pilot, propeller, glider, and engine.



Figure 8: Paramotor assembly with propeller, pilot, engine, and glider.

3.2.6 Blimps

The blimp was also considered for this project. Generally associated with the Hindenburg disaster, blimps are one of the safest, although rare, methods of air travel due to the use of inflammable gas and compartmentalization of the gas to prevent disaster in the case of a hull breach. Blimps offer an effective way to stay airborne for extended periods of time because they are positively buoyant and do not require wings for lift or rotors for vertical thrust or lift. However, the volume required to make the craft positively buoyant can be significant. Aerial Products, a blimp manufacturer, offers products [21] with maximum lift capabilities of 136 lbf starting at \$19000. Note that 136 lbf is noticeably below the required lift for this project and the price just for the blimp component, not including the structural, power, or motor components far exceed this project's preliminary budget. Some preliminary buoyancy calculations were performed to estimate the size needed for a blimp. Assuming a net craft and payload weight of 400 lbf, it was found that for an ideal, optimized balloon shape fitting into a 18ft x 9ft parking place, the balloon would have to be over 36 feet tall. This seems to be unreasonably large for an everyday commuter to navigate. First, to stay on the ground, additional weights, like sand bags, are needed, and then to return to the ground after flight, the blimp must be deflated. Then re-inflation, implying that a readily available source of the gas used to fill it up (most likely helium) is available, which is not the case for the common commuter.

3.2.7 Mosquito Ultralight

The Mosquito can be ordered as a kit in five separate segments and takes about 200 hours to assemble [22]. One of its aspects that interests buyers is its ability to autorotate, meaning that even when no power is applied to the engine, the main rotor blade will continue to spin in such a way that continues to produce thrust, potentially allowing the helicopter to make a safe landing in the case of an emergency. However, this type of landing is very demanding on the pilot and requires a great deal of skill. Although it is

technically an ultralight, the Mosquito necessitates a significant and sustained mental effort by the pilot for controlled flight because of the large amount of angular momentum present in the system, making for unavoidable gyroscopic effects. One obvious attribute of the Mosquito is its ability of VTOL. To qualify as an ultralight, the designers of the Mosquito were forced to discard the cockpit to decrease the weight of the vehicle, increasing the vulnerability of the pilot in the event of a crash or blade malfunction. Figure 9 below shows the Mosquito ultralight and an exposed pilot.



Figure 9: Mosquito ultralight with rider.

3.2.8 Firefly Ultralight

ECM's most likely contemporary ultralight competitor that complies with FAR 103 would be the Kolb Firefly, seen below in Figure 10. Constructed by Kolb Aircraft located in Phoenixville, Pennsylvania this fixed wing ultralight is an easy to build aircraft and is controlled by a 3-axis cable, push-pull tube system. Weighing 250 lbs empty, this aircraft is considered an ultralight by FAA standards. Also providing the ability of retracting wings and tail, this aircraft can be stored in a reasonable sized storage in just 15 minutes. Kolb Aircraft grants buyers additional options such as a full enclosure, a composite prop, lights, brakes and a ballistic parachute [23]. The Firefly comes standard with a 40 hp engine which gives it a top speed of 63 miles per hour. And with a price tag of around \$9,000 it's hard to beat this product for a sport enthusiast to enjoy flight without a license or a fortune. However, the team believes that the ECM design would be a superior product since with a 150 ft take off distance, the Firefly simply cannot be used in a number of different environments. Vertical takeoff and landing of the proposed multicopter design provides a versatile advantage that the firefly just can't provide [24].



Figure 10: Kolb's Firefly Ultralight in flight.

3.2.9 Carter Aviation

Carter Aviation Technologies out of Wichita Falls, Texas has developed a VTOL autogyro prototype called the 4-Place PAV (Personal Air Vehicle). Unlike most autogyro designs the 4-Place PAV uses a smaller 'pre-rotator' motor to spin the rotors at takeoff. To lift off, the pre-rotator is de-clutched and the rotor pitch is increased in order to catch the air. The propulsion propeller is activated and the rotors are switched to auto-rotation mode for forward flight. Also, as the speed of the vehicle increases the rotors slow down to reduce drag and the wings take strain of flight [25]. At full speed the 4-Place PAV acts as a fixed wing aircraft and it is designed to reach 245 mph at an altitude of 25,000 ft. It will have an expected empty weight of 2500 lbs, a jump takeoff weight of 4000 lbs and a rolling takeoff max weight of 5000 lbs. The Proof of Concept was able to fly at a test weight of 3800 lbs with a 45 foot diameter rotor and wingspan, and a 350 HP turbocharged Lycoming IO-540 engine. With a capacity to hold two pilots and two passengers and a designed lift to drag ratio of 15, the Carter PAV is at the forefront for new autogyro design. The Carter PAV's design characteristics are very advantageous to implement into an ultralight commuter vehicle. But with 2250 lb over the 250 empty weight limit and with its complicated vertical takeoff system, it may not be a viable way to create an ultralight aircraft [26]. The Carter 4-Place PAV can be seen in Figure 11.



Figure 11: Carter Aviation 4-Place PAV in flight.

3.3 Patents

Although the idea of a commuter multicopter is somewhat rare, a patent search yielded several results relevant to this project. The first describes the usage of redundant rotors in a common plane, generating lift and propulsion by adjusting the motor plane angle. Additionally, the motor speeds are monitored through a “failsafe network” [27]. Another patent comprises of “vertical takeoff and landing aircraft using a redundant array of independent rotors” where each rotor is electrically powered and controlled and all rotors are in the same plane of rotation. Figure 12 below shows what the author of the patent emphasizes the idea of *redundant* rotors. [28] A German patent outlines a similar aircraft to that in Figure 11; the aircraft can transport people or loads and is controlled by a signal processing unit without requiring outside input from a pilot. Unlike the two previous patents where the rotors are defined to be in a plane, this configuration applies to the “surface that is defined by the propellers,” a more general statement than a plane, as described previously [29]. Figure 13 displays this concept.

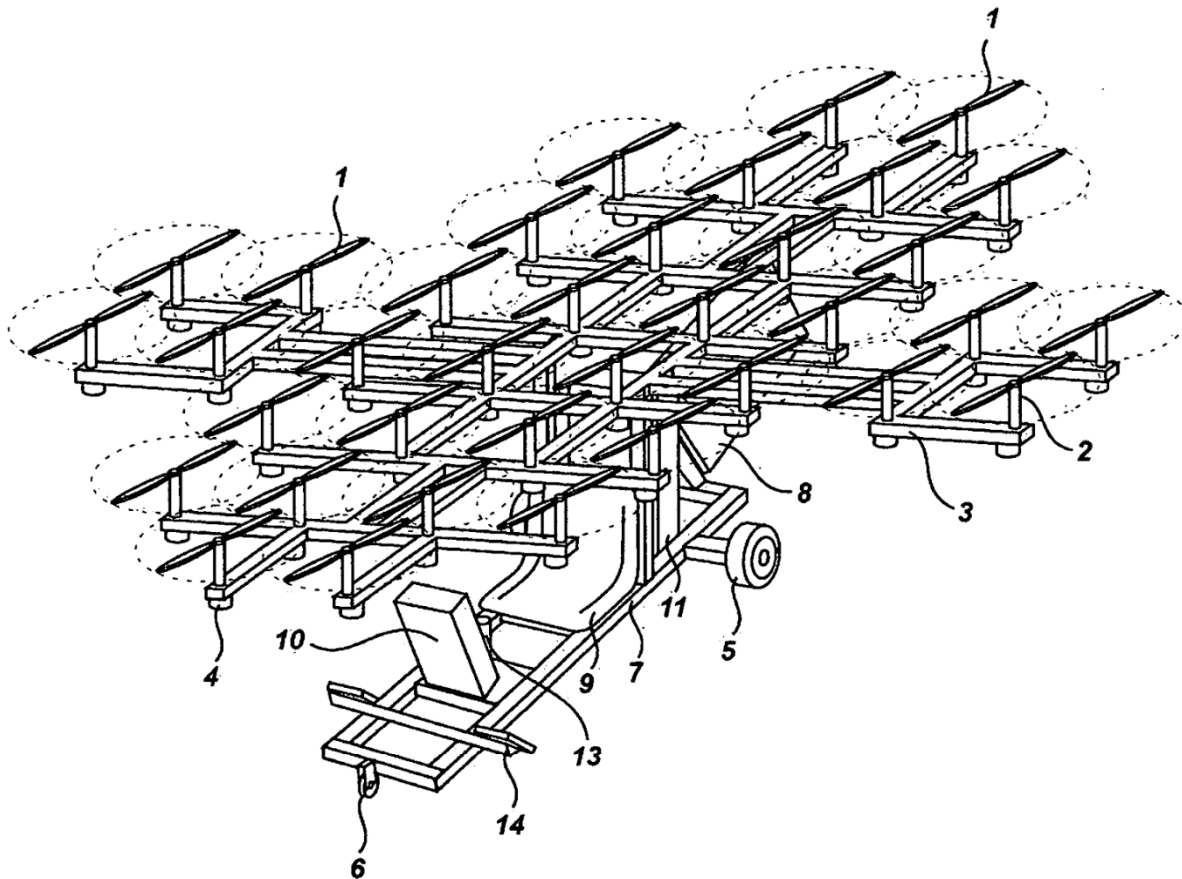
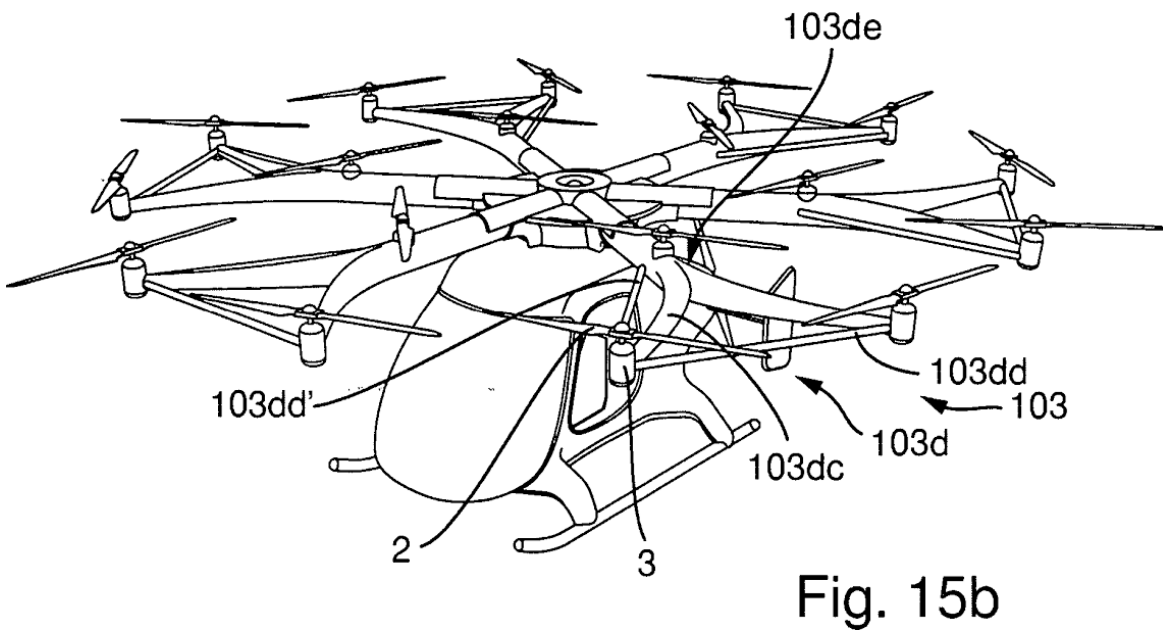
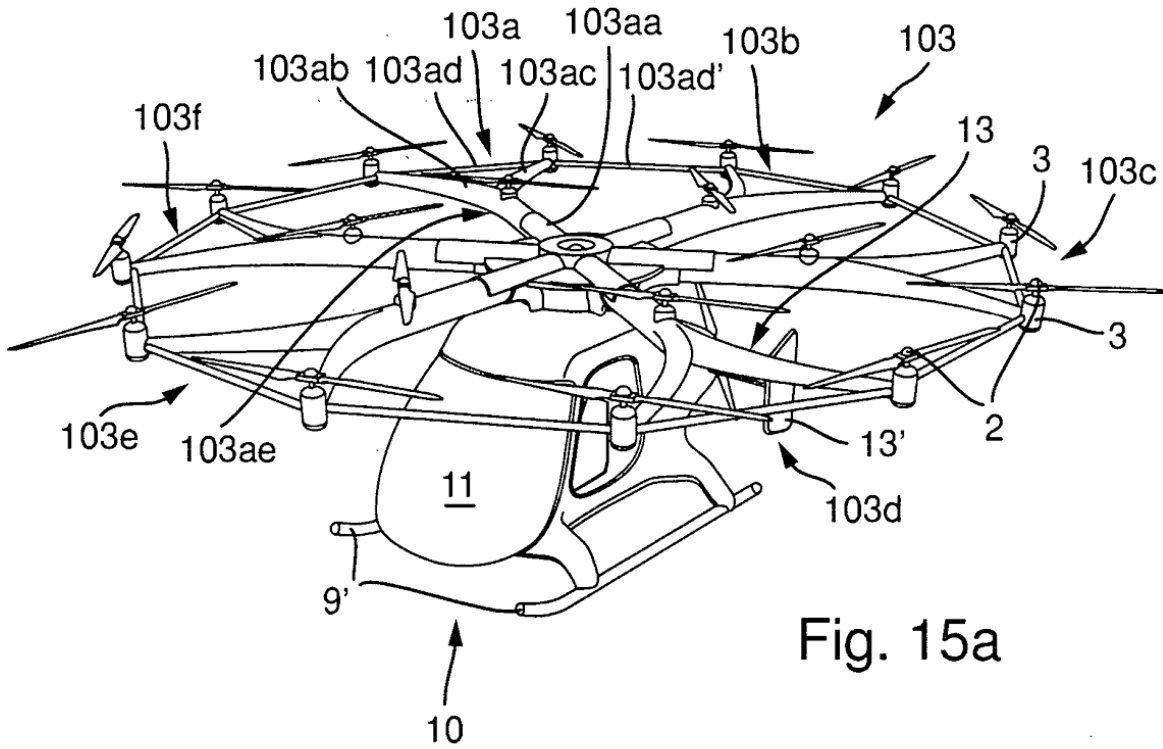


Figure 12: Multirotor with patented “failsafe network”



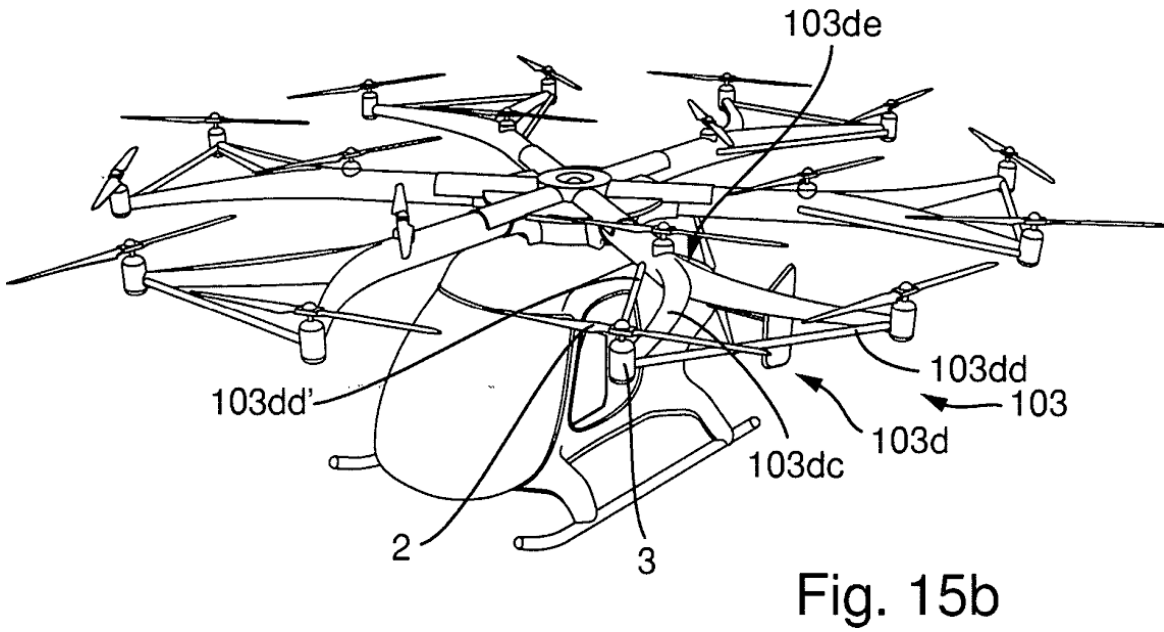
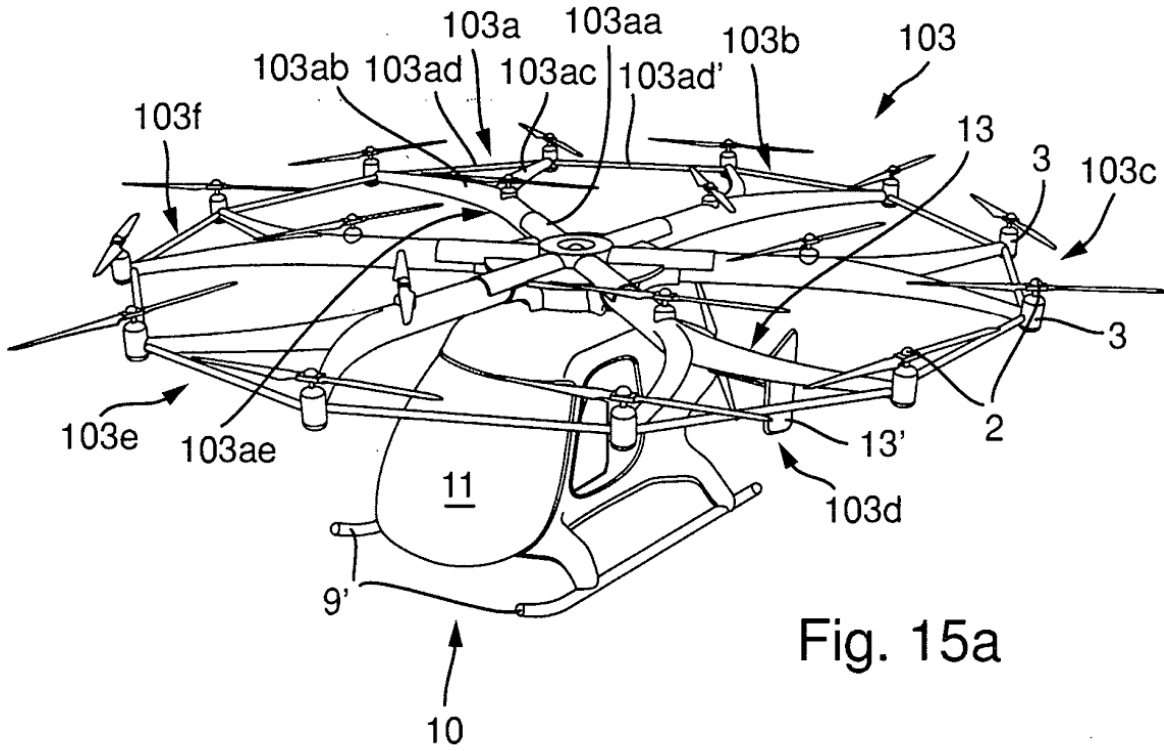


Figure 13: Patents for electric multicopter aircraft.

3.4 Subsystem Research

3.4.1 Flight System Dynamics and Controls

There were a number of flight systems that can be utilized to achieve the goals for this project, and each one varying significantly in system dynamics. The team began with the most basic principles for flight dynamics: the basic forces experienced. There were four major aerodynamic forces to consider in engineering design, and they include lift, weight, drag, and thrust. Lift is the upward force used to overcome the weight of the aircraft, while thrust can be used to both overcome weight and overcome the opposing force of drag. Three types of systems that are recognizable today are, quadcopters (multirotors), helicopters, and airplanes. Quadcopters are an interesting flying vehicle as they do not create lift, and often experience negligible drag due to their low speeds [30]. This means that the only primary experienced forces are weight and thrust, with thrust often being the only highly controllable variable [31]. The principle of balance and center of gravity also become highly important for quadcopters due to stability concerns. [31] Motion of a quadcopter follow the same controls of conventional aircraft: pitch, yaw, and roll, as can be seen in Figure 14.

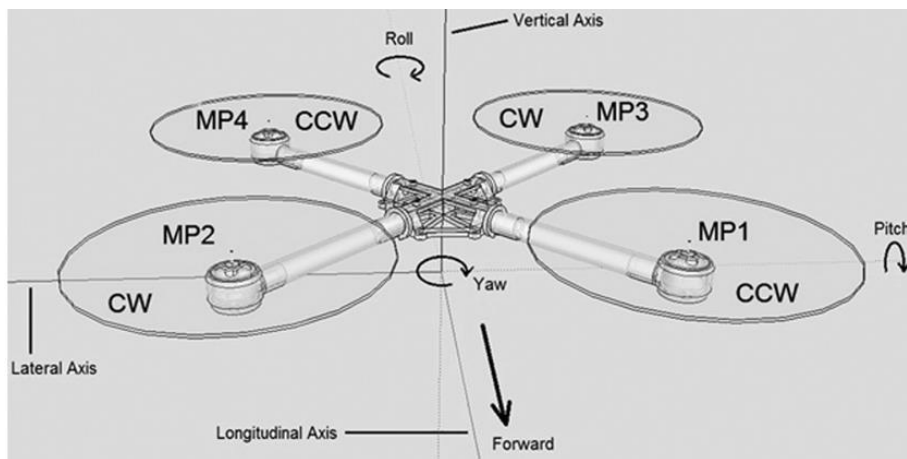


Figure 14: Quadcopter layout and possible directions of motion: roll, pitch and yaw [32].

To perform any of these maneuvers, all adjacent rotors must spin in opposite directions [31]. Clockwise spinning props are called “pullers” while counter-clockwise props are called “pushers”. To control pitch, one must decrease the speed of the front two rotors and increase the speed of the back rotors, making sure to keep a net-zero moment acting on the craft. [32] This will allow the vehicle to move forward through the air, while maintaining altitude. In order to yaw, or rotate in the horizontal frame, one must increase the speed of rotors in the direction of yaw, and decrease in the opposite direction. [32] For example, in order to yaw counter-clockwise, one would positively offset the counter-clockwise rotors and negatively offset the clockwise rotors. Finally, in order to roll, or bank the vehicle left or right, one must speed up the rotors in the opposite direction of roll and decrease in the direction of roll [32]. For example, to roll right, one would increase the speed of the two left rotors and decrease the speed of the two rights.

Helicopters are extremely complex systems overall, largely due to the fact that while airplanes want to fundamentally fly, helicopters do not [30]. A helicopter works by using a large main rotor blade (airfoil) to generate lift. In principle it does this the same as an airplane, by making air flow faster over the top than the bottom of the rotor blade, generating a pressure differential and lift. The difference here is that this is done through forcing the air over the rotor blades with a spinning motion [33]. A tail rotor on a helicopter counters the torque of the main rotor and keeps the aircraft from spinning in circles. To control a helicopter a pilot must use both hands and feet independently to fly the craft which requires extensive training. The cyclic pitch lever sits between the pilot's legs and can tilt the helicopter front, back, left, and right through varying pitch via a swashplate. The collective pitch lever allows one to gain or lose altitude. Lastly both feet are used to change the direction via the foot pedals. [30]

Airplanes experience the same aerodynamic forces of lift, weight, drag, and thrust. An airplane uses a fixed wing that, when air flows across it, creates a high pressure region below the wing and a low pressure area above the wing. This pressure differential caused by the wing is what creates lift. Unlike helicopters and quadcopters, airplanes vector their thrust to primarily oppose drag. Airplanes can't conventionally obtain VTOL because they must reach a certain velocity before the wings can generate enough lift to overcome their weight, but are naturally stable in the air. If an airplane loses power mid-flight it can continue to glide to a safe landing unlike helicopters and quadcopters. Airplanes use three main control surfaces to control the aircraft's roll, pitch, and yaw. The elevator, usually located at the rear of an airplane on the horizontal stabilizer, adjusts controls pitch. Ailerons, located on the wings adjust to control roll. The rudder, located on the vertical stabilizer at the rear, controls yaw. Most airplanes do not require any sort of electronic controller to stabilize and require much less pilot input to fly than helicopters.

3.4.2 R/C Control Systems

R/C multirotors have recently become extremely popular due to their advancement in control technologies. R/C multirotors are especially desirable because of their simplistic construction and limited number of moving parts; the only moving parts on multirotors are the propellers themselves. The reason for this is that all the degrees of freedom for a multirotor with four or more propellers can be controlled solely by changing the independent rotor speeds. This is structurally simpler than using the swashplates and anti-torque propellers used on helicopters [34]. However, creating a quadrotor control system that can detect and react accurately and quickly enough to provide for stable controllable flight is extremely difficult. With advancements and the lowering costs of electronic sensors and processors these systems are now commercially available.



Figure 15: An R/C Quadcopter.

Today's R/C multirotors like the one seen above in Figure 15 can perform acrobatic maneuvers, fly autonomously, hold position/altitude, and can be easily controlled due to the advances in electronic control systems. These controllers are programmed and built for your typical hobbyist multirotor in mind; however, the sensors and electronics used in these crafts are extremely capable. Current control boards for multirotors are extremely sensitive and can adjust motor inputs hundreds of times a second. Thanks to a growing community of hobbyists and professionals using multirotors for aerial photography and video control, technologies are getting better and better. Also, many of the most popular control boards use open-source code like the ArduCopter [35], AeroQuad [36], and OpenPilot [37], which allow the user to adjust the code based on their specific application. This makes these boards highly versatile and perhaps even adaptable to a larger platform like ours. While these R/C multirotors are small with respect to this project, the e-volo VC1 proves the same principles and layout can be used to make a full size aircraft capable of holding an occupant.

3.4.3 Actuator Disk Theory

Actuator Disk Theory (Momentum Theory) is a simplified model for the relationship between thrust and power for a propeller. The assumptions for Actuator Disk Theory are that the propeller is an infinitely thin disk that does not have any drag due to friction. In addition it is assumed that velocity of the air at the entrance and the exit is constant across the actuator disk. Using these assumptions and control volume analysis equations relating thrust and power can be derived. The most basic of all situations relevant to the project would be a single actuator disk in hover.

$$P = \sqrt{\frac{T^3}{2\rho A}}$$

The above equation is for a single rotor disk hovering. More complex calculations can be derived that account for the tilt of the rotor disk during forward flight as well as the velocity of the rotor. For comparing different designs with each other Actuator Disk Theory will work well since only the relative magnitudes are important as long as the calculated power is close to the actual power needed. Once the number of designs was reduced to two or three configurations, a more comprehensive model was used.

3.4.4 Ground Effect

All fixed wing and helicopter aircrafts experience the aerodynamic effects of ground effect. Ground effect refers to the phenomenon that allows aircraft to maintain altitude at slower airspeeds or rotor speeds when within one wingspan or rotor diameter of the ground. This performance gain is due to the change in flow pattern around the aircraft when close to the ground. This change in flow reduces downwash, upwash, and wingtip vortices providing a large decrease in induced drag.

One of the biggest perks of utilization of ground effect is the large increase in blade efficiency for rotorcraft, an important factor for maximizing energy use. This is accomplished by two aerodynamic phenomenon taking place within the ground effect. First, the entire airflow is altered by the ground interrupting the airflow underneath the craft. This reduces induced drag while simultaneously increasing the lift vector vertically [38]. Secondly, operating a rotorcraft near the ground reduces rotor tip vortices generation by adding a physical barrier [38]. This causes an increase in efficiency at the outer lengths of the rotor by minimizing the area affected by vortices as well as decreasing turbulence [38].

Ground effect is most significant when the wing or rotor is close to the ground. The reduction in induced drag exponentially decreases with wing proximity to the ground. When a wing is at a height equal to its

wingspan induced drag is reduced by 1.4%; at a one-fourth its wingspan, 23.5%; and at one-tenth, 47.6% [39]. This performance increase in ground effect allows aircraft to maintain lift at lower rotor speeds and airspeeds than those needed outside of ground effect. The Pilot's Handbook of Aeronautical Knowledge by the FAA cites the significance of ground effect and that it "must be considered during takeoffs and landings" [39].

For the team's applications, the team believes ground effect can be very advantageous in maximizing energy efficiency. ECM foresees future vehicle iterations being operated at heights near one effective rotor length from the ground. This would allow the commuter to bypass traffic in a lane directly above the standard flow of traffic. In these circumstances, the pilot can remain in the ground effect envelope to maximize efficiency of the craft. This of course provides numerous safety concerns, which would have to be addressed in accordance with state law and federal regulations. The largest concern amongst these is the hazard of operating flying craft near the proximity of drivers. In a more general sense, ground effect can always be utilized to initially decrease power necessary for lift off.

3.4.5 Power Systems

The team has researched many different power generation methods used in aviation and general commuter travel, with the most common method being the combustion engine. The combustion engine is split between two categories, Spark Ignition (SI) and Compression Ignition (CI) Engines. SI Engines use a fuel with high octane ratings for antiknock qualities. This engine requires a spark to ignite the fuel and is used in common ground vehicles. CI Engines, more commonly known as diesel engines, require a fuel that can ignite on its own under certain conditions.

There are many alternative fuels to replace conventional gasoline or diesel. Such fuels are listed in Appendix D. Here at Cal Poly, the team has access to reserves of Cal Poly produced methanol and dimethyl ether, SI and CI fuels, respectively. Methanol is a fuel with high octane ratings which will decrease knocking capabilities and increase compression ratios and power output. It is also much cleaner than conventional gasoline, producing CO₂ and water vapor as products. This can be a clean alternative to a fully electric aerial vehicle. Dimethyl Ether is an excellent replacement for D2 and other diesel fuels. Its high cetane and low octane ratings make it a high performing fuel and it combusts in a much cleaner fashion than D2. Both fuels are better performing than their conventional counterparts which can justify the placement and use of such a system on the project for power generation

Gas turbines or jet engines are another viable source of power generation. Gas turbines essentially compress air, mix it with a fuel, and ignite it to create a hot expanding gas that will spin a turbine for energy output. Industrial size gas turbines are out of the team's reach but micro turbine "gensets" are feasible. These miniature gas turbines can produce propulsion and rotary motion for a project of ECM's scale.

These systems rely on the fact that the fuel has very high energy density, as seen in Appendix C: Table 1 Fuel Density Chart, to offset the inefficiencies in the combustion process. Typical gasoline-powered commuter vehicles have a power delivery efficiency of approximately 20%. Batteries on the other hand are very efficient at delivering the power stored in them but have low energy density. Typical battery power delivery efficiencies are approximately 90% [40]. Advances in lithium ion and lithium polymer batteries have started to catch up to fuel in terms of energy density. The big difference between combustion power delivery and battery power delivery is that the combustion power delivery usually requires a more complex and lower efficiency system to deliver its power. A hybrid power delivery system takes some pros and cons from each system, but adds even more complexity. In cars it tends to be used for high efficiency power delivery at low speeds and high energy and power density for long distance and higher speeds.

3.4.6 Batteries

For this project, several viable battery options have been researched, including Lithium Polymer (LiPo), Nickel-Metal Hydride (NiMH), and Lithium-Ion (Li-Ion). Table 1 below shows the charge density and voltage per cell of the Li-Po, Li-Ion, and NiMH batteries.

Table 1: Battery Data

Battery	Charge Density, (Wh/kg)	Voltage Per Cell (V)
Li-Po	185	3.7
Li-Ion	126	3.6
NiMH	100	1.25

Note that the Li-Po offers a significant advantage in charge density, an essential characteristic for lightweight aircraft. High discharge rates are necessary in order for the vehicle to VTOL as well as for quick system response. The NiMH does poorly in this category and is recommended to be used at a 0.2C discharge rate [41]. The lifetime of the battery must be considered as well. Due to the corrosive nature of the battery, performance begins to degrade after the first use and only a certain number of charge/discharge cycles can be expected. How the batteries are utilized, stored, charged and discharged, determines the battery's usable cycles which can vary significantly depending on these conditions. Although not at the same scale as this project, most RC hobbyists find their Li-Po's to last between 150-200 cycles. Safety is another concern for batteries. If improperly stored or charged, the Li-Po's may catch on fire and, consequently, require a specialized charger to avoid such circumstances. For proper performance, battery balancers or regulators must be used along with the batteries. The purpose of battery regulators is to avoid overcharging or over discharging the cells within a battery where each cell does not have exactly the same charge. For example, if the lower voltage limit is 3.0V and a cell is at 3.0V, then the entire battery must be disconnected in order to avoid over-discharging that particular cell. However, with a regulator, charge can be redistributed evenly among the cells, allowing for maximum functionality from the battery (<https://focus.ti.com/lit/an/slyt322/slyt322.pdf>).

	NiCd	NiMH	Lead Acid	Li-ion	Li-ion polymer	Reusable Alkaline
Gravimetric Energy Density(Wh/kg)	45-80	60-120	30-50	110-160	100-130	80 (initial)

Figure 16: Energy density of common battery types (1Wh/kg = 3.6KJ/kg) [42]

For the project the team considered weight and fuel capacity carefully, as these criteria are mandated by Part 103 of the Federal Aviation Regulations. The weight of the combustion engine needs to be added into the calculation of energy density. The engine weight is usually not considered except in extreme cases (i.e. supermileage vehicles). The weight of the gas engine, as well as the conversion system (alternator, inverter, etc.), in the case of hybrid power, has to be considered and is not negligible. The team will also have to consider the possibility of using a tethered electric vehicle. This would severely limit the range and use of the vehicle, but would almost negate the weight of a power delivery system. A new technology has come out that is making "tethered" flight more viable, the laser power delivery system [43]. The technology is still in its early stages, so it might not have enough power density to power the devices that the team will use to create thrust, but it might eventually be able to significantly reduce the weight of aerial vehicles.

3.4.7 Ducted Fans

In modern aircraft, two fundamental methods exist to exhibit thrust using propellers: ducted fans and non-ducted fans. A duct is a cylindrical structure surrounding the propeller that guides airflow into and out of the propeller and acts to mitigate tip effects, as seen in Figure 17 below. In this context, tip effect refers to the vortices that occur at the tip of propellers or fixed-wing aircraft. As an introduction to this concept, consider the wing. Between the top and bottom of the wing, a pressure differential exists, and it is this separation of a higher and lower pressure that allows that airplane to fly. At the tip of the wing, however, this separation is absent and the high pressure air beneath the wing can escape to the lower pressure above the wing. This effect creates these tip vortices which can be detrimental to both propeller and fixed-wing aircraft as propeller blades travel through the vortices induced by other blades. Additionally, this leakage effect is parasitic to performance where the work done to compress the air freely escapes, illustrating a decrease in aircraft lift and thrust. Ducted fans seek to avoid this effect by sealing the pressure differential at the end of the propeller so minimal leakage occurs. For the duct to benefit aircraft performance, clearance between it and the propeller must be small, generally around 3% of the diameter of the fan [44]. In addition to negating tip effect, ducts can create lift from their physical structure. Observe in Figure 17 that the air traveling into the propeller is being accelerated from its initially static state while air on the outside of the propeller remains static. Consequently, a pressure differential is created that provides lift to the aircraft, although, depending on the shape of the duct, the lift may be inconsequential. It should be noted that ducts become detrimental at higher speeds because their presence inherently increases the drag of the aircraft, generally limited to several hundred miles per hour. If properly implemented, ducted can reduce power consumption to 70% of non-ducted fans for a given thrust, but the additional weight of the duct's structure must be considered in this comparison.

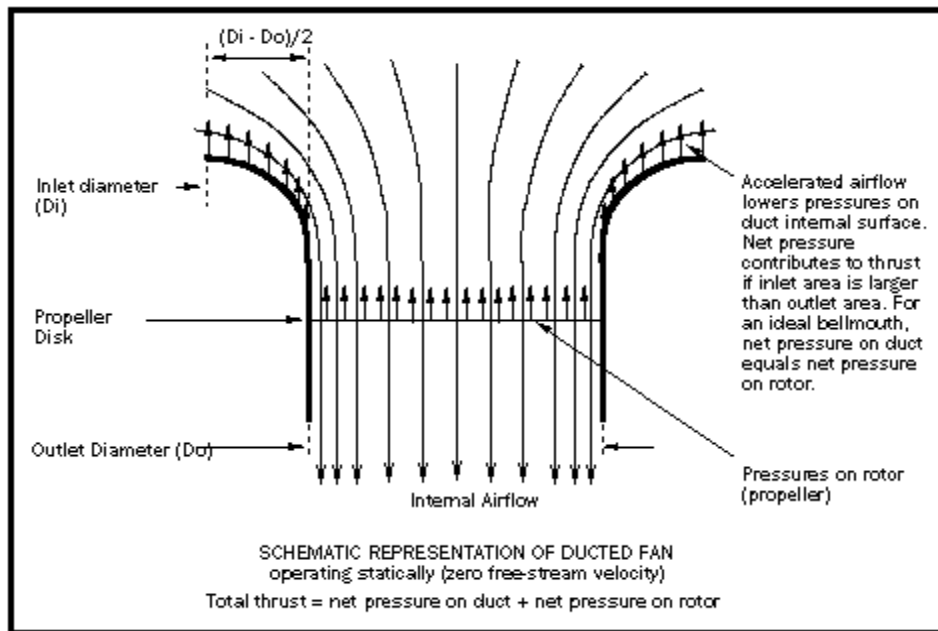


Figure 17: Model of airflow around a ducted fan [45].

3.5 Current Commuter Issues

This project is supposed to address the issues of the daily commuter and make his or her frequent travels to work, school, or making errands a more quick and enjoyable experience. To better understand how to meet these needs, research was conducted involving the distances traveled, the time taken, the cost to travel, and efficiency of the mode of travel that a commuter commonly encounters. First, the team will address how far the average American travels per year. The Federal Highway Administration (FHA) released the information shown below in Table 2 in September of this year, displaying the average annual and daily miles traveled by various age groups in the United States [46].

Table 2: Annual and Daily miles traveled by various age groups in the United States.

Age (years)	Annual Miles Traveled			Daily Miles Traveled		
	Male (mi)	Female (mi)	Total (mi)	Male (mi)	Female (mi)	Total (mi)
16-19	8206	6873	7624	22.5	18.8	20.9
20-34	17976	12004	15098	49.2	32.9	41.4
35-54	18858	11464	15291	51.7	31.4	41.9
55-64	15859	7780	11972	43.4	21.3	32.8
65+	10304	4785	7646	28.2	13.1	20.9
Average	16550	10142	13476	45.3	27.8	36.9

The table above indicates that for this project to be successful and to appeal to the average commuter, the machine must have a minimum range of about 35 miles. Another goal of this project is to decrease the time spent in traffic. According to a 2011 study done by Texas A&M, the average American commuter spends 38 hours a year in traffic. Consequently, this time spent in traffic costs the country 5.5 billion hours of waiting as well as 2.9 billion gallons of wasted fuel, \$121 billion in delay and fuel cost, and an additional 56 billion pounds of carbon dioxide emission. In this study, LA and San Francisco were in second and third place, respectively, for the most hours spent in traffic, both above 60 hours annually, equivalent to 1.5 work weeks [47]. This is indicative of California's relatively severe traffic problem. Therefore, it is reasonable to conclude that another mode of transportation capable of avoiding these significant traffic delays would be advantageous to the average American.

Although the majority of American's have adopted the automobile as their primary form of transportation, other (less popular) methods exist that allow commuters to avoid traffic-related delays. Because this project is focused on private, rather than public, transportation methods, the team researched the current private transportation market. This group includes cars, trucks, small aircraft, and small helicopters. These vehicles were chosen primarily to demonstrate their efficiency, an important criteria in a world demanding more energy conscious individuals and transportation. Table 3 below shows the miles per gallon rating of ground and aircraft machines. Note that "mpg" (or person-miles per gallon) is the number of individuals that can ride in the vehicle multiplied by the miles per gallon of the vehicle. This unit of measurement is widely used because if a passenger train is considered in these studies, its gas mileage is close to 0.15 mpg, but it can carry hundreds of people, meaning that it actually is a very efficient form of travel.

Table 3: Efficiency comparison of several ground vehicles and aircraft.

Vehicle	mpg	Number of Passengers	pmpg
2014 Toyota Prius	50	5	250
Ford F-150	20	5	100
PiperSport: Lighweight Plane	20	2	40.1
R-22: Lighweight Helicopter	16	2	31.0
HoverBike	12	1	11.5
Paramotor	15	1	15.0
Martin Jetpack	1.6	1	1.6

By no means is Table 3 considered an exhaustive list for vehicle efficiencies. The ground vehicles, the Prius [48] and F-150 [49], were chosen because they give a sense of the maximum and minimum range of efficiency while the PiperSport [50] and R-22 [51] were chosen because they could potentially be used as commuting aircraft that avoid ground traffic and are small enough for personal use. Additionally, some of the ultralights and other aircraft discussed earlier in this document are presented to provide some insight into the efficiency range of the competition of this project. Note that the Aero-X and Firefly ultralight are not presented because no efficiency information could be found and that specific “mph” values could not be found for some of the vehicles so a value was calculated by dividing the vehicle’s range by their fuel capacitance.

4 OBJECTIVES

For the sponsor, the team intended to deliver an ultralight vehicle design that meets all the requirements of Part 103 of the US Federal Aircraft Regulations for a powered vehicle. This vehicle would be a reasonably compact, single-seat multicopter with sustained flight and vertical takeoff and landing (VTOL) capabilities. It would be simple to operate, being no more complex to fly than a small quadrotor UAV. The vehicle would be as safe to operate as is feasible for an ultralight and feature propeller guards, an emergency shutoff feature, and sufficient electrical insulation to protect the user and bystanders. It will be durable enough to survive gentle regular use and be usable in both manned and unmanned flight. It would have a relatively small footprint, ideally being able to fit within two standard parking spaces or an area of similar size. Lastly, it must be designed to make use of as many commercial off-the-shelf parts as possible. The list of customer requirements can also be found in Appendix C: Project Requirements.

To meet the sponsors' requirements, implementation of the Quality Function Deployment (QFD) method was used in order to create a set of engineering specifications. The full document is included in Appendix C: Figure 1 and includes all of the details of the analysis. Then a list of all the requirements that were given to the team by the sponsor was drafted, as well as additional requirements that the team decided were crucial for success. These requirements are in bold and are located on the left side of the QFD. The group then proceeded to assign numerical values to signify the importance of each requirement on a scale of 1 to 10. It was fairly straightforward to decide upon values within the team, but assumptions were made in deciding the importance of each requirement to the sponsor. The group then graphically displayed the relative importance of each requirement on the far left of the QFD so the critical requirements could be emphasized.

On the right side of the QFD, the team assessed how well some of the competitors met the requirements given to the project. Again, a numerical value between 1 and 10 was assigned to each competitor for each requirement, and the results were plotted on the far right to aid with the analysis. Finally, the group came to the exciting part of the analysis: determining what engineering specifications the team would use to gauge the overall success of the project. The group came up with a lengthy list, and added the specs to the top of the QFD in bold. The team then assessed how closely related each customer requirement was with each technical specification. Closely related items were designated with a black circle, moderately related items with a white circle, slightly related items with a triangle, and the rest were left blank. This allowed the group to once again determine the relative importance of each specification, which is plotted in the lower section of the QFD.

After comparing the competitor's products to the teams' new specifications at the very bottom of the QFD, the team was able to decide upon numerical targets for each specification that, if met by the team, would make the project extremely competitive. These numbers were the main purpose of conducting the entire analysis, and will define how the team carries out future design decisions. Finally, the group indicated which of the requirements were closely related to each other by marking the intersection of the two in the very top of the QFD with a plus sign. If any of the requirements had too many plus signs, or if any customer requirement was satisfied by too many technical specifications, the specification was considered redundant and removed. After a lengthy analysis and several iterations, the team was able to decide upon a final list of target technical specifications, which are listed below in Table 4. The numerical values for these specifications were targets, not concrete requirements, and were subject to change upon further analysis.

Table 4: Target Engineering Specifications.

Spec #	Parameter Description	Target	Tolerance	Risk	Compliance
1	Uninterrupted Flight Time	10 minutes	- 0 minutes	High	Test
2	Fully Loaded Weight:Thrust Ratio	1 : 1.2	- 0	Medium	Test
3	Angular Deviation while Hovering	20 degrees	+ 0 degrees	High	Test
4	Degrees of Freedom in Control System	6	N/A	Medium	Inspection
5	Payload Weight Capacity	200 pounds	- 0 pounds	High	Test
6	Range of Remote Operation	100 feet	- 0 feet	Medium	Test
7	Vehicle Weight	254 pounds	+ 0 pounds	High	Test
8	Footprint	18 feet x 18 feet	+ 0 ft^2	Medium	Test
9	Percentage of COTS Parts	50%	- 0%	Low	Analysis
10	Minimum Design Factor of Safety	1.20	- 0	Low	Analysis
11	Ingress Protection Rating	3	- 0	Medium	Inspection
12	Number of Exposed Electrical Connections	0	N/A	Medium	Inspection

5 PROJECT PLANNING

5.1 Method of Approach

In order to reach the project's end goal, it was imperative that the team follows a structured approach to the solution. Much of the structure can be seen in Figure 18, the Formal Design Process, as established by the teams' senior project requirements. The main difference would be that the team members would carry out a majority of this process twice, resulting in a much more accelerated pace.

Formal Design Process

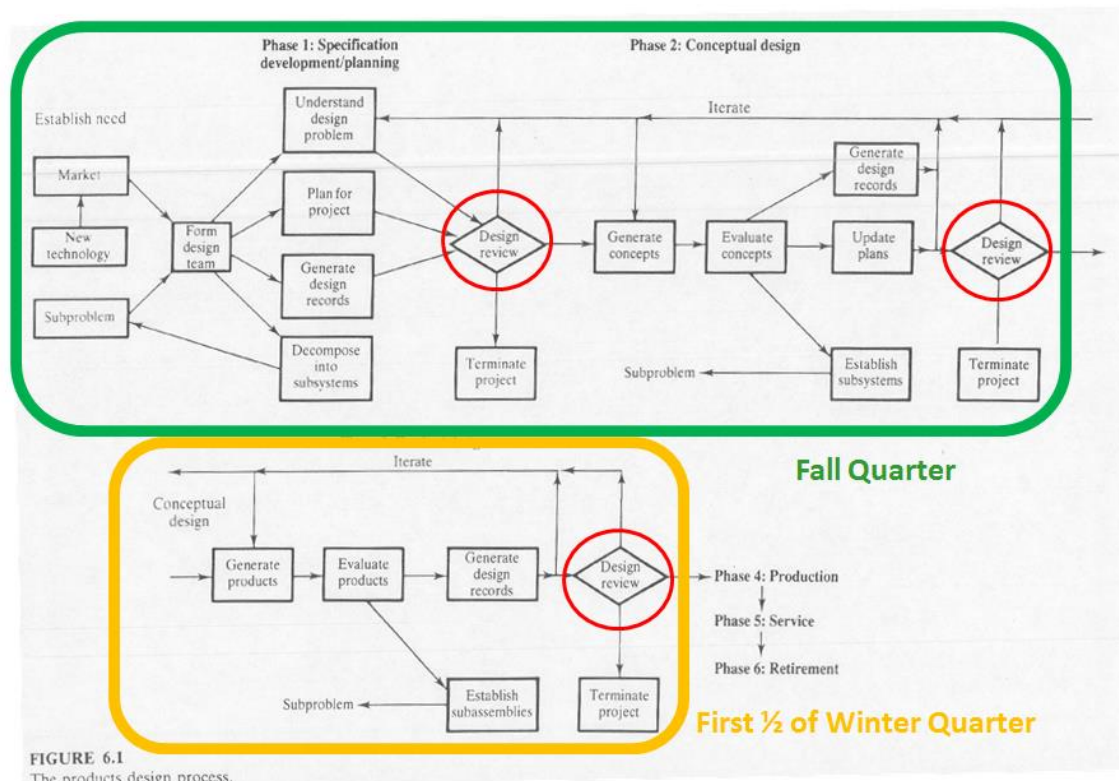


FIGURE 6.1
The products design process.

Figure 18: Formal design process as seen from Ullman's "The Mechanical Design Process" [52].

What follows is a breakdown of the process:

The team then completed Phase 1, which is specification development and planning. The group began with sponsor presentations, which led to the formation of the nine person team. Since then, the team has worked to build an organizational structure for the team activities and sponsor communication. In order to plan for the project, an extensive amount of the research was needed to acquire an understanding of what the project entails. This document marks the first of four design reviews, it encompasses the research, and the requirements and specifications that arose from it. Before beginning any conceptual design, the first job was to decide a generic project scope.

After consultation with the sponsor, Professor Fabijanac, and Professor Schuster, the team has decided to design a full scale prototype that meets the specifications outlined in this document, which will be fleshed

out in detail with preliminary analysis. This allows the group to provide the optimal engineering solution within the time frame, while allowing flexibility as a first iteration Cal Poly project. From here, work on the teams' behalf will lead to the final deliverables, which exist at three levels. If the group was not able to secure any additional funding, an engineering analysis with a feasibility study would be completed, utilizing the current budget for motor/prop/thrust testing. If the team was able to obtain a substantial amount of external funding, the group would design a scale model of the vehicle, in addition to the previously stated testing and engineering feasibility study. The most ideal option was to complete the feasibility study and then provide a full scale prototype that proves the plausibility of the concept. Regardless of funding, the initial analysis would be focused on a full scale vehicle, while the prototyping and production would be subject to a variable budget.

With this established, the team began Phase 2, beginning with concept generation and ideation. The group first focused on the top level design and functionality of the vehicle. From here the team began an initial evaluation and comparison of ideas, including decision matrices, subsystems to be evaluated and preliminary analyses to narrow down the options to an overarching system to be presented later in this report, marked design review 2. Upon approval of the PDR, the team began a phase which deviated from the standard senior project course timeline. This was Phase 3 (integrated conceptual design). Here, the group broke into smaller teams, each working on subsystems simultaneously in a horizontal integration technique. The team once again generated subsystem concepts, and performed concept evaluations. Team organization allowed for this independent subsystem work, and a subsystem Point of Contact (POC) kept each team informed of the others' work. After decision matrices had been evaluated within each sub-team, a final approval process began in which decision matrices and other tools were used to find which subsystems would complement each other the best to create the best system. Design review 3 summarized this work in the form of this document, to be issued to the sponsor for approval. This would mark design review 3.

Upon approval of the Critical Design Review, Phase 4 (product design), would be initiated. This phase tasked each sub-team to work on their subsystems, producing a detailed engineering analysis that would provide much of the basis behind the feasibility study and set up for production. Each sub-team was responsible for the design of the subassemblies within their subsystem. Numerous iterations lead to a final subsystem concept design to be integrated with the others for a final system. The sub-teams were dynamic and fluid, with members working with each other frequently and often to maintain compatibility of subsystems. This was the most crucial part of Phase 4. After the detailed analysis was completed, a final internal engineering review occurred in which final evaluation of subsystems and compatibility would take place. This lead into design review 4, the Final Design Report.

This completion and approval of the Final Design Report marked the beginning of Cal Poly's final phase of Senior Project, Phase 5 (production). This was where the decision as to which tier the project would end on would be decided. Provided adequate funding, the team began the production, fabrication, and testing of a vehicle, with a Project Update Report being sent to the sponsor approximately midway during the process to update on project status. Upon the completion of production, the sponsors received a Final Project Report and see the final results in person.

Throughout the process, the team worked to acquire funding, donation, sponsorship, and assistance in creating the process. This includes school resources such as the CIE, corporate resources, and the assistance of additional assistance from Cal Poly students and faculty, taking on a more multidisciplinary approach. This helped create visibility as well as increase the team chances of returning a final project in the top tier approach.

For the purposes of marketing and fundraising, there was an initial proof of concept test performed long before deadlines. The first test was a motor and propeller thrust test. To do this test, selection of motors and propeller to be used for the project were needed. This test demonstrated to investors that the planned design was feasible, and that the team would simply need more funding to make the full-scale vehicle a reality.

In order to ensure that the project design did not exceed the funding available there was deadlines in which a certain funding level would be needed or the project would shift direction to a lower cost goal. The first deadline was December 12th, 2014. At this time the team will determine if there was sufficient funding to design and build a full scale product, or if a small scale model or proof of concept testing was required. In order to continue to full scale, an estimation of \$10,000 of funding was needed to purchase materials or an equivalent amount of donated materials was required.

If the information in this document justified the acquisition of sufficient funding to go full scale, the team would determine if the project was able to build a working prototype out of the final material choices (i.e. expensive composites) or if needed, the group would build a proof of concept model out of less expensive materials. In order to build the prototype an estimated \$40,000 was required in total funding. These funding goals were not absolute and were subject to change with further development; the team would keep the sponsors up to date with any changes to the funding plans. The combined timeline was as follows:

November 18th, 2014	Preliminary Design Report
December 12th, 2014	First funding deadline (\$10,000 goal)
January 30th, 2015	Critical Design Report
February 6th, 2015	Second funding deadline (\$40,000 goal)
June 5th, 2015	Final Project Report

For a more detailed project timeline refer to Appendix C: Table 4 and Figure 2.

5.2 Construction Plan

The team started construction as soon as the project secured funding. The first construction task was to build a motor testing platform to carry the test plan detailed above. The team talked with the Electrical Engineering Department about using their motor testing equipment. At the same time the mounting brackets and sensor arrangement were manufactured. The team would have to order a large amount of parts even before testing was done to ensure longer lead time parts would arrive. If the testing went well and the motors were within their required specifications, parts ordered would be allowed to go through. If the testing shows the motors were not within their required specifications the group would have to redo testing with new motors and return or cancel original orders.

As the ordered parts came in the team would have to do testing and verification to make sure parts were not damaged in shipping or were outside of advertised specifications. Batteries could be tested the day that they were received with a digital multimeter. Motors and electronic speed controllers (ESC) would require a quick run through of the motor test plan in order to make sure there were no manufacturing defects or delivery damages. The main controller board would have to be programmed and tested for communication ranges and sensor accuracy. The team would split up into teams for structure, electrical systems and programming. If the group could split up the programming of the controller board, the assembly of the electrical circuits and the structure building they could be done roughly in parallel. The team would occasionally have to come together to do tests for multiple motors and make sure the

programming was working correctly. The full scale assembly of all the subsystems would have to have started on about February 19, 2015 and finish by around March 3, 2015. If all went well the team could immediately go from full scale assembly into testing until the end of Winter Quarter 2015. For a more detailed project timeline, refer to the Gantt chart in the Appendix C: Schedule/Gantt Chart. Note that these dates were subject to change and may deviate from those outlined in the Cal Poly Senior Project Syllabus for a schedule that is more conducive for this project.

5.3 Management Plan

Particular roles were assigned to individuals at the start of this project that have and will continue up to its end to facilitate functions critical to team organization and success. These roles were:

<i>Sponsor Communication:</i>	Marley Miller
<i>Meeting Documentation Organizer:</i>	Alex O'Hearn
<i>Information Retention and Organization:</i>	Blake Sperry
<i>Treasurer and Accountant:</i>	Sam Juday & Ike Sheppard
<i>Goal Tracking:</i>	Blake Sperry & Ike Sheppard

To account for the progress made with this project and to continue working efficiently and yielding exceptional results, the team structure has adopted a scheme of smaller teams working on the subsystems of the multicopter. Because the project was relatively large in scale and covers many ranges within the mechanical engineering discipline, this approach was necessary in order to have team members capable of sufficiently exploring component selection, design, and analysis. Therefore, the following subsystem teams were created with the respective persons:

- Structure:** Marley Miller, Sam Juday, Art Norwood, Alex O'Hearn
- Propulsion:** Blake Sperry, Ollie Kuntz,
- Controls/Electronics:** Kyle Kruz, Jarrell Washington, Ike Sheppard

These teams work independently but maintain communication through the use of cloud services for the most up-to-date versions, iterations of designs and decisions as well as meet every Tuesday, Thursday, and Sunday for collaborative meetings, team approval, and subsystem updates. The Tuesday and Thursday meetings are three hours (12:00pm - 3:00pm) each and were part of the Senior Project course, while Sunday meetings were four hours (4:00pm-8:00pm) long and has been implemented by the members of this project.

Apart from the subsystem design itself, each subgroup was responsible for designing and purchasing necessary testing equipment to verify their design before it was equipped into the final design. Additionally, upon the completion and submittal of this report, each subgroup made the necessary adjustments in their design or analysis to accommodate for any constructive feedback or considerations it received from this report's presentation to its lab advisor and sponsors. Once a cemented final design had been chosen and proper testing had been done, each subgroup was responsible for completing their respective subsystem in accordance with the major deadlines described by this project's Gantt chart and the Senior Project course syllabus. These deadlines are shown below.

Corrected, Finalized Design:	14 February, 2015
Begin Manufacturing:	27 February, 2015
All Testing Completed:	02 March, 2015
Completed Subsystem Assembly and Testing	24 April, 2015
Completed System Assembly	11 May, 2015

Finish System Stability/Hover Testing	27 May, 2015
Senior Design Expo	29 May, 2015
Final Project Report	5 June, 2015

Clearly there was still a great deal of work to do to attain this project's goals and was foreseeable that some subsystems may be completed before others or take longer than others. In such a case, the team had the ability to re-organize and prioritize some of the more cumbersome tasks that may surface in the coming months by temporarily reallocating members.

Funding was another key concern of this project. In order to reach the funding goals of this project, the entire team would assist in the application process for the two project-funding grants available at Cal Poly. Once the success of the applications was known, the team would adjust the goals and desired outcomes of the project accordingly. For a more detailed project timeline refer to Gantt chart in Appendix C: Schedule/Gantt Chart. Note that the Gantt chart in this report differs significantly from that in the Preliminary Design Report. These adjustments were made to account for some of the scheduling conflicts, the time allotted for some of project's tasks, and the requirement of additional tasks that have surfaced since the creation of the initial Gantt chart.

6 TOP CONCEPT DESIGNS

6.1 Design #1: Multicopter (under-body props)

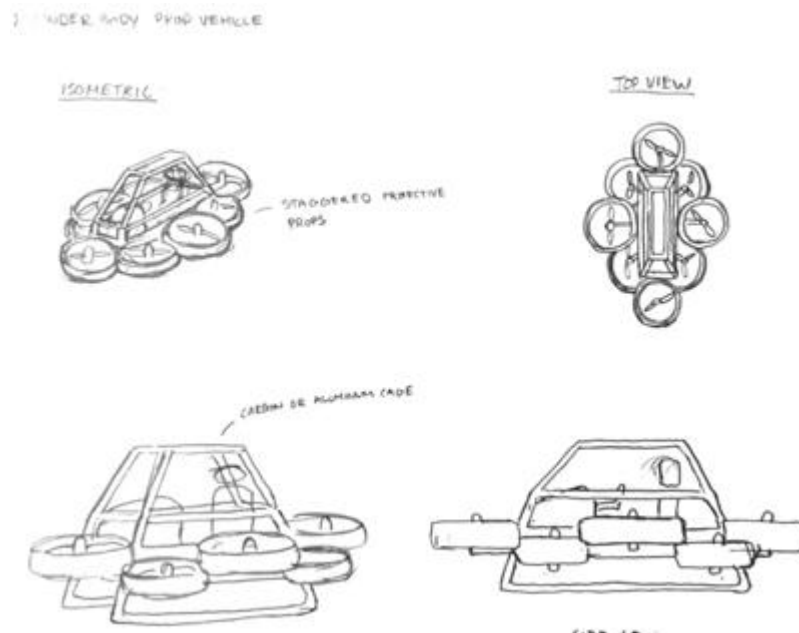


Figure 19: Multicopter (under-body props)

The first design mirrors the original intent of the sponsor very closely. It consists of a basic quadrotor layout, with several rotors on each arm. The pilot will be situated in the center of the vehicle, above the plane of rotors, yet low enough to maintain a low center of gravity to increase stability of the craft. The under body structure would allow for minimal landing gear weight and safer landings, since quadrotors often land with a significant horizontal velocity. Multicopter configurations also have excellent VTOL capabilities and are very steady when hovering, and their simplicity allows for an extremely lightweight structure. This arrangement has the additional aeronautical characteristic of ground effect which would help with sustaining lift.

The multicopter with under-body prop configuration met the some of this project's specifications. One of its critical abilities is VTOL which is necessary for the commuter to conveniently take off and land within the confines of a parking space. Similarly, because the propellers are close to the ground, a significant ground effect can be taken advantage of and applied as VTOL assistance. Due to the placement of the propellers, the implementation of a landing gear will be relatively simple because the landing mechanism could be fixed to the existing structure of the vehicle. Additionally, assuming that the control system will be similar to a common multicopter, then the unmanned operation of the vehicle will be relatively straightforward and allow for a responsive system, but it will be more complicated because the aircraft will be operating at an unstable equilibrium point. In the event of a single motor or propeller failure, this design would be able to compensate well because of the excess of props present. However, this concept suffers heavily on the safety side because the user could fall into the props or, if unshrouded, would face significant difficulties exiting the craft upon failure.

6.2 Design #2: Multicopter (overhead props)

OVERHEAD PROP VEHICLE (STANDING)

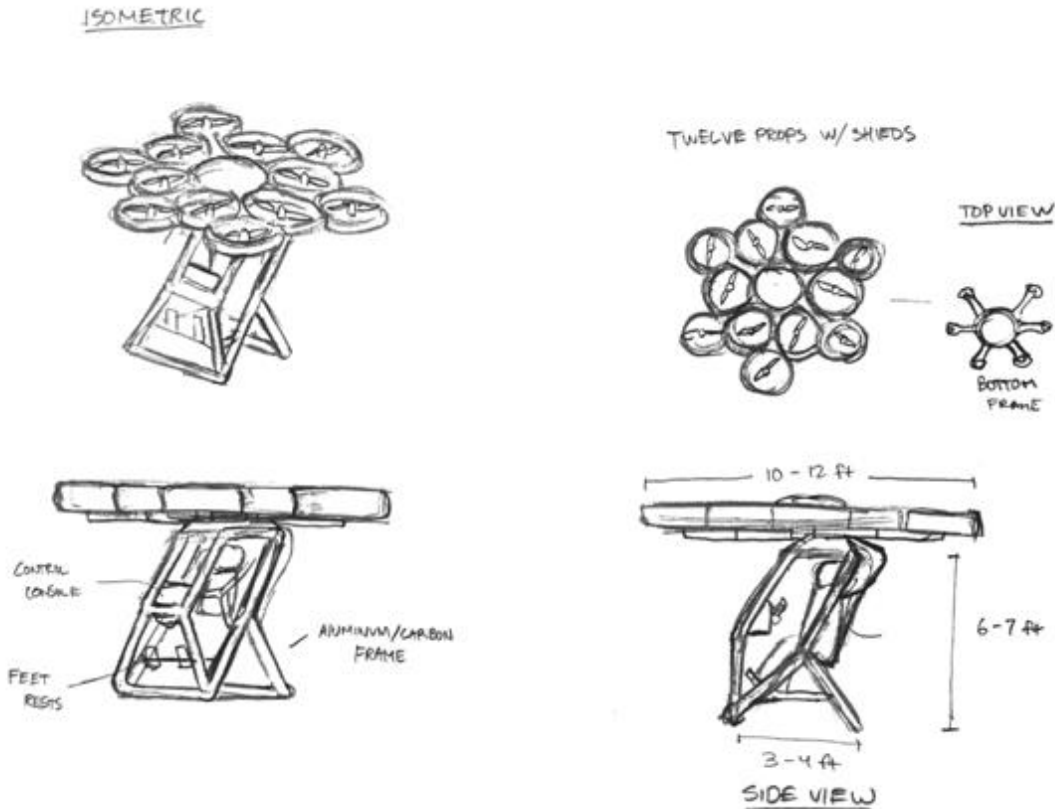


Figure 20: Multicopter (overhead props)

This design is very similar to the previous one, with the exception that the props are located above the pilot's head. The advantage of this layout is that the center of gravity would be below the rotors, indicating that the team would have a self-stabilizing system. This would make the controls design extremely easy, and would simplify the vehicle's operation as well. However, the redesign would call for much more structural material and reduced landing stability.

The overhead multicopter satisfies the design specifications much in the same way as the under-body props multicopter does. The only primary differences are in safety, VTOL capabilities, and weight. With the propellers above the user direct unintentional contact is much less likely. Having the propellers fully above the pilot helps prevent propellers from breaking and injuring the pilot and the pilot from falling into the propellers. The overhead multicopter is a great VTOL performer like a helicopter however with the elevated height of the propellers the vehicle can't make as much use of ground effect as the under-body propeller design. The structure of the overhead multicopter would be similar to the layout of the under-body multicopter except it would require more material to suspend a "cockpit" below the plane of the propellers. Because of this the overhead multicopter would weigh more than the underbody design, however should still meet the 254 lb limit.

6.3 Design #3: Hoverbike/Hoverboard

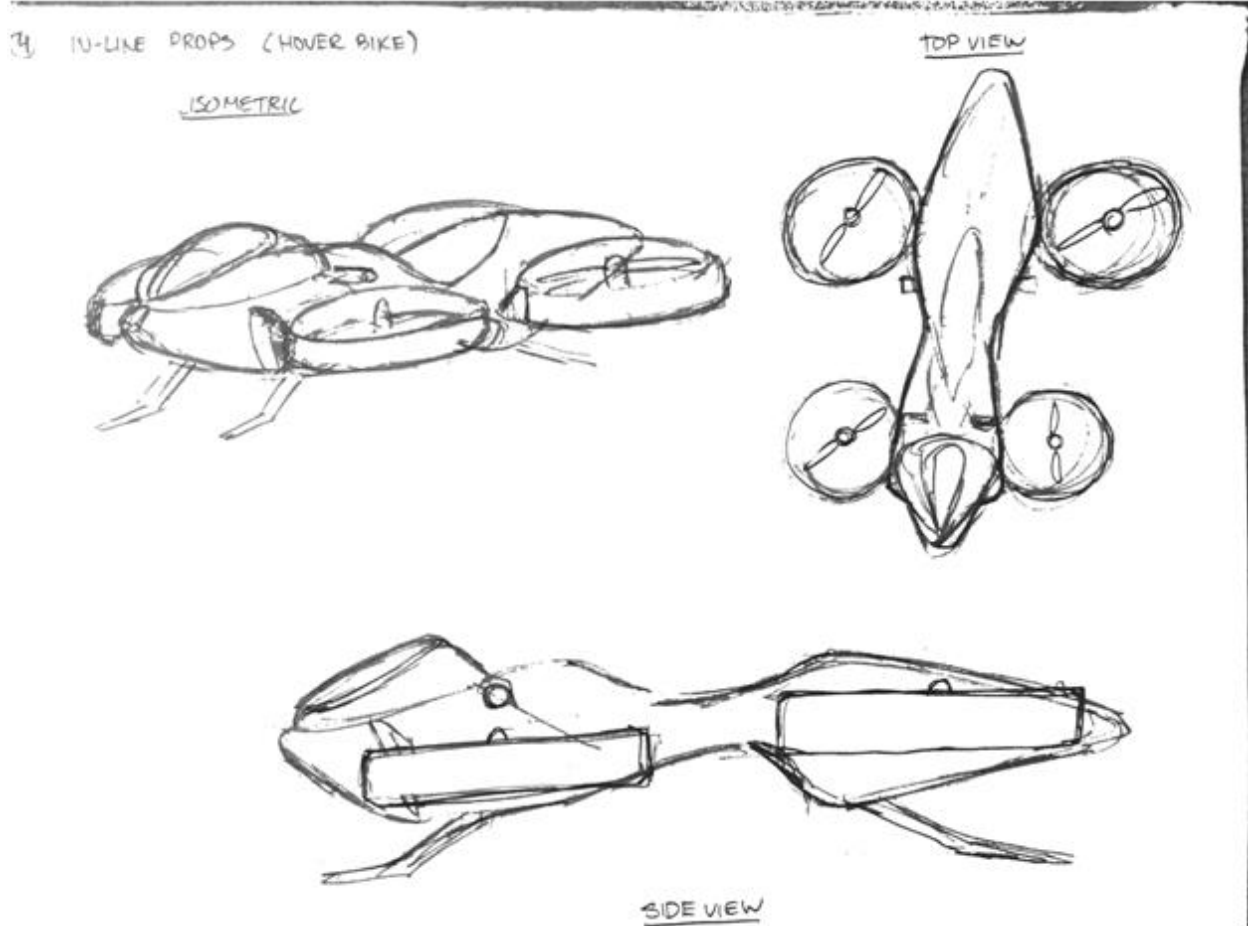


Figure 21: Hoverbike/Hoverboard

The hoverbike and hoverboard designs are radically different than the quadcopter configurations in that there are only two groups of synchronous rotors. This means that additional means of balancing the vehicle laterally is needed, presenting the team with a significant design challenge. However, creating an operational vehicle could mark the first vehicle of its kind. All specifications could be met with this configuration, but it would be difficult to create a working prototype.

This design's specifications benefit and suffer from many of the same attributes as the multicopter underbody prop configuration. However, this design would likely have between two and four props, where the failure of one could lead to a catastrophic failure because of the lack of redundant rotors available to compensate for this loss.

6.4 Design #4: Powered VTOL Gyrocopter

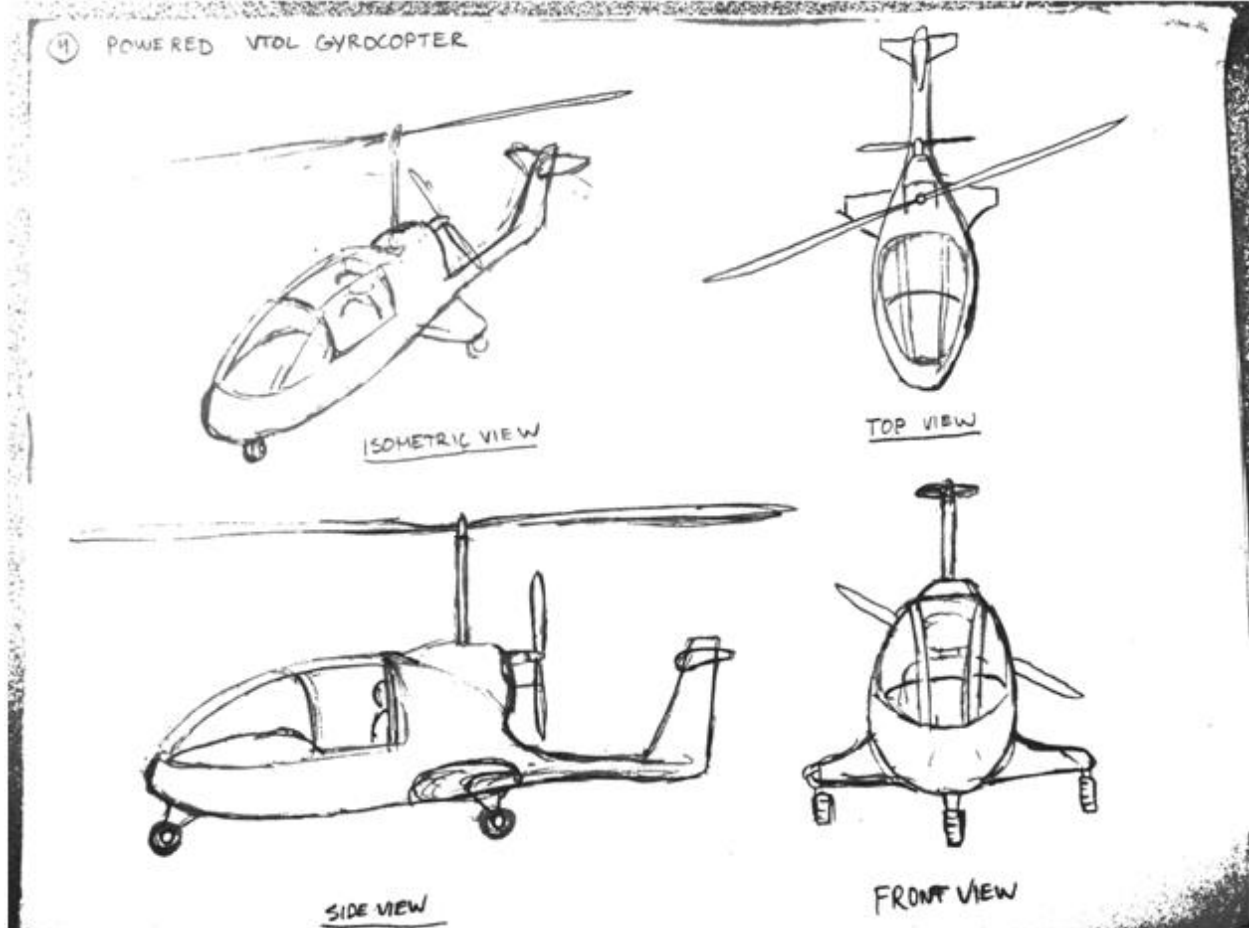


Figure 22: VTOL Gyrocopter

The gyrocopter is a very aged technology, dating back to before the helicopter was ever invented. However, it has very little visibility within the aviation community, yet still shows a lot of promise. The power is driven into a propeller at the rear of the vehicle, while an unpowered main rotor provides lift from the top. This lift is generated due to the angle at which the rotor is oriented and allows for a pretty impressive forward velocity. In order to satisfy the VTOL requirement, the team would have to implement a secondary motor or some means of powering the main rotor during takeoff and landing, which would definitely complicate things. However, the benefits in range and speed may outweigh the challenges that this design would impose.

The powered VTOL gyrocopter met all design specifications except it will not be able to hover midflight unless substantial power was to be diverted to the large rotor. The needed energy to power the large rotor would quickly deplete precious battery life. The large rotor would also need to be unshrouded in order to take advantage of autorotation which would further decrease the safety of the aircraft. This design would also be difficult to alter for unmanned capabilities; with a multistage VTOL process a complex control system will be needed. Gyrocopters are usually light compared to other aircraft so it wouldn't be too difficult to modify the design to follow FAR 103 ultralight requirements. Gyrocopters don't require a large fixed wing area and the rotor is high above the pilot which would give the aircraft a small footprint.

6.5 Design #5: Multi-Gyrocopter

⑥ MULTIGYROCOPTER (ALTERNATIVE DESIGN)

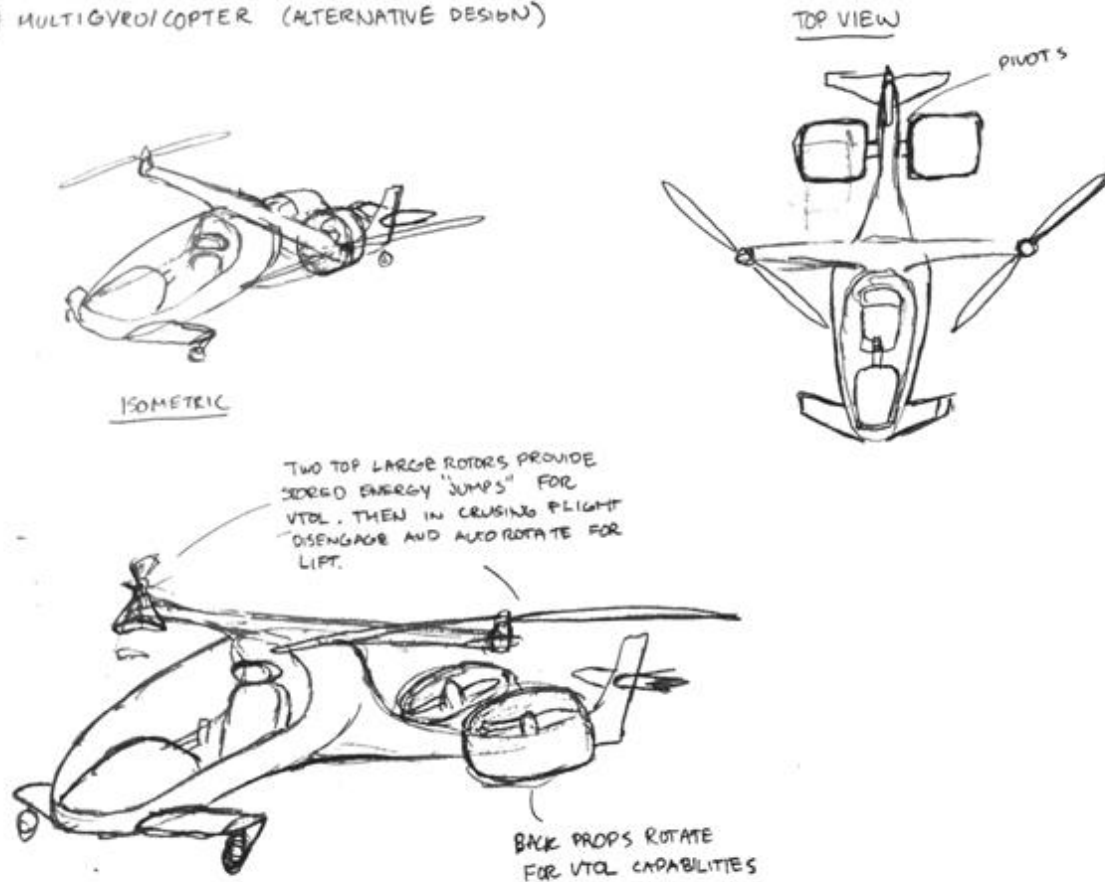


Figure 23: Multi-Gyrocopter

A multi-gyrocopter would operate in a very similar fashion to a traditional gyrocopter, except it would utilize the layout of a standard multicopter. In theory the four rotors would engage for VTOL and in cruising the two front two rotors would slow down and the back two would provide forward movement. The autorotor would have to be pitched back at a high angle in order to provide autorotation. The numerous rotors could improve stability and maneuverability, and such a design would definitely be groundbreaking. However, the multiple rotors would also complicate an already complicated VTOL system since each rotor would require some form of power.

Much like the powered VTOL gyrocopter mid-flight hover and unmanned flight would be difficult. The multi-gyrocopter would be safer than the powered VTOL gyrocopter due to redundant rotors and improved maneuverability. This comes at a price however, due to the larger structure to hold the additional rotors the footprint and weight of the vehicle would be greater.

7 CONCEPT DECISION PROCESS

Narrowing and selecting the design concept for this project was a five step process. The first step was weeding out ideas based on obvious feasibility issues. Next the remaining ideas were categorized and combined into fundamental concepts. Third, the fundamental concepts ran through a decision matrix and the top five were chosen for further analysis. The top five were investigated with quantitative research, ran through the decision matrix again, and the top two designs were chosen through debate and consensus. Finally the lead design idea was selected by an open-forum technical discussion by the team. See Appendix C: Tables 2 & 3 for Decision Matrices.

After the ideation stage there were dozens of design ideas that could possibly satisfy the requirements. The first method used to cut out design ideas was a go/no go approach. Each idea was briefly examined and either kept or thrown out based on build feasibility and ability to meet requirements. This first selection process removed roughly two thirds of the designs. Most designs removed in the go/no go stage were very far-fetched or overly ambitious for a 10 month project; it was important to narrow down scope in order to define success. This allowed the team to have a more manageable mission to achieve.

Many of the ideas were similar variants of each other, so design concept categories were created following the go/no go elimination. These categories were based off of primary method of lift generation. These categories were X-copter, fixed wing, autogyro, lighter-than-air, parachute, and combinations. Combinations included any idea utilizing more than one method of lift generation during flight. Many design concepts within their respective category were fundamentally the same and combined into one concept. These ideas were combined together into things like the inline prop concept. By categorizing and combining design ideas the fundamental concepts were found and used in the first decision matrix. Following is a breakdown of each category and their subgroups, the designs listed can be found in the decision matrices in Appendix C: Tables 2 & 3.

X-copter category housed all of the concepts that fell into the standard multicopter or multi rotor categories. This category included 5 different design ideas. Design 1 was the Under Body Prop Vehicle. This was categorized by a vehicle that had its props positioned underneath the pilot. Design 2 was the Over Head Prop Vehicle (Standing) characterized by the rider positioned in an upright standing position with the props above head. Design 3 was the Over Head Prop Vehicle (Sitting), which was the same as the previous design with the exception of having the user in a sitting or prone position. Design 4 was the In-line Props category, which consisted of all designs with a single row of props and controlled by shifting the center of gravity such as hoverbikes and hoverboards. The last option, Design 5, was a quad flap category consisting of a multi rotor with controllable trailing flaps to allow for gliding.

Fixed Wing category housed the concepts utilizing a fixed wing structure to generate and maintain lift. The two designs in this category were Design 1: N-Plane and Design 2: Folding Wings. N-Plane was categorized as any standard plane with n-number of wings as lifting surfaces. Folding wings were designs with wings that had the ability to minimize used space by either folding inward or telescoping. This would help with minimization of footprint.

The Autogyro category consisted of all concepts utilizing gyrocopter theory. These aircraft would include a large unpowered overhead prop that would spin due to forward motion of the vehicle from a rear facing propeller to create lift. Design 1 was the N-Gyro, characterized by any standard gyrocopter with N-number of unpowered blades atop to create lift. Design 2, N-Gyro w/ Power, included the same principles as Design 1, with the addition of detachable drive power to the above-head props. This would allow for VTOL capability in the form of "jump takeoff" when connected, and then standard gyrocopter operation when disconnected. Lastly, Design 3 N-Gyro w/ Ducted Fan Under, was an N-Gyro that achieved VTOL through a separate propulsion system, primarily a ducted fan or jet system.

The Lighter-Than-Air category consisted of any idea that created its lift by offsetting weight with the use of lighter-than-air gas such as helium or hot-air. Design 1 was a standard Blimp, using a large body filled with gas and a compartment for the driver. Design 2, N-Blimp, was an aircraft structure with numerous compartmentalized areas filled with gas in order to create lift.

The Parachute category housed ideas that incorporated parachutes to either help or completely create lift for the pilot. Design 1, Paramotor, consisted of ideas where the user had a large propeller strapped to their back to create forward propulsion and then a parachute to create lift. Design 2, N-Paraglider, were unpowered craft utilizing no direct power and numerous parachutes to create and control lift.

The Combination category included any design that incorporated at least two concepts from separate categories above. Design 1, Raft/N-Copter was the idea of combining multiple x-copter concepts as well as a lighter-than-air component. The idea was to have a craft similar to a naval Zodiac with a row of props on both sides, combining the in-line props and under body prop vehicle ideas. The craft itself would be filled with a gas to help reduce craft weight. Design 2, MutliGyro/Copter combined the X-copter and Autogyro categories. The idea was to have a multicopter system in which every one of the drive shafts could be disconnected, allowing for gyrocopter capabilities. Design 3, Blimp/MultiCopter were vehicle configurations that encompassed the X-copter and Lighter-Than-Air categories. The idea here was to have a multicopter design that offset some of its power needs by naturally decreasing the resultant weight force of the craft. Design 4, In-Wing Props, combined both the Fixed Wing and X-copter categories. These designs would see a fixed wing aircraft with propellers placed within the structure for VTOL capabilities. Lastly, Design 5, Rotating Props/Osprey, combines the X-copter and Fixed wing ideas once again, this time utilizing large propellers that can rotate 90 degrees in order to orient for thrust and lift.

The first decision matrix took all of the fundamental concepts and scored them based on how well they could meet certain design criteria. The design criteria were based on the customer requirements and other attributes the team deemed important to the project. The criteria were then weighted by importance, with safety, aircraft weight, and VTOL capabilities weighted the highest. The other criteria included, sustained cruise, UAV-capability, payload, midflight hover, control systems, footprint, durability, COTS use, flight ability, aesthetics, novelty, interest, and cost. The team as a group went through and scored each design in every criterion. The results of this initial decision matrix were sent to the project sponsors and returned with comments. The team then adjusted the decision matrix accordingly.

Utilizing the design matrix as a critical design criterion, the team chose the top scoring concepts along with a group favorite that scored a little lower, as the major contenders. The low scores of the Lighter-Than-Air, Parachute, and Fixed Wing categories helped rule out the categories completely. The issue with Lighter-Than-Air was based around initial hand calculations that estimated a craft height of approximately 17 feet. This footprint size was impractical. The parachute method virtually made any form of VTOL impossible, often requiring large open areas to take off. Fixed wing concepts were generally too large in width due to their width or became very mechanically difficult in order to reduce this width footprint. The team ended up with five ideas, renamed to better represent their purpose: Design 1: Multicopter (under body props), Design 2: Multicopter (overhead props), Design 3: Hoverbike/Hoverboard, Design 4: Powered VTOL Gyrocopter, Design 5: Multi-Gyrocopter.

Since these ideas' scores were so similar, the five ideas were considered to be at a tie going into the final round of comparisons. The first of the five to be eliminated was the Hoverbike/hoverboard category. The use of the group's preliminary excel database helped make this decision. Utilizing this, the team was able to see that in order to have the minimal props to be considered a bike or board; the craft would need very high-powered motors swinging massive props. The team then debated whether or not gyrocopters were an option to pursue. The idea had been successfully implemented before, and created the opportunity for

great efficiency based on disk area. The idea could achieve all of the specifications the team needed to satisfy in order to meet customer requirements. The group was quite polarized here. Novelty became the deciding factor for eliminating Powered VTOL Gyrocopter, as well as opportunity for testing. VTOL gyrocopters had not only been successfully created, but efficiently. The group decided they wanted to tackle a project that the United States has seen very little of. Along with this, the autonomous controls for this form of vehicle would be highly complicated and sophisticated. As operating the vehicle for testing would have to be autonomous, this may be over scoping for the project. For similar reasons, primarily system sophistication and project scope, Multi-Gyrocopter was eliminated.

Left with the two multicopter configurations, the team began from scratch once again trying to decide which configuration style of multicopter would best suit the customer's needs. Creating a pros and cons list for both led to the following major conclusions: Underbody would allow maximization of ground effect and minimization of weight, as well as the desired "look" of the multi-rotor people have come to expect. This came at the expense vehicle stability and increased safety needs to satisfy concerns. Overhead props would allow for a self-stabilizing vehicle configuration increasing prop safety at the expense of complicating landing, increasing tip sensitivity and blowing high velocity air directly at the pilot. After much debate, the team decided that the pros of the underbody design outnumbered those of the overhead design.

The team's concluding decision for the overall system structure is a Multicopter with Underbody Props, which is defined as a vehicle whose props remain under the shoulder line of the pilot. This allows room to play with body position in order to maintain a stable operating point. The biggest concern with this design will be keeping the pilot safe from the spinning props if a prop were to become disengaged, or if the pilot fell. Polishing of the group's excel database will allow for the optimization of motors and battery configurations in order to maximize flight time. The decision of the final system archetype allows for further analysis of subsystems as the team prepares to enter project Phase 3. A rough model of this system configuration can be found below in Figure 24.



Figure 24: Multicopter with underbody props.

8 PRELIMINARY DESIGN

Taking the preliminary calculations into account, the team formed a rough idea of the preliminary design for the project. The following represents the main concepts at the time of the Preliminary Design Review.

The model shown above in Figure 24 measures 11' by 11', which fits well within the size requirements of the project. As seen in the model, the team is planned (tentatively) on implementing a 12-rotor design, with 3 rotors per main arm arranged in a triangular pattern. This will allow for an implementation of a more simple control scheme for the vehicle. Each rotor would have been around 36" in diameter, putting the craft in the optimum operating range for the vehicle as predicted by the actuator disk theory calculations. Each arm was responsible for providing up to 175 lb_f of thrust, meaning that each propeller and motor must provide about 58 lb_f of thrust at maximum. Each rotor would have been shrouded in order to protect bystanders from walking into the props and to prevent the props from taking damage if the vehicle bumps into its surroundings. See Figures 25 and 26 below for a closer look of the prop configuration on each arm and the prop ring layout.



Figure 25: Grouping of propellers on each arm in preliminary design.

The method of integrating the shrouds and the motors into the vehicle were unknown at this stage in the project. Mounting them safely and securely presented a significant challenge for the team, in order to maintain minimal vehicle weight these components needed to be mounted in the lightest way possible.

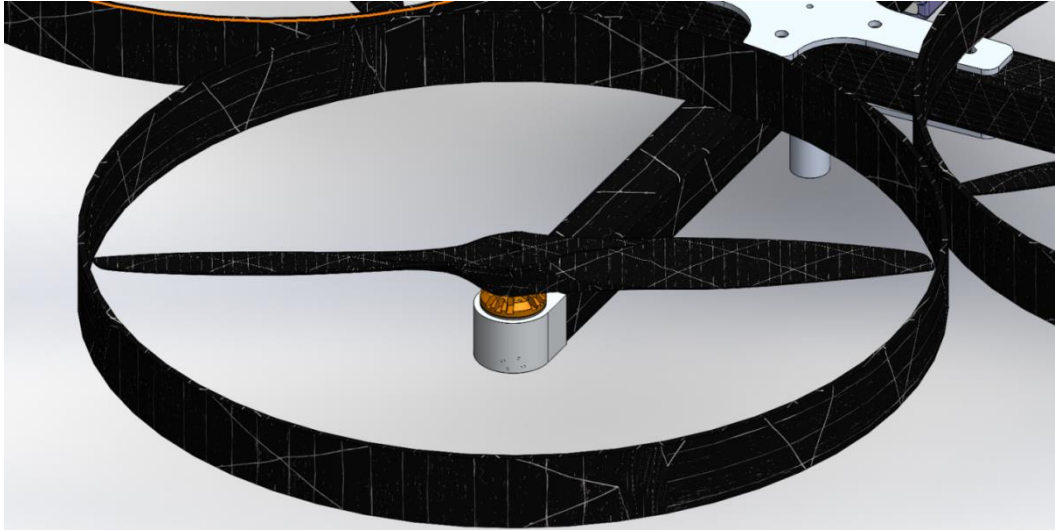


Figure 26: A closer look at the propeller and prop ring on the end of each arm.

Since storage space is at a premium with such a minimal design, the team encountered difficulty in specifying a location for batteries. The group tentatively decided to place them under each main arm, arranged in lines parallel to the arm. This allowed for the batteries to be out of the way of the operator and to distribute their weight along the craft evenly. It also allowed for the battery weight to counteract some of the thrust generated at the end of each arm by the propellers, reducing the bending moment acting on the arm (and therefore the stresses on the arm). However, it also provided additional challenges; the batteries needed to be protected from the ground and the design required the use of additional wire (being spread out throughout the vehicle). These issues resulted in some small amount of additional weight being added to the craft. The location of the batteries can be found below in Figure 27.

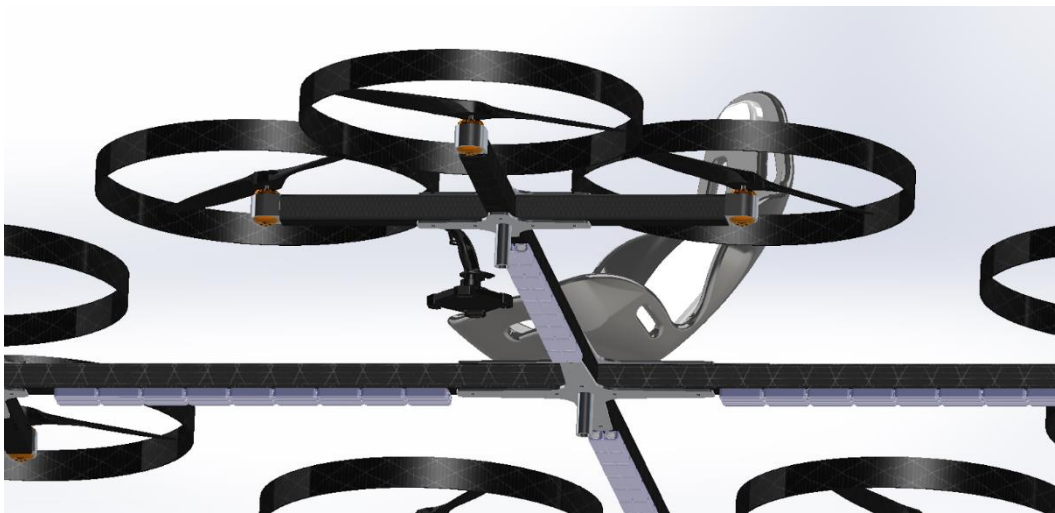


Figure 27: View of the underside of the vehicle showing landing gear and battery arrangement.

Provisions for landing the vehicle were a point of concern for the selection of the final concept design. As can be seen above in Figure 27, the team opted for a very simple landing gear setup consisting of short aluminum rods extending downward from the end of each main arm and from the center of the craft. The team liked this design for several reasons. First, the landing gear weighed very little, with all five cylinders (5" length x 1.5" OD x 0.25" thickness) weighing only a few pounds in total. The landing gear provided a lot of strength and stiffness since they were essentially stout aluminum rods welded to the aluminum plates holding the frame together. The design could be scaled as needed if testing and further evaluation

revealed additional strength or length was necessary. For example, the group knew that the landing gear rod as specified required a 2100 lb_f load at the end of the rod to yield in bending (assuming that the weld between the plate and the rod holds up); the landing gear would have need been revised if landing loads were determined to exceed this value (for instance, in windy conditions causing the vehicle to land with some significant component of horizontal velocity). The team could also adjust the length of the rods if it is determined that the low vehicle height (5" off the ground) jeopardizes the pilot's legs while landing or presents danger to the propellers, as the multicopter may kick up debris which could cause serious harm to the propeller blades if they should come into contact with it. A side view of the model showing the relative heights of the components can be seen below in Figure 28.

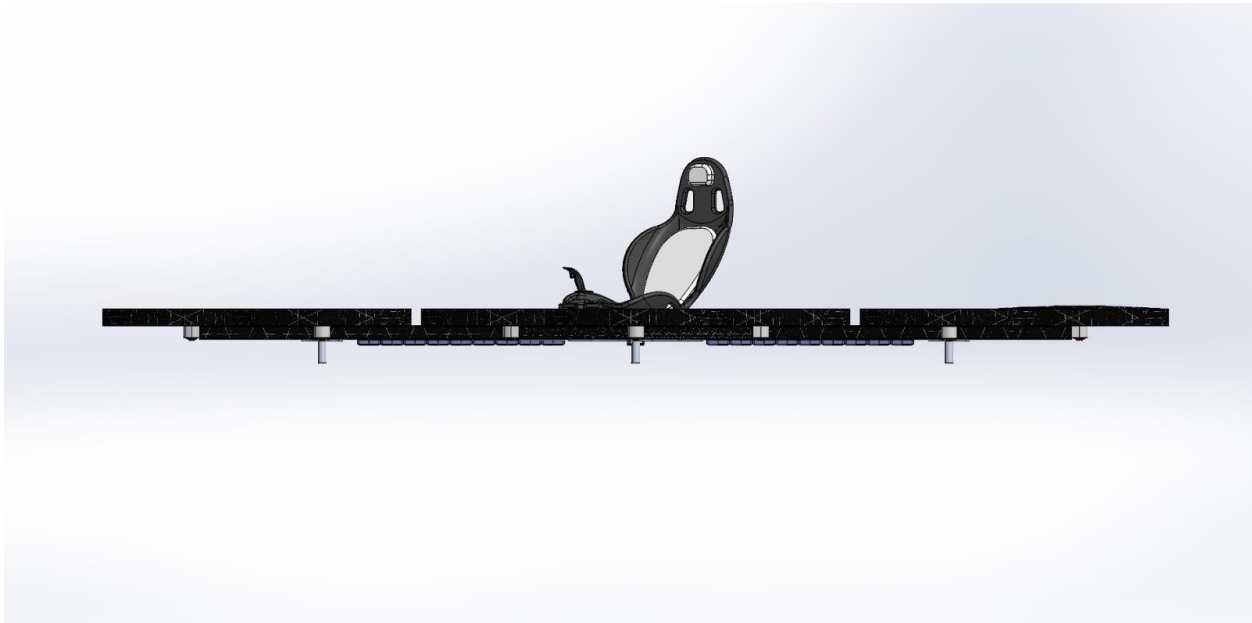


Figure 28: A side view of the preliminary design demonstrating the rough height of the design.

Regarding the construction of the frame, the team is looking into carbon construction to minimize the weight of the structure. The main arms were 6.5' long with a square cross-section measuring 2.5" x 2.5" x 0.125" thick. The team planned on using a layup schedule of primarily 0° plies oriented along the tubes, with several 45° and 90° plies added in for torsional rigidity and strength in the radial direction. This layup would be refined further on in the design process. In any case, this method gave a tip deflection of about 1.1" at maximum thrust and factor of safety for bending stresses of about 17. A point the team needed to investigate further was the vibration associated with the motors and the oscillation modes for the structure, but the design seemed (at first glance) to be adequately stiff enough, and all of the carbon tubes together would weigh about 33 lbs as specified. A rough initial layout of the frame can be seen below in Figure 29.



Figure 29: An initial layout of the model showing the main arms and smaller arms.

To attach the frame together, the team intended to use a thermosetting resin (like epoxy) to bond the carbon arms to the aluminum plate brackets. These brackets can be seen above in Figures 26-29 above at the joints between the arms. Using 0.25" thick aluminum plate for these brackets allowed for high strength at minimal weight; the various brackets as shown in the model weighed about 2-4 lbs depending on the configuration. Minimum bond lengths for the bond between the arm and the brackets needed to be investigated further, but the model featured over 12" of bond length for the main arms and about 5" of bond length for the smaller arms which both seemed like adequate starting points for bonding the parts together.

Lastly, the group intended to locate the pilot in the center of the craft as shown in Figure 29 above. The pilot's seat would be secured rigidly by means of bolts or other bonding techniques to the top plate attaching the main arms together, and the pilot's controls would sit near or integrated into the seat. This seemed to be the best way to add the seat and control interface into the vehicle without the addition of a significant amount of weight.

Using SolidWorks' built-in material data and the teams own Excel system performance sheets, the initial determination of an admittedly rough structure weight for the system (minus any batteries, electronics, wiring, or a seat) was about 156 lbs. This was of course a very rough estimate, but it indicated that the team was on the right track with the design (at least as far as weight is concerned). This value could be

reduced as alternative and superior ways of configuring the vehicle and arranging the components were found.

9 INITIAL MULTICOPTER CONFIGURATION EVALUATION

For preliminary calculations the team used basic models in order to produce a rough performance estimates. By compiling the results of each subsystem, the group was able to model the entire multicopter using an iterative process. A summary of the tool is shown below:

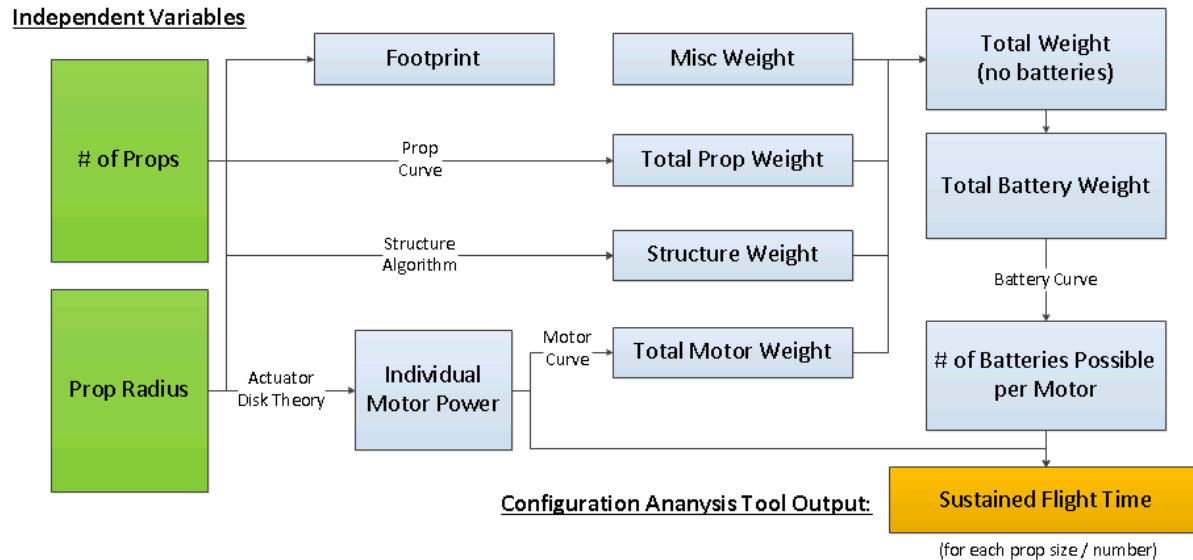


Figure 30: Overview of Configuration Analysis Tool

Propeller radius and the number of propellers were the two independent variables that all of the results were derived from. These independent variables were chosen because they have the greatest effect on performance and were easily relatable to the top level design constraints.

9.1 Tool Overview

The first constraint considered was the footprint of the multicopter. The requirements specified that the multicopter must fit within two parking spaces, which constitutes an 18ft. by 18ft. space. The approximate size of the multicopter was calculated for each combination of propeller radius and number of propellers. The approximate size was then compared to the maximum dimensions and any combinations that exceeded maximum dimensions were highlighted in red and eliminated, as shown below:

		Number of Props									
		1	4	6	8	12	16	12	16	24	32
Prop Radius (ft.)	1	2.0	4.1	5.6	6.1	8.2	10.6	5.6	6.1	8.2	10.6
	1.1	2.2	4.5	6.2	6.7	9.0	11.8	6.2	6.7	9.0	11.8
	1.2	2.4	4.9	6.8	7.3	9.8	13.1	6.8	7.3	9.8	13.1
	1.3	2.6	5.3	7.3	7.9	10.6	14.3	7.3	7.9	10.6	14.3
	1.4	2.8	5.7	7.9	8.5	11.4	15.5	7.9	8.5	11.4	15.5
	1.5	3.0	6.2	8.5	9.1	12.2	16.7	8.5	9.1	12.2	16.7
	1.6	3.2	6.6	9.0	9.7	13.1	18.0	9.0	9.7	13.1	18.0
	1.7	3.4	7.0	9.6	10.3	13.9	19.2	9.6	10.3	13.9	19.2
	1.8	3.6	7.4	10.1	10.9	14.7	20.4	10.1	10.9	14.7	20.4
	1.9	3.8	7.8	10.7	11.5	15.5	21.7	10.7	11.5	15.5	21.7
	2	4.0	8.2	11.3	12.1	16.3	22.9	11.3	12.1	16.3	22.9
	2.1	4.2	8.6	11.8	12.7	17.1	24.1	11.8	12.7	17.1	24.1
	2.2	4.4	9.0	12.4	13.3	18.0	25.3	12.4	13.3	18.0	25.3
	2.3	4.6	9.4	13.0	13.9	18.8	26.6	13.0	13.9	18.8	26.6
	2.4	4.8	9.8	13.5	14.5	19.6	27.8	13.5	14.5	19.6	27.8
	2.5	5.0	10.3	14.1	15.1	20.4	29.0	14.1	15.1	20.4	29.0
	2.6	5.2	10.7	14.7	15.7	21.2	30.3	14.7	15.7	21.2	30.3
	2.7	5.4	11.1	15.2	16.4	22.0	31.5	15.2	16.4	22.0	31.5
	2.8	5.6	11.5	15.8	17.0	22.9	32.7	15.8	17.0	22.9	32.7
	2.9	5.8	11.9	16.3	17.6	23.7	33.9	16.3	17.6	23.7	33.9
3	6.0	12.3	16.9	18.2	24.5	35.2	16.9	18.2	24.5	35.2	
3.1	6.2	12.7	17.5	18.8	25.3	36.4	17.5	18.8	25.3	36.4	
3.2	6.4	13.1	18.0	19.4	26.1	37.6	18.0	19.4	26.1	37.6	

Figure 31: Vehicle width in feet based on configuration

blue column titles indicate stacked props

Next the total power for the system was calculated for each combination. The model implemented was Actuator Disk Theory, which is based on control volume analysis of momentum and energy. Friction is ignored in this model to allow for simplicity. Since the model is only for the purpose of estimating the power required, the simplest case of hovering was considered. Forward movement and vertical movement require more power, but the calculations are considerably more complicated. To account for this, the team applied a substantial amount of excess payload capacity.

Equation 1:

$$P = \sqrt{\frac{T^3}{2\rho\pi r^2}}$$

Equation 1 shows the actuator disk equation for a single disk, where T is the thrust, p is the density of air, and r is the radius of the actuator disk. Since the team is designing a multicopter, Equation 1 needed to be modified to take into account multiple disks.

Equation 2:

$$P = \sqrt{\frac{T^3}{2\rho\pi N r^2}}$$

Equation 2 is the modified actuator disk theory, where N represents the number of actuator disks. To derive this equation the thrust was divided by the number of disks based on the assumption of equal

loading. The power then represented the individual power needed for each disk. Multiplying by the number of disks gave the total power shown in Equation 2.

Another modification that was made to the original actuator disk theory was made to account for differences between a vehicle with all props in a single plane and a vehicle with stacked props. Since the power required is directly proportional to the total area of disks, the team was able to derive the following simple relationship:

Equation 3:

$$P_{2N,stacked} = \frac{1}{2}P_{N,standard}$$

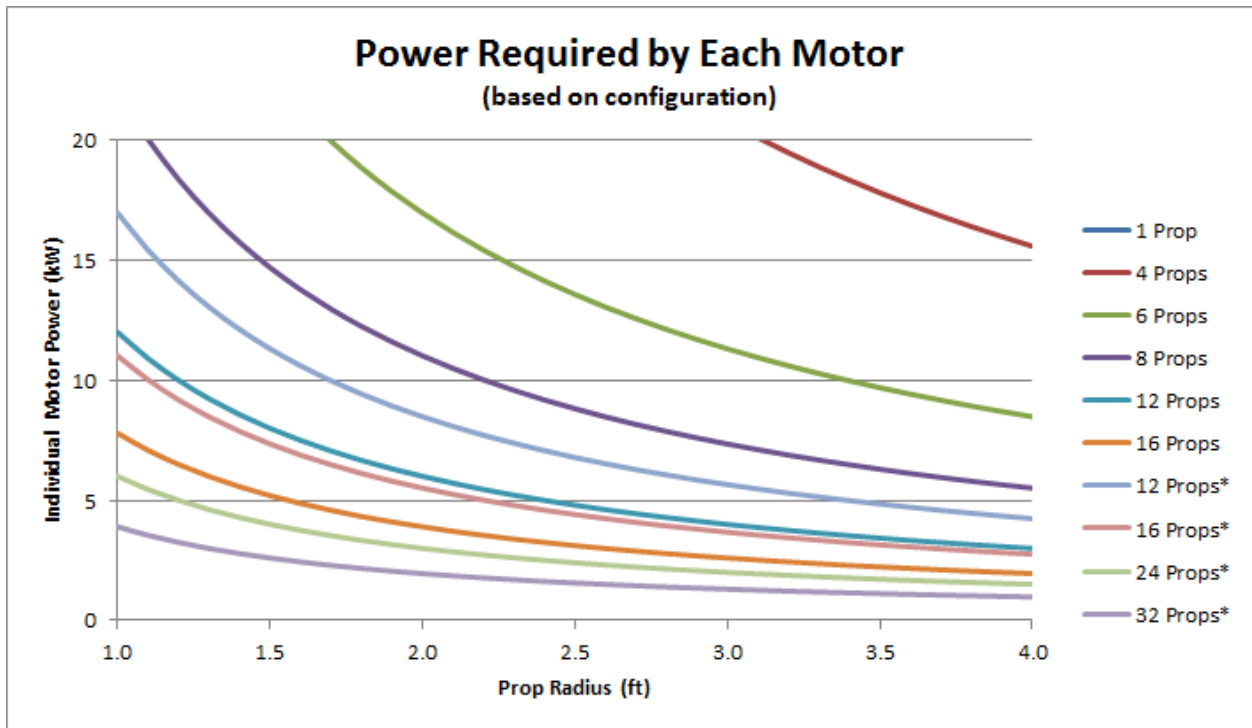


Figure 32: Individual motor power for various configurations of number and propeller size

an asterisk (*) indicates stacked props

The individual power for each disk was calculated, and a plot of the results is shown in Figure 32 above. Based on motor research, the maximum power for each disk was set to 10 kilowatts, and any configurations that exceeded the maximum power were eliminated, as shown below:

		Number of Props									
		1	4	6	8	12	16	12	16	24	32
Prop Radius (ft.)	1	498.6	62.3	33.9	22.0	12.0	7.8	17.0	11.0	6.0	3.9
	1.1	453.3	56.7	30.8	20.0	10.9	7.1	15.4	10.0	5.5	3.5
	1.2	415.5	51.9	28.3	18.4	10.0	6.5	14.1	9.2	5.0	3.2
	1.3	383.6	47.9	26.1	17.0	9.2	6.0	13.0	8.5	4.6	3.0
	1.4	356.2	44.5	24.2	15.7	8.6	5.6	12.1	7.9	4.3	2.8
	1.5	332.4	41.6	22.6	14.7	8.0	5.2	11.3	7.3	4.0	2.6
	1.6	311.7	39.0	21.2	13.8	7.5	4.9	10.6	6.9	3.7	2.4
	1.7	293.3	36.7	20.0	13.0	7.1	4.6	10.0	6.5	3.5	2.3
	1.8	277.0	34.6	18.8	12.2	6.7	4.3	9.4	6.1	3.3	2.2
	1.9	262.4	32.8	17.9	11.6	6.3	4.1	8.9	5.8	3.2	2.1
	2	249.3	31.2	17.0	11.0	6.0	3.9	8.5	5.5	3.0	1.9
	2.1	237.4	29.7	16.2	10.5	5.7	3.7	8.1	5.2	2.9	1.9
	2.2	226.7	28.3	15.4	10.0	5.5	3.5	7.7	5.0	2.7	1.8
	2.3	216.8	27.1	14.8	9.6	5.2	3.4	7.4	4.8	2.6	1.7
	2.4	207.8	26.0	14.1	9.2	5.0	3.2	7.1	4.6	2.5	1.6
	2.5	199.5	24.9	13.6	8.8	4.8	3.1	6.8	4.4	2.4	1.6
	2.6	191.8	24.0	13.0	8.5	4.6	3.0	6.5	4.2	2.3	1.5
	2.7	184.7	23.1	12.6	8.2	4.4	2.9	6.3	4.1	2.2	1.4
	2.8	178.1	22.3	12.1	7.9	4.3	2.8	6.1	3.9	2.1	1.4
	2.9	171.9	21.5	11.7	7.6	4.1	2.7	5.8	3.8	2.1	1.3
3	166.2	20.8	11.3	7.3	4.0	2.6	5.7	3.7	2.0	1.3	
3.1	160.9	20.1	10.9	7.1	3.9	2.5	5.5	3.6	1.9	1.3	
3.2	155.8	19.5	10.6	6.9	3.7	2.4	5.3	3.4	1.9	1.2	

Figure 33: Individual motor power for various configurations

blue column titles indicate stacked props

In order to estimate the weight of the motors, equations were developed that related the power output of the motors to the weight. These equations were made by plotting the weight and power output of multiple motors and fitting them with a trend line. Figure 34 shows the plotted motor data and the trend line for the motors. The same process was implemented to obtain figures relating the size of the batteries and the propellers to their weight.

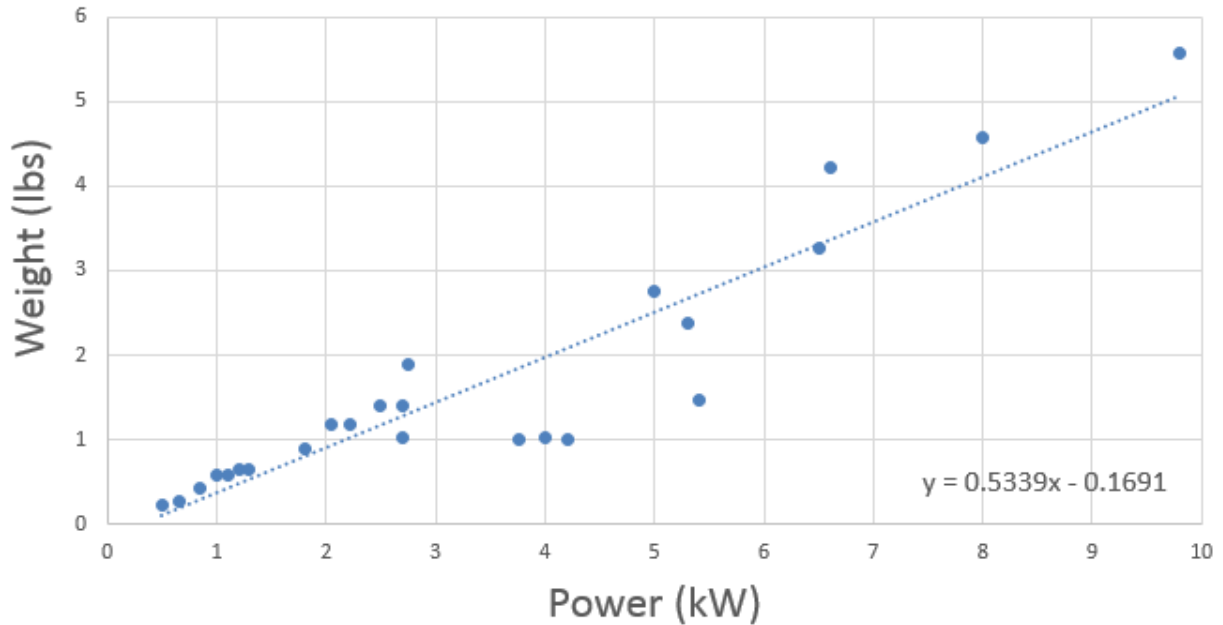


Figure 34: Motor weight vs power data and trend line used to model relationship

The structure was assumed to be made of carbon fiber tubing, with one arm extending radially to each propeller from a central hub. Each arm was assumed to have a constant cross section. The loading on the arm was the total thrust divided by number of arms and was placed at the end of the arm. The length of the arm was estimated based on geometry of the propellers. The size of each arm was determined using the Von Mises failure criterion, giving a total structure weight.

In order to determine the quantity of batteries that were allowable for each configuration was done by subtracting the weight of the structure, motors, props, wires, ESC's, seat, and miscellaneous structural components from the allowable 254 pounds. Combining this information with the group's motor power data and a typical value for battery energy density, the team was able to determine rough flight time estimates for every feasible configuration. The data is shown below in Figure 35:

9.2 Final Output and Analysis

		Number of Props									
		1	4	6	8	12	16	12	16	24	32
Prop Radius (ft.)	1	-1.4	-0.6	0.3	0.8	2.6	3.6	1.0	2.0	3.1	3.8
	1.1	-1.2	-0.3	0.7	1.2	3.1	4.1	1.4	2.4	3.6	4.4
	1.2	-1.1	0.0	1.0	1.6	3.5	4.7	1.8	2.8	4.1	4.9
	1.3	-0.9	0.3	1.4	1.9	4.0	5.2	2.1	3.2	4.5	5.3
	1.4	-0.8	0.6	1.8	2.3	4.4	5.7	2.5	3.6	4.9	5.8
	1.5	-0.6	0.9	2.1	2.7	4.9	6.2	2.9	3.9	5.4	6.3
	1.6	-0.4	1.2	2.5	3.1	5.3	6.7	3.2	4.3	5.8	6.7
	1.7	-0.3	1.5	2.8	3.4	5.7	7.2	3.6	4.7	6.1	7.1
	1.8	-0.1	1.8	3.2	3.8	6.1	7.6	3.9	5.0	6.5	7.5
	1.9	0.0	2.1	3.5	4.1	6.5	8.1	4.3	5.3	6.9	7.8
	2	0.2	2.4	3.9	4.5	6.9	8.5	4.6	5.7	7.2	8.2
	2.1	0.3	2.7	4.2	4.8	7.2	8.9	4.9	6.0	7.5	8.5
	2.2	0.5	3.0	4.6	5.1	7.6	9.3	5.2	6.3	7.8	8.8
	2.3	0.6	3.3	4.9	5.4	7.9	9.6	5.6	6.6	8.1	9.1
	2.4	0.8	3.6	5.2	5.7	8.2	10.0	5.9	6.9	8.3	9.3
	2.5	1.0	3.9	5.6	6.0	8.6	10.3	6.2	7.1	8.6	9.5
	2.6	1.1	4.2	5.9	6.3	8.8	10.6	6.5	7.4	8.8	9.7
	2.7	1.3	4.5	6.2	6.6	9.1	10.9	6.8	7.6	9.0	9.9
	2.8	1.4	4.8	6.5	6.9	9.4	11.2	7.1	7.9	9.2	10.0
2.9	1.6	5.1	6.8	7.1	9.6	11.4	7.3	8.1	9.3	10.2	
3	1.7	5.4	7.1	7.4	9.8	11.7	7.6	8.3	9.4	10.2	
3.1	1.9	5.7	7.4	7.6	10.0	11.9	7.9	8.5	9.5	10.3	
3.2	2.0	5.9	7.7	7.8	10.2	12.0	8.1	8.6	9.6	10.3	

Figure 35: Estimated flight time in minutes based on configuration

blue column headers indicate stacked props

Keep in mind that this tool was intended to portray *trends* in flight time, *not* accurate flight time data. This was the teams' best analysis for now; more accurate flight times would be determined in later iterations using test data. The red cells indicate that the corresponding configuration is not possible due to any of a wide variety of reasons.

The first analysis that the team conducted based on this data was whether implementing double stacked props would provide an advantage or not. The team noticed that analogous configurations (such as 16 stacked props and 8 planar props) have almost identical flight times. Having said that, double stacked props would cause various issues. First of all, the cost of the vehicle would skyrocket due to the fact that the group would have to buy twice as many motors, twice as many props, and so on. There would also be far more parts to deal with and added complexities to the required control scheme. Double stacked props are typically used when high thrusts are required in small areas where props are likely to stall, which would constitute high disk loading. The disk loading is not nearly as high as some single stacked commercial systems in use today, so double stacking the props would have been inappropriate.

The next decision to be made was how many props would be implemented. The prop radii for 8 prop configurations were extrapolated due to motor power limitations, and were therefore far too large for this application. The team also considered a 24 prop design based on trends from the data, but the group was not able to design a configuration with the footprint small enough. Also the structure would have to be intricate, and therefore too heavy, so 24 prop configurations were eliminated. The big decision was between 12 props and 16 props. The 16 prop design has 20% more flight time for equal prop sizes, but the 12 prop design can support much larger props than the 16. The larger props sizes result in a 15% increase in flight time, but prop inertia quickly increases with radius. This leads to poor response times from the controls, which may lead to safety concerns. Both configurations showed promise, and in the end the quantity of props was determined by the availability of motors in the market. The implementation of the Joby JM1S (discussed later in this document) brought the team to the selection of a 12 prop design.

The final decision to make was the actual prop size. The data showed that as prop size increases, efficiency and flight time go up as well. However, prop inertia also increases, leading to poor flight characteristics. Knowing this, the team estimated that the ideal prop size would be 36 inches in diameter, possibly less. Again, in the end this was decided by the availability of props, which is discussed later in this document.

9.3 Major Assumptions

The major assumptions made in the teams' model are as follows:

- All assumptions associated with Actuator Disk Theory (infinitely thin disks, no parasite drag, etc.)
- 1.5 factor of safety on thrust
- The Figure of Merit, M , from helicopter blade theory to be set at 0.7
- Disks do not interact, and overall thrust is superimposed
- Motor and prop inefficiencies are included in factor of safety
- All batteries discharge at equal rates
- 44V batteries
- 25 pounds of miscellaneous weight
- Carbon tubing has a linear density of 0.6 lb/ft
- 8oz ESC's
- Wire length = structure length
- Hobby props are implemented
- For double stacked props top and bottom motor power is equal

10 REVISIONS TO PRELIMINARY DESIGN

Compared to the preliminary design shown above (which was initially detailed for the preliminary design review), the team kept the main layout of the design the same as before but have introduced a number of significant changes to the individual components.

To start with, the team changed the tubing selection from square carbon tubing to round carbon tubing. The team was originally looking into square tubing as an alternative to round tubing because it was believed that it would make assembly of the craft easier and would allow the group to more precisely align the motors and propellers vertically, leading to a safer craft that would be easier to control. For these reasons the team started looking exclusively at square tubing for the structural components of the vehicle, but the group ran into a number of issues with this tubing. To begin with, not many manufacturers produce square profile carbon tubing, seriously limiting the selection of tubing sizes. In addition, the manufacturers that did produce square tubing in the approximate sizes that was needed refused to provide any information as to the layup schedules, material property data, or approximate stiffnesses and strengths of their tubing, reducing the design work to educated guesswork. They also commonly used carbon fiber weave fabric in the construction, leading the team to seriously doubt the ability of the tubes to withstand the worst-case loads the craft could encounter. Finally, the team was not able to locate any square tubing which could be epoxied inside of or over the square carbon tubing, meaning that it would be difficult make the center arm, or motor mounts without excessive difficulty and cost. This lead the team to again consider the round unidirectional carbon tubing, which the group had ample material data on and could find in a wide variety of sizes and wall thicknesses, meaning that it was more likely to find tubing that was strong enough for the project's needs. Addressing some of the difficulties of assembling the craft out of round tubing, the team developed a method of mounting components on the tubing mounts with brackets which could be used to hold landing gear, seats, and other additions as necessary. This did mean the team had to use caution when assembling the craft to ensure that the motors remain upright, but otherwise the group feels as though the round tubing was superior for the project's purposes.

The team also changed the main arms and spars to differently-sized tubes as it was realized that having the same size tubing for both components meant having a craft that was heavier than necessary. The motor spars don't need to be quite as strong as the main arms as their loading cases are smaller, so the team attempted to design the structure to provide the strength and stiffness necessary for proper operation while being relatively inexpensive and lightweight.

The team also significantly changed the mounts holding the vehicle together. In the preliminary design, the group envisioned using flat plates epoxied on the tops and bottom of the square tubes to hold the tubes in position and provide locations to mount the seat, landing gear, and other components of the craft. Not only is this design no longer feasible with round carbon tubing, but the team also felt as though the design was lacking in strength, as it would peel the epoxy holding the tubes and plates together and probably not perform very well in shear induced by tube torsion. The group elected to go with mounts made of round steel tubing which has been mitered and welded together to hold the carbon tubes together. This design gave more bond surface area between the mounts and the carbon tubes which provided a stronger joint between the two. It also resisted shear from tube torsion better than the previous design. The mitered tube mount design also weighed more than the flat plates, but the team did not feel as though the flat plate design would have worked satisfactorily in any case.

A new introduction from the preliminary design is the use of brackets in the craft's center and arm mount assemblies. When the team began the project the use of round tubes was a concern because of the difficulties involved in satisfactorily mounting components to them. After much thought on the matter the team conceived of a square bracket design that could sit around the tubes and be welded into place, providing a solid and versatile mounting place on which the group developed the rest of the craft and installed additional parts upon. Bolted on to the bracket assembly were plates for landing gear, seats, batteries, or other necessities, and between the plates and the mount there was a small space (roughly 1.5" by 4" by 4") for hiding control boards and sensors. The team especially like this idea because it provided some room for expansion in the future; if the group determined that the landing gear was not sufficient, that a replacement seat was needed with a different model, or an addition of some unforeseen component to the craft was required, the craft may have space available to do so on these brackets.

The team also changed the idea of the propeller rings in several fundamental ways. The team initially had assumed that the propeller rings would need to contain a propeller if it broke up during use and prevent the propeller from taking damage in the event that the craft bumped into another object during flight; in other words, a very tough and stiff propeller guard for each propeller was required. Not only was this assumption incorrect, as the sponsors have recently indicated to the group, but it also gave rise to extremely heavy composite propeller rings (more than 7 pounds per ring) being called for on the preliminary design. These rings added more than 84 pounds to the craft (about a third of the total allowable weight), and the entire team felt as though this was an unacceptable addition to a vehicle with such stringent weight limits. Therefore, the team talked to the sponsors and were instructed to design a set of propeller rings that would instead hold a mesh around the propeller; these were intended to help keep debris and small objects from being sucked into the propellers and thrown around during flight. The propeller rings in the final design were now only intended to provide a form for the mesh and so were no longer designed to be a structural element. While it may have seemed dangerous to not enclose the propellers in a rigid propeller ring, the nature of the ultralight requirements for the vehicle meant that the questionable protection the rings provide wasn't deemed to be worth their additional weight.

Finally, the team opted to use a commercially available RC controller system to fly the craft instead of building a unique control system into the craft. A control system built into the craft was deemed to introduce unnecessary weight as well as additional complexity and liability while in use, and a RC transmitter would be needed to perform unmanned tests on the vehicle, so instead the team planned on just having any potential rider flying the craft use an RC transmitter to control it. Later, a dedicated control system would be incorporated into the craft after testing was complete.

11 FINAL MULTICOPTER DESIGN

11.1 Structure

11.1.1 Layout

This design of the 12 prop Electric Commuter Multicopter consists of a fully specified structure and propulsion design. The craft is approximately 15.87' diagonal and 12'x12' square. The craft consists of a 4-way center mount with 4 main arms extending outwards. The operator sits in the seat at the center of the craft located on top of the center mount. The team designed this aircraft to consist of 12 propellers as to provide maximum efficiency within the project constraints. Therefore, at the end of each arm there are 3 synchronized propellers, oriented in a triangular fashion. These motors are attached by an arm mount with three smaller carbon fiber tubes, or spars, extending out of it. Then at the end of these individual spars is a motor mount, on top of which is the motor and propeller. Around each propeller is a carbon fiber ring with a metal grating to ensure human safety. Located on the underside of each arm mount and the center mount is a bracket assembly which holds the landing gear. This design is shown below in Figure 36.



Figure 36: Full Multicopter Design

11.1.2 Main Arms

The main arms are round tubes that connect the seat and center mount with the rest of the craft and are the basis for the structure. The tubes are from C-Tech and are 52" long and have an inner and an outer diameter of 2.500" and 2.746" respectively, providing a wall thickness of 0.123". At first, a similar tube from Rockwest Composites with an inner and outer diameter of 2.500" and 2.63", respectively, was chosen for the main arms of the craft. Ultimately the thicker tube from C-Tech was chosen because it significantly increased the factor of safety against failure at a cost of six pounds to the total weight. These tubes are constructed with unidirectional carbon fiber, therefore they are assumed to have a symmetrical layup schedule of three 0° plies and two 45° plies surrounding an additional 0° ply in the center. This assumption is discussed in the analysis section. See Appendix B-1 and Appendix D: Newport 301 Datasheet for more information and technical data on these tubes. Both the center mount and the arm mounts consist of steel tubes inserted into the ends of the carbon arms. These tubes are welded together at each junction and are attached to the carbon with epoxy bonds. Each main arm would weigh 3.11 pounds, according to manufacturer data. A depiction of the craft's main arms can be found below in Figure 37.

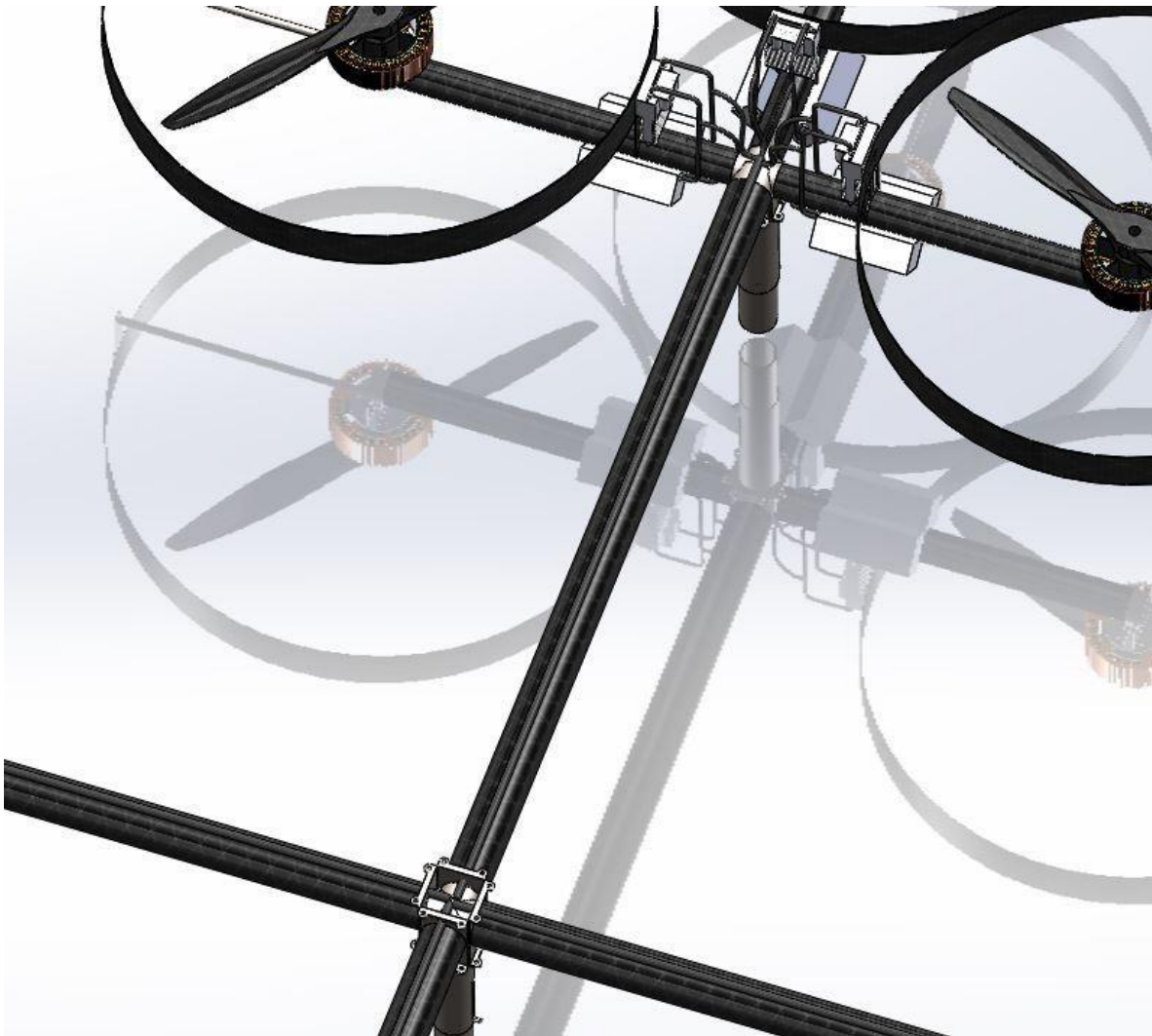


Figure 37: Main Carbon Fiber Spar

11.1.3 Motor Spars

The motor spars are round tubes from Rockwest Composites with a length of 22" and an inner and an outer diameter of 2.000" and 2.125", respectively, with a wall thickness of 0.0625". Like the main arms, the spars are also made out of unidirectional carbon fiber and are similarly constructed. See Appendix B-1 and Appendix D: GRAFIL 34-700 for more information and technical data on these tubes. The motor spars branch out from the arm mount and connect to the craft's motor mounts, holding the motors in place around the rider. As with the main arms, the spars slide over smaller steel diameter tubes of the arm mounts and motor mount and are bonded in place with epoxy. Each motor spar would weigh 0.50 pounds, according to manufacturer data. A depiction of the craft's motor spars can be found below in Figure 38.

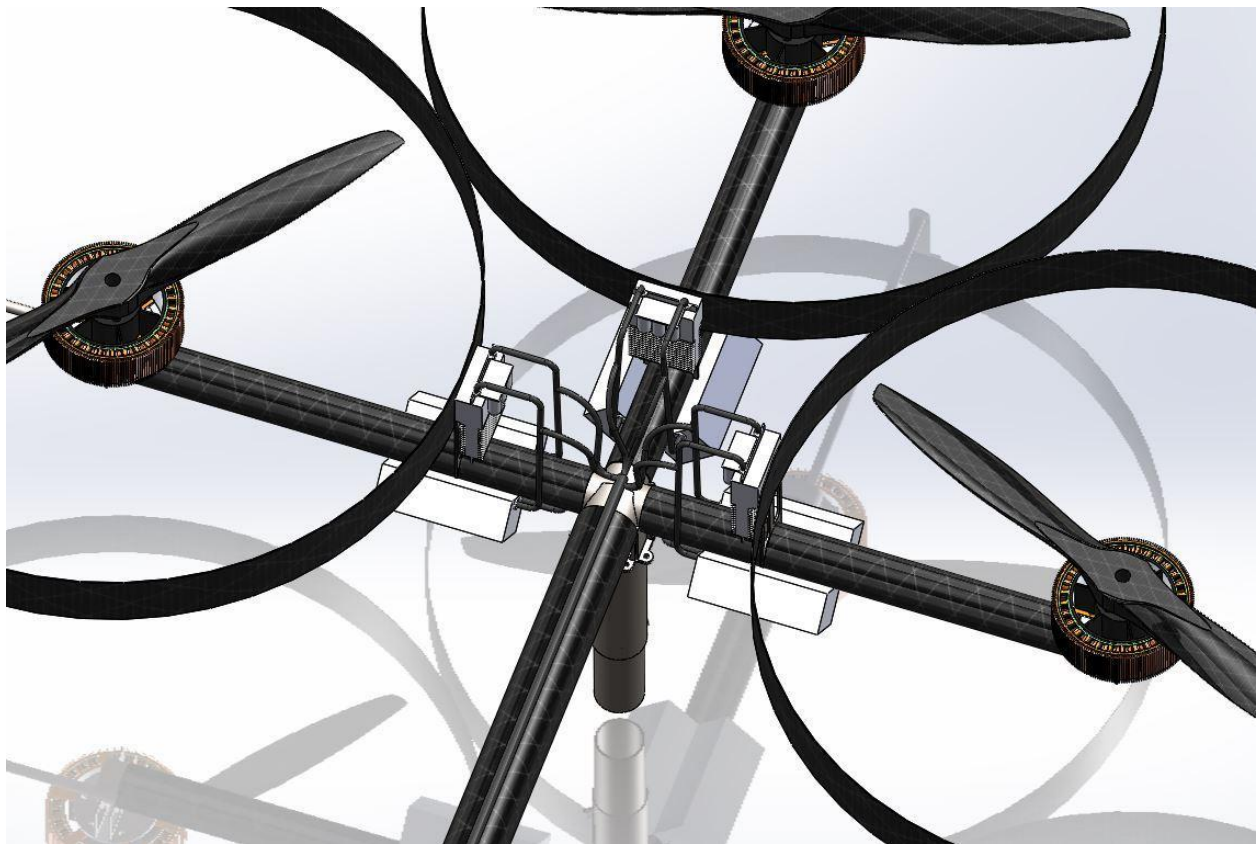


Figure 38: Auxiliary Carbon Fiber Spars

11.1.4 Center Mount

The center mount assembly holds the seat, main landing gear, and main arms in place and is the centerpiece of the vehicle, allowing for the standard “quadrotor” arrangement which is popular in smaller drones and UAVs. The center mount assembly is composed of three main components: the center mount, seat, and landing gear bracket assemblies. Shown below in Figure 39 is a bottom view of the craft’s center mount assembly.

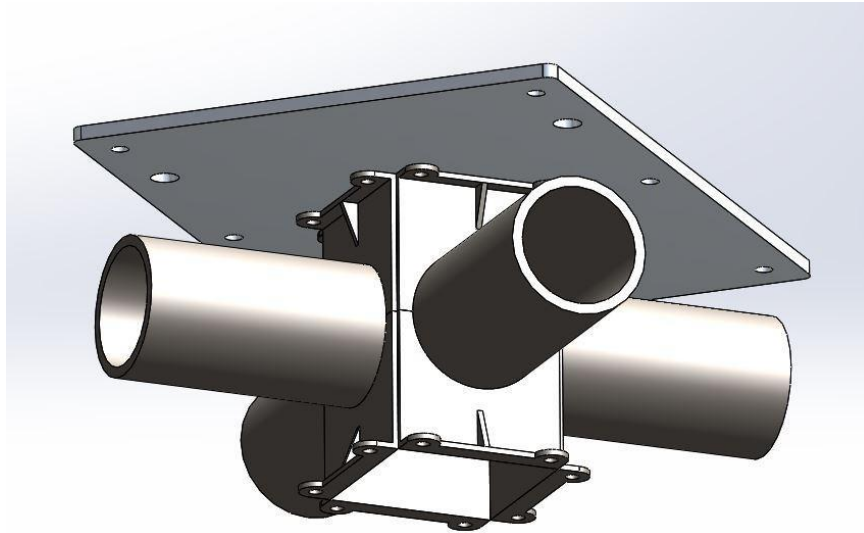


Figure 39: Bottom View of Center Mount Assembly

The center mount unit is constructed out of 4130 Chromoly steel tubing which is mitered and welded together to give it its plus sign shape. The mount measures 12”x12” along the tube axes, and the tubes have outer and inner diameters of 2.486” and 2.124”, respectively. This design should allow the tube ends to extend 4.50” inside each arm, providing plenty of bond surface for adhesion between the carbon main arms and the steel center mount. The diametric difference between the outside of the center mount tubes and the inside of the main arms should allow for the ideal bond thickness of 0.007” and will allow for the team to use a glass bead additive, known as Bond Line Control, in the epoxy to ensure a consistent separation gap and to prevent galvanic corrosion between the two materials. For more details on the bonding process and the materials used in this procedure, please see the ‘Materials Selection’ section below. The center mount should weigh 8.20 pounds, although it might be slightly more due to weld metal being added during the manufacturing process. Shown below in Figure 40 is the center mount unit.

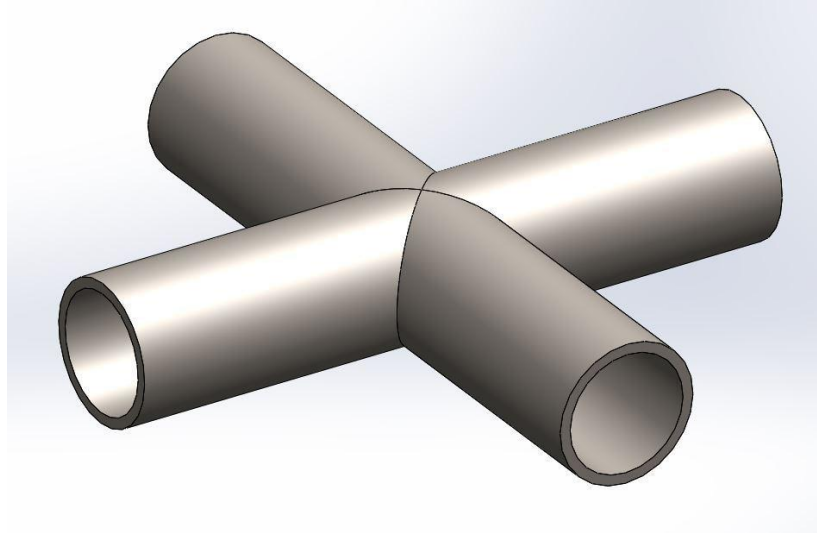


Figure 40: Steel Center Mount

Shown below in Figure 41 are the seat and landing gear bracket assemblies which surround the center mount. As one can see from the photo, the two bracket assemblies are in fact identical; this should help make these components relatively simple to manufacture. The bracket assemblies are each constructed out of 4 bracket walls made out of 12 gauge (0.1046" thick) plate steel (4130 Chromoly), and welded together into a square profile so that they sit around the tubes in the center mount. The brackets are then joined to the top and bottom of the center mount with fillet welds around the length of the contacting surfaces. Each bracket wall measures 2.50" tall by 3.00" wide and has an overhang of, 0.60"; this overhanging portion is what attaches to the landing gear in the center of the craft. For a closer look at these bracket walls please see Figure 41 below. The bracket walls should weigh 0.11 pounds each (though this may increase slightly with the addition of weld filler metal during the manufacturing process).

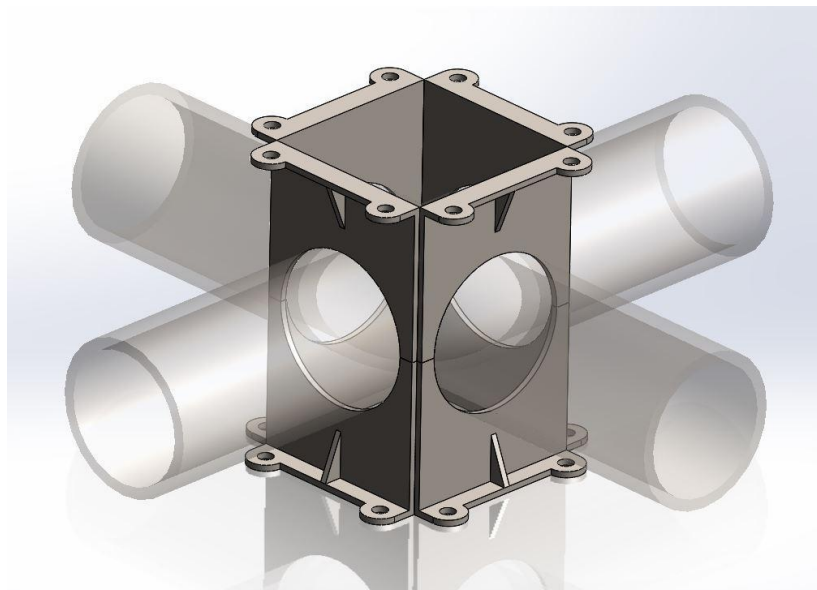


Figure 41: Center Mount Walls

On the bottom of the landing gear bracket, located under the center mount, a plate is bolted on to the bracket with 8 x 1/4"-20 Grade 5 bolts. This plate can be seen below in Figure 42. This should provide an adequate amount of strength and provide for secure mounting locations in case the team finds a need to

add additional components to the underside of the craft in the future. The plate is designed to be removable. The landing gear can be welded or otherwise attached to the plate as needed and can be replaced in the event of a rough landing. This plate is made out of 12 gauge 4130 steel plate, measures 4.40" wide by 4.40" tall, and should weigh 0.41 pounds.

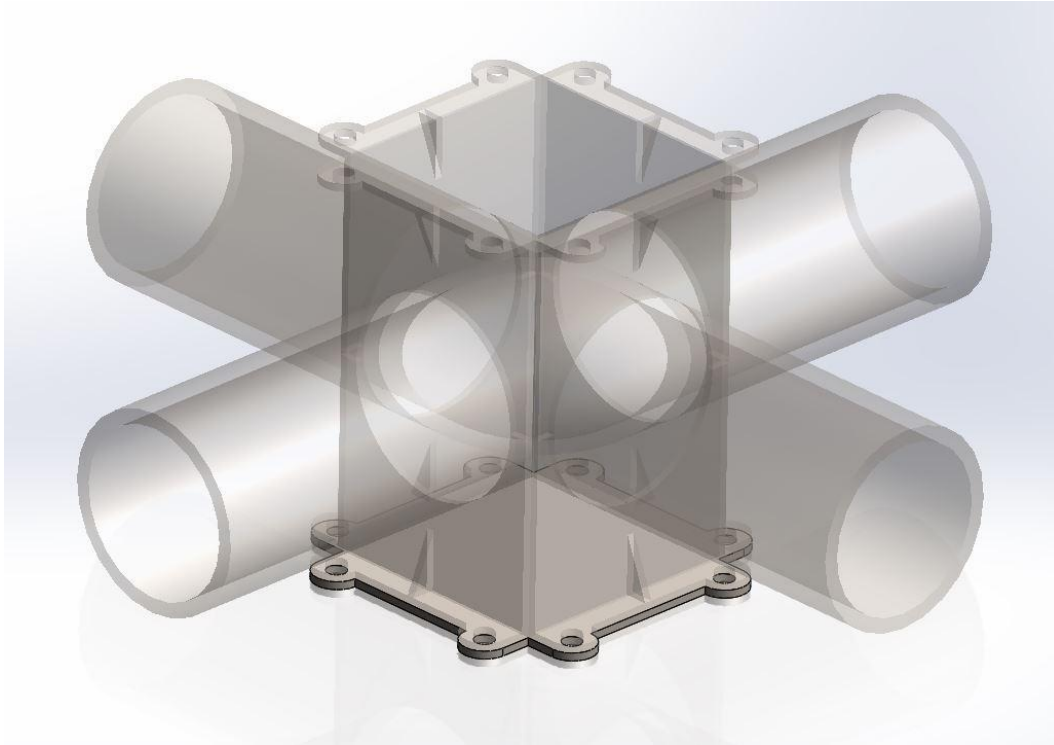


Figure 42: Center Mount Landing Gear Plate

11.1.5 Seat Plate and Seat

On the top of the seat bracket assembly (which is located above the center mount), an aluminum 6061-T6 plate is bolted to the top of the bracket with 8 x 1/4"-20 Grade 5 bolts. This plate can be seen below in Figure 43. This aluminum plate also has bolt patterns for attaching to the underside of the seat, which is a JEGS Pro High Back II racing seat, and for attaching of the seat belt, which is a 3" wide latch-style belt from SeatBeltPlanet.com. The designed seat plate should weigh 2.61 pounds and the seat itself weighs 13 pounds. The seat belt should weigh less than a couple of pounds; this information is not specified by the manufacturer, but they appear to be very lightweight and roughly the same size as other belts which should weigh a pound.

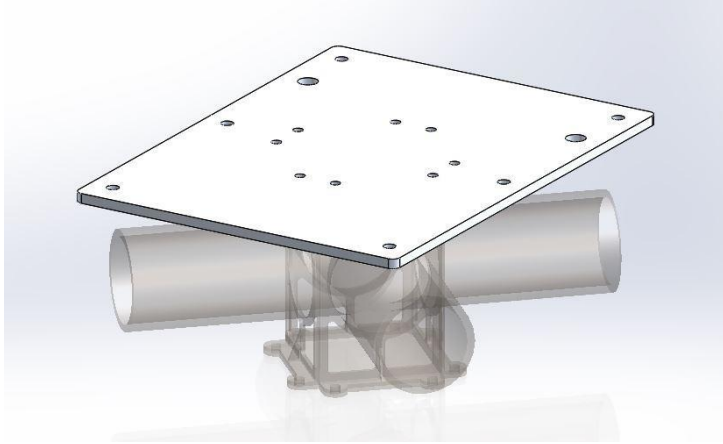


Figure 43: Seat Mounting Plate



Figure 44: Summit Lightweight Seat

11.1.6 Arm Mounts

The arm mount assembly is shown below in Figure 45. The arm mount assembly attaches the motor spars to each main arm in the craft. It is constructed in a similar fashion to the center mount assembly, employing both a bracket assembly and the arm mount. There are four arm mount assemblies total located throughout the craft (one per arm).

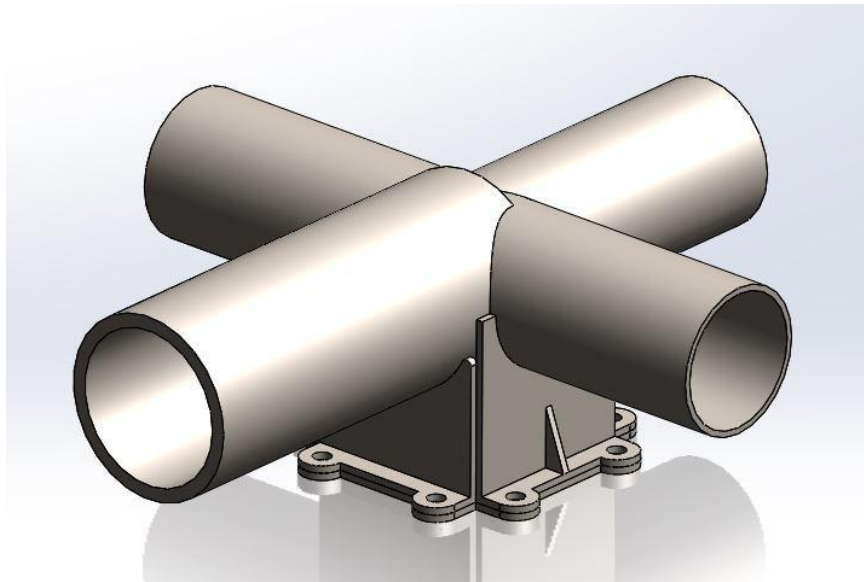


Figure 45: Arm Mount Assembly

Like the larger center mount, this component is constructed out of 4130 Chromoly steel tubing which was mitered and welded together. However, this mount is more complex because it requires tubes of two different sizes. The mount measures 10.50" by 9" along the axes of the tubes. Three of the tubes making up the mount have an outer diameter of 1.986" and an inner diameter of 1.870". These tubes slide inside the motor spars and bond in place with epoxy. The fourth tube is the same size as the tubes making up the center mount (with inner and outer diameters of 2.486" and 2.124" respectively), and it bonds in place inside the main arm. As with the center mount, there is a gap of 0.007" between the outer diameters of the steel tubes and the inner diameters of the carbon tubes to allow for optimum bond strength and the use of the glass bead additive with the epoxy. This mount should weigh 3.87 pounds (not including any additional weight from filler metal gained during welding).

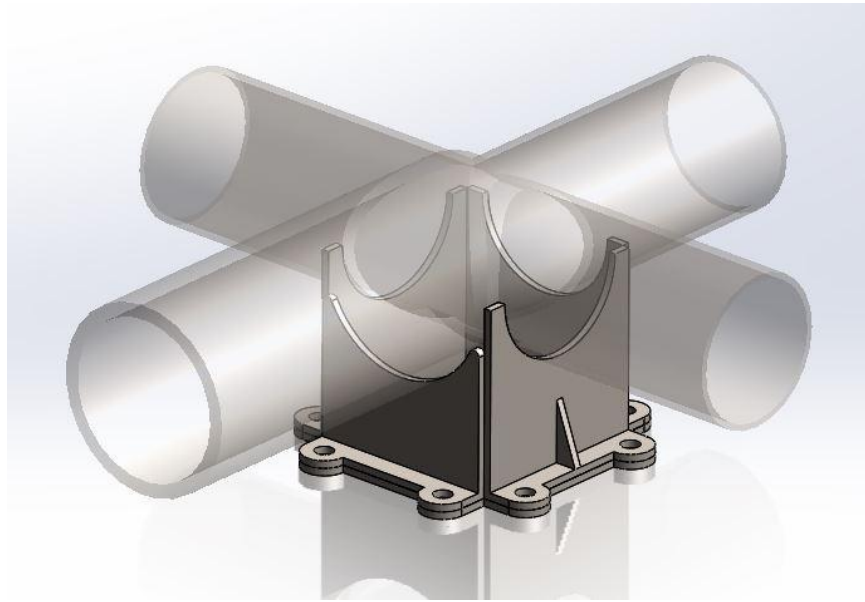


Figure 46: Arm Mount Walls

The arm bracket assembly is shown above in Figure 46. This assembly is needed in order to support the landing gear below the arm mount. It is constructed from 4 bracket walls which are welded together into a square profile like the brackets for the center mount, and it is made of 12 gauge plate steel (4130 Chromoly). In order to accommodate the different sizes of steel tubing which are joined together, three of the bracket walls are made to fit around the smaller diameter tubing of the arm mount, while the remaining bracket wall fits around the larger tube. The bracket walls for the smaller tubes weigh 0.10 pounds and measure 2.50" tall by 2.50" wide, while the bracket wall for the larger tube weighs 0.09 pounds and measures 1.96" tall by 2.50" wide. Both bracket walls also have an overhanging portion which bolts to the landing gear plate which sticks out 0.60" from the side of each plate. The bracket assembly is welded on to the arm mount with fillet welds all along the contacting surfaces.

On the bottom of the arm bracket is the arm assembly bracket's landing gear plate which is bolted onto the assembly with 8 x 1/4"-20 Grade 5 bolts. A similar plate can be seen above on the bottom of Figure 42. This plate serves to hold the landing gear for the arm and should provide for secure mounting locations in case the team finds a need to add additional components to the underside of the craft in the future. As with the center mount landing gear, the plate is designed to be removable; landing gear can be welded or otherwise attached to the plate as needed for quick repair or replacement. The plate is made out of 12 gauge 4130 steel plate, measures 3.90" wide by 3.90" tall, and should weigh 0.31 pounds.

11.1.7 Motor Mounts

Shown below in Figure 47 is the craft's motor mount assembly. There are 12 of these assemblies in the craft, one per motor, and they serve to keep the motor properly aligned and in place while also holding the propeller shrouds in position.

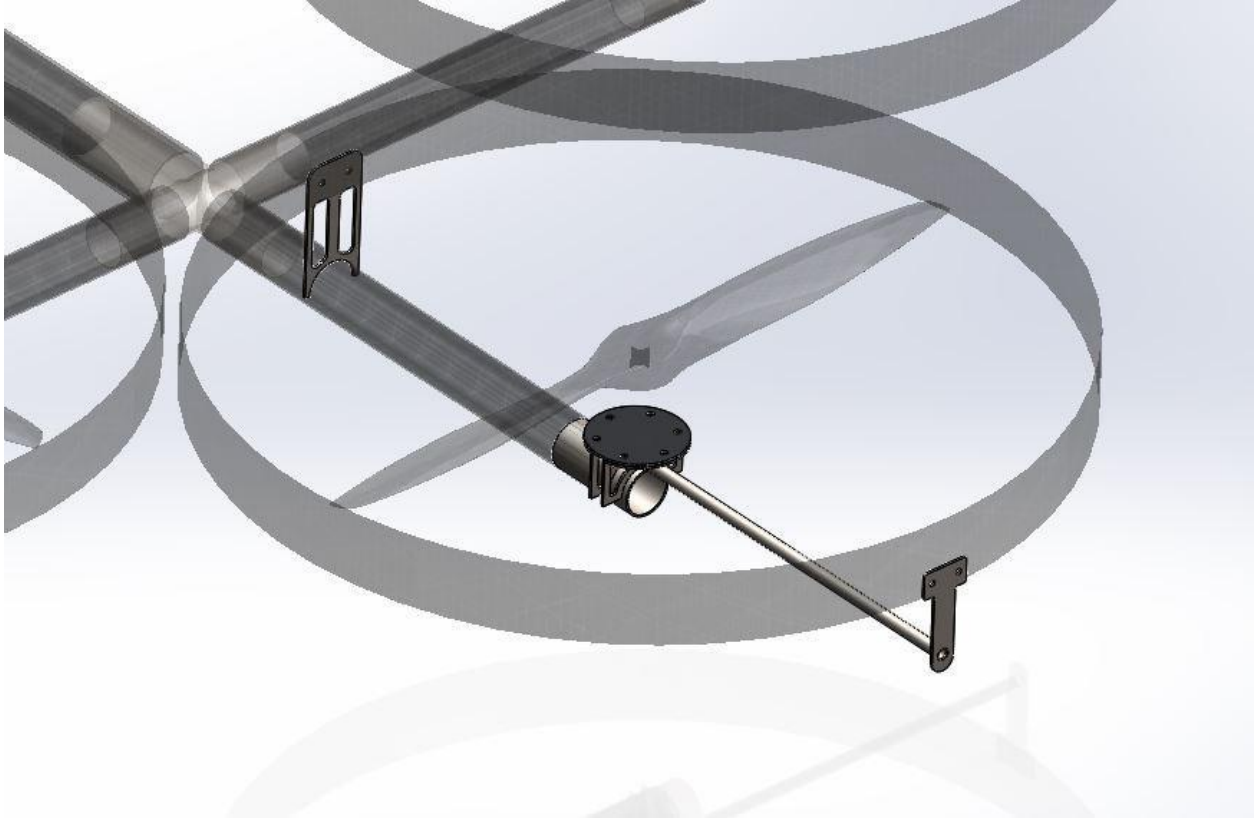


Figure 47: Motor Mount Assembly

The motor mount is shown below in Figure 48. The motor mount is what attaches the motors to the end of the motor spars, and it is constructed out of several different parts. The first is a section of the smaller-diameter 4130 steel tubing (also used in the arm mount above) which measures 4.00" long and has an outer and inner diameter of 1.986" and 1.870", respectively (after turning down the outer diameter by 0.014"). For a closer look at this section of tubing, please see Figure 48 below. This tubing should weigh 0.57 pounds. Three inches of this carbon tube slides inside the motor spar and is bonded in place with epoxy. The remaining inch of tubing holds the motor mount walls, which are constructed out of 12 gauge 4130 steel plate and measures 2.00" tall by 3.75" wide. These plates are welded on to the top of the short section of tubing. The top plates of the mount walls stick out 1.63" and have clearance holes for the purpose of bolting to the motor. These walls should weigh 0.22 pounds each.

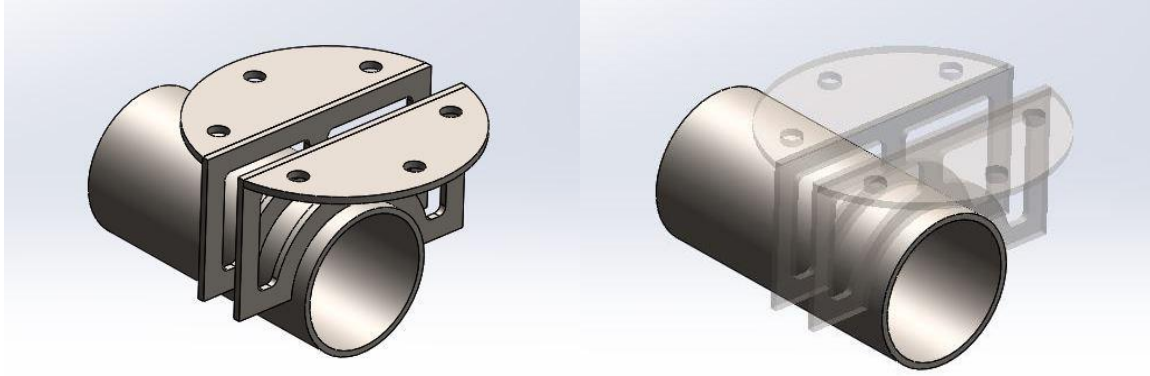


Figure 48: Close-up of Motor Mount

The propeller shroud spar extends off of the motor mount, which serves to hold a lightweight propeller ring and mesh assembly in place around the propeller itself. For a closer look at this component please see Figure 49 below. The shroud assembly is intended to prevent the propellers from hitting debris towards the user or bystanders at high speeds and to keep the propeller from sucking in small objects which could damage it. The propeller shroud isn't intended to protect the craft from crashes or contain the propeller in the event of a catastrophic propeller failure. The shroud spar is constructed out of thin walled 4130 steel tubing and is welded onto the surface of the outward-facing motor mount wall directly above the 4130 steel tubing. The spar measures 16.25" long and has inner and outer diameters of 0.444" and 0.500", respectively, and it would weigh 0.19 pounds. At the end of the spar, a narrow mounting plate of 12 gauge 4130 plate steel is welded. This plate is 2.00" wide and 4.50" tall, and serves to hold one side of the propeller ring in place. The plate has two mounting holes; through these holes the propeller ring is screwed into place, and the use of two mounting holes restricts the ring from rotating or translating in space. This mounting plate would weigh 0.15 pounds.

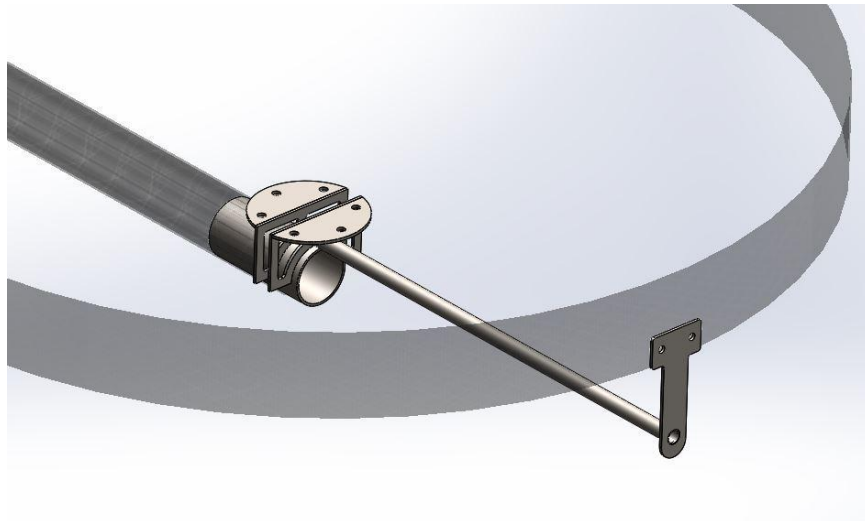


Figure 49: Propeller Shroud Spar

The inner ring mount on the other side of the propeller ring holds it in place, see below in Figure 50. This mount attaches to the propeller ring and to the motor spar connected to the motor mount assembly, and it serves to help lock the propeller ring in place when used in tandem with the other ring mount. The mount is constructed out of 0.10" thick 4130 steel Chromoly steel plate and measures 5.45" tall by 2.53" wide. It is bonded directly to the motor spar with epoxy; this should provide the component enough strength to rigidly hold the propeller ring in place but not enough to stay on in the event of a significant direct impact where it may cause damage to the motor spar (again, the propeller ring and mounts are not designed to protect the craft from crashes or collisions). The motor spar propeller ring mount should weigh 0.22 pounds.

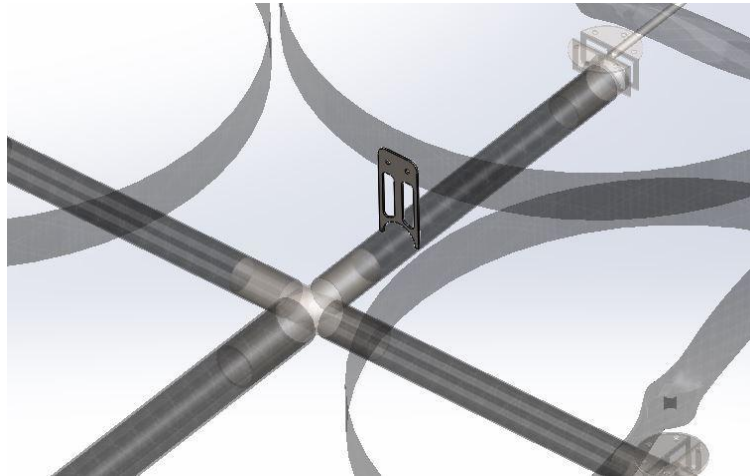


Figure 50: Inner Prop Ring Bracket

The propeller rings are shown below in Figure 51. The propeller rings are constructed out of braided carbon fiber tape and have an outer diameter of 33.00", a nominal wall thickness of 0.096", and a height of 2.00". They will serve to provide a form for a mesh shroud which should help prevent the propellers from sucking in debris and throwing it at bystanders or the user. The team was planning on getting 1/2" square bird netting for the mesh. It should also help prevent the user or a bystander from touching the craft's propellers (especially with their fingers) and should keep larger debris from impacting and damaging the propellers during use. Each propeller ring should weigh 1 pound.

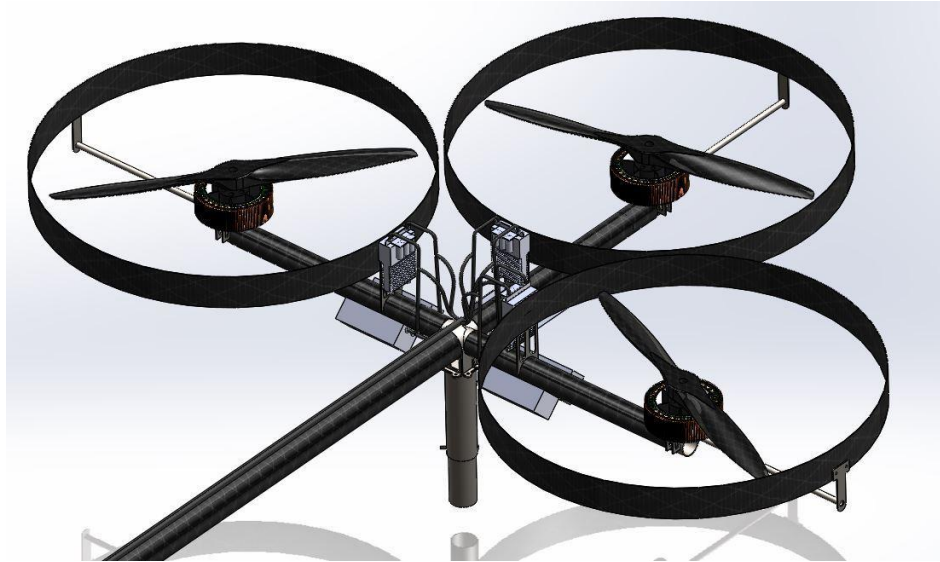


Figure 51: Propeller Rings

11.1.8 Landing Gear

The landing gear system for the vehicle is visible on the underside of the craft, shown below in Figure 52. The system makes use of 5 sets of landing gear: one set under the center mount assembly and one set under each arm mount assembly. Each set of landing gear is identical and uses a helical compression spring as the method of cushioning the landing impact. A steel tube encases and guides spring compression while a smaller steel tube compresses the springs and slides within the larger tube (telescoping).



Figure 52: Underside View of the Landing Gear

An exploded view of the landing gear assembly is shown below in Figure 53. The large tube that encases the spring is a stock 4130 steel tube that would be cut to 8.75" in length, it has an inner and outer

diameter of 2.5" and 2.310" respectively. This tube would be welded onto the bottom each arm mount assembly and center mount. The slot in tube is 4.5" long and 0.25" wide and would be machined out. A clevis pin would be placed through the smaller tube and through this slot. The pin and slot will guide the smaller tube and prevent the smaller tube from falling out once the aircraft leaves the ground. The slot is also designed for when the landing gear is assembled and experiencing no load the spring will be compressed by 3/16". This will keep the clevis pin from sliding and help prevent the assembly from moving around in flight. The slot is also longer than travel of the spring by 0.13". This is to allow extra room when the spring is compressed to ensure the load transferred from the ground to the structure is through the compressed spring and not the pin in the slot.

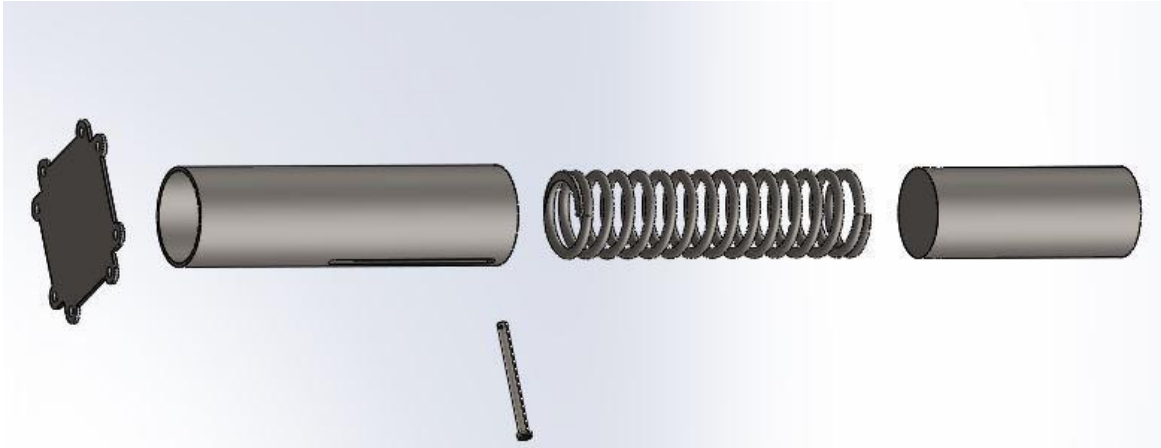


Figure 53: Exploded View of the Landing Gear Assembly

The spring has an unsprung length of 8.00" and a compressed length of 3.63", providing 4.37" of travel. The spring is made of tempered steel and has an outer diameter of 2.187", giving 0.0615" of clearance between the inner wall of the tube encasing the spring and the spring itself. This clearance prevents the spring from buckling and minimizes lateral movement of the spring. The spring has a wire diameter of 0.250", a spring constant of 61.8 lbs/in, and a maximum load of 274.0lbs. The spring was selected based on the maximum force on a single landing point that would cause failure in the structure. That force, with a factor of safety, came out to 256lbs. The team did not want a spring to have a maximum spring force much greater than the force that could break the structure, nor did the team want a spring that would be too soft and let the landing gear "bottom out" before the failure load. Having the maximum spring force be similar to the failure load provides more protection against hard landings by allowing the utilization of the spring's entire travel.

The smaller telescoping tube is stock tubing made of 4130 steel cut to a length of 5.50". The tube has an outer diameter of 2.25" and an inner diameter of 2.010" with a wall thickness of 0.083". The hole in the small tube has a diameter 0.25" and is for the clevis pin. The hole is located 0.50" from the face that contacts the spring. The plate on the end of the tube that contacts the spring is cut from the same 0.10" thick 4130 chromoly plate used in the mounts of the structure. The plate would be cut to the same diameter of the small tube, 2.25". The plate would be welded to the tube. If the spring gets fully compressed the smaller tube will extrude from the larger tube by 0.50".

The clevis pin is stock from McMaster Carr and made of 18-8 stainless steel. The pin has a usable length of 2 9/16" and would have a minimum clearance of 0.002" in a 0.25" hole. The manufacturer specifies to use a 1/16" cotter pin for the clevis pin.

Each landing gear assembly weighs 3.83lbs, accounting for 19.15lbs of the total craft's weight.

11.2 Propulsion

11.2.1 Propellers

The final propeller selection is 12 30"x10" carbon fiber propellers from the Precision Pair Series manufactured by Xoar. The team as requested that Xoar have these propellers custom made for the team, as 30"x10" are not a standard diameter and pitch for Xoar. As the propellers aren't commonly available for purchase, the exact specifications of the product are unknown other than the specified pitch and diameter. Based on other propellers from the Precision Pair Series, the expected weight of the 30x10 propellers should be between 90 and 100 grams per unit. This would add a system weight of 2.7 lbs. Each propeller comes with a pre-drilled center hole, as well as pre-shipping balancing. The cost per pair of propellers is \$349.

11.2.2 Motors

The two motors that were be considered were the JM1S motor from JobyMotors and the Turnigy RotoMax 80CC motor. In order to make a final selection, testing would be completed on the Turnigy RotoMax, already in the team's possession, for a proper comparison.

The JM1S is a high quality electric in-runner aircraft motor designed and manufactured by Joby Motors. It uses high copper fill-rate to create a high torque constant which provides high torque at low RPM. Although this motor is slightly overpowered for the team's purposes, the Joby motor with 2T Wye winding provides excellent efficiency of up to 90% and over 80% for the desired operating range of 35lbs to 80lbs thrust per motor with a 30x10 propeller. At a nominal RPM of 6000 and a continuous torque of 9.6 ft-lb (13 N-m), these motors can provide a continuous power of 8.2 kW and a max peak output of 12.6 kW. The unit weights 1.8 kg (4 lbs) a unit with a diameter of 6 in (154 mm) and height of 2.1 in (53.1 mm). This will give a total system weight addition of 48 lbs. The full data sheet for the motor is included in Appendix D: Joby Motor. Included with the data sheet is testing data for the motor with several different propellers. This test data proves that the motor will work for the craft's applications. Each motor comes at a price of \$1140.

The Turnigy RotoMax 80CC motor is a hobby motor designed for large scale hobbyist RC planes. Each motor weighs 4.2 lbs (1.92kg), which would contribute a total weight addition of 50.4 lbs. The motor has a rated max continuous output of 6.6kW, and costs \$282 per motor. The data sheet for the motor is included in Appendix D: Turnigy RotoMax 80cc. Forum data online as well as videos provide evidence of the unit outputting at least 32 lbs of thrust when powered with 6s batteries. This motor is the low cost option, and was tested to validate their possibility of use for the project. The test plan and setup can be found in section 20.2: Propulsion Test Plan.

With the test data for the Rotomax motor collected, it is still the team's current recommendation that the JM1S be utilized for this project, now or for future iterations. Joby's motors are highly reliable and efficient, meant to endure long term use. The hobbyist motors such as the Turnigy RotoMax generally aren't meant for continuous use and will likely require frequent maintenance or replacement. There is also the aspect of customer service, which Joby has proved highly dependable; the group's communications have been answered swiftly and promptly. On the other hand, there is no direct line of contact with the Turnigy RotoMax motor makers or suppliers, Hobby King. The team believes that what you lose in monetary savings you get back in the form performance, reliability, and longevity.

11.2.3 Batteries

The choice of batteries is limited by a couple parameters. The nominal voltage 51.8 Volts (14s batteries) are limited by the voltage required by the ESC and the motors. The current draw needed provides a minimum for the discharge rating of the battery. Off-the-shelf batteries don't come in 14s packs, so in order to get to a 14s packs you generally need to put two 7s batteries in series. Putting batteries in series adds the voltages, but keeps the capacity and discharge rating of a single battery.

There are higher voltage limits from certain ESCs (i.e. Alien 420A 24s ESC), but the limiting factor is more likely going to be the motors. The off-the-shelf motors the team has been looking at have all been rated up to 51.8 Volts. The Joby motors (JM1S) can work with higher voltage, but they are more expensive.

The discharge rating is split into two ratings: peak discharge rating and maximum continuous rating. The peak discharge rating is to account for spikes in current and shouldn't be used for rating the usable discharge current of the battery. The maximum continuous rating is the usable rating for discharge current, but in actual use you should still have a margin of safety between the maximum continuous current draw of your system and the maximum continuous discharge rating of the battery. Batteries will tend to lose capacity and start heating up even at the maximum continuous rating. The discharge rating is given as a C rating. You can multiply the capacity of the battery by the C ratings to give a current rating in amps. If you put more battery packs in parallel the capacities can be added, which gives an overall higher discharge current and more flight time.

The plan is to fill the remaining weight of the craft (up to 254 lbs) with batteries after all the other weights are accounted for. The minimum the team would like to fly with is at least a single 14s battery pack per motor in order to not over discharge the batteries. Batteries would be put onto each arm to directly service the motor closest to them. The batteries would then be connected in parallel with the wiring explained below to make sure that the batteries are evenly discharged. If the batteries are discharged unevenly the craft could have a motor cut out at an inopportune time.

11.2.4 Wire

For this project, two types of wire are required: power and signal. The power wiring will be used to connect the ESCs, batteries, and motors. The signal wiring will be used to transfer a servo signal from the flight controller to the ESC. The ESC will then interpret the signal to determine how power to supply to the motor.

Considerations for the selection of power wiring include its weight per length, ampacity (amps it is able to carry), and the temperatures to be encountered at operating and extreme operating conditions. Because the motors of this project require thousands of watts, thicker wiring is required to prevent the wiring heating up due to the large amount of current flowing through it. Note that wire with large cross section will have less internal resistance than similar wire with a smaller cross section. This increase in wire cross-section makes for a heavier wire. Thus, the amount of power wire the team will implement onto the project must be minimized. With several of the craft's cable-routing schemes, it was found that the weight of the cables rivaled that of the structure of the craft. Therefore, all of the power components (ESC and batteries) were clumped together into a module located at the end of each arm of the craft rather than having all of the batteries placed directly under the pilot. See Appendix D: 8AWG Power Cable for further information on wire sizing.

Additionally, because the motors will be run at relatively high currents during both operating and max conditions (~150amps), the wiring selected must also accommodate these high ampacity demands as well as keep its insulation intact. It can be difficult to find such wiring because it is on the edge of the power requirements of the hobby world and there is certainly there is large diameter industrial cable that can operate at such power settings but their temperature they are supposed to operate in, or at least that their data values are taken from, are all closer to 90°C, too conservative for the team's applications.

Table 5: NEC Table 310.16 for Covered Wires

Size AWG or kcmil	Temperature Rating of Conductor [See Table 310.13(A).]						Size AWG or kcmil
	60°C (140°F)	75°C (167°F)	90°C (194°F)	60°C (140°F)	75°C (167°F)	90°C (194°F)	
	Types TW, UF	Types RHW, THHW, THW, THWN, XHHW, USE, ZW	Types TBS, SA, SIS, FEP, FEPB, MI, RHH, RHW-2, THHN, THHW, THW-2, THWN-2, USE-2, XHH, XHHW, XHHW-2, ZW-2	Types TW, UF	Types RHW, THHW, THW, THWN, XHHW, USE	Types TBS, SA, SIS, THHN, THHW, THW-2, THWN-2, RHH, RHW-2, USE-2, XHH, XHHW, XHHW-2, ZW-2	
	COPPER			ALUMINUM OR COPPER-CLAD ALUMINUM			
18	—	—	14	—	—	—	—
16	—	—	18	—	—	—	—
14*	20	20	25	—	—	—	—
12*	25	25	30	20	20	25	12*
10*	30	35	40	25	30	35	10*
8	40	50	55	30	40	45	8
6	55	65	75	40	50	60	6
4	70	85	95	55	65	75	4
3	85	100	110	65	75	85	3
2	95	115	130	75	90	100	2
1	110	130	150	85	100	115	1
1/0	125	150	170	100	120	135	1/0
2/0	145	175	195	115	135	150	2/0
3/0	165	200	225	130	155	175	3/0
4/0	195	230	260	150	180	205	4/0
250	215	255	290	170	205	230	250
300	240	285	320	190	230	255	300
350	260	310	350	210	250	280	350
400	280	335	380	225	270	305	400
500	320	380	430	260	310	350	500
600	355	420	475	285	340	385	600
700	385	460	520	310	375	420	700
750	400	475	535	320	385	435	750
800	410	490	555	330	395	450	800
900	435	520	585	355	425	480	900
1000	455	545	615	375	445	500	1000
1250	495	590	665	405	485	545	1250
1500	520	625	705	435	520	585	1500
1750	545	650	735	455	545	615	1750
2000	560	665	750	470	560	630	2000

The National Electrical Code (NEC) lays out conservative ratings for ampacities for wiring in buildings for covered wires for use in building walls, as shown in Table 5. The NEC also lays out a rating for wiring in free air, as shown in Table 6. These ratings are still fairly conservative considering the fact that the team wants to minimize the weight of wires on the craft and the ratings in the tables below and above are for very long term use and. They also only go up to 90° C rated insulation. Insulation rating can be 125 degree Celsius rated for PVC and up to 150 or 200 degrees Celsius for silicone rubber and Teflon insulation. Wire ratings can go above that as well with exotic insulation. The higher insulation ratings allow for more ampacity for a given gauge. This means the wires can take more heat before they fail. The problem with using silicone insulation is that it has worse abrasion resistance than PVC and polyethylene (90° C rated insulation). The way to get around this would be to buy wire with fiberglass wrapped wire,

which adds weight and cost or put fiberglass wrapping on portions of the wire that are most likely to be in contact with rough surfaces.

Table 6: NEC Table 310.17 for Wires in Free Air

Size AWG or kcmil	Temperature Rating of Conductor [See Table 310.13(A).]						Size AWG or kcmil
	60°C (140°F)	75°C (167°F)	90°C (194°F)	60°C (140°F)	75°C (167°F)	90°C (194°F)	
	Types TW, UF	Types RHW, THHW, THW, THWN, XHHW, ZW	Types TBS, SA, SIS, FEP, FEPB, MI, RHH, RHW-2, THHN, THHW, THW-2, THWN-2, USE-2, XHH, XHHW, XHHW-2, ZW-2	Types TW, UF	Types RHW, THHW, THW, THWN, XHHW	Types TBS, SA, SIS, THHN, THHW, THW-2, THWN-2, RHH, RHW-2, USE-2, XHH, XHHW, XHHW-2, ZW-2	
	COPPER			ALUMINUM OR COPPER-CLAD ALUMINUM			
18	—	—	18	—	—	—	—
16	—	—	24	—	—	—	—
14*	25	30	35	—	—	—	—
12*	30	35	40	25	30	35	12*
10*	40	50	55	35	40	40	10*
8	60	70	80	45	55	60	8
6	80	95	105	60	75	80	6
4	105	125	140	80	100	110	4
3	120	145	165	95	115	130	3
2	140	170	190	110	135	150	2
1	165	195	220	130	155	175	1
1/0	195	230	260	150	180	205	1/0
2/0	225	265	300	175	210	235	2/0
3/0	260	310	350	200	240	275	3/0
4/0	300	360	405	235	280	315	4/0
250	340	405	455	265	315	355	250
300	375	445	505	290	350	395	300
350	420	505	570	330	395	445	350
400	455	545	615	355	425	480	400
500	515	620	700	405	485	545	500
600	575	690	780	455	540	615	600
700	630	755	855	500	595	675	700
750	655	785	885	515	620	700	750
800	680	815	920	535	645	725	800
900	730	870	985	580	700	785	900
1000	780	935	1055	625	750	845	1000
1250	890	1065	1200	710	855	960	1250
1500	980	1175	1325	795	950	1075	1500
1750	1070	1280	1445	875	1050	1185	1750
2000	1155	1385	1560	960	1150	1335	2000

Another big consideration for the wiring was which conductor material to use. The best conductor in terms of conductance per are is silver, but it is denser than copper and only slightly more conductive. This makes copper good for most cases. Aluminum is also a very common conductor. It is less conductive than copper, but it is considerably less dense, so it has better conductivity per weight. This made it a good choice for the craft's application. There are also some cases where nickel conductors are used for high temperature applications, but nickel is heavier, less conductive, and would have interfered with the craft's motors and batteries due to its ferromagnetic properties.

The batteries, motors and ESCs came with copper wiring which was connected such that it was difficult to replace. The team was, therefore, stuck with the wiring for those portions. The team wanted to connect the batteries packs on each arm in parallel to balance the battery capacities, which required running wire along the length of the craft. The team used 8 AWG copper wire with silicone insulation in order to save weight and get away from connecting dissimilar metals. The use of the 8 AWG wire was based on a couple manufacturer's claims of and a few charts getting close to a 200A rating for the wire. The team planned on testing the wire along with the motor test and if the manufacturer's specification were too low the wire would heat up to an unacceptable level. If this was the case the team would go with higher gauge aluminum wire, but that came with its own concerns. The first concern was galvanic corrosion, when you connect two dissimilar metals you can cause increased corrosion rates in one of the metals (i.e. the aluminum). This can be mitigated by antioxidant pastes/coating that contain a metal that will corrode before the aluminum. The other concern was a difference in thermal expansion coefficients between

copper and aluminum. This would cause the aluminum and copper wires to detach over time as they expand and contract. This could be mitigated by bimetallic connectors, which allow you to connect copper wires to copper a copper lug and aluminum wire to an aluminum lug and the lugs are connected such that they aren't affected by the thermal expansion. Bimetallic connectors generally come with an antioxidant coating as well.

11.2.5 Stacked Prop Configurations

The theoretical efficiency of the vehicle was only limited by the amount of area that it could encompass with its props. With this in mind, the team decided to investigate the effects of adding a second layer of propellers above the existing ones. The team was able to analyze the stacked system with the same actuator disk theory as before, just modified slightly. The power draw per pound of thrust from the top prop remained unaltered, since all changes to the fluid flow were downstream of the prop. As for the bottom prop, the team was still able to model it as an infinitely thin disk inputting power into a fluid in order to change its momentum. The only difference is that the incoming air has a higher initial velocity than the still air being pulled in by the top propeller. The team was able to deduce that if the props with greater pitch were mounted on the bottom in order to accommodate the greater fluid flow similar or better efficiencies could be achieved. The team decided to conservatively model the stacked props as a single prop with twice the actual area, providing much greater efficiencies within the same overall footprint. Unfortunately, the added components proved to be too heavy to justify their implementation, since comparable configurations had almost identical predicted flight times (i.e. 24 stacked props vs. 12 planar props). Given this information, the only differences were more appealing aesthetics, greater control complexity, and much greater vehicle cost. Therefore, the team decided to stick with a planar prop configuration.

11.3 Controls

11.3.1 Multicopter Dynamics

Dynamic variations for multicopter movement are very dependent on number of rotors as well as structural placement of the rotors. The team has narrowed the design on propulsion side to either a 12 or 16 rotor configuration, dynamic design was based off of the two x-copter designs up for consideration; each configuration had two sensible and similar solutions. The first solution was the "Clustered Quadcopter" control scheme. Here, the direction of motion of each of the motors on a spar would match. When facing forward in the craft the directions would be as follows:

Forward Right Cluster (FR): Clockwise (CW)
Forward Left Cluster (FL): Counter Clockwise (CCW)
Rear Right Cluster (RR): Counter Clockwise (CCW)
Rear Left Cluster (RL): Clockwise (CW)

This configuration worked independently of rotor numerical configuration; both the 12 and 16 rotor models would work the same. The only change would be in the level of redundancy.

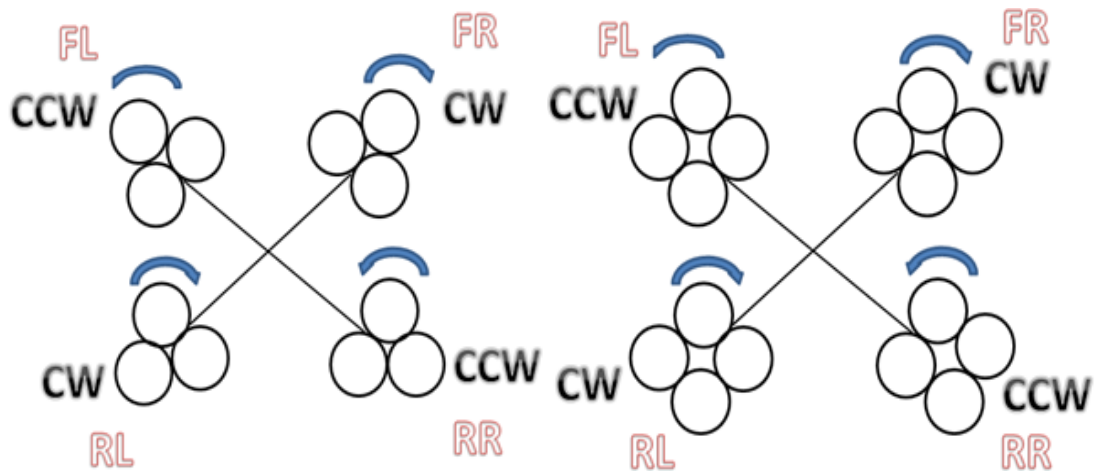


Figure 54: Diagrams for the 12 (left) and 16 (right) clustered quadrotor configurations

The second configuration was known as the “Independent Vehicle” control scheme. This scheme treats each cluster of motors as if they were an independently controlled vehicle while alternating to keep vehicle stability. This model is a bit more confusing as well as varying for each configuration. For the 16 rotor configuration, when facing forward in the craft, the directions would be as follows:

Forward Right Cluster: Front Right Motor: CCW Front Left Motor: CW Rear Right Motor: CW Rear Left Motor: CCW	Forward Left Cluster: Front Right Motor: CCW Front Left Motor: CW Rear Right Motor: CW Rear Left Motor: CCW
Rear Right Cluster: Front Right Motor: CCW Front Left Motor: CW Rear Right Motor: CW Rear Left Motor: CCW	Rear Left Cluster: Front Right Motor: CCW Front Left Motor: CW Rear Right Motor: CW Rear Left Motor: CCW

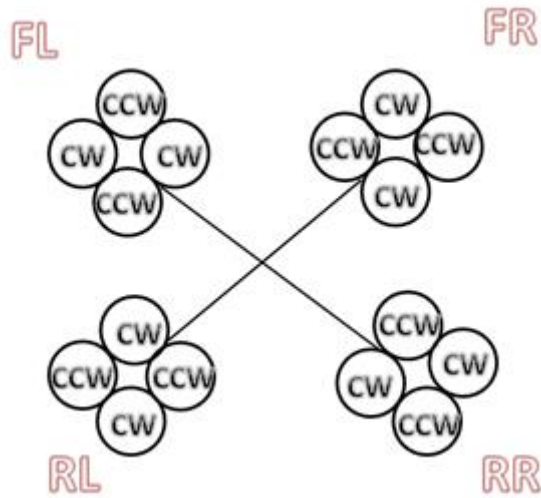


Figure 55: Diagram for the 16 rotor configuration of the “Independent Vehicle” control scheme

In the 12 rotor configuration there will likely be a triangular formation of rotors on each spar. In this model, when facing forward in the craft, the directions would be as follows:

Forward Right Cluster: Point Motor: CCW Base Motors: CW	Forward Left Cluster: Point Motor: CW Base Motors: CCW
Rear Right Cluster: Point Motor: CW Base Motors: CCW	Rear Left Cluster: Point Motor: CCW Base Motors: CW

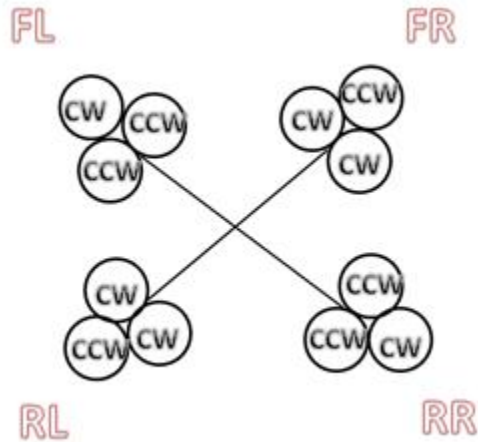


Figure 56: Diagram for the 12 rotor configuration of the “Independent Vehicle” control scheme

The pros of the “Clustered Quadcopter” configuration included its extreme simplicity when compared to the other configuration, as well as ease of adaptability of available software for use in this formation; this configuration was in the end, the same a regular quadcopter, with the exception that the thrust loading is split between three motors per arm. The pros of the “Independent Vehicle” configuration were primarily in improvement of redundancy. If any of the motors gave out, the likelihood of a motor of the same spinning orientation also giving out at the same time is decreased. In the event that the craft’s banked battery system fails a “two + one” orientation would fail instead of an entire cluster of similar motor spinning orientations.

In the end, the team decided to error on the side of simplicity and chose the “Clustered Quadcopter” in the 12 rotor configuration. The team believed that the redundancy increases were not large enough to outweigh the benefit of system simplicity; particularly with the group’s lack of professional stability software or stability software designers. After the team picked the “Clustered Quadcopter” configuration it could specify how to achieve elevation, pitch, roll and yaw. For simplicity, each of the motor clusters was assigned a designator:

- Forward Right Cluster: CP1
- Forward Left Cluster: CP2
- Rear Right Cluster: CP3
- Rear Left Cluster: CP4

In order to elevate, the total thrust of the system must overcome the weight of the aircraft and rider. This is accounted for through equivalent increase of thrust on all motors:

$$\text{Thrust (T)} = \text{CP1} + \text{CP2} + \text{CP3} + \text{CP4}.$$

In order to pitch the craft forward, and therefore create forward movement, one must thrust the rear facing clusters with a higher load than the front. If thrust is only increased in the back, the vehicle would pitch forward as well as elevate which is not a desired result from a controls standpoint. Therefore, in order to maintain the moment balance, the front motors must increase and rear motors decrease by an identical offset. The following was implemented, the offset changing until the vehicle pitches a maximum 30°:

Forward Pitch	Backward Pitch
CP1= T+Offset CP2= T+Offset CP3= T-Offset CP4= T-Offset	CP1= T-Offset CP2= T-Offset CP3= T+Offset CP4= T+Offset

In order to perform a roll, the motor cluster opposite the direction of travel must thrust harder than the rest. Once again, in order to maintain torque balance, one cannot just increase the thrust on one side; this will cause the aircraft to elevate while rolling. To accommodate this, both sides must change; opposing motors increased by an offset and same side decreased by the same offset. The following was implemented, the offset changing until the vehicle banks by 20°:

Left Turn	Right Turn
CP1= T+Offset CP2= T-Offset CP3= T+Offset CP4= T-Offset	CP1= T-Offset CP2= T+Offset CP3= T-Offset CP4= T+Offset

The execution of a yaw is similar to that of roll, only diagonal clusters must match. Once again, the aircraft cannot stay at a steady altitude if thrust is only increased on the two diagonal motor clusters. The following was implemented, the offset increasing until the yaw is clocked at 20°/s:

Counter Clockwise Rotation	Clockwise Rotation
CP1= T-Offset CP2= T+Offset CP3= T+Offset CP4= T-Offset	CP1= T+Offset CP2= T-Offset CP3= T-Offset CP4= T+Offset

11.3.2 User Interface

Just as important as any technical aspect of Electric Commuter Multicopter, was the user interface (UI) with which the user or pilot engages the aircraft. The VC1 utilized a simple RC transceiver to receiver interface, resembling the control scheme of your standard RC quadcopter. What follows is a breakdown of the different user interfaces including mapped controls:

11.3.2.1 Saitek X52 Flight Control System

The Saitek system is an advanced flight simulator flight control system reminiscent of what would be used for PC gaming or official flight simulators. This fighter pilot approved set up comes in two pieces, the throttle unit and joystick unit. An abundance of different control inputs as well as complete customization and button mapping allows for an experience that could be tailor perfectly for this aircraft. The throttle would remain in the middle “neutral” position to keep the aircraft at “idle” or at lift off capacity thrust. Throttle up would increase the thrust, while the throttle down would decrease the thrust. The rest of the actions would be mapped to the joystick. The forward and backward movement of the joystick would cause the aircraft to pitch in that direction. The side the side movement of the joystick would cause the aircraft to strafe or roll in the corresponding direction. Twisting the joystick CW or CCW would turn the aircraft in a flat plane, that corresponding direction. The sensitivity in which the joystick is manipulated would work to either slow or speed up these movements. The safety covered switch button would serve as an emergency engine out trigger, protected from accidental engagement by the safety mechanism. An optional feature which the team hoped to implement was the utilization of the sticks three bottom button for “cruise control” abilities. The idea here was to have the left switch engage idle condition, middle switch place the aircraft at 1 ft hover, and the right at 5ft, which would clear the majority of consumer vehicles. The team hoped to see this utilized as part of “pre-flight” check in. Lastly, the joystick’s main trigger would be used for optional height lock; depressing the trigger while throttling would bring the system back to hover, and the user would then place the throttle lever back at neutral. The system cost \$129.99.



Figure 57: The Saitek X52 Flight Control System

11.3.2.2 Xbox 360 Controller

A large portion of the young adult and adult population is familiar with the landmark design of Microsoft's Xbox 360 controller for video games. Due to its commonality and familiarity, the team decided to pursue the option for a transmitter input for the aircraft. The ergonomic design feels great and would be a comfortable way of controlling the vehicle. The right trigger would be utilized to increase height of the aircraft by varying thrust. The left trigger would serve as a means of decreasing this. The bumpers would be assigned the same controls, but in finer increments, used as a trim for the vehicle. The left joystick would control pitch with forward and backward movement, while left and right movement would cause a strafe or roll in that direction. The right joystick would be used to yaw the vehicle towards the direction of movement (i.e. right for clockwise movement). The face button would serve as a "cruise control" purpose, the most important of these being Y placing the user at idle. X would take the user to 1 ft, Y to 5 ft, and B to 10 ft. The unit costs \$39.99.



Figure 58: Microsoft's Xbox 360 console controller

11.3.2.3 Mad Catz F.L.Y. 5 Stick for PC

The F.L.Y. 5 Stick is a joystick and miniature throttle aimed at PC and PS3 users for video games and flight simulator use. The combination stick and throttle unit minimizes size in combination and provides programmable control. The basic controls would match that of the Saitek system. Throttle neutral at middle and increasing or decreasing thrust with forward or backward throttle respectively. Forward or backward movement of the joystick would cause the vehicle to pitch, while lateral movement would cause a strafe or roll. A rotation of the joystick would cause a yaw as well, in its respective direction. The bottom buttons would be set for "cruise control," from left to right being set at idle, 1 ft., 5 ft., and 10 ft., respectively. The trigger would once again serve as an optional height lock. The unit costs \$59.99.



Figure 59: The Mad Catz F.L.Y 5 Stick for PC and PS3

11.3.2.4 Spektrum Dx6 Transmitter

Spektrum is renowned as one of the largest producers of functional, affordable RC transmitters and receivers. Being completely customizable it allows the team to map the controller with an optimized control scheme for user input. The 6 in the name represents the 6 channels which are programmable for different functions; only 4 channels are necessary for regular multicopter control, expanding team control expansion. With the built-in ability to communicate with a receiver directly out of the box, this unit was the simplest to integrate. The left stick would control forward and backward movement with a respective movement. Rotating the left stick in either a clockwise or counter clockwise direction would cause the aircraft to yaw in that direction. The right stick would control pitch with forward and backward movement, and roll or strafe with a lateral movement to either side. The switches at the top of the controller would serve as “cruise control” once again, front left idle, back left 1 ft., front right, 5 ft., back right 10 ft. This package comes at \$229.99.



Figure 60: Spektrum Dx6 transmitter

11.3.2.5 Decision

It was the team's recommendation that the Saitek X52 Flight Control System be utilized for the aircraft system. Many considerations were taken into account here, including the larger cost for the systems implementation. The biggest deciding factor was dual module set up; having the throttle unit and joystick unit separate allows a comfortable user interface. The throttle module would attach to an arm unit which can be attached to either the left or right side of the seat. The joystick could be mounted to the seat and placed comfortably between the users legs. This would allow for a more natural feel than a single user interface unit which would require an uncomfortable location, between the pilot's legs. Secondly, the team believed that the system was very intuitive and "feels" like the way a user would want to pilot the craft. It utilized motions and gestures that are synonymous to the movement of a vehicle. The team was targeting those with "some" technical background as the base consumer market most interested in this project. The team believed that the resemblance to flight simulator controls as well as advanced video game flight control will be beneficial. The Xbox 360 controller came in second as an alternate choice for the sponsors, if they believed it would be more familiar for them and costumers. These controls are familiar for the most recent generation, but it does not resemble something that should control an aerial vehicle.

11.3.3 System Communications

From the beginning, the team knew it did not want to follow the VC1 route and use a standard transmitter and receiver system. The VC1 felt unintuitive and clunky in control, which meant it's something the team could easily improve upon with the group's solution. The biggest issue to overcome was that the majority of the control units available are meant to be used as a USB controller for either a game console or PC. Therefore, these units did not have the functionality of transmitting to a receiver. The closest to this technology is Bluetooth capabilities, which the reliability is questionable for such applications. The other option would have be to wire directly into the system, which might have been the most practical if not for the fact that as students at Cal Poly, the team would not be able to test the vehicle directly, and would have to remove the controller interface to operate the system remotely. The solution was to adapt an off the shelf system to work for the craft's purposes. The method most commonly used by the online forum RC community spoke of using a USB to PPM cable to transform the user inputs into something readable by a transmitter. This would route the signal through a standard RC receiver, such as the Spektrum receiver which is mentioned earlier at a price of \$75.99.



Figure 61: CompuFly USB to PPM converter

The issue here was, the group would still be using the RC transmitter unit, and therefore adding unnecessary weight. Therefore unless another method could be utilized, the VC1 route would have been the best possible solution. A method of mitigating this need was next on the agenda. After research, a transmitter module called the Scherrer LRS TX7000 Lite was found. This small lightweight transmitter module was a low weight long range system designed for UAV applications, offering 20 km of

transmittance range. It also came with a receiver for a price of \$269.99. When coupling this with the Saitek control interface with the Scherrer transmitter and linked via a CompuFly cable, the team believed that it would be possible to integrate a USB device into the system to create an intuitive and removable flight system for the aircraft.



Figure 62: Scherrer LRS Tx7000 Lite transmitter and receiver set

11.3.4 Microcontrollers

When searching for microcontrollers, the team focused on searching for systems that were open-source, adaptable, output heavy, and equipped with advanced sensor capabilities. After much discussion, the team narrowed down the selection to three different controllers:

11.3.4.1 Open Pilot Revolution Flight Controller

The OpenPilot Revolution is an advanced, high speed flight controller with a highly supported open-source platform. The system easily allows 12 outputs, as verified through schematics and online directions from their own manual. It utilizes the STM32F4 32-bit microcontroller as the main processor, running at a speed of 168 Mhz. Utilizing the MPU-6000 for 3-axis gyro and 3-axis accelerometer, the controller can give very accurate feedback. An onboard pressure sensor/altimeter can provide an altitude sensitivity of 10cm. A magnetometer provides accurate heading information as well. For \$174.95, the team received all of this as well as a GPS module and OPLink Modem for advanced communications.



Figure 63: Open Pilot Revolution Hardware Bundle

11.3.4.2 APM 2.6 Set Flight Controller

The APM 2.6 Flight Controller is one of 3D Robotics flagship flight controllers. Based off of the open source Arduino coding platform, this highly supported platform is great for conventional quadcopters. Meant to support 8 motors, the system is expandable via motor shields to achieve the craft's base number of 12. It contains a 3-axis gyro and accelerometer as well as barometer for altitude sensing. Although the system is very well supported, it has a slower microcontroller chip and it has a less versatile arrangement of input/output pins. The package comes at a price of \$239.98.



Figure 64: 3D Robotic's APM 2.6 Set Flight Controller

11.3.4.3 HoverflyOPEN

The HoverflyOPEN is a highly advanced open-source flight controller platform, utilizing a Parallax Propeller microcontroller. This microcontroller provides high multi-purposing capabilities as it 8 core, usually unheard of for RC flight controller purposes. The system can accommodate 12 motors, although it is meant for less. Once again the system provides gyro and accelerometer readings for stabilization purposes. Although this controller is great and highly advanced, it is the least widely known and therefore supported system.

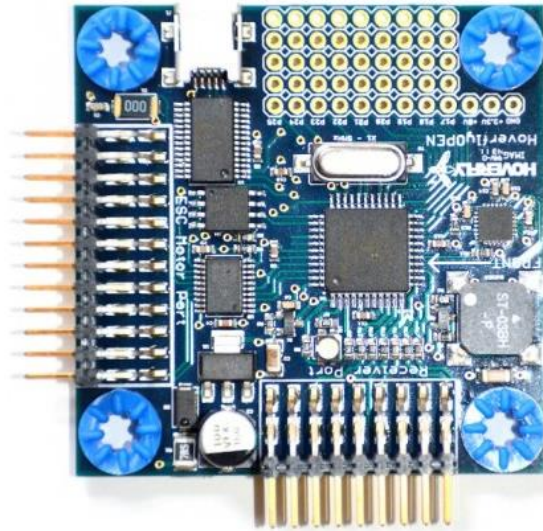


Figure 65: HoverflyOPEN Flight Controller

11.3.4.4 Decision

After much consideration, the team selected to move forward with the OpenPilot Revolution. The largest determining factor was that it was the only microcontroller that offered 12 outputs out of the box, with a built in option for creating the configuration using the open source OpenPilot GCS software suite. This alone, was almost enough to convince the team of this decision. As the board is highly supported, it has a large following online as well as forum support, which might have been willing to provide the team with help on the project; this could have really come in handy if addition peripherals were needed or a modification of the base software was required. The pricing on the unit was a bargain as well, coming with such high speed components as well as a GPS module which could have come very handy during the team's testing. The 168 Mhz speed would also provide zippy response time, which was a must with the momentum lag that the system would be experiencing from spinning large propellers. A side note, in order to power the microcontroller, the team would need to add a simple battery eliminator circuit. Overall, it was believed this microcontroller would serve the current team as well as those who may continue with this project in the future.

11.3.5 OpenPilot GCS

As touched on before, the OpenPilot Flight Controller comes with its own nice software suite called OpenPilot GCS to help setup the board for your specific vehicle. This software and its nice GUI allowed for easy configuration of up to 12 motors, along with their direction of spin, speed, as well as other functions. It also allowed the setting of sensitivity and limits to the pitch, roll, and yaw axes. This capability from helped greatly reduce controls set-up time as well as insert a level of confidence in the microcontroller use. The configuration tab allowed more than just this, it also allowed stability refinement. The software will also perform various data logging functions and displays them in a convenient manner in the Scopes tab. Other features include a Flight Data screen that shows vehicle position, relative clocking, and height as well as other information. The program would also allow the team to save the data once a board has been calibrated. Lastly, you can fly a flight simulator using a computer and the team's control scheme, which would help the craft's system testing.



Figure 66: Screenshot of Flight Data tab for the OpenPilot GCS software

11.3.6 Peripheral Add-Ons

Currently, as no one had recorded an attempt at using a COTS microcontroller to build a large scale multicopter, the team did not have reliable data on how accurate the gyroscope, accelerometer, altimeter, or magnetometer would be. The main issue was that if the flight controller is placed at the center of the craft it might not have been sensitive enough to control properly, a huge deflection out at the arms would cause a small deflection at the middle. The feedback of the microcontroller would have to be very sensitive to be able to accurately control the craft. The team planned to test the unit as is, but also planned for the possibility of a lack of necessary sensitivity. If this deficiency was present, the group would attach a gyroscope and magnetometer to the arm mount of CP1, CP2, and CP3. This would deliver feedback from the actual position of the worst deflections, the gyroscopes would provide a rate of change and the magnetometer would update the gyroscope with the absolute heading. The team believed that these sensors added to a Serial Peripheral Interface Bus, would serve as the needed motion clocking for the entire system.

12 COST

To estimate the cost of the craft, the team first created a spreadsheet with material and products necessary for the construction of the craft. The team allowed for an adequate amount of extra material (usually 10-20%) for components which would be manufactured so that spare material to produce replacements or revise a part if the need arose. A closer look at this spreadsheet can be found on the next page

In this spreadsheet, the team multiplied the cost of each component by the quantity required for the project and then applied a tax of 7.5% to the cost for each item. Estimations of the shipping costs for each product were calculated, using the vendor's own checkout system to obtain accurate quotes wherever possible. Finally, the team added the tax-adjusted costs for each set of items and the shipping for all orders together to obtain the grand total. This total represents the least amount of funding that was felt it is possible to complete this project with. With all costs for materials factored in, the team calculated a grand total of \$30700. The cost breakdown by section is listed in Table 7.

Table 7: Cost breakdown by section

	Cost
Structure	\$4693.41
Power/Controls	\$6932.23
Propulsion	\$16130.00

The team also needed to hire a welder to weld the craft's components together, due to the skill required to complete this task. It was estimated that this would cost approximately \$100 per hour, and an estimated 10 hours of welding time to produce the parts, resulting in a total cost of about \$1000 for welding services.

The majority of the cost for this project came from the propulsion and energy storage components. The Joby motors alone cost \$13700, and if Turnigy Rotomax motors were to be implemented, savings would have been over \$10000. The feasibility of using these motors would later be determined through the motor tests.

Table 8: Cost Analysis

Part or Raw Material	Implemented in P/N	Qty	Unit Cost	Shipping	Cost
Motor Spar	ECM-1-S0-1002	4	192.79	N/A	771.16
Main Arm	ECM-1-S0-1001	4	412.68	N/A	1650.72
Compression Spring	ECM-1-S0-0904	5	12.53	N/A	62.65
Seat Plate	ECM-1-S1-1104	1	30.88	16.13	30.88
Seat	ECM-1-S1-1105	1	218.95	11.58	218.95
Epoxy Resin (Rings)	ECM-1-S1-1307	2	27.95	32.96	88.86
Epoxy Hardener (Rings)	ECM-1-S1-1307	1	32.95	N/A	32.95
Epoxy for all carbon-steel joint	ECM-1-S1-1102	1	272.69	19.95	272.69
Biaxial Carbon Weave (Rings)	ECM-1-S1-1307	430	1.51	57.57	649.3
Large diameter 4130 tubing	ECM-1-S1-1102	1	153.02	N/A	153.02
Small diameter 4130 tubing	ECM-1-S1-1102	2	80.22	N/A	160.44
Seat Belt	ECM-1-S1-1105	1	29.95	5	29.95
4130 12 gauge plate large	ECM-1-S1-1104	1	144.74	N/A	144.74
4130 12 gauge plate small	ECM-1-S1-1104	1	46.32	N/A	46.32
4130 12 gauge plate small	ECM-1-S1-1103	1	34.74	N/A	34.74
4130 Landing gear guide tube	ECM-1-S0-0902	1	90.93	N/A	90.93
4130 Landing gear inner tube	ECM-1-S0-0902	1	62.15	N/A	62.15
Landing gear pin	ECM-1-S0-0903	1	8.53	N/A	8.53
Cotter Pins	ECM-1-S0-0903	1	7.77	N/A	7.77
Netting	ECM-1-S1-1303	1	125.95	N/A	125.95
Structure Bolt	ECM-1-H0-2501	1	12.01	N/A	12.01
Structure Nut	ECM-1-H0-2601	1	6.74	N/A	6.74
Prop Ring Bolt	ECM-1-H0-2502	2	8.06	N/A	16.12
Prop Ring Nut	ECM-1-H0-2602	2	7.92	N/A	15.84
Flight Controller Board	ECM-1-P1-1706	1	174.95	N/A	174.95
Electronic Speed Controller	ECM-0-P1-1801	12	206.91	16.3	2482.92
Red 8AWG Power Cable	ECM-1-P1-1705	40	1.89	14.51	75.60
Black 8AWG Power Cable	ECM-1-P1-1705	40	1.89	0	75.60
Power Cable Connectors	ECM-1-P1-1705	50	5.1	24.63	255
Signal Wiring	ECM-0-P1-1801	2	9.99	4.95	19.98
Signal Connectors	ECM-0-P1-1801	1	59.95	0	59.95
7s LiPo Battery	ECM-1-P0-1601	24	130.96	N/A	3143.04
LiPo-Safe Battery Pouch	ECM-1-P0-1601	12	8.63	0	103.56
150W Soldering Gun	ECM-1-P1-1705	1	15.88	0	15.88
Voltage Regulator	ECM-1-P0-1601	1	37.99	5.99	37.99
USB to PPM	ECM-1-P0-1708	1	67.82	2.25	67.82
Control Module (UI)	ECM-1-P0-1709	1	149.99	0	149.99
Transmitter and Receiver	ECM-1-P0-1710	1	269.95	0	269.95
Xoar Carbon Propellers	ECM-1-P1-1401	7	350	140	2450
Joby Motor	ECM-1-P0-1501	12	1140	540	13680
				Grand Total	30729.13

13 WEIGHT

One of the most significant aspects of the team's design was the aircraft's weight, due to keeping the craft within ultralight classification. To calculate a detailed total weight of the craft with no actual real parts to weigh, 3D models of all parts were created with SolidWorks. With an accurate collection of parts, mass properties of the approximate materials were found. Parts with materials not explicitly expressed in SolidWorks or were not accurately determined within the program were estimated with known values of real material properties. Wire weight was found by a slightly different method by creating a SolidWorks 3D model of wire layout on the craft. The wire length was then gathered through dimensioning and with a known value of the wire's weight per length. The parts and their corresponding weights were summed together to find a total weight of the structure using an excel spreadsheet. This value was found to be roughly 175 lbs, with roughly 3 lbs added for additional miscellaneous weight. Due to the weight value found only by means of computer approximation, this value is not concrete and in no way reflects the final value but provides a method to analyze the craft with acceptable accuracy.

With the calculated multicopter weight, battery weight could be found by subtracted the total weight from the max ultralight weight of 254 lbs. The battery weight was calculated to be 79 lbs and with a known weight of an individual battery of 2.2 lbs the total available battery is 36. With an approximately known number of batteries, an estimated flight time could be calculated with an estimated energy density value in seconds per pound of battery. This calculation was found with information gathered from Joby motor's test data.

Table 9: Weight Analysis

ECM P/N	Description	Weight (lbs)	Number of Parts	Total
ECM-1-S0-0901	Landing Gear REV	3.83	5	19.15
ECM-1-S0-0902	Landing Gear Guide Tube			
ECM-1-S0-0903	Landing Gear Pin			
ECM-1-S0-0904	Landing Gear Spring			
ECM-1-S0-0905	Sleeve			
ECM-1-S0-1001	2.50" diameter x 52" Carbon fiber tube	3.11	4	12.44
ECM-1-S0-1002	2.00" diameter x 22" Carbon fiber tube	0.57	12	6.84
ECM-1-S1-1101	Bracket Wall on Center Mount	0.11	8	0.88
ECM-1-S1-1102	Center Bracket	8.15	1	8.15
ECM-1-S1-1103	Landing Plate on Center Mount	0.41	1	0.41
ECM-1-S1-1104	Mounting Plate for Seat/Control System/etc	2.6	1	2.6
ECM-1-S1-1105	Seat for passenger	6	1	6
ECM-1-S1-1107	Center Mount Bottom	0.08	4	0.32
ECM-1-S1-1201	Bracket Wall for small tube in Arm Mount	0.16	12	1.92
ECM-1-S1-1202	Bracket Wall for large tube on Arm Mount	0.13	4	0.52
ECM-1-S1-1203	Landing Plate on Arm Mount	0.13	4	0.52
ECM-1-S1-1204	Arm Mount with three small, one large steel tubes	3.87	4	15.48
ECM-1-S1-1300	Motor Alignment Plate	0.11	12	1.32
ECM-1-S0-1301	Steel Tube for Motor Mount	0.57	12	6.84
ECM-1-S1-1302	Bracket Wall on Motor Mount	0.22	24	5.28
ECM-1-S1-1303	Carbon Ring surrounding Props	1	12	12
ECM-1-S1-1304	Outer Prop Ring holder	0.15	12	1.8
ECM-1-S1-1305	Spar to hold outer prop ringholder	0.19	12	2.28
ECM-1-S1-1306	Inner Prop Ring Holder	0.22	12	2.64
ECM-1-P1-1401	30in Prop.SLDPRT	0.2	12	2.4
ECM-1-P0-1501	Joby Motor	4	12	48
ECM-1-P0-1601	LiPo battery	N/A	N/A	0
ECM-0-P1-1801	ESC	1	12	12
			Individual battery weight	2.233
			Total	172.79
			Total battery weight	81.21
			Number of batteries	36

14 SAFETY

14.1 Critical Design Hazard Checklist

The Critical Design Hazard Checklist is a pdf document in Appendix C: Table 4 that lists many of the hazards associated to their respective subgroups; such as, structures, propulsion, and controls. The list is a portion of the FMEA created to analyze the potential failure modes. On the far right of the document is a new column addressing the action taken in the design to mitigate the hazard or potential failure mode. The hazards listed in the PDR (beginning section of this report) is listed in the Critical Design Hazard Checklist and addressed with technical detail.

14.2 Structure

The main structure safety hazards arise from poor construction of the craft and minor damage from transportation and use. The craft must be constructed with precision and care to ensure it will hold up to normal operating conditions. Having too large of clearances in the bonds between the mounts and carbon tubes, too small or improper welds, or having improper epoxy ratios could result in failure under loads less than the structure is designed to withstand. Having the low factor of safety of 1.2 allows little to no error in construction.

Many hazards can be caused by regular use and transportation of the system. For example during transportation the craft would be set on its side and one of the shrouds could deform enough to interfere with a spinning prop. However, this small deformation would not be easily noticeable without close inspection. If the user fails to check the shrouds and props before use the prop will strike the shroud and can cause serious damage to the aircraft and/or injury to the user or bystanders. Many small things that are not easily noticeable without inspection can cause serious damage and injury. Landing gear could become misaligned after a few hard landings, propeller mounts can come loose, mesh over the props could break and interfere with the props, and seat and seat belt bolts could loosen. All of these hazards can be avoided with a thorough pre-flight check, and is required before the aircraft is turned on.

14.3 Propulsion

The safety hazards associated with the propulsion system of this project are numerous for both its circuitry and rotating objects. Extreme caution would be taken with the circuitry, where high currents (up to 200 amps) and voltages (51.8 volts) would be encountered. Unexposed connections between wiring and visible air gaps between positive and negative leads were necessary. Lithium Polymer (LiPo) batteries require extreme caution because they catch fire easily. As such, when charging and storing the batteries they would be placed into fireproof LiPo safe bags in an area with non-flammable materials to avoid secondary fires. Additionally, before any of the electrical equipment would be attached to the craft, extensive testing regarding the current draw and discharge rate of the battery as well as its temperature and temperature of the power wiring for periods of maximum thrust would be done to verify that no limits were breached.

With motor-propeller assemblies capable of outputting 60 lbf of thrust and rotating at 6000 rpm (under extreme cases) stable testing equipment and motor fixtures were needed. For example, the thrust could push back or knock over the test fixture, potentially breaking propeller and motor or the propeller could loosen from its attachment to the motor and become a projectile, or a natural frequency of the assembly could be reached and could shake the assembly apart. Therefore, every step would be taken to ensure propellers are mounted securely to the motors but mistakes can always happen. Thus, whenever in operation, testing participants would stand sufficiently far away from the craft or behind some other structure to avoid any propellers that may break and become projectiles.

In the case that any propellers began spinning out of control, be it error from the controller, battery, or wiring, an emergency full-stop switch would be used to cut all power to the craft.

14.4 Controls

There were no immediate dangers from the controls system to be used on this craft because it would likely be a printed circuit board (PCB) with voltages and currents well below hazardous levels. However, once connected to other power components, like the ESC, batteries, motors, and final craft, stability would be essential to avoid craft or personnel damage. Thorough understanding of the OpenSource software accompanying the flight controller was necessary. The control system could have been susceptible to noise from the large voltages and currents running through the craft. Therefore, implementation of shielding or hardware and software filters would be necessary to provide stable flight control.

15 DESIGN ANALYSIS

15.1 Structure

15.1.1 Loading Cases and Assumptions

The team wanted to keep a normal use case in mind for all of the design analysis. Since the craft's primary function would be hovering for tests, the team wanted to base the analysis on the loading the craft would see during hover. Because of the way that the components were chosen to be assembled together and experience loading, some of the analysis work would overlap in these sections.

In the team's analysis, a number of assumptions were made about how the craft would be used. The craft's motors were assumed to each have a maximum output of 62.5 pounds of thrust under normal usage, yielding a total thrust of 750 pounds for the vehicle. This estimate represents a 0.65 g net acceleration upwards, much faster than the team planned to allow a human rider to actually accelerate, since the limitations of the final craft's vertical net acceleration was set to 0.2 g at maximum. Designing to the maximum thrust that the vehicle could output helped ensure that there was nothing the rider could reasonably do during normal flight that would cause a failure of the craft.

The team assumed a rider weight of 200 pounds, a value agreed upon between the group and the sponsors at the beginning of the project, and a total vehicle weight of 254 pounds (the maximum weight allowable for an ultralight aircraft in the United States). The combination gives the team a total flight weight of 454 pounds. This assumed that the craft was fully loaded with batteries and the payload; this is almost certainly a conservative estimate.

The team also assumed that the craft would be landed gently each time it is used, hitting the ground no faster than 5.7 feet per second (or 3.9 miles per hour). This represented dropping the craft with the bottom of the landing gear starting 6 inches above level ground. This drop assumed that the motors weren't still spinning while the craft landed, while in reality they would continue to spin and generate lift while the craft approached the ground, slowing the craft's descent. The team did not feel as though this impact velocity was unreasonable considering the weight and scope of the craft; this vehicle was more intended to serve as a test platform rather than a consumer ready product, and it would be treated accordingly.

In addition to these, it was originally planned to ensure that some of the components in the craft could withstand several worst-case loading conditions which simulated accidents and crashes; however, the team decided to scrap this analysis concept due to the impractical nature of designing a lightweight aircraft to survive a severe crash. The aerospace industry doesn't typically design for surviving crashes, and the team felt as though it would be unrealistic to assume that a design for this scenario was needed. This craft was instead designed to meet a minimum safety factor of 1.2 under what the group considered to be normal use. Wherever it was feasible with the steel parts, components were designed for infinite life criteria with 95% confidence in addition to the desired safety factor.

15.1.2 Main Arms and Motor Spars

The team selected the motor arms and spars by looking for tubing with inner diameters in the 2"-3" range that were sold in the lengths needed. From preliminary calculations the team knew that carbon fiber tubing in that approximate size was needed in either square or round profiles to have an adequate amount of strength, and that changes could be made to the outer diameter as needed to get more

strength out of a certain sized tube. After doing preliminary calculations and searching for similarly sized square carbon fiber tubing, the team determined that carbon fiber tubes fitted over steel mounts would be preferred, as stock round steel tubes could be easily found (which have their tightest tolerances on their outer diameter) to fit inside a mandrel-formed carbon fiber tube (which have their tightest tolerances on their inner diameter). With this in mind, a number of potential candidates were found for the motor spars and main arms that would fit over stock sized steel tubes.

To analyze the main arms and motor spars, the team first had to get an idea of the layup schedule for the tubes. The layup schedule and material information for carbon tubes is usually not given out to customers by the manufacturer, but Rockwest Composites provided information on one of their large diameter tubes which the team was considering using for the main arms of the vehicle. This tubing had a 2.500" nominal inner diameter and a 2.628" outer diameter and was constructed out of 11 plies of unidirectional carbon fiber. The fibers were arranged with three 0° plies and a pair of ±45° plies arranged symmetrically around a 0° ply, providing a tube that was relatively strong in bending but would also resist some torsional loading applied to it. The team used MATLAB code supplied by a composites professor at Cal Poly to estimate the strength and stiffness of the tube given its layup schedule and the material properties of the carbon fiber used by Rockwest Composites. For all of the carbon fiber tubes for which little composition data was collected, the team assumed the use of a layup schedule pattern similar to Rockwest's, as it was understood that it's a fairly common tube built primarily for bending applications.

The team originally intended to design the carbon tubes with respect to three different criteria. First, the team wanted to limit their linear and angular deflections and keep the craft sufficiently stiff. Next, they had to comfortably survive the normal usage loading conditions that were anticipated during testing or regular usage. Finally, the tubes were desired to be able to survive a worst-case bending load and a worst-case torsion load, simulating the craft landing on some surface other than flat ground.

Because the team already had estimates for the mechanical properties of unidirectional carbon fiber tubing, those mechanical property estimates were used to select a good tubing combination for the main arms and motor spars. A MATLAB program was then written which required the following inputs: the material property data (determined by the tube's properties code) and the tubing dimensions for both the main arms and the motor spars. The program would then calculate the total vertical and angular deflections of the tubes at their endpoints during normal use, the maximum stresses on each component during normal use, and the total weight of the carbon fiber tubing for the entire craft. This program relied on the input of data for a pair of different tubes, as it determined the total deflection values by the superposition of the two tubes. The program was used to compare many different combinations of different carbon fiber tubes together, allowing the selection of what the team felt was a good set of tubes. For more information on the team's program, please see the MATLAB Code for Stiffness section in Appendix B-11.3.

The team desired that the craft be stiff enough so that the tips of the outermost motor spars (the ones directly in line with the main arms) would deflect angularly less than 8° from horizontal. This amount was based on the assumption that at least 99% of the motors' thrust would be pointing directly upwards while the craft was in use. In essence, this means that with a tip angular deflection of 8°, up to 1% of the craft's total thrust could be in the horizontal direction, making the craft drift around while hovering. It was impossible to totally prevent the tips of the motor spars from deflecting, so the team felt as though this was an acceptable specification to design around. Because the group was not sure about how much weight each arm would be supporting or where that weight would be located or distributed, the weight of the structure itself was ignored and focus was primarily set on the effects of thrust from the motors for these calculations. This means that the calculations were conservative, as the weight on each arm would directly counter the motor thrust which would be deflecting the arms of the craft.

In all, the team looked at 1", 2", 2.5", and 3" size tubes in a variety of wall thicknesses. Based on the calculations, the group initially chose 2.500" x 2.628" x 52" round carbon fiber tubing for the main arms and 2.000" x 2.125" x 22" round carbon fiber tubing for the motor spars, thinking they provided a good compromise between stiffness, strength, cost, and weight. A relatively large tube size was chosen for the motor spars, the stiffness of this component was actually more significant than its strength; otherwise the team would have gone with a much smaller tube size. Both of these tubes were sold at Rockwest Composites.

Three major loading conditions for normal usage were desired for testing for the main arms. First, maximum loads that the main arms could handle in bending, assuming the beam was loaded in a cantilever configuration with a point mass at the free end, were determined. This would be useful for determining the maximum loads the arms could withstand during landing, as the impact forces from landing would act at the ends of the main arms. It was estimated that the tubes could support about 1100 pounds before failure in bending using the data from the MATLAB code. This seemed acceptable given that the peak calculated forces during landing were estimated to be approximately 270 pounds during normal use.

The group then attempted to model the loading that the main arms would see with normal use (ie. when the craft hovers). In this case, the three motors on the motor spars branching out from each arm thrust at a constant force of 62.5 pounds. To simulate this, the max thrust of the three motors were combined (187.5 pounds) and placed at the end of the tube, then the moment caused by the motor spar was found which is directly in line with the main arm. The team's calculations with these combined loads indicated that the stress on the craft's main arm would be about 35 ksi, easily within the realms of survivable loading.

The team wanted to determine the stresses that would be placed on the main arms during tube torsion. Torsion was not anticipated on the main arms; if the craft was balanced properly and if each cluster of three motors were run at the same speeds, there should have been little to no torsion acting on the craft during any kind of normal use. For the normal use case, the team originally calculated the stresses expected to be seen on the main arm if it were being twisted by both of the side motors (the motors not in line with main arm) spinning in opposite directions; this was to simulate wiring one or more of the motors improperly and having it spin in the wrong direction, generating thrust upwards and creating a force couple around the main arm. However, the group came to believe that this wasn't a situation that was likely to be seen, as each motor's connections would be carefully tested before attempting to run it, and even when the team would first test it, the motors would be ramped up very slowly to ensure the motors were all spinning properly. Therefore, it was decided that the tube torsion loading case would instead be modeled as having one of the two side motors firing at full thrust while the other is turned off. This model would simulate the loss of one of the side motors due to an electrical issue; because of how this multicopter will likely be controlled, losing one motor in one cluster would require the other two motors in the cluster to compensate for the lost motor. It was found that the loads placed on the main arm by this tube torsion were extremely small and resulted in no significant shear stress being placed on the tubes.

Lastly, the team analyzed the vibration that the arms might be subjected to. Because of their length, it was foreseeable that a natural frequency could be reached during the craft's operation from an excitation frequency induced by the motors that would potentially cause the craft to become unstable, unable to land, or cause the multicopter to shake itself apart. In this analysis, models were developed to approximate the stiffness of the arms in bending and in torsion where the subsequent natural frequency was compared to the range of RPMs the motors are expected to operate in. Note that in this analysis, the motor RPM is the excitation frequency and was predicted to be between 4000-4500 RPM for hover. The bending natural frequency was modeled in several ways. The first method assumed the arm to be a massless carbon fiber cantilever beam rigidly fixed to the center bracket with the mass of the motors and batteries placed at its end. All other values used to find the stiffness, like Young's Modulus, shear

modulus, beam dimensions, and the linear density of the beam were taken from the analysis used to determine the failure modes described in the earlier sections. In the second model the arm was assumed to have a mass and all other parameters stayed the same. The results of the first and second models were natural frequencies of 400 RPM and 397 RPM respectively. There are two observations to be made from these results. The first is that adding the mass of the beam to the model had almost no effect on its natural frequency because the added mass was relatively small compared to the total mass of the components at the tip of the beam. The next observation was that the first natural frequency was sufficiently far from the excitation frequency. The differences in frequencies also showed that the vibration mode of the arm that would be close to 4000 RPM would be corresponding to small oscillation amplitudes because the inertia of the system would restrict anything resembling large displacements.

Analysis continued with the second and third natural frequencies of the beam. An exact model for this analysis could not be developed so an approximation was created, where distributing the point mass along the length of the beam provided reasonable results. Using this method, the first, second, and third natural frequencies were found to be 2060 RPM, 12910 RPM, and 36160 RPM respectively. These values are still reasonably far away from the expected operating conditions of the motors. However, the results of this method could be improved upon with experiment and finite element vibrational studies.

As mentioned early, the next step in vibration analysis was the torsional natural frequency of the arm. Here, the arm was approximated as a torsional spring. The spars were assumed to be rigid attachments to the torsional spring. The motors on the motor spars were assumed to contribute to the torsion applied to the arm and the third motor on the motor spar that extends parallel with the arm was assumed not to contribute to the torsion of the beam; this was because the line of action of any load applied by this motor to the torsional spring would act through the center of the arm, so there can be no additional torsional moment created by this motor. The result of this analysis yielded a natural frequency of 536 RPM, which, similar to the bending analysis above, is sufficiently far from the excitation frequency for the craft's purposes. For hand calculations and further analysis, refer to Appendix B-13.

Next, the team analyzed the tubing selected for the motor spars. The loading conditions commonly seen by these components are far less severe than those of the main arms, making their analysis rather simple. During normal use the motor spars shouldn't see any significant torsion, as there is no place on the motor mounts or propellers where significant lever arms are found or where torque has been generated in a direction along the tubes. For the normal usage loading case, the stress placed on the spars when a motor thrust upward at the end of the spar was determined. Under this loading condition, the tubes see a 1375 in-lbf torque, translating to a shear stress of 2131 psi which was initially assumed was easily survivable by the carbon tubes.

However, the group was later informed that the tube calculations were based off the incorrect assumption that the $\pm 45^\circ$ plies in the tubing would aid in resisting bending; theoretical calculations usually take these layers into account when deriving a tube's strength and stiffness, but real-world testing of these estimates would seem to indicate that it was more realistic to assume that the $\pm 45^\circ$ plies do nothing to resist the bending forces applied to the tube. Similarly, the team was advised to treat the 0° plies as though they would do nothing to resist torsional loads. Essentially, it was advised to look at only the 0° plies in the tube when calculating bending stresses and stiffnesses, and to look only at the $\pm 45^\circ$ plies when calculating shear stresses. The team was also told not to expect to obtain the theoretical maximum strength of the material within the tubing. Instead, assuming a yield strength of 100 ksi, as laboratory testing indicated was commonly the most strength one could obtain from the particular fiber used in the tubes, was sufficient. With this corrected, the tubing analysis calculations changed significantly.

Rerunning the team's MATLAB codes with the relevant parameters adjusted, the team found that the stiffness of the system decreased slightly for every pairing of carbon fiber tubes. It was found that the combo that was selected initially wasn't quite stiff enough to keep the angular deflection at the tips of the motor spars from exceeding 8° with the set minimum factor of safety of 1.2.

The team also determined that the main arm in fixed-end loading conditions could actually withstand only 381 pounds at maximum when taking into account having effectively 4 fewer carbon fiber plies and a lower yield strength. The group also recalculated the stresses for the hovering loading case and found that the stresses on the main arm from regular use were actually much higher than originally calculated, but were still within acceptable limits given the set safety factors. However, the craft's stresses from torsion became far higher and actually dropped below the acceptable factor of safety to about 1. These revelations indicated that a new tube for the main arm would have to be chosen.

The motor spars, however, were not affected significantly by these revelations. Because the selection of this component was driven primarily by bending stiffness rather than absolute strength and higher stiffness in carbon fiber is more resource-intensive to obtain than higher strength, the motor spars end up having a rather large safety factor. Under normal usage loading cases, the selected tubing for motor spars have a factor of safety of 9.33; please see Appendix B-1.4 for this calculation. Because it is still stiff enough to for the craft's purposes, this tube size was used in the final design.

With this new information in mind, the team set about trying to find a new tubing size which would replace the 2.500" x 2.628" x 52" tubes. The group eventually found a tube manufacturer named C-Tech that sells unidirectional carbon fiber tubing with the same size inner diameter (2.500") but with drastically thicker outer walls. The new tubing has an outer diameter of about 2.760", making for walls that were approximately double the thickness of the previous tubes. It was assumed that they are constructed in a similar manner to the other tubing produced by Rockwest but simply with more 0° and $\pm 45^\circ$ plies, as they are constructed primarily for bending. The team sent C-Tech an enquiry about providing a tube recommendation given the craft's loading cases and if they would supply a layup schedule for the 2.500" x 2.760" tubes. C-Tech recently responded informing the team that their tubes are made to order. They also stated that a 2.500" x 2.736" x 52" with a 1:1 ratio of 0° and $\pm 45^\circ$ plies would be able to withstand a 500lb cantilevered load and should be able to survive the craft's maximum normal loading conditions with the specified factor of safety of 1.2. This response from C-Tech occurred after the larger 2.500" x 2.760" tubing was chosen from them and the analysis was completed.

According to the team's calculations, the 2.500" x 2.760" tubes would be able to withstand a cantilever end load of 850 pounds (for a factor of safety for landing of 3.15), have a factor of safety for bending under normal usage of 3.76, and have a factor of safety for torsion of 3.38. See Appendix B-1 for these calculations. The response from C-Tech stating that their slightly thinner walled tube with less 0° plies than what was assumed could withstand the calculated loading case helped the team validate the calculations and provides further assurance the tubes would be able to withstand the specified loading conditions.

They are not significantly more expensive than the thinner tubing that were originally looked at before and they take the calculated factors of safety up to levels the team is more comfortable with without adding a significant amount of weight (the replacement tubes add only 3 pounds to the total structure). The group felt that this was more than adequate for the project's usage and would provide peace of mind while testing the craft. The team was still getting quotes for custom tubes made by Rockwest to see if an equivalent set of tubes for a lower price could be found, as currently the custom tubes selected were expensive to ship to the group's location.

15.1.3 Center Mount Assembly

After selecting the carbon fiber tubing, the team began the selection process for the steel tubing that would be used for the craft's center mount. The project's requirements included that the tubing had to have the same nominal outer diameters as the nominal inner diameters (2.500" and 2.00") of the carbon fiber tubing. It was also desired to have the steel tubing and the weld metal joining it together, have a safety factor of at least 1.2 for unlimited life with a 95% confidence.

The process started by locating tubing from a variety of metal suppliers which sold tubing in 2.500" and 2.000" nominal outer diameters. The team intended to find a variety of tubes for each size with different wall thicknesses, which would allow for a selection tubes for the main arms and the motor spars with the right balance between strength and weight. Analyzing the different available sizes under the calculated loading cases would point to a favorable size tube. As noted in the Materials Selection section above, it was decided to look specifically at 4130 Chromoly tubing, as it would provide relatively high strength while still being weldable and machineable. Because of the welding procedures that the large steel tubing would be undergoing, it was also decided to treat the steel as annealed for the purposes of mechanical properties. This was for safety reasons; as noted earlier, the thin-walled tubing may not experience a significant degradation of strength during the welding process, but the group did not have access to any convenient way to ensure this at Cal Poly (like a heat treating oven), so it was decided to be conservative with the tubing estimates.

The primary loading cases on the center mount arose from the thrust of the motors and from loads encountered during landing. Using the loads from normal use applied to the main arm and spars, the maximum shear loads and bending moments were determined which would be applied to the steel tubes in the center mount assembly.

First, the team analyzed the bending and shear stresses that the tubing in the mounts would see from hovering. Looking at a single arm assembly extending off of the center mount, equivalent loads at the base of one of the steel tubes were modeled assuming that the three motors on the arm were thrusting with 62.5 pounds of thrust each. The equivalent moment applied on the tube was approximately 11,130 lbf-in, and the equivalent shear load was 187.5 pounds. With these values in mind, the group analyzed the available steel tube sizes to see if a size which could adequately resist these loads with the minimum factor of safety and confidence level without weighing too much could be found. Based on the material property research for annealed 4130 Chromoly steel, a material endurance limit of 40 ksi and a yield strength of 50 ksi was assumed; this translated to an allowable stress of on the tubes of 28.9 ksi with the craft's safety factor and a 95% confidence level.

The most suitable tubing size that was found for this mount has a 2.500" outer diameter and a 2.124" inner diameter. The stresses on these tubes from hovering due to the bending moments were found to be about 15.1 ksi (the shear stresses were found to be so small that their inclusion had negligible effect on the team's calculations, and so they were eliminated). This calculation provided a factor of safety of 2.30 for hovering loads.

Next, the team analyzed the tubes under landing conditions. Once again an equivalent bending moment at the base of the steel tube in the center mount was formed, but this time modeling a 270 pound force applied to the arm mount at the end of the main arm. This translated to a 14,040 lbf-in bending moment, generating a factor of safety of 1.51 for landing loads. For a closer look at the tube selection calculations, please take a look at the Steel Tube Selection Calculations section in Appendix B-2.

Next, analysis of the welded joints and determination of the necessary weld profiles for the center mount were required. The team began by finding the weld length along the edges of the mitered steel tubing in order to estimate the average shear stresses on the welds under the hovering and landing loads discussed above. It was determined that 9.56" of weld length for each tube section in the center mount was needed.

No standard model could be found online or in Shigley's to estimate stress for welds which joined two mitered tubes together. In order to predict the stress in the weld, six separate models of the joint were used to estimate the conditions in the actual weld. Two of the models were unrealistically conservative while two were unrealistically magnanimous. These four models produced a range which the actual weld should fall within. The remaining two models were believed to be the most representative of the joint and from the analysis did fall within the range produced by the other four models.

Based on the thickness of the material being joined (0.181" for both tubes), a weld size of 0.125" was assumed, as it was the minimum weld size for joining materials with a thickness less than 0.25 [Shigley's table 9-6]. Each of the six models used this assumption. Preliminary calculations of weld stress took into account both shear due to bending and shear forces. It was found that shear forces not due to bending had a negligible effect on the total shear stress experienced by the weld joint. For all six models, therefore, it was assumed shear stress not due to bending is negligible.

The first model analyzed assumed that the weld joint was a flat circle all around the tube instead of having curves due to mitering [Shigley's Table 9-2 #9]. The actual dimensions of the welded tube were used, 2.486" for the diameter of the tube. For this model the shear stress in the weld is 26.8ksi, which fails for E60XX, E70XX, E80XX, and E90XX electrodes. This model had a weld length of 7.8" compared to the actual weld length of 9.56". This was one of the unrealistically conservative models as it does not account for the increased weld length due to the mitered tube profile. Therefore it was assumed that the mitered tube weld has less stress than this model.

The second model was the same as the first except the radius was increased so that the weld length in the model would be the same as actual weld length. This model had a shear stress of 17.9ksi in the weld. This is below all the allowable shear stresses for the considered electrodes. Compared to all the other models this was considered the most representative of the actual weld being that it was circular and had the same weld length. However, given the increased radius, and in turn a greater resistance to bending, the actual weld was assumed to have slightly more stress than the tubes in this model.

The third model assumes the weld was two vertical parallel welds undergoing the same bending moment [Shigley's Table 9-2 #2]. The two vertical welds in this model had the same height as the diameter of the tube, 2.486". This makes a weld length of 4.972". The shear stress this model produced was 31.6ksi, above the allowable shear stress for most electrodes. This model was the most conservative as it exerted the same bending moment as the other models on a much shorter weld length of 4.972".

The fourth model was based on the double vertical weld model of the last model but accounted for the actual 9.56" weld length of the joint. This made the height of each vertical weld 4.87". The stress for this case is 8.7ksi. This case would easily survive all of the calculated loading and certainly have an infinite fatigue life under normal operating conditions. This model is extremely magnanimous; the model assumes the full weld length and relatively has a much higher moment of inertia because it has twice the height. This drastically increased the weld's ability to resist bending and therefore had a much lower stress because of it. This is the most liberal model and is assumed to represent the best case for the welded joint.

The fifth model was similar to the previous two; it had two parallel welds about the same axis that the bending moment was about [Shigley's Table 9-2 #3]. This model used the diameter of the large steel tubes (2.486") as the length of the two horizontal welds as well as the distance between them. The stress this model predicted the weld to experience under normal use was 21.2ksi. While this model only had 4.972" of weld length it is assumed to be reasonably accurate; this model represented the portion of the tube that doing the most to resist the applied bending moment (the top and bottom of the pipe). However, considering this model had about half the weld length as the actual component, it was assumed the actual weld joint will develop less stress than this model.

The sixth model used the same horizontal parallel model as the last model but accounted for the actual 9.56" weld length. The length of the each horizontal weld was 4.78" and the distance between them is the diameter of the tube, 2.486". This model predicted a shear stress of 11.0ksi in the weld. This case was also a liberal estimate as it puts more material at the top and bottom of the weld which aid in resisting bending. It can be assumed that the actual weld sees greater stresses than this model.

From the six models a range from 17.9ksi to 21.2ksi was established from models two and five. Models two and five were the predicted models to produce the closest values to the actual weld. This assumption was confirmed because models two and five had values that did lie in the middle of stresses the conservative and magnanimous models produced. As discussed earlier the actual weld was thought to have a higher stress than seen in model two but less stress than seen in model five. The average of these two values was taken and the shear stress in the weld of the center mount during normal use was estimated to be about 20ksi.

From this value in order to meet the required minimum factor of safety of 1.2 an E80XX or greater series electrode had to be used, which has a maximum allowable shear stress of 24ksi. This allowable shear stress is supplied by the AISC welding code and has a 1.44 safety factor built in. If this built in safety factor was accounted for an E60XX electrode could be used with a factor of safety of 1.3. However, for the sake of keeping to safety and assuming there is a reason there is a built in factor of safety an E80XX or greater electrode was recommended for this weld. It should also be noted that a 0.125" weld size was assumed for all calculations and is a minimum weld size according to AISC code. If it is possible to increase the weld size that would decrease the stress in the weld and allow the use of a lower grade electrode or increase the factor of safety with the use of an E80XX or greater electrode.

Using the maximum allowable shear stress using an E80XX electrode calculated above, 20ksi, was calculated the maximum allowable landing force the center mount weld could withstand. The landing force was applied as a point load at the end of the 52" main carbon tube creating a moment. Using the average moments of inertia in models two and five, the maximum allowable force at an arm mount was 256lbs. This was the weakest component of the craft in terms of the worst landing condition, and is what the landing gear is specified for. Please see the attached welding calculations in Appendix B-3.

For the center mount weld, infinite fatigue life is desirable. Based on the stress calculations for the weld and using an E80XX electrode, which was at the minimum factor of safety of 1.2, infinite life under these conditions was unlikely. The fatigue strength using the tube and weld properties at the center mount was calculated with an E60XX series electrode, and was calculated to be 26.1ksi and the corrected fatigue stress at the weld was calculated to be 25ksi. This condition does meet infinite life but not with a factor of safety of 1.2. In order to meet a 1.2 safety factor an E100X type electrode must be used, providing a factor of safety of 1.31. Therefore assuming a weld size of 0.125" an E100X electrode was recommended if to provide infinite life at the center mount under normal operating conditions. Again the weld size could be increased if possible to increase the factor of safety or allow for the use of an E60XX, E70XX, E80XX, or E90XX electrode. See Appendix B-4 for these calculations.

For the bracket assembly, the team wanted to analyze the craft's components based on landing loads and rider weights encountered during normal use. The group envisioned the bracket seeing loading from the seat plate and the landing gear. For the seat plate, the rider could place his weight off-center on the seat, causing the entire seat plate to place a bending moment on the assembly. The landing gear could also load the bracket axially with up to 270lbf and could place a bending moment on the bracket when landing with a horizontal component of velocity.

The team first designed the bracket walls making up the center bracket assembly by making them solid with no cutouts; however, it was decided to skeletonize them upon realizing that the welded box-profile bracket assembly would be far stronger than what was required and would weigh a significant amount more than was necessary. The cross-sectional moment of area was determined of the box structure in terms of the widths of the 12 skeletonized struts making up the bracket walls, then a numerical function solver was used to determine the maximum allowable bending moment that could be placed on the assembly by either the seat plate or the landing gear assembly. The team calculated that the width required for the struts was about 0.037" to survive indefinitely and with 95% confidence for a 1200 in-lbf bending load (the bending moment placed on the assembly when the 200 pound rider weight is placed at the very edge of the seat plate). This design was theoretically possible but was smaller than what the team felt was reasonable for cutting with a CNC plasma cutter or welding, so the group opted to go for 0.2" wide struts. This technique cuts several pounds off the weight of the craft while retaining a large factor of safety ($n = 5.5$) for the seat loading conditions. The axial loading from the rider was found to be insignificant, resulting in a compressive stress of only 830 psi.

However, for rough landing load conditions (which are expected while testing the craft), the team found that the skeletonization of the brackets was not practical. During landing, the craft is expected to see up to a 250 lbf horizontal end load on the landing gear as this would represent the craft's landing at a slight angle or with a small component of horizontal velocity. With this loading and a 13.35" landing gear length, a max bending moment of 3340 in-lbf would be seen, resulting in a stress of over 111 ksi on the craft's skeletonized brackets. Without the cutouts, a stress of 24.6 ksi was expected to be seen, providing a factor of safety for infinite life of 1.41 with 95% confidence. Therefore, the group intended to go with non-skeletonized brackets for all of the bracket walls in the craft, as the team simply does not feel as though the weight savings are worth the risk.

Lastly, the team had to calculate the required bond length between the carbon and the steel tubing. Since epoxy would be used to bond the materials together, a way to calculate the shear stress on the adhesive layer from the bending moments applied to the tubes under normal use was required. To do this, the group first determined the maximum line load from a moment applied to a round tube. Using this line load and an allowable average shear strength of epoxy, the required length of the bond surface for the joints was calculated. More information on these calculations can be found in the Bond Length Calculations section in Appendix B-6. Using a conservative average allowable stress of 1000 psi, the required bond lengths for the large and small tubes to be 2.86" and 0.44" were determined, respectively. Using 4" and 3" bond lengths for these components provided factors of safety of 1.77 for the large tube and 6.85 for the small tube. This did seem to indicate that the smaller tube should be shortened, as the initial estimated bond length was found by multiplying the tube diameter by 1.5. The team was wary of having less than 3" of bond length holding the motor spars in place, this idea will be investigated in future tests.

15.1.4 Arm Mount Assembly

After completing the center mount design analysis and large diameter steel tube selection process, the group had to make sure the selected steel tubing had to be sufficient for the arm mount assembly. The team did not expect to encounter any serious issues with this component, as it encountered much smaller loads than the center mount, and the component was planned to be built using the same large diameter

tubing from which the center mount was made. This could be revised in the future, as the larger tubing on the arm mount could have a smaller inner diameter than on the center mount in order to save a small amount of weight while remaining strong enough for the craft's purposes. However, the group decided to use the same tubing in order to eliminate the risk of getting the two sizes mixed up (which could have catastrophic results for the craft).

The team also needed to select a small steel tubing size for use with the motor spars. To do so, the same approach was used to select the larger diameter tubing. First, the equivalent shear and moment loads were found on the small diameter tubing from one of the motors thrusting upwards at maximum output on the end of a motor spar. This yielded a moment of 1375 lbf-in and a shear force of 62.5 lbf. Neglecting the shear loading because it was so small, the group then searched for the thinnest-walled tubing that would survive this load with a factor of safety of 1.2 and 95% confidence. The team was also recommended to not select tubing with wall thicknesses less than 0.050" as this would make the tubing excessively difficult to weld together. With this in mind, a tube with a 2.000" outer diameter and a 1.870" outer diameter was eventually found which proved to be the best fit of all the tubes analyzed. With a 1375 in-lbf moment applied to the tube, the max stress on the tube was calculated to be approximately 7430 psi, yielding a factor of safety of 3.64. With a wall thickness of 0.065", going with thinner-walled tubes would most likely have meant going below the 0.050" wall thickness threshold, so the team was fairly confident that it wouldn't be possible to go much thinner than with this selection.

For the section of larger diameter tubing the arm mount, the stresses on the tube were checked just to be sure that the tube selection was reasonably safe. A bending stress of 1870 psi was obtained, yielding a factor of safety above 10 for this component. The maximum shear stress obtained from operating one of the side motors independently was only 935 psi (from a torque of 1375 in-lbf), which was so small that it could be safely neglected. Again, this part could be replaced by slightly thinner tubing to save some weight but the group opted to use the same tubing for both the center and the arm mounts.

The team didn't envision any torque being placed on the small diameter tubes by the motor spars, as there isn't any place for a significant load to generate a large torque on the tubes. It was estimated that the small diameter tubing could withstand about 5000 in-lbf of torque, meaning that the carbon tubes and the adhesive bonding the tubes together would likely fail before the steel tubing does.

The stress in the welds that connect the mitered tubes were then analyzed. Under the maximum loading condition the maximum moment the weld experiences was the 1375 in-lbf defined above. The same models used for the welds in the center mount were used to estimate the stress in the weld, again assuming a 0.125" weld size and neglecting shear forces other than bending. First the circular model was used [Shigley's Table 9-2 #9], changing the radius of the tube from 0.993" to 1.216" to account for the actual weld length. Using this model the stress in the weld is predicted to be 3.34ksi. This provides a safety factor of 5.38 using an E60XX electrode and a factor of safety of 7.19 using an E100X. Considering these high factors of safety it was assumed the welds in the center arm mount, including the one connecting the main tube to the mount, will meet the 1.2 safety factor against failure and fatigue strength. See Appendix B-7 for these calculations.

15.1.5 Motor Mount Assembly

The motor mount assembly consisted of multiple design considerations. The prop ring spar was 16.25" in length with a downward force at the outer end, holding half of the prop ring's weight and the outer prop mount weight. The bending stresses in the spar due to this moment were insignificant, so failure would not occur unless a high impact was involved. The fillet welds at either end of this rod are another scenario of potential failure. With a wall thickness of .03" corresponding to a minimum weld bead height of .125",

the stresses in the bead due to shear and bending moments were well below the yield strength of the weld material used. However the wall thickness of this tube needed to be increased to .05" to weld it properly. The increase in wall thickness improved the factor safety, so it is safe to assume the .05" would not fail under these conditions. More information on these calculations can be found in Appendix B-8.

The motor mount walls were skeletonized to save weight, but buckling in the thin walls and failure in the weld bead along the underside of the hemispherical platform was a design consideration requiring critical analysis. The buckling criteria was applied to the skeletonized cross sectional area because of the lack of material opposing the axial load. The total moment of inertia was calculated of the three columns that make up the geometry of this cross section with respect to the axis parallel to the length. After calculation, the critical load to buckle one wall is approximately 28.8 kip, 2 orders of magnitude greater than the load being designed for.

These bracket walls would not experience any bending due to their orientation with respect to the propellers. They sit directly underneath the motor and props, therefore axial loading was the main force taken into consideration. However, when analyzing the semicircular platform attached horizontally to the vertical skeletonized wall, bending from the bolts on the horizontal plate could cause concerning stress in the fillet weld attaching the horizontal and vertical pieces together. After calculation the stresses in the weld bead due to bending were significantly less than the yield strength of the welding material, therefore the weld should take most if not all of the stress without failing. More information on these calculations can be found in Appendix B-5.

15.1.6 Landing Gear

The purpose of the landing gear is to soften landings and allow for reasonably high vertical landing speeds without compromising the structure. Under the team's analysis, the weakest element of the aircraft's structure was determined to be the center mount welds. Under the defined worst landing loading case, these welds could only withstand a static force of 256lbs concentrated at one of the landing gear sets. With the helical spring telescoping design, the more travel the vehicle had, the faster the craft can land. However, too long of landing gear introduced the potential issues of tipping and large bending forces on the landing gear mount if the craft landed with a lateral velocity. A spring with an unsprung length of 8", 4.37" of travel, a spring constant of 61.1lb/in, and a maximum force of 271lbs when fully compressed was chosen for the landing gear based on this criteria.

Assuming the spring is linear, the average force one landing gear set can see is 135lbf before the landing gear bottoms out. Knowing this average force using work-energy the maximum vertical speed for landing was determined as well as an equivalent "drop height." Drop height is the greatest height the aircraft can be dropped with no upward thrust and expect to experience no damage. The maximum vertical speed and drop height assume negligible lateral forces on the landing gear. Using work energy in conjunction with potential and kinetic energy the maximum drop height was calculated to be slightly over 6". The maximum vertical landing speed rating was calculated by using the basic freefall physics equations from 6", and was calculated to be 5.672ft/s (3.9mph). See Appendix B-10.1.

Buckling for both the spring and the smaller telescoping tube in the landing gear was also considered. Since the spring was rated for 271lbf and is guided by the larger tube, the spring wouldn't fail due to buckling under normal operating conditions. Using the Euler buckling equations, the maximum allowable force for the smaller telescoping tube was calculated to be about 3E6lbf. In addition, the slenderness ratio for this member indicates that the member should fail in compression before buckling occurs. With the maximum rated load of 271lbf, the smaller telescoping tube had a factor of safety of 132 in compression.

For the weld connecting the large telescoping tube to the landing gear plate, the team calculated the maximum allowable lateral force at the bottom of the landing gear when fully extended. When the landing gear was fully extended it is 13.5" long and with a lateral force at the bottom creates a bending moment at the weld. To obtain the allowable lateral force the flat circular weld model was used as it represents these conditions. Using this model, the maximum lateral force at the bottom of the landing gear causing the weld to fail was 800lbs with the 1.2 factor of safety. This lateral force was much greater than the lateral force the brackets above connecting the landing gear plate to the arm/center mounts can withstand. Having the brackets break was not desirable and could cause severe damage. It is much more preferable to have the landing gear snap off as it is easier to repair and can prevent further damage. To ensure that the landing gear weld breaks before the brackets under lateral loads at the landing gear, it is likely that the larger telescoping tube must be tack welded to the plate. See Appendix B-10.2 for these calculations.

Because of the bolting pattern, the team had difficulties with calculating the expected stresses on the landing gear plates while taking landing loads. A three point bending model analysis of the plate with a 270 lbf peak landing load shows that the plate would develop approximately 49100 psi of stress, too high for it to be able to endure indefinitely. However, this model ignores the fact that the landing gear plate was actually rigidly secured from all sides and that the landing load isn't applied to the direct center of the plate, providing a very conservative stress estimate. The team elected to run a finite element analysis study to estimate the stresses that the plate would actually see. The SolidWorks model was imported into ABAQUS as a linear shell model and the plate was meshed with 1596 quadratic reduced integration elements. For the load, a pressure load was placed on a partition which represented the contact surface of the landing gear spring on the plate and placed 270 lbf in total on the plate. For the boundary conditions, an encastred boundary condition was placed on the 8 bolt holes and the flanges around them in order to simulate the plate being bolted down by the bolt holes. Running the model, it was immediately seen that the stresses in the plate are unnaturally elevated around the bolt hole flanges; this was believed to be due to the choices in the model and boundary conditions and do not reflect reality. Instead, the team was interested in the maximum stresses located in the main body of the plate. Examining the plate, it was estimated that the plate should see about 10 ksi, yielding a factor of safety for fatigue life of 1.98 with a factor of safety of 1.2 and 95% confidence. Please see Figure 67 below for a look at the plate model and the stress distribution throughout it.

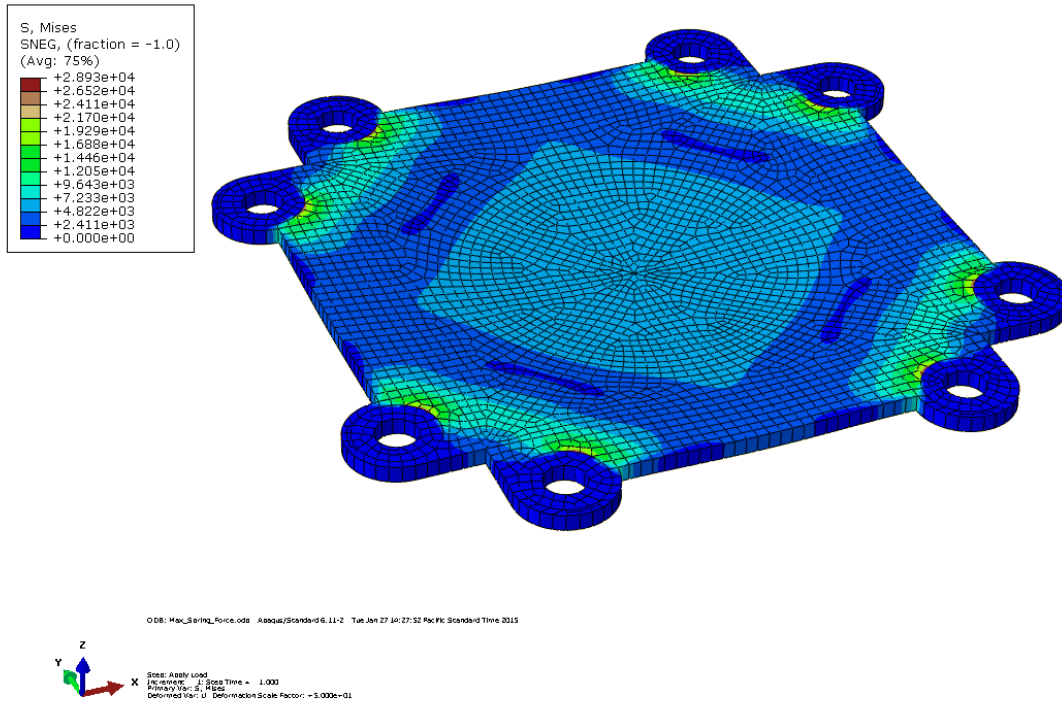


Figure 67: Finite Element Analysis of Landing Gear Plate under Maximum Loading Conditions

15.2 Propellers

15.2.1 Dimensions

The two dimensions to consider for the propeller were diameter and pitch. The operating conditions where the propellers were compared was at a combined thrust of 600lbs in hover. The 600lbs of thrust was determined by the 1.2 thrust to maximum weight ratio specified in the design requirements. The team also chose to analyze at hovering conditions because of the ease of calculations and testing. All test data found was a static thrust test, and any testing the team would perform would be a static thrust test. The final design was expected to move slowly through the air. As a result the operating conditions for the propeller would always be close to a hover situation.

The first parameter to be selected for the team’s design was the diameter. Based on actuator disk theory and JavaProp models it was determined that the largest propeller that could be used would offer the best efficiency. The only limiting factor on propeller size was that the tip speed needed to be below .85 Mach. The largest propellers that were commercially available and applicable for the project were 36” propellers. At this diameter the propeller would have to spin at 7100 RPM for the tip speed to become a relevant factor. The team did not plan on running near 7100 RPM, so tip speed was not relevant for the group’s considerations.

The structure stiffness requirements ended up being the limiting factor on the propeller size. Above 30” the structure could not provide the required strength; the craft became larger for an increase in propeller size and the craft’s current structure design couldn’t get much larger without compromising several of the calculated factors of safety. Further discussion of structure strength and analysis could be found in the

design analysis section above for structures. Due to the strength limitations, the maximum possible diameter of 30" was selected.

The pitch of the propeller is related to the speed at which the propeller is designed to move through the air. Since the team's multicopter was not going to move through the air at relatively high speeds, lower pitch propellers were theoretically better for the craft's application. The theory was confirmed with thorough JavaProp modeling. Table 10 shows the results of the JavaProp models.

Table 10: Effect of pitch on power consumption

Diameter	Pitch	Thrust	RPM	Power
(in)	(in)	(lb)	(1/min)	(kW)
34	10	50	6242	5.975
34	11	50	5985	5.928
34	12	50	5764	5.994
34	13	50	5569	6.126
34	14	50	5414	6.213

As shown above, the higher pitch propellers generally require more power for a constant thrust. Since the JavaProp models matched with theory, the minimum propeller pitch available, 10", was selected.

15.2.2 Material

The two options for the propeller material were carbon fiber and wood. Carbon fiber is lighter, stiffer, stronger, and more expensive than wood. The lightness of the prop was the most important factor to the project since weight reduction was vital wherever feasible. At the size considered carbon fiber propellers could be as little as half the weight of wooden propellers. In addition to saving weight for more batteries, lower weight propellers would also have a quicker response time as they present a lower inertia for the motors to spin up. This faster response time would allow for quicker and more precise control of the aircraft.

The stiffness of the propeller is related to the efficiency of the propeller. The higher the stiffness of the propeller, the more efficient it would be. However, the less stiff propellers are able to dampen out shocks encountered from maneuvering and wind gusts. For this application the team determined that higher efficiency was significantly more important than any shock absorbing qualities that may come with lower efficiencies.

The strength of the propeller is a factor in crashes. A stronger propeller may not break in minor crashes. However, if the propeller does not break, the impact forces of the crash are all absorbed by the main structure. The main structure would be very difficult to repair or replace, and needed to be protected whenever possible. Therefore weaker propellers could act as a sacrificial weak link; this would be preferred since propellers are relatively cheap and easy to replace. However, a weaker propeller would

also more likely become a flying projectile during a crash so it could be slightly more dangerous in certain circumstances.

Ultimately the efficiency, weight, and control advantages of carbon fiber outweighed the potential strength disadvantages it had. Price was the only reason that wooden propellers would be considered. The two quotes the team received were \$350.00 per pair of carbon fiber propellers, and \$218.00 per pair of wooden propellers.

15.2.3 Number of Propellers

The number of propellers was first approximated by the configuration analysis tool, discussed on page 48. The results of the configuration analysis tool showed that the ideal number of propellers would be 16 propellers, with 12 propellers being a slightly less optimal configuration.

Test data for the JM1S motor found in Appendix D: JM1S Test Data showed that 12 propellers would be a slightly better configuration. Table 11 shows a comparison of 12 and 16 propellers based on the test data.

Table 11: Comparison of 12 and 16 propeller power consumption and weight

Number of Motors	Total Thrust	Thrust per motor	Power per motor	Total Power	Motor and ESC Weight
[-]	(lbs)	(lbs)	(kW)	(kW)	(lb)
12	600	50	6536	78432	59.6
16	600	37.5	4364	69824	79.5

As shown in Table 11 above the 16 propeller configuration used 12% less power than the 12 propeller configuration. However, the additional weight of 4 motors and ESCs would take away approximately 20% of the available battery weight, and the additional wire and structure weight would take up even more. The power savings gained through adding additional propellers was counteracted by the increase in weight and the overall flight time was decreased.

The final propeller selection is 12 30"x10" carbon fiber propellers from the Precision Pair Series from Xoar. The propellers are not commonly available for purchase so the exact specifications of the product are not known other than the pitch and diameter. Based on other propellers from the Precision Pair Series, the expected weight of the 30x10 propellers should be between 90 and 100 grams each.

15.2.4 Propeller Analysis

Upon receiving the Turnigy motor and observing the small mounting pattern through which the bolts would keep the propeller in place, it was observed that a calculation of bearing stress on the propeller by the bolts was required to insure that at high torque, the propeller would not fail. Both the Joby and Turnigy motors had similar mounting patterns; therefore the calculations were made for a circular hole pattern of 44mm in diameter. Under a continuous 13 N-m of torque (the Joby motor's operating load), 93.27 psi of bearing stress was produced by each bolt on the propeller. For a peak torque of 20 N-m, 144.2 psi of

bearing stress was produced. In shear, beechwood has a shear strength of approximately 2100 psi, indicating that the props would have a factor of safety of 14.6 for the worst possible condition. Although the team does not have the shear properties of the carbon fiber props that were purchased, it is a safe assumption that it is stronger than the wooden props used for testing.

15.3 Motor

The required motor characteristics of the motor were initially estimated for several propellers in the size range that was considered using JavaProp. The propellers that were modeled were 32"x18", 34"x13", and 36"x10" propellers. These models were initially selected to cover the range of diameters and pitches that were in the size range indicated by the configuration analysis tool discuss on page 57. The results of the JavaProp simulations are shown in Table 12.

Table 12: Motor performance requirements estimates

Propeller	Torque	RPM	Power
[-]	(N-m)	(1/min)	(kW)
32 x 18	13.5	4500	6.5
34 x 13	10	5500	6
36 x 10	10	6500	7

Using the performance requirements shown in Table 12 two motors were selected as a high and low cost option. The low cost option was the 80CC Turnigy RotoMax Brushless outrunner motor. The specifications are shown in Appendix D: Turnigy RotoMax 80cc. The higher-cost option was the JM1S motor from Joby Motors. The Joby Motor had test data with the propeller that the team is using, so it was known that it would work for this application. The JM1S motor specifications are listed in Appendix D: Joby Motor. The test data for the JM1S is listed in Appendix D: JM1S Test Data.

The 80CC Turnigy Rotomax motor was tested to determine if it could be a satisfactory low cost substitute for the JM1S. The test plan and setup is in Appendix C: Propeller Test Plan. If the 80CC Turnigy Rotomax motor was able to closely match the performance of the JM1S motor, the 80CC Turnigy RotoMax motor would be selected for the project. However, for any commercial development of this project, the JM1S would be the recommended motor.



Figure 68: Mounted wooden propeller on Joby JM1S motor

Although the test data was held as reliable, it was believed that mathematically constructing the model and comparing it with the test data would play as a good validation of the team's results. A MATLAB program file was used to first give a contour reference visual the craft's final parameters for actuator disk theory method. This could be utilized to verify that the motors would provide the power necessary for the craft's configuration. This data is also available in table format should the user wish to view it, similar to the table presented in from the initial multicopter configuration tool as first utilized during PDR. The tool predicts that the multicopter's required power ranges from 4.5 to 7 kW as expected.

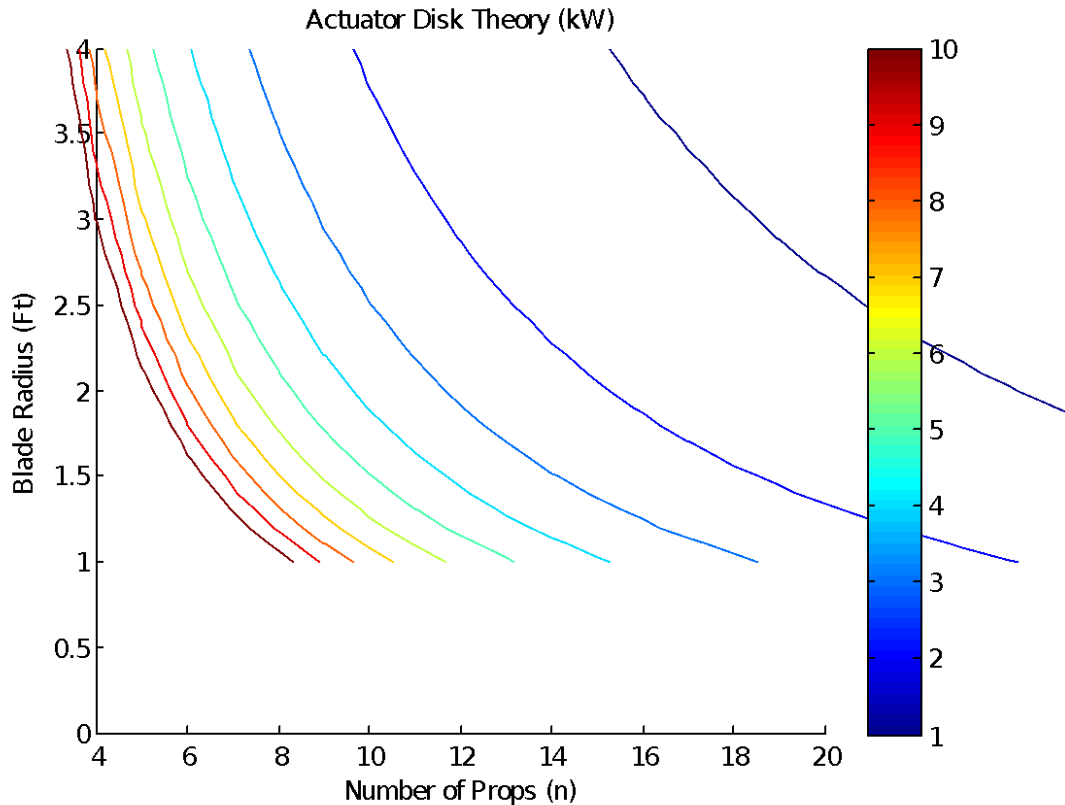


Figure 69: Actuator disk theory contour plots generate in MATLAB program, showing power in terms of blade radius and propeller number

Second, and more importantly, using a JavaProp configuration, contour curves for thrust vs normalized air speed were generated with contours of RPM. This served three purposes; first, it verified that with the system in place, thrust loads could be mathematically generated at similar RPM to that of actual Joby test data. This is an important propulsion validation, as it indicates that the team can trust their test data. Secondly, it verified that, for a large multicopter at high speeds, the thrust is a heavily dependent on RPM and very loosely correlated with speed, something that the group was very unsure about during research. This means that at the low forward speeds this aircraft might go through, the team would not have to worry about generating tremendous amounts of additional thrust, only making sure that the vertical component was equivalent. Lastly, it partially validates the use of JavaProp as a design tool, as the thrust coefficients and advanced ratio values outputted corresponded with test results.

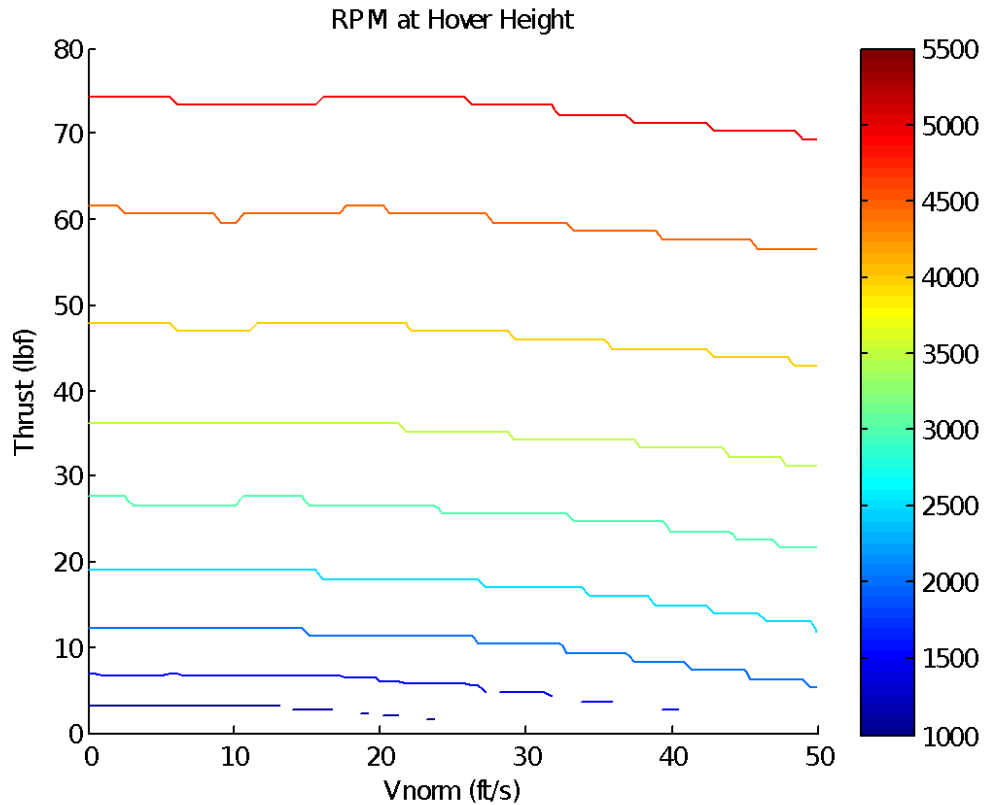


Figure 70: RPM at Hover Height, showing contours of RPM over a range of thrust and velocity (normalized). This helps validate mathematically the experimental results presented by Joby

During an aircraft performance class, creating motor models displaying efficiency as a function of torque and speed was frequent activity. Cal Poly's Dr. Robert McDonald provided the team with a copy of a rubberized motor model which would allow for the use of specifications to create a motor model that could then be taken to a motor manufacturer for fabrication. He had given permission to learn the tool through trial and error and for it to be utilized, along with the rest of the team generated code, for future users. The team recommends using a motor model for both COTS and custom motor applications. The included model is one of the Joby motor that has been selected for possible system integration. In order to use it, one would first generate the RPM at Hover Height for the system they wish to use and then pick off the correct RPM. One caveat is that one must either have a good idea of the system torque required (comparable test data) or consult with a manufacturer to get an idea. With this, and the maximum necessary RPM, one can create a motor model which the user could present to a motor manufacture and ask for manufacturing capability of that motor. The easiest use of the program is when performance data is known from a manufacturer, and you can pick a necessary thrust and find the corresponding torque and RPM as the operational points, and then design a motor for particular efficiency to request for fabrication. The main purpose of this component, was to provide future users a starting point for custom motor fabrication.

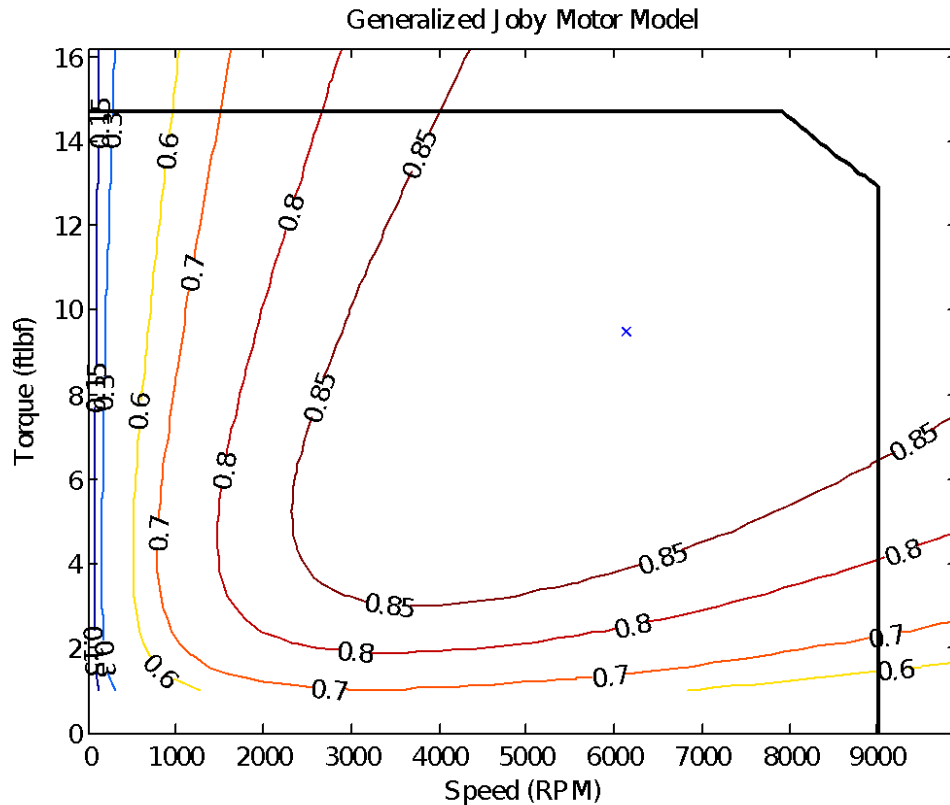


Figure 71: Generalized Joby Motor model with an efficiency at 89%, torque of 9.5 ft-lb, and RPM of 6134. The “K” factors are determined based off of motor max RPM and torque

Lastly, as the tool was partially generated before the project's final design conditions were determined, a verification test was performed to test the program's use. In order to do this, a known smaller scale quadcopter was modeled mathematically to see if the RPM as a function of thrust versus normalized velocity would produce similar results to that of the listed data. The results matched quite closely, revealing that quadcopter in question could reach the pounds of thrust required per motor it had advertised, as well as giving extra assurance of the program's capabilities. This verification was performed on the IRIS+ multicopter by 3D Robotics.

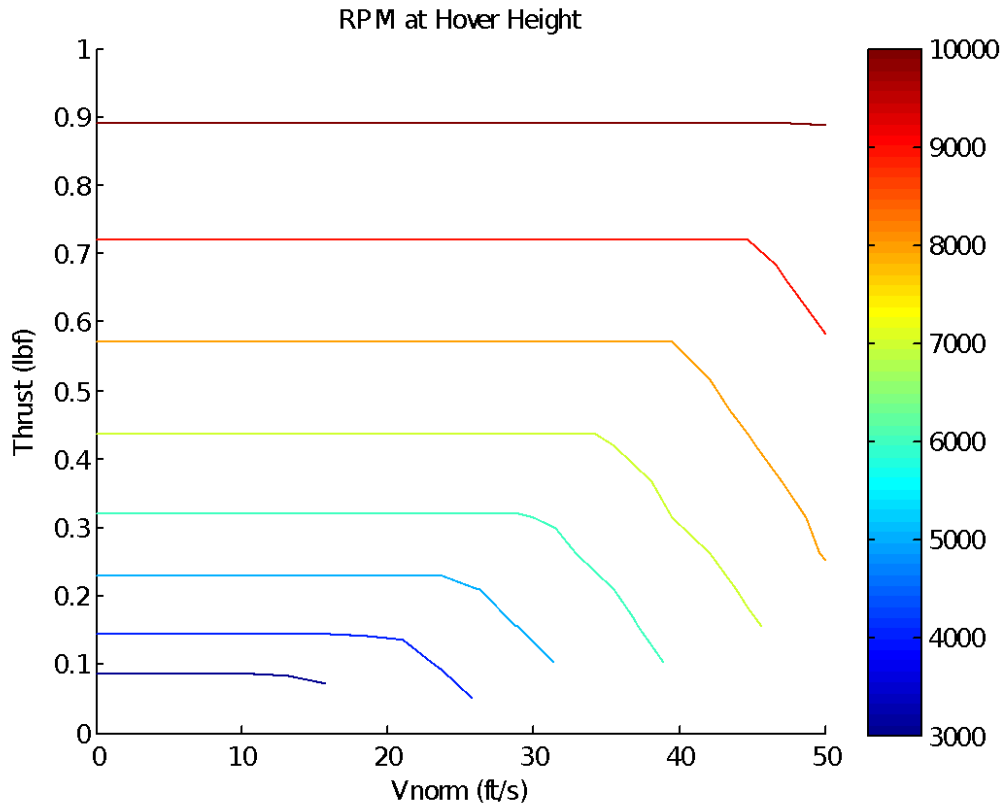


Figure 72: RPM at Hover Height, showing contours of RPM over a range of thrust and velocity (normalized) for the 3D Robotics IRIS+ multicopter. The results are comparable to the data provided by 3D Robotics and validates the program

The code contains a basic skeleton code for blade element theory calculations for future users, but is currently non-functional, due to mathematical errors and lack of approximations. The code as well as a brief instruction manual for both the design code and rubberized model is presented in Appendix C: MATLAB Design Program.

16 MATERIAL SELECTION

With arguably the most important engineering requirement aside from student and user safety being to produce a craft which weighs less than 254 pounds (please see Regulations section above), the team was immediately restricted in the choices of materials which could be used for this vehicle. Therefore, most of the craft's design choices place an emphasis on lightness rather than large safety factors. This was a difficult decision for the group, but ultimately the team's priorities mostly lie in meeting the absolute weight requirements set by the sponsors. There are some concessions to this rule; this craft represents the best design which could be built and tested by the current team members. Because of the limited experience with impact protection, composite design, and advanced fabrication methods, this design doesn't necessarily reflect how the group would advise an electric commuter multicopter to be produced if it were to be made professionally on an industrial scale. That being said, the team's primary driving force in this project is the final weight of the craft, and it shows in the material selections.

16.1 Unidirectional Carbon Fiber Tubing

The main structural elements of the craft (the main arms and motor spars) would be constructed out of unidirectional carbon fiber and would be produced professionally by trustworthy composites companies. From the very beginning of the project the team started looking at unidirectional carbon tubing for its extremely high strength to weight ratio, excellent fatigue life and damping properties, and its relatively high specific stiffness. In essence, unidirectional carbon tubing make for excellent beam material, especially for the craft's uses. Using unidirectional carbon fiber tubing brings its own disadvantages and difficulties, however; the group would have to be very mindful during the design work to consider tube torsion, impact loading, and preserving the structural integrity of the tube lest the team cracks the main arms and spars and ruin their mechanical properties. These issues are seen reflected throughout the project's design. The carbon fiber tubing does not directly take any of the impact loading from landing and was sized to withstand a conservative case of tube torsion just to be on the safe side. The group ran checks on the tubing with programs designed to determine their effective stiffnesses and strengths See Appendix B-1, using conservative material data based on real-world testing performed at Cal Poly.

The team initially considered producing the project's own carbon fiber tubing; this was ruled out as it would be extremely difficult for the team members to safely and cost-effectively produce the tubes in a timely manner. Purchasing the tubing was agreed to be the best option given the circumstances of the project.

16.2 Epoxies and Bond Line Controller

The team planned to use a lot of epoxy to bond this craft together. For all of the joints between carbon fiber and steel surfaces, 3M Scotch-Weld 2216 2-part epoxy would be used to bond the components together. This type of epoxy has come recommended by several composites companies for use with their tubing, and according to Rockwest composites and 3M it should have no issues bonding the craft's carbon tubes to the steel mounts. This epoxy has 90 minutes of work life, providing plenty of time to complete the bonds and ensure that the components are positioned correctly before it starts to cure. The estimated adhesive layer thickness should be about 0.007" for all bonds between carbon fiber and steel surfaces.

For building the propeller rings, the group planned to use West System's 105 Resin with their 206 hardener. This is a 2-part marine epoxy system that should cure relatively slowly (20 to 25 minutes of pot life and 10 to 15 hours until it cures to solid state, according to the manufacturer), providing plenty of time to construct the rings. The resin would be added to the tape at a ratio of 1:1 by mass, and the epoxy and resin mixture would be formed at a ratio of 3.5 parts resin to 1 part hardener. This is the same epoxy and hardener pairing and the same ratios that Cal Poly's Human Powered Vehicle team uses in their wet layups while making carbon fiber bicycle fairings, so the team was confident that it should work using similar materials and procedures.

To help prevent galvanization between two electronegativity dissimilar materials when bonded together with epoxy, the team planned to make use of 0.007" Bond Line Controller from Rockwest Composites in the Scotch-Weld 2216 epoxy mixtures. This product is essentially a collection of small glass beads with outer diameters of 0.007" which separates and insulates the two materials being bonded together. Bond Line Controller will be added in to the 2216 epoxy and hardener at a ratio of 2 grams of Bond Line Controller per 2.7 oz of epoxy mixture and mix it thoroughly before applying it to the bond surfaces.

16.3 Carbon Fiber Tape

The propeller rings were to be made from a dry carbon fiber braided tape purchased from Rockwest Composites. The team selected this tape based on its dimensions, weight, and cost. The tape comes from the manufacturer in 2" wide by 0.024" thick strips cut to whatever length is ordered; in this case the group plans to purchase 430 feet of tape in order to make the craft's 12 propeller rings. The tape is biaxially braided with fibers arranged in a +/- 25° configuration. This should provide an acceptable amount of axial stiffness and strength compared to a conventional cloth weave, which would have fibers arranged in a +/- 45° or 0°/90° configuration. It also makes manufacturing the carbon rings extremely simple, as it will eliminate the need to cut very long continuous lengths of carbon cloth precisely (something that would be extremely difficult for the team to do). Instead, all that is needed to be done is wet the dry tape with epoxy and wrap it around the steel ring form until the desired wall thickness for the propeller rings has been reached. The carbon tape weighs less and is far stiffer and stronger than a comparable fiberglass tape, one of the competitive options for a ring material. Thin walled aluminum and steel rings were also looked into, but the team does not feel as though these are valid options considering the weight they add to the craft. The carbon fiber tape would be combined with a 2-part marine epoxy adhesive to form a stiff structure.

16.4 4130 Chromoly Tubing

The team opted to use 4130 cold drawn Chromoly steel tubing for the center, arm, and motor mounts. 6061-T6 tubes were first researched for use in these structural mounts due to its low weight and relatively high strength to weight ratio. However, a wealth of issues led the team to pursue steel tubing rather than aluminum.

First, aluminum has no calculable fatigue life. This means that part failure would most likely be seen on the craft if it was tested and used for a long enough time. This worried the group immensely, as the team feels reasonably confident in the craft's structural loading analysis but don't know enough about how the craft will be used or how much vibration it will see to say with certainty how long the vehicle should last. Significant vibration could cause a significantly shortened lifespan when using aluminum tubing, especially with lower safety factors. 4130 Chromoly, being a steel, can be designed to withstand a given load more or less indefinitely with a fair degree of certainty, and there is plenty of testing data which corroborate these findings. The craft's steel tubing components were designed to meet infinite fatigue life criteria with 95% confidence, something that couldn't be guaranteed with confidence for aluminum parts.

The team was also concerned with the structural properties of the material, given that the tubes were going to be mitered and welded together to form the different mounts. T6-temper 6061 aluminum is fairly strong for its weight, but after being welded the material can become annealed and lose its temper, returning its structural and mechanical properties back to the aluminum's annealed state. At its natural annealed strength (designated as aluminum 6061O), this becomes more and more likely the thicker the material sample gets; with the large tubing sizes necessitated by the use of aluminum tubing (as opposed to the sizes that would be used with an equivalent strength steel tube), the team is certain that the material would require post-weld heat treatment to restore it to its original strength. The relatively sizes of the brackets means that this isn't something that can be performed on campus, and no nearby heat treatment facilities were able to be located for parts to be treated professionally. The group could opt to have them sent across the state or country to have them professionally heat treated at a heat treatment facility, but this was seen as a less than ideal solution given the expense and potential turnaround times for the components. With 4130 tubing, the team can get away with far thinner wall thicknesses for an equivalent strength tube. The group consulted several welding professors in the IME department on the use of 4130 steel tubing for the project, and they advised the team that the issue of the steel properties changing with thin walled tubes was a non-issue due to the way that thin steel tubes cool and forms microstructures. In any case, the craft's steel tubing was selected such that even if the tubing becomes fully annealed the required minimum safety factor of 1.2 will still be met for infinite life with 95% confidence under the normal usage cases (essentially treating the local welded material in the tubes as hot rolled).

The team found that there wasn't a significant weight reduction when using 6061-T6 aluminum compared to a similarly capable 4130 tubing. For example, the center mount and the arm mounts each were about 1 to 2 pounds heavier when designed using 4130 tubing instead of 6061-T6. However, this doesn't take into account any factors of safety for infinite life (because it is not possible to design aluminum to have infinite life). Structurally, 4130 is three times stiffer than aluminum, meaning that the group also can plan on having less arm deflection with the steel tubing, and it is far easier to weld and bond with epoxy than aluminum or many other kinds of steel, requiring no special treatment aside from sanding the weld locations before welding. The team feels as though, all factors considered, the 4130 tubing is the project's best solution for the mount assemblies.

16.5 4130 Steel Plate

The team opted to use 12 gauge 4130 steel plate for all of the center, arm, and motor mount bracket assemblies as well as landing gear plates. Because the group made a decision to go with 4130 steel tubing and if the brackets and the mounts were to be welded together, steel plate was needed as the building material for the bracket walls. This decision is preferred in order to avoid drilling bolt holes in the craft's mounts and unnecessarily weakening them. For simplicity the group decided to go with thin 4130 plate steel; a large sheet of 12 gauge plate steel (approximately 0.109" thick) will be purchased and a CNC plasma cutter will be used to cut out all the bracket walls and flat components.

The plate steel arrives in an annealed state, providing a yield strength of 50 ksi. The steel in the plate components doesn't have to be as strong as the steel for the mounts, so this is acceptable. Using 4130 plate steel rather than a different steel means that welding the bracket assemblies will not require any special considerations nor will it drastically change the properties in the weld joint beyond what is expected during the welding process.

16.6 6061-T6 Aluminum Plate

While the team opted to use 4130 Chromoly steel for most of the structural components, 6061-T6 aluminum could be used for the seat plate. The seat plate is a relatively important component in the craft but doesn't see any severe sort of loading cases during normal use, will not see significant cyclic loading, and doesn't get welded to anything, meaning that the team can take full advantage of the material properties of the heat treated aluminum. It should also be easier to drill the bolt holes and fillet the edges of the plate with this material as opposed to steel.

16.7 Welding Filler Metal

For the welded joints between the steel tubes, the design required a filler metal meeting or exceeding ER100XX classification for tensile strength to meet the project's required factors of safety for fatigue life with 95% confidence. This requirement was based primarily off the major loading cases of the welds for the center mount (the part with the most intensive weld loading), as the welds on this mount are placed in shear when the tubing bends. This may be able to change with an increased weld size and will depend on input from the welding instructor.

16.8 Netting

The team intended to purchase PollyNet Premium bird netting with a 0.5" gap size to drape around the carbon fiber propeller rings in order to meet the project's requirement of fully enclosed propellers. The 0.5" gap size should keep large objects out, and the material has a tensile strength of 10 lbf per strand (with two strands per inch of netting) and weighs 8.5 pounds per 1000 square feet. To mesh over all of the rings would require about 170 square feet of netting, resulting in the addition of 1.45 pounds to the craft. The group plans to zip-tie the netting tightly around the rings, keeping the material out of the way of the propellers and allowing for repair and replacement of sections of netting easily. If the group decided to reduce the size of the gaps to keep foreign material out of the way of the propellers or that more strength was needed out of the netting, the team could have laid down an additional layer of netting over the first or use hardware cloth (a denser-packed metal mesh) instead of the bird netting. It was preferred to avoid this latter option, as the hardware cloth weighs 15 pounds per 100 square foot, meaning that an additional 21.1 pounds would be added to the craft to protect it. In any case, going with a mesh size much smaller than 0.5" would significantly impede airflow to the propeller, so 0.5" mesh is favored if it can be easily used.

17 CONSTRUCTION PLANS

17.1 Structure

17.1.1 Main Arms

The team planned to purchase the tubes which make up the main arms directly from C-Tech. All tubes would be custom made for each order allowing the team to use them without modification. Four main arms were planned to be purchased for the vehicle at a length of 52 inch.

To repair a carbon fiber main arm in the event of a catastrophic crack or injury to the tubing which impacts the structural integrity of the craft, the team recommends completely replacing the entire arm. To do so, the user (or manufacturer) would first cut the arms in half and separate any wiring running down the arm from the main arm tube. Then, using a hammer or impact device, they would crack the carbon tubing down its lengths until it splits from the tube. The tubes would then be separated from the arm and center mounts, using torsion to destroy the tubing if necessary (as the steel tubing will survive far greater torsional loads than a cracked carbon fiber tube). Next, the arm and center mount bond surfaces will be ground down to remove the remaining layer of epoxy on the steel tubes, using a harsh cleaning agent like acetone to soften the epoxy if this becomes necessary. The surfaces will be cleaned, sanded, and then cleaned again with acetone in order to prepare them to accept a new epoxy bond; this procedure can be found detailed below in the Craft Assembly section. A new main arm will then be epoxied in place on the arm and center mounts, completing the structural repairs. Finally, the wiring and other components removed previously can be reattached to the main assembly.

17.1.2 Motor Spars

The spars would be purchased from Rockwest Composites and the team would cut them to length. The carbon tubing which makes up the spars comes in 70" lengths, meaning that there will be about 4" of waste per tube to cut three 22 inch motor spars. The group planned to construct 12 motor spars for the vehicle.

Motor spars can be repaired in the same fashion as the main arms. First, however, the team would need to detach the propeller rings from the ring mounts so that the arm assembly can be removed properly, then the wires and electrical components from the broken motor spar would be removed. The broken spars would then be cut in half, fractured with impact loading, and twisted off the steel tubes. The steel surfaces would be ground down to remove the epoxy layer, and then sanded and cleaned to prep for a new layer to bond in the new motor spar. Finally, the replacement spar would be glued into place following the procedure below in the Craft Assembly section.

17.1.3 Center Mount

To make the center mount, first the team would need to measure the inside diameters of the carbon tubes and determine how much material will be needed to be removed off the steel tubes to fit them inside the carbon tubes properly. The group planned to provide around 0.007" of clearance between the tube walls for an optimal adhesive bond thickness. In order to produce this clearance, the steel tubing would be placed inside a lathe and the diameter will be turned down very slightly to the required size; the tubes come at a nominal outer diameter of about 2.50", so the exact amount removed would likely vary from tube to tube. With the tubes turned down to the right diameter, the group would then miter them using tools available at the hangar and tack them together with butt welds, taking care to ensure they are lined

up precisely. After checking the piece, all of the contact surfaces would be welded to finish the part. Only one center mount for the vehicle is planned to be constructed in total.

17.1.4 Center Mount Bracket

The center mount bracket was planned to start out as a large sheet of 12 gauge 4130 plate steel. The team planned to cut out the bracket wall components and the center mount landing gear plate on a CNC plasma cutter (located in Paso Robles) and weld each bracket wall assembly together with fillet and square groove welds. The four bracket walls would be positioned together on the center mount, then they would be bolted to the craft's landing gear plate, and then they would be tacked together. The group would then fillet weld the bracket together along all contacting surfaces after ensuring it fits the center mount properly. The center mount bracket would then be fillet welded to the center mount around the contacting surfaces, completing the center mount assembly. Four bracket walls were planned to be constructed in all, making for a total of one center mount bracket for the vehicle.

17.1.5 Seat Plate and Seat

The seat plate were to be constructed out of a 12" x 12" x 0.25" plate of 6061-T6 purchased from OnlineMetals.com. The team planned to locate and drill the mounting holes using a drill press and the corners would be filleted with a band saw. The seat plate would then be bolted to the top of the center mount assembly.

The group planned to purchase the seat directly from the manufacturer and bolt it to the seat plate after construction of the rest of the craft is finished. Because of the nature of the built-in seat mounting inserts, slight modification of the underside of the seat would be needed in order to bolt on to the seat plate. The nuts holding the seat plate attachment bolts for the center mount would stick into the polyethylene seat slightly and this would necessitate the removal of a small amount of material from the bottom of the seat with a Dremel. This shouldn't impact the structural properties of the seat, but if this procedure was determined to be unsafe after inspection, then the seat would be raised higher above the plate with nuts and longer bolts.

17.1.6 Arm Mount

The arm mount would be made in a fashion similar to the center mount. The team planned to measure the inner diameters of the motor spars and the main arms and to turn the outer diameters of the 4130 tubing down to give 0.007" of clearance between the tube walls for each tubing size. The three smaller diameter tubes would be mitered and welded together, taking care to ensure that they are straight and level with each other. The larger diameter tube would have a semicircular notch cut into the end that is to be welded; this notch would have the same diameter as the outer diameter of the smaller tubing. The smaller diameter tubing assembly would then be tacked inside of the notch in the larger diameter tubing and then the entire mount would be checked to ensure that it is level and straight. Once that is done the group planned to liberally weld the two pieces together, completing the arm mount. Four arm mounts were planned be constructed in total for the vehicle.

17.1.7 Arm Mount Bracket

The arm mount bracket was to be constructed very similarly to the center mount bracket. The team planned to cut the bracket walls and the landing gear plate for the bracket out of the 4130 steel plate, and each individual bracket wall would then be welded together with fillet and square groove welds. Then, the four bracket walls would be welded together while bolted to the landing gear and sitting on the arm mounts to ensure that each bracket fits the mount properly. Lastly, the arm mount bracket would then be welded to the arm mount, completing the arm mount assembly. Four arm mount brackets were planned to be constructed in total for the vehicle.

17.1.8 Motor Mounts

To construct the motor mounts, the team planned to first cut a section of the smaller-diameter steel tubing to length and to turn the outside diameter down slightly to give a 0.007" clearance between the inside of motor spars and outer diameter of the steel tubing. The group would then cut out the parts for the motor mount bracket walls from the 4130 steel plate. These bracket walls would be carefully welded together with fillet and square groove welds. A steel template with the motor bolt pattern was intended to be used to hold the bracket walls together in the correct orientation, and then the motor mount bracket walls would be tack welded to the steel tube. After verifying that the mount is assembled and aligned correctly, the

bracket walls could then be fillet welded to the steel tube. The team planned to produce 12 motor mounts in total for the vehicle.

17.1.9 Inner & Outer Ring Mounts

The propeller ring would be supported by two 4130 steel mounts, both cut out of a large steel plate of AISI 4130 by a CNC Plasma Cutter. The mount closest to the center of the vehicle, the inner ring mount is attached to both the corresponding spar and the prop ring. The hemispherical geometry at the bottom of the ring mount would wrap around the spar, and epoxy would hold the two together at the joining geometries. The strength of the epoxy would be sufficient in congruence to the light load of the carbon ring, implying that this assembly would be stable. Two Stainless Steel 12-24 3/4" long Pan Head Slotted machine screws would insert through a small piece of 20 gauge steel, through the rings, and through the two .25" holes in the ring mount with a Stainless Steel Hex Nut 5/16"-24 at the end.

The ring mount on the other side has a different geometry due to the assembly of parts. The outer ring mount would have the same attaching process to the prop ring as the inner ring mount. However, the outer ring mount would be inserted and welded at its bottom to a .5" steel tube that extends out from the motor mount bracket walls. This steel ring spar would provide minimum support to the ring; the ring is designed for countering outside interference from people, and to not withstand a thrown propeller. Hence the strength of the ring spar was not a critical concern in our design.

17.1.10 Propeller Rings

The team planned to construct the propeller rings out of a long roll of carbon fiber tape which is 0.024" thick and 2" wide. First a template would be formed out of a thin steel band that is cut to 2" wide and 105" long. This template would be secured end to end to produce a steel ring with a diameter of 33". Then the carbon fiber tape would be soaked with marine epoxy (not the two part epoxy that was used for the structure joints; please see the Materials Selection section below for more information) and wrapped tightly around the outside of the steel ring 4 times, giving a wall thickness of about 0.096". When the epoxy had cured, the tape would be cut off of the steel template and the tape would be removed from the inside of the carbon ring. Lastly, the group would cut several thin sheets of 20 gauge steel (about 2" wide by 2" tall and 0.036" thick) which would be epoxied on to the inner and outer surface of the ring where it is to be attached to the propeller ring mounts. The team would then drill a pair of horizontal holes through these steel sheets and through the carbon fiber ring; this would allow the propeller rings to be screwed directly to the mounts without destroying the carbon fiber, as the shear forces encountered by the ring would be resisted by the steel sheet instead of by the carbon fiber (which is much weaker in shear than steel). This procedure was planned to be done a total of 12 times to produce the 12 propeller rings needed for the vehicle. Each propeller ring was estimated to weigh about a pound.

17.1.11 Landing Gear

The landing gear was planned to be constructed by first cutting the stock tubes to their specified lengths for the landing gear. The stock 2.5" x 2.310" 6ft 4130 from long tube for the larger guide tube was to be cut into five 8.50" tubes. The smaller 2.5" x 2.12" 3ft 4130 tubing would be cut into five 5.50" long tubes.

Second, the slot in the guide tubes would be machined out. This slot was to be 4.5" long, have a width of 0.25", and would start 4" from one of the sides. The slot would be on both sides of the tube and the axis connecting the two slots would pass through the center point of the tube. The slot would be cut on a mill with a 0.25" diameter end mill with ideally a length of at least 2.5". The >2.5" length would allow the slot to be cut without resetting the part, ensuring the slot holes are in alignment. An extra-long end mill would have to be purchased for this. This long end mill method would not have to be used as some slop would

be acceptable for the pin. Starting 4" (measured at the center of the end mill) from the end of the tube provides the assurance that the both sides of other end of the slot will line up precisely, as no axial movement will be necessary to start the cut. This is important because when the landing gear is fully assembled in the unsprung position the pin will be perpendicular to the tube. In addition to this the smaller tube would be parallel with the larger tube and normal to the ground in level flight.

Third, the guide tube would be welded to the landing gear plate. The end of the tube that is 4" from the slot is the face welded to the plate. The guide tube will not fully be welded around its circumference. Instead it will be welded with five tack welds. This was intended to allow the landing gear to break off under a high lateral force instead of further damaging the aircraft. As strength can be managed with the number of tack welds the any effective electrode for welding 4130 steel will suffice. An E100X type electrode would most likely be used as it is what is used in other welds on the aircraft. Note the team does not anticipate any distortion from welding to affect the alignment of the slot as it is minor welding and the slot is located 4" away.

Fourth, the 12" x 12" 0.10" thick 4130 Chromoly plate would be cut with a CNC plasma cutter to produce five 2.25" diameter circles. These circles would then be welded to the smaller telescoping tube concentrically. The weld would be several tack welds. Any electrode for welding 4130 could be used, again an E100X would most likely be used. Once the part is cooled the welds would be ground down to ensure a clearance fit for telescoping.

Fifth, the smaller telescoping tube would have a 0.25" drilled through its entire diameter. This hole was to be located 0.50" from the face of the welded on plate. The hole would be cut using a drill press. In order to ensure the hole passes through the entire diameter of the tube, the tube would be mounted, marked for drilling, and then aligned to the drill bit. Ideally the drill bit would be long enough to drill through both sides of the tube without remounting the part. Considering the outer diameter of the tube would be 2.25" this shouldn't be an issue. The 0.25" clevis pin would then be inserted to test fit before attempting final assembly.

Finally, the landing gear would be assembled by inserting the spring into the larger telescoping guide tube. Next the smaller telescoping tube would be inserted into the larger tube with the plate side of the smaller tube contacting the spring in the tube. The smaller tube would be pushed to compress the spring, the hole in the smaller tube could then be aligned with the slot on the larger tube, and then the clevis pin would be inserted to hold the assembly together. Note 12lbs of force would be required to compress the spring in order to make the slot and hole line up for the pin.

17.1.12 Craft Assembly

The team planned to begin craft assembly when all major components (mounts, brackets, and carbon tubing) had been built. To assemble the craft, the outer surface of the exposed steel tubes in the center mount assembly and the radius of the inside lip of the steel tubing would be roughened up using a hand file; this would help prevent stress concentrations in the epoxy near the end of the steel tubing. Afterwards, the group would clean the tubing with acetone to ready them for accepting epoxy. The inside 4 inches of the carbon fiber tubes could also be roughened up and cleaned with acetone. Then, a small amount of epoxy resin and hardener would be mixed up and Bond Line Controller would be added to the mixture. This epoxy mixture would be spread lightly over the prepared steel surfaces, and then the four main arms would be slid over the corresponding steel tubes. The assembly would then be let to sit for 2 days while the epoxy cures.

While this assembly is curing, the team would similarly prepare the steel tubing outer and inner surfaces in the four arm mount assemblies and the inside surfaces of the 12 motor spars with an abrasion treatment and an acetone bath. The epoxy resin, hardener, and Bond Line Controller would then be

mixed up in 4 small batches; one batch for each of the arm mount assemblies. Then the epoxy mixture would be spread over the smaller-diameter steel tubing in the arm mounts and the motor spars would be slid over the steel tubes. With this completed for all four arm mounts and attached motor spars, the team would let them sit for 2 days while the epoxy cures.

After the arm assemblies cure, the team intended to bond the 12 motor mounts into place inside the motor spars. This would be done with the same approach as detailed above to prepare the steel tubing surfaces and the outer ends of the motor spars with sandpaper, hand filing, and an acetone bath. The group would again mix up 4 small batches of epoxy resin, hardener, and Bond Line Controller, one batch at a time for each arm mount assembly. For each arm mount assembly, the group planned to lightly coat the outer surfaces of the motor mount's steel tubes with epoxy mixture and then slide them into their corresponding motor spar ends. After each arm assembly was combined, the team intended to flip the assembly over and place it on a flat surface to ensure that the top plates of the three motor mounts would remain flat with respect to each other and with respect to the arm assembly. This would keep the motor mounts all perfectly parallel to each other and oriented correctly so that the 12 motors would not thrust the craft in slightly different directions. These assemblies would sit for an additional 2 days as the epoxy cures.

After the center mount assemblies and the arm assemblies have cured, the components would then be bonded together. As before, the inner and outer surfaces of the larger-diameter arm mount tubes would be prepared with sandpaper and hand filing before washing the surfaces down with an acetone bath. The team would also sandpaper the inside of the main arms and wash them with acetone where they would be joined with the arm mounts. Mixing up more epoxy resin, hardener, and Bond Line Controller, the group would lightly coat the outer surfaces of the steel tubes with the epoxy mixture and then slide them into the prepared ends of the main arms extending out from the center mount assembly. At this point, the craft would be sitting on the center mount and arm mount brackets, which would allow the team to keep it upright and relatively level. This would be completed in a level and flat environment while constantly checking the flatness and levelness of the motor mounts and the arms and spars. The craft would be adjusted, lifting up certain sections if needed, until the team was satisfied that the craft was as level as possible. The craft would then be allowed to sit for 2 days as the epoxy within it cures. After this point the main structural assembly of the craft would be completed.

After the craft cures the team would lift the entire craft up gently and set the arms down on raised and padded surfaces. The landing gear assemblies would install the landing gear assemblies onto the bottom of the bracket assemblies with bolts. After ensuring that the landing gear is assembled correctly, the craft would be lifted up and placed on the ground. At this point, the seat mount and seat would be bolted to the top of the center mount assembly.

The 12 propeller ring inner mounts would then be added to the assembly. The team would locate the spots on the motor spars where the mounts need to be bonded on and lightly abrade those locations, and afterwards the group would clean the surfaces with acetone. Then the contact surfaces of the inner mounts would also be abraded and cleaned. A small amount of epoxy resin, hardener, and Bond Line Controller would be mixed and applied to surface of the motor spars. The group would then place the mounts in position on the epoxy and tape them into an upright position to ensure they stay in position while the epoxy cures. These parts would be left in place for 2 days before being moved to ensure that the epoxy cures fully. If the apparent joint strength for this inner mount was satisfactory, additional carbon fiber tape (the same material which was used to build the propeller rings) would be purchased. The tape would then be wrapped around the base of the mount rigidly and around the motor spar to add additional strength. This component isn't a structural element, and it is preferred that it break off the craft in the event of an accident rather than damage the motor spar, but it also needs to stay on the motor spar securely enough to where it can hold its propeller ring in place safely under low to moderate loading conditions. These components would be left to sit for 2 days so that the epoxy could cure.

After the epoxy has cured the propeller rings would be installed, screwing them in place through their mounting holes and into the propeller ring mounts. After this stage installation of the motor could be done by bolting them into place on the motor mounts.

17.2 Propulsion

17.2.1 Propellers

The propellers that were to be used are manufactured by Xoar. The propellers are part of the Precision Pair Series, and are being custom made for this project. Once shipped the only additional work to be done to the propellers would be to drill the six mounting holes for the propeller. These holes would be concentric around the shaft hole. Drilling these holes would require high accuracy to ensure that the propeller remained in balance and would fit onto the motor. Drilling templates are available and would be used since a mistake could render a propeller useless.

The propeller would have to be balanced if it seems to vibrate when the motor starts to rotate. The process would require a leveled test setup with a motor and a propeller attached to it. The team would attach a gyroscope to the motor and it would show the vibrations as rotational rate measurements, which can be read. The team would add small weight to different portions of the propeller until the gyroscope measurements go to zero meaning the propeller was balanced. Maintenance of the propellers would involve balancing them. Sometimes, out of the box, the propellers can be imbalanced and will cause the motor-prop assembly to gyrate. This would be corrected through the applying epoxy or tape to the propeller to adjust its center of gravity to eliminate any gyroscopic effects. Anything further than rebalancing would be unreasonable because rotating objects require extreme attention to detail, and adjustment of any of the propellers' dimensions makes for a substantial challenge because of its intricate geometry.

17.2.2 Motors

The selected motors to be purchased would be fully operational, but would need some soldering to be connected to the ESC. They would need to be bolted to the mounting brackets and have their wiring connected to be operational. This is a large standout of a motor system not requiring gears or a gearbox, and a large reason for the team's exclusion of those applications. The motors would not be expected to receive substantial repairs because disassembly of these motors is generally discouraged and any substantial damage would require the purchase of a new motors.

17.2.3 Wire layout/Circuit diagram

Because of the high power applications of this project, up to 6800W for each of the twelve motors, some of the standard wires that would come with the electrical components may not be rated for this application where the assumed max current draw through the power wires is to be 200 amps. Consequently, some of these wires may need to be replaced. The sequence to replace these wires involves first desoldering the old wire from its respective electrical component. Then the new wire would be stripped, tinned, and soldered onto said electrical component. Once replaced, connectors would need to be attached to the wire so that components, like the motor, ESC, and batteries could be easily connected and disconnected. Heat shrink would then be placed over the connector to eliminate the possibility of direct exposure to the power circuitry. Because the 8AWG wires that would be used in this project are relatively large, they act as heat sinks when the soldering iron is applied to heat them. From manufacturing experience for the electrical components for the thrust test, it was found that 50W soldering irons do not produce enough heat for this procedure. To compensate for this, two 50W soldering irons should be sufficient but two people would need to work on one soldering joint, making for significant production inefficiencies,

especially when this process will have to be repeated for all twelve motors. Therefore a higher power soldering gun close to 150W would be used to assist in the solder process. The wiring would need to be checked for maintenance. The silicone wire is not very abrasion resistance, so wires could wear down to dangerous levels over time. The wire would need to be checked before and after each test as well as wrapping the wire in fiberglass for any sharp corners. If a wire's insulation is worn down the team would likely patch the worn insulation with Kapton tape or replace the section of wire depending on the degree of wear.

17.3 Controls

Because the flight controller was not made by this team and was instead purchased, the assembly of the control circuitry was relatively straight forward. This involved configuring the flight controller to use twelve of its I/O ports as outputs. These twelve output servo signals go to the twelve ESCs who then determine the current to supply to their respective motor. Note that it is not guaranteed that the flight controller would work on such a large craft because small deviations from hover may be more difficult to pick up by the controller. Thus, if the controller does not initially work, additional gyroscopes will have to be placed at the ends of the arms where angles and angle changes from pitch and roll will be more prominent. In this case, additional signal circuitry would be necessary connect the gyroscopes to the flight controller as well as configuring the controller to interpret these signals correctly. To avoid many of the problems with signal interference that are associated with analog signals, the gyroscopes, if used, would use digital communication to send information. Additionally, the flight controller would need to have power. The flight controller would require a Battery Eliminator Circuit (BEC) that would take the 51.8Volts in the power circuitry and convert it into a voltage reasonable to run the controls circuitry.

Depending on the magnitude of effects of electromagnetic interference from the motor, the signal wires going along the arms of the ESC would have to be twisted and/or magnetic bead will have to be added to reduce interference. The antenna for communication with the controls would have to be outside the main box to deal with potential interference from the metal and carbon fiber. There are shielded antenna extension wires that can be purchased for just this purpose, but the team would have to do testing to make sure that communication with the craft is retained at all times.

18 EXPECTATIONS AND FUTURE PLANS

Creating a full-scale working prototype of a manned multicopter commuter vehicle has remained at the heart of this project throughout its development. Despite expectations, team members have been fully aware of the financial needs of the project. Its large scale, numerous components, and safety concerns have made it difficult to keep the project's total cost below its initial funding resources. Attempts made to find new financial supporters but in the end the funds to make the full-scale model were not procured quickly enough to agree with the senior project's schedule. Therefore, options other than "full-scale" were necessary. The below sections detail the two additional options this project could have followed after failing to procure the appropriate full-scale funds, as well as the full-scale option. These options include an extensive testing and feasibility study, providing proof of viability of as many of the structural, propulsion and control systems as possible. Further options expand upon this with either the build of a scale model verifying the viability of full-scale prototype, or a full scale model providing a full scale proof of design concept. Note that to verify some of the components of the full-scale design, some aspects of these two options would be carried out whether or not additional funds were received. In the end, the team only had enough funding to complete most of Options 1 and 2 below, but future senior project groups may be able to expand upon these options in the future.

18.1 Option 1

Option 1 entailed extensive testing of the main components that make the Electric Commuter Multicopter what it is. For instance, 3-point bending of carbon fiber tubes, thrust data for the selected motor and carbon fiber prop configuration, and power output of different motors are various tests that the team planned on conducting. This simplified the entire project to a feasibility study, which would provide supporting evidence to the theoretical calculations to prove the design will be successful. This will serve as a baseline for future ECM teams to start from if the project returns to Cal Poly, San Luis Obispo in the ensuing years. However, this option did not include a prototype or a scaled prototype to show to the educational system or the transportation industry that there is an alternative form of small scale transportation in the form of personal multicopters. Until a full prototype is built and operated, the idea of an ultralight vehicle for the daily commuter and its validity will be limited.

This option was primarily based on the assumption of no additional funding from outside sponsors. With the funds donated to the project at this time, there wasn't confidence that anything more than a feasibility study was achievable. This option instead requires the essential materials from the ECM final design: primary and secondary equipment. Primary equipment includes carbon tubes, propellers, motors, and controls equipment. Secondary equipment includes testing materials, such as metals, wood framing, or wires, as well as technical testing equipment, which possibly entails generators, a DAQ, and various thermal and regulation supplies. However, to reiterate the importance of funding, the various tests were tentative on the amount of monetary resources available.

18.2 Option 2

Option 2 consisted of creating a scale model. Part of the difficulty and interest of this project is that the performance of aircraft this size in this category are often considered poor. Thus, in terms of propulsion, a scaled model would provide little insight. However, the controls scheme and structural components used in the model would yield some intuition development on how the full-scale craft would operate. The stability of the craft with the selected motor configuration would yield the most useful results where the wireless communication and data logging could be documented extensively and readily applied to the full scale model. However, dynamic and impact loads found in the model would, at best but unlikely, be scaled accordingly for comparison with to the loads expected from the full-scale craft, similar to the inconclusiveness of the propulsion at scale.

With this project's current funding resources or a relatively small increase in funding, a high-performance scaled model multicopter could have been built. However, independent of additional funds, a small,

hobbyist-style twelve rotor multicopter was built because it was essential to validate the craft's controls on a smaller model before its implementation onto the full-scale design for safety reasons. This multicopter was funded by money allocated by MESFAC. A scaled model would merely provide better estimates of the loads experienced by the craft and its in-flight energy consumption. However, the success of the scale model does not verify that a commuter multicopter adhering to project specifications is feasible, but it will provide a strong argument for or against final conclusions.

18.3 Option 3

Option 3 consisted of manufacturing and constructing the full scale Electric Commuter Multicopter, which encompasses the design specifications detailed in the Critical Design Analysis of this document. It would have either proven or disproven the design and the validity of a 254lb aerial vehicle, as well as the feasibility study. This would have had a significant engineering impact at Cal Poly and proven there are alternative ways of small scale transportation available to the transportation industry and average people. To clarify, this design is dangerous and the engineering team does not recommend it for commercial use until regulatory safety inspection of the FAA commence and all safety hazards are mitigated.

This option was based on receiving the full additional funding from outside sponsors as by referencing the cost analysis, Table 8.

19 ADDITIONAL DESIGN CONSIDERATIONS

19.1 Hexcopter Configuration

After deciding upon a twelve prop configuration, several prop layouts were discussed. The major alternative to the traditional quadcopter layout was a modified hexcopter layout, depicted below:

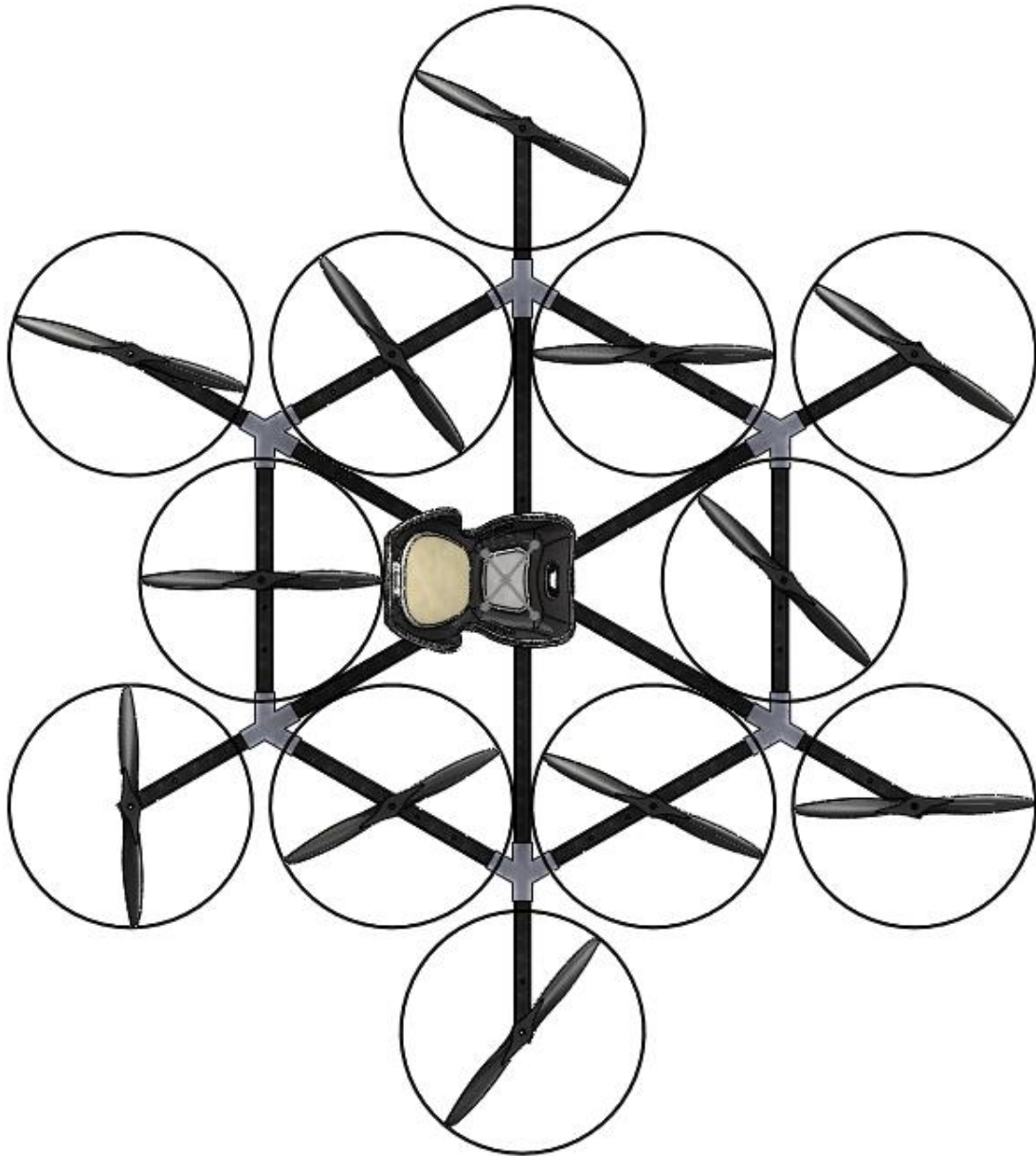


Figure 73: Top View of Hexcopter Concept

The Pros:

The connecting spars between arms would greatly increase the structure's stability and integrity. A large scale quadcopter has very large variable forces at the end of its spars, meaning that all of the vibrational energy is channeled through isolated carbon spars. This is concerning from a strength standpoint, but also from a deflection standpoint. This more interconnected hexcopter design would damp out vibrational energy by dispersing it between adjacent arms, resulting in smaller deflections and reduced impacts on fatigue life and overall vehicle control compensation.

The interconnecting spars also serve to eliminate most of the torsional bending that would arise due to imbalanced motors, non-centered loading, or gusts of wind. The layup schedule of most of the carbon tubes is heavily favored towards bending loads rather than torsional loading.

The hexcopter layout also allows the team to position the props in a much more compact fashion, which means that the craft's disk loading is much better. Therefore, the team would see an increase in efficiency and therefore flight time by adding more utilized disk space; the larger the disk area, the smaller the volume of air that must be accelerated to provide a given amount of thrust. This corresponds to less power used.

Finally, the compactness of this design means that it's possible to accommodate much larger props without exceeding the maximum footprint size. The model below contains 36 inch props and is still well within the required 18ft x 18ft maximum footprint. The reason that much larger props are desired is that a much higher thrust for the same electrical power supplied to the motors can be achieved. This would therefore decrease the amount of power necessary to achieve any singular thrust. However, larger props might theoretically require larger motors, which would drive the weight and cost of the structure up. If smaller props were selected, this design is still favorable due to the greatly reduced footprint area.



Figure 74: Hexcopter Concept

The Cons:

The primary concern with this design is the increased weight. Although comparable in overall carbon length, implementation of six auxiliary brackets will be required rather than four, and several of the motor mounts would have to be larger to interface with the middle of the interconnecting spars.

A large secondary concern with this design is the difficulty in control implementation. Thrust and yaw would be decently easy to implement, but roll and pitch would be difficult. The design would have to work in a modified hexcopter configuration, but symmetry concerns might disorient the rider as well as make the system less stable.

Most of the brackets would also be much more difficult to design and manufacture due to the acute angles between most of the spars. It wouldn't be impossible, but for the scope of the project, the team agreed that 90 degree angles would be more ideal.

The issue of entering and exiting the craft was also brought up. This concept would have to incorporate some means for the pilot to traverse or move the props.

19.2 Non-Traditional Quadcopter Control Scheme

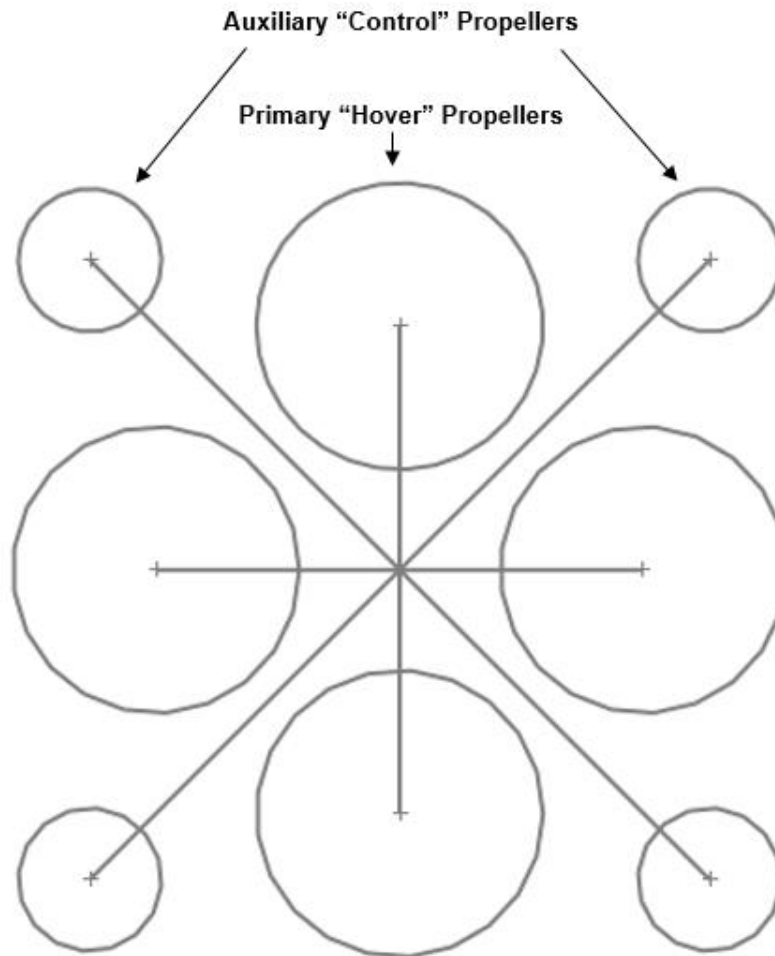


Figure 75: Non-Traditional Quadcopter Control Scheme

Another additional configuration was to take advantage of the large number of props required for the vehicle to diverge from conventional methods of controlling a multicopter. The idea was to design several primary "hover" props to operate at hover thrust and peak efficiency when supporting the entire vehicle weight in hover. Then several smaller auxiliary "control" props would embody a traditional quadcopter control scheme. These props would likely operate lower than their peak efficiency, but the relative size of the motors would make these losses negligible. The idea is very promising, but initial concerns that were not immediately answered led to the moving forward of the team's final design. One main concern is that the design is meant to be used by a commuter, or somebody that is going to spend a large majority of their time in the air moving forwards. This would mean that the rear hover prop would be providing the majority of the offset thrust for pitch, rather than the two motors used in an x-copter configuration. This would limit pitch sensitivity and response time. Also, for the four auxiliary motors and props to be capable

of maneuvering a 254 pound craft, a relative loss in roll and yaw sensitivity would be seen. This would make the aircraft less maneuverable. These important considerations eliminated this alternative design.

19.3 Alternative Landing Gear Designs

These are the landing gear designs that did not make the cut. Implementing a landing gear into the design proved to be an area full of contradicting interests. A solution was needed that would allow the vehicle to land in a comfortable fashion that would not cause any damage or harm to the craft or the pilot, even when the landing was more violent than anticipated. However, the existing weight of the already minimalistic structure dictated that the landing gear had to be extremely lightweight. Several designs were considered, but most were discarded due to their excessive weight.

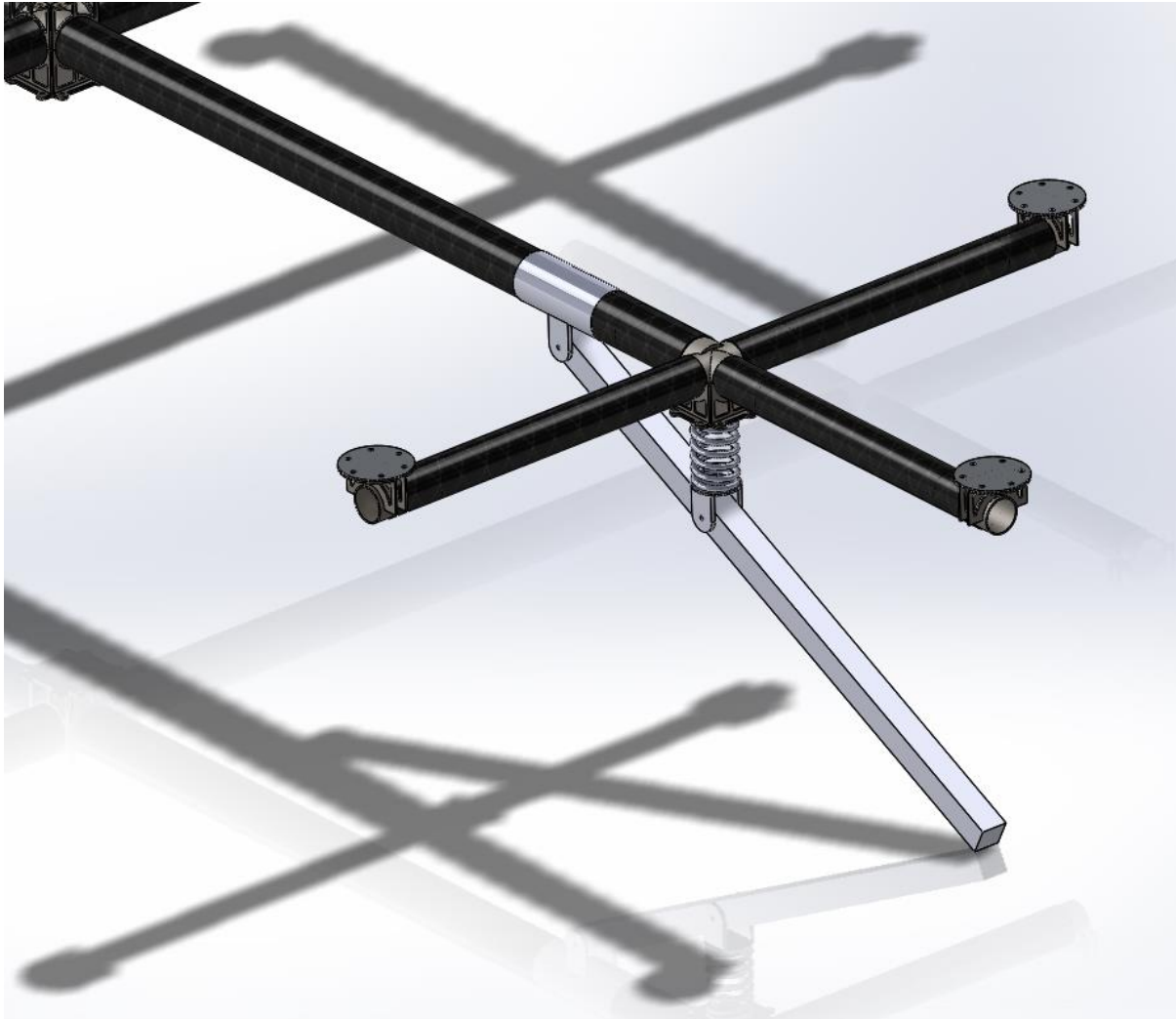


Figure 76: Landing Gear Preliminary Design 1

The first option (Figure 76) uses a long arm to exploit the small allowable deformations of the large springs. Many springs that can handle the loads that will be seen in the event of an aggressive landing have only 2, maybe 3 inches of travel. Such a large change in velocity in such a short distance would result in G-forces capable of crippling both the craft and the rider. This design would allow for upwards of 8 inches of travel with a spring that only provides 2 inches. As mentioned before, this design was eliminated due to its substantial weight.



Figure 77: Landing Gear Preliminary Design 2

Another attempt to achieve large deflections while withstanding large loads was the implementation of a central leaf spring array. The center mount would be taking most of the impact upon landing because all of the pilot's weight is directly above the bracket. The original design for the leaf spring was a single, curved continuous piece of spring steel, but due to manufacturing concerns, the team was forced to use something like the system depicted in Figure 77. Four pieces of spring steel would be welded to the central landing gear plate, and a cross-shaped reinforcement would be welded between the arms. This would not only allow the structure to deform along the longer members via bending, but also allow the cross section to absorb energy through elastic elongation. This design is decent for the calculated loading conditions, but once again proved to be too heavy to implement.

19.4 Multicopter Control Interface

In the initial design of the craft, the manner in which the pilot interfaces with the control system in an ergonomic way was not incorporated. The team has since then designed structural components that will help the user control the aircraft in a way that is comfortable and adjustable for an average adult pilot's needs.

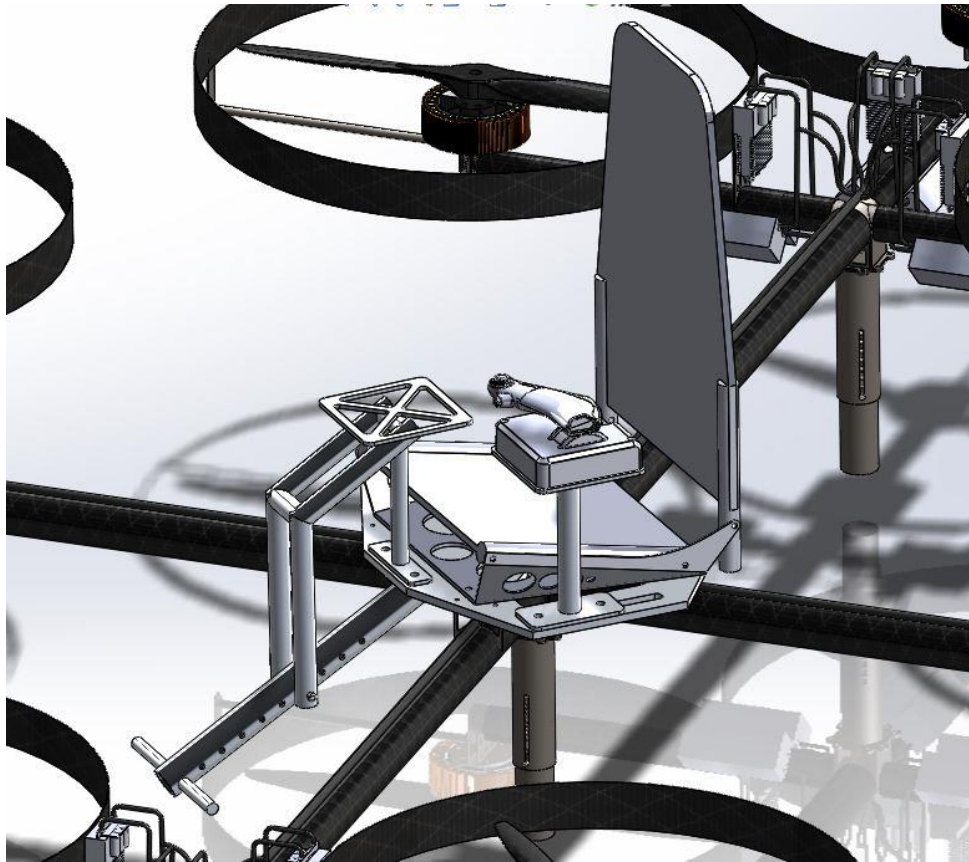


Figure 78: Full controls interface assembly placed on full scale vehicle.

The first component that was redesigned was the seat plate. In order to integrate the necessary pieces to the seat in a condensed fashion, the seat plate was configured to allow access to a foot rest, throttle stand, a joystick stand, joystick fork and the new selected flight seat. The seat plate's width was enlarged to accommodate the two side slots for the throttle stand. The plate's length was also increased to allow room for a four bolt pattern for the foot rest tube. The modified design can be seen in the following image.

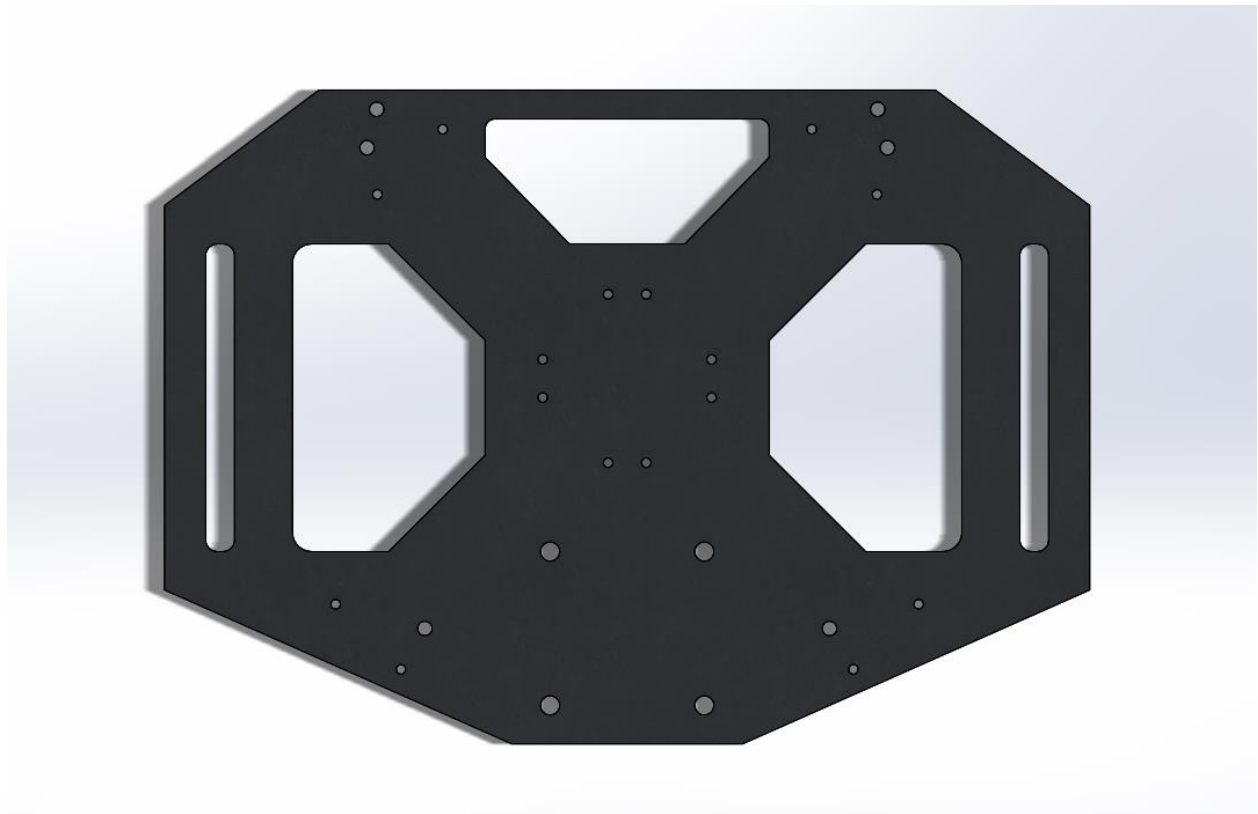


Figure 79: Solid model of the revised seat plate structure, extended to allow room for the throttle stand, foot pegs, and joystick stand.

The increased surface area of the plate brought additional problems of stress concentrations and large moment forces so to help, four wall structures will be bonded to the crafts spars to hold the weight. This can be seen in the following figure.

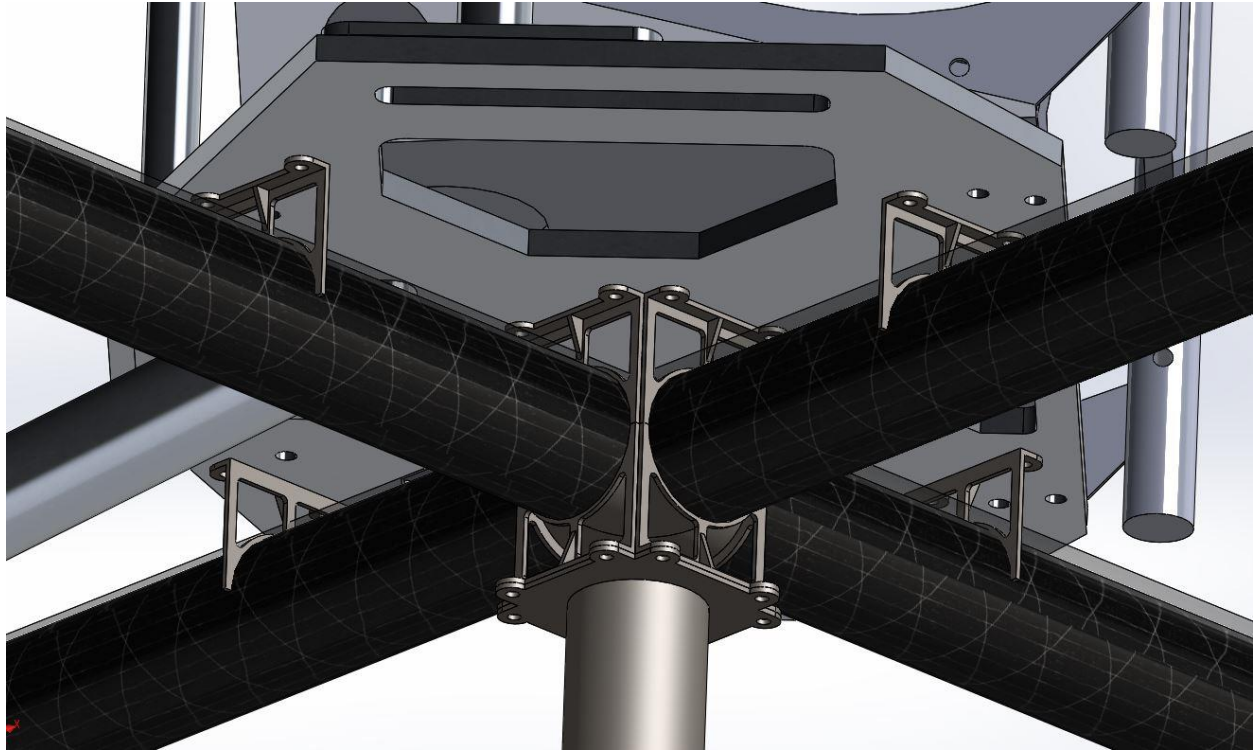


Figure 80: Underside view showing the additional plate to spar support braces.

To allow for a comfortable flying experience the user's legs must be supported and not allowed to dangle freely. A support tube was designed to protrude down and in front of the seat plate far enough away from the seat to allow for the pilot's leg length. It was assumed that the rider would not put a high load on the leg pegs due it being a simple rest, so a large moment is not expected. To allow for various leg lengths, holes would be placed at equal distances along the tube. The foot pegs could be removed and placed at different holes according to the rider's height. This is shown in the following image.

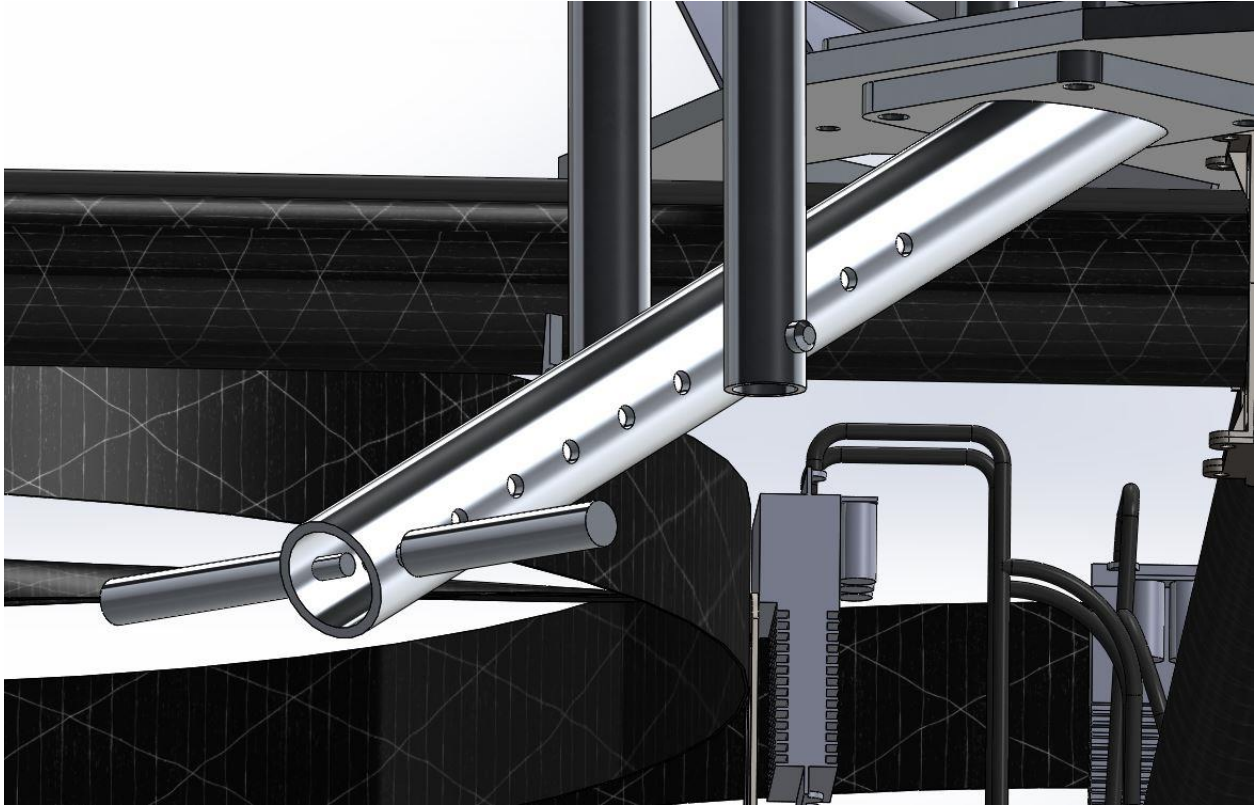


Figure 81: View of the rider leg support tube as well as adjustable foot pegs.

A joystick fork was designed to allow easy access to the seat when the user sits down. The fork would be hinged along the foot rest tube so it can swivel forward to allow room for the pilot. A tightening mechanism similar to a quick release skewer on a bikes wheel hub would be used to tighten the fork on the support tube. The fork's holes would be the same diameter as the foot pegs so it can be adjusted along with the foot pegs. When the pilot is situated on the flight seat the joystick could then be brought down to connect with the joystick stand. To allow the Saitek x52 joystick to be attached to the fork, a plate would be welded to one end of the fork and the joystick could be secured to the plate. The joystick fork can be seen in the below image.

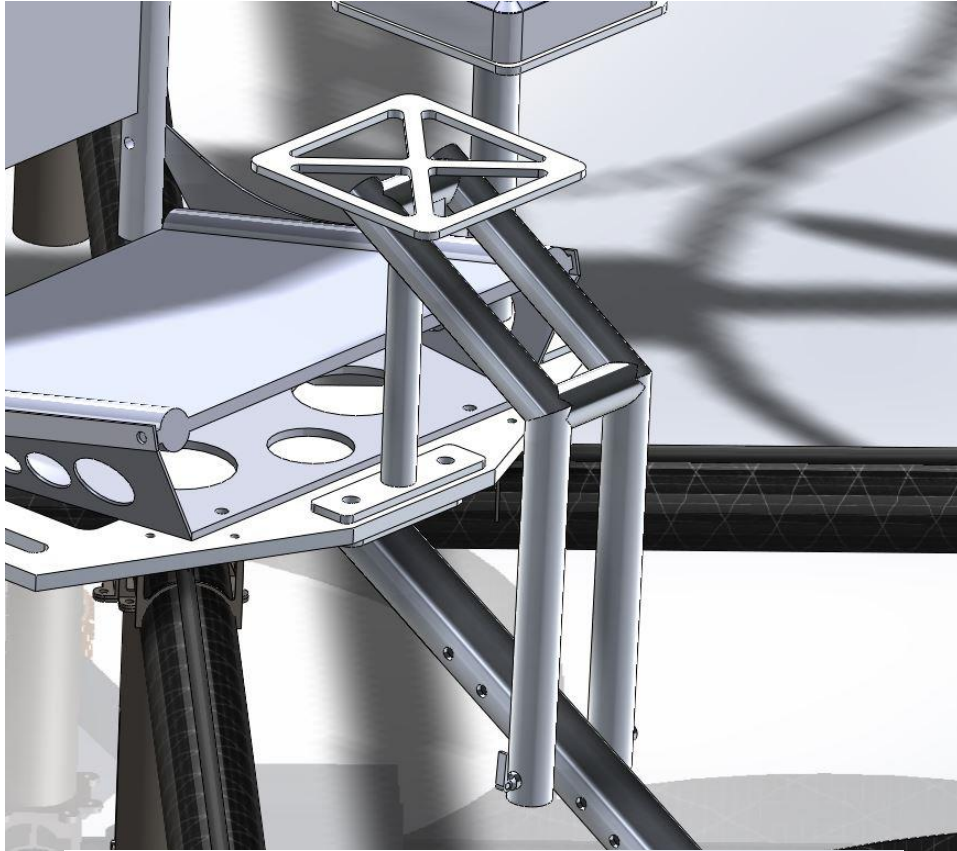


Figure 82: Solid model of the joystick fork, which allows the user to rotate the joystick plate away from the user during entry and re-entry.

The joystick stand is bolted down to the front of the seat plate using the front two cut for the leg support tube. This component was designed to be tall enough for an average adult, so that the joystick could be controlled comfortably. The joystick stand used a spring activated mechanism to allow for the joystick fork to snap into the place. To allow for the pilot to leave the aircraft the user would just have to disengage the springs via a button on the side and the fork would be released and lifted. The joystick stand is shown below.

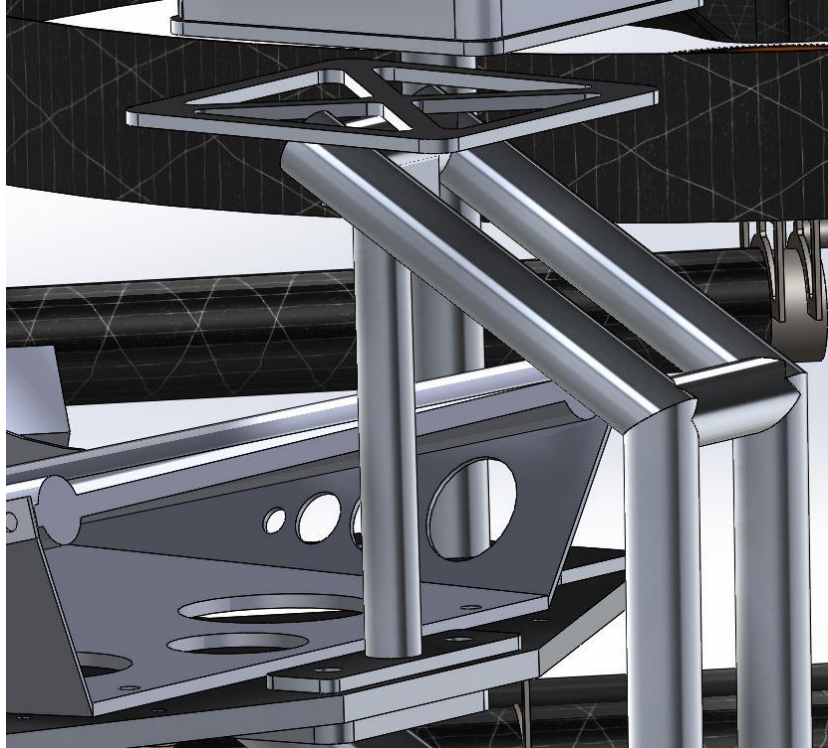


Figure 83: Joystick stand used to lock down the joystick fork for operational use

The throttle stand was designed to accommodate the Saitek x52 throttle. The stand would be connected to a base piece where two t-slot bolts with screw head tops, allowing for a dolly movement along the slot axis for adjustability. Slots are available on both sides to accommodate both left and right handed users of the throttle. The throttle stand can be seen in Figure 84.

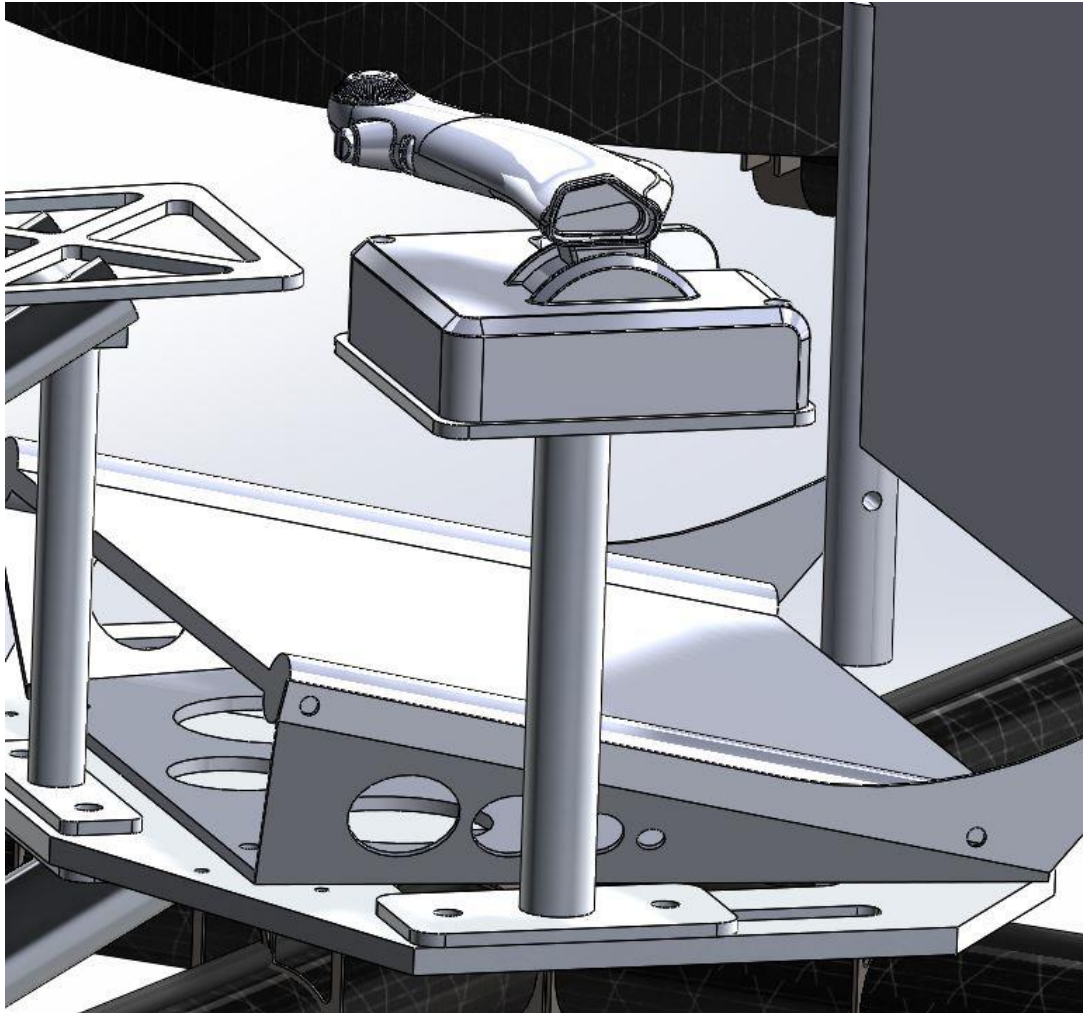


Figure 84: View of the vehicle's throttle stand positioned over its slot for easy adjustability.

The components mentioned above were designed to be made from Aluminum 6061 alloy to provide the necessary strength and weight for an ultralight aircraft. The estimated additional weight of these components is near 11 lbs. This weight would take away from the battery weight needed for the initial the estimated flight time. The new crafts weight would be 193.5 lbs allowing room for 27 Li-Po batteries, effectively decreasing our flight time to roughly 7.5 minutes. This data is shown in table 13.

Table 13: Approximate weight the control components add to the multicopter’s total weight.

Component	Material	Weight (lb)
Leg Support	Aluminum 6061	3.09
Throttle stand	Aluminum 6061	2.21
Joystick stand	Aluminum 6061	0.89
Joystick fork	Aluminum 6061	2.74
Feet Pegs	Aluminum 6062	0.36
Center seat Mount Wall	ASI 4340 Steel	0.44
Saitek x52	Plastic	1.1
New Seat Plate	Aluminum 6061	12.66
Total Control Component Weight		23.49
Structure weight		170
Total Craft weight		193.49
Total battery Weight		60.51
Individual Battery Weight		2.23
# of Batteries		27.13
Flight time/Battery Pounds (s/lbs)		7.4
New Fight time (min)		7.4629

19.5 Communication Modifications

In the original CDR, the full user interface setup included the use of a Scherrer TxRx700 Lite for communications with a transmitter that would be connected to the Saitek control system via a CompuFLY USB to PPM converter. After further research into the topic, it was discovered that the USB to PPM would work backwards from what it was originally assumed it would do; rather than convert USB signals from a joystick to a PPM signal used by the receiver, it would convert a PPM signal from a transmitter to a USB signal that would then be compatible with the joystick via a computer. This created an expensive over complicated system whose only purpose would be to effectively hack the Saitek transmitter we were using. From here a much simpler solution was found, utilizing telemetry kit with the Mission Planner system the team was already using. The telemetry kit consisted of two telemetry units which could communicate between one another; one plugged into the TELEM port of the Pixhawk, the other into a USB slot of the computer. This allows for a very customizable experience with easy setup and reliable connectivity. It also allows for the connection of a transmitter and receiver for backup fail safe. For RC applications such as the miniature multicopter, this set up is highly recommended. For the actual full sized vehicle, we recommend building an actual converter that uses separate control board to convert a direct USB signal into a PPM signal and then feeding that directly into the Pixhawk. Figure 85 shows an image of the telemetry kit.



Figure 85: NEEWER 3DR telemetry kit including both modules, two antenna, and the telemetry port connector.

19.6 Microcontroller Modifications

The original CDR specified the use of the OpenPilot Revolution as the control board for the full sized craft. Original testing intent was to purchase and use the OpenPilot Revolutions as part of the miniature testing. The company producing the microcontrollers is a hobbyist funded kickstarter, and they had gone into a cycle of low to no production. Upon request we received confirmation that a board was being manufactured for us. After a few further interactions, all contact was lost and the team was left having to find an alternative route. Speaking with a contact at 3DR, the team was assured that a Pixhawk could be utilized for our application, with even the possibility of independent control. This fact, as well as availability, and team familiarity with the platform spurred the purchase and testing of the mini with the Pixhawk. In order to get the vehicle off the ground, the decision to bank each arm of motors as one input into the Pixhawk was chosen. This allowed the use of all 12 motors, but the Pixhawk to think it was configured in the standard x-copter configuration. Further experimentation with the Pixhawk, including mixing, may allow for the independent control of all 12 motors, but time and programming constraints hindered efforts in this regard. For the full size craft, the team stands behind recommendation to use an OpenPilot Revolution, but if the unit continues to be difficult, the use of the Pixhawk in its current configuration, or expanded upon via mixing would be acceptable.

19.7 Pilot Protective Structure

Safety for the pilot should always remain paramount and to insure this a structure to protect the pilot is highly advised. If the project objective of ultralight regulation were to be modified one option to protect the user is designing and building a fiberglass or carbon fiber fairing which provides a shield from flying debris and high velocity wind. This fairing would not provide complete protection from a catastrophic crash but it could mitigate the effects of an uncontrolled fall to the ground. An alternative design would include a type of roll cage, preferably formed from carbon fiber to decrease overall structure weight. Carbon fiber would be the most costly option and would result in a complicated manufacturing process

but its strength and weight benefits outweigh these negatives. Alternatively the roll cage could be fabricated from an alloy such as aluminum, however this would increase the structure weight dramatically. This roll cage could also incorporate skids which would avoid the design of separate landing gears. A roll cage design can be seen in Figure 86.



Figure 86: One possible roll cage design constructed from carbon fiber added to the final multicopter structure.

20 TEST PLAN

In the immediate future, the team intends to run several tests in order to validate the results of the analysis. These should be completed before purchasing components for the construction of any prototype. The following sections entail the test reports from the Structures, Propulsion, and Controls groups. The test reports explain the purpose, procedure and their respective results.

20.1 Structure

20.1.1 Abstract

The Structures team designed and implemented two tests, the 3-point bend test and cantilever beam test, to validate determine whether the Electric Commuter Multicopter structure would withstand the applied loads and design parameters.

The 3-point bend test was to determine the effective flexural modulus of the main arm. This value is to predict the failure mode of the arm and to ensure that the tip deflection does not exceed the value specified by the problem definition. A viable method of testing was used, however it is prone to error. The carbon arm was simply supported by two steel jack stands that had minimal structural deflection during testing; however, the jack stands were prone to instability because of wobbling, impacting the results of the test. Weights were suspended over the middle of the carbon fiber arm and a dial indicator was placed on each side of the midline to measure the deflection of the tube for a given load. The data generated from this test allowed us to form an estimate for the flexural modulus of the tube.

The 3-point bend test results did not coincide with the manufacturer's specifications. The carbon tube manufacturer, C-Tech, specified a flexural modulus of 11 msi, but the experiment indicated a flexural modulus of 8.23 msi. However, this does not mean the carbon fiber arm needs to be replaced or redesigned; the flexural modulus still allows for angular deflections within the acceptable parameters (below 8.1 degrees) for our purposes with a safety factor of 1.5.

The cantilever beam test was designed to simulate the 271 lb loading condition on the end of a fixed 52" carbon fiber arm. This would test the strength of the center mount welds, carbon to steel joint connection, and the carbon fiber arm. A steel test jig was designed and built to hold the setup in place during the loading. The only facility that could withstand this test was Room 135 in Building 192, because it has a Strong Floor to bolt the test jig to.

The cantilever beam test proved to be beneficial in a variety of ways. The center mount welds and the carbon arm proved to be strong enough to take the loading and even survived a 500 lb test end load. However, the carbon to steel bonds did not pass the test; at 250 lbs the adhesive bond delaminated and failed.

20.1.2 Three-Point Beam Test

20.1.2.1 Purpose

The Electric Commuter Multicopter senior project team intended to perform a 3-point bending test to determine the effective flexural modulus of the main arm. This would allow us to verify that the custom-made carbon fiber tubing from C-Tech would perform as intended during operation of the vehicle. The stiffness of the carbon main arms is important for the design of the craft because it ensures that the thrust of the motors is not directed significantly in the horizontal direction (which would cause drift of the vehicle and general loss of thrust) and serves to keep the vibrations inherent in the craft from developing and oscillating

20.1.2.2 Equipment

Listed below is the equipment we used for the **3-point** test:

- Grizzly G9849 magnetic base and dial indicator
- 52 inches of large diameter carbon tubing (2.500" ID x 2.746" OD)
- 210 lb of weight plates
- 40 feet of 550 cord
- Level
- 2 automotive jacks
- 4 cinder blocks

Shown below in Table 14 is a cost estimate for the experiment. The total expenditures for the experiment totaled about \$440.

Table 14: Cost estimate for the three point bend test.

Cost Analysis			
Item	Quantity	Unit Price	Total Cost
Carbon Tube 2.5" x 2.7598" x 78.7402"	1	\$412.68	\$412.68
Grizzly G9849 magnetic base and dial indicator	1	\$27.45	\$27.45
Total Cost			\$440.13

20.1.2.3 Setup & Procedures

For the 3-point test, our 52" carbon fiber tube experienced a point load at the midpoint with one pinned support load at either end. Shown below in Figure 87 is our experimental test setup.



Figure 87: Experimental apparatus for the three-point bend test. Note the pair of dial indicators on either side of the load.

Each end was supported by automotive jack stands spaced 50" apart. The ends of the carbon tube were loosely tied in place with 550 cord to prevent it from rolling around during the test. To apply the point load, we hung weights from the center of the beam with 550 cord and lowered them safely down with one person on either side of the beam while a third person held the carbon tube lightly to prevent it from being grabbed and rotated by the paracord. To measure the displacement of the carbon fiber arm, the team used two Grizzly G9849 magnetic bases and dial indicators. These devices were capable of measuring up to an inch of displacement with a resolution of 0.001", more than precise enough for our purposes. We placed the tips of the dial indicator system directly below the centerline of the tube but offset from the 550 cord and weight, then measured the distance along the tube from the jack stands to the dial indicators. The weights were tied together in pairs so that they could be easily hung over the tube without the risk of overloading the paracord.

We then began applying the loads to the tube, placing one set of weights on the marked center of the beam. The displacements from the dial indicators were read, then the load was increased with the addition of more weights. We repeated this procedure until we had used all of our weights (a total of 210 lbs), then the pairs of weights were removed one at a time. When all the weights were removed, we checked the system for zero; if the dial indicators didn't return to within 0.003" of zero, we threw away the data points from that trial. After several trials being thrown away, we eventually obtained data for two trials with 44 total data points. We then used beam theory for a simply supported beam to calculate the applied stresses and strains at the locations of the dial indicator tips and divided the applied stress by the calculated strain to obtain an estimate for the flexural modulus of the tube.

20.1.2.4 Safety Concerns & Solutions

The risk factor of this test was miniscule enough that minimal safety precautions were needed. Human safety was ensured, therefore safety glasses were mandated to prevent any debris coming in contact with the user's eyes. Also, no user was allowed to be under the hanging weights due to the possibility the system collapses.

The system was comprised of two steel jack stands holding up the carbon tube as you can see in Figure 87. The carbon fiber tube was anchored to the steel stands by utilizing 550 cord and wrapping the steel and carbon. This served more as a safety precaution than a structural purpose. With the applied loads in the middle, this kept the carbon tube stable on the steel stands, preventing roll and slip of the tube.

20.1.2.5 Expected Results

From the three-point bend test on the main carbon tube we obtained different deflection values for different loads. This data would be used to calculate the flexural modulus of the main arm, assuming that the material stays in the linear elastic range (we do not expect to exceed the linear elastic range for the tubing). We expect this calculated flexural modulus to be roughly between 11 and 13 msi, which we calculated using a simple volume fraction analysis. The estimate of 11 msi neglects the stiffness that may be added by the $\pm 60^\circ$ plies in the tube, while the 13 msi estimate optimistically assumes that those plies will have proportionately lower but still significant stiffness.

20.1.2.6 Testing Results

Shown below in Figure 88 is the stress-strain curve for our tube under 3 point bend test conditions. The data from the 3-point bend test indicates a flexural modulus of about 8.2 msi, as can be seen by the regression line for the combined data set. Worth noting is the spread of the data at each applied load, seen in the figure as the horizontal clusters of data points at each stress level. This indicates a lack of repeatability and consistency in the testing, and this assessment is backed up by the large confidence interval we calculated for the flexural modulus. The true modulus of the tube (as found by our test) exists within the bounds of 7.51 to 8.88 msi with 95% confidence.

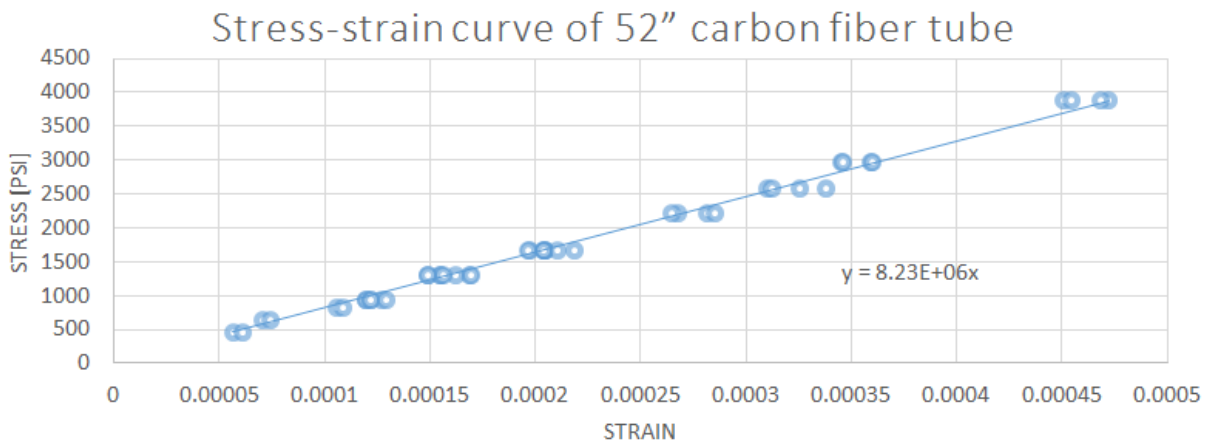


Figure 88: Stress-strain curve for the carbon fiber main arm during three point bend testing

The estimated flexural modulus obtained by our three point bend test is much lower than the range of predicted values, being about 30% lower than our conservative estimate of 11 msi. This outcome was most likely due to our test apparatus not being stiff enough for the loading applied to the tube; the deflection measured by the dial indicators was most likely a combination of the tube deflection and the

deflection of the automotive jack stands. To test this assumption, an experiment was commissioned by the team to be carried out in Cal Poly's Experimental Methods of Design course (ME 410) which would replicate the test but replace the dial indicator measurements with measurements from strain gauges. This testing resulted in a new estimate for the flexural modulus of 12.0 ± 0.05 msi with 95% confidence. The stress-strain curve for test can be found below in Figure 89. This new value falls right in between our estimates of 11 to 13 msi for the flexural modulus. We are inclined to accept the results of this new test over the results from our own testing because of the general quality of the new data (which exhibited perfect repeatability and no observable hysteresis) and because the strain readings from the new test are actual measurements of strain and are not estimated from beam theory; this means there was less estimation required to obtain the final modulus estimate. For more information on the testing methodology and results of this new test, please see Appendix C: General References and Tables.

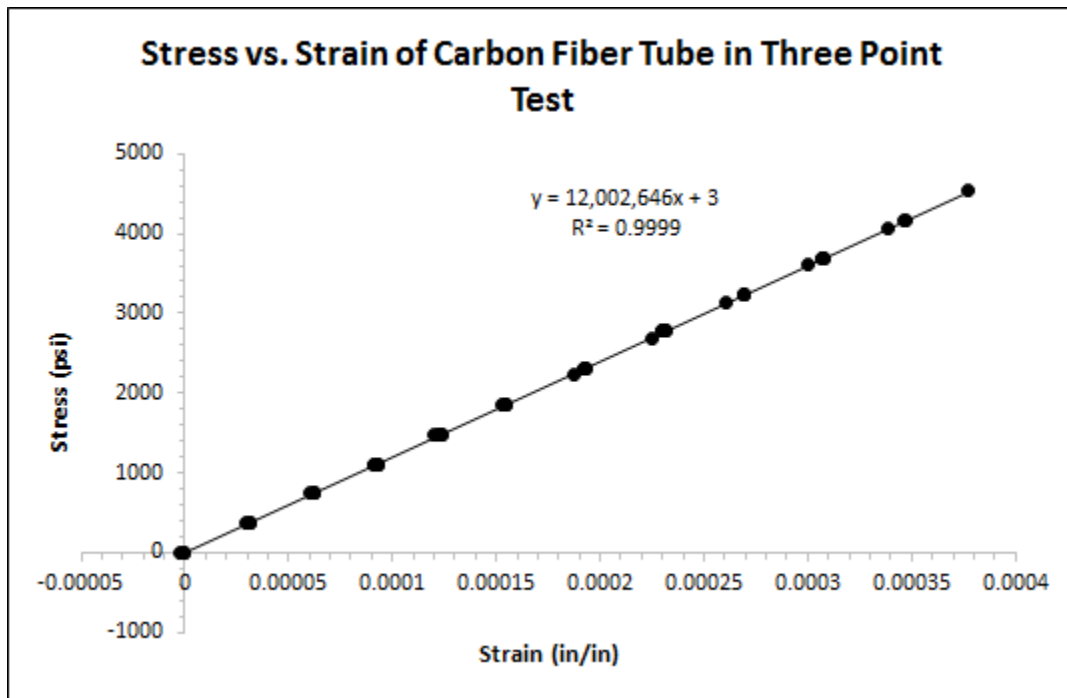


Figure 89: Stress-strain plot for the tube during the three point bend test utilizing strain gauges.

20.1.2.7 Conclusion

The initial 3-point test outputted a flexural modulus of 8.23 msi, far below our original estimated value of 11 msi. The discrepancy of these values may be caused by problems in our test method and the lack of stiffness in our test apparatus. For clarity, an additional test with strain gauges was performed by one of our team members in ME 410 (*Experimental Methods of Design*). From this test a flexural modulus of 12 msi was obtained. We are convinced that this value better represents the performance of the tube, as the strain gage method is in general a much more accurate method of obtaining structural performance estimates than our own method. From this the team concluded that this carbon fiber arm, with a flexural modulus above 11 msi (the conservative value used in our stiffness calculations and assumed as the minimum acceptable performance for our custom tubes), is stiff enough for use in our vehicle design.

20.1.3 Cantilever Beam Test

20.1.3.1 Purpose

The Electric Commuter Multicopter senior project team planned to perform a cantilever beam test on the center mount and main arm for further structural analysis. Specifically, this test was intended to verify a maximum load capacity for the center mount welds and the adhesive bonds attaching the carbon fiber main arm to the center mount. The team used audible and visual cues during the cantilever bending test to determine failure of the main arm and center mount assembly. This test was intended to be carried out before beginning the production and assembly of the center mount or other main structural components of the vehicle.

20.1.3.2 Equipment

Listed below is the equipment that was used for the cantilever beam test:

- 2.5' of 4130 chromoly tubing (2.500" OD x 2.124" ID)
- 52" of large diameter carbon tubing (2.500" ID x 2.746" OD)
- 1/16" X 36" ER70S-2 Harris® ER70S-2 Carbon Steel TIG Welding Rod
- 3 Black Oxide Steel Studs (0.5" x 7.5")
- 550 cord
- Scotch-Weld 2216 (1 oz. mixed, later substituted with Hysol 9462)
- Bond Line Controller, 0.007" variety
- Steel test jig fixture
- Weight Scale
- Automotive jack
- Strong Floor Room

Shown below in Table 15 is a cost analysis of the test fixture. The total cost for the test came out to be about \$420, not including the cost of the carbon fiber tube which we had already purchased.

Table 15: Cost Analysis of the Test Fixture for Cantilever Beam Test

Cost Analysis			
Item	Quantity	Unit Price	Total Cost
10 GA. (.135 thick) Steel Sheet Hot Rolled Steel Sheet	1	\$67.52	\$67.52
Black-Oxide Steel Adjusting and Positioning Stud, 1/2"-13 Thread, 7-1/2" Overall Length, 1-1/2"& 1-1/2" Thread Lengths	3	\$2.24	\$6.72
4130 Alloy Steel Round Tube, 2.500" OD, .188" Wall Thickness,	2	\$153.02	\$306.04
Carbon Tube 2.5" x 2.7598" x 78.7402"	1	Included in 3-Point Test Plan	Included in 3-Point Test Plan
Scotch-Weld 2216 Epoxy	1	\$18.75	\$18.75
1/16" X 36" ER70S-2 Harris® ER70S-2 Carbon Steel TIG Welding Rod	1	\$10.40	\$10.40
Bond Line Controller .007"	1	\$9.99	\$9.99
Total Cost			\$419.42

20.1.3.3 Setup & Procedures

For the cantilever beam test, the team first assembled and welded together the center mount (without any brackets) and bonded it to the carbon fiber main arm. A model of our center mount can be seen below in Figure 90.

The test fixture that held the center mount assembly in place during the test was a custom designed and manufactured steel apparatus made by the team. This steel test fixture, shown below in Figures 91 and 92, is made out of $\frac{1}{4}$ " low carbon sheet steel with a yield strength of 38 ksi. The fixture was designed to hold the carbon tube parallel to the ground and above an automotive jack stand and a 500 lb scale. During use, the test fixture places a maximum of 315 lb on each of the screws located at the back of the bottom plate under full loading conditions (a 270 lbf load at the end of the carbon main arm). This places a maximum pullout force of 315 lbf on the steel rails of the strong floor, well below their rated load capacity of 500 lbs. For more information on the analysis of the test fixture, please see Appendix B: Engineering Analysis and Hand Calculations. For more details on the test fixture, please see the provided engineering drawing in Appendix C.

The procedure is comprised of bolting the test fixture to the strong floor, attaching the center mount assembly to the rigid test fixture, and positioning the automotive jack directly under the opposite end of the 52" carbon fiber arm. Under the automotive jack is a scale measuring the force applied by the automotive jack onto the carbon fiber tube. The automotive jack will be operated until a load of 270 lbs is applied at the tube end or until premature center mount failure occurs.

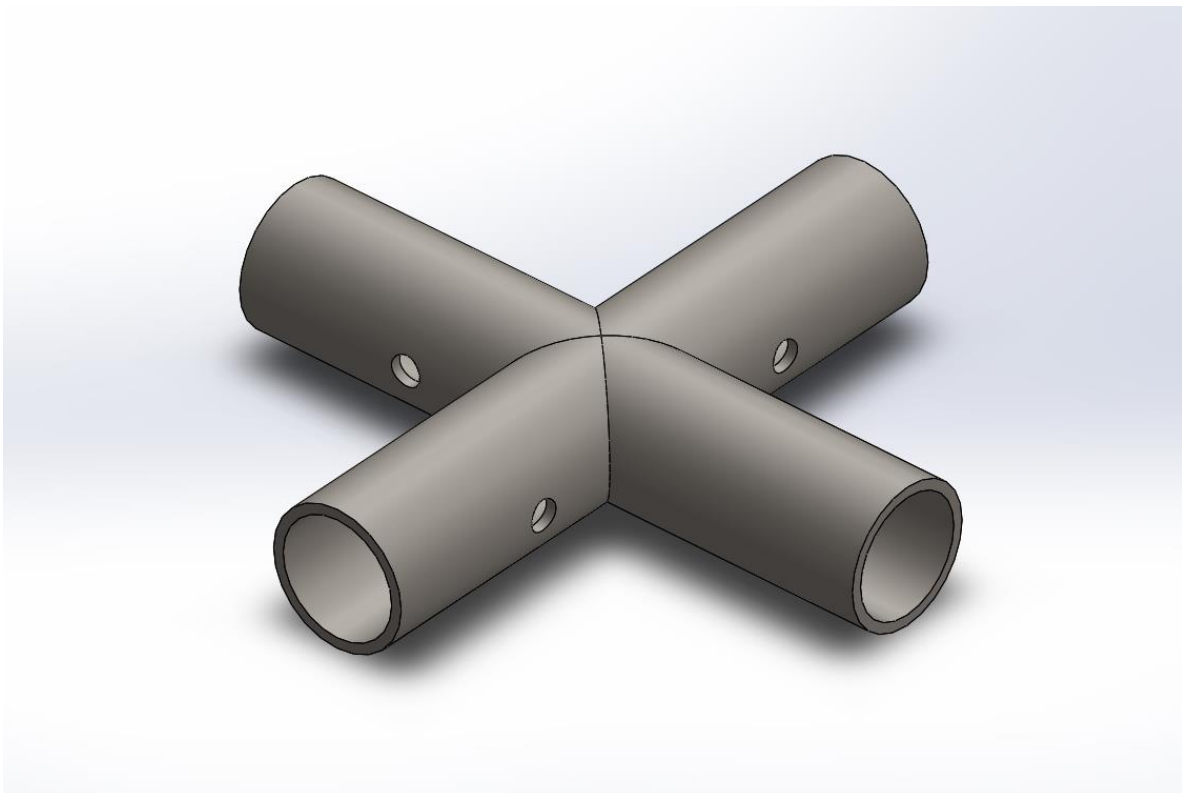


Figure 90: Steel Center Mount Test Piece.

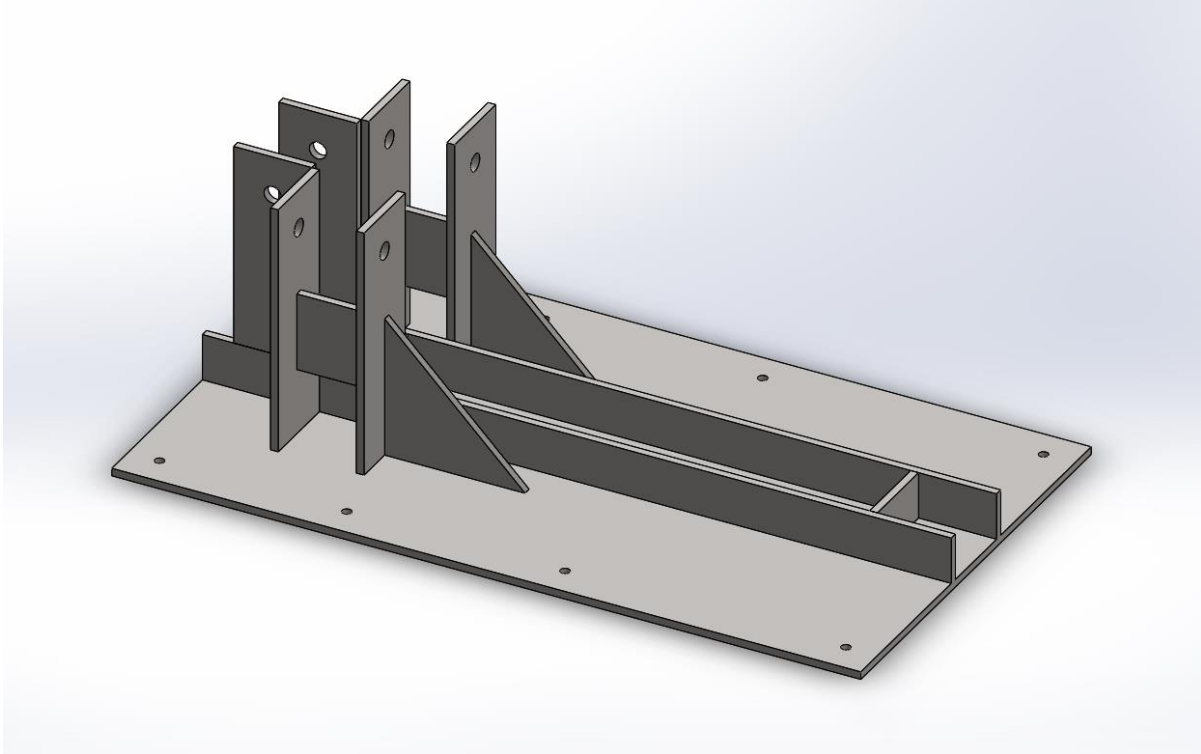


Figure 91: Cantilever beam test jig

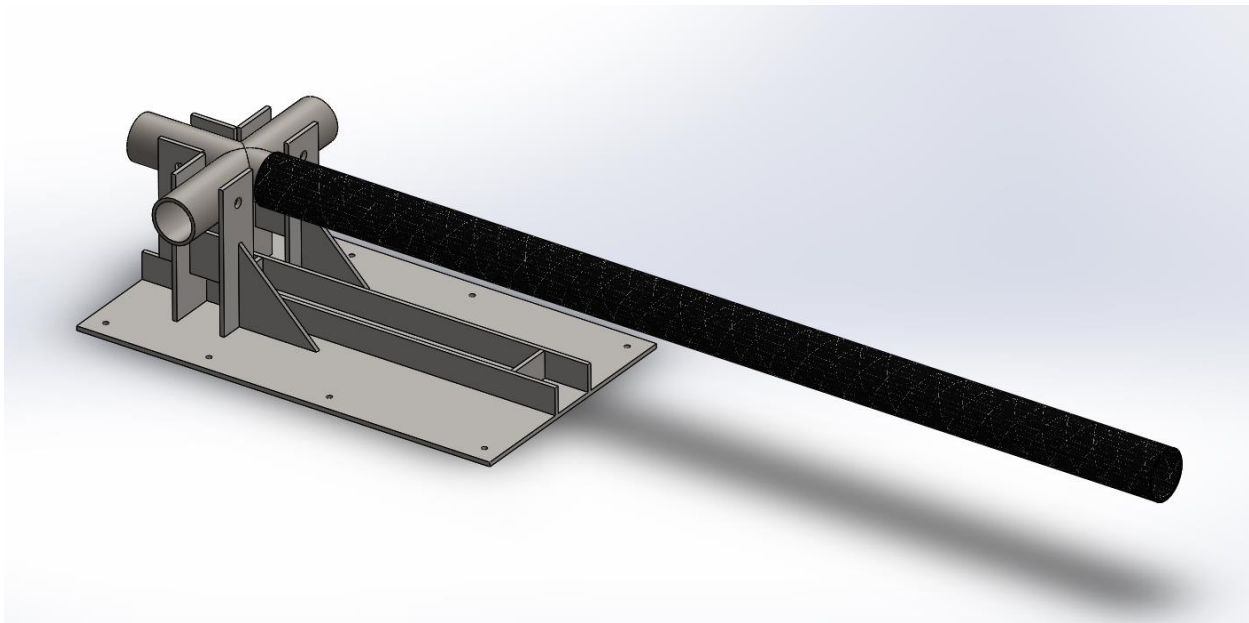


Figure 92: Cantilever beam test assembly illustrating one quadrant of the Electric Commuter Multicopter with a 52" carbon fiber tube, center mount and test fixture.

20.1.3.4 Safety Concerns & Solutions

This test was a test-to-failure, and therefore there was the significant possibility of failure and the increased risk of injury. The first scenario predicts the 4130 chromoly center mount welds failing. Due to the upward force of the automotive jack onto the carbon fiber arm, this would cause an upward and

backward acceleration toward the opposing end of the apparatus. To mitigate the possibility of injury, operators and supervisors located themselves away from the test setup in the direction of the automotive jack operator. Care was taken to ensure that the automotive jack operator increased the level of the jack from a location extending from the tip of the carbon fiber tube and in the opposite direction of the test fixture.

The next component to fail would be the adhesive bonds between the center mount and carbon fiber tube. Slipping would occur axially more than tangentially, therefore the possibility of the carbon fiber tube detaching entirely from the center mount is likely. This could cause injury if the operator or supervisors are near the test system or directly in line with the tube. To mitigate these possibilities, the operator during the test was located to the side of the tube and wore safety glasses and a face shield.

During testing, if the test supervisor feels that a situation is unsafe, they have the authority to stop the test at any time and take the appropriate actions necessary to ensure that it is safe to continue testing. If any individual is injured during the test, the test supervisor will have the authority to summon medical attention or send the injured person to a medical center. If it is determined that medical attention is required, the test supervisor will be responsible for calling 911 or the appropriate emergency number. If the test supervisor is injured during the test, the secondary test supervisor will receive the responsibilities of the test supervisor. In the case of a fire, the local fire department will be called immediately, no matter how small the fire is. If any portion of the test setup breaks, no further testing commence until the cause of failure can be identified and fixed to prevent future failures and potential incidents.

20.1.3.5 Expected Results

In the cantilever bend test, when applying the test load to simulate landing we expected the entire apparatus to survive. At a minimum loading of 310 lbs the welds in the center mount were expected to fail, based on the predictions for the stresses induced in the welded joints between the steel tube sections making up the center mount. The bond between the carbon and steel was expected to fail at a loading of 425lbs using a moderate estimate of 2000 psi of average shear strength for the bond surface. Overall, the test was expected to demonstrate that the center mount and tube assembly should hold up to the rigors of actual use.

20.1.3.6 Testing Results

The cantilever beam test gave us several key pieces of information about our vehicle design. First, the adhesives bond between the center mount and carbon main arm failed prematurely with a 247 lbf end load. At that point, the epoxy bond delaminated suddenly with a very audible cracking noise. Examining the bond at this point, it became clear that the bottom surface of the steel center mount had peeled away from the carbon main arm. The nature of the failure was such that the tube could continue to carry the load applied but that cyclic loading of any significant magnitude would completely break any remaining epoxy bond between the two tubes.

Running calculations on the failure load of the bond, we obtained an average bond shear strength of 581 lbf over the length of the bond. This is far lower than the 2000 psi of shear strength that we expected to see for this connection, and it indicates that bond peeling is the driving factor in bond strength for a tube to tube connection such as ours. We had assumed that the bond could be adequately modeled with a line load around the edge which placed the adhesive bond in shear stress, but instead we observed that the bending and deformation of the carbon tube under significant loading can cause higher stresses to develop in the bond. This highlights the need for future senior project teams working on the Electric Commuter Multicopter project to examine this connection more closely and perhaps even to run non-linear finite element analysis on the bond to aid in their redesign process. In any case, the connection between the main arms and the center mount needs a redesign; this could take the form of using a tougher epoxy, designing for a longer bond length, or using a different attachment method altogether. For the sake of testing the center mount and main arm, we decided to continue the application of load on the end of the main arm despite the delamination of the epoxy bond. The center mount and the main arm

survived testing at both the 247 lbf load and at the required 271 lbf end load with no adverse effects or observed yielding. For the sake of completeness, we then took the loading up to 500 lbf before backing off the load entirely.

The center mount survived the 500 lbf load with no observable adverse effects. It did not appear to yield during the test and the welds remained functional, giving us high hopes for the feasibility of our design. However, the carbon fiber main arm exhibited audible ply cracking at loads 350 lbs and above, indicating that the main arm was not entirely unaffected by the load. Also worth noting is the tube was still functional and did not exhibit yielding when returning to a zero load state. These results indicate to us that the assembly could likely survive end loads well above the required 271 lbf during usage, but that it would not be able to do so repeatedly. This means that, in the event of an emergency situation where a main arm is overloaded, a pilot of the aircraft might be able to land safely without the craft coming apart.

20.1.3.7 Conclusion

The 52" carbon fiber arm with a layup schedule of $[\pm 60/0_6/\mp 60/0]_s$ and the center mount welds will suffice for this application. However, the adhesive bond will not. An epoxy with a greater strength should be researched and analyzed.

20.2 Propulsion

20.2.1 Abstract

The performance test of the Turnigy Rotomax 80cc motor took place on February 28th, 2015 between 1100 and 1400. The purpose of the test was to determine if the Turnigy Rotomax motor would be a suitable low cost substitute of the JobyMotors JM1S. The results of the test showed that the Turnigy Rotomax 80cc motor was not a suitable alternative for a fully loaded test. The maximum continuous thrust of the motor is around 30lbs, compared to the 50lbs required for a fully loaded test. Due to the thrust limitations the Turnigy Rotomax 80cc motor would only be suitable for a craft carrying 100lbs of payload.

20.2.2 Introduction

The purpose of this test was to determine if the Turnigy Rotomax 80cc motor will be a suitable low cost alternative to the JM1S motor. Based on test data from the JobyMotors for a 30x10 propeller a motor will need to supply 8N-M of torque at 4500 RPM. The JM1S motor from JobyMotors would also be able to accelerate the propeller at a rate of 250 RPM/s. In order to use the Turnigy Rotomax 80cc motor, its performance must be able to closely replicate the JM1S motor's performance.

20.2.3 Experimental Apparatus and Procedure

The test setup schematic is shown in Figure 93. Figure 94 is a photo of the test setup (additional photos can be found in the propulsion test pictures in Appendix C). The thrust of the propeller will create a moment around the hinge. The scale will provide the reaction force offsetting the moment created by the propeller, and will then be able to record the thrust of the propeller. A non-contact tachometer was used to measure the rotation speed of the propeller. The scale measured the force produced by the propeller. A voltmeter, and ampmeter recorded the battery outputs. The voltmeter, clampmeter, tachometer, and scale were all filmed to record the data.

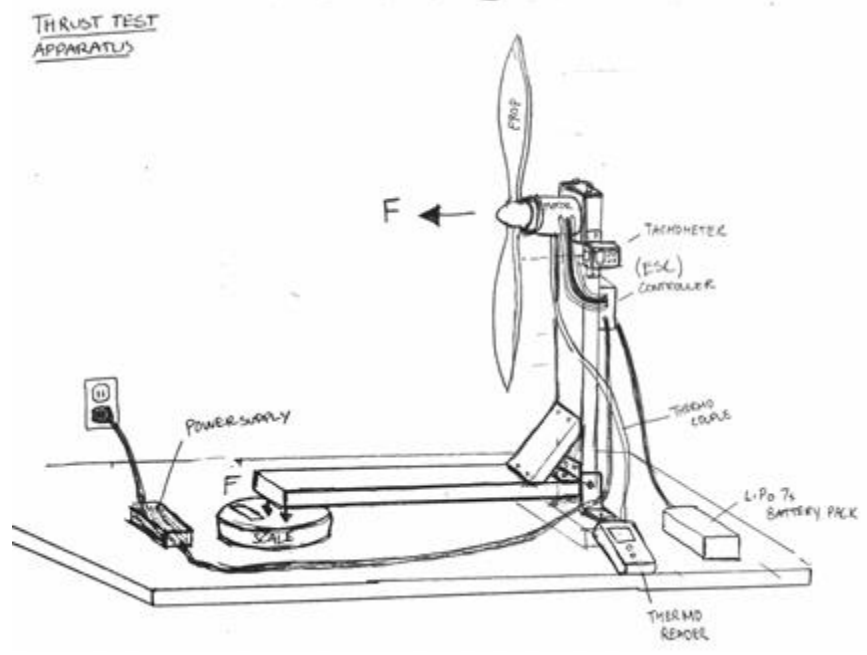


Figure 93: Motor test schematic.



Figure 94: Motor test setup

The first test was a general performance and system calibration test. To perform the first motor test the motor speed was slowly throttled through its power range. Using this curve the desired setting which leads to 50 lbs of thrust was determined. This test also served as the initial balancing test to ensure that catastrophic vibrations did not occur.

The second test was the propeller acceleration test. This test was performed by setting the throttle about 20% below the 50 lbs thrust operating point, and then increasing the throttle to the 50 lbs thrust operating point and measuring the response time. The throttle was then increased another 20 percent and the response time will be recorded.

The third test was the steady state test at the 50 lbs thrust operating point. We ran the motor for the remainder of the motor life (we expect only a few minutes) to test if the motor can maintain the load for a sustained time. The final temperature of the motor was measured to check if the motor overheated. The power draw of the motor was recorded during this test as well.

For a complete step by step list of how the tests were conducted please see Propulsion Test Step by Step Procedures document in Appendix C. Due to the motor being destroyed during the second test the third test was not able to be completed, but the motor failure during test two allows test two to function as test 3.

20.2.4 Results and Discussion

The measurements instruments were all filmed and the videos were synchronized and the measurements were recorded at each second. The complete raw data can be found in Propulsion Test Raw Data document in Appendix C. Figure 95 shows a plot of the thrust as a function of time.

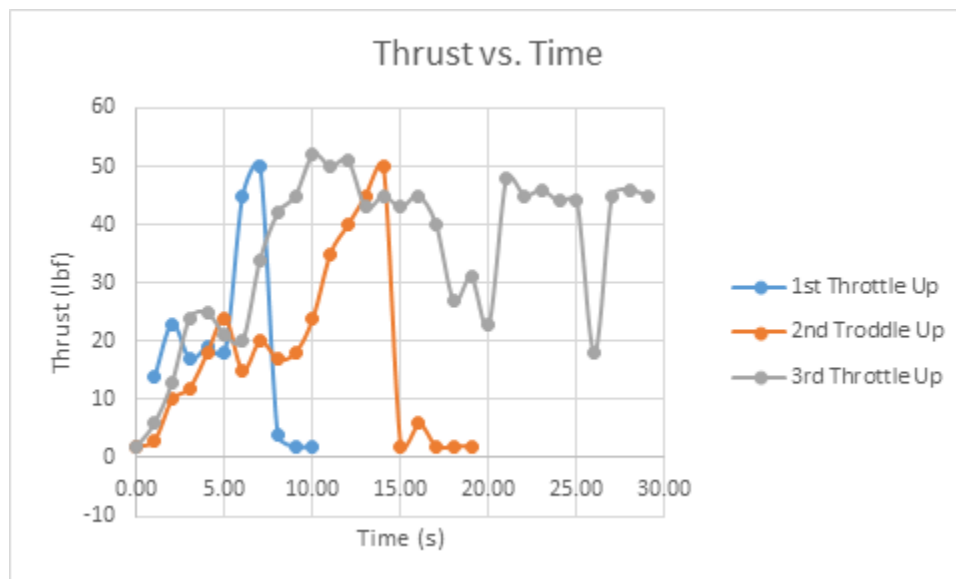


Figure 95: Thrust vs. time for the three throttle ups

Figure 95 shows that the motor reached a maximum thrust of approximately 50 lbf. The motor also was able to increase its thrust from 20 lbf to 50 lbf in 2 seconds, which would correspond to an acceleration of 741 RPM/s.

The motor performance at the rated load is listed in Table 16. The motor performance is based on data from the third throttle up, approximately after 7 seconds into the test.

Table 16: Motor performance at rated max conditions

Time (s)	Voltage (V)	Current (A)	Thrust (lb _f)	Power (W)
7.08	50.14	152.9	38	7666.406

The maximum rated load conditions occurred during the large acceleration period during the third throttle up. At this point in time the motor would be drawing more current and outputting more power than it would at steady state because it is accelerating the propeller. This is reflected by the large power draw for the thrust provided.

If the Turnigy Rotomax 80cc motors were to be used, the maximum thrust possible would be 450lbs for a short period of time. The motors would likely be able to run continuously at 30 lbf thrust conditions which would correspond to 360 lbs of thrust for the entire craft. The Turnigy Rotomax 80cc motor was able to greatly surpass the acceleration of the JM1S motor showing that the acceleration of the motor is mostly related to the ESC.

The Turnigy Rotomax 80cc also appears to be significantly less efficient than the JM1S motor. A direct comparison of the motor efficiencies is not possible because the Turnigy Rotomax 80cc motor was never ran continuously at one speed, so the acceleration of the motor always played a significant impact on the power draw. However, comparing the range of efficiencies to the JM1S motor data found in Appendix 3 it is quite clear that the Turnigy Rotomax 80cc motor is less efficient.

20.2.5 Improvements for Future Tests

The first improvement would be to use a more finely controlled throttle. During the test the thrust of the propeller could not be finely adjusted. Due to jumps in throttle data for the entire operating range was not gathered. For this test we used the joystick of a remote control. The reason for using the joystick is that the integration of the control into the system was very simple. However, the joystick did not allow for easy and accurate control of the throttle percentage. For future tests a knob throttle is recommended for use. The knob would allow for more movement over the throttle range which would allow for finer adjustment. The knob would also allow for greater repeatability since the position of the throttle could be marked and repeated for future tests.

An improvement for test safety would be to check the amperage rating of the circuit breaker. The circuit breaker used for this test was a 200A circuit breaker. However, the precise trip is not clear. Upon further research the trip current appears to be 300A. If it were possible a circuit breaker with a lower trip current would allow for greater protection against burning another. The circuit breaker during this test was not tripped thus its current interrupting abilities were not validated. While the circuit breaker was not tested there is confidence that it would function correctly.

If possible future tests should use a DAQ. While the test results were adequate to verify the performance of the motor, the specific performance data of the motor will contain large uncertainties. As a result the predicted performance of the motor based on the test is approximate. Also extracting the data from the tests will prove quite difficult since each value will need to be read at specific times from the videos. A DAQ would allow much more accurate results, however, would require considerably more work during setup, much more expensive equipment, and should only be used if highly accurate data is needed

The general construction of the test setup should be improved, in both materials and construction techniques. The video shot from the side of the propeller shows that the structure was bending during the test. The bending is likely what caused the large fluctuations in thrust indicated by the scale.

A more expensive tachometer should be used for further tests. The tachometer we used appeared to be very inaccurate and slow to change. Comparing the thrust vs RPM of our test and the JM1S test data shows very little similarity. Since the thrust vs RPM should be independent of motors, and the thrust measurement is reasonably accurate the RPM measurements must have significant errors.

20.2.6 Other Notes

Very little vibration was noticed during the test. Based on this observation the risk of vibration is significantly less than expected for the full multicopter assembly.

The propeller produced a significant amount of noise. During testing of the full assembly ear protection will be required.

The test confirmed why the overhead prop configuration was not practical. The propeller was blowing debris on the ground up to 20ft away, and would have almost certainly blow something into the pilot at high velocity during flight causing injury.

20.2.7 Conclusion

The purpose of this test was to determine if the Turnigy Rotomax 80cc motor would be a suitable low cost replacement for the JM1S motor. Due to the max thrust limitations of the Turnigy Rotomax 80cc motor, it is not suitable for use in the fully loaded craft. However, the motor could be suitable for an unloaded or lightly loaded craft test. The expected constant thrust of the motors is expected to be approximately 360lbs. With the multicopter weighing 254lbs, an additional 100lbs of payload could be carried during testing and the Turnigy Rotomax 80cc motors should be able to provide sufficient thrust for that purpose.

20.3 Controls

20.3.1 Purpose

The Electric Commuter Multicopter team performed a control system test to test the controls system for the multicopter on a smaller scale before the team builds a full scale prototype; the scale model was called the Mini for the purposes of this report. This testing was split into multiple parts to Test Different parts of the flight controller board and motor/propeller configurations for the multicopter. The main goal of this test were to see if a dodecacopter (12-rotor multicopter) can be controlled correctly by the flight controller. The sensors, like the accelerometer and gyroscope, were tested for sensitivity to small angular deflections similar to those expected on the main craft by the Mini. A summary of the Mini's attributes are presented in the Setup and Procedure section of Test D.

20.4 Manufacturing

20.4.1 Introduction

An integral part of the ECM project was the design, manufacture, and test of the mini multicopter; in order to test not only the controls system, but the tactile feel and performance of a dodecacopter. As funding was scarce, the vehicle was designed to be as cost effective as possible, particularly limiting the use of high performance structural components, to keep the vehicle to a purchasable budget. Funding for the vehicle came almost exclusively from the Cal Poly MESFAC fund, with a few additional items being purchased with awarded CPconnect funds.

20.4.2 Component Selection

As mentioned before, the system was designed to be a cost effective as possible, while still providing quality performance that would allow us to perform all required tests. Motor, ESC, and battery selection were based off of a sample quadrotor provided by one of the ECM team members. Using this model to help get a first estimate of motor KV as well as required battery power, all of the components were chosen. The base structure was designed completely out of aluminum plating and square tubing. All mounting components were created out of acrylic plate. A few different iterations packages were created and then run with the eCalc xcopterCalc to derive hypothetical performance characteristics and help hone in on the final assembly build. The results of the final eCalc model are shown below in Figure 96. It predicts a hover flight time of 9.8min and a payload of 6200g. These values are compared to the experimental results in the Testing section.

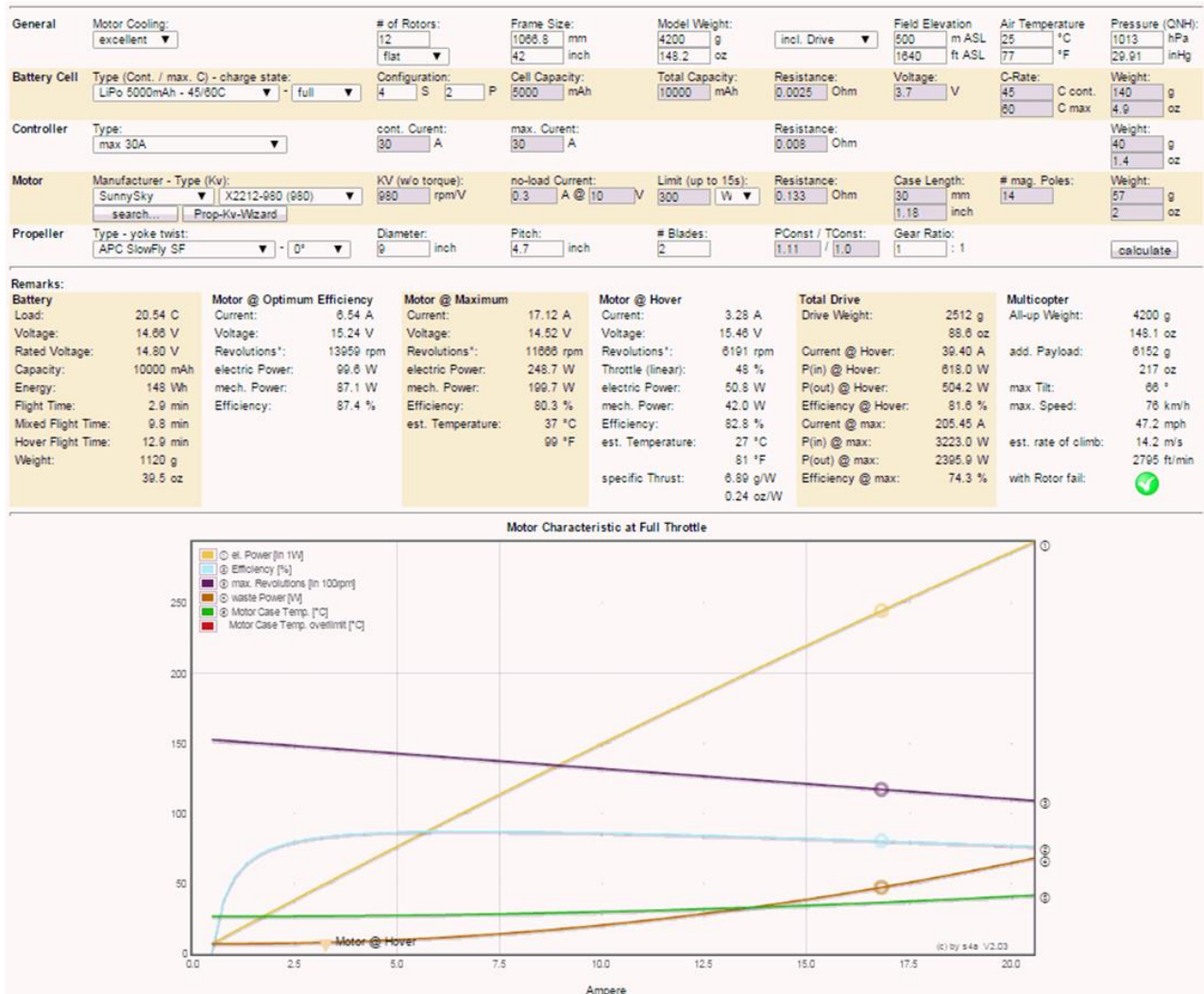


Figure 96: eCalc xcopterCalc hypothetical performance characteristics.

The structural components were mostly COTS parts, using rectangular aluminum tubing for the motor spars and motor arms, 1/8" aluminum sheet for the motor mounts and arm mounts (eventually changed to 1/4" acrylic sheet), and M3 steel screws and nuts as fasteners. A concern for aluminum tube selection was tube thickness and weight. Several calculations were made to predict the failure of several were

there times the weight of the craft was assumed to land on the end of one of the arms. The 1/16" wall thickness aluminum tubes were found to be sufficient for this loading case with a factor of safety of 1.67 where the critical position were at the screws holding the arm mounts to the motor arms. Attempting to keep weight low and robustness high, these tubes met the criteria for the Mini. A full list of the final components can be found in the Budget section below in Table 17.

20.4.3 Microcontroller and Calibration

After numerous attempts to receive an OpenPilot Revolution, the team decided to try a different microcontroller for use with the miniature build; it was more important to see if a configuration could work with twelve rotors than having the correct microcontroller, and the team was not left with many options. After reconsidering research, it was decided that the Pixhawk would be purchased via MESFAC funds, with the motors being banked together in clusters of three. Although having independent control of each motor is favorable, the team knew that stabilization and stability should still be functional, as the Pixhawk controlled motors via its orientation in space (gyroscopes and accelerometers).

20.4.4 Fabrication

Once all parts were received, all the components had to be machined for use on the mini craft. First, the entire system was modeled in SolidWorks as solid models. This allowed for the creation of drawings for fabrication, as well as placement of components in the full assembly and their mating regions. The motor mounts and arm mounts were initially cut out by water jet company in San Luis Obispo. However, the tolerances for the water cutting process yielded sloppy edges on ours. It was then decided not to use the aluminum sheet and instead use 1/4" acrylic, which was readily available and could be easily cut by the Mustang 60' laser. The stock square aluminum tube was drilled in the machine shops by team members themselves. A solid model of the final assembly is shown below in Figure 97.

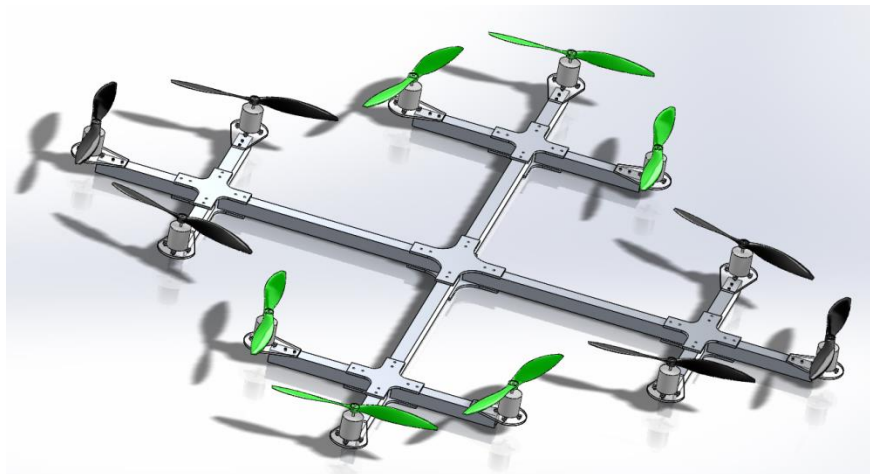


Figure 97: SolidWorks assembly solid model of the structural components of the mini multicopter including motors and propellers for prop spacing.

20.4.5 Assembly

Once all the components were cut and drilled, the structure was then assembled in full. A power distribution board was then created to bank power between the two sets of 4S battery packs, each consisting of two 2S battery packs in series. The motors were then installed, along with the ESCs. The propellers were then installed in the X copter format, with the right forward right motors and rear left motors installed with CCW props and the forward left and rear right installed with CW props. Once the entire system was hooked up, a full calibration was performed via the Mission Planner GUI interface. A picture of the final build of the vehicle is included in Figure 98. The entire system is quite complicated,

and has a lot of wiring and internal infrastructure that is complex in nature. Figure 99 provides a simplified schematic of how the system works as a whole.

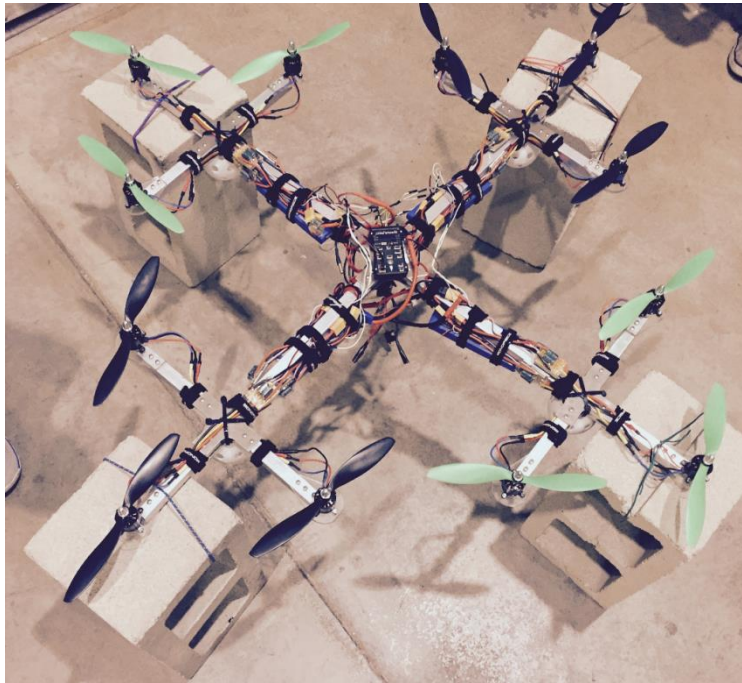


Figure 98: Final fully assembled mini multicopter with electronics fully installed.

A detailed schematic of the Mini's circuitry is provided in Appendix A. A simplified circuit diagram is shown below in Figure 99.

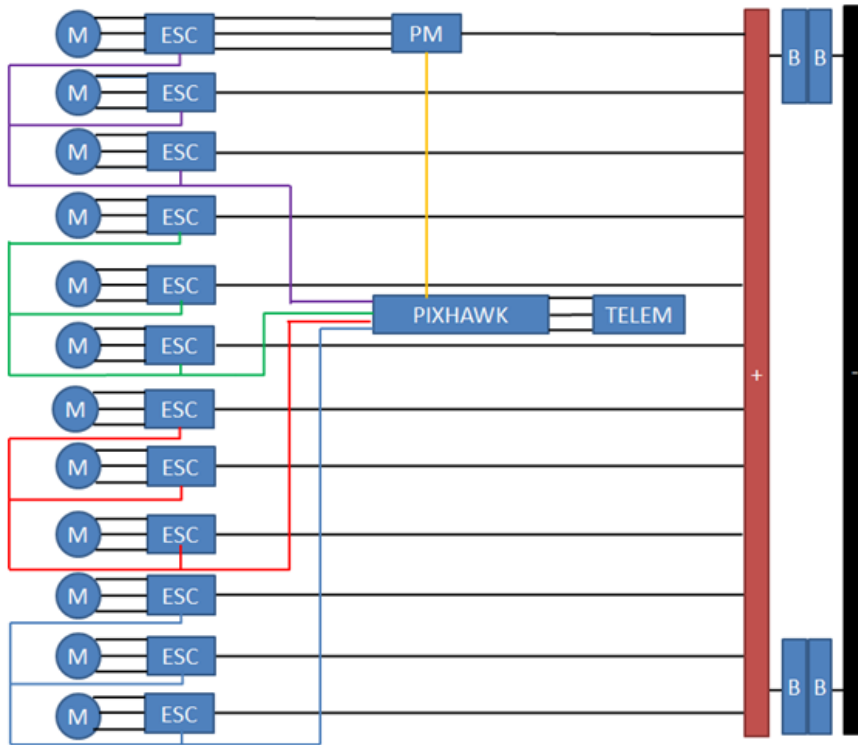


Figure 99: Simplified circuit diagram of the Mini drone.

20.5 Budget

The table below summarizes the expenses accumulated from the building and testing the Mini. Item names, models, and unit prices have been tabulated along with the total cost of the project, including taxes and shipping. Note that there are two motors shown here; the D2830 motors were the initial selection for the Mini but they were found to be poorly designed because the motor shaft was fixed to the motor housing through a set screw that had no key. They result was a significant amount of slippage and unusable motors. The next motors selected were the SunnySky's which worked properly and have been implemented into the final design of this project.

Table 17: Summary of component selection and cost for the Mini

	Component	Name	Quantity	Unit Price	Total (including taxes and shipping)
Propulsion	Motor	D2830-11 1000kv Brushless x12	12	\$10.45	\$1,246.67
	Motor	SunnySky X2212 KV980 II Brushless Motor	12	\$19.95	
	Prop CCW (Black)	Slow Fly Electric Prop 9047 SF CCW	2	\$3.16	
	Prop CW (Black)	Slow Fly Electric Prop 9047 SF CW	2	\$3.16	
	Prop CCW (Green)	Black CCW Prop	2	\$3.16	
	Prop CW (Green)	Black CW Prop	2	\$3.16	
Electronics and Controls	ESC	Turnigy Multistar 35 Amp	12	\$13.94	
	Battery	Turnigy Nano-Tech 5000mah 2S	4	\$17.53	
	Programming Card	Programming Card	1	\$8.70	
	Receiver and Transmitter	DX6i 6CH DSMX Radio System	1	\$165.98	
	PPM Encoder	3DRobotics PPM Encoder	1	\$24.90	
	Flight Controller	PixHawk Flight Controller for Autonomous Vechicles	1	\$199.99	
	Connectors	XT60 Connectors	1	\$14.31	
Velcro Straps	Hook and Loop Fastening Cable	1	\$31.01		
Structure	6061 Aluminum Tube	1/16" Wall Thick, 3/4"x3/4"x 3' Long	5	\$9.02	
	Stainless Steel Screws	Pan Head Phillips Machine Screw, M3 Size, 30MM Length, .5MM Pitch	1	\$10.80	
	Stainless Steel Nuts	Type 18-8 Hex Nut, M3X0.5 Thread Size, 5.5MM Wide, 2.4MM High	1	\$5.55	
	Acrylic Sheet	1'x2'x1/8" Arcylic sheet	1	\$20.00	
	Aluminum Sheet	12"x24"x125" (1/8") ALUMINUM SHEET 6061-T6	1	\$30.35	

20.6 Testing Equipment

This section of the test plan lists the components that were used in the subtests of the primary and secondary controls tests. Several of the tests required the same equipment so, to eliminate redundancy, the testing equipment may refer to another test.

20.7 Summary of Tests

20.7.1 Test A: Motor Drive Test

- OpenPilot Revolution
- Power supply 35V, 5amp
- (1,6,12)x35A Multistar ESC w/BEC
- (1,6,12)xD2830-11 Motor
- Transmitter
- Receiver
- Computer
- 14AWG power wire
- 22AWG servo wire
- Dodecaopter structure
- Power distribution board
- Safety Glasses

20.7.2 Test B: Propeller Thrust Interference Test

- Materials from Test A
- 35lb cinder block
- Scale
- Video recording device

- Mission Planner software
- Materials from Test G

20.7.3 Test C: Floating Tether Test

- Materials from Test A
- 10 foot tether x2
- 35lb cinderblock weight to hold craft x4
- Mats to cover area craft is expected to operate in

20.7.4 Test D: Redundancy Testing

- Materials from Test A and d

20.7.5 Test E: Disturbance Test

- Materials from Test A and d

20.7.6 Test F: User Interface Test

- Materials from Test A and d
- Saitek controller set
- 3DR Telemetry kit
- Laptop

20.8 Setup and Procedure

The setup and procedure of each primary and secondary controls test are described below. Sketches have been provided for clarity of how the test was performed and how its materials were used. For a step by step reference of these tests, please see our Controls Test Procedures section in Appendix C.

20.8.1 Test A: Motor Drive Test

The motor drive test involved running motors with the servo tester and then controlling them with the flight controller. In the servo tester section, first one motor, then six motors, then twelve motors were tested unloaded, i.e. without propellers. The one-motor test had the power distribution board (PDB) connected to the ESC and the ESC would in turn be connected to the “out” port of the servo tester through its servo signal wire. It would then be connected to the motors through the motor power cables. The PDB was connected to the four 2s LiPo batteries in a series and parallel configuration. For clarification, if the batteries were labeled 1 through 4, batteries 1 and 2 were connected in series and batteries 3 and 4 were also connected in series. Then the ground cable of batteries 1 and 3 were connected and the power cable of batteries 2 and 4 were connected. The power distribution board had a total of sixteen connections: two for battery power, two for battery ground, and the remaining twelve connecting both power and ground to the ESC’s. In the first test, with only one motor, only one of the twelve PDB connectors was used. Next, the servo tester was powered by a power supply at its “in” port. When on, the ESC’s vibrated the motors to make a beeping sound indicating that they were armed. Once all components are on, the user varied the servo tester from its zero state up to full throttle observing the response of the motors. This verified that the ESC, battery, servo signal interface between these components worked for one motor. Next, six then twelve motors were tested using the same procedure as described above by connecting the additional ESC’s to the PDB and to the respective “out” ports of the servo tester. When the servo tester was turned up, all the motors responded in similar manner. Note, as there are not enough output pins on

the servo tester or the flight controller to control each motor individually, the servo signals of the ESC's were soldered together, essentially causing multiple motors to be treated and controlled as one.

In the next section of this test the flight controller was used with the receiver and transmitter to control the motors. The flight controller was powered from the ESC's battery eliminator circuit (BEC) with the receiver getting power from the RC port of the flight controller. The transmitter was used to throttle up the first motor. Five more motors and ESCs were added and the transmitter was used to throttle up all six motors. Then six more motors were added, running a total of twelve motors. As noted previously, there are not enough output pins on the flight controller to control the twelve motors individually so four sets of three servo signal wires were soldered together in order to properly control twelve motors.

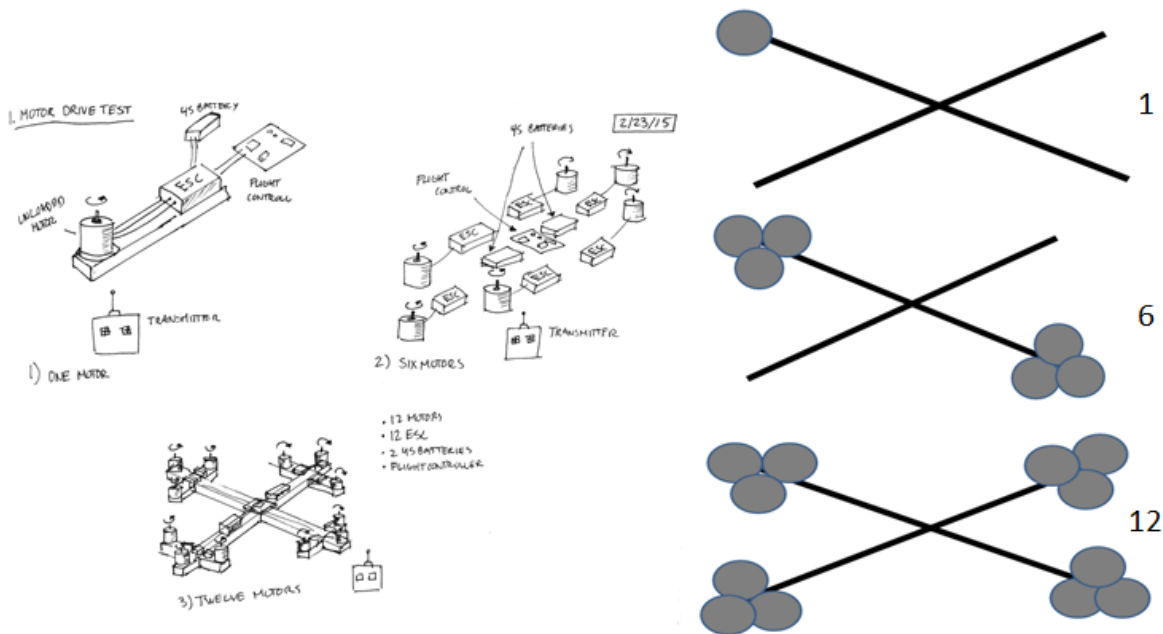


Figure 100: Schematic of 1, 6, and 12 motor drive tests

20.8.2 Test B: Propeller Thrust Interference and Maximum Thrust Test

This test involved determining the reduced thrust experienced by placing propellers in close vicinity to one another. A standard household scale was used in this test. A 35lb cinder block was placed on the scale with the craft strapped to the cinder block with rope. The total weight of the cinderblock and craft was first measured and the reduction of weight was measured when the motors were turned on. To provide several points, the motor thrust was recorded at approximately 40%, 50% and 60%. Prior to turning the craft on, in the Mission Planner controller radio tab, the minimum and maximum radio values of the Saitek were recorded. The minimum value corresponds to 100% thrust and maximum corresponds to 0% thrust. The Radio value changed as the Saitek was throttled up. These values were normalized to determine the percent thrust the motor is operating.

In the first part of this test, one propeller was attached to each arm of the craft, making four mounted propellers in total. The craft was then turned on and throttled up from 0% up to 40%, 50%, and finally 60% throttle, the weight from the scale was measured at each of these intervals. The craft was then turned off. The thrust per motor was then found by taking the initial weight of the system and subtracting

the weight of the system with the motors at the respective thrust values and then dividing that number by four because there are four motors. The above procedure was then repeated with eight propellers (two on each arm) and finally twelve propellers (three on each arm). Figure 101 below shows a slightly modified setup of this test as well as simple diagram. The difference is that rather than the motors attached to a board they were mounted on the craft structure and evenly distributed, producing a purely axial load on the scale and allowing for more accurate measurement of the resulting thrust.

For the maximum thrust test, the twelve propellers remained attached to the craft. To avoid ground effects, the craft was turned upside down so that it thrust directly upwards. This was a safety precaution because the craft was pushing into the ground rather than trying to lift off, reducing the risk of the craft flying into bystanders. The flight controller could not be used for this test as its software will not operate the craft while it is upside down. Therefore, the servo tester was needed in order to throttle up the motors. To record the maximum thrust value, the same technique as that described above was used but the weight recorded on the scale increased rather than decreased.

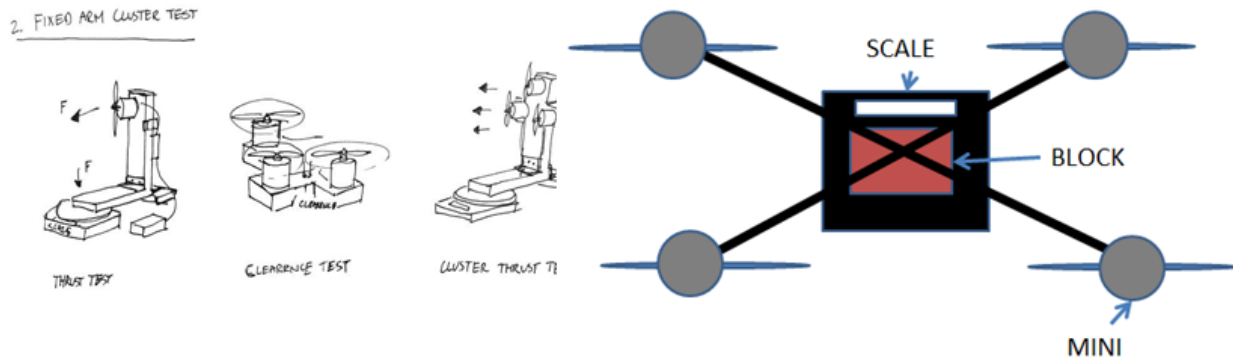


Figure 101: Schematic of the fixed arm cluster test with 1 and 3 motors.

20.8.3 Test C: Floating Tether Test

The floating tether test was performed by first covering the expected operating region of the craft with mats to avoid damage to both the craft and operational property. Then, one of the 10 ft tethers was attached to one arm of the craft. The other end of the tether was attached to two of the 35 lb cinderblocks. The cinder block was placed several feet away from the craft. The same was done on the opposite arm of the craft. These two attachments allow for operating in a square in order to test the thrust, pitch, and roll characteristics of the craft. The advantage of having the craft attached on two sides rather than just one connection directly underneath was that in the event of in-flight malfunction, the craft would not fall onto the cinder blocks holding it down. Additionally, there was redundancy implemented in that if one tether breaks, another was present to hold the craft in the specified area. However, the disadvantage was that it was more challenging to test the yawing ability of the craft without getting the craft tangled; this wasn't seen as a critical element in this test.

Once constrained, and all personnel were wearing eye protection and completely out of the range of operation of the craft, the operator flew the craft and observed the response and stability for a given controller input. A summary of the Mini's flight characteristics are presented below in Table 18.

Table 18: Summary of Mini multicopter measured and expected flight characteristics.

Weight (lbs)	Footprint (without props)	Expected Flight Time, (min)	Expected Payload Capacity, (lbs)	Number of Rotors
11	42in X 42in	8	7	12

Because this test required the craft to fly, additional care was taken to minimize the risk of damaging property or harming others in the event of an in-flight malfunction. This test was performed inside the gym with the Mini tethered to the ground. The personnel attending the flight remained a sufficient distance (20 ft) from the craft while it was in flight. Additionally, access to the flight facility was restricted to those participating in the test. A 10 ft tether was attached to several 35 lb cinderblocks, limiting the craft's movement to a 10 ft radius. Figure 102 provides a simplified overview of the flight parameters that were tested.

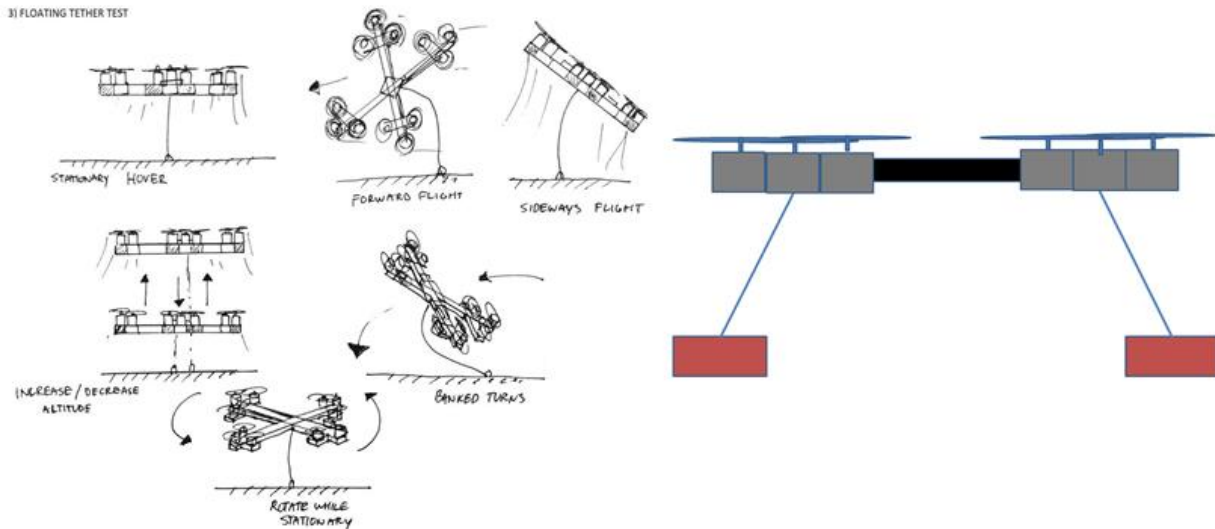


Figure 102: Floating tether Test Flight patterns.

The following tests (Tests D through F) required the same flight space with the same safety precautions as those described by Test C.

20.8.4 Test D: Redundancy Testing

The redundancy test validated the control system's ability to compensate in the case of a single motor failure. The dodecaopter was run with twelve loaded motors, like the floating tether test, however, one motor was disconnected from its ESC prior to operation. The dodecaopter was slowly revved to hover, then subsequently the motors were throttled to full thrust. This simulated the event of a motor failure for the aircraft. The dodecaopter then tried to compensate for a loss of a motor and the stability of the craft was visually inspected.

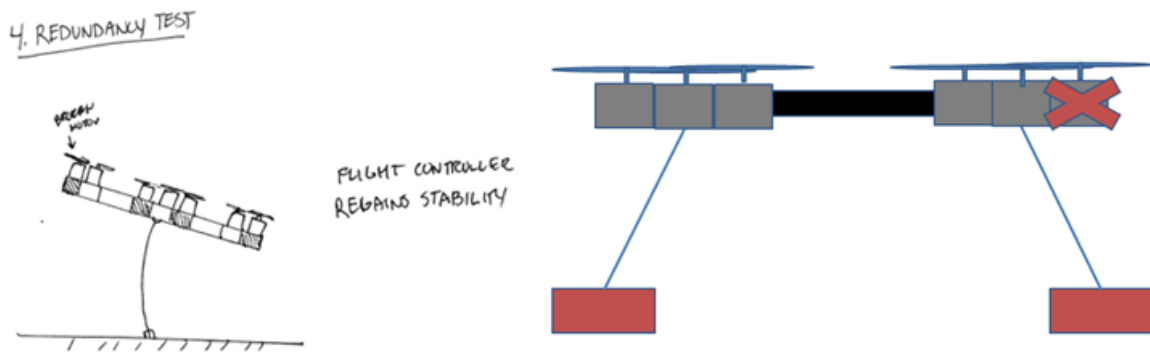


Figure 103: Redundancy test schematic showing kill-fuse.

20.8.5 Test E: Disturbance Test

The disturbance test was used to verify that the flight controller could provide a stable hover with an outside disturbance such as gusts of wind or a light impact. The dodecopter was fully loaded and brought to a 5 ft hover. Control stability was tested by inducing a physical load on the system by straining the copter by its tethers; this simulated the copter being restricted by an outside force. The success of the control system was visually inspected.

20.8.6 Test F: User Interface Test

The user interface test involved configuring the Saitek with a telemetry device, and transferring the user input to the dodecopter via the Mission Planner application on a laptop. This test verified that the user could control the craft from a non-standard RC controller; it is a go/no-go test. Additionally, the intuitiveness of the controls system was determined. If an experienced multicopter user would struggle to learn to control the craft with the Saitek configuration, a new scheme would be adapted with the possibility of reverting to a standard RC transmitter device. The results of this test was the feedback of the user and overall performance and feel of the test. This was hard to quantify, but is an important and intuitive test.

20.9 Data Acquisition

Below, the techniques and resources to be used for collecting data of the primary and secondary test is described.

20.9.1 Test A: Motor drive test

The motor drive test was mostly a go/no go test to see if the interface between the motors, ESCs, flight controller, receiver, and transmitter worked. More extensive testing of current draw and thrust was recorded in the fixed arm cluster part of this test. It also involved a check for vibration problems ensuring the craft did not shake itself apart. This part of the testing was done entirely by visual and audio inspection.

20.9.2 Test B: Propeller Thrust Interference and Maximum Thrust Test

In the Mission Planner Radio tab, the maximum and minimum radial thrust values of the Saitek was recorded. These are more or less arbitrary numbers and must be normalized to get a thrust percentage. A video recording device was placed on the scale in order to record the thrust. For the four, eight, and

twelve propeller tests, the Saittek throttle was moved from approximately its 40% throttle position to its 50% and finally to its 60% with one individual recording the Radio value at each of these approximate thrust settings. The throttle was left at its respective value for several seconds to allow the scale to come to equilibrium. By applying the respective thrust percentage, number of motors, and net thrust recorded, a thrust per motor value was found.

For the maximum thrust test, the same technique to record thrust was used as the propeller thrust interference. The only difference is that the craft was now thrusting into the ground rather than trying to lift off, it increased the load seen by the scale rather than reducing it.

20.9.3 Test C: Floating Tether Test

The quantitative data to be measured from this test was the total flight time of the craft. This was done using a stopwatch. Time began when the craft lifted off and ended when the craft needed to return to the ground due to low batteries. Care was taken to set minimum battery settings in the ESC's so as not to run the batteries too low and ruin them.

The qualitative data that was recorded during this test was the general performance of the control system to maintain stable flight during the test. The performance of the control system was rated by the observers, and pilot. A complete failure of the control system corresponded to the multicopter not being able to maintain a stable hover, and not being able to perform any of the maneuvers. A complete pass for the control system corresponded to the multicopter maintaining stable hover, and being able to smoothly complete each maneuver in succession without loss of stability. The performance of the multicopter was assessed through a pass or failure of each maneuver.

20.9.4 Test D: Redundancy Testing

This test was validated via both visual and tactile methods; if delays occurred, or stabilization time seemed substantial, the response time was measured. If the time to compensate was too substantial, modifications to the control system were implemented to reduce response time. The test was filmed to capture any changes in the aircraft's behavior during flight. The rest of the test information was provided by the pilot, and their judgment of the craft's ease of use after motor failure. The importance of this test was the ability for the microcontroller to compensate well in a motor out scenario with minimal operator help.

20.9.5 Test E: Disturbance Test

Much like the redundancy test, the disturbance test required a mostly visual and tactile evaluation of the vehicle's ability to stabilize after a significant disturbance to the system. If the time for compensation was substantial, the response time was measured. If the time to compensate was too substantial, modifications to the control system were implemented to reduce response time. The test was also video recorded for future analysis. The rest of the information was also provided by the pilot, whose judgment categorized the craft's ease of use during disturbance loading.

20.9.6 Test F: User Interface Test

As stated before, the proper implementation of the Saittek user interface was judged on a no/no-go basis. This conclusion was reached by operating the dodeca-copter at no-load and observing that it complied with the user's inputs. Satisfaction of the user during testing was evaluated through feedback provided during in-flight operations. Feedback involved an oral or written description of the user's experience of the Test Controls.

20.10 Expected Results

In the expected results sections below, the desired results and outcome of each primary and secondary test is outlined.

20.10.1 Test A: Motor drive test

The expected result was twelve running motors. The visual and audio inspection could yield a bad motor or ESC that were repaired, replaced, or otherwise dealt with in future tests.

20.10.2 Test B: Propeller Thrust Interference and Maximum Thrust Test

From eCalc, an RC calculator, the expected specific hover thrust was 6.89 g/W. This value was for the full 12-prop configuration. Therefore, it was expected that 4 motors will deliver one-third of this value and 8 motors will deliver two-thirds of this value or 1.90 lb/motor. Additionally, independent of the eCalc result, the twelve motor configuration was expected to have three times the thrust of the four motor configuration. Any significant deviation from this result was indicative of prop-wash between propellers and, although the results cannot be scaled, may predict some of the losses expected with the actual full-scale craft.

Also from eCalc, the maximum payload was expected to 6200 g or 13.6 lb. This value was expected to be close to that found in the maximum thrust test.

20.10.3 Test C: Floating Tether Test

From our eCalc simulations, the expected flight time for our Mini vehicle at hover was 9.8 min. A value reasonably close to this was expected during our tests.

The flight controller was expected to be able to maintain stable hover, and we hoped that it would allow for the easy control of the multicopter. The controller was also expected to not be able to exceed the maximum values input to the controller as listed above in Figure 103 above.

20.10.4 Test D: Redundancy Testing

In the event of a motor failure the flight controller was expected to successfully compensate for the loss of one motor. The stability of the craft would fluctuate then become steady once the controller increased the thrust in neighboring motors. In the case of loss of significant altitude or a crash, a reassessment of the flight controller and connections would ensure success in a future tests.

20.10.5 Test E: Disturbance Test

The flight controller was expected to provide stabilization when a disturbance affects the flight of the craft. The stability of the craft should fluctuate then steady once the controller increases the thrust in neighboring motors to compensate for the disturbance. In the case of loss of significant altitude or a crash, a reassessment of the flight controller and connections will ensure success in a future tests.

20.10.6 Test F: User Interface Test

The Saittek user interface was expected to be successfully implemented into the dodecacopter's controller scheme and that it would yield a more intuitive flight experience than an equivalent standard RC transmitter. If results indicated a poor ability to implement the Saittek or that it would not assist the user's flight experience, another controller interface would be considered or the RC transmitter would be adopted.

20.11 Safety Concerns and Solutions

The safety concerns and their solution from the primary and secondary controls tests are described below.

20.11.1 Test A: Motor drive test

The main safety concerns for this part of the test were electrical. Good electrical connections were made between the ESC and motors and between the batteries and ESCs. Also, correct wiring for signals between the flight controller and ESCs was ensured beforehand. A clean bench was required for this test to avoid unintentional interference.

20.11.2 Test B: Propeller Thrust Interference and Maximum Thrust Test

Several parameters were accounted for to maintain safety throughout the fixed arm cluster test. First, during the static interference portion, it was verified that the motors are off/disconnected so that they do not turn on while being spun by hand. Second, the dodeca-copter structure was securely mounted to the test fixture so that it did not break free. To avoid any hazards, experiment participants maintained a 10 ft distance from propellers. Electrical concerns were present as well, however, they were addressed in the “motor drive test” section.

20.11.3 Test C: Floating Tether Test

Several parameters were accounted for to maintain safety throughout this test. First, the dodeca-copter structure was securely mounted to the test fixture so that it does not break free. To avoid any hazards, experiment participants maintained a 10 ft distance from propeller. Electrical concerns were present as well, however, they were addressed in the “motor drive test” section.

20.11.4 Test D: Redundancy Testing

In addition to the previously identified safety concerns, there was the hazard of the multicopter flying out of control and striking a test operator or a passerby. In order to protect everyone the multicopter was tethered to the ground by two 10 ft tethers. A circle extending 20ft from the tether base was marked on the ground. Once the test began, no test operators were allowed to enter the circle. In order to protect the public, at least one person was assigned as a lookout. The lookout was responsible for warning anyone not associated with the test of the safety hazard and preventing them from entering the circle. If at any time someone enters the circle the multicopter was immediately landed (assuming it is safe) and the circle would be cleared before the test could continue.

20.11.5 Test E: Disturbance Test

Due to the fact that motor function was disturbed mid-flight, some flight characteristics were unforeseen and the craft could potentially crash. Only one team member could be near the multicopter during flight to prevent tethers from interfering with the propellers themselves. The other team members remained at a significant distance away from the test area. As a result of the high probability of a crash, cushioned padding was placed around the dodeca-copter.

20.11.6 Test F: User Interface Test

Dangers for this test resulted only from the dodeca-copter batteries as well as unloaded motors. Therefore, the same safety procedure and precautions described by the “Motor drive test” section were adapted to fit this test.

20.12 Safety Equipment

The safety equipment to implement the safety solutions described in the previous section has been placed into a bulleted list for each primary and secondary test.

20.12.1 Test A: Motor drive test

- Electrical tape or other insulation

20.12.2 Test B: Propeller Thrust Interference and Maximum Thrust Test

- Electrical tape
- Small wall to separate operator from craft

20.12.3 Test D: Floating Tether Test

- Tethers
- Cinderblocks
- Protective eye-wear
- Mats to cover area of operation
- Look-out

20.12.4 Test D: Redundancy Testing

- Smartphone (video/stopwatch)
- Adequate distance
- Tether
- Padding

20.12.5 Test E: Disturbance Test

- Smartphone (video/stopwatch)
- Adequate distance
- Tether
- Padding

20.12.6 Test F: User Interface Test

- Safety glasses

20.13 Results and Analysis

Below, the results of tests A through F are summarized with the analysis methods used to investigate the experimental data.

20.13.1 Test A: Motor drive test

The results of the motor drive test are as follows. As stated in the Setup and Procedure section, first one then six then twelve motors were run with the servo tester and then with the receiver and transmitter. In both of these tests, all of the motors were controllable and received a “Go” grade indicating that the next steps in the controls test plan could begin.

Table 19: Result of Go / No Go Test For 1, 6, and 12 motors

Motor Configuration	1	6	12
Go/No Go	Go	Go	Go

These results conclude that the motor, ESC, flight controller, receiver, and transmitter interface work together and indicate the craft would be flyable in the twelve motor configuration.

20.13.2 Test B: Propeller Thrust Interference and Maximum Thrust Test

The results of the propeller thrust test are somewhat conclusive at higher thrust percentages. Figure 104 below shows some of the general trends seen from the test. The data was curve-fit with a second-order polynomial. At lower thrust percentages the thrust per motor is larger for the two-third and three-third motor configuration while at larger thrust percentages the thrust per motor is largest for the one-third motor configuration. Additionally, the maximum thrust test yielded a result of 27lbs.

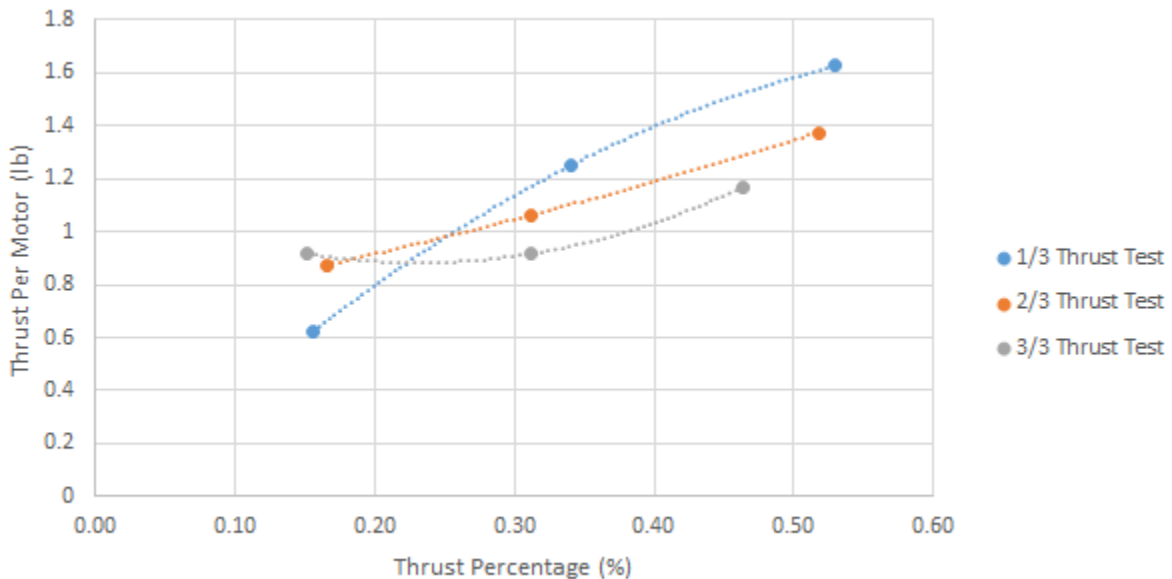


Figure 104: Effect of prop interference on thrust per motor.

For each test, the voltage of the LiPo batteries was recorded to keep track of the decrease in power as well as to make sure the LiPo's did not drop below their respective cutoff voltage. The voltages are shown in Table 20.

Table 20: Recorded voltages at each motor configuration test

Voltage at Beginning of Test (V)	15.48	15.36	15.22
Motor Configuration	1/3	2/3	1

The results of the propeller thrust test are as follows. There appears to be a general trend in the data indicating that with an increase in number of propellers, there is a decrease in thrust per motor due to propeller interference particularly at higher thrust percentages. The discrepancy seen at lower thrust percentages may be a result of the test setup and the scale used. The scale used was a simple bathroom scale whose accuracy can be speculated. Additionally, the cinder block placed on top of the scale could not sit completely flat due to some of the contours of the scale which would make the resulting thrust

values vary, although not significantly. For a more conclusive test, more thrust values need to be collected; most likely a range from 20% to 100% would suffice. To get a more accurate value, now that the interference has been identified, the test would need to be repeated with larger Joby motors. Additionally, the tests were performed with the LiPo batteries used to operate the craft. Overtime, batteries decay in the power they can provide to a certain load, as shown in **Table 20** and that may be the result of the trend seen here as the one-third thrust test was performed first, then the two-third, and finally the full thrust. To avoid this, the motors should be powered by a DC power supply to ensure constant power is provided to the motors for each test.

20.13.3 Test C: Floating Tether Test

The data collected from the floating tether test was the flight time of the craft. This value is shown below in Table 21. The flight time was found to be 14 minutes and the flight operator found the craft to be stable in hover and remain stable during any reasonable maneuver attempted.

Table 21: Flight time and flight operations results

Flight Time (min)	Stable Hover	Maneuverability
14	Pass	Pass

The results of the floating tether test indicate that treating all three motors on one arm as one motor is possible and keeps the craft stable in hover and in simple flight operations. This was a major assumption in control of the multicopter and indicates that it may be possible to apply the flight controller and motor control layout to a larger-scale craft. Additionally, the recorded flight time exceeds the predicted value found from eCalc by over 40%. eCalc is a relatively reliable program and is used by much of the RC community. The significant difference between the experimental and predicted results most likely stems from the use of twelve motors rather than the four which are usually used for multicopter configurations. Due to the propeller interference present found in test C it was expected for the craft to have a lower flight time than the eCalc prediction. The reason for this miscalculation could be that while in flight, the craft spent the majority of its time in the ground-effect region which would reduce the power required to maintain hover. In further testing, this possibility can be avoided if the craft is operated outside and not tethered so that it can maintain sufficient distance from the ground and provide a better estimate to the actual flight time of the craft as it will most likely be flown outside in its use.

20.13.4 Test D: Redundancy Testing

The redundancy testing passed without complications. The motor was disconnected from the ESC before arming the system. The system was then armed, team members placed in position, and flight initiated. Visually, there was a slight increase in vehicle drift, but the pilot could account for this with user input. The pilot's testimony revealed that the change in vehicle operation was near negligible at all times of flight. The microcontroller could successfully compensate for the loss of a motor. Visual inspection during operation and afterward via video allowed insight into system interaction; the microcontroller could not see the loss of a motor, but could measure a change in inclination via the gyroscope and accelerometer within the craft. The PID controller would then tell the three motors on the side of inclination to increase until the craft was level. This would increase the RPM of the two motors left, until the craft was level. The increase in speed on the affected arm was highly noticeable.

20.13.5 Test E: Disturbance Test

The disturbance testing partially passed through the disturbances induced by the restraint tethers. The system was armed, team members placed in position, and flight initiated. The craft was brought to a low hover, and then thrust up and taken to a radial corner of the tether to induce a tethering load. Visually, it could be seen that the craft speeds up the rotors of the vehicle side being restricted. At times, this compensation was too drastic, and would create unpredictable flight characteristics. This would then

usually partially stabilize. From the standpoint of the pilot, the unpredictable behavior made the craft hard to fly in these conditions, but could be controlled with pilot skill. At high thrust loads, the compensation by the microcontroller would overshoot by large margins, and cause the craft to rocket into the air at high speeds in an arc restricted by the tethers. This was dangerous for the craft as it took the vehicle to an almost 90 degree from horizontal orientation, where zero thrust can be generated. The microcontroller kept the vehicle from flipping over, but it was the pilot's job to reorient and stabilize the craft. This validated that the microcontroller would likely be able to account for small disturbances due to environmental conditions, but rely on pilot input for large disturbances such as impact or crashing.

20.13.6 Test F: User Interface Test

The user interface testing passed without complications, as well as surpassing all expectations during setup. The first step was to calibrate the Saitek throttle and joystick in the Pixhawk compatible Mission Planner. This was quite simple and allowed for intuitive control mapping as well as input reversal. After calibration was completed, the telemetry module had to be installed. The laptop portion of the kit was plugged into the Mission Planner laptop and drivers were installed, while the other module was plugged into the TELEM port of the pixhawk. After setting the module to the correct channel, the telemetry units bound immediately. This was tested numerous times to test for reliability with satisfactory results. Once the system connected, it took a flip of a switch to arm the vehicle. The throttle ran incredibly smooth, allowing one to hold throttle much easier than with an RC transmitter. The joystick module ran very smoothly, but had a slight delay to the input; this didn't alarm the team too much as there was a fully customizable joystick calibration suite that could be used for implementation on a loaded test. Overall, the control scheme felt effective and intuitive, and would serve as a great on vehicle companion for the full vehicle or test flight apparatus with virtual reality equipment included.

20.14 Conclusion

The goal of the controls testing was to prove that the team could use a flight controller to control a craft with twelve motors in a safe and easy-to-control manner. From these results, the selected flight controller and motor layout could be used on the full scale craft. The flight controller performed well, it controlled all twelve motors and it made the craft stable if the calibration was well done. The ability to control a large craft with 30 inch propellers and 52 inch arms versus the Mini with 9 inch propellers and 21 inch arms remains untested. A full-scale or similar size craft is needed to validate the controller for this project.

21 RECOMMENDATIONS

The following literature thoroughly explains two paths and their respective recommendations the next ecm team can take. The first path, alluding to the following 'structure', 'propulsion', 'controls', and 'ecm team' sections, gives suggestions to improve upon the current ecm design. The second path, 'other designs', gives guidance towards a new design with different parameters, if the new ecm team wanted to go that direction.

21.1 Structures

21.1.1 Loading Cases: Dynamic, Static, and Vibration

It is the team's understanding that manned aircrafts are designed with strict standards. For a manned multicopter such as the one presented in this senior project, loading cases and strength standards have not been developed due to the novelty of the design. When designing the structure, only rudimentary load cases were considered. Such loads entailed maximum thrust, maximum angular tip deflection, basic vibrational analysis, torsional load due to motor loss, and the maximum landing rating. However, the maximum landing rating was not determined by estimating what the aircraft could experience in a worst case landing, but by what the welds could withstand if the craft landed on one arm. While this load was considered a reasonable worst case expectation, it was found implicitly rather than explicitly. The landing load should have been determined without regard to other design loads, then the welds should have been designed to those standards rather than the other way around.

The design conditions, such as a maximum eight-degree deflection at the tip of the furthest from center spar, were also chosen arbitrarily. An eight degree deflection results in 1% difference in thrust and was chosen to be the largest acceptable variation. This one percent change value was chosen with no previous knowledge of actual performance characteristics under that condition. Regarding the stiffness of the craft, this was the only governing criteria. Other considerations such as vibrations and flight controller sensitivity should be considered for stiffness of the design and probably have more effect on performance than minimal thrust variation.

The only vibrational criterion was that the natural frequency of the craft should not be near the operational frequency of the motors. The vibration due to sudden accelerations, impact, and all other operational conditions were not considered. Critical vibrational conditions and their resulting magnitudes should also be analyzed in order to help determine necessary craft stiffness.

Further research and testing should be performed to determine accurately what loads the craft will see in order to produce a reliable structure. A dynamic loading analysis of landing on one arm is strongly recommended and will most likely drive much of the design.

21.1.2 Different Adhesives/Torsional Shear

If bonding carbon tubes to steel mounts or use of any other critical structural bonding is used in the next design iteration, further adhesives analysis needs to be performed. Typically adhesives fail in peel, much like what occurred in the ECM's cantilever bend test. The bond between the carbon and center mount was justified using an equation that estimates the necessary bond length given a particular load. The premature bond failure in the cantilever beam test suggests that the bond length equation is not applicable and/or there are more variables or imperfections that are not being considered. Stress concentrations at the ends of the carbon tube and steel tube were not considered and may have affected the bond.

In addition, torsional loading should be analyzed and tested for the center mount and main arm bond as it is a design load and was not performed on this design, because peel was assumed to be the initial failure.

The epoxy used for the bond was suggested by human power vehicle, a Cal poly club that frequently bonds composites. While this may have been an acceptable epoxy for their application further research should be performed in order to find and validate an epoxy for this application.

21.1.3 Different Layup Schedule of Main Arms and Spars

The main carbon arms of the ECM were manufactured with a layup schedule to provide maximum strength in bending and enough strength to resist the maximum expected torsional load. The layup schedule used was determined in collaboration with c-tech to tailor the tube to our needs. The main calculations used to determine the layup schedule only considers the number of zero degree plies for bending and non-zero plies for torsional, not the ply's location in the laminate. The final layup schedule was then produced to resemble the layup schedule used in the carbon tubes used for the spars of the ECM. Experimentation with layup schedules using FEA or a Matlab program should be used to find a layup schedule to effectively meet the design requirements. It should be noted that composite tubes under bending should have a 90 degree ply on the outside to prevent the plies from peeling.

21.1.4 Carbon Fiber/Composite Mounts

Much of the structural weight came from the steel mounts, joining the critical components of the structure. These joints were the most difficult portion to manufacture, and the bond between the carbon arms and steel is a critical issue because the lack of appropriate adhesives and its premature failure. The team recommends looking into carbon wrapped joints to decrease weight and eliminate the steel to carbon bond. Steel mounts were chosen because they allowed a "modular" construction. If a carbon tube were to be damaged, that tube alone could be broken off the steel mount and replaced. With an all carbon construction, if a single tube is damaged the entire craft is compromised. Also when using carbon mounts, impact resistance needs to be considered as carbon is not regarded for its integrity after impact. If landing gear is attached to these mounts, like in the ECM, the mounts need to handle the landing impact. Regardless, lowering the weight of the structure using all carbon would allow the use of thicker carbon tubes resulting in higher strength and stiffness and/or flight times could be increased

21.1.5 Redesign Landing Gear

The landing gear contributes to much of the structural weight with their steel construction. In addition the landing gear does not provide shock absorption for landing that isn't normal to the ground. The landing gear is likely to fail or "catch" the ground in this condition. When a larger prototype is produced it is strongly recommended a new landing gear system be designed that is lighter and allows the craft to land in different ways, much like the wiffle balls allow the mini.

21.1.6 Stress Concentration Analysis/FEA

This is an aerial vehicle; therefore each critical part that enhances the performance and integrity of the craft should be thoroughly analyzed. Finite element analysis was performed on the center mount and its assembly because the respective loading cases made that the most critical of components. However, finite element analysis should have been continued on other parts, such as the spar mounts, motor mounts, and especially the epoxy joints between main arms and center mount in order to investigate the complex interactions between the components.

21.1.7 Disassembly, Potted Inserts & Attachments

A problem with the current design is that the aircraft has a large footprint of 12ft x 12ft and it cannot be disassembled without breaking off the carbon components. The next ECM iteration will find it convenient to have a design that can be disassembled, however, this will require an in-depth design and analysis. Attachment points are always difficult to implement with a carbon frame, and the intricate parts that this

would require would inevitably lead to stress concentrations and opportunities for delamination or fiber fracture.

Potted inserts are a feasible way to attach other components to composites. They are usually used in composite structures with a honeycomb core, so thickness of the laminate structure may be a design factor. However, it is imperative to note that a hole in any composite is detrimental to its stiffness and strength. The overall properties of the laminate will be significantly compromised

21.1.8 Minimize Footprint/Compact Propellers

An initial design parameter was to limit the size to a traditional parking space. This changed rapidly after realizing the feasibility of such a parameter with the design. However, that shouldn't discourage other iterations to research ways to make the design more compact. This iteration had to abide by many different constraints while designing and learning. Future teams may have more time and the ability to condense the project while still moving it forward.

21.2 Propulsion

21.2.1 Improve the Thrust Test Rig

The current thrust test rig gave the team some good data to work with, but did not provide results as accurately as they had hoped. One issue was that we did not use an actual data acquisition system, so even though we did our best to synchronize the start of the test for each set of data, they may not have been aligned perfectly. A DAQ would eliminate this possible discrepancy in the data. Another detail to consider is that the interface between the moment arm and the scale did not have a roller joint in between it, meaning that some lateral forces were induced as the motor was powered up. Finally, it would be ideal if the test rig arm had the same geometry as the actual vehicle so that the drag forces would be representative of what would be encountered during flight.

21.2.2 Reanalyze the Number and Size of Propellers

The number and size of the propellers should be reanalyzed based on changes made to the rest of the craft. The initial optimization tool used a very simple linear density and a total length of carbon tubing needed based on a quad copter configuration to estimate the weight of the structure. As a result, the smaller branches of the structure that support one motor are significantly oversized, and the structure weight was significantly overestimated. This nuance was particularly noticeable in the high propeller count configurations. The 32 propeller configuration was eliminated because the structure was calculated to be over 100 lbs, which is not possible with the weight constraints. Using a better structure weight estimate will allow for larger and/or more propellers to be used to maximize the disk area. This in turn will allow for greater efficiency during flight. In general, configurations that are an even number, and a square number subtracted from a larger square number (i.e. $32=36-4=62-22$) or number that allows for efficient circular packing patterns are the best configuration and should be the focus of further analysis.

21.2.3 Analyze the Propeller Pitch

The pitch for the propellers was selected based on the theory that pitch is related to the speed at which a propeller is designed to move through the air. Since the craft will be hovering or moving sideways through the air the axial velocity of the propellers would always be small. In order to select a propeller that was designed for speeds closest to these conditions the smallest available pitch for the selected diameter was selected. Further analysis needs to be done to ensure that this logic is correct. Furthermore the pitch of the propeller is involved in the thrust vs rpm relationship. High pitch propellers will move more air and will produce more thrust at a given rotation speeds. High pitch propellers also have more drag so more torque

will be necessary to turn the propeller. If a motor that offers significant weight or efficiency benefits at very slow speeds is available changing to a high pitch propeller may offer better flight times.

21.2.4 Using Different Motors

The Joby motors being used are slightly oversized for the 30x10 propellers being used, however they are still an excellent option for future designs. Additional research into available motors should be done to allow for the selection of a motor that better matches its performance requirements. A few sources that would be a good places to start are hacker motors, KDE direct motors, and alien power systems. Motors for electric go-karts could potentially work, but the previously recommended motor brands should be considered first since they are designed for planes/quad-copters and other applications that are much more closely related to their use in this project. Low cost hobby motors, such as the Turnigy Rotomax brand should be avoided if possible due to the lack of technical specifications, resulting in easy destruction of the motor during the required testing.

Along with using different motors, different voltages should be considered as well. High voltage motors will allow for lower currents, smaller wires, and lower voltage drops which degrade performance. However, low voltages are better suited to the slow rotation speeds that are ideal for high efficiency. Further research will need to be done into the costs and benefits of varied motor voltage. Ideally a motor manufacturer will be able to manufacture a custom wound motor for the specified operating conditions.

21.2.5 Multi-Blade Propellers and Stacking Propellers

The number of blades on the propeller should be better analyzed. The standard configuration is a 2 blade propeller. Two blade propellers tend to be more efficient for the same thrust, but provide less thrust per area. Propellers with more blades allow for smaller propellers to be used to produce the same thrust. Since the tip speed of the propeller is strongly related to the noise produced, the slower tip speeds on the smaller propellers will produce significantly less noise. Unfortunately there are significantly fewer commercially available options for propellers with more than 2 blades so finding an appropriate propeller could be difficult.

Stacking propellers also allows for noise reduction and increases the thrust per area at the cost of lower efficiency. Stacking propellers is ideally suited for when the disk loading is so high that achieving the necessary pressure difference across one propeller is not possible, and the propeller begins to stall. Double stacking propellers allows for the pressure difference to be achieved in steps which allows for propellers to operate more efficiently in these scenarios.

Due to the difficulty in designing, analyzing, and implementing, the double stacked propeller configuration should be a last resort. If the footprint becomes a limiting factor for the craft and disk loading greater than the capability of a 2 blade propeller, higher number blade propellers should be considered first. Similar is true if noise reduction is desired, the simplicity of increasing the number of blades makes it the desired option of the two.

Based on initial research, it appears that neither option is appropriate for the craft at this time. However, further research into both options needs to be done. When the design of the craft is more finely set and the final selection of components is being made, the option to switch to a smaller 3+ bladed propeller may allow for smaller components to be used saving weight and making up for the efficiency loss. Research into these options should be considered low priority as single stacked 2 blade propellers are the standard and are well suited for the application.

21.2.6 Consider Thrust Loss Due to Neighboring Propellers

Research and testing needs to be done to determine the thrust lost due to propellers in close proximity, and the effect that propeller rings will have on performance. As the propellers rotate, they create

turbulence that extends off the end of the propeller. The turbulence will be directly in the rotation path of the neighboring propeller and will almost certainly reduce the efficiency of the neighboring propeller. Propeller rings may eliminate this problem by blocking the turbulence of propeller from interfering with another propeller.

There are additional sources of efficiency loss in our system. Propellers work by accelerating air to create a pressure difference. Simple conservation of mass shows that the intake area of a propeller must be significantly bigger the exit area (and certainly larger than the propeller itself). Since the propellers are overlapped, their intake areas will overlap. If the propellers are able to simply act as one large propeller and form an effective intake area equal to the theoretical size required, the efficiency loss should not be too significant. The more likely scenario is that the overlapping intake areas effectively restrict the airflow to each propeller or cause non-ideal velocity gradients for the propellers. A restricted air flow would reduce the efficiency because in order to produce the same thrust, the air would need to be accelerated much more and would use more energy. Non-ideal velocity gradients would also affect the efficiency of the propellers because the blade angle would no longer be properly suited for the flow speed.

Analysis of these effects will certainly require CFD, which would likely be unreasonable for a senior project. Testing for the thrust loss should be relatively easy. Testing would include a simple test jig with multiple propeller located in close proximity. The propellers would be turned on one at a time and the thrust produced measured. This test should be done before significant work is done to size the propellers because the loss of lift will significantly change the results.

21.2.7 Determine the Benefits of Carbon Fiber Propellers

Carbon fiber propellers are more ideal for the craft than wooden propellers in every way except that in a collision wooden propellers are more likely to break possibly saving the structure of the craft from absorbing the full force of the crash. The magnitude of the advantages need to be quantified to determine if the extra cost for carbon fiber propellers is worth it. The main advantages of carbon fiber propellers is that high quality propellers are lighter (cheap carbon fiber propellers can potentially be heavier than wood) which will save weight, and allow for a quicker response time, and lower required torque for a set response time. The carbon fiber propellers are also stiffer which will increase efficiency. Xoar boats a 37% weight savings by switching to carbon fiber but does specify an efficiency increase. Carbon fiber propellers are absolutely recommended from a performance standpoint, but the efficiency benefits should be known to justify the additional cost.

21.2.8 Reanalyze Configuration Tool

Our current configuration analysis tool was intended to give us a ballpark estimate of which motor count and prop size would give us the maximum possible flight time. We spent quite a bit of time creating the tool using purely theoretical relations and data, and expected to create a second iteration once we had test data to support or refute our original claims. Seeing as we finished testing right before senior expo, we were not able to update our predictions, but we are sure that the program could use some attention.

Several areas that need to be improved are; the structure weight estimate, wire weight estimate, propeller weight curve, motor weight curve, and battery weight curve. The structure weight estimate needs to be modified to take into the varying size of the structure component based on craft size, not just the length of tubing required. The wire estimate needs to be updated for the final battery placement. The propeller weight curve should be redone for the Xoar propellers and similar models instead of the smaller propellers initially used. The same is true for the motor weight curve and battery weight curve.

21.2.9 CFD

Our analysis of double stacked props was based upon actuator disk theory, which is essentially a rudimentary application of basic momentum equations. It works very well for individual props, but likely

lacks the ability to predict the behavior of two props stacked on top of each other. Such a configuration would have incredibly complex interactions, and would only be able to be fully analyzed using computational fluid dynamics (CFD). It may turn out that our conclusions about the inefficiencies of stacking props were way off base.

21.3 Controls

21.3.1 Increase Mini Flight Time

The current iteration of the miniature prototype (the mini) was built using the small mechanical engineering student fee allocation committee budget as the primary concern. If the mini were redone or another larger prototype were built, then other concerns like flight time, thrust, range, footprint, payload capacity, and maneuverability might become more of a concern. If flight time was brought out to be a primary concern for example, the footprint could be expanded and larger, efficient propellers powered by slower spinning motors could be used. The configuration was also based on the full sized craft the team designed, so other configurations with a different number of propellers and different spacing's could be used.

21.3.2 First Person View (FPV goggles)

The mini is currently flyable with a typical RC transmitter and flight control system. This system allows the mini to be flown while it is line of sight of the pilot controlling it. The addition of first person view (FPV) goggles and a corresponding camera system on the mini would allow the mini to be flown out of line of sight. That, along with the flight control system joystick and throttle similar to one implemented on a full craft, would allow for a realistic flight simulation setup. This setup would allow the pilot to fly the craft prior to a manned flight without risking their health.

21.3.3 Battery Charging/Testing

The current system for charging batteries requires the use of an undersized charger owned by the Cal poly robotics club. The mini only has 4 batteries, but it still takes an hour and a half to completely charge. If the craft is scaled up, more batteries will be added and charging will become a problem. A new battery charging system should be implemented with a high power charger from a manufacturer like iCharger or Thunder Power RC. In order to get enough power to the charger to allow it to charge the batteries quickly a high-powered dc power supply will need to be used. The batteries need to be tested for maximum discharge characteristics. When the team did the Rotomax motor testing the upper range of current draw was tested with the batteries specified for the full craft. The batteries showed swelling indicative of an over discharge situation. The team believes this is due to the individual cells in the battery packs being rated for a maximum discharge current, but when the cells are put into a battery pack that maximum safe discharge current should be lowered. A proposed battery testing document has been written up by the team.

21.3.4 Calibration - Long Arm

The calibration of the mini requires placing the front, back, left, right, top and bottom of the flight controller on a flat surface to calibrate the accelerometer and gyroscope. The 3-axis compass needs to be calibrated by spinning the flight controller at least once around the x, y, and z axes. The process of calibrating requires a very flat surface or the mini will constantly drift in one direction during flight. The team saw this drifting action when testing the mini. With the full sized craft, any amount of drift will be amplified by the long arms of the craft. This drift amplification might be mitigated by the addition of an accelerometer, gyroscope, and compass for each arm on the full sized craft. The team would also recommend all calibrations be carried out with a surface that is known to be level.

Mentioned earlier in the report, it may be found that, once built, a full-scale craft will not be controllable with standard flight controller due to the significant distances from the hub of the craft to the arms and the notable deflection of the arms that is expected in normal flying conditions. To increase the effectiveness of the flight controller it may be necessary to apply additional accelerometers to the arms of the craft in order to better estimate its current position and allow for more accurate control. There will be challenges to properly interface and calibrate these external accelerometers to the with the flight controller's built-in accelerometers but it may be a necessary step in order to have a functioning, stable full-scale craft. This is also mentioned in the additional flight controller modules section.

21.3.5 Steps Towards Outdoor Flight

The current legislation restricts the flight of any model aircraft or unmanned aerial vehicles (UAV) on or around Cal poly campus. The FAA is currently discussing the flight of UAVs on campus with the chancellor of the CSU system. The requirements for flight by a public agency (Cal poly) are that a certificate of waiver or authorization be filled out before the mini or the full craft can be flown as a UAV in outside flight. The mini can be flown inside buildings for testing as long as the owner or operator of the building gives permission. This team was able to get permission to fly in Cal poly's recreation center that were extremely helpful in the flight experiments carried out there. If no luck is found there, here is a list of other possible inside locations for flight testing:

- Aero hangar (building 4)
- Bonderson high bay (building 197)
- Simpson lab (building 187)
- Ground level of grand avenue parking structure (building 130)
- Ground level of poly canyon village parking structure (building 271)
- Farm shop (building 9)

21.3.6 Additional Flight Controller Modules (GPS, etc.)

At this time, the mini only has the ability to maintain stability and can relay minimal telemetry data within a short range. Attempts were made to connect a Bluetooth module to the flight controller in order to transfer data and set control gains remotely, but there was little success however, the mini and the full craft could use extra sensors to allow for extra functions. A GPS module could be added to allow position hold and the ability to tell it to go to waypoints on a map. The built-in barometer could be used to allow either craft to hold its altitude. A pitot tube could be added to measure air speed. Sonar, laser, or radar distance sensors could be added to allow for the avoidance of other aircraft and more accurate altitude hold close to the ground or to make a map of the environment around the aircraft. As we recommended in the calibration section above more stability sensors could be added at different places on the craft. The Pixhawk flight controller allows for the addition of a GPS, pitot tube, and some distance sensors fairly easily, but the addition of more stability sensors isn't as easy. They would need to be added to an i2c, can, or serial port and additional programming would be required to add the extra sensors into the flight control algorithm.

21.3.7 Different Flight Controller

The original choice for flight controller was the OpenPilot revolution, but due to the fact that a single person is manufacturing that flight controller the team wasn't able to order it. The OpenPilot was the team's preferred choice due to the ease of making more customized flight configurations. The Pixhawk and the OpenPlot flight controllers have some fairly similar hardware, prices, and extra sensor modules. The biggest difference is the software used on the flight controllers. There is a possibility due to similarities in hardware that the OpenPilot software could be used with the Pixhawk software. The other

option is to make a customized flight controller board with OpenPilot hardware and load the software or make a completely custom flight controller and develop new software for it as well.

21.3.8 Other Power Sources

Batteries are the easiest way of getting power to a flying vehicle, but they have limited capacity and add to the craft weight. It is recommended that alternative systems of power be looked into. The only way to guarantee near-infinite flight time would be to build a tethered power system for the craft, but be solely for testing purposes. Another possible way of powering the craft is to use a specially tailored solar panel-like device to beam power with a near-infrared laser. This system is being worked on by Lasermotive and it is still in the early stages of development. Another possibility of power source is a hybrid system with an internal combustion engine powering an electrical generator, which would then power the craft. This system relies on the high energy density of fuels relative to batteries to make up for the inefficiencies of the combustion cycle. The hybrid system was initially removed as an option for powering flight because of the difficulties of properly connecting the electrical and mechanical energy domains as well as the significant weight from the addition of an engine but teams are still encouraged to research the area and look for possible applications.

21.3.9 Custom Battery Packs

As was mentioned in the battery charging/testing some of the commercial off-the-shelf batteries specifications are inflated or wrong. The battery specifications could be tightly controlled if the batteries were ordered as a custom pack from a company that does battery packs. The pack's final weight and cost might be able to be cut down as well.

21.3.10 Asymmetric Weight Distribution Testing

In the testing of the mini and in the team's designs of the full craft the team tried its best to balance the weight of the crafts evenly. If the crafts were used for payload testing asymmetric weight distribution should be tested. The craft might need to be calibrated differently depending on what type of payload.

21.3.11 Disturbance Testing (wind, etc.)

In the mini testing, one motor was turned off and it was found that it could compensate for at least one motor being unusable. In the mini testing, there were no tests for large disturbances like wind or objects hitting the craft because operation was limited to indoors. If the full craft were made disturbances would have to be accounted for with extra sensors or tested for extensively.

21.3.12 Hard-Wiring Controls

The control system for the mini is an option between a RC transmitter and a flight control system joystick and throttle. Either control system could be ported over to a larger craft, but they are both limited by wireless transmission. The flight control system joystick and throttle could be hard-wired if the usb data were translated into pulse width modulation (pwm) or pulse period modulation (ppm) that the flight controller uses as a control signal. The flight control system would also need 5 volt power because it would no longer be getting power through usb.

21.4 ECM Team (Future Project Direction)

21.4.1 Multidisciplinary Project (CSE, EE, AERO, ME)

In order for this project to be successful, the team suggests that future groups be multidisciplinary. To handle the various aspects of designing a multi-rotor aircraft, a team consisting of electrical engineers, computer science engineers, mechanical engineers and aerospace engineers would be ideal. Even though much was accomplished utilizing only mechanical engineers, it would be very beneficial to have specific experts focus on the various areas that they are accustomed to. Researching unfamiliar aspects of aero/multicopter design such as electrical power systems and programmable flight controllers was an inefficient use of the group's time given the scope of the project. These small specialized teams could then tackle their respective areas in a timelier manner.

However, a multidisciplinary team would inevitably create complexities when it comes to communication and integrating the various subsystems within the design. A project management role is recommended to guide the project, communicate between various groups, and to mitigate any issues that arise.

21.4.2 Smaller Senior Project

Smaller groups or smaller senior projects to make the Electric Commuter Multicopter as a whole will allow for a more efficient and better performing design. In the current state the group struggled with setting meetings and other scheduling limitations associated with large groups. In addition one person could not have a full understanding of the entire project. When someone worked on multiple sections of the project focused one section at a time, the other section of the project suffered because that person possessed vital information. As a result entire sections of the project were temporarily stuck because one person was working on another section leaving individuals without anything productive to do.

Smaller groups would also allow for a more in-depth design on specific components. A small group would be able to focus on their individual task, and learn everything relating to that task. In the large group every person wanted to know what the other groups were doing and as a result no one was able to focus purely on their task. This phenomenon also slowed design because everyone wanted to have their input on a design. As a result a subgroup spent considerable time proving or disproving the validity of designs to the rest of the group which possessed less familiarity with the design area. Given no time constraints this would produce better results, but for a senior project where the design time frame is considerably limited, the time spent discussing designs as a group just limited the ability of subgroups to progress through the design process decreasing the quality of the final design.

21.4.3 Larger Senior Project

It would be unwise for the next senior project to deviate from what works without a legitimate reason to justify doing so. The ECM team worked together as a unit with no set leader in place to guide the project along. Each critical decision that affected the team was brought to the attention of the group and was discussed until a consensus was reached. Though slightly inefficient, this system works well if the people on the team are rational and understanding. If there is a certain person that does not embody these traits, the project's path could take an interesting and potentially bad route.

While the large group seems to work well, a hands on advisor could be very beneficial. One of the big learning opportunities in this project was the experience of working in a large group. Engineers will be required to work in groups of more than two or three in industry, and the nine person experience is very valuable. Having a more hands on advisor would help the project keep advancing while the team learn how to work as part of a nine person group.

21.4.4 Advertising (Outside Financing)

This project has the potential to make history by designing and building something the collegiate level has never seen before. The success of this project will benefit the Cal poly name and increase the prestige of the college of engineering. Success is the ultimate goal, but there is no success if there is no need for it. This project should be known and given a presence within the aerial vehicle community, and advertisement is the way to do just that. If done correctly, advertising this project's triumphs and accomplishments will influence the project's continuation and encourage the team members to do their best engineering.

There are many ways to advertise a project like this and it is fairly easy with today's digital media. Digital media is a potentially viral source of advertisement, and if used properly can make headlines within days. Obtaining help from the journalism and graphic communications departments at Cal poly will help get the ball rolling within the Cal poly community. In addition, a Facebook, twitter, and Instagram pages are all excellent forms of digital media. T-shirts are also a great way of getting the ECM name out there.

21.4.5 Objective Defined/Clarity

The design of a project is contingent upon the problem definition and the it's respective parameters. This iteration of ECM did not have a clearly defined problem definition by the sponsors, which made it hard to design to their needs. Though it is primarily out of the engineer's control, it is recommended to advocate for a clear and explicit problem definition and parameters.

21.4.6 Set Standards/Formatting

For convenience and efficiency a set standard for documents should be established. This pertains to weekly status reports; meeting agendas; and the preliminary, critical, and final reports.

21.4.7 Objective Defined/Ultralight Regulation

In order to create a concise scope for the project, a clear objective for the Electric Commuter Multicopter must be defined. Currently, ECM is in a conflicted state where its purposes cannot be truly met due to restrictions of ultralight aircraft from far 103. The inability of flying within populated areas negates the main goal of avoiding congested roadways and cutting commuting time. To solve this problem, the team recommends clearly defining the main objective of this aircraft. Either stay within the ultralight guidelines and create a hobbyist vehicle for recreational use, or ditch the far 103 requirement altogether and try to form a new type of commuter vehicle. All of this is subject to the future stance of the FAA regarding aerial commuter vehicles and multicopter use, so until the rules change, team ECM believes that a non-ultralight electric multicopter would be a more viable project. Without far 103, alternative materials and components could be selected, or a structural redesign could take place, both of which could increase performance and safety.

21.4.8 Monetary Transparency/Outside Financing

First and foremost, an adequate budget must be provided if this project is to be continued. Unfortunately for the current team, the necessary funding needed to build a manned multicopter was not available through the sponsors. The initial design budget was priced at around \$35,000 but alternative smaller designs can be done with around \$5,000 to \$10,000. A clear budget would greatly benefit the scope and success of an ambitious project such as this. This team was able to acquire some funding through the university and we would also recommend continuing this trend with the addition of a sponsor budget. If funding through a sponsor such as Lawrence Livermore national labs/NASA Ames does not occur, outside financing is required. To allow for further exploration in an ECM project, communication to various

organizations and companies is highly advised and either through advertising or use of company products; an arrangement can be made for financing.

21.4.9 Increased Sponsor Interaction

To insure project goals are met in a yearlong timeline, a sufficient amount of sponsor interaction is required. The team suggests a period of no more than two weeks between status updates to provide the necessary sponsor feedback and direction for the project. There were times where contact with the sponsor was difficult and the time lost meant that the project was in a state of limbo where we needed the necessary permission to continue along a certain path. Timely responses is key in order to continue to accomplish the demanding goals in such a compact schedule. The team also recommends a point of contact for the sponsors. This eliminates sponsor ambiguity of who to contact and also the possibility of contacting the sponsor more than once about the same topic.

21.4.10 Implementing Good Data Management Practices

With addition to and changes in project direction, the ECM team advises an established way of storing and formatting team data. Team members must keep up on logging in work time and providing adequate work within their log book. The current team uses google drive to store all the team's work, which has worked very well for our needs. However, Microsoft OneDrive may prove even more useful for a future team. Formulating a Gantt chart early on with concrete deadlines and goals will highly benefit a team working towards completing a complicated project such as this one. Allocating team members to work times where small teams can accomplish goals in scheduled times is also advised. The earlier these suggestions are completed, the more that can be achieved.

21.5 Other designs

21.5.1 Design Parametric Study for Varying Payloads

Throughout the year, our sponsors seemed a little shaky on the required payload capacity. We originally designed to carry a passenger with minimal gear (200 lbs), but found out later that we may have only needed to accommodate a carrying capacity of 70 lbs for payload testing to be done by either Lawrence Livermore or NASA Ames. If this were the case, it may be a good idea to add a third independent variable to the configuration analysis tool: payload capacity. Reduced payload would greatly reduce the amount of power draw from the batteries, and may redistribute where our priorities lie with respect to weight. If this were to be accomplished, an output of max flight time vs. Payload could be presented to the sponsors, giving them better insight on what they would be getting out of a requested design.

21.5.2 Gyrocopter (if VTOL is not a requirement)

One of the main issues with a manned multicopter is its lack of glide in case of power loss, to combat this the team suggests incorporating the aspects of gyrocopters in a new multicopter design. To somehow introduce propeller autorotation in the design would allow for a type of glide to a safe landing area. To incorporate this component along with VTOL capabilities would obviously increase mechanical and electric complication within an already highly complicated aircraft but the additional safety aspects of automation should not be ignored.

21.5.3 Over-body Vehicle Research

Orienting the props above the user shifts the overall center of gravity below the plane of props. This in turn means that when the vehicle is tilted on any axis, a corrective moment results, and the craft tends to lean towards equilibrium. Essentially, raising the props above the user creates an inherently stable

system. However, doing so will likely result in a heavier structure, which is why we originally dismissed the idea.

21.5.4 Truss Structure

A truss structure should be considered in future iterations. The current structure is a simple cantilever design. The cantilever is simple to build and analyze. However the cantilever design caused very high bending moments to be developed in the center mount and the spar causing the need for very strong and heavy components. A truss structure would allow the load to be supported by two force members which could offer a much better strength to weight ratio since the truss members are better situated to resist a moment.

The drawback of the truss structure is that for a carbon fiber frame a significant source of weight is the connecting pieces. A truss structure would require more connections which may increase the weight. However, since the truss structure would be supporting the loads with two force members the connecting pieces would not need to support moments and would be significantly smaller and simpler than the currently used connecting pieces. The small, simple components would save time and money during manufacturing and the individual weight savings may offset the increase in the total weight of structural components.

Since the loading on the craft structure is not reversed the truss components will always carry their load in tension or compression. The predictability of the load will allow for the tension components to potentially be replaced with very light weight and high strength rope (dyneema, spectra or vectran are recommended). The lightweight and aerodynamic benefits from the small cross section of rope should be advantageous over carbon tubes.

21.5.5 Fairing/Roll Cage

Safety for the pilot should always remain paramount and to insure this a structure to protect the pilot is highly advised. If the project objective of ultralight regulation were to be modified one option to protect the user is designing and building a fiberglass or carbon fiber fairing which provides a shield from flying debris and high velocity wind. This fairing would not provide complete protection from a catastrophic crash but it could mitigate the effects of an uncontrolled fall to the ground. An alternative design would include a type of roll cage, preferably formed from carbon fiber to decrease overall structure weight. Carbon fiber would be the most costly option and would result in a complicated manufacturing process but its strength and weight benefits outweigh these negatives. This roll cage could also incorporate skids which would avoid the design of separate landing gears.

22 CONCLUSION

The Electric Commuter Multicopter project was given to the Mechanical Engineering Department of Cal Poly, San Luis Obispo by Bob Addis and Bill Bruner of Lawrence Livermore National Laboratory. The concept of an aerial vehicle as a commuting transportation device was meant to eliminate traffic congestion and reduce commuting time for the user, granting him more freedom in daily travel. Specific parameters such as Federal Aviation Administration regulations and safety requirements needed to be met, which then restricted the number of feasible designs that could ultimately be considered. In addition, we weren't able to obtain funding from LLNL, limiting the efficiency of the team throughout the quarter and the manufacturing of a full scale prototype. From discussions with the sponsors throughout the academic year, this project would eventually become more of a feasibility study, keeping in mind the initial requirements of the project.

To meet the needs of this project, our team of 9 mechanical engineers sought help from other departments within the University. The Computer Engineering, Computer Science, Aerospace Engineering, and Business Administration Departments were contacted. Though enthusiastic about the project, these departments couldn't be of any substantial help. As a result, the ECM team divided into three groups to analyze the main systems of the design: Structure, Propulsion, and Control System. Though these groups were distinct, each member had some involvement within each group.

With the help of funds from Cal Poly, the team was able to perform testing on the structural components, propulsion system, and the flight control system. These tests validated the design and highlighted areas that needed to be improved in future years.

The goal of the structural team was to produce a low weight, safety factored carbon fiber and steel structure. The low weight structure was necessary to meet the 254lb maximum weight requirement of the team to meet ultralight regulations. This made the use of carbon fiber tubes for the main frame a necessity, offering exceptional strength and stiffness at a very low weight. Steel mounts join the frame together and account for a large portion of the aircraft's weight. While these mounts do cost the structure in terms of weight, they also provide easy mounting points for components, good impact resistance compared to carbon, are within the team's capability to produce, and offer a solid platform for welding and epoxy bonding. A propeller safety ring system consisting of both carbon fiber rings and lightweight mesh provide additional safety to the user, craft, and bystanders by helping keep foreign debris from being pulled into the rotors and shot outwards.

The team has confidence that the components selected will satisfy the requirements with a couple exceptions. The epoxy used for the carbon to steel joints did not work for this application, therefore the epoxy for composite to metal joints needs immediate research and analysis. A vibrational analysis for the structure needs attention as well.

The propulsions team focused on analyzing the performance of the motors and propellers. The research focused on using Actuator Disk Theory to relate test data from one propeller to another. JavaProp, a propeller modeling program was also used to try and estimate the performance of commercially available propellers, and the motor performance requirements for a given propeller. The propulsion also researched battery and speed controller selection to ensure the entire propulsion system is compatible. The propulsion team decided that 12 30X10 propellers spun by the Joby JM1S motor powered by two 7S Li-Po batteries in series was the best propulsion system. During testing the propulsion team identified several areas that will need much more advanced analysis techniques such as CFD and examining overlapping intake areas. Identifying these areas will allow future teams to focus their efforts only on the critical areas.

The goal of the controls team was to develop and test an inexpensive, fully-functioning control system that would allow for vehicle navigation and control as well as provide an intuitive human machine interface. To this end, the team opted to use an OpenPilot Revolution flight controller with 12 outputs and speed of 168 MHz, communications via a telemetry kit and personal computer running the OpenPilot

GCS software, and user interface via the Saitek X52 flight control system. This allows for easily modifiable control of the craft with an input device that can be mounted on the craft or held in hand for testing and VR practice, with a range of approximately 20 km. For the final vehicle, communications would be hardwired into the system via a USB to PPM crafted with an independent control board. The flight controller comes with the OpenPilot GCS software suite for ease of programming. Most importantly, all major components are COTS, reducing the cost tremendously from a custom aircraft control system. Testing on a small scale went successfully, and taught the team a lot of valuable information. The future now requires the next step of testing with a full scale vehicle and verifying the scaling of controls principals.

The Electric Commuter Multicopter team set a foundation for the project and the iterations to come. The original design requirements were found to be ambitious however unreachable given not enough financial capital and a thin technological limit. With altered design requirements in the coming year the chance of success for future teams is very likely.

23 ACKNOWLEDGEMENTS

The ECM team would like to thank the following Cal Poly staff for their support and guidance through this senior project.

- Dr. Fabijanic, Advisor, ME
- Dr. Mello, Composite Design, ME
- Dr. Schuster, Senior Project Coordinator, ME
- Dr. McDonald, Propulsion & Motor Implementation, AERO
- Kevin Williams, Welding & Manufacturing, IME
- Robyn Claborn, ASI-Asst. Dir. Ops, Recreation Center

24 REFERENCES:

- [1] United States. US Department of Transportation. Federal Aviation Administration. *103-7 The Ultralight Vehicle*. N.p.: Federal Aviation Administration, 1984. Web. 5 Oct. 2014. <[http://rgl.faa.gov/Regulatory_and_Guidance_Library/rgAdvisoryCircular.nsf/list/AC%20103-7/\\$FILE/Signature.pdf](http://rgl.faa.gov/Regulatory_and_Guidance_Library/rgAdvisoryCircular.nsf/list/AC%20103-7/$FILE/Signature.pdf)>.
- [2] "Federal Aircraft Regulations, Part 103:." *FAR Part 103*. The Ultralight Home Page, n.d. Web. 5 Oct. 2014. <<http://www.ultralighthomepage.com/FAR.part103.html>>.
- [3] "Chapter 14: Airspace." *Pilot's Handbook of Aeronautical Knowledge*. N.p.: Federal Aviation Administration, 2008. 14-1-4-10. *Pilot's Handbook of Aeronautical Knowledge*. Federal Aviation Administration, 2008. Web. 12 Oct. 2014. <http://www.faa.gov/regulations_policies/handbooks_manuals/aviation/pilot_handbook/media/PHAK%20-%20Chapter%2014.pdf>.
- [4] "Background of Ultralight Historical." *Human'Air*. Human'Air, n.d. Web. 19 Oct. 2014. <<http://www.human-air.net/en/ulmhistoric>>.
- [5] "E-volo | Aviation Pioneering – Aviation Future." *Evolo* RSS. N.p., n.d. Web. 20 Oct. 2014. <<http://www.e-volo.com/information>>.
- [6] "E-volo | VC1 – Proof of Concept." *Evolo* RSS. N.p., n.d. Web. 20 Oct. 2014. <<http://www.e-volo.com/information/vc1-proof-of-concept>>.
- [7] "E-volo | VC200 – the First Volocopter to Carry Two People." *Evolo* RSS. N.p., n.d. Web. 20 Oct. 2014. <<http://www.e-volo.com/ongoing-developement/vc-200>>.
- [8] "E-volo | How Long Can The Volocopter Fly?" *Evolo* RSS. N.p., n.d. Web. 20 Oct. 2014. <<http://www.e-volo.com/information/how-long-can-you-fly>>.
- [9] Malloy, Chris. "THE HOVERBIKE." – *MA Hoverbike*. N.p., n.d. Web. 17 Oct. 2014. <<http://www.hover-bike.com/MA/the-hoverbike/how-you-can-own-it/>>.
- [10] DeRoche, Mark. "The Aero-X - Aerofex." *Aerofex The AeroX Comments*. Aerofex Corp, n.d. Web. 17 Oct. 2014. <<http://aerofex.com/theaerox/>>.
- [11] Lewis, Jeff. "Autogyro History and Theory." *Autogyro History and Theory*. N.p., 4 Jan. 2002. Web. 16 Nov. 2014.
- [12] "The Butterfly LLC - The Ultralight Butterfly Specifications." *The Butterfly LLC - The Ultralight Butterfly Specifications*. N.p., n.d. Web. 17 Nov. 2014.
- [13] Cartier, Kerry. "Popular Rotorcraft Association :: Gyroplane FAQs." *Popular Rotorcraft Association :: Gyroplane FAQs*. N.p., n.d. Web. 16 Nov. 2014.
- [14] Dodson, Brian. "Redesigned Martin Jetpack Deliveries Expected to Start in 2014." *Redesigned Martin Jetpack Deliveries Expected to Start in 2014*. Gizmag, 28 Sept. 2013. Web. 20 Oct. 2014. <www.gizmag.com/martin-jetpack-p12/29215>
- [15] "The Martin Jetpack – Fly the Dream." *The Martin Jetpack*. N.p., 2013. Web. 20 Oct. 2014. <www.martinjetpack.com>
- [16] "BlackHawk Kestrel Paramotor Frame." BlackHawk Paramotor, 2011. Web. 16 Oct. 2014. <<http://www.blackhawkparamotor.com/cages/blackhawk-kestrel-paramotor/>>.

- [17] "Paramotor FAQ." *Flying High Paramotors*. N.p., n.d. Web. 16 Oct. 2014. <<http://flyhighparamotors.com/paramotor-f-a-q/>>.
- [18] "Scout Paramotors Innovative Features - Scout Paramotors USA." *Scout Paramotors USA*. Team Fly Halo, 2014. Web. 16 Oct. 2014. <<http://scoutparamotorsusa.com/scout-paramotors-innovative-features/>>.
- [19] "Learn to Fly." *Bhpa.co.uk*. British Hang Gliding & Paragliding Association, n.d. Web. 16 Oct. 2014. <http://www.bhpa.co.uk/sport/bhpa/learn_to_fly/>.
- [20] "Frequently Asked Questions." *Paramotor FAQ : Adventure Replies to All Questions*. N.p., n.d. Web. 16 Oct. 2014. <<http://www.paramoteur.com/faq>>.
- [21] "Heavy Lift Nylon Blimps | Blimps." *Heavy Lift Nylon Blimps | Blimps*. N.p., n.d. Web. 17 Nov. 2014.
- [22] "Mosquito Aviation - Home of the Ultimate Ultralight Helicopter : New ! Carbon Fibre Tailrotors." *Mosquito Aviation - Home of the Ultimate Ultralight Helicopter : New ! Carbon Fibre Tailrotors*. N.p., n.d. Web. 21 Oct. 2014. <<http://www.innovator.mosquito.net.nz/mbs2/cftr.asp>>.
- [23] "Kolb FireFly, Kolb FireFly Part 103 Legal Ultralight Aircraft, Kolb FireFly Ultra Lite Plane, Ultralight News Newsmagazine." *Kolb FireFly Ultralight, Kolb FireFly Part 103 Legal Ultralight Aircraft, Kolb FireFly Ultra Lite Plane, Ultralight News Newsmagazine*. Ultralight News, n.d. Web. 20 Oct. 2014. <<http://www.ultralightnews.com/ssulbg/firefly-thenewkolbaircraft.html>>
- [24] "Kolb Aircraft Firefly 103 Legal Ultralight." *Kolb Aircraft Firefly 103 Legal Ultralight*. N.p., Sept. 2011. Web. 20 Oct. 2014. <www.kolbaircraft.com/firefly.htm>
- [25] Page, Lewis. "Personal Air Vehicle' VTOL Jump-copter in Key Flight Test." • *The Register*. N.p., 24 Jan. 2011. Web. 16 Nov. 2014.
- [26] "Carter Aviation Technologies, An Aerospace Research & Development Company." *Carter Aviation Technologies*. Carter Aviation Technologies, 2014. Web. 16 Nov. 2014.
- [27] "Patent WO2013174751A3 - Method for Controlling an Aircraft in the Form of a Multicopter and Corresponding Control System." *Google Books*. N.p., n.d. Web. 17 Nov. 2014.
- [28] "Patent US20060266881 - Vertical Takeoff and Landing Aircraft Using a Redundant Array of Independent Rotors." *Google Books*. N.p., n.d. Web. 17 Nov. 2014.
- [29] "Patent DE102012202698A1 - Vertical Take-off and Landing Aircraft for Transporting People or Loads, Has Signal Processing Unit Performing Position Control Such That Aircraft Is Horizontally Located in Space without Pilot's Control Inputs or Remote Control." *Google Books*. N.p., n.d. Web. 17 Nov. 2014.
- [30] Brain, Marshall, and William Harris. "How Helicopters Work." *HowStuffWorks*. HowStuffWorks.com, n.d. Web. 19 Oct. 2014. <<http://science.howstuffworks.com/transport/flight/modern/helicopter.htm>>.
- [31] Norris, Donald. "Flight Basics." *Build Your Own Quadcopter: Power up Your Designs with the Parallax Elev-8*. N.p.: McGraw-Hill/TAB Electronics, 2014. N. pag. *Safari Tech Books Online*. Web. 18 Oct. 2014. <http://proquest.safaribooksonline.com/book/hardware-and-gadgets/9780071822282/2-quadcopter-flight-dynamics/ch02lev1sec1_html>.
- [32] Norris, Donald. "Quadcopter Controls." *Build Your Own Quadcopter: Power up Your Designs with the Parallax Elev-8*. N.p.: McGraw-Hill/TAB Electronics, 2014. N. pag. *Safari Tech Books Online*. Web. 18 Oct. 2014. <http://proquest.safaribooksonline.com/book/hardware-and-gadgets/9780071822282/2-quadcopter-flight-dynamics/ch02lev1sec2_html>.

- [33] Krasner, Helen. "How Do Helicopters Fly? Lift, Drag, and Thrust." *Decoded Science*. N.p., 21 Nov. 2012. Web. 20 Oct. 2014. <<http://www.decodedscience.com/how-do-helicopters-fly/20418>>.
- [34] Gibiansky, Andrew. "Quadcopter Dynamics, Simulation, and Control Introduction." (n.d.): n. pag. *Andrew Gibiansky*. Andrew Gibiansky, 23 Nov. 2012. Web. 2 Oct. 2014. <<http://andrew.gibiansky.com/downloads/pdf/Quadcopter%20Dynamics,%20Simulation,%20and%20Control.pdf>>.
- [35] "APM Copter." *ArduCopter*. 3D Robotics, n.d. Web. 20 Oct. 2014. <<http://copter.ardupilot.com/>>.
- [36] "AeroQuad - The Open Source Quadcopter / MultiCopter." *AeroQuad*. AeroQuad Open Source Project, n.d. Web. 20 Oct. 2014. <<http://aeroquad.com/content.php>>.
- [37] "OpenPilot.org – The Next Generation Open Source UAV Autopilot." *OpenPilot*. Open Pilot Foundation, 2013. Web. 20 Oct. 2014. <<http://www.openpilot.org/>>.
- [38] Cantrell, Paul. "Ground Effect." *Helicopter Aviation*. Paul Cantrell, n.d. Web. 18 Nov. 2014.
- [39] "Chapter 4: Aerodynamics of flight." *Pilot's Handbook of Aeronautical Knowledge*. N.p.: Federal Aviation Administration, 2008. 14-1-4-10. *Pilot's Handbook of Aeronautical Knowledge*. Federal Aviation Administration, 2008. Web. 17 Nov. 2014. <http://www.faa.gov/regulations_policies/handbooks_manuals/aviation/pilot_handbook/media/PHAK%20-%20Chapter%2014.pdf>.
- [40] Cascio, Jamais. "Open the Future: Record Battery Energy Density in Context [Updated]." *Open the Future: Record Battery Energy Density in Context [Updated]*. N.p., 27 Feb. 2012. Web. 20 Oct. 2014. <http://www.openthefuture.com/2012/02/record_battery_energy_density.html>
- [41] "All About Batteries." *Ni-MH Batteries (Nickel Metal Hydride)*. N.p., 16 Feb. 2013. Web. 18 Nov. 2014.
- [42] "What's the Best Battery?" *Advantages and Limitations of the Different Types of Batteries*. Battery University, n.d. Web. 19 Oct. 2014. <http://batteryuniversity.com/learn/article/whats_the_best_battery>
- [43] Nugent, Tom. *Laser Power for UAVs*. Tech. N.p.: LaserMotive LLC, 2010. Print. <<http://lasermotive.com/wp-content/uploads/2010/04/Wireless-Power-for-UAVs-March2010.pdf>>
- [44] Akturk, Ali, and Cengiz Camci. "ASME DC | Journal of Turbomachinery | Tip Clearance Investigation of a Ducted Fan Used in VTOL Unmanned Aerial Vehicles-Part I: Baseline Experiments and Computational Validation." *ASME DC | Journal of Turbomachinery | Tip Clearance Investigation of a Ducted Fan Used in VTOL Unmanned Aerial Vehicles-Part I: Baseline Experiments and Computational Validation*. N.p., 26 Sept. 2013. Web. 18 Nov. 2014.
- [45] www.esotec.org/hbird/HTML/DuctMyths_F.html
- [46] "Average Annual Miles per Driver by Age Group." *Average Annual Miles per Driver by Age Group*. United States Department of Transportation - Federal Highway Administration, 26 Sept. 2014. Web. 17 Oct. 2014. <<https://www.fhwa.dot.gov/ohim/onh00/bar8.htm>>.
- [47] Schrank, David, Bill Eisele, and Tom Lomax. "Urban Mobility Report." (n.d.): n. pag. INRIX Traffic Data, Dec. 2012. Web. 17 Oct. 2014.
- [48] "Compare Side-by-Side." *Fueleconomy.gov*. US Department of Energy, 2014. Web. 17 Oct. 2014. <<http://www.fueleconomy.gov/feg/Find.do?action=sbs&id=34489>>.
- [49] "F-150 STX." Ford, 2014. Web. 17 Oct. 2014. <<http://www.ford.com/trucks/f150/trim/stx/>>.

- [50] *Pilot's Operating Handbook*. N.p.: PiperSport Distribution Inc., 03 Oct. 31. PDF.
- [51] "R22 BETA II Helicopter." *Robinson Helicopter Co.* N.p., n.d. Web. 17 Oct. 2014. <http://www.robinsonheli.com/rhc_r22_beta_ii.html>.
- [52] Department of Mechanical Engineering. *ME 428-429-430 Senior Design Project Lecture #1 Budget, Travel, Research*. San Luis Obispo: California Polytechnic State University, n.d. PPT.
- [53] Maekawa, Shoji, Kouichi Shibasaki, Toyotoshi Kurose, Toshiyuki Maeda, Yoshitaka Sasaki, and Tatsuya Yoshino. "Tear Propagation of a High-Performance Airship Envelope Material." *Journal of Aircraft* 45.5 (2008): 1546-553. Web.
- [54] Boundy, Bob, Susan W. Diegel, Lynn Wright, and Stacy C. Davis. *Biomass Energy Data Book*. Appendix A. N.p.: US Department of Energy, 2011. Print.<http://cta.ornl.gov/bedb/appendix_a/Lower_and_Higher_Heating_Values_of_Gas_Liquid_and_Solid_Fuels.pdf>
- [55] Steiger, Jon N. "The Ultralight Home Page." *The Ultralight Home Page*. N.p., n.d. Web. 20 Oct. 2014. <<http://www.ultralighthomepage.com>>
- [56] Department of Mechanical Engineering. *ME428/ME429/ME430 Senior Project Reference Book and Success Guide*. San Luis Obispo: n.p., 2014. Department of Mechanical Engineering, Sept. 2014. Web. 14 Oct. 2014.
- [57] *Renewable Energies*. By Art MacCarley. Germany, Munich. July-Aug. 2014. Performance.
- [58] "Commercial / Business Aerospace Testing Services." *Aerospace Testing*. Dayton T. Brown Inc., 2014. Web. 17 Nov. 2014.
- [59] "195 Epoxy Resin/206 Slow Hardener." (2013): n. pag. West System. Web. <http://www.westsystem.com/ss/assets/Product-Data-PDFs/TDS%20105_206.pdf>.
- [60] "Black Max Comfortlite Folding Seat." Black Max, 2003. Web. <<http://www.blackmaxbrakes.com/comfortlite-seat>>.
- [61] "Bow Tie Cotter Pin." *McMaster-Carr*. N.p., n.d. Web. <<http://www.mcmaster.com/#bow-tie-cotter-pins/=vtsjtr>>.
- [62] "Compression Springs." *McMaster-Carr*. N.p., n.d. Web. <<http://www.mcmaster.com/#compression-springs/=vtsodn>>.
- [63] "Easy-to-Weld 4130 Alloy Steel." *McMaster-Carr*. N.p., n.d. Web. <<http://www.mcmaster.com/#alloy-steel-sheets/=vtsd7p>>.
- [64] "Easy-to-Weld 4130 Alloy Steel/ Round Tubes--Unpolished (Cold Drawn)." *McMaster-Carr*. N.p., n.d. Web. <<http://www.mcmaster.com/#alloy-steel-hollow-rods/=vtsqgb>>.
- [65] "Extreme-Strength Hex Nuts- Grade 9." *McMaster-Carr*. N.p., n.d. Web. <<http://www.mcmaster.com/#catalog/121/3183/=vtsxm9>>.

- [66] "Grafil 34-700." Grafil Inc., n.d. Web.
<http://www.rockwestcomposites.com/fckeditor_assets/attachments/2F270%2F34-700.pdf%3F1386700840>.
- [67] "Hex Nuts." *McMaster-Carr*. N.p., n.d. Web.
<<http://www.mcmaster.com/#catalog/121/3184/=vtsvjp>>.
- [68] "High-Strength Steel Cap Screws." *McMaster-Carr*. N.p., n.d. Web.
<<http://www.mcmaster.com/#catalog/121/3121/=vtsx52>>.
- [69] "Material Safety Data Sheet: West System 105 Epoxy Resin." (2013): n. pag. Web.
<<http://www.westsystem.com/ss/assets/MSDS/MSDS105.pdf>>.
- [70] "Material Safety Dta Sheet Scotch-Weld (TM) Epxoy Adhesive 2216 B/A, Gray." 3M, 2008. Web.
<http://multimedia.3m.com/mws/mediawebserver?mwsld=SSSSSuUn_zu8l00x4x_x482ePv70k17zHvu9lxtD7SSSSSS-->.
- [71] "Newport 301 Product Data Sheet." *Newport Adhesives and Composites, Inc.* (2006): n. pag.
[Http://www.specmaterials.com/pdfs/Newport301CureData.pdf](http://www.specmaterials.com/pdfs/Newport301CureData.pdf). Web.
- [72] "Pan Head Slotted Machine Screws." *McMaster-Carr*. N.p., n.d. Web.
<<http://www.mcmaster.com/#catalog/121/3003/=vtsuiw>>.
- [73] "Scotch-Weld Epoxy Adhesive 2215 B/A." *Technical Data* (2009): n. pag.
[Http://multimedia.3m.com/mws/media/1539550/3mtm-scotch-weldtm-epoxy-adhesive-2216-b-a.pdf](http://multimedia.3m.com/mws/media/1539550/3mtm-scotch-weldtm-epoxy-adhesive-2216-b-a.pdf).
- [74] "PJP-T 2PJP-T 28 Precision Pair Carbon Fiber Propeller For Electric Multicopter or Fixed Wing Application." Xoar, n.d. Web. 08 Feb. 2015.<<http://www.xoarintl.com/rc-propellers/precision-pair/PJP-T-28-Precision-Pair-Carbon-Fiber-Propeller/>>
- [75] "JM1S." Joby Motors. Joby Motors, n.d. Web. 08 Feb. 2015.
<<http://www.jobymotors.com/public/views/pages/products.php>>.
- [76] "Revolution Hardware Kit." - OpenPilot Store. N.p., n.d. Web. 08 Feb. 2015.
<<http://store.openpilot.org/home/21-revolution-hardware-kit.html>>.
- [77] "Turnigy Dlux 250A HV 14s 60v ESC (AR Warehouse)." HobbyKing Store. N.p., n.d. Web. 08 Feb. 2015.<http://www.hobbyking.com/hobbyking/store/__57873__Turnigy_dlux_250A_HV_14s_60v_ESC_AR_Warehouse_.html?strSearch=Turnigy+dlux+250>.
- [78] "PRC Silicone Wire by the Foot - 8 AWG." ProgressiveRC. N.p., n.d. Web. 08 Feb. 2015.
<<http://www.progressiverc.com/prc-silicone-wire-by-the-foot-8-awg.html>>.

- [79] "Castle Creations - CCBUL6.5X3 6.5mm Bullet Conn 13G/8G 200A (3) - CC BULLET 6.5MM." Active Powersports. N.p., n.d. Web. 08 Feb. 2015. <http://www.activepowersports.com/castle-creations-ccb6-5x3-6-5mm-bullet-conn-13g-8g-200a-3-cc-bullet-6-5mm/?gclid=Cj0KEQIA0aemBRC8p87zv_mc5qYBEiQAIeEMQU-wFRG-q10AdUaYiYc4n_t8ZX31nPpv2liJnwywqSsaAhsL8P8HAQ>.
- [80] "Turnigy Nano-tech 5000mah 7S 65~130C Lipo Pack (AR Warehouse)." HobbyKing Store. N.p., n.d. Web. 08 Feb. 2015. <http://www.hobbyking.com/hobbyking/store/uh_viewItem.asp?idProduct=59238>.
- [81] "150 Watt 120 Volt Soldering Iron with Chisel Style Tip." Amazon. N.p., n.d. Web. 08 Feb. 2015. <<http://www.amazon.com/Watt-Volt-Soldering-Chisel-Style/dp/B008MG9H3A#productDetails>>.
- [82] "Turnigy Dlux 10A (10~60V) HV SBEC." HobbyKing Store. N.p., n.d. Web. 08 Feb. 2015. <http://www.hobbyking.com/hobbyking/store/__24753__Turnigy_dlux_10A_10_60V_HV_SBEC.html>.
- [83] "Scherrer UHF Tx Rx 700 Lite." Hobby Wireless. N.p., n.d. Web. 08 Feb. 2015. <http://hobbywireless.com/scherrer-uhf-long-range-rc-c-98_100/scherrer-uhf-tx-rx-700-lite-p-1538.html>.
- [84] Agarwal, Bhagwan D., Lawrence J. Broutman, and K. Chandrashekhara. Analysis and Performance of Fiber Composites. New York: Wiley, 1980. Print.

Electric Commuter Multicopter

Engineering Part and Assembly Drawings

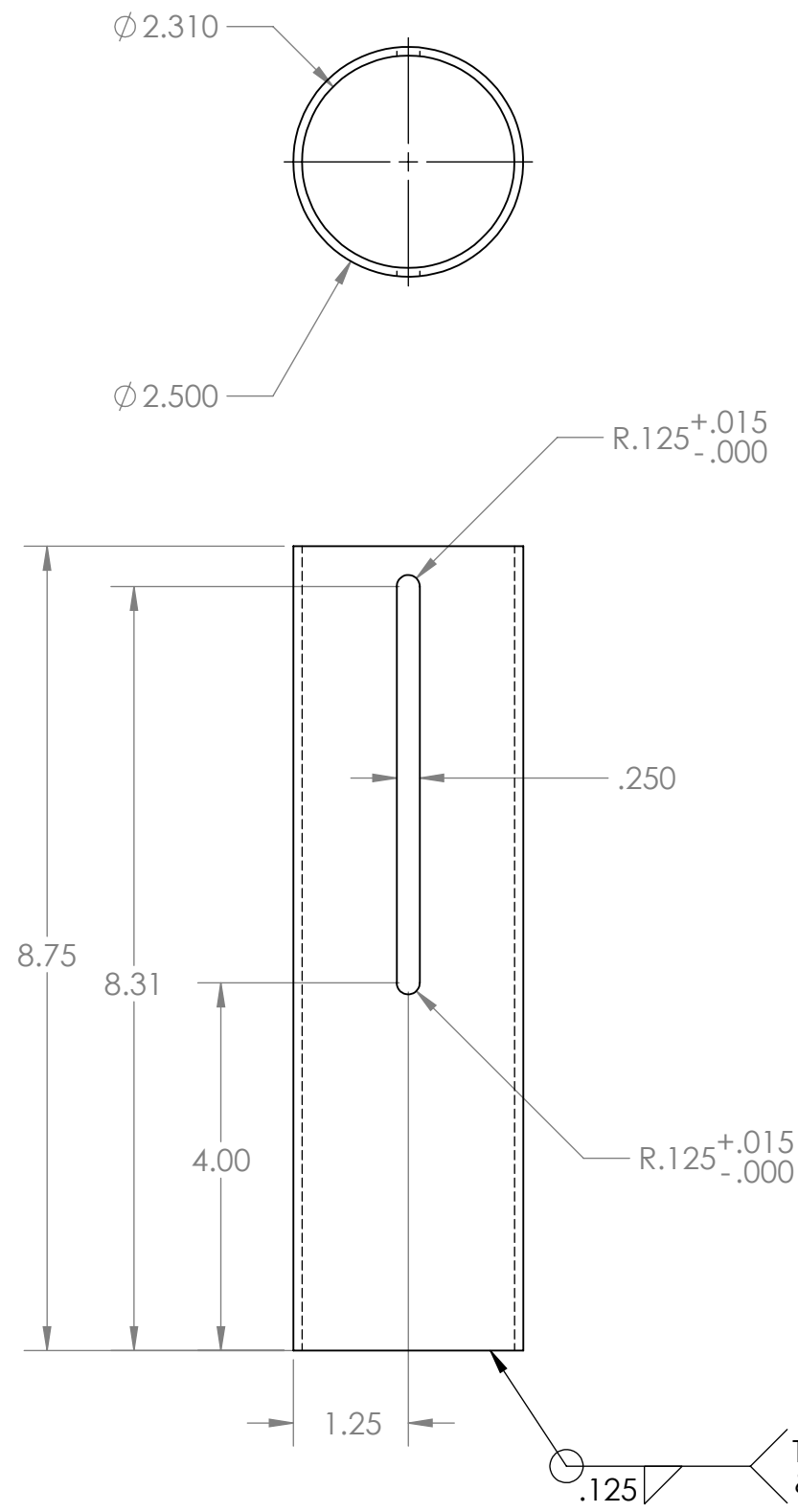
Notes:

Unless otherwise specified,

All tolerances are $\pm 0.010''$

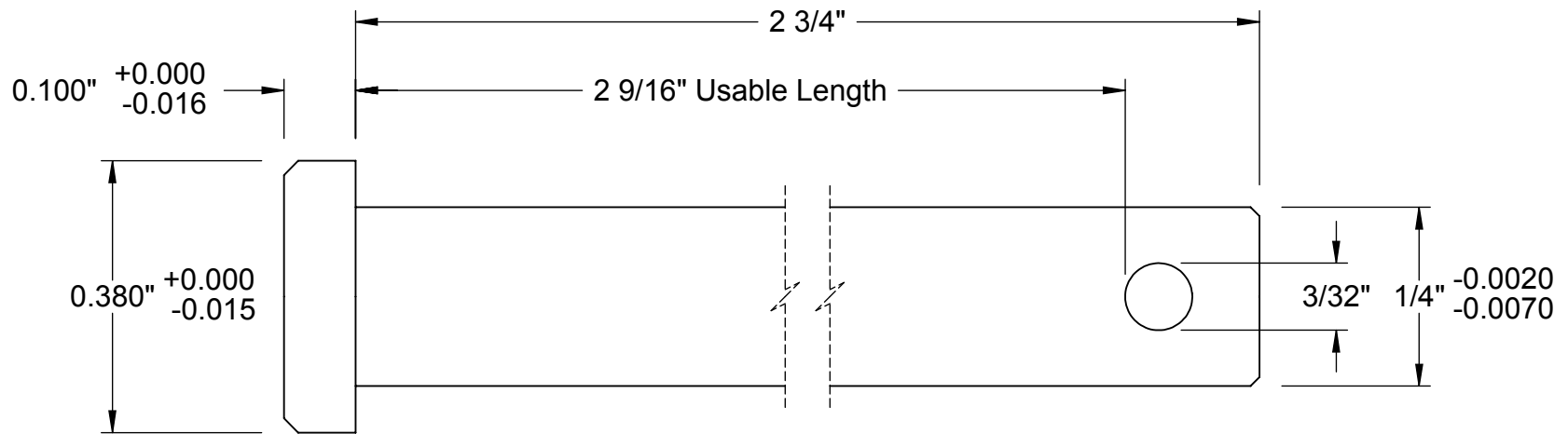
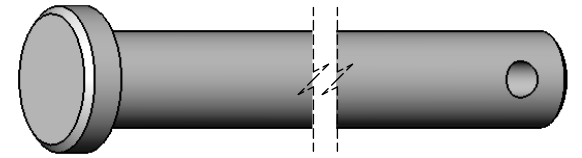
Units are inches and pounds

Positional tolerances on holes is $\pm 0.005''$

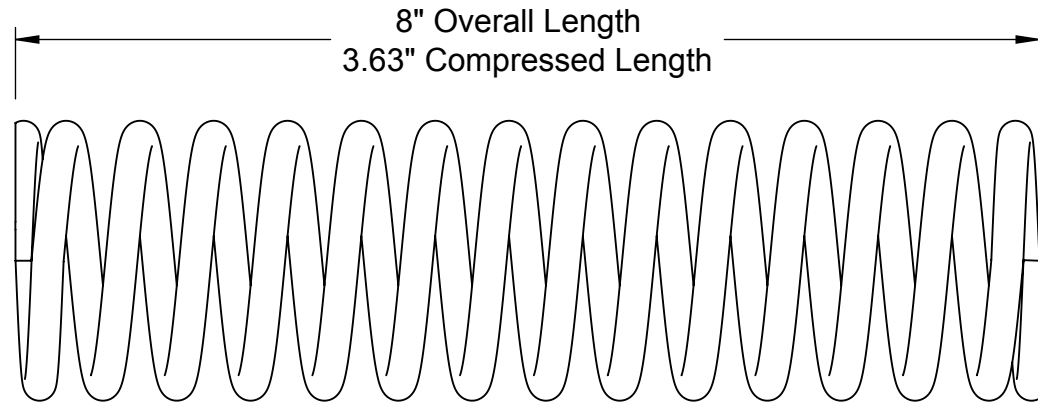
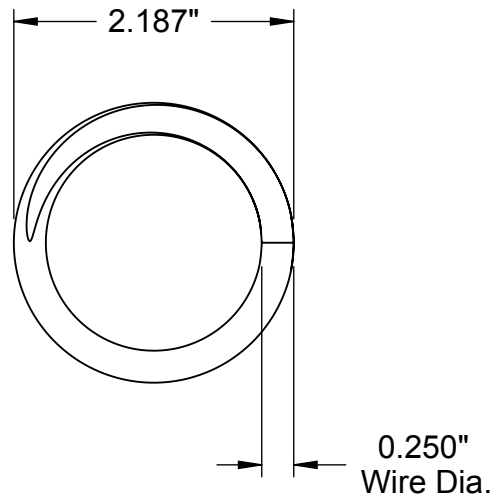
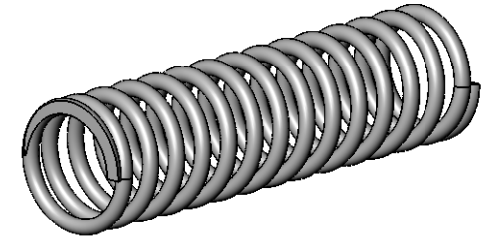


PROPRIETARY AND CONFIDENTIAL
 THE INFORMATION CONTAINED IN THIS DRAWING IS THE SOLE PROPERTY OF ELECTRIC COMMUTER MULTICOPTER TEAM. ANY REPRODUCTION IN PART OR AS A WHOLE WITHOUT THE WRITTEN PERMISSION OF ELECTRIC COMMUTER MULTICOPTER TEAM IS PROHIBITED.

		UNLESS OTHERWISE SPECIFIED:		NAME	DATE		
		DIMENSIONS ARE IN INCHES		DRAWN	MM	1/30/15	TITLE: LANDING GEAR GUIDE TUBE
		TOLERANCES:		CHECKED	OK	1/30/15	
		TWO PLACE DECIMAL ± 0.01		ENG APPR.			
		THREE PLACE DECIMAL ± 0.014		MFG APPR.			
		INTERPRET GEOMETRIC TOLERANCING PER:		Q.A.			SIZE B
		MATERIAL: 4130 CHROMOLY		COMMENTS:			
		FINISH					REV A
NEXT ASSY	USED ON	DO NOT SCALE DRAWING					SCALE: 1:2
							WEIGHT: 1.71
							SHEET 1 OF 1



McMASTER-CARR <small>CAD</small> http://www.mcmaster.com © 2012 McMaster-Carr Supply Company <small>Information in this drawing is provided for reference only.</small>	PART NUMBER 92390A175
	Clevis Pin



McMASTER-CARR CAD

PART
NUMBER

96485K164

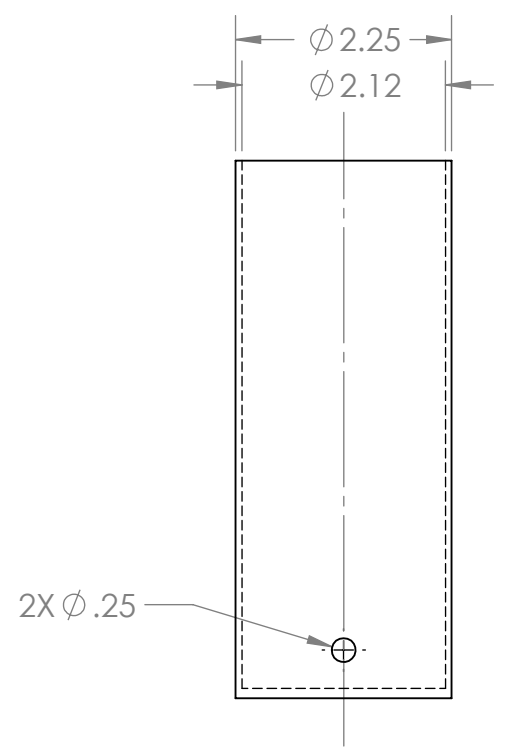
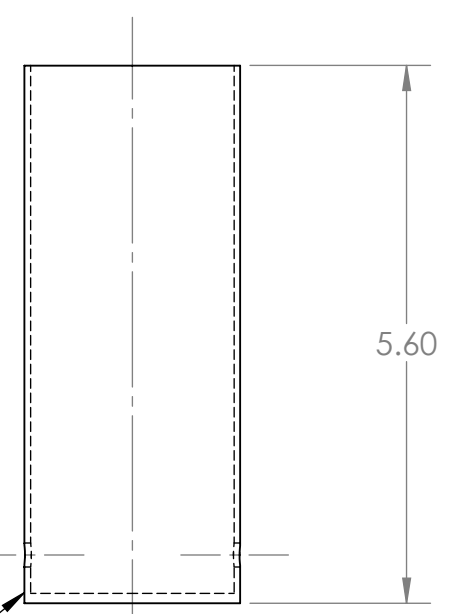
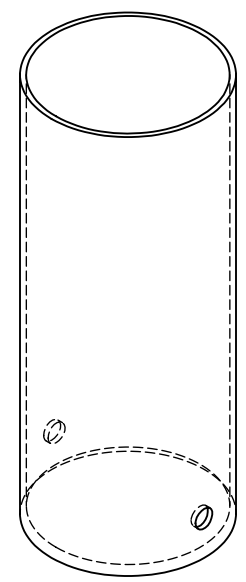
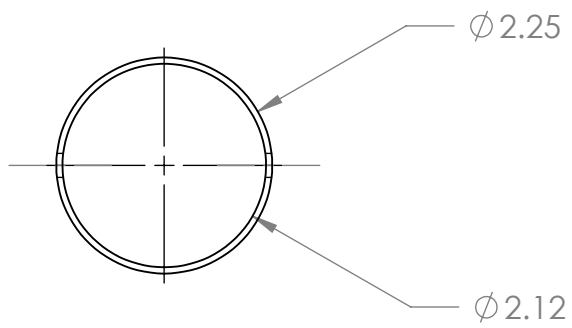
<http://www.mcmaster.com>
© 2012 McMaster-Carr Supply Company

Spring-Tempered Steel
Compression Spring

Information in this drawing is provided for reference only.

8 7 6 5 4 3 2 1

D
C
B
A

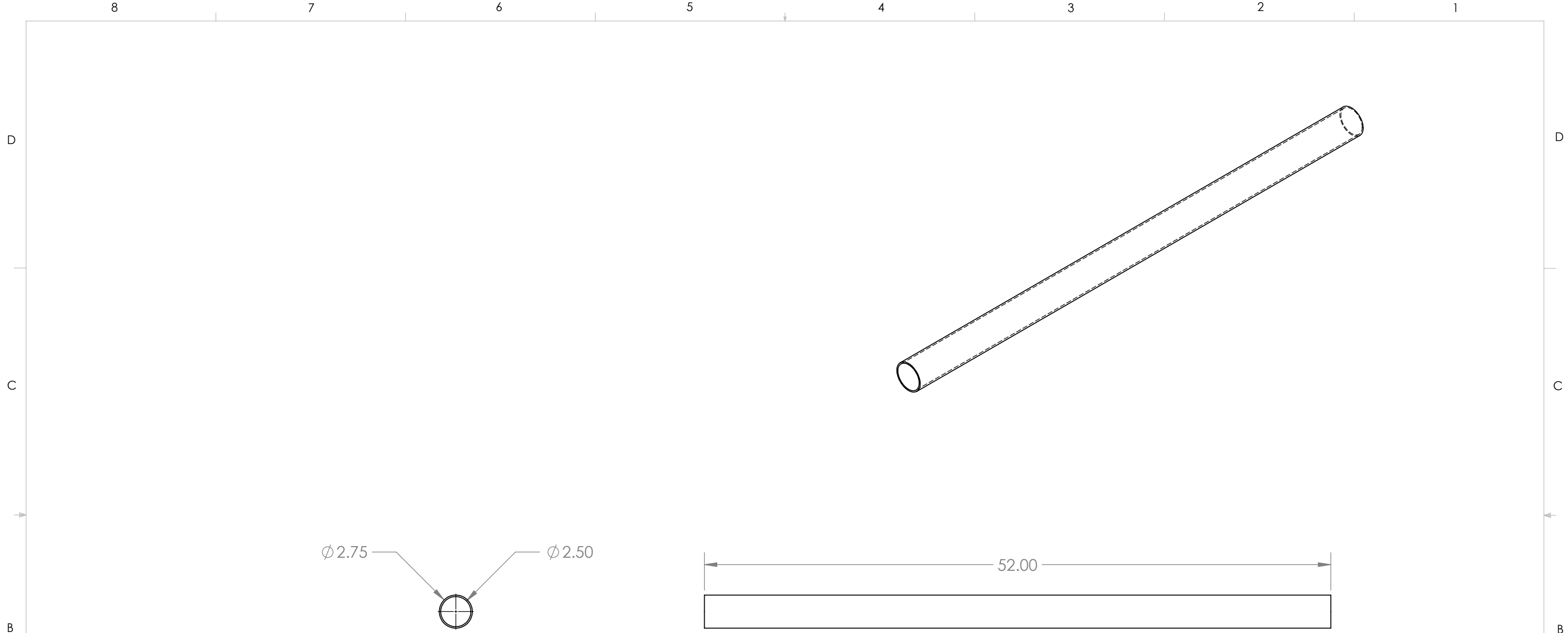


PROPRIETARY AND CONFIDENTIAL
 THE INFORMATION CONTAINED IN THIS DRAWING IS THE SOLE PROPERTY OF ELECTRIC COMMUTER MULTICOPTER TEAM. ANY REPRODUCTION IN PART OR AS A WHOLE WITHOUT THE WRITTEN PERMISSION OF ELECTRIC COMMUTER MULTICOPTER TEAM IS PROHIBITED.

		UNLESS OTHERWISE SPECIFIED:					
		DIMENSIONS ARE IN INCHES TOLERANCES: ±0.01		DRAWN	ARTHUR	1/29/15	
				CHECKED	MM	1/30/15	
				ENG APPR.			
				MFG APPR.			
		INTERPRET GEOMETRIC TOLERANCING PER:		Q.A.			
		MATERIAL 4130 CHROMOLY		COMMENTS: STEEL TUBE PURCHASED FROM MCMASTER CARR. END CAP IS STEEL PLATE PURCHASED FROM MCMASTER CARR.			
		FINISH					
NEXT ASSY	USED ON			TITLE: LANDING GEAR SLEEVE			
APPLICATION		DO NOT SCALE DRAWING		SIZE	DWG. NO.	REV	
				B	ECM-1-DS0-0905	A	
				SCALE: 1:2	WEIGHT: 1.36 lbs	SHEET 1 OF 1	

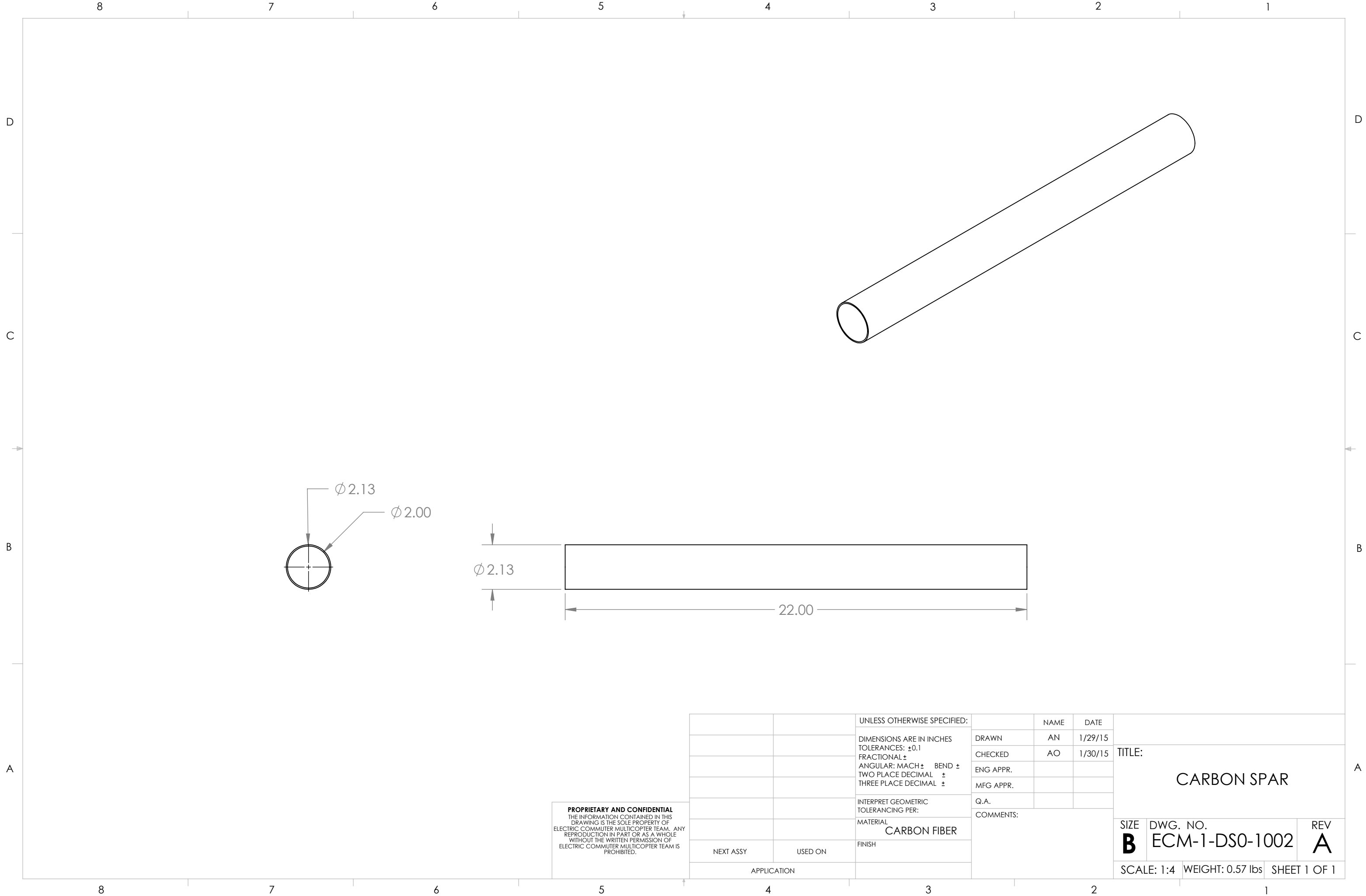
8 7 6 5 4 3 2 1

D
C
B
A



PROPRIETARY AND CONFIDENTIAL
 THE INFORMATION CONTAINED IN THIS DRAWING IS THE SOLE PROPERTY OF ELECTRIC COMMUTER MULTICOPTER TEAM. ANY REPRODUCTION IN PART OR AS A WHOLE WITHOUT THE WRITTEN PERMISSION OF ELECTRIC COMMUTER MULTICOPTER IS PROHIBITED.

		UNLESS OTHERWISE SPECIFIED:		NAME	DATE	TITLE: <h1>MAIN ARM</h1>	
		DIMENSIONS ARE IN INCHES	DRAWN	MM	1/25/15		
		TOLERANCES:	CHECKED	AO	1/30/15		
		INNER DIAMETER ± 0.010	ENG APPR.				
		OUTER DIAMETER ± 0.020	MFG APPR.				
		INTERPRET GEOMETRIC TOLERANCING PER:	Q.A.			SIZE B	
		MATERIAL: CARBON FIBER	COMMENTS: PURCHASED DIRECTLY FROM ROCKWEST COMPOSITES AND CUT TO LENGTH.				DWG. NO. ECM-1-DS0-1001
		FINISH: NONE					REV A
	NEXT ASSY	USED ON				SCALE: 1:2	
	APPLICATION					WEIGHT: 3.11 lbs	
						SHEET 1 OF 1	



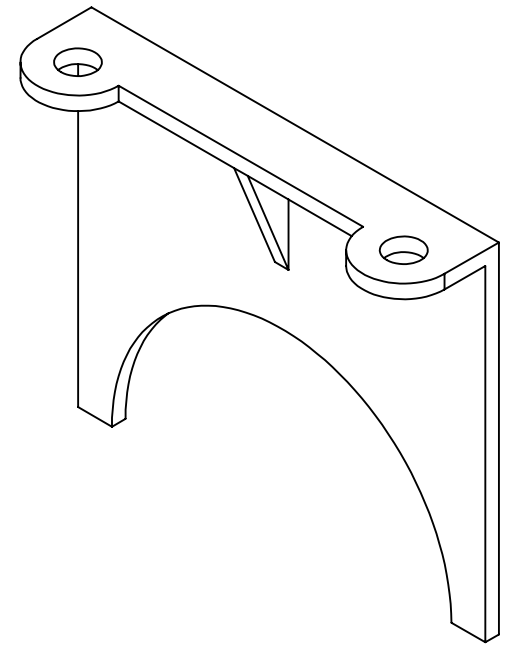
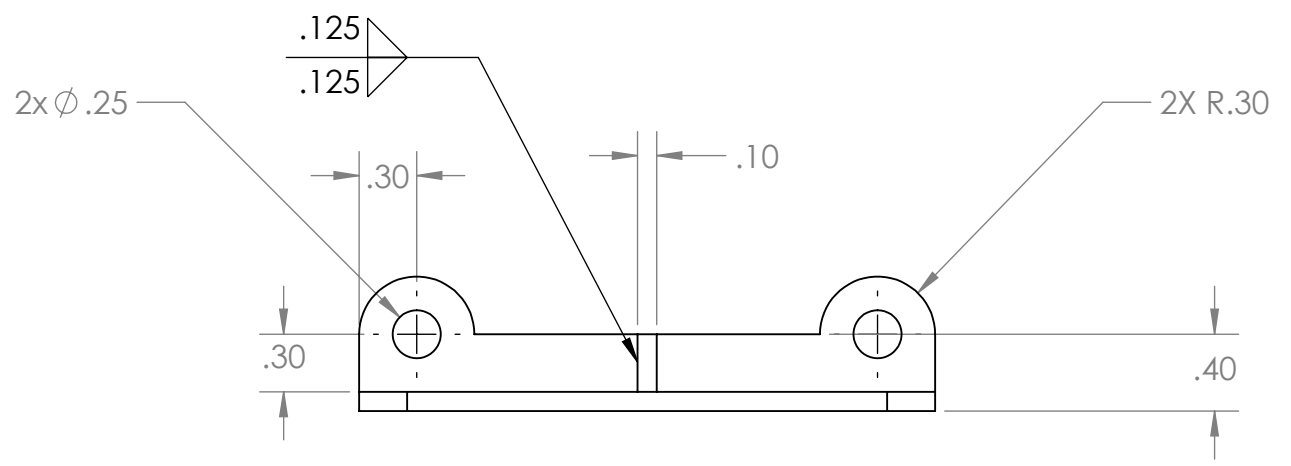
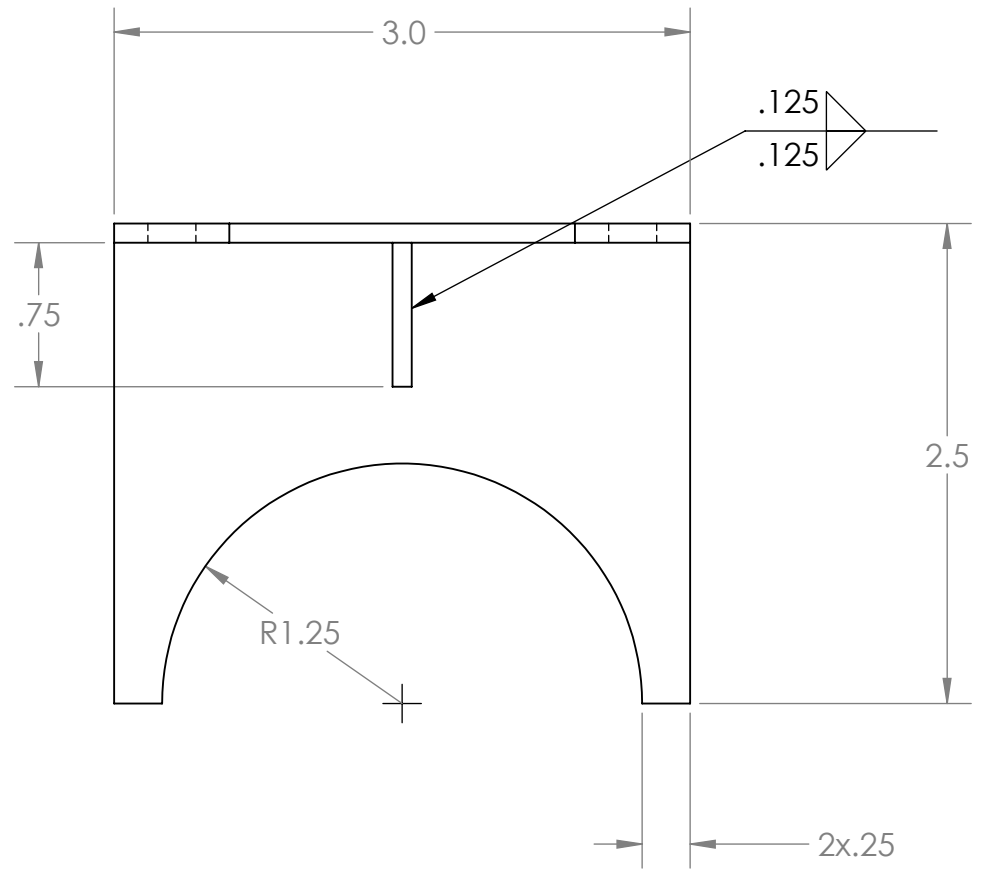
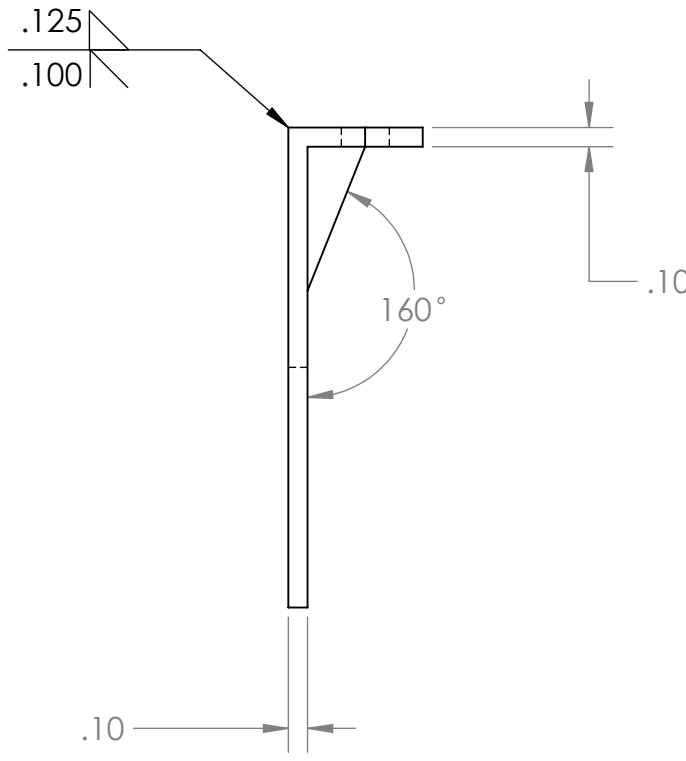
PROPRIETARY AND CONFIDENTIAL
 THE INFORMATION CONTAINED IN THIS DRAWING IS THE SOLE PROPERTY OF ELECTRIC COMMUTER MULTICOPTER TEAM. ANY REPRODUCTION IN PART OR AS A WHOLE WITHOUT THE WRITTEN PERMISSION OF ELECTRIC COMMUTER MULTICOPTER TEAM IS PROHIBITED.

		UNLESS OTHERWISE SPECIFIED:		NAME	DATE	TITLE: CARBON SPAR
		DIMENSIONS ARE IN INCHES	DRAWN	AN	1/29/15	
		TOLERANCES: ± 0.1	CHECKED	AO	1/30/15	
		FRACTIONAL \pm	ENG APPR.			
		ANGULAR: MACH \pm BEND \pm	MFG APPR.			
		TWO PLACE DECIMAL \pm	Q.A.			SIZE DWG. NO. REV B ECM-1-DS0-1002 A
		THREE PLACE DECIMAL \pm	COMMENTS:			
		INTERPRET GEOMETRIC TOLERANCING PER:				
		MATERIAL				SCALE: 1:4 WEIGHT: 0.57 lbs SHEET 1 OF 1
		FINISH				
	NEXT ASSY	USED ON				
	APPLICATION					

8 7 6 5 4 3 2 1

D
C
B
A

D
C
B
A



PROPRIETARY AND CONFIDENTIAL
 THE INFORMATION CONTAINED IN THIS DRAWING IS THE SOLE PROPERTY OF ELECTRIC COMMUTER MULTICOPTER TEAM. ANY REPRODUCTION IN PART OR AS A WHOLE WITHOUT THE WRITTEN PERMISSION OF ELECTRIC COMMUTER MULTICOPTER TEAM IS PROHIBITED.

		UNLESS OTHERWISE SPECIFIED:		NAME	DATE	TITLE: CENTER MOUNT WALL	
		DIMENSIONS ARE IN INCHES		DRAWN	BLAKE S.		1/26/15
		TOLERANCES:		CHECKED	OHEARN		1/27/15
		FRACTIONAL ± 1/4		ENG APPR.			
		ANGULAR: ± 5°		MFG APPR.			
		ONE PLACE DECIMAL ±.05		Q.A.			
		TWO PLACE DECIMAL ±.01		COMMENTS:			
		INTERPRET GEOMETRIC TOLERANCING PER:					
ECM-1-S1-11	CENTER MOUNT ASSY	MATERIAL 4130 CHROMOLY					
NEXT ASSY	USED ON	FINISH UNSPECIFIED					
APPLICATION							
SIZE	DWG. NO.	REV					
B	ECM-1-DS1-1101	A					
SCALE: 1:1	WEIGHT: 0.111lb	SHEET	OF				

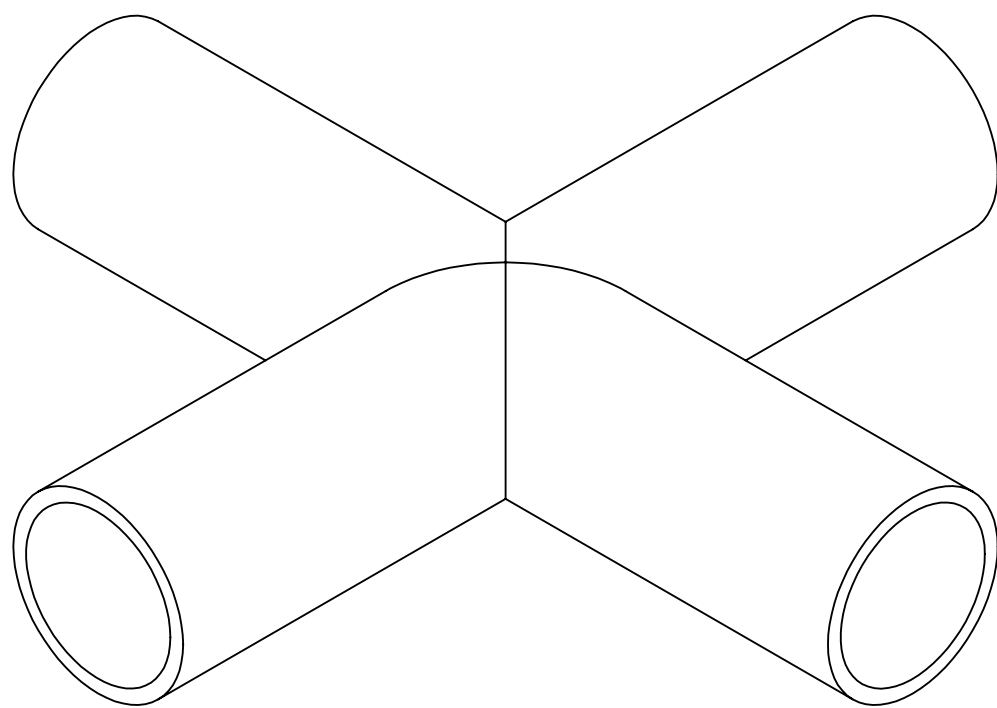
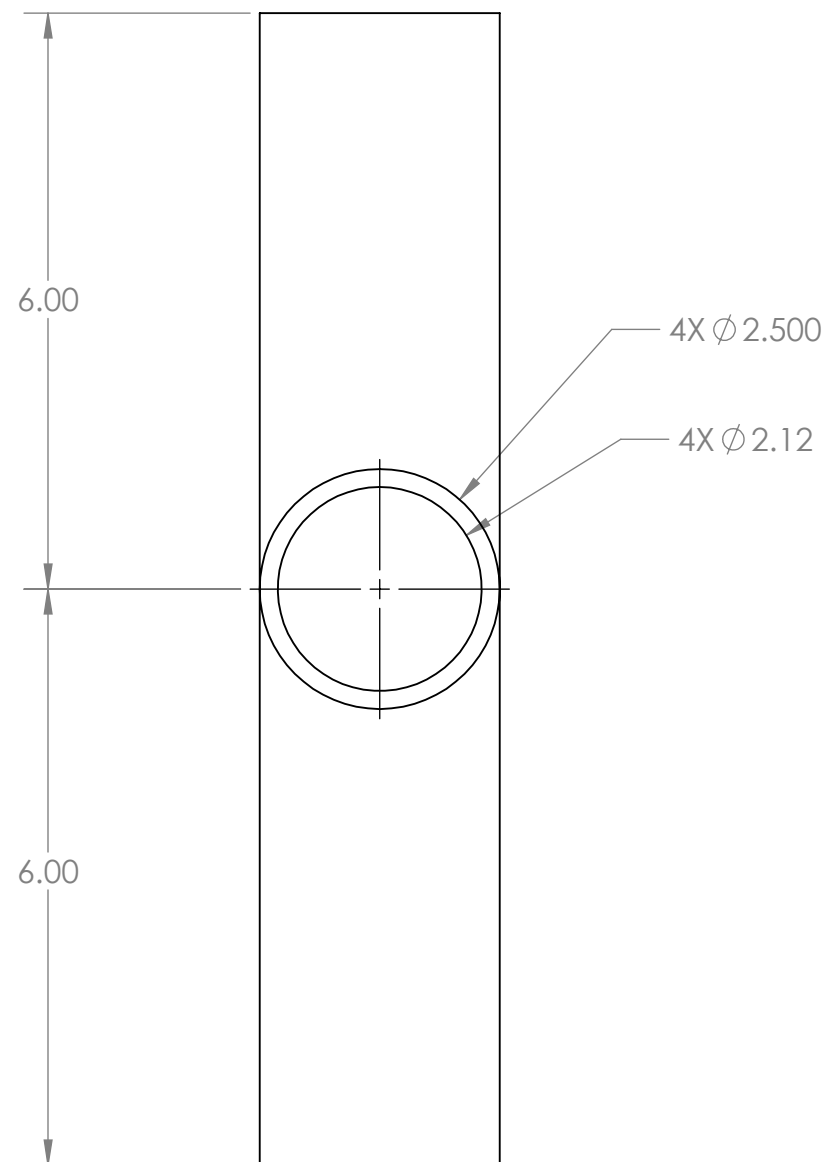
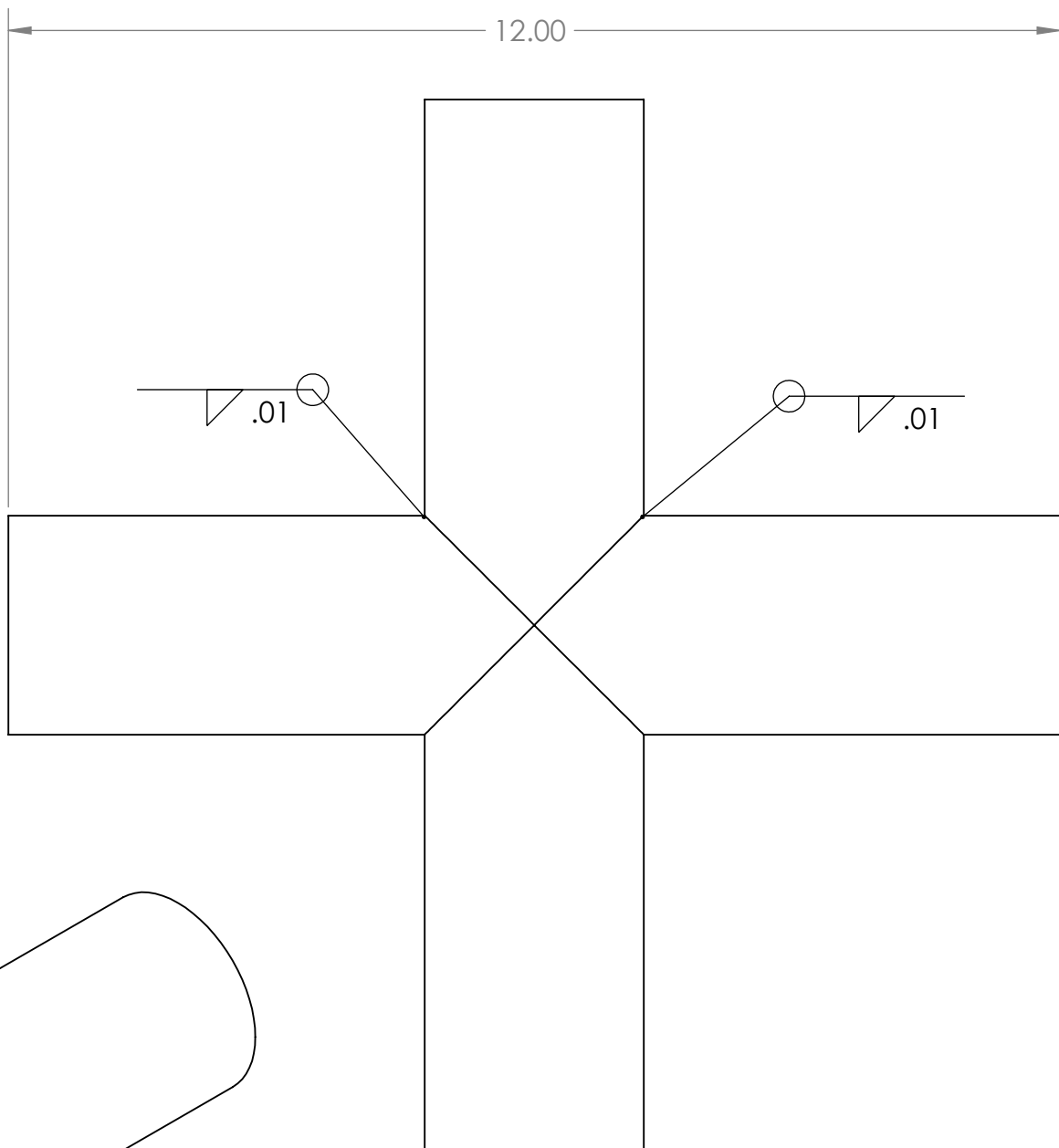
8 7 6 5 4 3 2 1

8 7 6 5 4 3 2 1

D
C
B
A

D
C
B
A

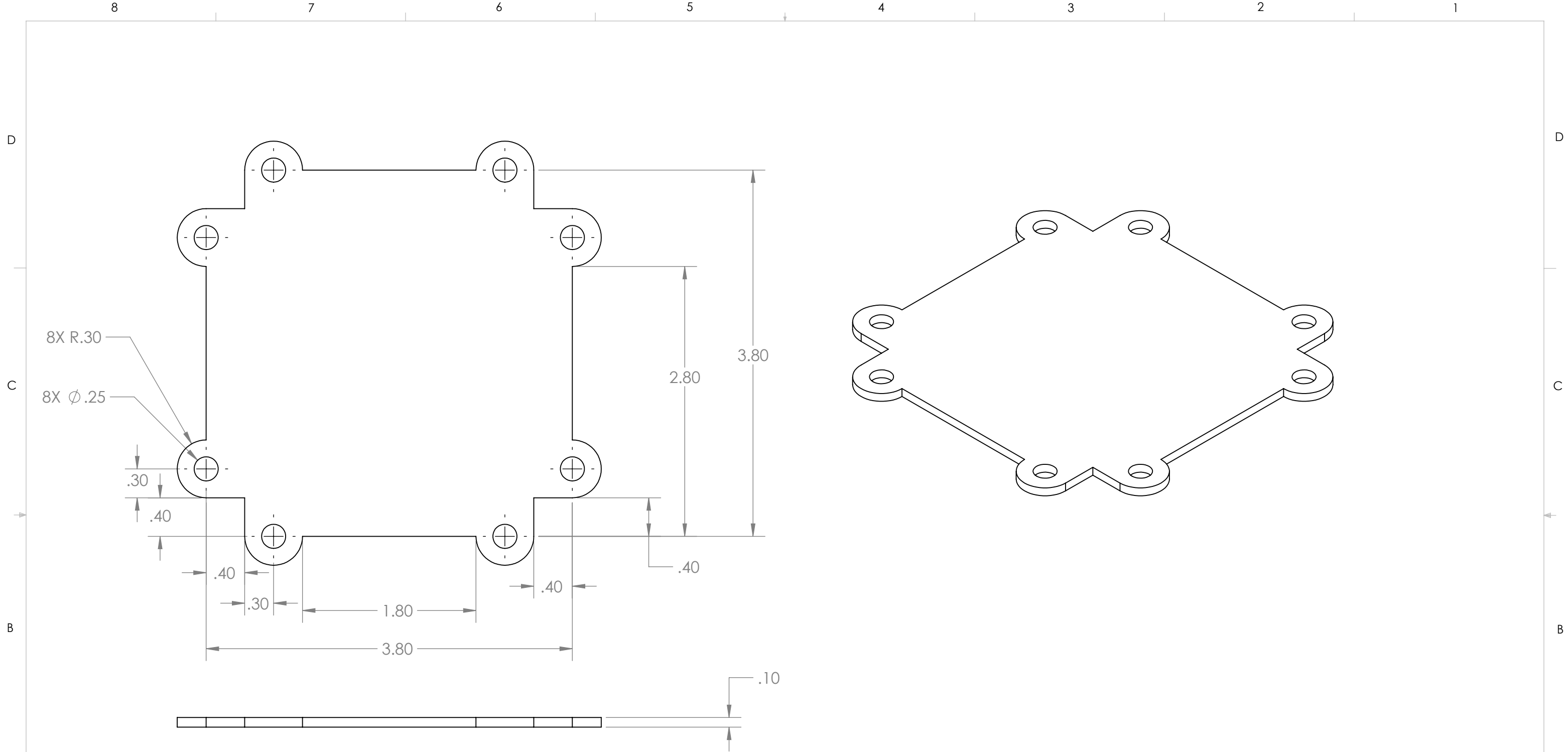
PART IS
AXISYMMETRIC



PROPRIETARY AND CONFIDENTIAL
THE INFORMATION CONTAINED IN THIS
DRAWING IS THE SOLE PROPERTY OF
ELECTRIC COMMUTER MULTICOPTER TEAM. ANY
REPRODUCTION IN PART OR AS A WHOLE
WITHOUT THE WRITTEN PERMISSION OF
ELECTRIC COMMUTER MULTICOPTER TEAM IS
PROHIBITED.

		UNLESS OTHERWISE SPECIFIED:		NAME	DATE		
		DIMENSIONS ARE IN INCHES		DRAWN	BLAKE S.	1/26/15	TITLE: CENTER BRACKET
		TOLERANCES:		CHECKED	OHEARN	1/30/15	
		FRACTIONAL ± 1/4		ENG APPR.			
		ANGULAR: ± 5°		MFG APPR.			
		TWO PLACE DECIMAL ±.01		Q.A.			SIZE DWG. NO. REV B ECM-1-DS1-1102 A
		THREE PLACE DECIMAL ±.003		COMMENTS:			
		INTERPRET GEOMETRIC TOLERANCING PER:				SCALE: 1:2 WEIGHT: 8.15lb SHEET OF	
ECM-1-S1-11	CENTER MOUNT ASSY	MATERIAL 4130 CHROMOLY					
NEXT ASSY	USED ON	FINISH UNSPECIFIED					
APPLICATION							

8 7 6 5 4 3 2 1



PROPRIETARY AND CONFIDENTIAL
 THE INFORMATION CONTAINED IN THIS
 DRAWING IS THE SOLE PROPERTY OF
 ELECTRIC COMMUTER MULTICOPTER TEAM. ANY
 REPRODUCTION IN PART OR AS A WHOLE
 WITHOUT THE WRITTEN PERMISSION OF
 ELECTRIC COMMUTER MULTICOPTER TEAM IS
 PROHIBITED.

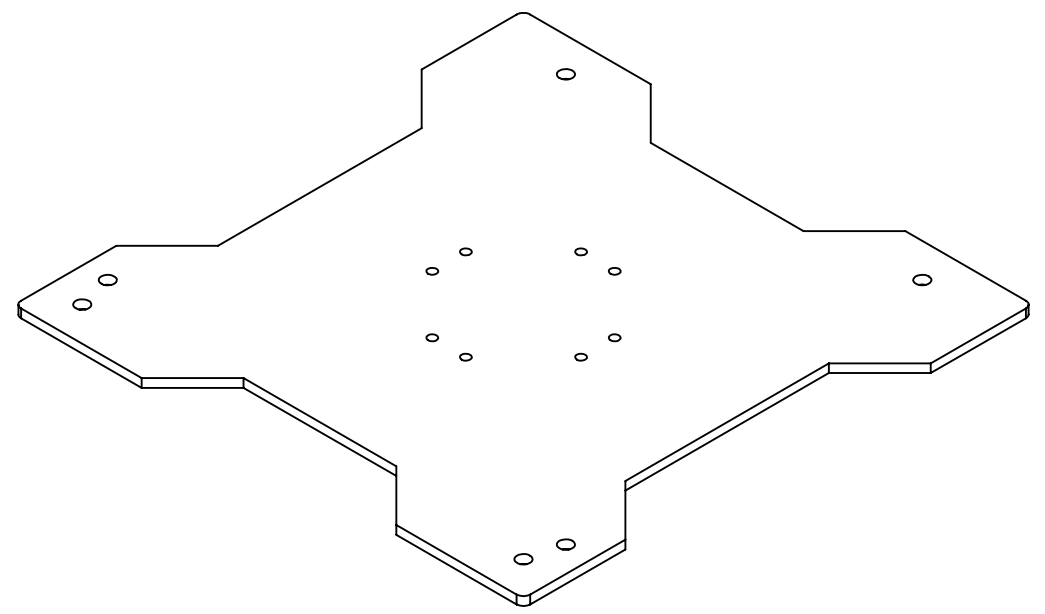
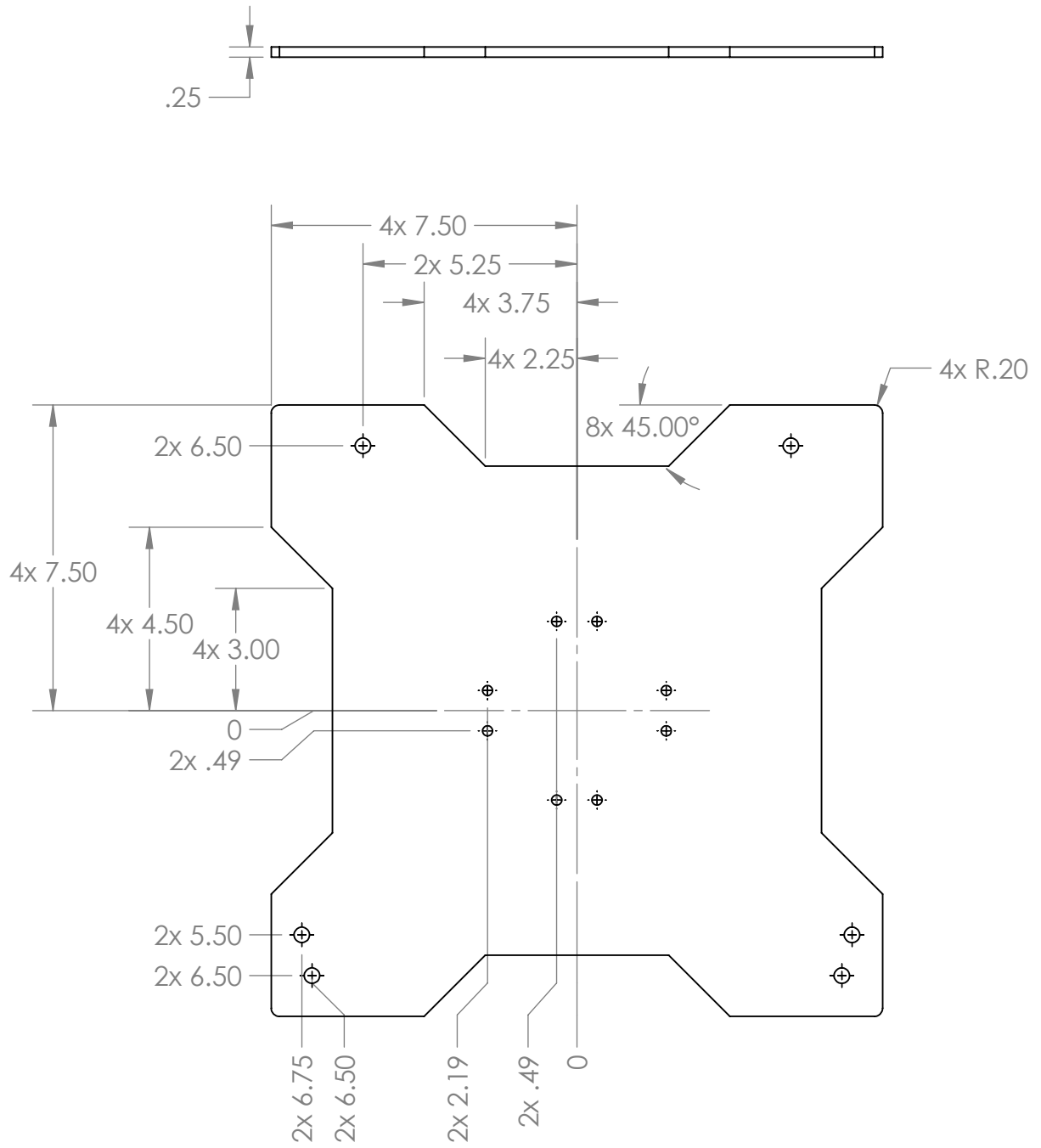
		UNLESS OTHERWISE SPECIFIED:		NAME	DATE
		DIMENSIONS ARE IN INCHES		DRAWN	AO
		TOLERANCES:		CHECKED	1/30/15
		FRACTIONAL ±		ENG APPR.	
		ANGULAR: MACH ± BEND ±		MFG APPR.	
		TWO PLACE DECIMAL ±		Q.A.	
		THREE PLACE DECIMAL ±		COMMENTS:	
		INTERPRET GEOMETRIC TOLERANCING PER:		UNITS: LBS & INCHES UNLESS OTHERWISE SPECIFIED	
		MATERIAL		SIZE	DWG. NO.
		4130 chromoly		B	ECM-1-DS1-1103
		FINISH		REV	A
NEXT ASSY	USED ON			SCALE: 1:1	WEIGHT: 0.41
APPLICATION				SHEET 1 OF 1	

Title:
 Landing Plate
 on Center
 Mount

8 7 6 5 4 3 2 1

D
C
B
A

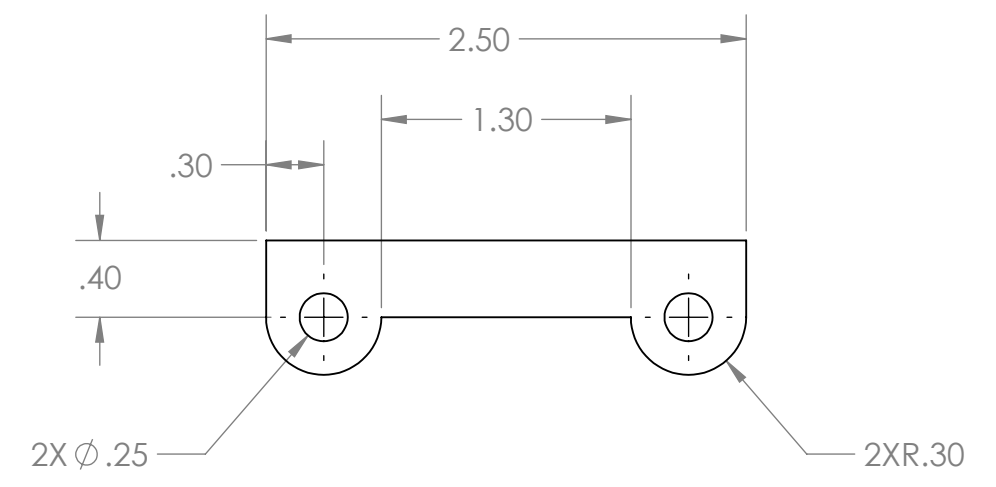
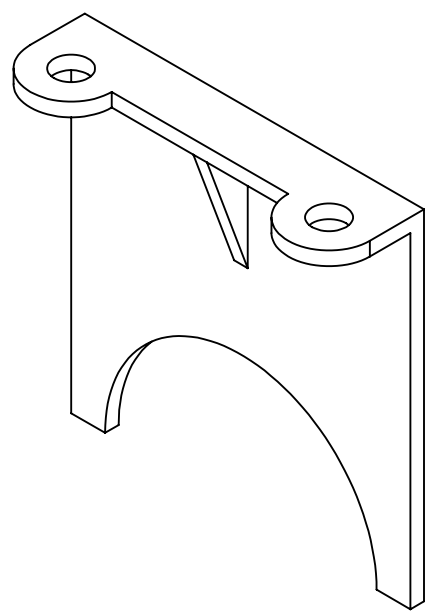
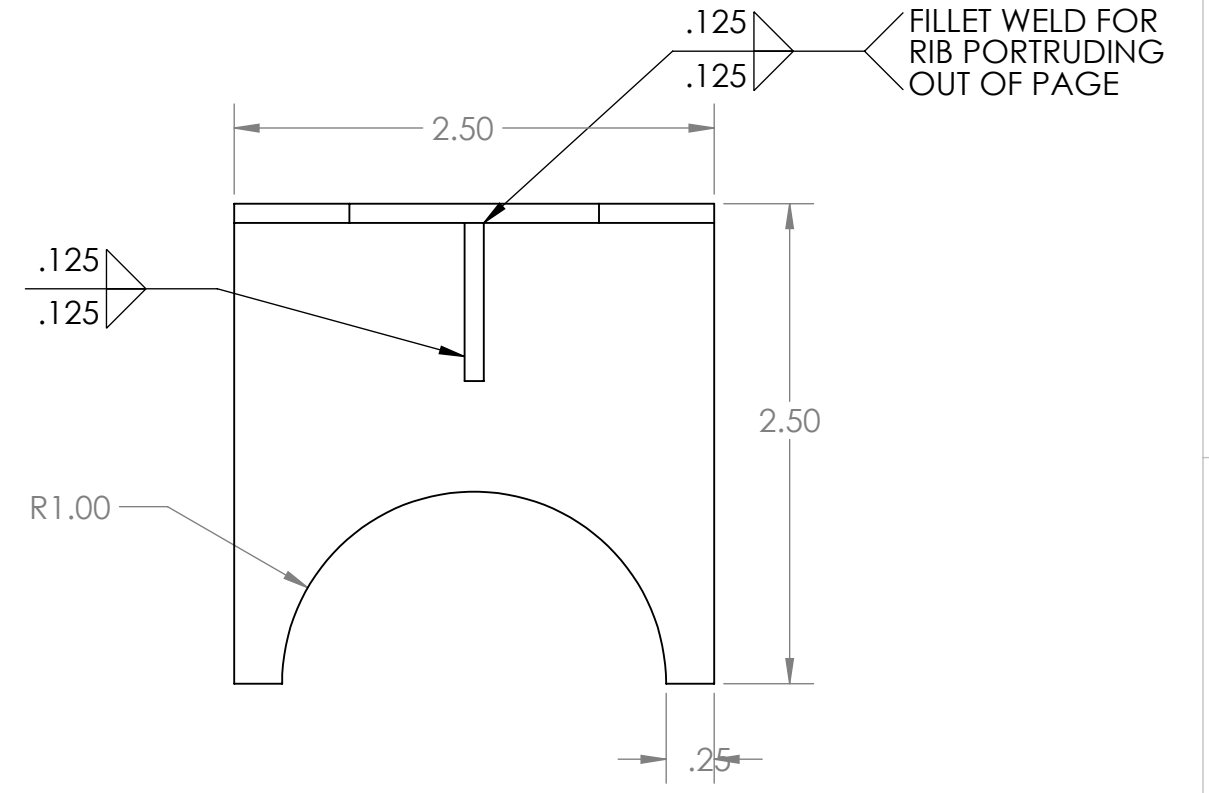
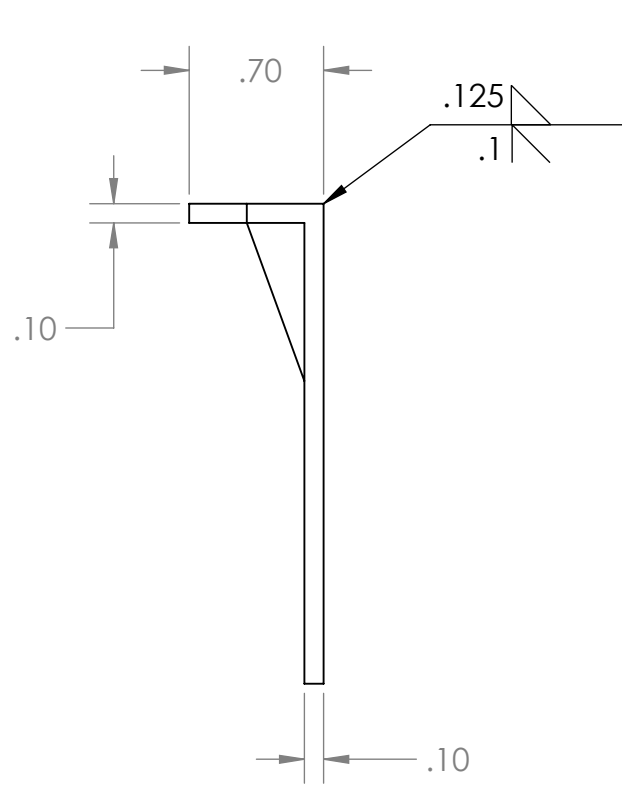
D
C
B
A



PROPRIETARY AND CONFIDENTIAL
 THE INFORMATION CONTAINED IN THIS
 DRAWING IS THE SOLE PROPERTY OF
 ELECTRIC COMMUTER MULTICOPTER TEAM. ANY
 REPRODUCTION IN PART OR AS A WHOLE
 WITHOUT THE WRITTEN PERMISSION OF
 ELECTRIC COMMUTER MULTICOPTER TEAM IS
 PROHIBITED.

		UNLESS OTHERWISE SPECIFIED:				TITLE:	
				NAME	DATE	ECM-1-DS1-1104	
				DRAWN	JW 1/30/2015		
				CHECKED	AO 1/30/15		
				ENG APPR.			
				MFG APPR.		SIZE DWG. NO. REV	
				Q.A.		B ECM-1-DS1-1104 A	
				COMMENTS:		SCALE: 1:4 WEIGHT: 4.5 lbs SHEET 1 OF 1	
NEXT ASSY		USED ON		MATERIAL			
				6061-T6			
				FINISH			
				NONE			
APPLICATION							

8 7 6 5 4 3 2 1

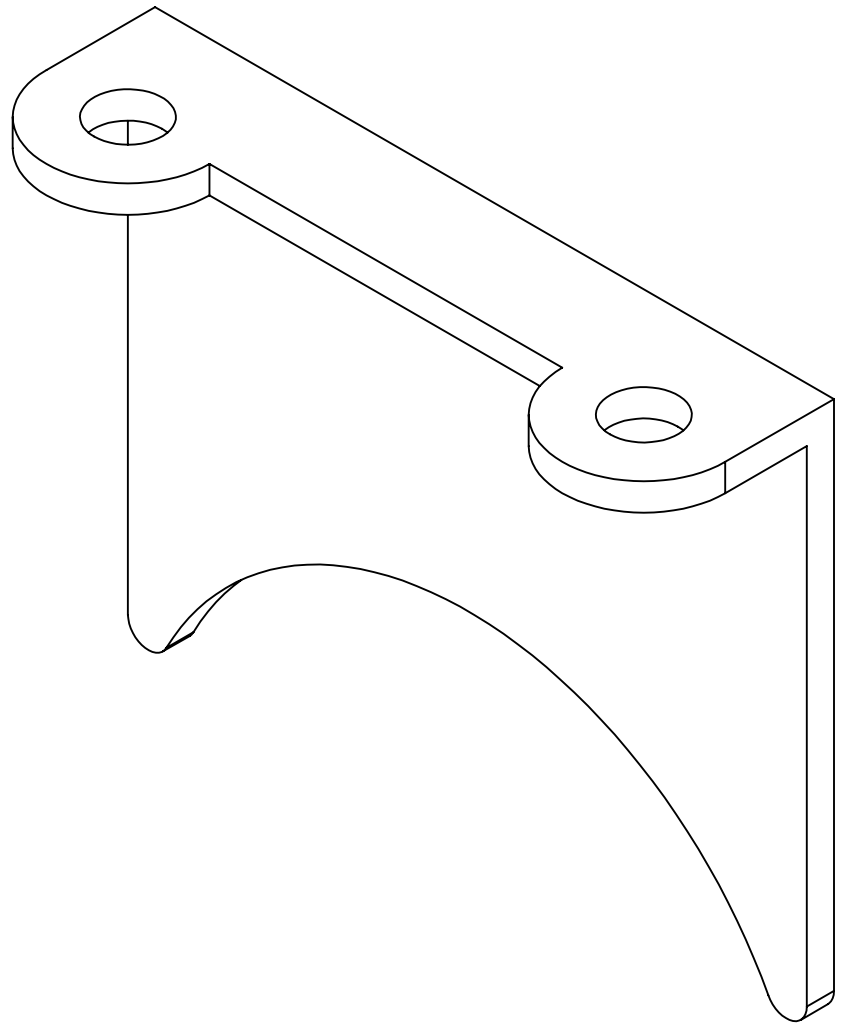
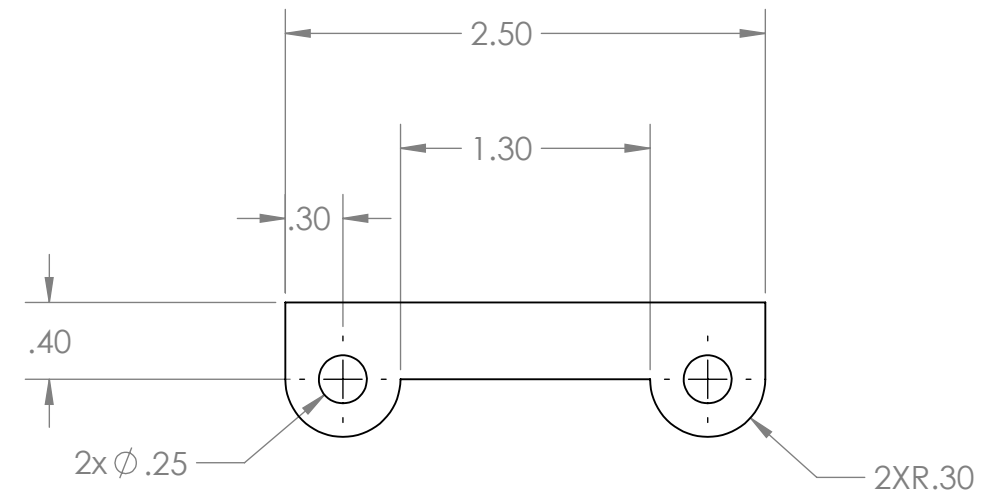
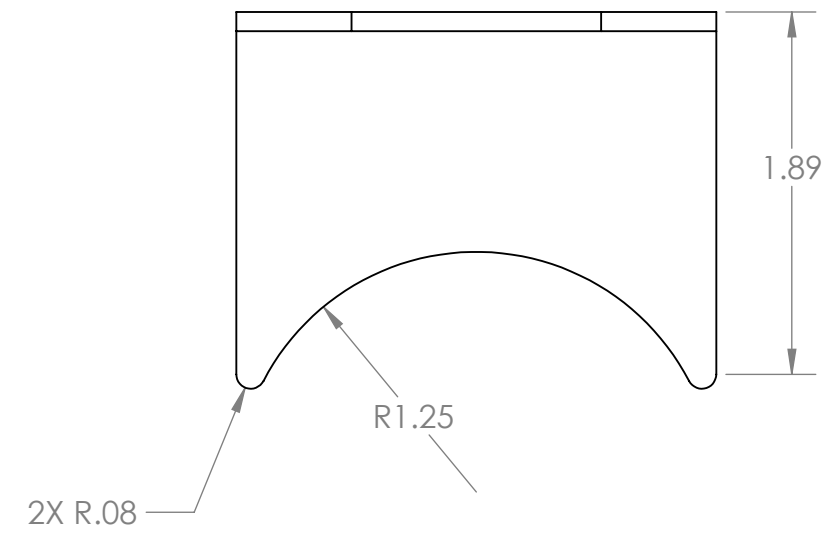
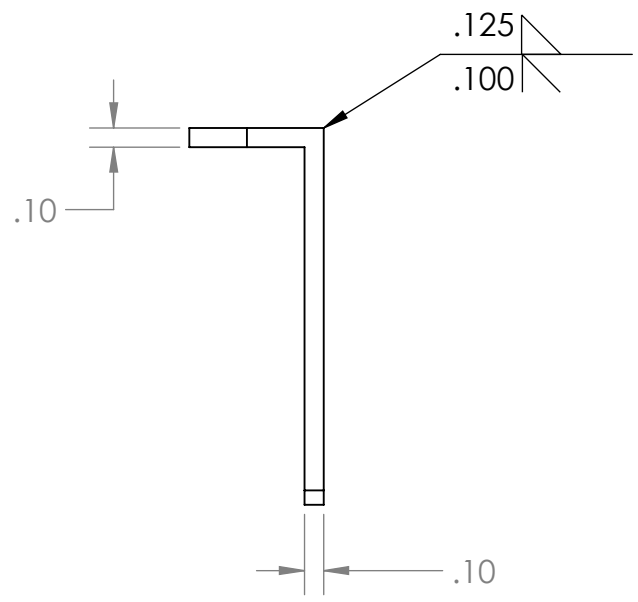


PROPRIETARY AND CONFIDENTIAL
 THE INFORMATION CONTAINED IN THIS DRAWING IS THE SOLE PROPERTY OF ELECTRIC COMMUTER MULTICOPTER TEAM. ANY REPRODUCTION IN PART OR AS A WHOLE WITHOUT THE WRITTEN PERMISSION OF ELECTRIC COMMUTER MULTICOPTER TEAM IS PROHIBITED.

		UNLESS OTHERWISE SPECIFIED:		NAME	DATE	TITLE: BRACKET WALL FOR SMALL TUBE IN ARM MOUNT
		DIMENSIONS ARE IN INCHES TOLERANCES: ±0.1 FRACTIONAL ± ANGULAR: MACH ± BEND ± TWO PLACE DECIMAL ± THREE PLACE DECIMAL ±		DRAWN	ARTHUR 1/29/15	
		INTERPRET GEOMETRIC TOLERANCING PER:		CHECKED	AO 1/30/15	
		MATERIAL		ENG APPR.		
		4130 CHROMOLY		MFG APPR.		
NEXT ASSY	USED ON	FINISH		Q.A.		SIZE
APPLICATION				COMMENTS:		B
						DWG. NO.
						ECM-1-DS1 -1201
						REV
						A
						SCALE: 1:1
						WEIGHT: 0.16 lbs
						SHEET 1 OF 1

8 7 6 5 4 3 2 1

D
C
B
A



PROPRIETARY AND CONFIDENTIAL
 THE INFORMATION CONTAINED IN THIS DRAWING IS THE SOLE PROPERTY OF <INSERT COMPANY NAME HERE>. ANY REPRODUCTION IN PART OR AS A WHOLE WITHOUT THE WRITTEN PERMISSION OF <INSERT COMPANY NAME HERE> IS PROHIBITED.

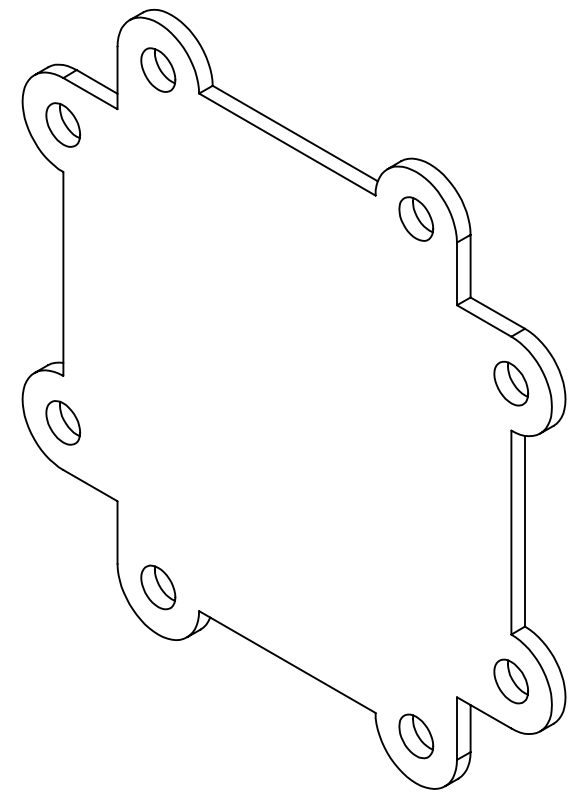
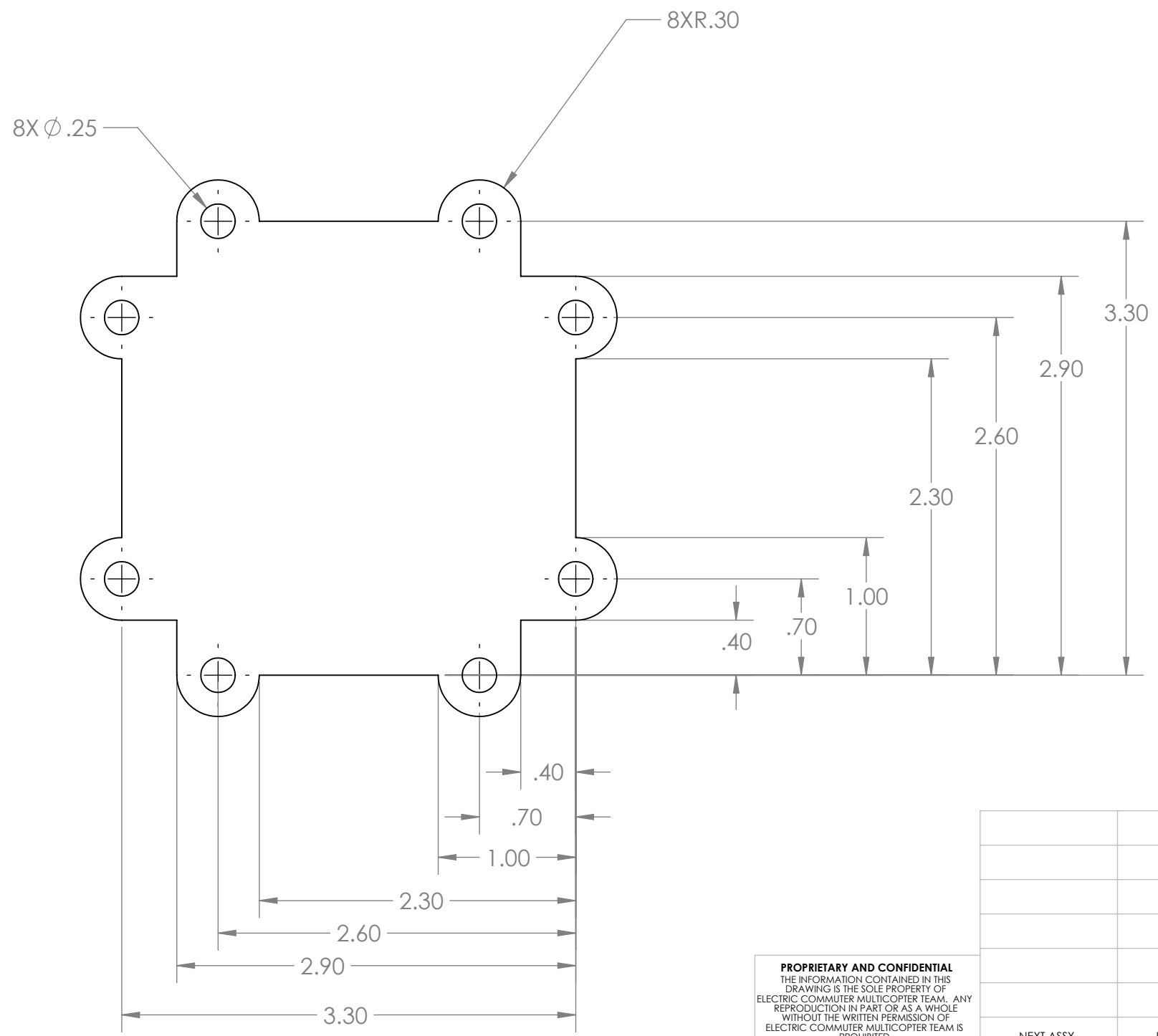
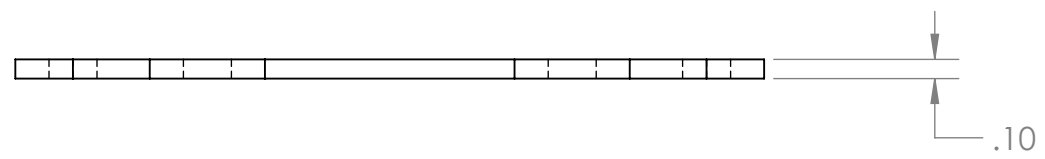
		UNLESS OTHERWISE SPECIFIED:		NAME	DATE	TITLE: BRACKET WALL FOR LARGE TUBE ON ARM MOUNT	
		DIMENSIONS ARE IN INCHES		DRAWN	ARTHUR		1/29/15
		TOLERANCES:		CHECKED	AO		1/30/15
		FRACTIONAL ±		ENG APPR.			
		ANGULAR: MACH ± BEND ±		MFG APPR.			
		TWO PLACE DECIMAL ±		Q.A.			
		THREE PLACE DECIMAL ±		COMMENTS:			
		INTERPRET GEOMETRIC TOLERANCING PER:					
		MATERIAL					
		4130 CHROMOLY					
		FINISH					
NEXT ASSY	USED ON						
APPLICATION							
SIZE	DWG. NO.	REV					
B	ECM-1-DS1-1202	A					
SCALE: 2:1	WEIGHT: 0.13 lbs	SHEET 1 OF 1					

8 7 6 5 4 3 2 1

8 7 6 5 4 3 2 1

D
C
B
A

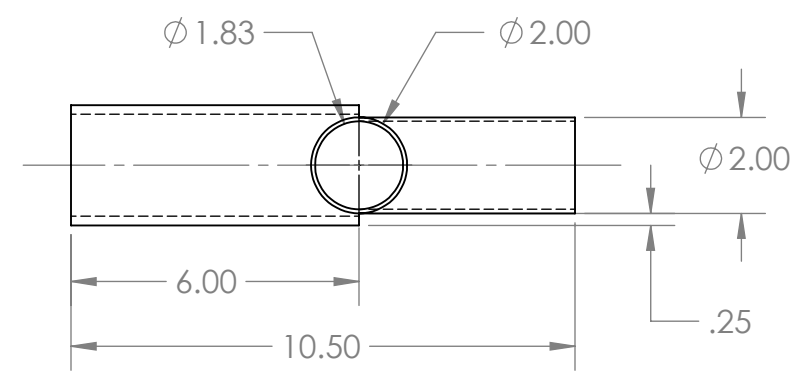
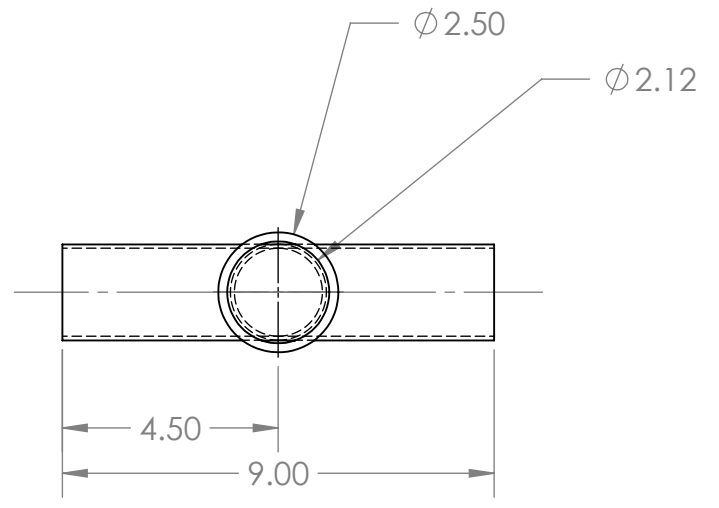
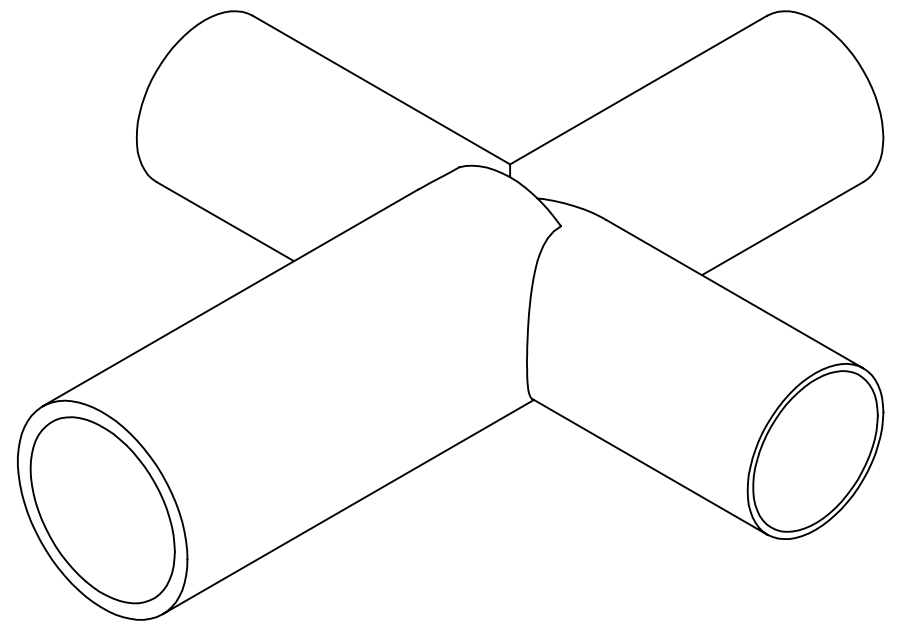
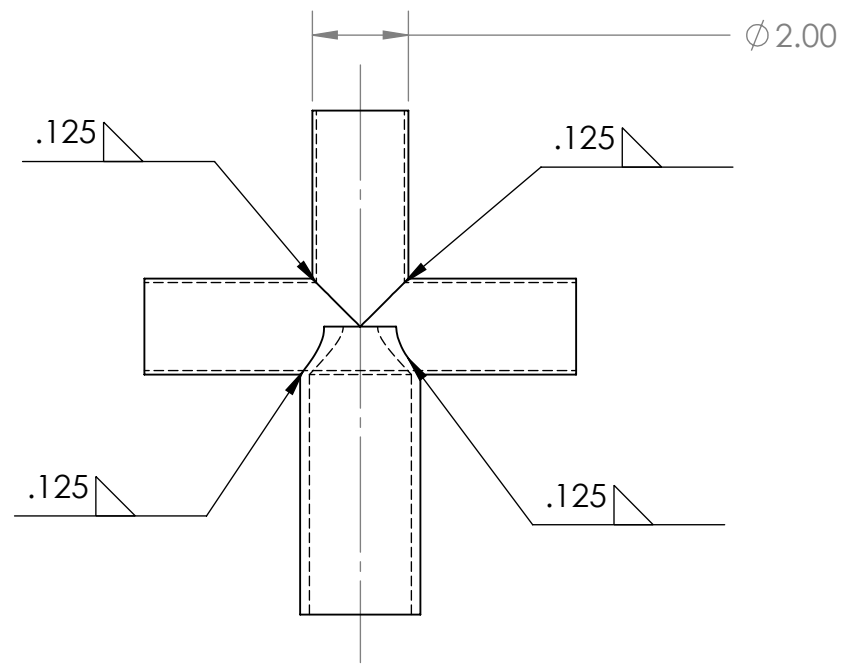
D
C
B
A



PROPRIETARY AND CONFIDENTIAL
 THE INFORMATION CONTAINED IN THIS DRAWING IS THE SOLE PROPERTY OF ELECTRIC COMMUTER MULTICOPTER TEAM. ANY REPRODUCTION IN PART OR AS A WHOLE WITHOUT THE WRITTEN PERMISSION OF ELECTRIC COMMUTER MULTICOPTER TEAM IS PROHIBITED.

		UNLESS OTHERWISE SPECIFIED:		NAME	DATE
		DIMENSIONS ARE IN INCHES TOLERANCES: \pm 0.1 FRACTIONAL \pm ANGULAR: MACH \pm BEND \pm TWO PLACE DECIMAL \pm THREE PLACE DECIMAL \pm		DRAWN	ARTHUR 1/29/15
		INTERPRET GEOMETRIC TOLERANCING PER:		CHECKED	AO 1/30/15
		MATERIAL 4130 CHROMOLY		ENG APPR.	
NEXT ASSY		USED ON		MFG APPR.	
APPLICATION		DO NOT SCALE DRAWING		Q.A.	
				COMMENTS:	
TITLE: LANDING PLATE ON ARM MOUNT					
SIZE	DWG. NO.			REV	
B	ECM-1-DS1-1203			A	
SCALE: 1:1		WEIGHT: 0.13 lbs		SHEET 1 OF 1	

8 7 6 5 4 3 2 1



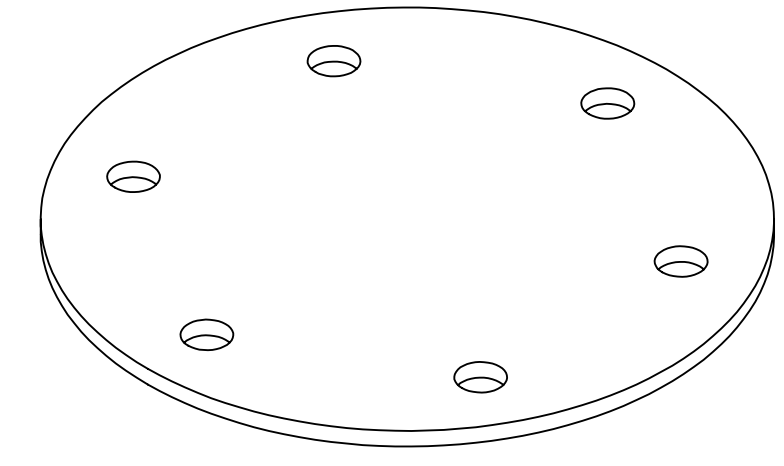
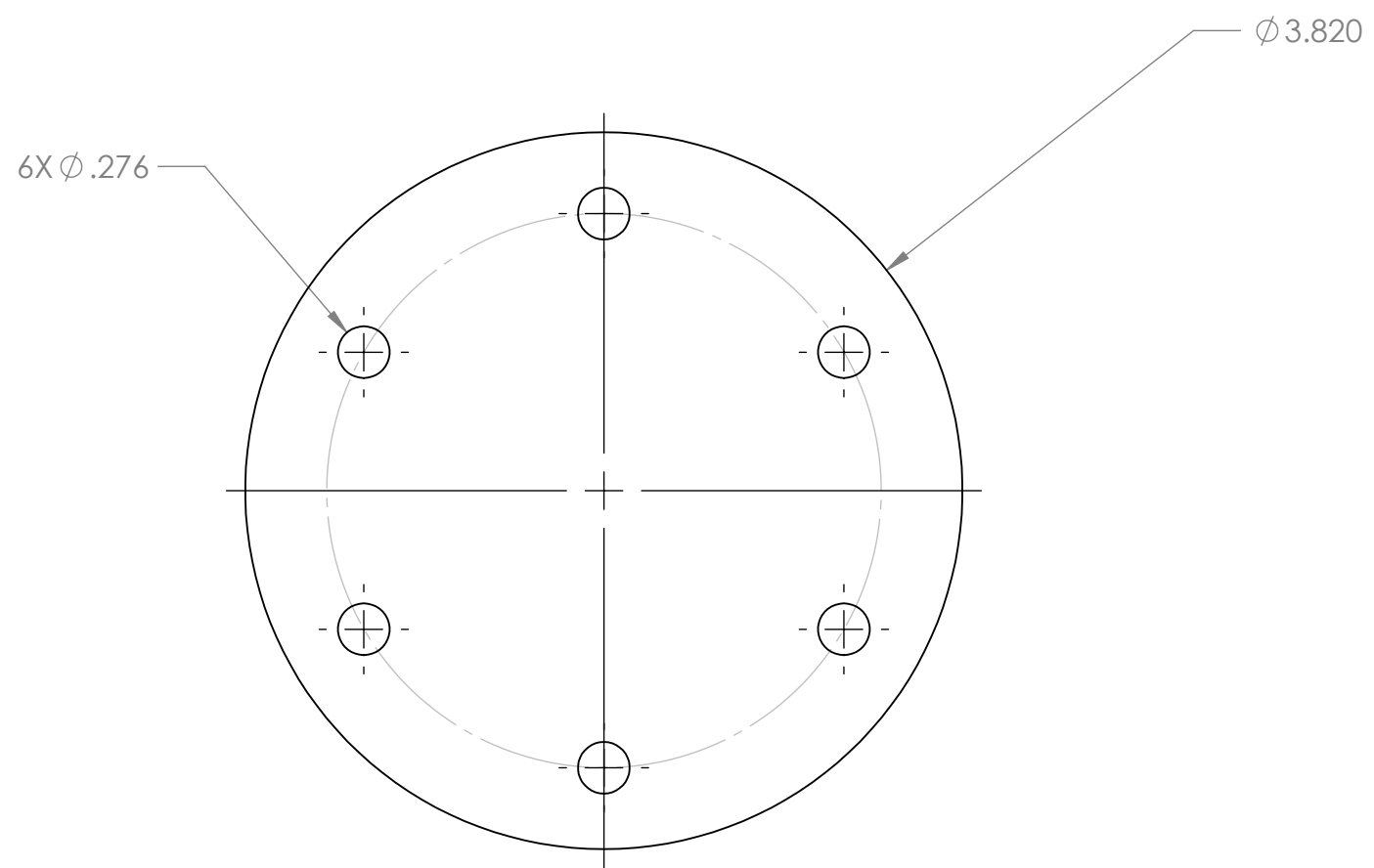
PROPRIETARY AND CONFIDENTIAL
 THE INFORMATION CONTAINED IN THIS DRAWING IS THE SOLE PROPERTY OF <INSERT COMPANY NAME HERE>. ANY REPRODUCTION IN PART OR AS A WHOLE WITHOUT THE WRITTEN PERMISSION OF <INSERT COMPANY NAME HERE> IS PROHIBITED.

		UNLESS OTHERWISE SPECIFIED:		NAME	DATE	TITLE: ARM MOUNT WITH THREE SMALL, ONE LARGE STEEL TUBES
				DRAWN	ARTHUR 1/29/15	
				CHECKED	AO 1/30/15	
				ENG APPR.		
				MFG APPR.		
		INTERPRET GEOMETRIC TOLERANCING PER:		Q.A.		SIZE DWG. NO. REV B ECM-1-DS1-1204 A
		MATERIAL 4130 CHROMOLY		COMMENTS:		
		FINISH				SCALE: 1:4 WEIGHT: 3.87 lbs SHEET 1 OF 1
NEXT ASSY	USED ON					
APPLICATION						

8 7 6 5 4 3 2 1

D
C
B
A

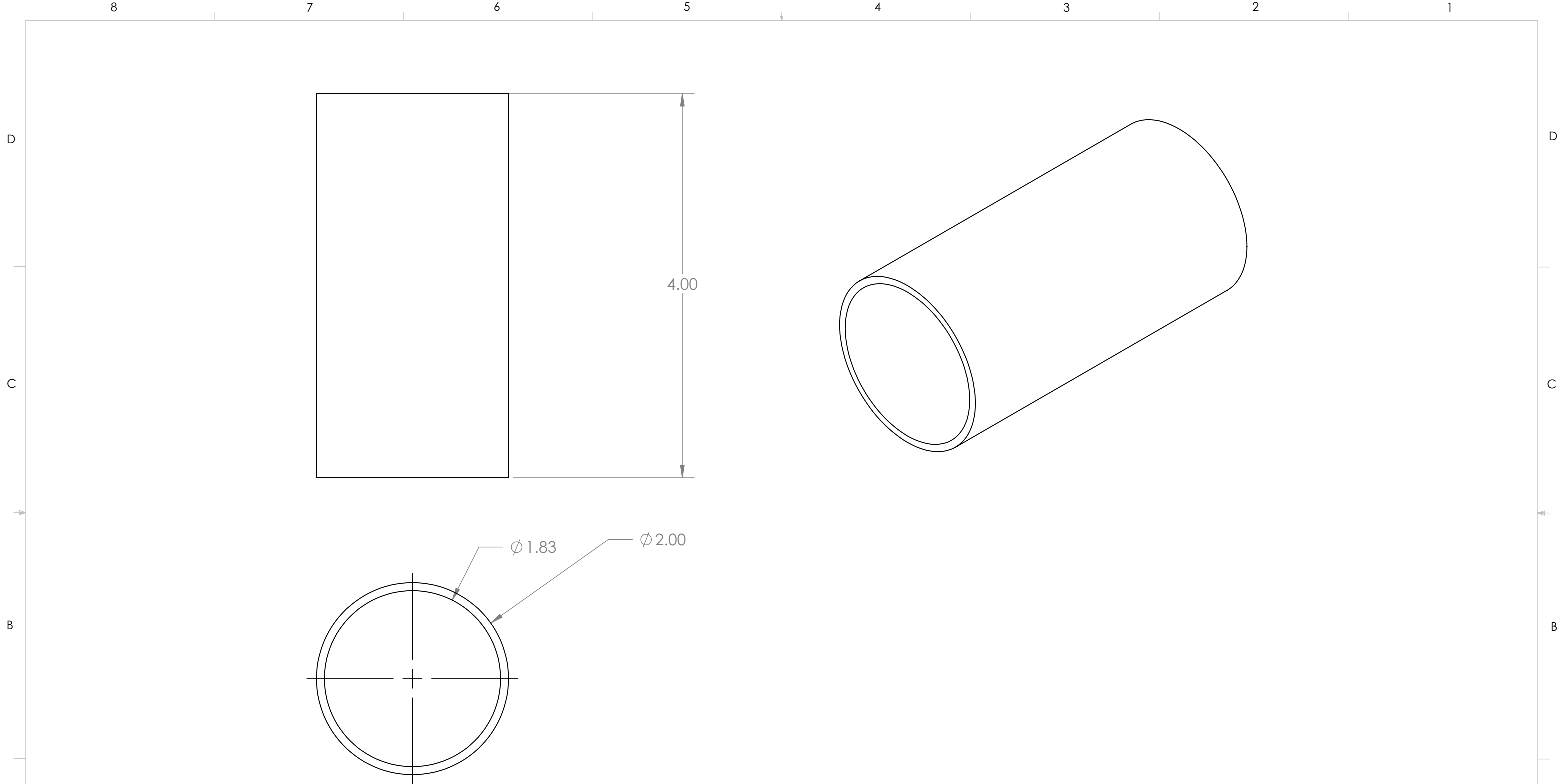
D
C
B
A



PROPRIETARY AND CONFIDENTIAL
 THE INFORMATION CONTAINED IN THIS
 DRAWING IS THE SOLE PROPERTY OF
 ELECTRIC COMMUTER MULTICOPTER TEAM. ANY
 REPRODUCTION IN PART OR AS A WHOLE
 WITHOUT THE WRITTEN PERMISSION OF
 ELECTRIC COMMUTER MULTICOPTER TEAM IS
 PROHIBITED.

		UNLESS OTHERWISE SPECIFIED:		NAME	DATE	TITLE: Motor Aligning Bracket
			DRAWN	AO	1/30/15	
			CHECKED	MM	1/30/15	
			ENG APPR.			
			MFG APPR.			
		INTERPRET GEOMETRIC TOLERANCING PER:		Q.A.		SIZE DWG. NO. REV B ECM-DS1-1301-1 A
		MATERIAL	AL-6061			
		FINISH				SCALE: 1:1 WEIGHT: .11 SHEET 1 OF 1
NEXT ASSY	USED ON					
APPLICATION		DO NOT SCALE DRAWING				

8 7 6 5 4 3 2 1



PROPRIETARY AND CONFIDENTIAL
 THE INFORMATION CONTAINED IN THIS DRAWING IS THE SOLE PROPERTY OF ELECTRIC COMMUTER MULTICOPTER TEAM. ANY REPRODUCTION IN PART OR AS A WHOLE WITHOUT THE WRITTEN PERMISSION OF ELECTRIC COMMUTER MULTICOPTER TEAM IS PROHIBITED.

		UNLESS OTHERWISE SPECIFIED:	NAME	DATE	TITLE: MOTOR MOUNT TUBE	
			DRAWN	AO		1/30/15
			CHECKED	MM		1/30/15
			ENG APPR.			
			MFG APPR.			
		INTERPRET GEOMETRIC TOLERANCING PER:	Q.A.		SIZE DWG. NO. REV B ECM-1-DS0-1301 A	
		MATERIAL	COMMENTS:			
		FINISH				
NEXT ASSY	USED ON				SCALE: 1:1 WEIGHT: .57 SHEET 1 OF 1	
APPLICATION						

8 7 6 5 4 3 2 1

8 7 6 5 4 3 2 1

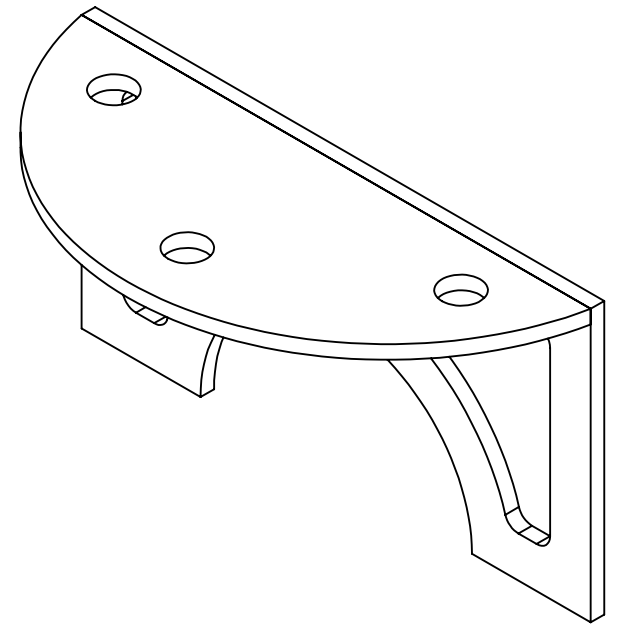
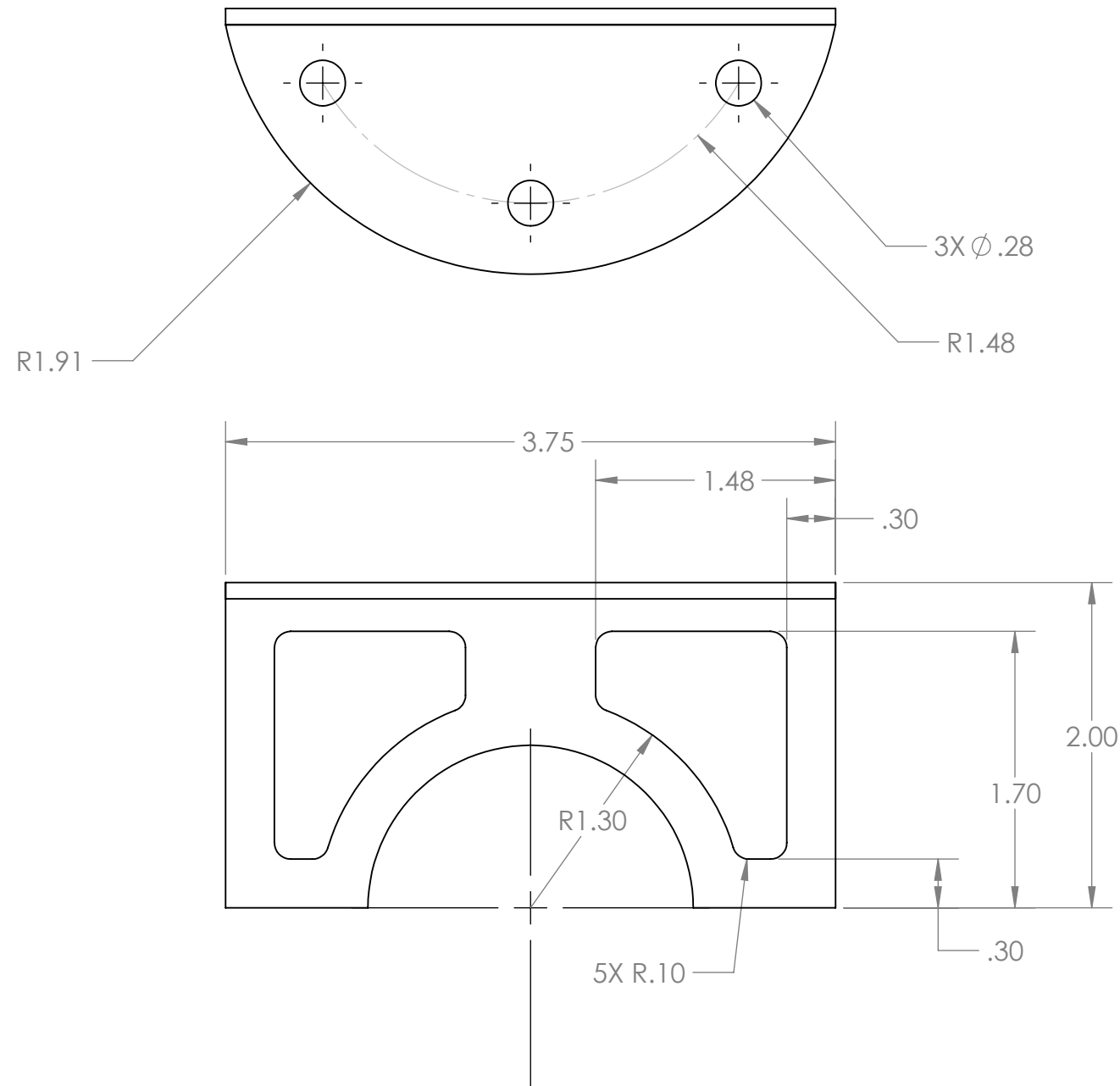
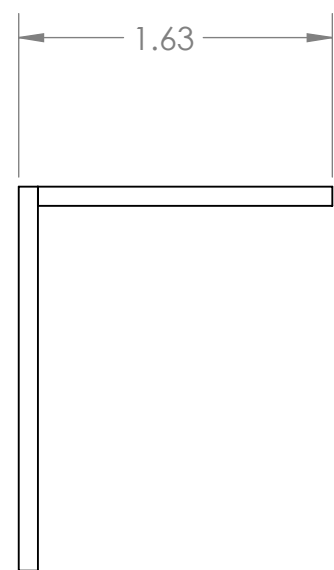
D
C
B
A

D
C
B
A

8 7 6 5 4 3 2 1

D
C
B
A

D
C
B
A



PROPRIETARY AND CONFIDENTIAL
THE INFORMATION CONTAINED IN THIS DRAWING IS THE SOLE PROPERTY OF <INSERT COMPANY NAME HERE>. ANY REPRODUCTION IN PART OR AS A WHOLE WITHOUT THE WRITTEN PERMISSION OF <INSERT COMPANY NAME HERE> IS PROHIBITED.

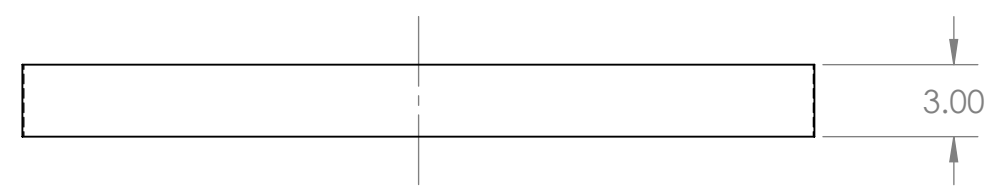
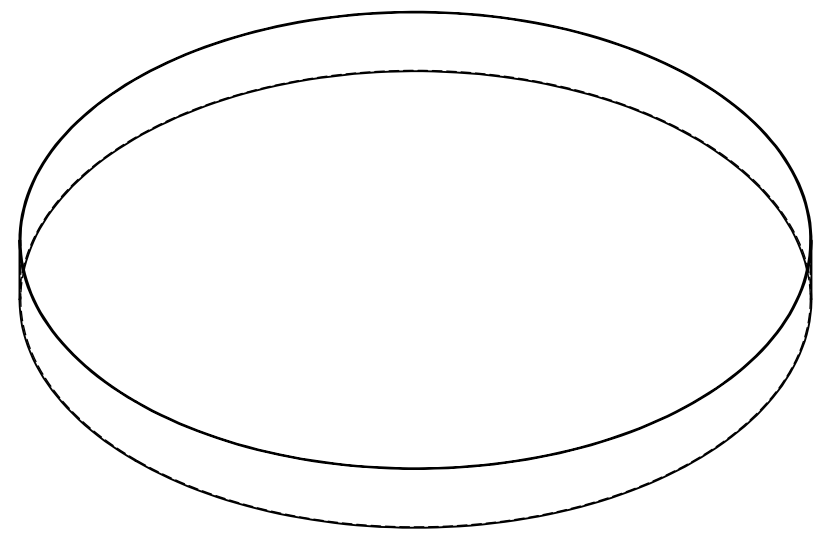
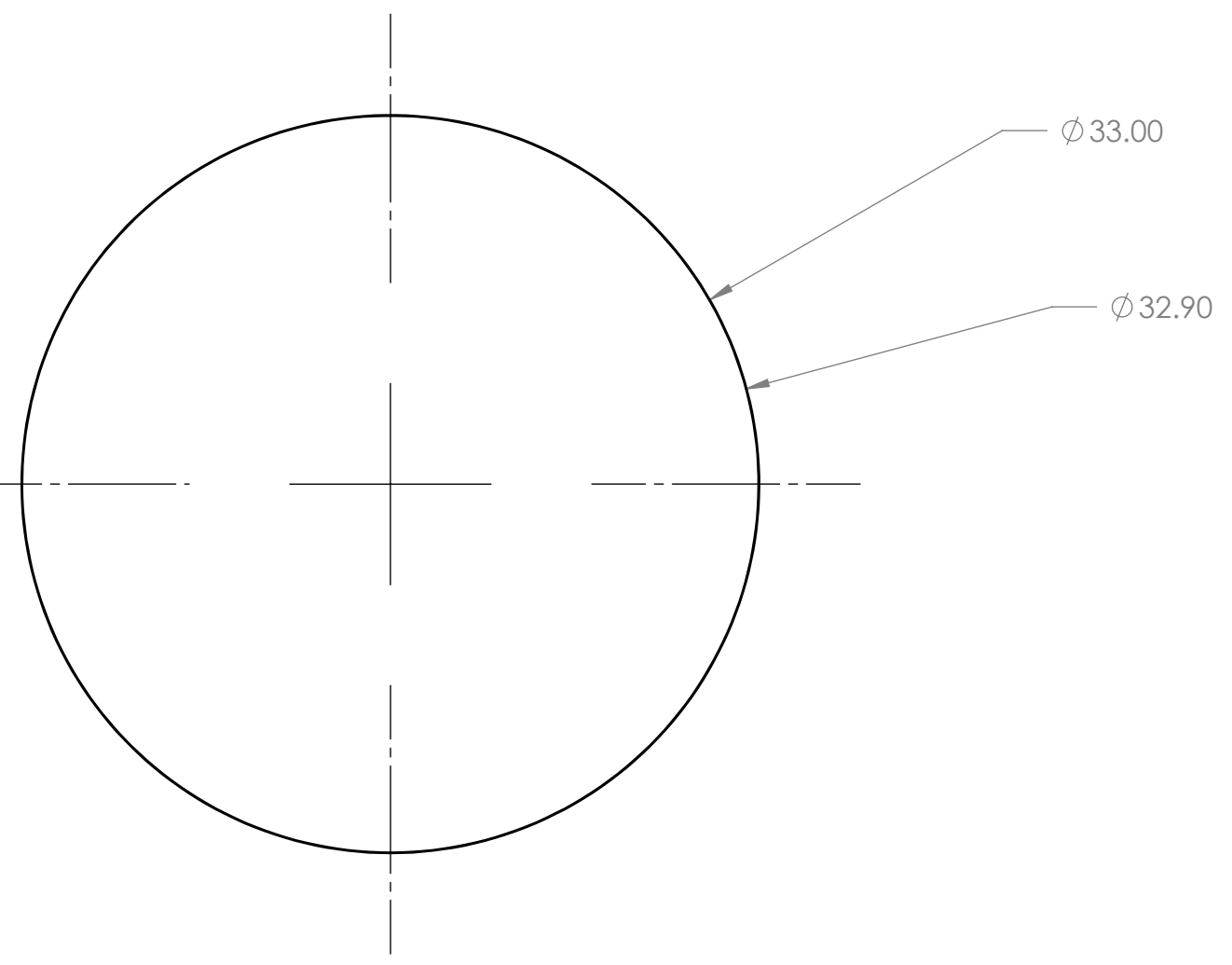
		UNLESS OTHERWISE SPECIFIED:		NAME	DATE
		DIMENSIONS ARE IN INCHES		DRAWN	AO 1/30/15
		TOLERANCES:		CHECKED	MM 1/30/15
		FRACTIONAL \pm		ENG APPR.	
		ANGULAR: MACH \pm BEND \pm		MFG APPR.	
		TWO PLACE DECIMAL \pm		Q.A.	
		THREE PLACE DECIMAL \pm		COMMENTS:	
		INTERPRET GEOMETRIC TOLERANCING PER:			
		MATERIAL			
		AISI 4130			
		FINISH			
NEXT ASSY	USED ON				
APPLICATION		DO NOT SCALE DRAWING			
		TITLE:		Motor Mount Bracket Wall	
SIZE	DWG. NO.	REV			
B	ECM-1-DS1-1302	A			
SCALE: 1:1	WEIGHT: .22	SHEET 1 OF 1			

8 7 6 5 4 3 2 1

8 7 6 5 4 3 2 1

D
C
B
A

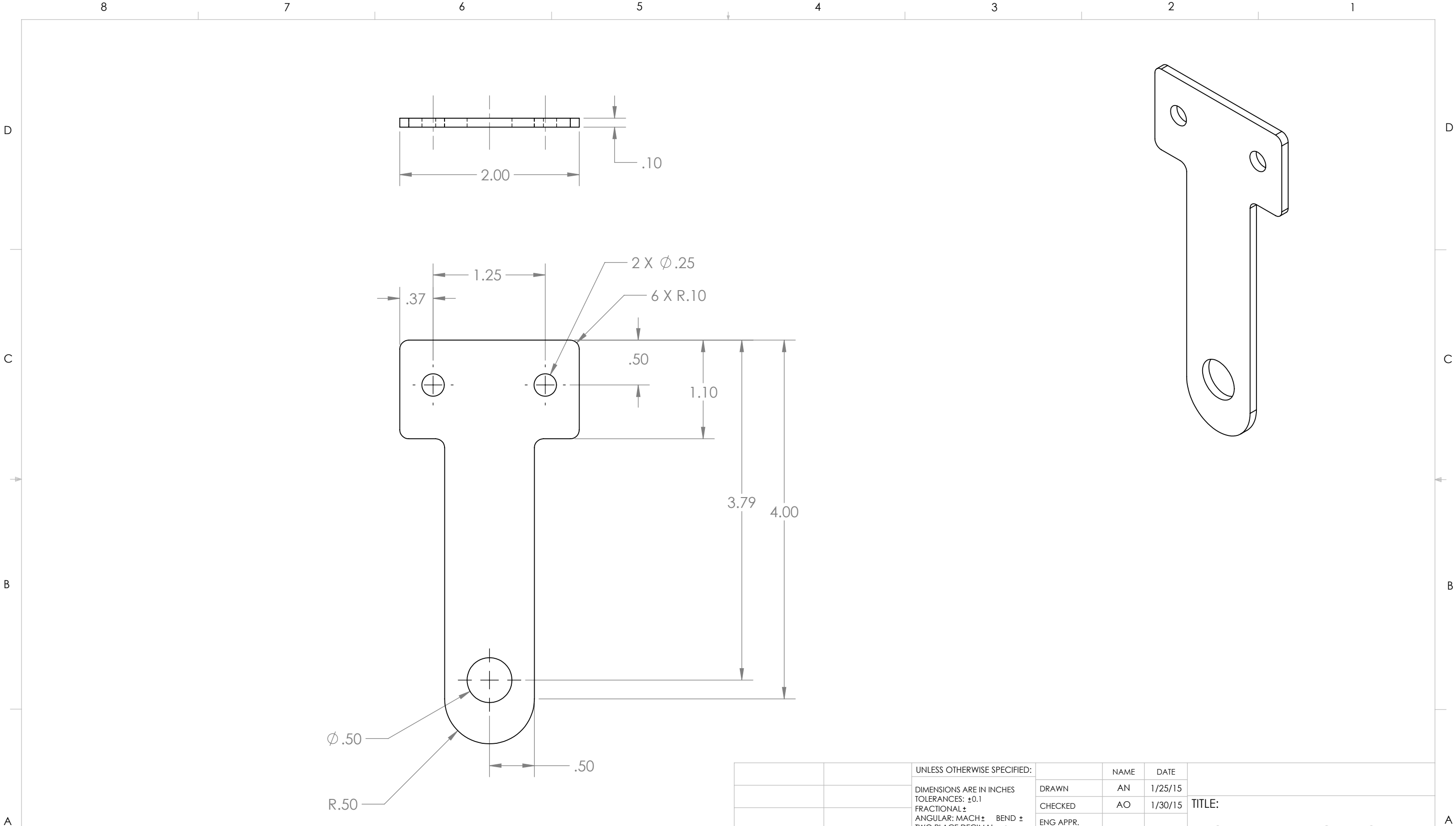
D
C
B
A



PROPRIETARY AND CONFIDENTIAL
 THE INFORMATION CONTAINED IN THIS
 DRAWING IS THE SOLE PROPERTY OF
 ELECTRIC COMMUTER MULTICOPTER TEAM. ANY
 REPRODUCTION IN PART OR AS A WHOLE
 WITHOUT THE WRITTEN PERMISSION OF
 ELECTRIC COMMUTER MULTICOPTER TEAM IS
 PROHIBITED.

		UNLESS OTHERWISE SPECIFIED:		NAME	DATE	TITLE: PROP RING
			DRAWN	AN	1/25/15	
			CHECKED	AO	1/30/15	
			ENG APPR.			
			MFG APPR.			
		INTERPRET GEOMETRIC TOLERANCING PER:		Q.A.		SIZE DWG. NO. REV B ECM-1-DS1-1303 A
		MATERIAL CARBON FIBER		COMMENTS:		
NEXT ASSY	USED ON	FINISH				SCALE: 1:8 WEIGHT: 1 lb SHEET 1 OF 1
APPLICATION						

8 7 6 5 4 3 2 1



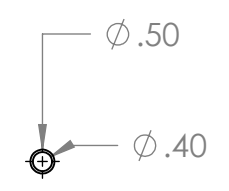
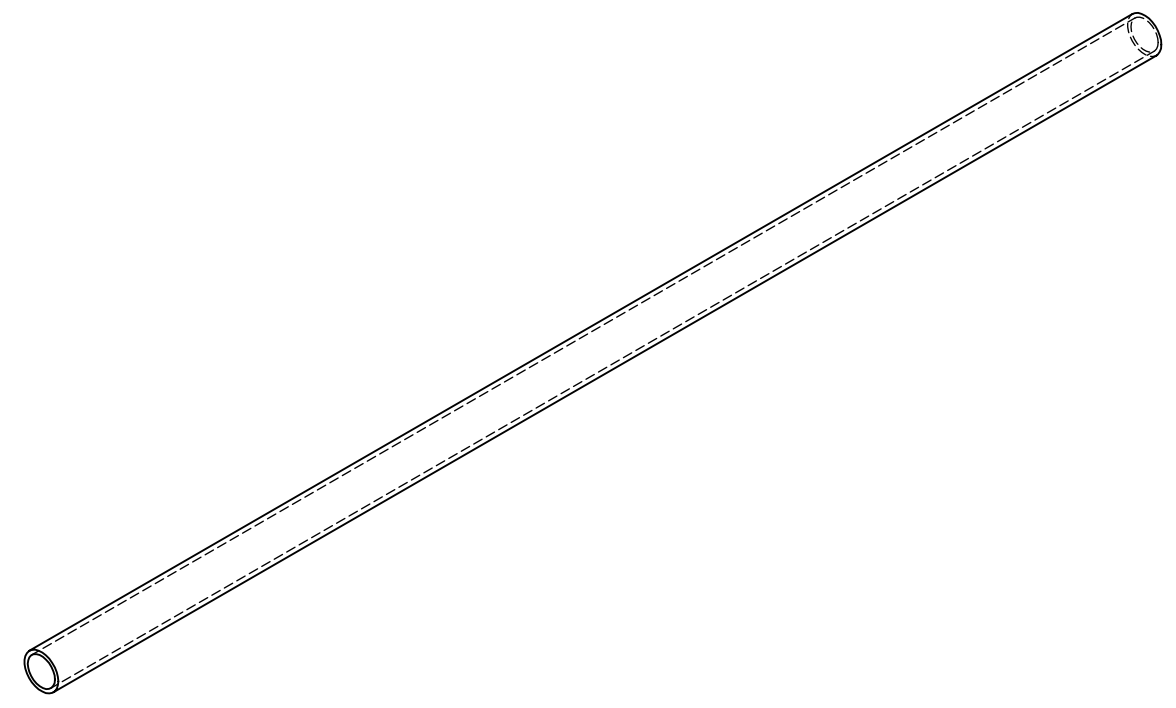
PROPRIETARY AND CONFIDENTIAL
 THE INFORMATION CONTAINED IN THIS DRAWING IS THE SOLE PROPERTY OF ELECTRIC COMMUTER MULTICOPTER TEAM. ANY REPRODUCTION IN PART OR AS A WHOLE WITHOUT THE WRITTEN PERMISSION OF ELECTRIC COMMUTER MULTICOPTER TEAM IS PROHIBITED.

		UNLESS OTHERWISE SPECIFIED:				NAME	DATE
		DIMENSIONS ARE IN INCHES		DRAWN	AN	1/25/15	
		TOLERANCES: ± 0.1		CHECKED	AO	1/30/15	
		FRACTIONAL \pm		ENG APPR.			
		ANGULAR: MACH \pm BEND \pm		MFG APPR.			
		TWO PLACE DECIMAL \pm		Q.A.			
		THREE PLACE DECIMAL \pm		COMMENTS:			
		INTERPRET GEOMETRIC TOLERANCING PER:					
		MATERIAL		4130 CHROMOLY			
NEXT ASSY		USED ON		FINISH			
APPLICATION							
				TITLE:			
				OUTER RING MOUNT			
SIZE	DWG. NO.		REV				
B	ECM-1-DS1-1304		A				
SCALE: 1:1		WEIGHT: 0.15 lb		SHEET 1 OF 1			

8 7 6 5 4 3 2 1

D
C
B
A

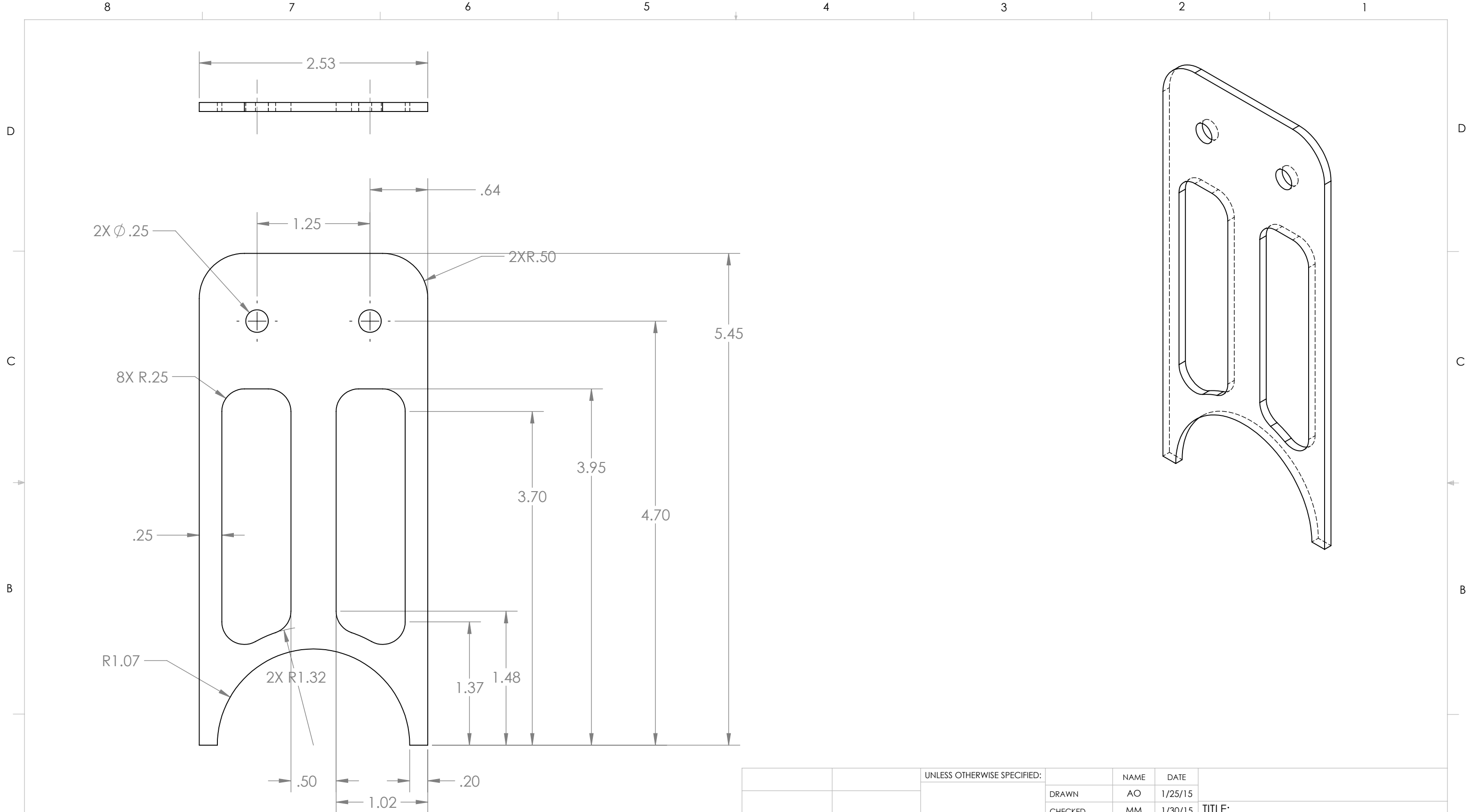
D
C
B
A



PROPRIETARY AND CONFIDENTIAL
 THE INFORMATION CONTAINED IN THIS
 DRAWING IS THE SOLE PROPERTY OF
 ELECTRIC COMMUTER MULTICOPTER TEAM. ANY
 REPRODUCTION IN PART OR AS A WHOLE
 WITHOUT THE WRITTEN PERMISSION OF
 ELECTRIC COMMUTER MULTICOPTER TEAM IS
 PROHIBITED.

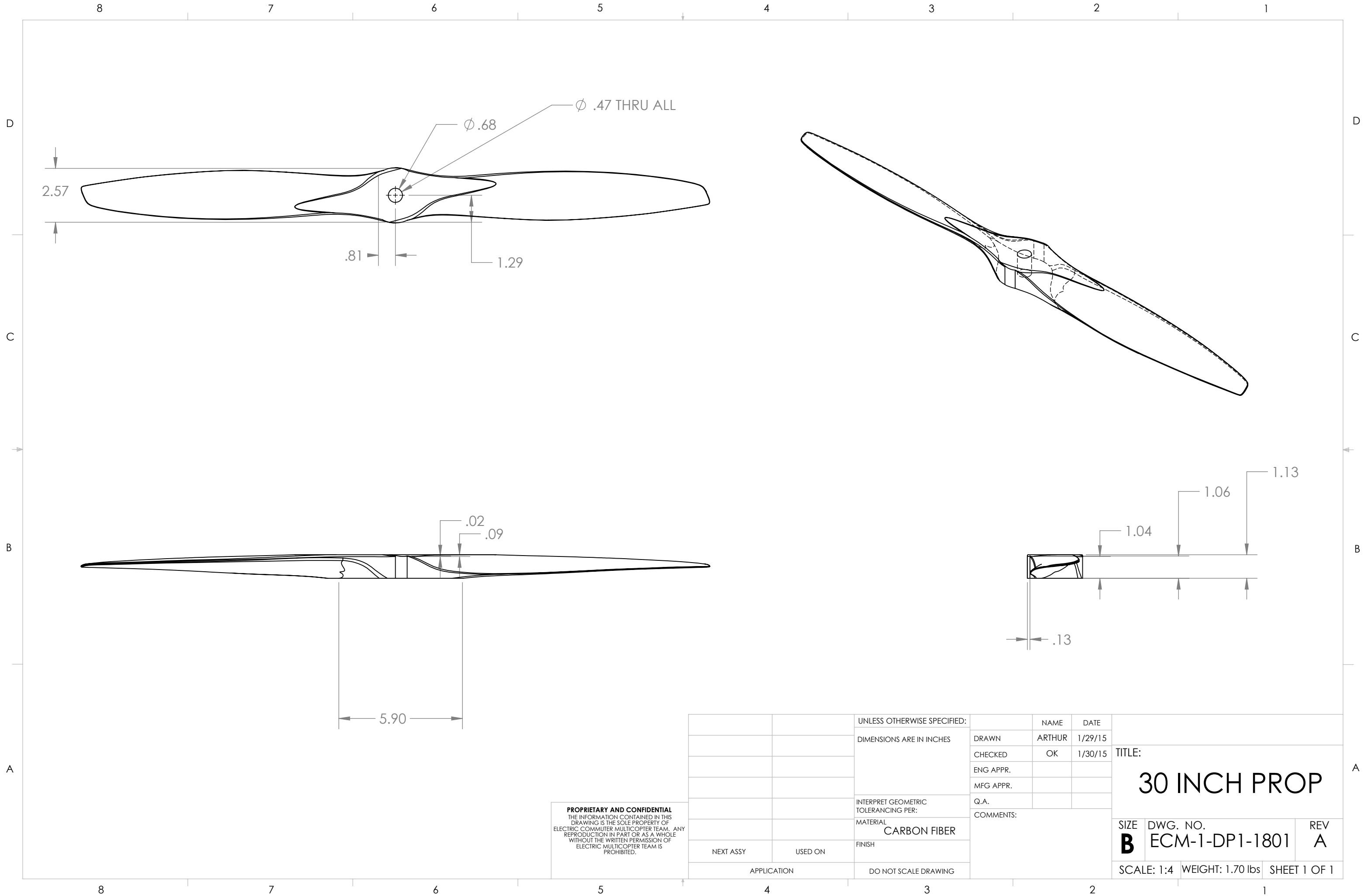
		UNLESS OTHERWISE SPECIFIED: DIMENSIONS ARE IN INCHES TOLERANCES: ±0.1 FRACTIONAL ± ANGULAR: MACH ± BEND ± TWO PLACE DECIMAL ± THREE PLACE DECIMAL ± INTERPRET GEOMETRIC TOLERANCING PER: MATERIAL 4130 CHROMOLY FINISH		NAME	DATE	TITLE: <h1 style="text-align: center;">RING SPAR</h1>
			DRAWN	AN	1/25/15	
			CHECKED	AO	1/30/15	
			ENG APPR.			
			MFG APPR.			
			Q.A.			
			COMMENTS:			
NEXT ASSY	USED ON		SIZE	DWG. NO.	REV	
			B	ECM-1-DS1-1305	A	
APPLICATION			SCALE: 1:4	WEIGHT: 0.19 lbs	SHEET 1 OF 1	

8 7 6 5 4 3 2 1



PROPRIETARY AND CONFIDENTIAL
 THE INFORMATION CONTAINED IN THIS DRAWING IS THE SOLE PROPERTY OF ELECTRIC COMMUTER MULTICOPTER TEAM. ANY REPRODUCTION IN PART OR AS A WHOLE WITHOUT THE WRITTEN PERMISSION OF ELECTRIC COMMUTER MULTICOPTER TEAM IS PROHIBITED.

		UNLESS OTHERWISE SPECIFIED:		NAME	DATE	TITLE: INNER RING MOUNT	
				DRAWN	AO		1/25/15
				CHECKED	MM		1/30/15
				ENG APPR.			
				MFG APPR.			
				Q.A.			
				COMMENTS:			
				INTERPRET GEOMETRIC TOLERANCING PER:			
				MATERIAL			
				4130 CHROMOLY			
				FINISH			
NEXT ASSY	USED ON					SIZE DWG. NO. REV	
						B ECM-1-DS1-1306 A	
APPLICATION		DO NOT SCALE DRAWING		SCALE: 1:1		WEIGHT: 0.22 lbs	
						SHEET 1 OF 1	

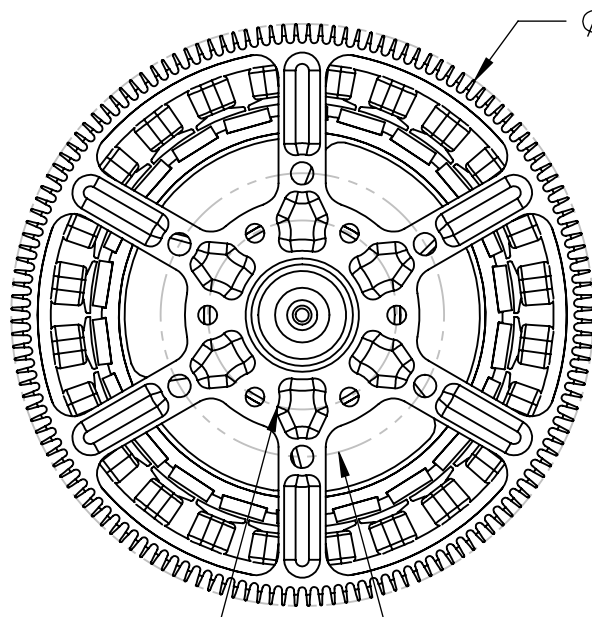
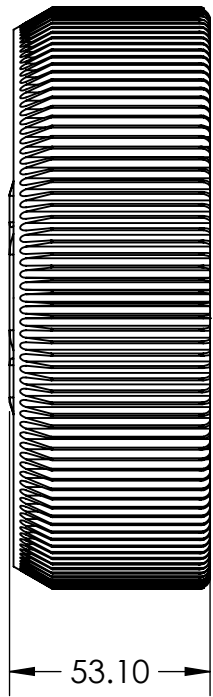


PROPRIETARY AND CONFIDENTIAL
 THE INFORMATION CONTAINED IN THIS
 DRAWING IS THE SOLE PROPERTY OF
 ELECTRIC COMMUTER MULTICOPTER TEAM. ANY
 REPRODUCTION IN PART OR AS A WHOLE
 WITHOUT THE WRITTEN PERMISSION OF
 ELECTRIC MULTICOPTER TEAM IS
 PROHIBITED.

		UNLESS OTHERWISE SPECIFIED:		NAME	DATE	TITLE: 30 INCH PROP
		DIMENSIONS ARE IN INCHES	DRAWN	ARTHUR	1/29/15	
			CHECKED	OK	1/30/15	
			ENG APPR.			
			MFG APPR.			
		INTERPRET GEOMETRIC TOLERANCING PER:	Q.A.			SIZE DWG. NO. REV B ECM-1-DP1-1801 A
		MATERIAL CARBON FIBER	COMMENTS:			
NEXT ASSY	USED ON	FINISH				SCALE: 1:4 WEIGHT: 1.70 lbs SHEET 1 OF 1
APPLICATION		DO NOT SCALE DRAWING				

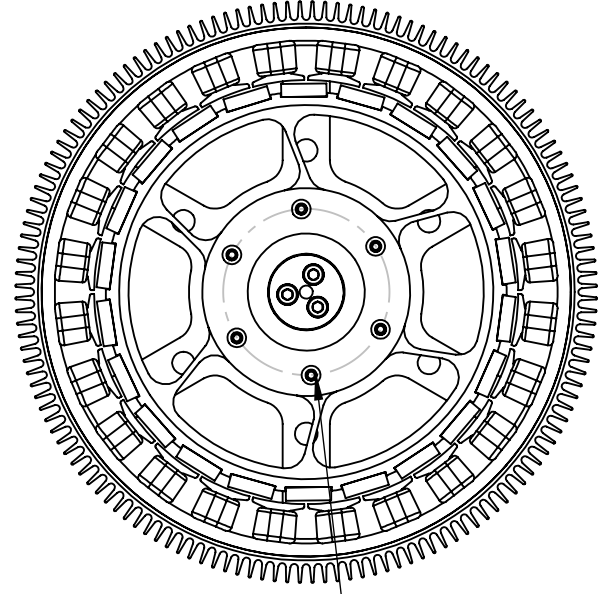
A
B
C
D
E
F
G
H
I
J
K
L
M
N
O
P
Q
R
S
T
U
V

A
B
C
D
E
F
G
H
I
J
K
L
M
N
O
P
Q
R
S
T
U
V



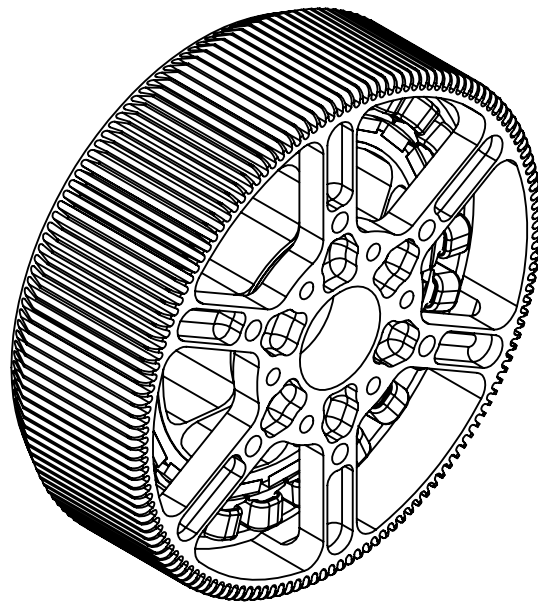
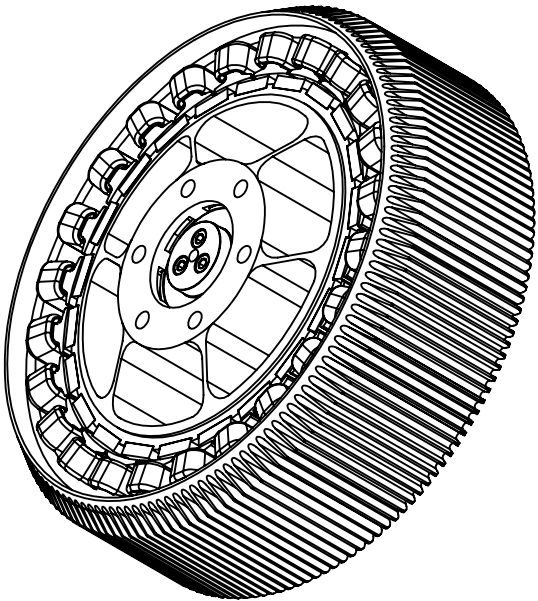
Mounting Pattern
 $\phi 50$
 6x M6 Tapped

$\phi 154$ OD



Mounting Pattern
 $\phi 75$
 6x M6 Thru

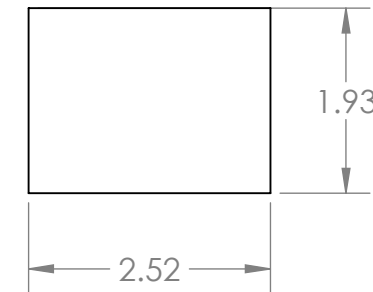
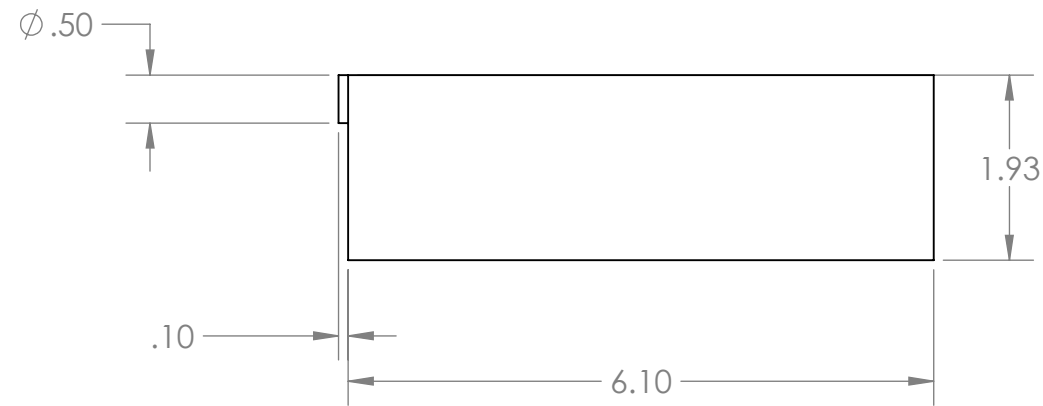
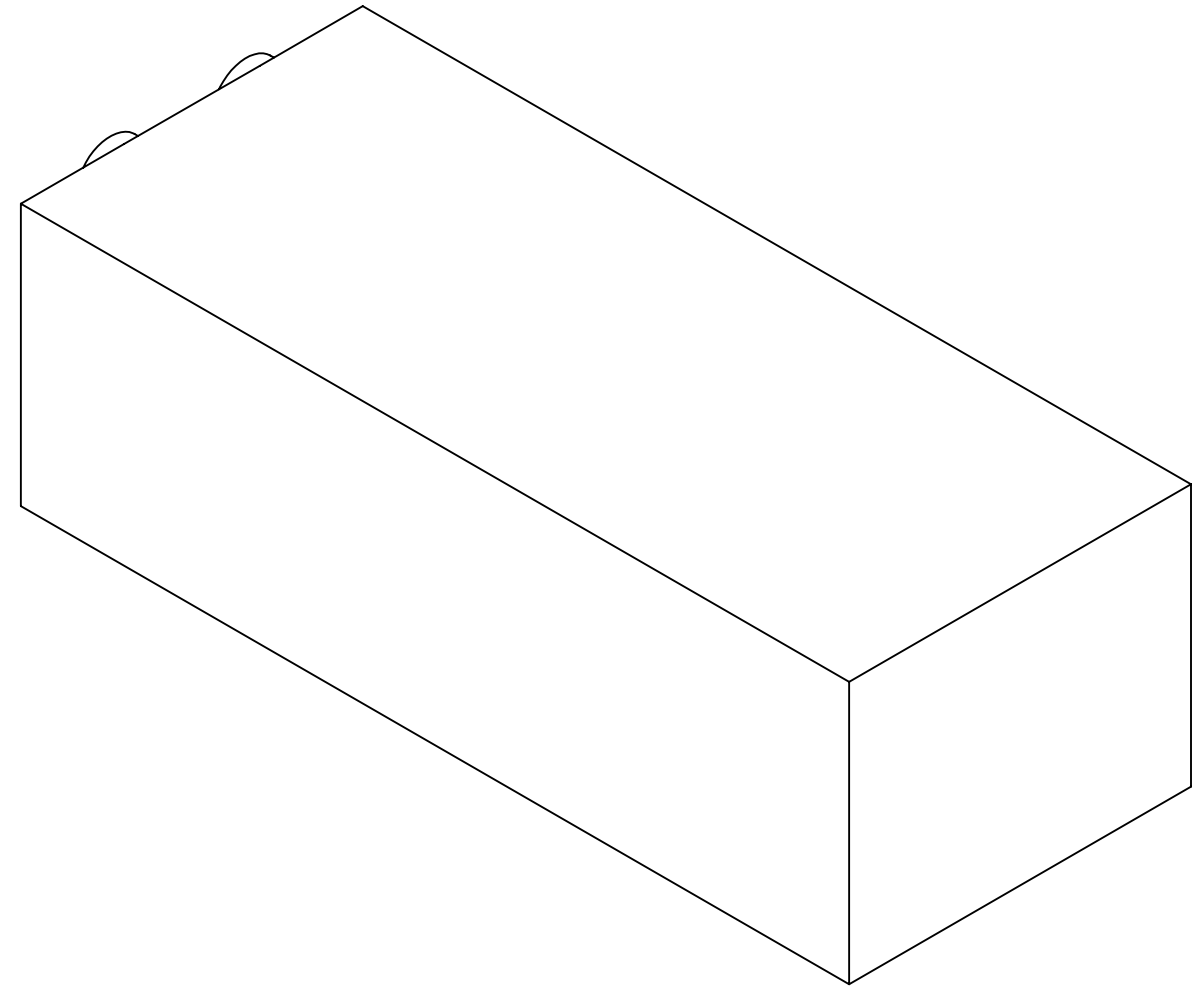
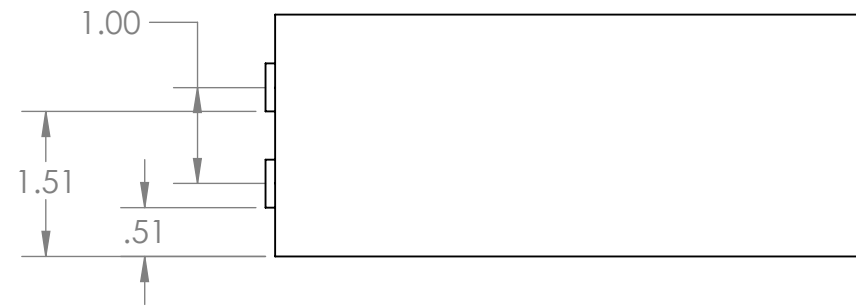
Mounting Pattern
 $\phi 44$
 6x M5 Tapped



340 Woodpecker Ridge
 Santa Cruz, CA 95060
 +1 (831) 426-3733

TITLE: JM1S		
DWG. NO.		
DRAWN	AUTHOR Scott MacAfee	DATE 11/18/13
REVA-01	Standard Tolerances in MM (Unless Otherwise Specified) Linear Dimensions: X.XX +/-0.05mm X.XXX +/-0.010mm Angular Dimensions: +/-0.5 degree	
<small>PROPRIETARY NOTICE: This document is the property of Joby Aviation Inc. and contains confidential, proprietary information. Neither it nor the information contained therein shall be disclosed to or duplicated nor used by others except as authorized by Joby Aviation Inc in writing.</small>		
Material:		SHEET 1 OF 1

Color: Anodized Orange Finish: Sand Blasted Weight: GRAMS



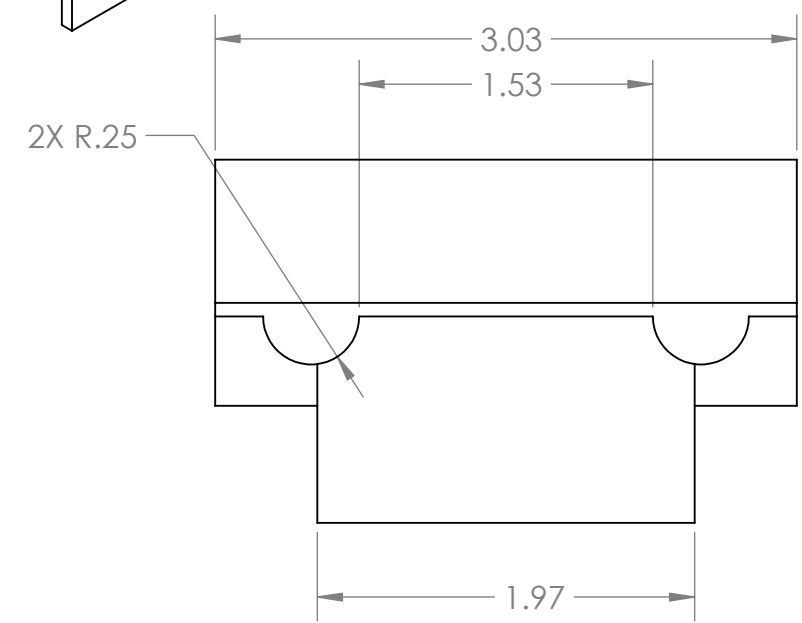
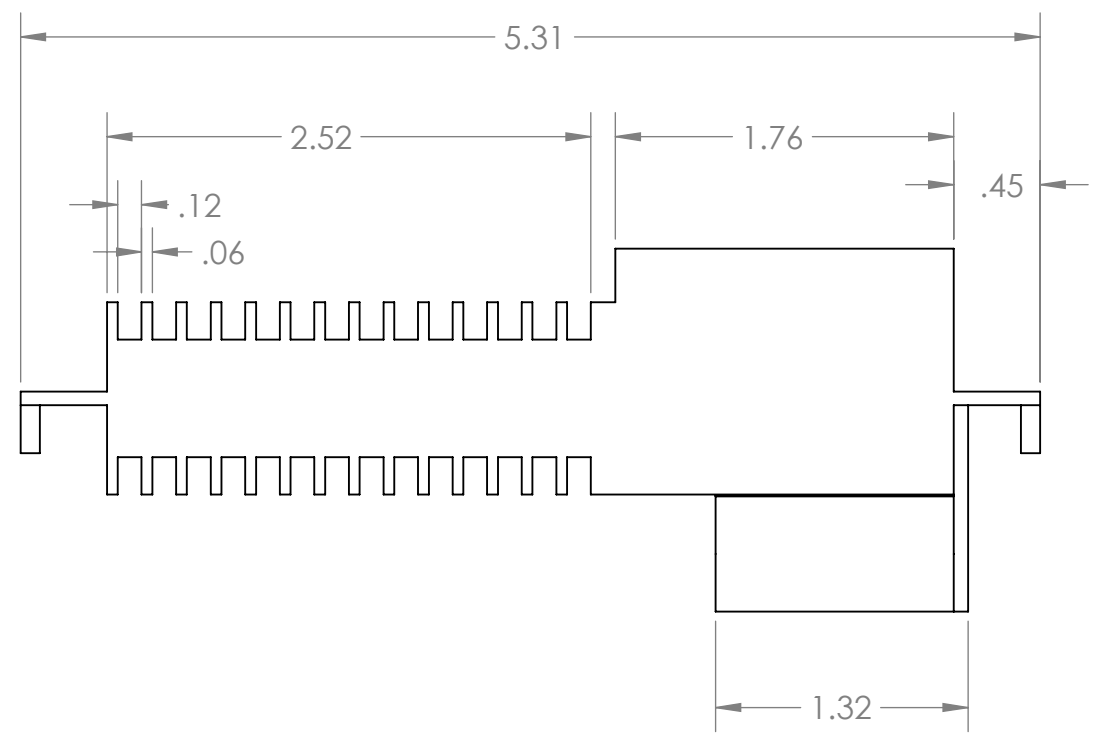
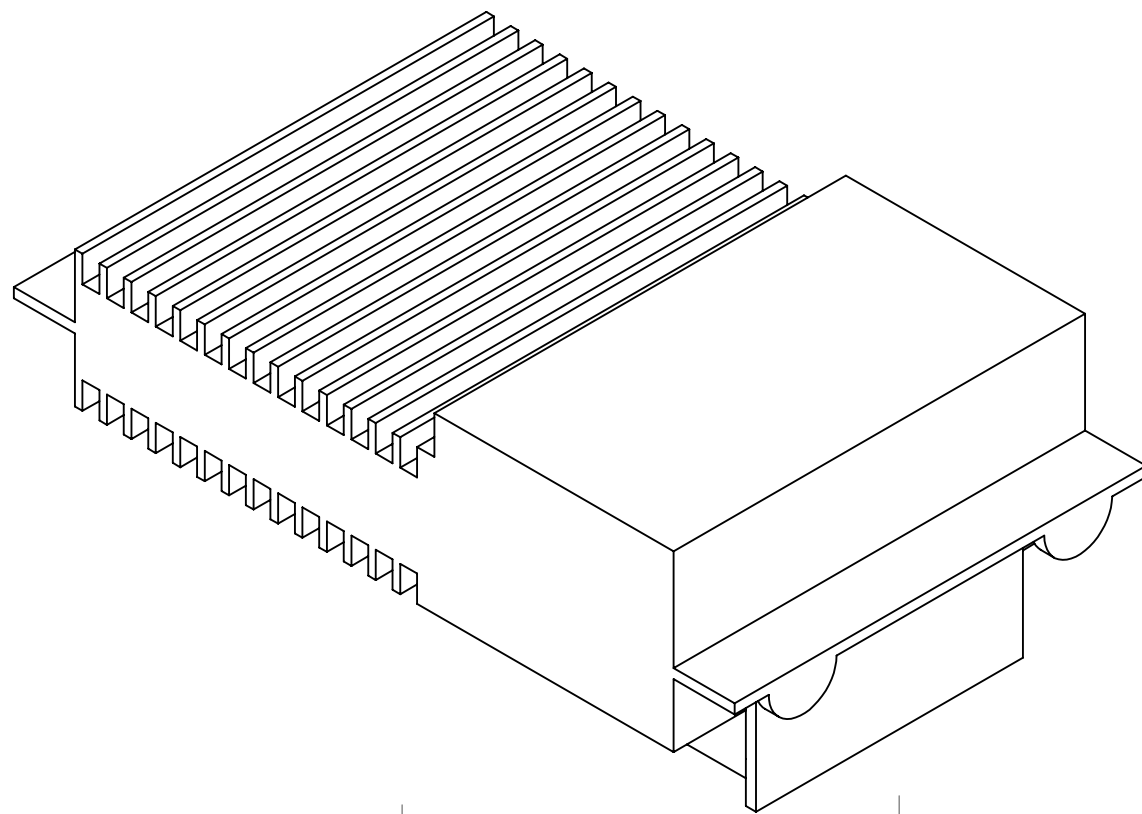
PROPRIETARY AND CONFIDENTIAL
 THE INFORMATION CONTAINED IN THIS DRAWING IS THE SOLE PROPERTY OF ELECTRIC COMMUTER MULTICOPTER TEAM. REPRODUCTION IN PART OR AS A WHOLE WITHOUT THE WRITTEN PERMISSION OF ELECTRIC COMMUTER MULTICOPTER TEAM IS PROHIBITED.

		UNLESS OTHERWISE SPECIFIED: DIMENSIONS ARE IN INCHES	NAME	DATE	TITLE: 7s LiPo Battery	
			DRAWN	ARTHUR		1/29/15
			CHECKED	OK		1/30/15
			ENG APPR.			
		INTERPRET GEOMETRIC TOLERANCING PER:	Q.A.			
		MATERIAL LITHIUM-ION POLYMER	COMMENTS:			
		FINISH				
NEXT ASSY	USED ON					
APPLICATION		DO NOT SCALE DRAWING				
			SIZE	DWG. NO.	REV	
			B	ECM-1-DP0-1601	A	
			SCALE: 1:2	WEIGHT: 2.2 lbs	SHEET 1 OF 1	

8 7 6 5 4 3 2 1

D
C
B
A

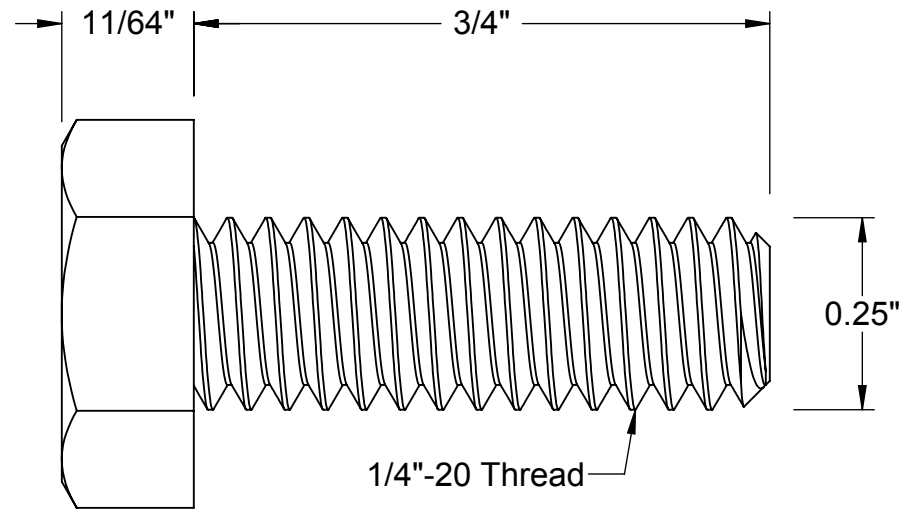
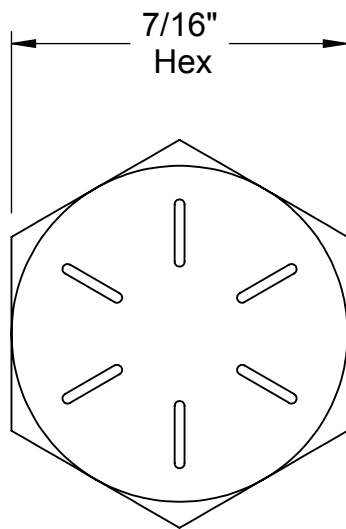
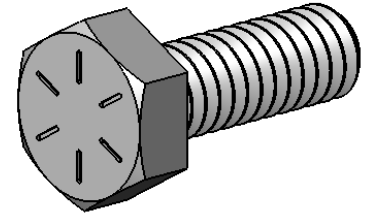
D
C
B
A



PROPRIETARY AND CONFIDENTIAL
 THE INFORMATION CONTAINED IN THIS
 DRAWING IS THE SOLE PROPERTY OF
 ELECTRIC COMMUTER MULTICOPTER TEAM. ANY
 REPRODUCTION IN PART OR AS A WHOLE
 WITHOUT THE WRITTEN PERMISSION OF
 ELECTRIC COMMUTER MULTICOPTER TEAM IS
 PROHIBITED.

		UNLESS OTHERWISE SPECIFIED:		NAME	DATE	TITLE: ESC
			DRAWN	AO	1/30/15	
			CHECKED	MM	1/30/15	
			ENG APPR.			
			MFG APPR.			
		INTERPRET GEOMETRIC TOLERANCING PER:		Q.A.		SIZE B DWG. NO. ECM-1-DP0-1801 REV A
		MATERIAL		COMMENTS:		
NEXT ASSY	USED ON	FINISH				
APPLICATION		DO NOT SCALE DRAWING				SCALE: 1:1 WEIGHT: 1 SHEET 1 OF 1

8 7 6 5 4 3 2 1



McMASTER-CARR CAD

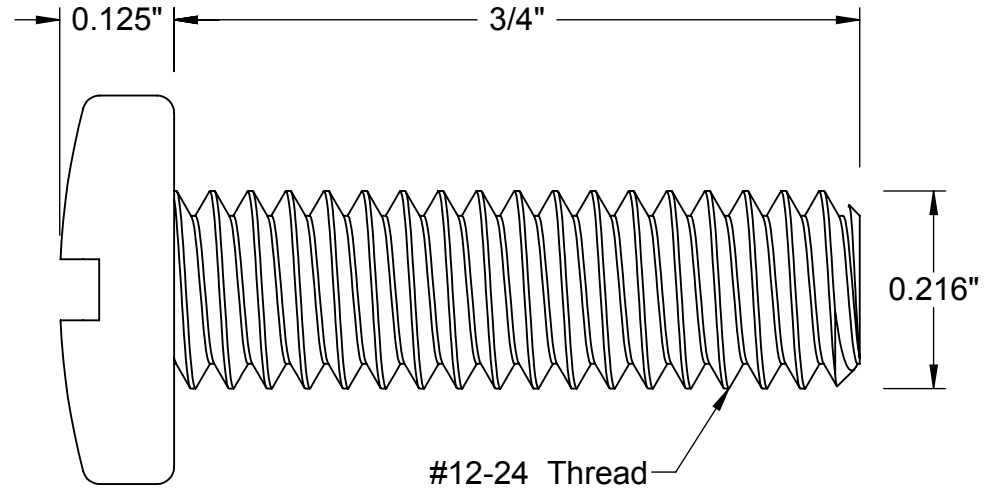
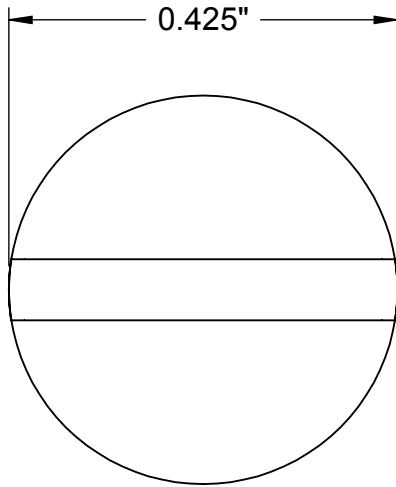
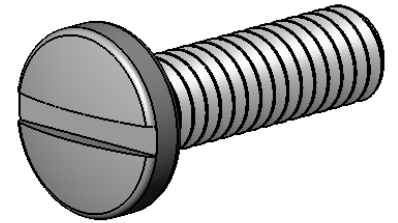
PART
NUMBER

92620A540

<http://www.mcmaster.com>
© 2014 McMaster-Carr Supply Company

High-Strength Steel
Cap Screw-Grade 8

Information in this drawing is provided for reference only.



McMASTER-CARR CAD

<http://www.mcmaster.com>

© 2012 McMaster-Carr Supply Company

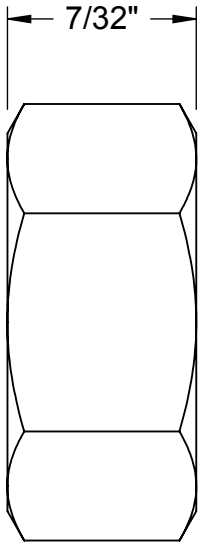
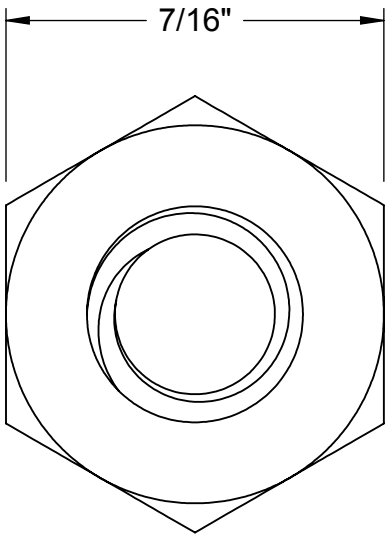
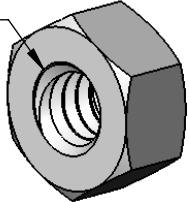
Information in this drawing is provided for reference only.

PART
NUMBER

91792A294

Pan Head Slotted
Machine Screw

1/4"-20 Thread



McMASTER-CARR CAD

<http://www.mcmaster.com>

© 2015 McMaster-Carr Supply Company

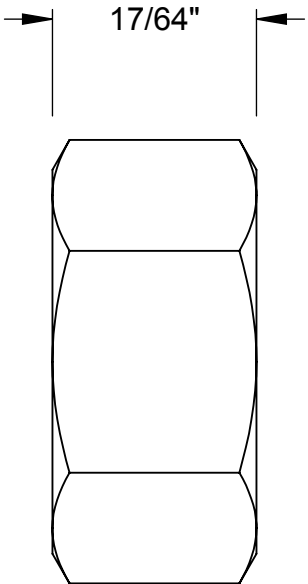
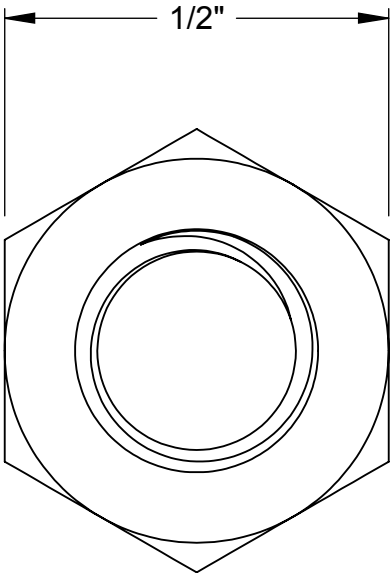
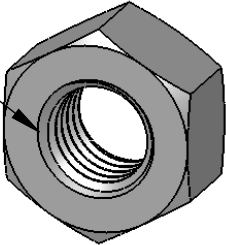
Information in this drawing is provided for reference only.

PART
NUMBER

93827A211

Hex
Nut

5/16"-24 Thread



McMASTER-CARR CAD

<http://www.mcmaster.com>
© 2009 McMaster-Carr Supply Company

Information in this drawing is provided for reference only.

PART
NUMBER

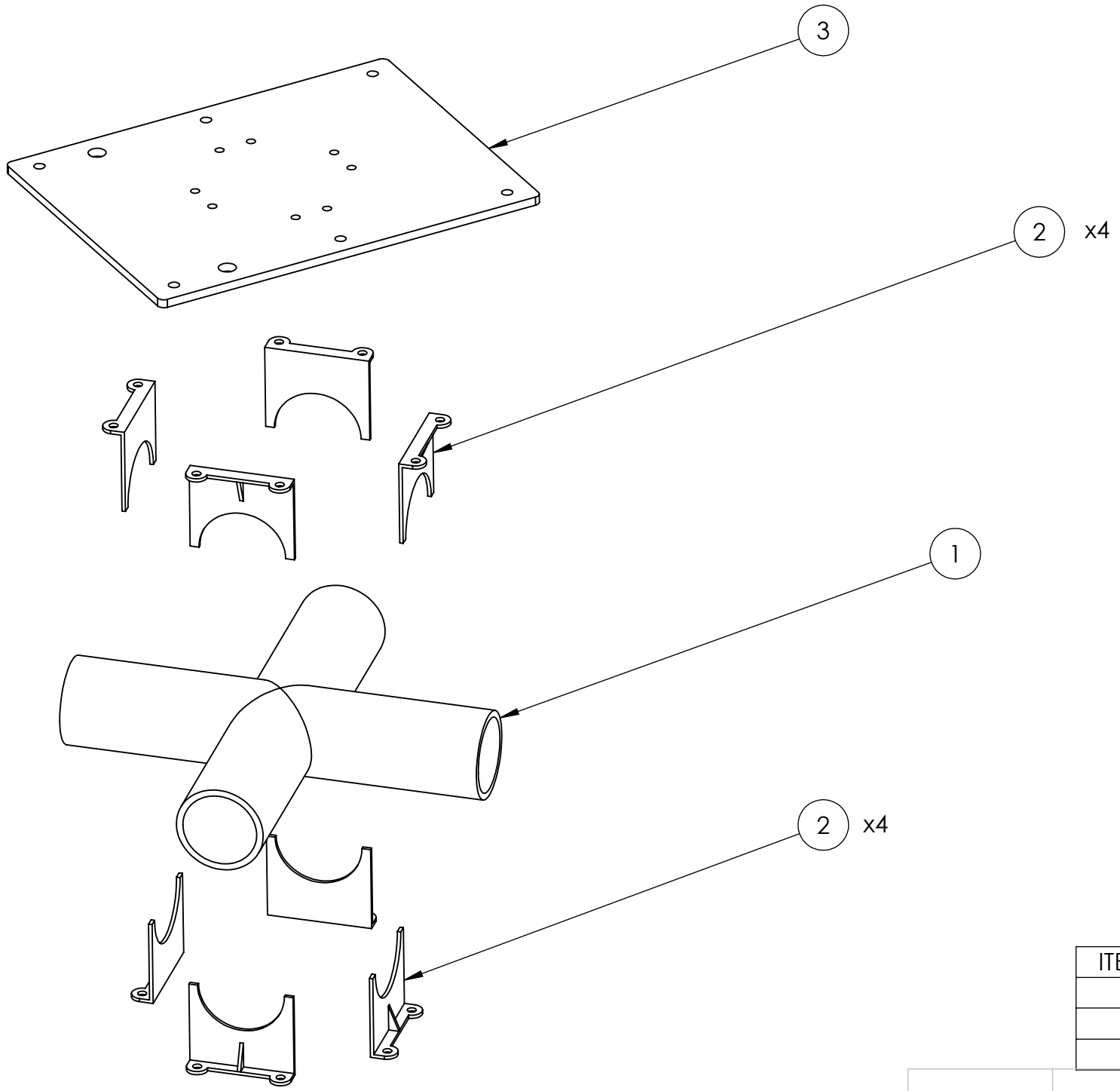
94804A315

Type 316 Stainless Steel
Hex Nut

8 7 6 5 4 3 2 1

D
C
B
A

D
C
B
A

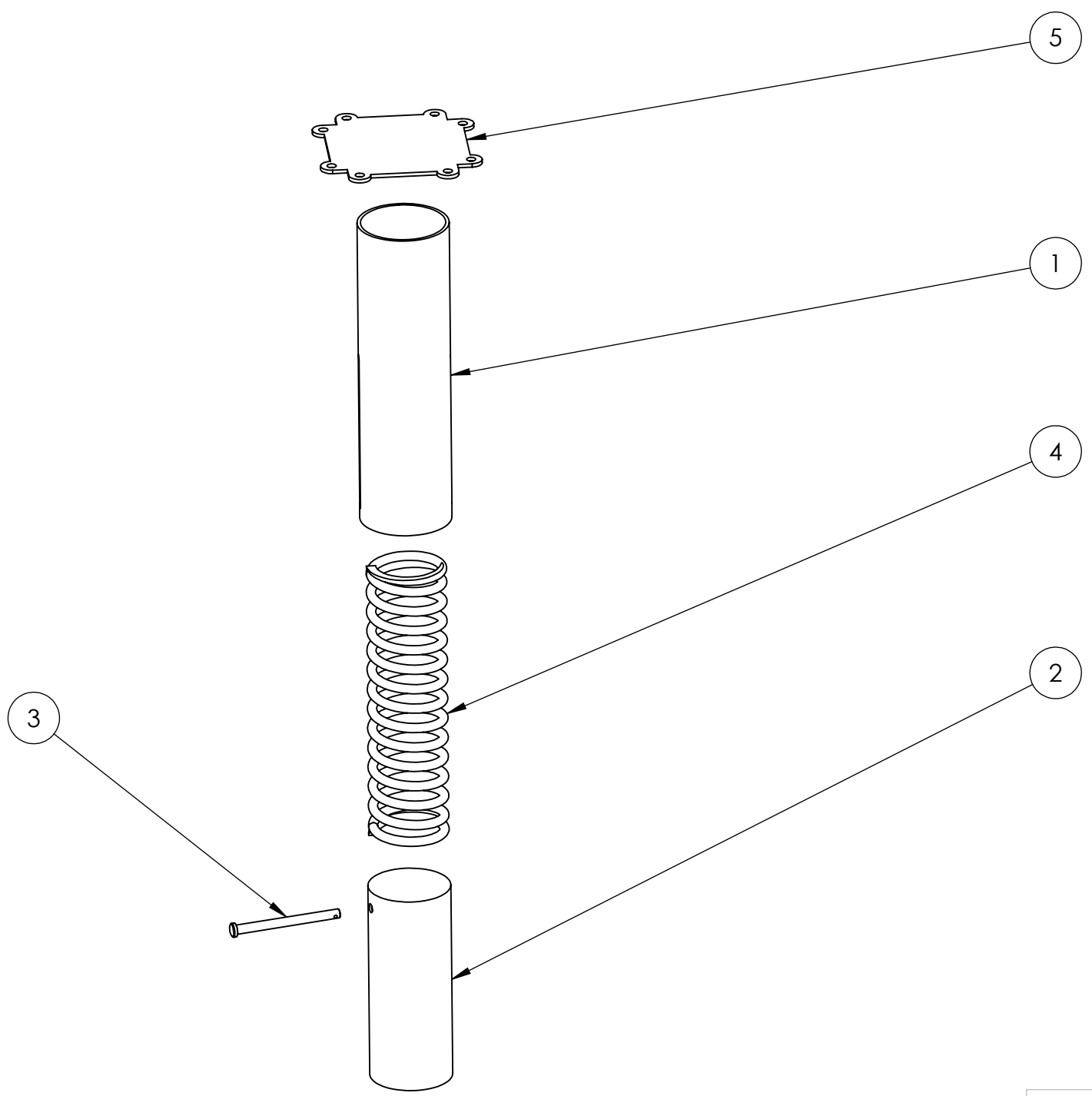


ITEM NO.	PART NUMBER	DESCRIPTION	QTY.
1	ECM-1-S1-1102	CENTER BRACKET	1
2	ECM-1-S1-1101	CENTER MOUNT WALL	8
3	ECM-1-S1-1104	SEAT PLATE	1

PROPRIETARY AND CONFIDENTIAL
 THE INFORMATION CONTAINED IN THIS DRAWING IS THE SOLE PROPERTY OF <INSERT COMPANY NAME HERE>. ANY REPRODUCTION IN PART OR AS A WHOLE WITHOUT THE WRITTEN PERMISSION OF <INSERT COMPANY NAME HERE> IS PROHIBITED.

ECM-1-A1-0001	MULTICOPTER ASSY	NAME	DATE	TITLE: CENTER MOUNT ASSEMBLY
NEXT ASSY	USED ON	DRAWN	BLAKE S. 1/29/15	
APPLICATION		CHECKED	MARLEY 1/30/15	
DO NOT SCALE DRAWING		ENG APPR.		
		MFG APPR.		
		Q.A.		SIZE B DWG. NO. ECM-1-DA1-0002 REV A SCALE: 1:4 WEIGHT: 12.2lb SHEET 1 OF 1
		COMMENTS: LANDING GEAR PLATES ARE INCLUDED IN LANDING GEAR ASSEMBLY.		

8 7 6 5 4 3 2 1



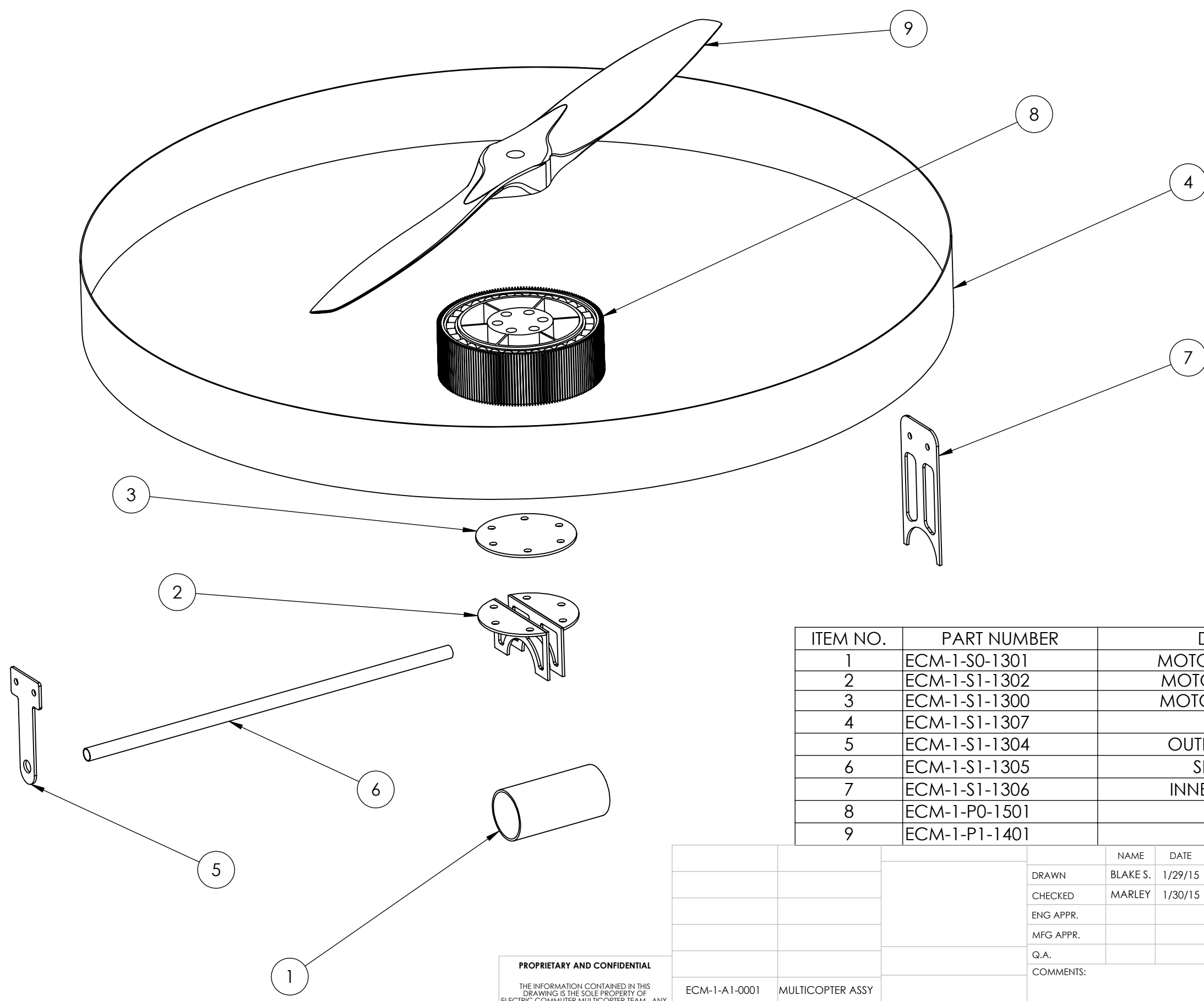
ITEM NO.	PART NUMBER	DESCRIPTION	QTY.
1	ECM-1-S0-0902	LANDING GEAR OUTER TUBE	1
2	ECM-1-S0-0905	LANDING GEAR TIP	1
3	ECM-1-S0-0903	LANDING GEAR BOLT	1
4	ECM-1-S0-0904	LANDING GEAR SPRING	1
5	ECM-1-S1-1103	LANDING GEAR PLATE	1

PROPRIETARY AND CONFIDENTIAL
 THE INFORMATION CONTAINED IN THIS DRAWING IS THE SOLE PROPERTY OF ELECTRIC COMMUTER MULTICOPTER TEAM. ANY REPRODUCTION IN PART OR AS A WHOLE WITHOUT THE WRITTEN PERMISSION OF ELECTRIC COMMUTER MULTICOPTER TEAM IS PROHIBITED.

ECM-1-A1-0001	MULTICOPTER ASSY	NAME	DATE	TITLE: LANDING GEAR ASSEMBLY
NEXT ASSY	USED ON	DRAWN	BLAKE S. 1/29/15	
APPLICATION		CHECKED	MARLEY 1/30/15	
		ENG APPR.		
		MFG APPR.		
		Q.A.		SIZE B DWG. NO. ECM-1-DA1-0005 REV A SCALE: 1:4 WEIGHT: 3.83 lbf SHEET OF
		COMMENTS: LOCKED TOGETHER WITH COTTER PIN THROUGH CLEVIS PIN		

8 7 6 5 4 3 2 1

D
C
B
A

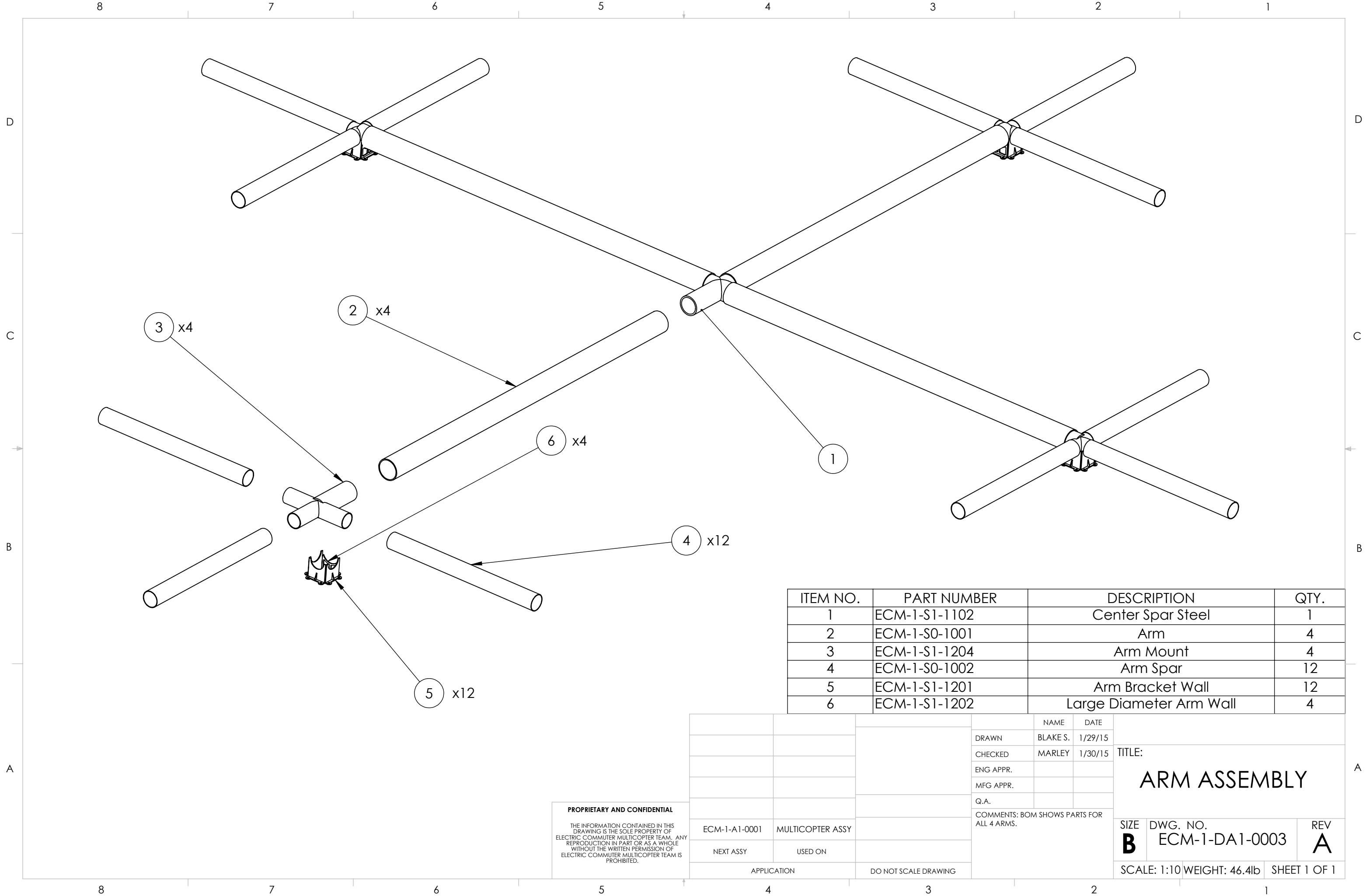


ITEM NO.	PART NUMBER	DESCRIPTION	QTY.
1	ECM-1-S0-1301	MOTOR MOUNT INSERT	1
2	ECM-1-S1-1302	MOTOR MOUNT WALL	2
3	ECM-1-S1-1300	MOTOR MOUNT PLATE	1
4	ECM-1-S1-1307	PROP RING	1
5	ECM-1-S1-1304	OUTER RING MOUNT	1
6	ECM-1-S1-1305	SHROUD SPAR	1
7	ECM-1-S1-1306	INNER RING MOUNT	1
8	ECM-1-P0-1501	JOBY JM1S	1
9	ECM-1-P1-1401	PROP	1

PROPRIETARY AND CONFIDENTIAL
 THE INFORMATION CONTAINED IN THIS DRAWING IS THE SOLE PROPERTY OF ELECTRIC COMMUTER MULTICOPTER TEAM. ANY REPRODUCTION IN PART OR AS A WHOLE WITHOUT THE WRITTEN PERMISSION OF ELECTRIC COMMUTER MULTICOPTER TEAM IS PROHIBITED.

ECM-1-A1-0001	MULTICOPTER ASSY	NAME	DATE	TITLE: MOTOR ASSEMBLY
		DRAWN	BLAKE S. 1/29/15	
		CHECKED	MARLEY 1/30/15	
		ENG APPR.		
		MFG APPR.		
		Q.A.		SIZE DWG. NO. REV B ECM-1-DA1-0004 A
		COMMENTS:		
NEXT ASSY	USED ON	SCALE: 1:4 WEIGHT:		SHEET OF
APPLICATION		DO NOT SCALE DRAWING		

8 7 6 5 4 3 2 1



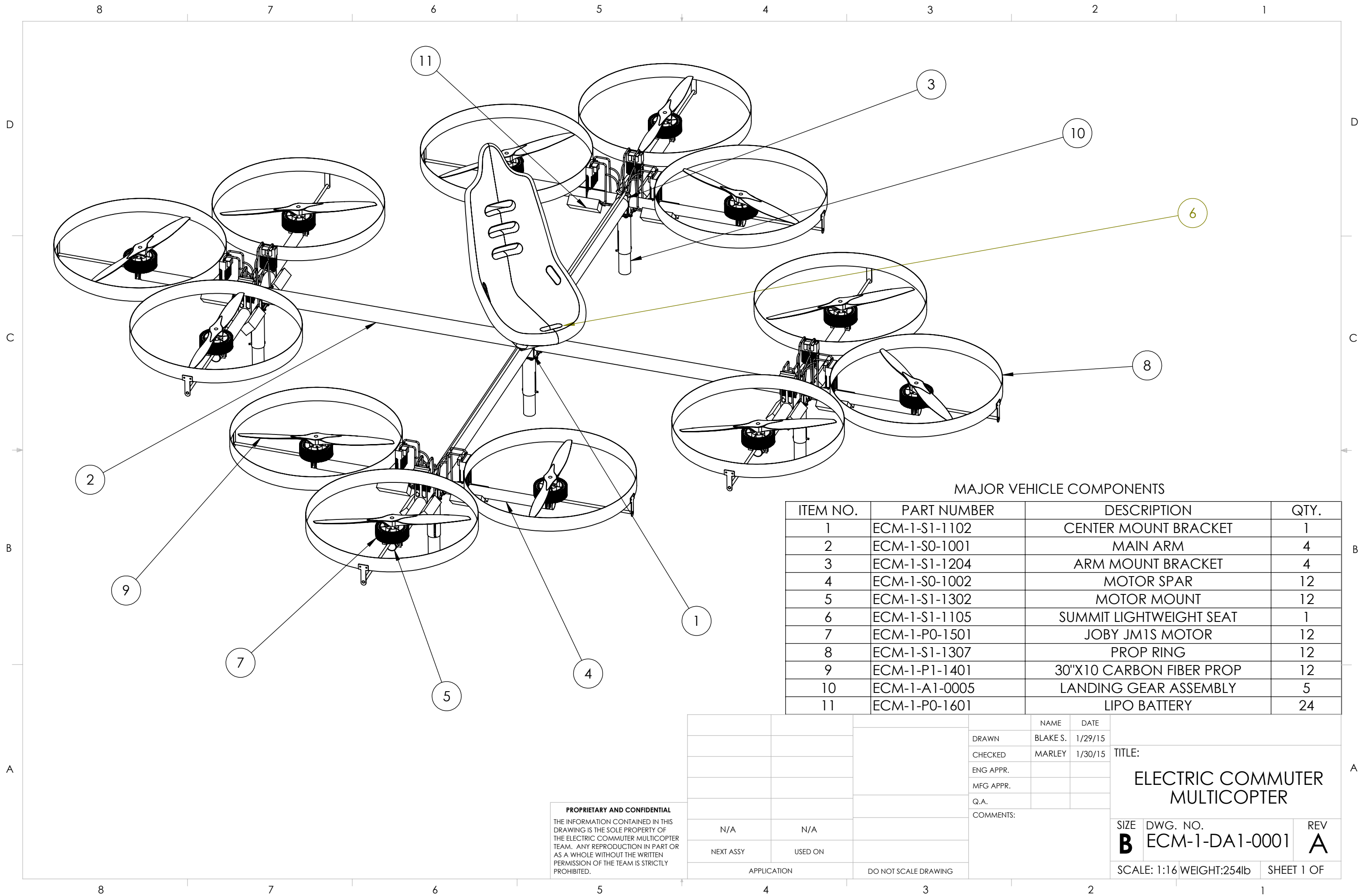
ITEM NO.	PART NUMBER	DESCRIPTION	QTY.
1	ECM-1-S1-1102	Center Spar Steel	1
2	ECM-1-S0-1001	Arm	4
3	ECM-1-S1-1204	Arm Mount	4
4	ECM-1-S0-1002	Arm Spar	12
5	ECM-1-S1-1201	Arm Bracket Wall	12
6	ECM-1-S1-1202	Large Diameter Arm Wall	4

PROPRIETARY AND CONFIDENTIAL
 THE INFORMATION CONTAINED IN THIS DRAWING IS THE SOLE PROPERTY OF ELECTRIC COMMUTER MULTICOPTER TEAM. ANY REPRODUCTION IN PART OR AS A WHOLE WITHOUT THE WRITTEN PERMISSION OF ELECTRIC COMMUTER MULTICOPTER TEAM IS PROHIBITED.

ECM-1-A1-0001	MULTICOPTER ASSY
NEXT ASSY	USED ON
APPLICATION	DO NOT SCALE DRAWING

NAME	DATE
DRAWN BLAKE S.	1/29/15
CHECKED MARLEY	1/30/15
ENG APPR.	
MFG APPR.	
Q.A.	
COMMENTS: BOM SHOWS PARTS FOR ALL 4 ARMS.	

TITLE: ARM ASSEMBLY		
SIZE B	DWG. NO. ECM-1-DA1-0003	REV A
SCALE: 1:10	WEIGHT: 46.4lb	SHEET 1 OF 1

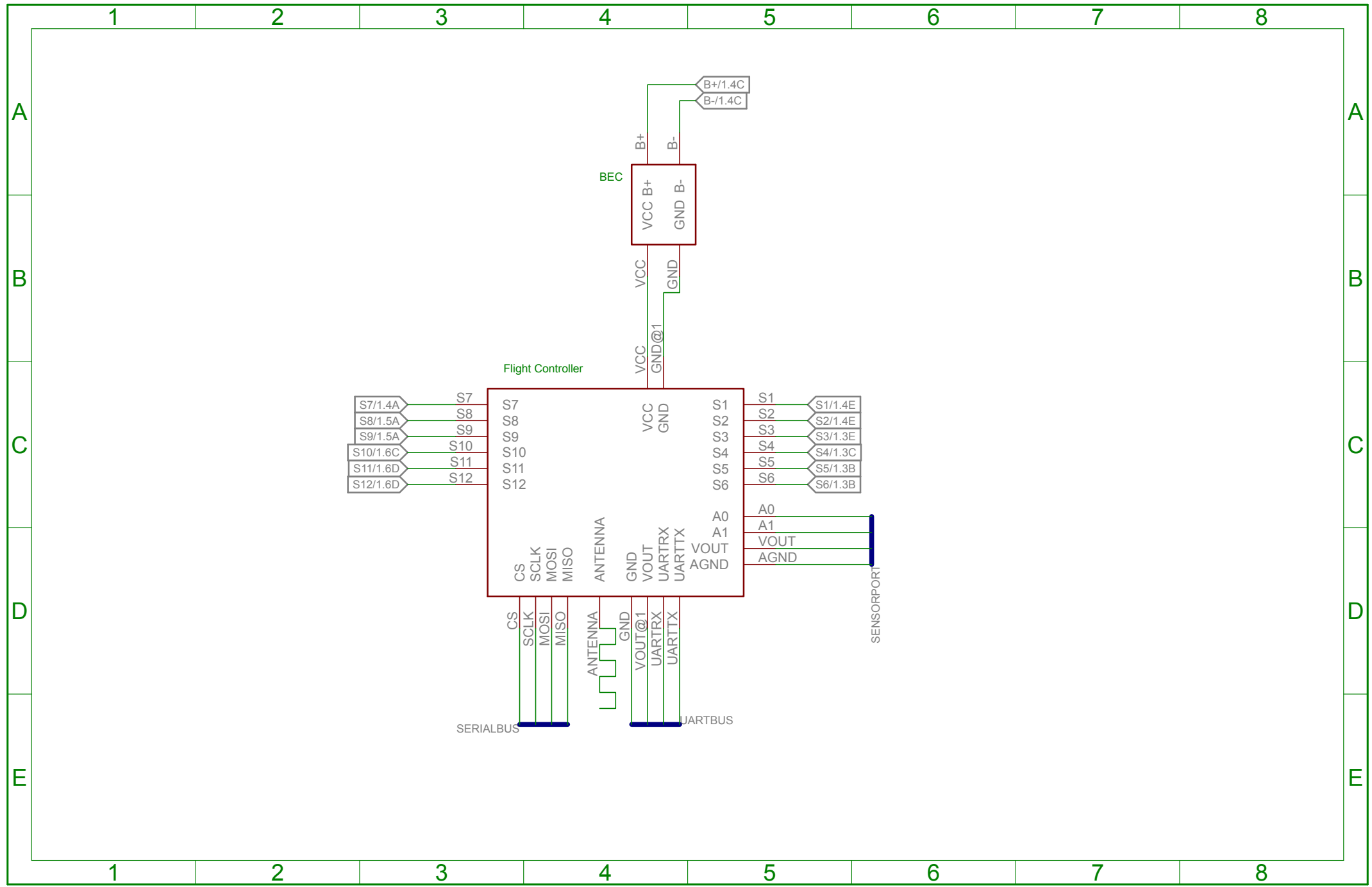


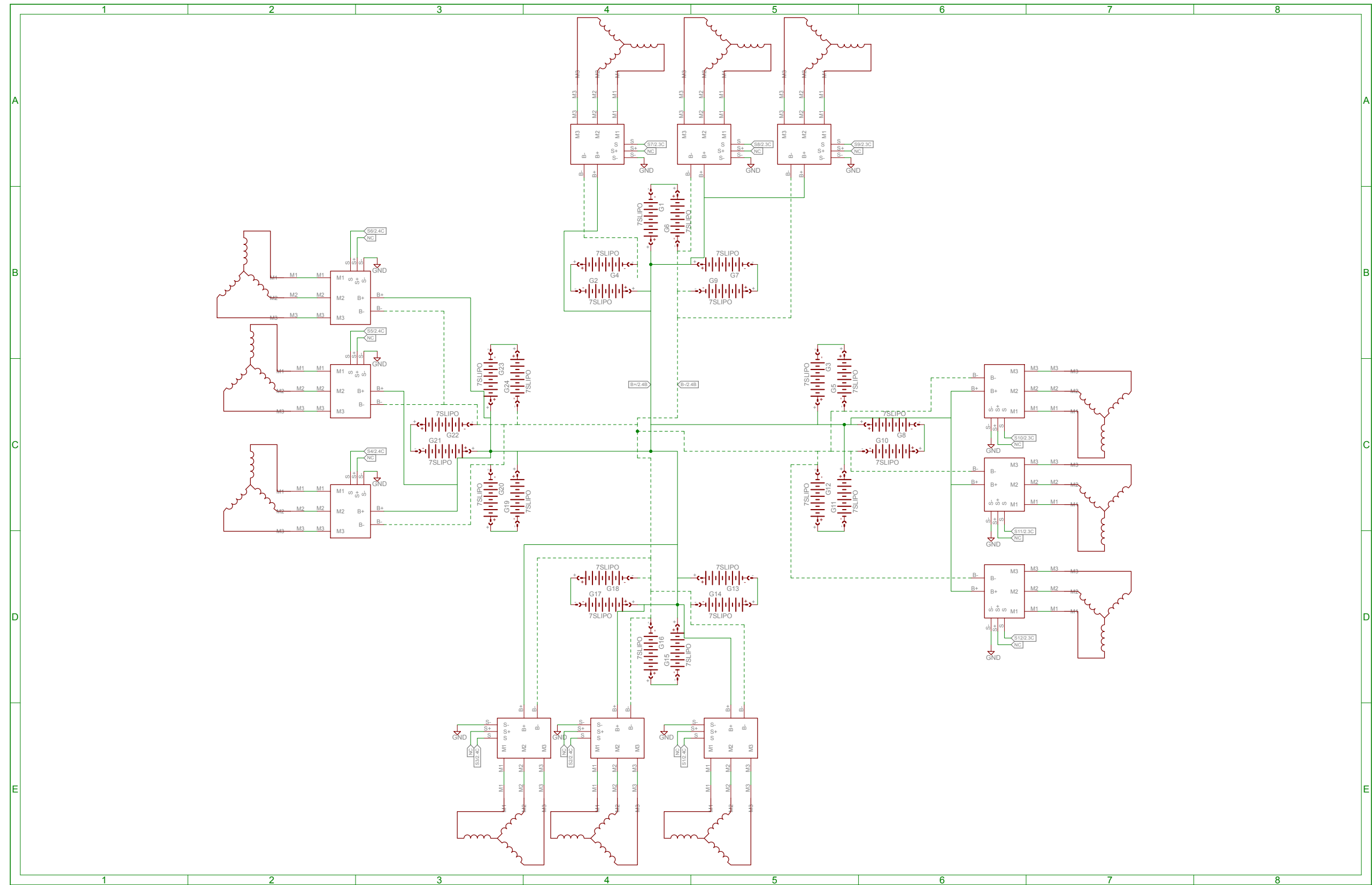
MAJOR VEHICLE COMPONENTS

ITEM NO.	PART NUMBER	DESCRIPTION	QTY.
1	ECM-1-S1-1102	CENTER MOUNT BRACKET	1
2	ECM-1-S0-1001	MAIN ARM	4
3	ECM-1-S1-1204	ARM MOUNT BRACKET	4
4	ECM-1-S0-1002	MOTOR SPAR	12
5	ECM-1-S1-1302	MOTOR MOUNT	12
6	ECM-1-S1-1105	SUMMIT LIGHTWEIGHT SEAT	1
7	ECM-1-P0-1501	JOBY JM1S MOTOR	12
8	ECM-1-S1-1307	PROP RING	12
9	ECM-1-P1-1401	30"X10 CARBON FIBER PROP	12
10	ECM-1-A1-0005	LANDING GEAR ASSEMBLY	5
11	ECM-1-P0-1601	LIPO BATTERY	24

PROPRIETARY AND CONFIDENTIAL
 THE INFORMATION CONTAINED IN THIS DRAWING IS THE SOLE PROPERTY OF THE ELECTRIC COMMUTER MULTICOPTER TEAM. ANY REPRODUCTION IN PART OR AS A WHOLE WITHOUT THE WRITTEN PERMISSION OF THE TEAM IS STRICTLY PROHIBITED.

		NAME	DATE	TITLE: ELECTRIC COMMUTER MULTICOPTER
		DRAWN	BLAKE S. 1/29/15	
		CHECKED	MARLEY 1/30/15	
		ENG APPR.		
		MFG APPR.		
		Q.A.		SIZE DWG. NO. REV B ECM-1-DA1-0001 A
		COMMENTS:		
N/A	N/A			SCALE: 1:16 WEIGHT:254lb SHEET 1 OF
NEXT ASSY	USED ON			
APPLICATION		DO NOT SCALE DRAWING		





Appendix B

Electric Commuter Multicopter

Engineering Analysis and Hand Calculations

APPENDIX B-1

CARBON TUBE DEFLECTION & STRESSES

ECM HAND CALCS

FIND : DEFLECTION/ANGULAR DEFLECTION AT TIP, STRESS (BENDING & TORSIONAL) ON CARBON TUBES UNDER NORMAL OPERATION. (MAX THRUST)

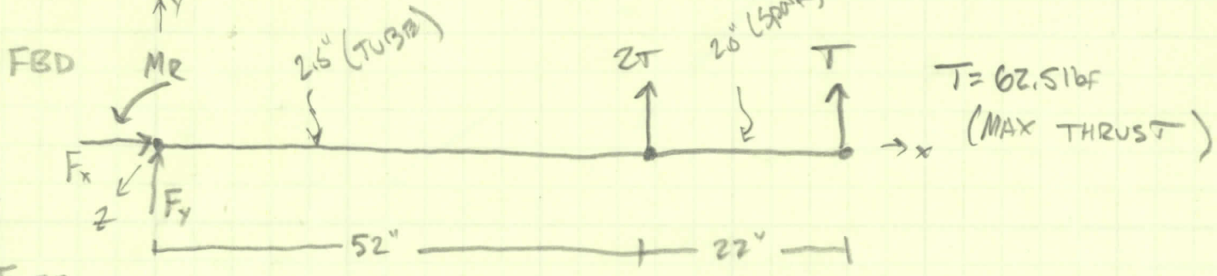
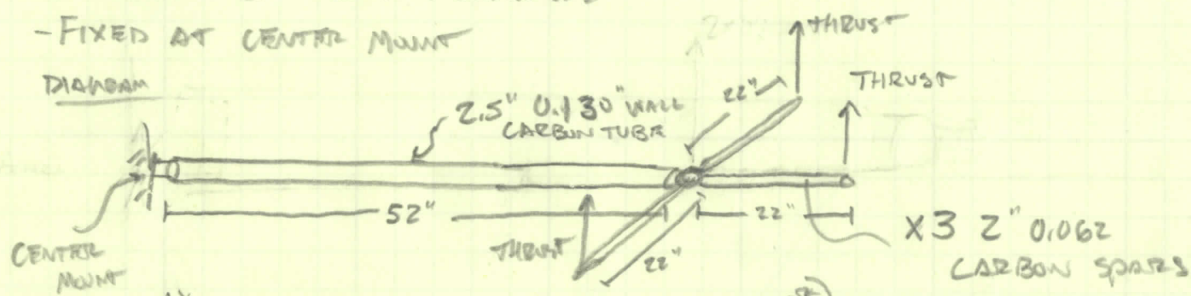
ASSUMPTIONS : - SHEAR STRESS NEG. LL BENDING STRESSES
 - $\sigma_{ULTIMATE} = 100 \text{ ksi}$ (CONSERVATIVE FIGURE PROVIDED BY)
 - $\tau_{ULTIMATE} = 11 \text{ ksi}$ (CONSERVATIVE FIGURE BASED ON TEST RESULTS ON ROUND TUBES IN TORSION FROM REPORTS ONLINE)

MAIN TUBE : 14, 0° plys
 8, 45° plys
 SPAR : 7, 0° plys
 4, 45° plys

- $E_{TUBE} = 18.2 \text{ Msi}$ (PROVIDED BY TUBE MANUFACTURER)
 - DIMENSIONS OF MOUNTS NEGLIGIBLE
 - FIXED AT CENTER MOUNT

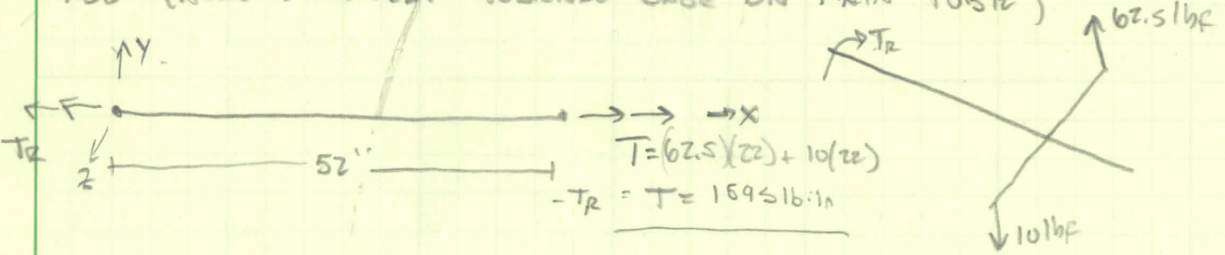
$E_{SPAR} = 14.1 \text{ Msi}$

DIAGRAM



$F_x = 0$
 $F_y = -187.5 \text{ lbf}$
 $MR = -(52)(2T) + 74(T)$
 $MR = -11125 \text{ lb}\cdot\text{in}$

FBD (ASSUME WORST TORSIONAL CASE ON MAIN TUBE)

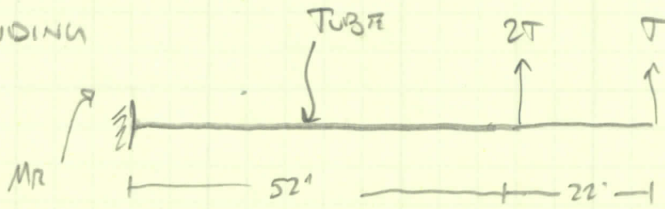


$T = (62.5)(22) + 10(22)$
 $-T_R = T = 1595 \text{ lb}\cdot\text{in}$

42-381 50 SHEETS EYE-EASE® - 5 SQUARES
 42-382 100 SHEETS EYE-EASE® - 5 SQUARES
 42-389 200 SHEETS EYE-EASE® - 5 SQUARES
 National Brand

TUBE - MAX NORMAL OPERATING CONDITION

BENDING



$$T = 62.5 \text{ lb}$$

$$M_R = 11125 \text{ lb}\cdot\text{in} \quad (\text{MAX MOMENT IN TUBE})$$

CALCULATING MAX STRESS IN TUBE DUE TO BENDING

$$\sigma_{\text{MAX}} = \frac{MC}{I}$$

$$M = 11125 \text{ lb}\cdot\text{in}$$

$$C = \frac{D}{2} = \frac{2.5 + (2 \times 0.130)}{2} = 1.38 \text{ in}$$

CALCULATING MOMENT OF INERTIA

$$I = \frac{\pi}{4} (\Gamma_o^4 - \Gamma_i^4) \quad (\text{FOR ROUND TUBES})$$

* FOR BENDING ONLY APPLY 0° PILES TO THICKNESSES IN CALCULATING I *

$$\Gamma_o = 1.38 \text{ in} - 0^\circ \text{ PILES LOCATED USUALLY AT OUTSIDE}$$

$$\Gamma_i = 1.38 - (0.005454(14))$$

$$\Gamma_i = 1.304 \text{ in}$$

$$I = \frac{\pi}{4} (1.38^4 - 1.304^4)$$

$$I = 0.578 \text{ in}^4$$

$$\sigma_{\text{MAX}} = \frac{(11125 \text{ lb}\cdot\text{in})(1.38 \text{ in})}{0.578 \text{ in}^4}$$

$$\sigma_{\text{MAX}} = 26.6 \text{ ksi}$$

$$\text{FACTOR OF SAFETY} = \frac{100}{26.6} = \underline{3.76}$$

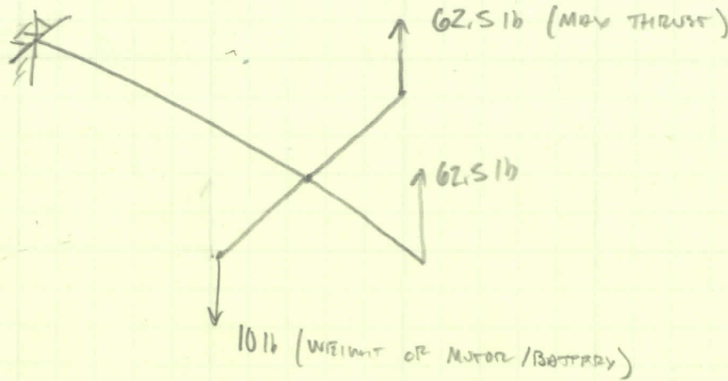
APPENDIX B-1.2

MAIN CARBON TUBE TORSIONAL STRESS

ECM HAND CALCS

TUBE - MAX SHEAR LOAD

ASSUME ONE MOTOR DIES, OPPOSITE MOTOR AT FULL THRUST



MAX TORQUE ON TUBE

$$T = 1595 \text{ lb}\cdot\text{in}$$

CALCULATION MAX TORSIONAL SHEAR STRESS

$$\tau_{\text{max}} = \sqrt{\left(\frac{T \cdot r}{J}\right)^2 + \left(\frac{V}{A}\right)^2}$$

$$T = 1595 \text{ lb}\cdot\text{in}$$

$$r = 1.37 \text{ IN (RADIUS OF MOST OUTER 45° PLY)}$$

$$J = \frac{\pi(D_o^4 - D_i^4)}{32} \quad (\text{ONLY ACCOUNT FOR THICKNESS DUE TO } \pm 45^\circ \text{ PLYS})$$

$$D_o = 2.74 \text{ IN}$$

$$D_i = 2.74 - (6(0.005454)(2))$$

$$D_i = 2.658 \text{ IN}$$

$$J = \frac{\pi(2.74^4 - 2.658^4)}{32}$$

$$A = \pi r_o^2 - \pi r_i^2$$

$$A = 0.1709 \text{ IN}^2$$

$$V = 125 - 10 = 115 \text{ lb}$$

$$J = 0.672 \text{ IN}^4$$

$$\tau_{\text{max}} = \sqrt{\left(\frac{1595 \text{ lb}\cdot\text{in} \cdot (1.37 \text{ IN})}{0.672 \text{ IN}^4}\right)^2 + \left(\frac{115 \text{ lb}}{0.1709 \text{ IN}^2}\right)^2}$$

$$\tau_{\text{max}} = 3.25 \text{ KSI}$$

$$\text{FACTOR OF SAFETY} = \frac{11}{3.25} = 3.38$$

$$\tau_{\text{max}} \text{ FOR } 2.5'' \times 0.064'' \text{ WALL} = 6.9 \text{ KSI}$$

THIS WAS THE

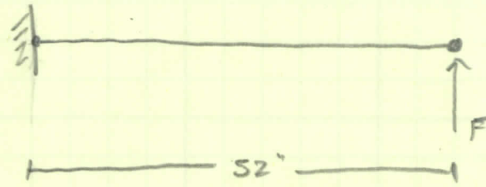
$$F.S. = 1.6$$

ORIGINAL TUBE THAT WAS PICKED FOR THE MAIN TUBE

MAIN CARBON TUBE STRENGTH, USED TO ESTIMATE MAX LANDING SPEED

WORST LANDING CASE FOR CARBON TUBES

→ CRAFT LANDS WITH NO LATERAL MOVEMENT BUT WITH AN ANGULAR VELOCITY OR DISPLACEMENT (ONE LANDING WHEEL HAS GROUND FIRST WHILE THE REST OF AIRCRAFT IS STILL AIRBORNE)



MAX ALLOWABLE STRESS

$$\sigma_{allow} = 100 \text{ ksi}$$

FIND ULTIMATE LANDING FORCE

$$\sigma_{allow} = \frac{Mc}{I}$$

$$I = 0.576 \text{ in}^4 \text{ (ONLY } 0' \text{ PLAYS FOR BENDING)}$$

$$c = 1.30 \text{ in} \quad I, c \text{ VALUES CALCULATED EARLIER}$$

$$100,000 \frac{\text{lb}}{\text{in}^2} = \frac{52 \text{ in} (F) (1.30 \text{ in})}{0.576 \text{ in}^4}$$

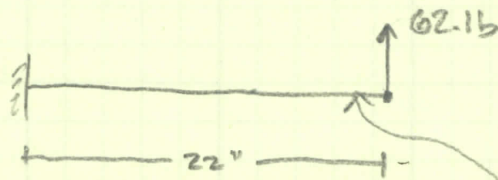
$$F_{max} = 805 \text{ lbs}$$

→ Apply 1.2 Factor of Safety

$$F_{allowable} = 670 \text{ lb}$$

↖ MAX LANDING FORCE (CARBON TUBE) WILL BE DICTATED FOR

SPAR - MAX BENDING STRESS AT MAX OPERATING CONDITION (MAX THRUST)



$$M = (22 \text{ in})(62.15)$$

$$M = 1375 \text{ lb}\cdot\text{in}$$

CARBON SPAR 2.0" ID 2.125" OD

WALL = 0.062"

↑ MANUFACTURED SPAC

MAX STRESS

$$\sigma = \frac{Mc}{I}$$

$$c = r_o = \frac{OD}{2} = \frac{2.125}{2} = 1.0625 \text{ in}$$

$$\sigma_{\text{max}} = \frac{(1375 \text{ lb}\cdot\text{in})(1.0625 \text{ in})}{0.13629 \text{ in}^4}$$

$$\rightarrow \sigma_{\text{max}} = 10.7 \text{ ksi}$$

↓ ONLY THICKNESS OF 0° PLYS ↓

$$I_{\text{SPAR}} = \frac{\pi}{4} (r_o^4 - r_i^4) \quad r_o = 1.0625 - (7/0.005454)$$

$$= \frac{\pi}{4} (1.0625^4 - 1.0243^4)$$

$$I_{\text{SPAR}} = 0.13629 \text{ in}^4$$

$$r_i = 1.0625 - 0.032170$$

$$\text{FACTOR OF SAFETY} = \frac{100 \text{ ksi}}{10.7 \text{ ksi}}$$

$$\rightarrow \text{F.O.S.} = 9.33$$

CALCULATING MAX ALLOWABLE FORCE AT TIP OF SPAR

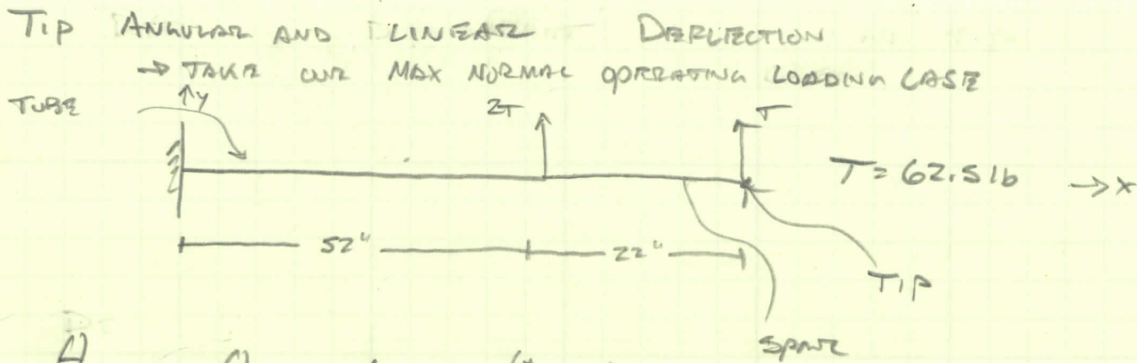
$$\sigma_{\text{STRENGTH}} = 100 \text{ ksi}$$

$$100,000 = \frac{(22 \text{ in})F(1.0625 \text{ in})}{0.13629 \text{ in}^4}$$

$$F_{\text{MAX}} = 583 \text{ lb}$$

Apply 1.2 Factor of Safety

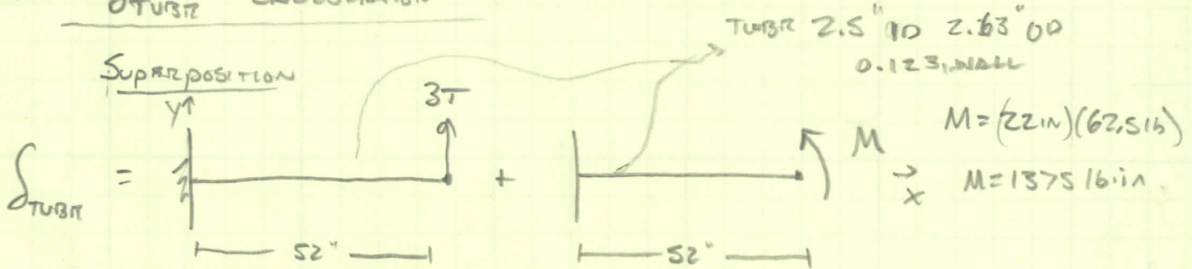
$$\rightarrow F_{\text{ALLOWABLE}} = 485 \text{ lb}$$



$$\theta_{TOTAL} = \theta_{TUBE} + \theta_{SPAC} \quad (\text{ANGULAR})$$

$$\delta_{TOTAL} = \delta_{TUBE} + \delta_{SPAC} + L_{SPAC}(\theta_{TUBE}) \quad \begin{matrix} \text{IN [RAD]} \\ \text{IN [RAD]} \end{matrix}$$

→ δ_{TUBE} CALCULATION



$$\delta_{TUBE} = \frac{(3T)(L)^3}{3EI} + \frac{ML^2}{2EI} \quad (\text{BEAM DEFL}) \quad I = 0.578\text{IN}^4 \quad (\text{ONLY } I_x \text{ FOR BENDING})$$

$$\delta_{TUBE} = \frac{(3)(62.5\text{LB})(52\text{IN})^3}{3(18.2\text{E}6 \frac{\text{LB}}{\text{IN}^2})(0.578\text{IN}^4)} + \frac{(1375\text{LB}\cdot\text{IN})(52\text{IN})^2}{2(18.2\text{E}6 \frac{\text{LB}}{\text{IN}^2})(0.578\text{IN}^4)}$$

$$\delta_{TUBE} = 0.835\text{IN} + 0.177\text{IN}$$

$$\delta_{TUBE} = 1.01\text{IN}$$

→ θ_{TUBE} CALCULATION

SAME SUPERPOSITION

$$\theta_{TUBE} = \frac{(3T)L^2}{2EI} + \frac{ML}{EI}$$

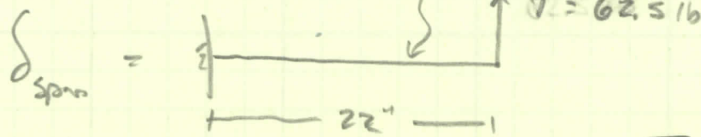
$$\theta_{TUBE} = \frac{3(62.5\text{LB})(52\text{IN})^2}{2(18.2\text{E}6 \frac{\text{LB}}{\text{IN}^2})(0.578\text{IN}^4)} + \frac{(1375\text{LB}\cdot\text{IN})(52\text{IN})}{(18.2\text{E}6 \frac{\text{LB}}{\text{IN}^2})(0.578\text{IN}^4)}$$

$$\theta_{TUBE} = 0.02409\text{rad} + 0.00678\text{rad}$$

$$\theta_{TUBE} = 0.03087\text{rad} \left(\frac{180^\circ}{\pi\text{rad}} \right) = 1.77^\circ$$

δ_{spar} CALCULATION

2.0" ID 2.125" OD



$$\delta_{\text{spar}} = \frac{(T)(22)^3}{3EI}$$

 $I = 0.13629 \text{ in}^4$ (ONLY 0° PLYS FOR BENDING)

$$\delta_{\text{spar}} = \frac{(62.5 \text{ lb})(22 \text{ in})^3}{3(19.1 \text{E}6 \frac{\text{lb}}{\text{in}^2})(0.13629 \text{ in}^4)}$$

$$\rightarrow \delta_{\text{spar}} = 0.0852 \text{ IN}$$

 θ_{spar} CALCULATION

$$\theta_{\text{spar}} = \frac{(T)(22 \text{ in})^2}{2EI}$$

$$\theta_{\text{spar}} = \frac{(62.5 \text{ lb})(22 \text{ in})^2}{2(19.1 \text{E}6 \frac{\text{lb}}{\text{in}^2})(0.13629 \text{ in}^4)}$$

$$\rightarrow \theta_{\text{spar}} = 0.00581 \text{ rad} \left(\frac{180^\circ}{\pi \text{ rad}} \right) = 0.333^\circ$$

CALCULATING TOTAL LINEAR DEFLECTION AT TIP

$$\delta_{\text{TOTAL}} = \delta_{\text{TUBE}} + \delta_{\text{spar}} + L_{\text{spar}}(\theta_{\text{TUBE}})$$

$$\delta_{\text{TOTAL}} = 1.01 \text{ IN} + 0.0852 \text{ IN} + (22 \text{ IN})(0.03041 \text{ rad})$$

$$\rightarrow \delta_{\text{TOTAL}} = 1.78 \text{ IN}$$

CALCULATING TOTAL ANGULAR DEFLECTION AT TIP

$$\theta_{\text{TOTAL}} = \theta_{\text{TUBE}} + \theta_{\text{spar}}$$

$$\theta_{\text{TOTAL}} = 1.77^\circ + 0.333^\circ$$

$$\rightarrow \theta_{\text{TOTAL}} = 2.10^\circ$$

STEEL TUBE SELECTION CALCSA130 CHROMOLY STEELANNEALED PROPERTIES: $S_{ut} = 80 \text{ ksi}$, $S_y = 50 \text{ ksi}$

$$S_e' \approx 40 \text{ ksi}$$

$$S_e = K_a K_b K_c K_d K_e S_e'$$

$$S_e = (0.8151)(0.9212)(0.868)(40 \text{ ksi}) = 27.04 \text{ ksi}$$

$$W/n = 1.2 \rightarrow S_e = 22.53 \text{ ksi}$$

LARGE TUBING: $ID = 2.124''$, $OD = 2.500''$

$$I_x = \frac{\pi}{4} \left(\left(\frac{2.5''}{2} \right)^4 - \left(\frac{2.124''}{2} \right)^4 \right) = 0.9184 \text{ in}^4$$

$$\sigma_{max} = \frac{M_y}{I} = \frac{(14040 \text{ lbf-in})(1.25 \text{ in})}{(0.9184 \text{ in}^4)} = 19109 \text{ psi} \quad (\text{LANDING LOADS})$$

$$n = \frac{27.04 \text{ ksi}}{19.09 \text{ ksi}} = 1.415 > 1.2 \checkmark \rightarrow \text{LARGE TUBING SHOULD WORK}$$

SMALL TUBING: $ID = 1.870''$, $OD = 2.000''$

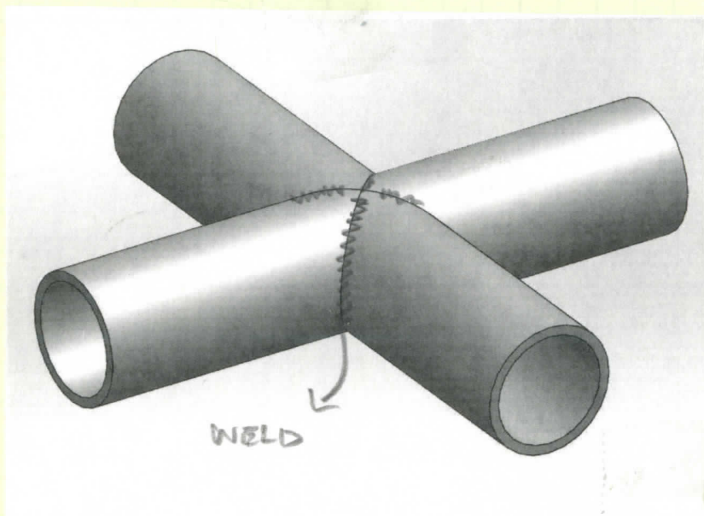
$$I_x = \frac{\pi}{4} \left(\left(\frac{2.000''}{2} \right)^4 - \left(\frac{1.870''}{2} \right)^4 \right) = 0.1851 \text{ in}^4$$

$$\sigma_{max} = \frac{(1375 \text{ lbf-in})(1 \text{ in})}{(0.1851 \text{ in}^4)} = 7428 \text{ psi} \quad (\text{HOVERING LOADS})$$

$$n = \frac{27.04 \text{ ksi}}{7.428 \text{ ksi}} = 3.640 > 1.2 \checkmark \rightarrow \text{SMALL TUBING SHOULD WORK}$$

THERE FOR, WE WILL USE 2.500" OD x 2.124" ID
AND 2.000" OD x 1.870" ID TUBING.

FIND: STRESS IN WELDS IN THE CENTER MOUNT
UNDER MAX NORMAL OPERATING LOADING



TUBES: 2.496" OD
2.124" ID
0.181" WALL
4130 CARBON STEEL

- 9.56" OF WELD LENGTH

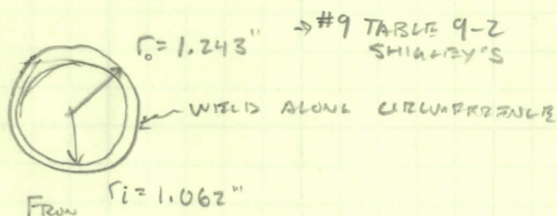
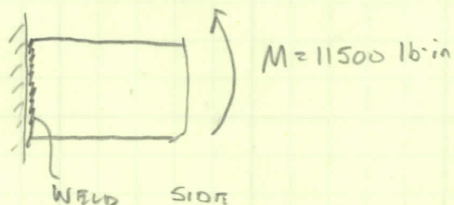
- FOR WELDS JOINING MATERIAL
LESS THAN 1/4" ASSUME
WELD SIZE (THROAT)
OF 1/8" (0.125")

- SHEAR NOT DUE TO BENDING
NEGLECTABLE

→ NO STANDARD MODEL TO FIND STRESS IN WELDS BETWEEN
MITERED TUBES.

CALCULATED USING FIVE STANDARD MODEL TO ESTIMATE THE
STRESS IN THE WELD

MODEL 1 ASSUME WELD AREA IS A FLAT TUBE IN BENDING



$$\sigma = \frac{MC}{I} \quad (\text{pg 487 SHIGLEY'S})$$

M = 11500 lb-in, SAME MOMENT
CARBON TUBE EXPERIENCES UNDER
THIS LOADING CONDITION

$$I = 0.707 h I_w \quad (\text{pg 487})$$

h = WELD THROAT

I_w CALCULATED USING SHIGLEY'S TABLE 9-2 pg 496

$$I_{w, \text{rect}} = \pi r^3 \quad \rightarrow \quad I = 0.707 (0.125 \text{ in}) (\pi (1.243 \text{ in})^3)$$

$$I_w = \pi (1.243)^3 \quad I = 0.533 \text{ in}^4$$

$$\sigma_1 = \frac{(11500 \text{ lb-in})(1.243 \text{ in})}{0.533 \text{ in}^4}$$

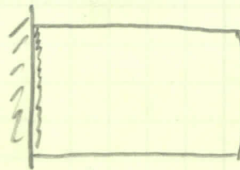
$$\sigma_1 = 26.8 \text{ ksi} \quad (\text{FAILURE USING E60, E70, \& E80 ELECTRODES})$$

THIS MODEL IS EXTREMELY CONSERVATIVE, IT DOES NOT ACCOUNT
FOR THE INCREASED WELD LENGTH DUE TO THE MITER.

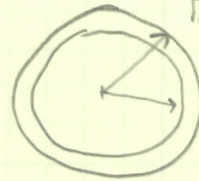
WE CAN ASSUME THE MITERED TUBE WELD HAS LESS STRESS THAN THIS.

MODEL 2

USE SAME CIRCLE MODEL, EXCEPT RADIUS OF CIRCLE IS INCREASED TO ACCOUNT FOR ACTUAL WELD LENGTH. ASSUME CIRCUMFERENCE = WELD LENGTH.



$M = 11500 \text{ lb}\cdot\text{in}$



$r_o = \frac{9.56}{2\pi} = 1.52 \text{ in}$

$r_i = 1.339 \text{ in}$

$\tau_2 = \frac{M r}{I}$

$I = \pi r^3 = \pi (1.52^3)$

$I = 0.707 (1.125 \text{ in}) (\pi (1.52 \text{ in}^3))$

$I = 0.975 \text{ in}^4$

$\tau_2 = \frac{(11500 \text{ lb}\cdot\text{in})(1.52 \text{ in})}{0.975 \text{ in}^4}$

$\tau_2 = 17.9 \text{ ksi}$

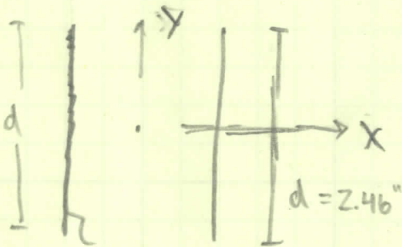
THIS MODEL SHOULD BE CLOSE TO OTHER ACTUAL WELD

ELECTRODE	E60	E70	E80
FACTORS OF SAFETY	1.006	1.173	1.34

MODEL 3

USING A PARALLEL LINE WELD MODEL # 2 TABLE 9-2 SHILLEY'S

FOR THIS MODEL THE OUTER DIAMETER IS THE HEIGHT OF LINES



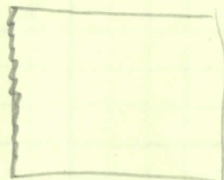
WELDS

$\tau_3 = \frac{M c}{I}$

$I = \frac{d^3}{3}$

$I = 0.707 (1.125 \text{ in}) \left(\frac{2.496 \text{ in}^3}{3} \right)$

$I = 0.4526 \text{ in}^4$



$M = 11500 \text{ lb}\cdot\text{in}$

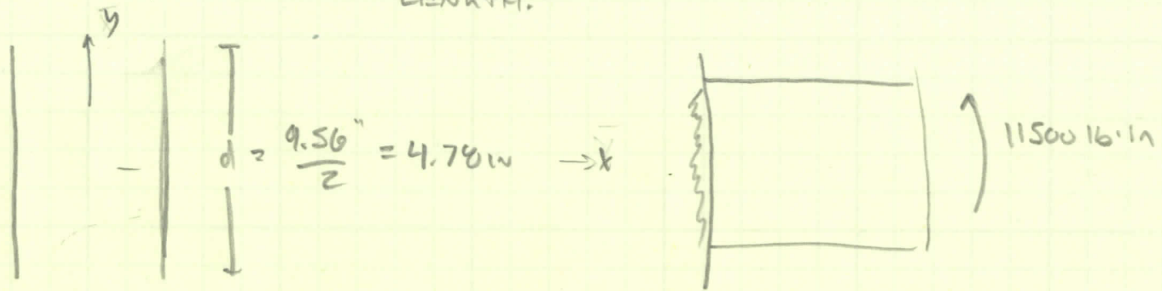
$\tau_2 = \frac{(11500 \text{ lb}\cdot\text{in})(1.243 \text{ in})}{0.4526 \text{ in}^4}$

$\tau_2 = 31.6 \text{ ksi}$

FAILURE W/ E60, E70, E80

THIS MODEL IS ALSO EXTREMELY CONSERVATIVE AS THE TOTAL WELD LENGTH IS ONLY 4.9 IN AS OPPOSED TO THE ACTUAL 9.56 IN.

MODEL 4 SAME PARALLEL LINE MODEL BUT USING
 $d = \frac{9.56}{2}$, ACCOUNTING FOR THE ENTIRE WELD
 LENGTH.



$$\tau_4 = \frac{Mc}{I}$$

$$\tau_4 = \frac{(11500 \text{ lb-in})(2.435 \text{ in})}{3.217 \text{ in}^4} = 8.7 \text{ ksi}$$

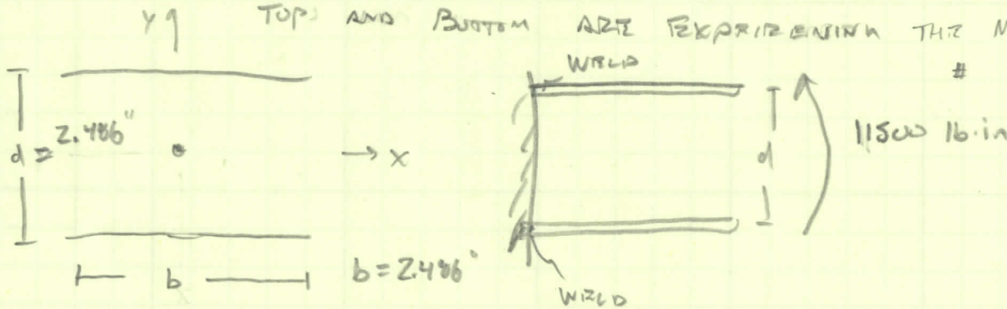
$$I_{u4} = \frac{bd^3}{3}$$

$$I = 0.707(0.125 \text{ in}) \left(\frac{4.76}{3} \right)^3$$

$$I = 3.217 \text{ in}^4$$

THIS WOULD BE A BEST CASE
 MODEL BUT ALLOWS US TO CREATE
 A RANGE THAT OUR WELD FALLS WITHIN

MODEL 5 PARALLEL LINE MODEL BUT BENDING ABOUT A
 DIFFERENT AXIS, AS IN THE ACTUAL WELD THE
 TOP AND BOTTOM ARE EXPERIENCING THE MOST STRESS



$$\tau_5 = \frac{Mc}{I}$$

$$\tau_5 = \frac{(11500 \text{ lb-in})(1.243 \text{ in})}{0.679 \text{ in}^4}$$

$$I_{u5} = \frac{bd^2}{2}$$

$$I = 0.707(0.125 \text{ in}) \left(\frac{2.406 \text{ in} \times (2.406 \text{ in})}{2} \right)$$

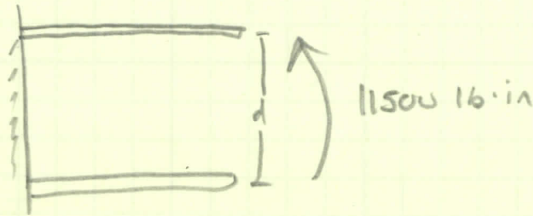
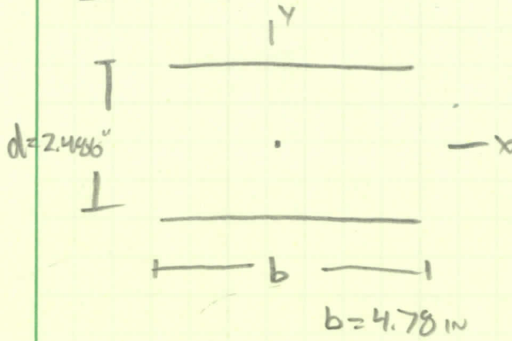
$$I = 0.679 \text{ in}^4$$

$$\tau_5 = 21.1 \text{ ksi}$$

THIS IS AGAIN CONSERVATIVE BUT
 BY ONLY USING 4.972 IN OF WELD
 LENGTH. HOWEVER, PROBABLY FAIRLY
 ACCURATE SINCE THIS MODEL WITH
 THE TWO PARALLEL PLATES HAS
 THE BEST ABILITY TO RESIST BENDING.

ELECTRODE	E60	E70	E80
FACTOR OF SAFETY	0	0	1.14

MODEL 6 SAME AS MODEL 5, BUT USING ACTUAL WELD LENGTH



$$I_{u_b} = \frac{bd^2}{2}$$

$$I = 0.707(0.125 \text{ in}) \left(\frac{4.78(2.446)^2}{2} \right)$$

$$I = 1.305 \text{ in}^4$$

$$\tau_b = \frac{(11500 \text{ lb-in})(1.243 \text{ in})}{1.305 \text{ in}^4}$$

$$\tau_b = 11.0 \text{ ksi}$$

AGAIN WOULD BE CONSIDERED A BEST CASE BUT DOES HELP NARROW THE RANGE

DETERMINING STRESS IN WELD FROM MODELS

MODEL 2 & 5 REPRESENT THE WELD MOST CLOSELY THE ACTUAL WELD SHOULD NOT HAVE LESS STRESS THAN MODEL 2 AND SHOULDN'T HAVE MORE THAN MODEL 5.

FROM THIS THE ESTIMATED STRESS IN THE WELDS UNDER MAX NORMAL LOADING IS

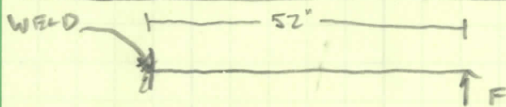
$$\tau_{\text{WELD}} \approx 20 \text{ ksi}$$

GIVEN THE FACTOR OF SAFETY FOR THE CRAFT AN E80 ELECTRODE MUST BE USED.

$\tau_{\text{MAX E80}} = 24.0 \text{ ksi}$ ← DEFINED IN BOOK AND HAS A BUILT IN FACTOR OF SAFETY OF 1.44

$$\text{FACTOR OF SAFETY} = \frac{24}{20} = 1.2$$

MAX ALLOWED FORCE AT LANDING POINT FOR WELD



$$I = \frac{I_z + I_y}{2} = \frac{0.975 + 0.679}{2} = 0.827$$

$$\tau = \frac{Mc}{I} = (1.243 \text{ in})$$

$$F_{\text{MAX ALLOWABLE}} = 256 \text{ lbs}$$

$$20,000 = \frac{(52 \text{ in})(F)(1.243 \text{ in})}{0.827 \text{ in}^4}$$

FIND: FATIGUE STRENGTH IN CENTER JOINT WELD

$$\tau_{weld} = 20 \text{ ksi (UNDER MAX NORMAL CONDITION)}$$

FOR E80 ELECTRODE $S_{UT} = 80 \text{ ksi}$

$$K_{FS} = 1.25 \text{ (FROM SHIPLEY'S TABLE 9-5 PG 490)}$$

→ MOST STRESS IN WELD DUE TO A BENDING MOMENT IS OCCURRING AT THE TOP AND BOTTOM OF JOINT WHERE IT IS A BUTT WELD, HOWEVER A FILLET BEINGS ON THE SIDES, BUT THEY ARE ON THE NEUTRAL AXIS WHERE THERE IS LITTLE TO NO STRESS.

$$K_a = 1.347 (80 \text{ ksi})^{-0.085} = 0.923$$

TABLE 6-2 PG 288, GROUNDED

$$K_b = 0.91 (2.486 \text{ in})^{-0.157} = 0.789 \text{ FROM (6-20) PG 288}$$

$$K_c = 1 \quad K_e = 0.897$$

$$K_d = 1 \quad K_f = 1$$

$$S_{sc} = (0.923)(0.789)(1)(1)(0.897)(0.5)(80)$$

$$\rightarrow S_{sc} = 26.1 \text{ ksi}$$

$$\tau'_{allow} = K_{FS} \tau_{weld} = 1.25(20)$$

$$\rightarrow \tau'_{allow} = 25 \text{ ksi}$$

(FOR INFINITE LIFE)

$$\text{Factor of Safety} = \frac{26.1}{25} = 1.044$$

FOR WELD MEETING INFINITE FATIGUE LIFE

DOES NOT MEET PROJECT'S FOS OF 1.2

WITH E90XX ELECTRODE

$$S_{sc} = (0.923)(0.789)(1)(1)(0.897)(0.5)90$$

$$S_{sc} = 29.4 \text{ ksi}$$

$$F.S. = \frac{29.4}{25} = 1.18 \neq 1.2$$

→ E90 ELECTRODE NECESSARY TO MEET

WITH E100X ELECTRODE

$$S_{sc} = 32.7$$

$$F.S. = \frac{32.7}{25} = 1.31 \checkmark$$

TO MEET INFINITE LIFE A E100X

ELECTRODE IS NEEDED, OR WELD SIZE INCREASED. EITHER FOR A WAY TO USE A E60, E70, E80, E90 ELECTRODE, WELD STRESS NEEDS TO

BE DECREASED OR RELIABILITY IS LOWERED.

Motor Mount Wall page 1FIND

- 1) • Calculate the Per for buckling in the bracket walls
- 2) • Calculate stresses τ_{weld} in weld at top of wall to hemispherical platform

Assume

- 1) a • Most critical area to analyze is the skeletonized cross section due to less material
- 2) • Weld bead at bottom of motor mount wall to motor mount is negligible b/c it only experiences shear. The top hemispherical platform connected to the vertical wall experiences bending in addition to shear. Therefore analyze this

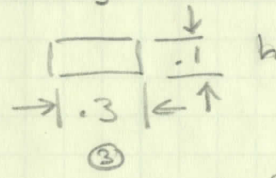
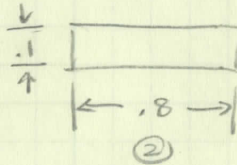
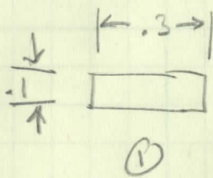
ANALYSISBuckling

$$P_{cr} = \frac{C\pi^2 EI}{L^2}$$

$$C = 1.2$$

$$E = 30 \times 10^6 \text{ psi}$$

$$I = I_1 + I_2 + I_3$$



$$I_1 = I_3 = \frac{bh^3}{12}$$

$$= \frac{(0.3)(0.1)^3}{12}$$

$$= 2.5 \times 10^{-5} \text{ in}^4$$

$$I_2 = \frac{bh^3}{12}$$

$$= \frac{(0.8)(0.1)^3}{12}$$

$$= 6.667 \times 10^{-5} \text{ in}^4$$

$$I = (2.5 \times 10^{-5} \text{ in}^4) \times 2 + 6.667 \times 10^{-5} \text{ in}^4$$

$$I = 1.167 \times 10^{-4} \text{ in}^4$$

$$P_{cr} = \frac{(1.2)(\pi^2)(30 \times 10^6 \text{ psi})(1.167 \times 10^{-4} \text{ in}^4)}{(1.2 \text{ in})^2}$$

$$= 28.8 \text{ kip} \leftarrow \text{this is the force to buckle one bracket over designed} = \text{good}$$

MOTOR MOUNT WALL

page 2

$$\tau_{\text{weld}} = \tau' + \tau''$$

$$\tau = \frac{V}{A} \quad \tau'' = \frac{Mc}{I}$$

$$\tau'' = \frac{Mc}{I}$$

$$M_1 = M_3 = \left(\frac{62.5}{6}\right)(.22 \text{ in})$$

$$= 2.29 \text{ lbf-in}$$

$$M_2 = \left(\frac{62.5 \text{ lbf}}{6}\right)(.96 \text{ in})$$

$$= 10 \text{ lbf-in} \rightarrow M = (2.29 \text{ lbf-in}) \times 2 + 10 \text{ lbf-in} = 14.58 \text{ lbf-in}$$

$c = .96 \text{ in} \leftarrow$ will take the largest distance for design purposes

$$I = .707 h I_0$$

$$I_0 = \frac{d^3}{12}$$

$$= \frac{(3.75 \text{ in})^3}{12} = 4.39 \text{ in}^3$$

$$h = .125 \text{ in}$$

$$I = .707 (.125 \text{ in})(4.39 \text{ in}^3)$$

$$= .388 \text{ in}^4$$

$$\tau'' = \frac{(14.58 \text{ lbf-in})(.96 \text{ in})}{.388 \text{ in}^4}$$

$$= 36 \text{ psi}$$

This is a negligible value for bending, and shear will be smaller in value therefore this will not fail.

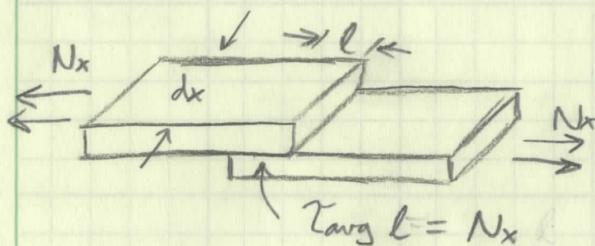
In addition, since this weld will not fail it

is safe to conclude our assumption the bead at the bottom of the bracket attached to the motor mount will not fail as well.

BOND LENGTH CALCULATIONS

LINE LOAD ON TUBE: $N_x = \frac{My}{\pi r^3}$

$$N_{x_{max}} = \frac{M}{\pi r^2}$$



$\tau_{avg} \approx 1000 - 4000$ PSI
 \rightarrow WE WILL USE $\tau_{avg} = 1000$ PSI

$$\tau_{avg} l = N_x = \frac{M}{\pi r^2}$$

$$l = \frac{M}{\tau_{avg} \pi r^2} \rightarrow \text{REQUIRED BOND LENGTH}$$

LARGE TUBES: $M = 11125$ lbf-in (HOVERING)

$$l = \frac{11125 \text{ lbf-in}}{(1000 \text{ PSI})(\pi)(1.25 \text{ in})^2} = 2.266 \text{ in}$$

WE DECIDED ON $l \approx 1.5 \cdot ID \approx 4$ in OF OVERLAP

$$n = \frac{4 \text{ in}}{2.266 \text{ in}} = 1.765 > 1.2$$

$M = 14040$ lbf-in (LANDING)

$$l = \frac{14040 \text{ lbf-in}}{(1000 \text{ PSI})(\pi)(1.25 \text{ in})^2} = 2.860 \text{ in}$$

$$n = \frac{4 \text{ in}}{2.860 \text{ in}} = 1.399 > 1.2 \rightarrow 4" \text{ OVERLAP SHOULD BE OKAY}$$

BOND LENGTH CALCULATIONSSMALL TUBES

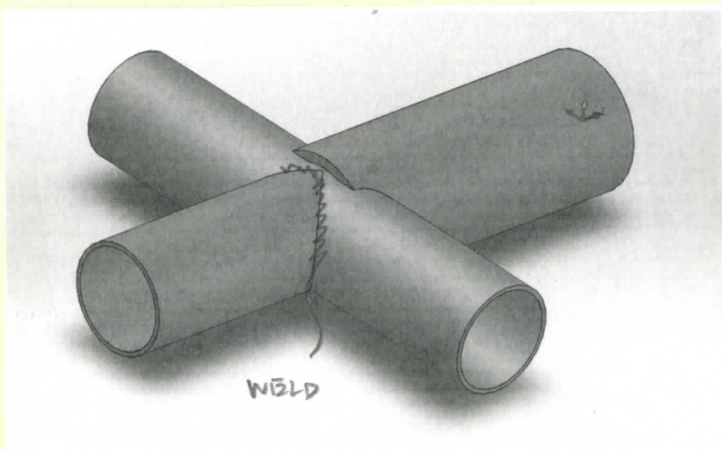
$$M = 1375 \text{ lbf-in (HOVERING)}$$

$$l = \frac{1375 \text{ lbf-in}}{(1000 \text{ PSI}) \pi (1.00 \text{ in})^2} = 0.438 \text{ in}$$

WE SELECTED $l = 3 \text{ in} \approx 1.5 \cdot \text{ID}$

$$n = 6.854 > 1.2 \checkmark \rightarrow 3'' \text{ OVERLAP SHOULD BE FINE}$$

FIND: STRESS IN WELDS IN THE ARM MOUNTS UNDER MAX NORMAL OPERATING LOADING.



TUBES: 1.906" OD
1.970" ID
0.058 WALL

- 7.64" OF WELD LENGTH

- ASSUME 1/8" WELD SIZE

- SUBSTR NEGLIGIBLE NOT DUE TO BENDING

→ LIKE CENTER MOUNT WILL USE THE TWO MOST ACCURATE MODELS.

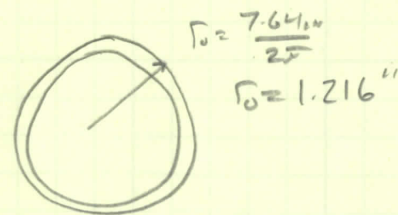
MODEL 1 ASSUME FLAT TUBE IN BENDING W/ CIRCUMFERENCE EQUAL TO WELD LENGTH.



$$M = (22') (62.514)$$

$$M = 137516 \text{ in}$$

$$h = 0.125 \text{ in}$$



$$\sigma = \frac{Mc}{I}$$

$$I_0 = \pi r^3 = \pi (1.216^3)$$

$$I_2 = 0.707 h I_0 \quad (\pi (1.216^3))$$

$$I = 0.707 (0.125 \text{ in}) (\pi (1.216^3))$$

$$I = 0.500 \text{ in}^4$$

$$\sigma = \frac{(137516 \text{ in}) (1.216 \text{ in})}{0.500 \text{ in}^4}$$

$$\sigma = 3.34 \text{ ksi}$$

$$\sigma_{allow} = 18.0 \text{ ksi}$$

E60XX

→ F.S. OF 5.38 W/ E60XX ELECTRODE

→ NO FURTHER ANALYSIS REQUIRED
FACTOR OF SAFETY OF 1.2 IS ALL REACHED IN EXCESS.

→ BASED ON ANALYSIS OF CENTER MOUNT WELDS INFINITE LIFE WILL ALSO BE MET FOR THIS WELD

Weld Stress for Ring Spar - page 1

FIND τ_{weld} ANALYSIS

pg 489 in Shigley

$$\tau_{\text{weld}} = \tau' + \tau''$$

$$\tau' = \frac{V}{A} \quad ; \quad \tau'' = \frac{Mc}{I}$$

$$\tau'' = \frac{(12.675 \text{ lbf-in})(.25 \text{ in})}{I}$$

$$I = 0.707hI_0$$

$$\begin{aligned} I_0 &= \pi r^3 \quad \text{for circular geometry} \\ &= \pi (.25)^3 \\ &= 0.0491 \text{ in}^3 \end{aligned}$$

$h = .125''$ for thickness less than .25''

$$I = .00434 \text{ in}^4$$

$$\tau'' = \frac{(12.675 \text{ lbf-in})(.25 \text{ in})}{.00434 \text{ in}^4}$$

$$\tau'' = 730.26$$

$$\begin{aligned} \tau' &= \frac{V}{A} \quad ; \quad A = 1.414 \pi h r \\ &= \frac{.78 \text{ lbf}}{.13882 \text{ in}^2} \\ &= 5.618 \end{aligned}$$

$$\begin{aligned} \tau_{\text{weld}} &= 730.26 + 5.618 \\ &= 735.88 \text{ psi} \end{aligned}$$

According to Shigley, τ_{weld} cannot exceed corresponding weld material stress which is 24 ksi due to other design parameters of other components, using the same welding material will reduce cost.

Stresses in Shroud spar page 1Find

- Stresses at end of beam
- Will it fail?

 τ_{max} BendingASSUME

- $a = 1.2g$
- neglect torsion
- weight of the spar is negligible
- prop ring weight held by two supports.

ANALYSIS τ_{max} for hollow tube, by Shirley Table 3-2

$$\tau_{max} = \frac{ZV}{A}$$

$$V = F_{tot} = F_{ring} + F_{ringmount}$$

$$F_{ring} = \frac{(1.00 \frac{lbm}{2})(1.2)(32.174 \frac{ft}{s^2})}{32.174 \frac{lbm \cdot ft}{s^2}}$$

1 lbf

$$F_{ring} = .6 \text{ lbf}$$

$$F_{ringmount} = \frac{(.15 \text{ lbm})(1.2)(32.174 \frac{ft}{s^2})}{32.174 \frac{lbm \cdot ft}{s^2}}$$

1 lbf

$$F_{ringmount} = .18 \text{ lbf}$$

$$V = F_{tot} = .6 \text{ lbf} + .18 \text{ lbf}$$

$$V = .78 \text{ lbf}$$

$$\tau_{max} = \frac{Z(.78 \text{ lbf})}{.0914 \text{ in}^2}$$

$$= 17 \text{ psi}$$

$$A = (\pi r_{out}^2 - \pi r_{in}^2)$$

$$= (\pi (.5^2 - .47^2))$$

$$= .0914 \text{ in}^2$$

Conclusion: This is negligible

After communicating with manufacturing technicians
0.05" wall thickness will be used for proper welding.
This does not hurt our design, it improves it.

page 2

To Find σ_{bending}

$$\sigma_{\text{bending}} = \frac{Mc}{I}$$

$$I = \frac{\pi}{64} (.5^4 - .47^4)$$

$$= 6.727 \times 10^{-4} \text{ in}^4$$

$$M = (.78 \text{ lbf})(16.25 \text{ in})$$

$$= 12.675 \text{ lbf-in}$$

$$c = .25 \text{ in}$$

$$\sigma_{\text{bending}} = \frac{(12.675 \text{ lbf-in})(.25 \text{ in})}{6.727 \times 10^{-4} \text{ in}^4}$$

$$= 4.71 \text{ ksi}$$

S_y for 4130 annealed is $\approx 50 \text{ ksi}$

Van Mises stress for plane stress

$$\sigma' = (\sigma_A^2 - \sigma_A \sigma_B + \sigma_B^2)^{1/2}$$

σ_B is negligible; theoretically zero

$$\sigma' = \sigma_A$$

$$\therefore \text{S.F.} \approx 10$$

Conclusion: This piece can withstand common bending moments

After communicating with manufacturing techs,

0.05" wall thickness will be used for proper welding

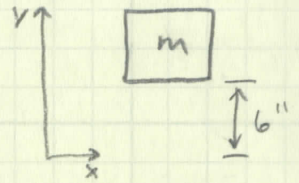
This does not hurt our design, but improves it

LANDING FORCES

6 INCH DROP: $d = \frac{1}{2}gt^2 + V_0t + d_0$

$$\frac{1}{2} \text{ ft} = \frac{1}{2}gt^2 \rightarrow t = \sqrt{\frac{1 \text{ ft}}{32.174 \text{ ft/s}^2}} = 0.1763 \text{ s}$$

$$V = gt = (32.174 \text{ ft/s}^2)(0.1763 \text{ s}) = 5.672 \text{ ft/s}$$



$$KE = \frac{1}{2}mV^2 = \frac{1}{2}(454 \text{ lbm})(5.672 \text{ ft/s})^2 = 7303.5 \frac{\text{lbm ft}^2}{\text{s}^2} \left[\frac{\text{lb}}{\text{lbm} \cdot 32.174 \text{ ft/s}^2} \right]$$

$$= 227 \text{ lbf} \cdot \text{ft}$$

WORK-ENERGY: $F_{\text{ave}} d = KE$

$$F_{\text{ave}} d = 227 \text{ lbf} \cdot \text{ft} \rightarrow \text{CHOOSING DISTANCE CHANGES AVERAGE FORCE EXPERIENCED WHILE LANDING.}$$

NOTES

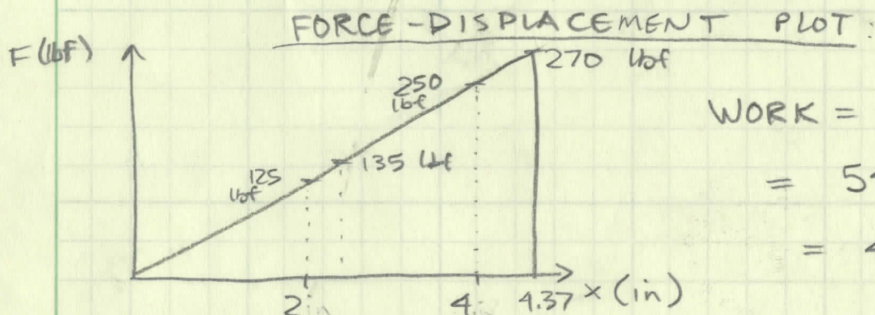
- INDUSTRIAL SHOCK ABSORBERS PROVIDE F_{ave} CONSTANTLY OVER THEIR TRAVEL, BUT THE TRAVEL IS SHORT ($\approx 2''$).
- SPRINGS HAVE LONGER TRAVEL DISTANCES BUT INCREASE F OVER THEIR DISPLACEMENT.
- SPRINGS CAN BE MADE TO WORK FOR US IF WE USE A LONGER TRAVEL AND A LOWER k .

• 5 SETS OF LANDING GEAR ON THE CRAFT

OUR SELECTION: 8" LONG, 2.187" WIDE (OD), 3.63" COMPRESSED, TRAVEL = 4.37", $k = 62.5 \text{ lbf/in}$

$$F_{\text{ave}} = \frac{227 \text{ lbf} \cdot \text{ft}}{4.37 \text{ in}} \left[\frac{12 \text{ in}}{\text{ft}} \right] = 623.3 \text{ lbf}$$

FORCE SEEN BY EACH UNIT: $\frac{623.3 \text{ lbf}}{5} = 124.7 \text{ lbf}$
(ON AVERAGE)



WORK = AREA UNDER CURVE

$$= 540 \text{ lbf} \cdot \text{in} @ 4.37 \text{ in}$$

$$= 45 \text{ lbf} \cdot \text{ft} \text{ PER LANDING GEAR UNIT.}$$

→ 225 lbf-ft IN TOTAL

SPRING SHOULD DRASTICALLY REDUCE IMPACT FORCES.

→ $F_{\text{max}} \approx 270 \text{ lbf}$

APPENDIX B-10.2

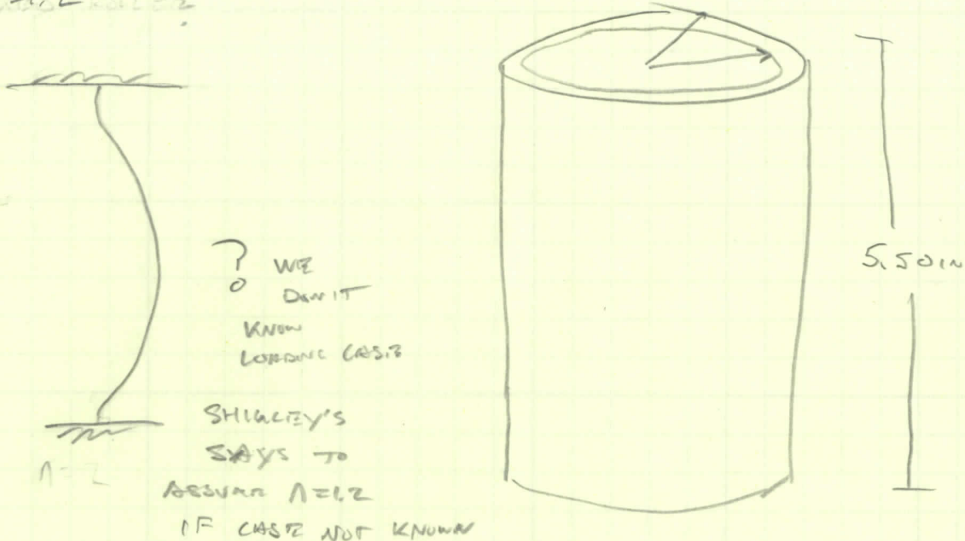
LANDING GEAR FORCES AND STRESSES

TEAM HAND CALCS

FIND: MAXIMUM FORCE ALLOWED BEFORE BUCKLING ON LANDING GEAR

ASSUME $n=1.2$

$r_o = 1.125 \text{ in}$
 $r_i = 1.06 \text{ in}$



$$F_{MAX} = \frac{1.2^2 EI}{L^2}$$

$$I = \frac{\pi}{4} (1.125^4 - 1.06^4)$$

$$F_{MAX} = \frac{(1.2)^2 \pi^2 (30 \times 10^6) (0.2665 \text{ in}^4)}{(5.50)^2}$$

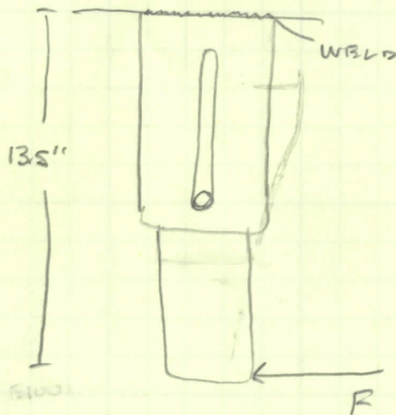
$$I = 0.2665 \text{ in}^4$$

$$F_{MAX} = 3 \times 10^6 \text{ lbs}$$

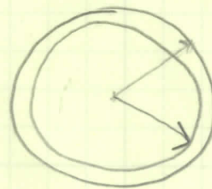
→ SLENDERNESS RATIO CONCLUDES TUBE SHOULD BE TREATED AS PURE COMPRESSION MEMBER.

→ BUCKLING IN THE SPRING UNDER COMPRESSION WILL ALSO NOT OCCUR FOR THE SAME REASONS.

FIND: MAX HORIZONTAL FORCE WELD CAN SURVIVE ON LANDING GEAR



TUBE TOP VIEW



$r_o = 1.25 \text{ in}$
 $r_i = 1.155 \text{ in}$

$$I_o = \pi r^3$$

$$I = 0.707 (1.25 \text{ in}) (\pi (1.25^3 \text{ in}^3))$$

$$I = 0.54226 \text{ in}^4$$

ASSUME USING E1000 ELECTRODE
 $\sigma_{TENS} = 30 \text{ ksi}$
 $\sigma_{MAX} = \frac{Mc}{I}$

$$30,000 = \frac{F(13.5 \text{ in})(1.25 \text{ in})}{0.54226 \text{ in}^4}$$

$$F_{MAX} = 964 \text{ lbs}$$

$$F_{ALLOWABLE} = 800 \text{ lbs}$$

Apply Factor of Safety

COMPRESSION STRESS, SMALLER THAN SLIPPING TUBE

$$\sigma = \frac{F}{A}, \frac{27116 \text{ lbf}}{0.446 \text{ in}^2}$$

$$A = r_o^2 - r_i^2$$

$$A = \pi (1.25^2 - 1.06^2)$$

$$A = 0.446 \text{ in}^2$$

$$\sigma = 607.6 \text{ psi}$$

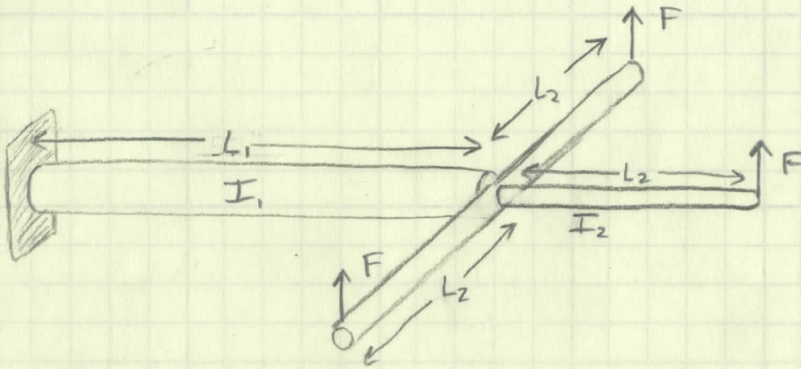
$$F.S. = 131.7$$

MATLAB CODE FOR STIFFNESS CHECKS

→ ESTIMATES DEFLECTIONS OF EACH TUBE IN ARM ASSEMBLY. IGNORES STEEL COMPONENTS (WHICH ARE STIFFER THAN CARBON FIBER)

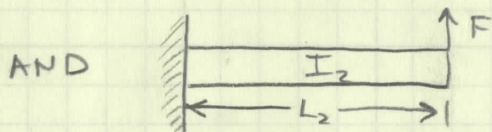
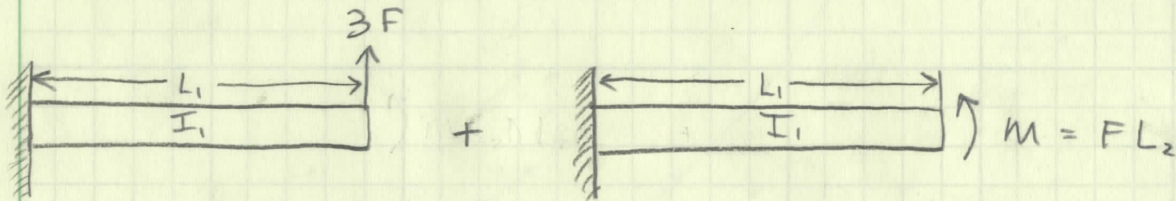
SEE ATTACHED CODE AND VERIFICATION

MODEL

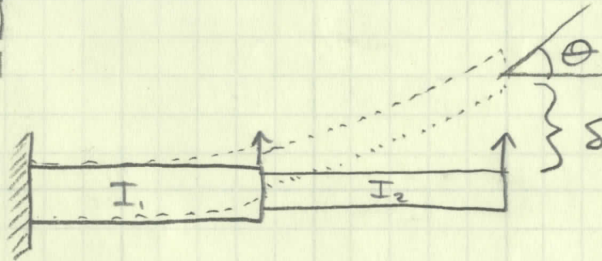


F = MOTOR THRUST

MODELED AS:



SUPERPOSITION:



WHERE $\theta_{FORCES} = \frac{PL^2}{2EI}$, $\theta_{MOMENTS} = \frac{ML}{EI}$, $\delta_{MOMENTS} = \frac{ML^2}{2EI}$,
 $\delta_{FORCES} = \frac{PL^3}{3EI}$

$\theta_{2END} = \theta_1 + \theta_2 + \delta_{2END} = \delta_1 + \delta_2 + \theta_{2END} L_2$

$\theta_{2END} = \left(\frac{3FL_1^2}{2EI_1} + \frac{20L_1L_2}{EI_1} \right) + \left(\frac{FL_2^2}{2EI_2} \right) \rightarrow$ ANGULAR DEFLECTION AT THE END OF THE FURTHEST MOTOR SPAR

$\delta_{2END} = \left(\frac{3FL_1^3}{3EI_1} + \frac{L_1^2L_2F}{2EI_1} \right) + \frac{FL_2^3}{3EI_2} + \theta_{2END} L_2 \rightarrow$ LINEAR DEFLECTION AT END OF FURTHEST MOTOR SPAR

CARBON TUBE/SPAR STRUCTURE VALIDATION

CARBON PROPERTIES:

USING ASH/3501-6 UNIDIRECTIONAL

PLY THICKNESS = 0.0052 IN

DENSITY = 0.057 lb/in³

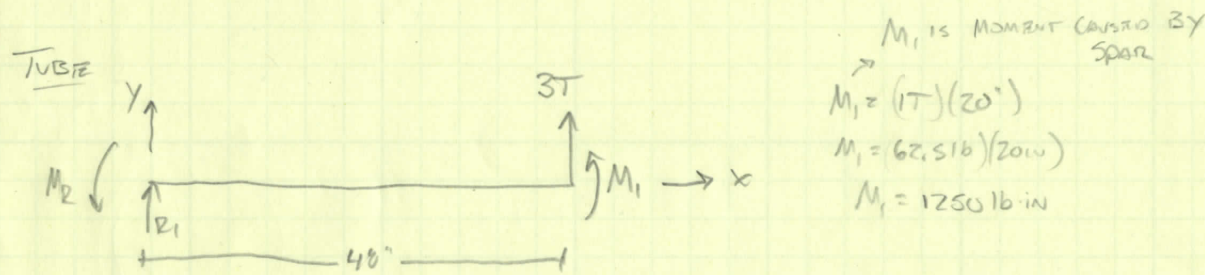
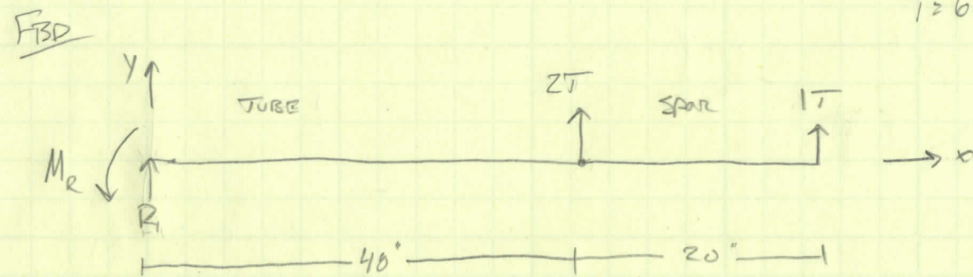
LONGITUDINAL MODULUS = 20.0 x 10⁶ psi

VERIFIED WITH DR. MALLO'S EFFECTIVE STIFFNESS CALCULATOR

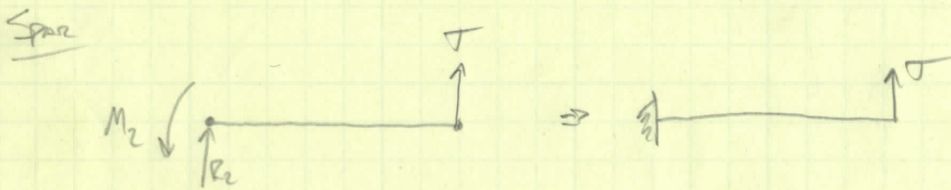
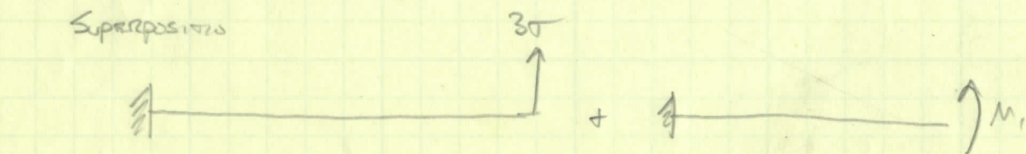
FOR UNIDIRECTIONAL CARBON TUBES, EFFECTIVE STIFFNESS UNDER SHEAR + BENDING IS THE LONGITUDINAL MODULUS.

E_x = 20.0 x 10⁶ psi

T = 62.5 lb



M₁ IS MOMENT CAUSED BY SPAR
 M₁ = (T)(20")
 M₁ = 62.5 lb(20 in)
 M₁ = 1250 lb-in



* FOR VALIDATION TUBE AND SPAR HAVE EQUAL PROPERTIES AND GEOMETRIES

LINEAR & ANGULAR DEFLECTION @ END OF TUBE

$$\delta_{TOTAL} = \frac{(3T)(L)^3}{3EI} + \frac{(M_1)L^2}{2EI} \quad \theta_{TOTAL} = \frac{(3T)L^2}{2EI} + \frac{M_1L}{EI}$$

M₁ = 1250 lb-in

T = 62.5 lb

L = 48 in

E = 20.0 x 10⁶ psi

r_o = D/2 = 3.63 in = 1.815 in

r_i = D/2 = 3.5 in = 1.75 in

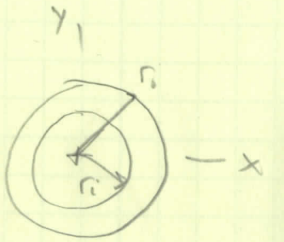
I = 1.1569 in⁴

MOMENT OF INERTIA (AREA) FOR ROUND TUBE

I_x = I_y = $\frac{\pi}{4}(r_o^4 - r_i^4)$

I_x = $\frac{\pi}{4}(1.815^4 - 1.75^4)$

I_x = 1.1569 in⁴



$$\delta_{TOTAL} = \frac{3(62.5 \text{ lb})(48 \text{ in})^3}{3(20 \times 10^6 \text{ lb/in}^2)(1.1569 \text{ in}^4)} + \frac{(1250 \text{ lb-in})(48 \text{ in})^2}{2(20 \times 10^6 \text{ lb/in}^2)(1.1569 \text{ in}^4)}$$

δ_{TOTAL} = 0.2987 in + 0.06224

δ_{TOTAL} = 0.3610 in

$$\theta_{TOTAL} = \frac{3(62.5 \text{ lb})(48 \text{ in})^2}{2(20 \times 10^6 \text{ lb/in}^2)(1.1569 \text{ in}^4)} + \frac{(1250 \text{ lb-in})(48 \text{ in})}{(20 \times 10^6 \text{ lb/in}^2)(1.1569 \text{ in}^4)}$$

θ_{TOTAL} = 0.009335 + 0.00259

θ_{TOTAL} = 0.011928 rad $(\frac{180^\circ}{\pi \text{ rad}}) = 0.68345^\circ$

δ & θ FOR SPAR

$$\delta_{SPAR} = \frac{(62.5 \text{ lb})(20 \text{ in})^3}{3(20 \times 10^6 \text{ lb/in}^2)(1.1569 \text{ in}^4)}$$

$$\theta_{SPAR} = \frac{(62.5 \text{ lb})(20 \text{ in})^2}{2(20 \times 10^6 \text{ lb/in}^2)(1.1569 \text{ in}^4)}$$

δ_{SPAR} = 0.0072 in + θ_{TOTAL}(20") θ_{SPAR} = 5.402 x 10⁻⁴ rad $(\frac{180^\circ}{\pi})$

δ_{SPAR} = 0.0072 in θ_{SPAR} = 0.0309°

TOTAL LINEAR & ANGULAR DEFLECTION

δ_{TOTAL} + δ_{SPAR} = δ
 δ = 0.60676 in

θ = θ_{TOTAL} + θ_{SPAR}
 θ = 0.714403°

VALIDATED ✓

National Brand

National Brand

APPENDIX ^B A-11.3MATLAB TUBE
DEFLATION CODE

ECM HAND CALC

Carbon Tube Calculator

ECM - ME429 Winter Quarter 2015

Contents

- [Material Properties](#)
- [Calculations](#)

Material Properties

Units: Inches, Pounds (Force),

```

% Carbon Tube Properties

% Lengths
L1 = 48;      % [in] length of arm with larger diameter
L2 = 20;      % [in] length of spar with smaller diameter

% Dimensions
s1 = input('input large tube dimensions [in], ex 3.5 x 3.163 x 72" is [3.5 3.63 48]: ');
    % [in] large tube dimensions
s2 = input('input small tube dimensions [in]: ');      % [in] small tube dimensions
density1 = input('input weight density for large tube, [lbm/ft]: ')/12;      % [lbm/inch]
density
density2 = input('input weight density for small tube, [lbm/ft]: ')/12;      % [lbm/inch]
density

% Here we convert [lbm/foot] to [lbm/inch], and it is assumed that
% [lbf/inch] = [lbm/inch]

E = 20*10^6; % [psi] modulus of elasticity

% Wall Thicknesses
t1 = (s1(2) - s1(1))/2; % wall thickness of large tube
t2 = (s2(2) - s2(1))/2; % wall thickness of small tube

% Mass
m1 = density1*L1;      % [lbm] mass of large tube
m2 = density2*L2;      % [lbm] mass of large tube

% Total Mass
mass=4*(m1+(3*m2));      % [lbm] mass of carbon structure

% Moments of Inertia
ri1 = s1(1)/2;      % Inner radius large tube
ro1 = s1(2)/2;      % Outer radius large tube
I1 = .25*pi*(ro1^4 - ri1^4); % Area Moment of inertia large tube

ri2 = s2(1)/2;      % Inner radius small tube

```

APPENDIX ~~B~~ A-11.2MATLAB TUBE
DEFLECTION CODE

ECM HAND CALCS

```
ro2 = s2(2)/2; % Outer radius small tube
I2 = .25*pi*(ro2^4 - ri2^4); % Area Moment of inertia small tube
```

```
.Error using input
Cannot call INPUT from EVALC.
```

```
Error in CarbonTubel_5 (line 14)
```

```
s1 = input('input large tube dimensions [in], ex 3.5 x 3.163 x 72" is [3.5 3.63 48]: ');
% [in] large tube dimensions
```

Calculations

```
% Need: Angular (and maybe linear) deflection of both tips
% stresses/strains
% factor of safety for deflection (8 degrees) and stress/strain
% weight of tubes per arm (include all three spars)
%
% Start with calculating moment of inertias of both tubes, then use
% [weight/foot] to calculate total weight (arms are 48", spars are 20").
% Use Shigley's deflection formulas

thrust = 62.5; % [lbf] per motor

% Large Tube
theta1F = (3*thrust*L1^2)/(2*E*I1); % [rads] angular deflection due to thrust of large tube
theta1M = (20*thrust*L1)/(E*I1); % [rads] angular deflection due to moment of large tube
theta1 = theta1F + theta1M; % [rads] total angular deflection of large tube

delta1F = (3*thrust*L1^3)/(3*E*I1); % [inches] linear deflection due to thrust of large tube
delta1M = (20*thrust*L1^2)/(2*E*I1); % [inches] linear deflection due to moment of large tube
delta1 = delta1F + delta1M; % [inches] total linear deflection of large tube

moment1 = 3*thrust*48+thrust*68; % [lbf*inch] moment on large tube from normal use
stress1 = (moment1*ro1)/I1; % [psi] stress from normal use, (My/I)

theta1degrees = 180*theta1/pi

% Small Tube
theta2F = (thrust*L2^2)/(2*E*I2); % [rads] total angular deflection (due to thrust) of small tube
theta2 = theta2F + theta1; % [rads] total angular deflection of small tube

delta2F = (thrust*L2^3)/(3*E*I2); % [inches] total linear deflection (due to thrust) of small tube
delta2 = delta1 + delta2F + L2*theta1; % [inches] total linear deflection of small tube

moment2 = thrust*20; % [lbf*inch] moment on large tube from normal use
```


APPENDIX A-11.3
B

ECM HAND CALCS

```
stress2 = (moment2*ro2)/I2; % [psi] stress from normal use, (My/I)
```

```
theta2degrees = 180*theta2/pi
```

```
M1=30864; % [lb*in]
```

```
stress11=(M1*ro1)/I1
```

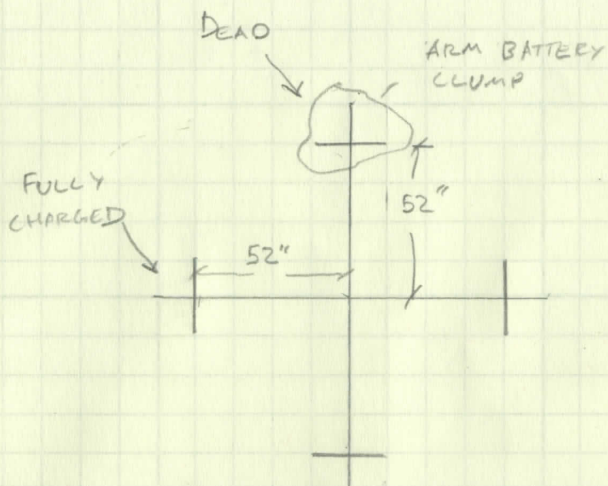
```
M2=9080.4; % [lb*in]
```

```
stress22=(M2*ro2)/I2
```

Published with MATLAB® R2014a

TO LINK ARM BATTERY CLUMPS IN PARALLEL

STRUCTURE / WIRE LAYOUT



FIND

MAX AMP DRAW ASSUMING
1 ARM BATTERY CLUMP IS
DEAD

MAX Δ VOLTAGE FOR 19S . .

$$\text{MAX} \rightarrow \text{CHARGE PER CELL} \quad -4.2 \text{ V} \quad \times 14 = \quad 58.8 \text{ V}$$

$$\text{CUT-OFF CHARGE} \quad -3.5 \text{ V} \quad \times \quad 49 \text{ V}$$

$$\Delta V = 58.8 \text{ V} - 49 \text{ V}$$

$$= 9.8 \text{ V}$$

\Rightarrow OHMS LAW: $V = IR$

$$I_{\text{max}} = \frac{V_{\text{max}}}{R}$$

NEED R \rightarrow ASSUME 8 AWG COPPER

FROM THELEN. DS AWG COPPER WIRE CHART

$$8 \text{ AWG} \left| \begin{array}{l} \text{Weight} \\ \text{length} \end{array} \right. \left[\frac{\text{lbs}}{1000 \text{ ft}} \right] = 4.753 \text{ lbs}/1000 \text{ ft}$$

$$\frac{\text{Resistance}}{\text{length}} \left[\frac{\Omega}{1000 \text{ ft}} \right] = 0.67 \text{ } \Omega / 1000 \text{ ft}$$

OUR LENGTH FROM THE DEAD BATTERY CLUMP TO THE FULLY CHARGED CLUMP IS $2.52' = 104''$

THUS,

$$I_{max} = \frac{9.8V}{\left(0.67 \frac{\Omega}{1000ft}\right) \left[104in\right] \left[\frac{1ft}{12in}\right]}$$

$$I_{max} = 1687 \text{ Amp}$$

← WE DON'T NEED THIS MUCH
→ DECREASE BY INCREASING RESISTANCE TERM BY INCREASING GAGE (SMALLER WIRE)

WEIGHT ADDED TO STRUCTURE

$$\left(47.53 \frac{lbs}{1000ft}\right) \left(52in\right) \left(4\right) \left[\frac{1ft}{12in}\right] = 0.824 \text{ lbs}$$

OR, ASSUME MAX CURRENT = 200 A FOR MOTOR

$$R = \frac{V_{max}}{I_{max}}$$

$$= \frac{9.8V}{200A}$$

$$= \frac{0.049 \Omega}{\left(104in\right) \left[\frac{1ft}{12in}\right]}$$

$$= 0.005654 \frac{\Omega}{ft}$$

$$= 5.654 \frac{\Omega}{1000ft}$$

REFERENCING PREVIOUS CHART, THIS RESISTANCE VALUE CORRESPONDS TO

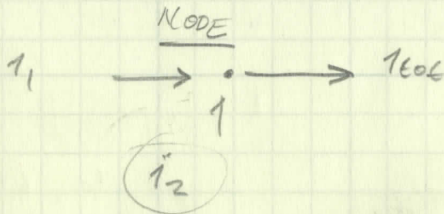
$$\text{AWG 16 WITH } W/L = 8.56 \text{ lbs}/1000ft \Rightarrow 0.148 \text{ lbs}$$

$$R/L = 42 \frac{\Omega}{1000ft}$$

NOTE THIS SEEMS LIKE AN UNREASONABLE METHOD BECAUSE THE 16 GAGE IS NOWHERE CLOSE TO RATED FOR 200 AMP

ANOTHER APPROACH

ASSUME ONE BATTERY CLUMP IS DRAWING $\frac{1}{3}$ OF ITS POWER / CURRENT FROM THE OTHER BATTERY CLUMPS, WHERE THE MOTOR REQUIRES 200 AMP TO OPERATE.



$$i_{tot} = i_1 + i_2, \quad i_2 = \frac{1}{3} i_{tot}$$

$$i_2 = \frac{1}{3}(200 \text{ Amp})$$

$$i_1 = \text{CURRENT DRAW FROM IMMEDIATE BATTERY} = 66.7 \text{ amp}$$

$$i_2 = \text{CURRENT DRAW FROM DISTANT BATTERIES}$$

$$i_{tot} = \text{TOTAL CURRENT GOING TO MOTOR}$$

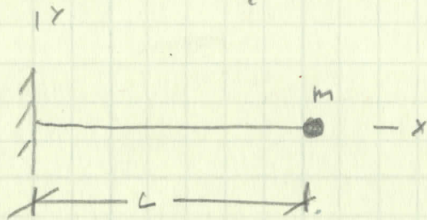
⇒ CHECK WEIGHT FOR 12 AWG (RATED FOR 90 AMP)

$$W/L = 7.81 \text{ lb}/1000 \text{ ft} \left(104 \text{ in} \right) \left[\frac{14}{12 \text{ in}} \right] (4)$$

$$= 0.271 \text{ lbs}$$

CONCLUSION

- POWER WIRE WILL NOT ADD SIGNIFICANT WEIGHT TO STRUCTURE
- FOR SAFEST APPROACH, WE WILL USE THE 8 AWG FOR CONSISTENCY OF CABLING, LESS HEAT GENERATION + SAFETY FROM MOST EXTREME CURRENT LOADING CASE OF 200 AMP, WHERE ALL CURRENT TO POWER MOTOR IS PROVIDED THROUGH THE "TRANSMISSION LINES"



$$\omega_n = \sqrt{\frac{3EI}{mL^3}}$$

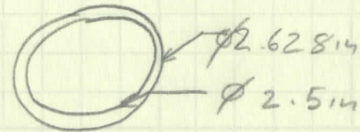
TUBE DIMENSIONS
FROM COMBO 7

$$E = 13.4 \times 10^6 \text{ psi}$$

$$I_z = \frac{\pi}{4} (r_o^4 - r_i^4)$$

$$= \frac{\pi}{4} \left(\left(\frac{2.628 \text{ in}}{2} \right)^4 - \left(\frac{2.5 \text{ in}}{2} \right)^4 \right)$$

$$= 0.4239 \text{ in}^4$$



$$m = \# \text{ MOTORS} \times \text{mass MOTORS}$$

$$\rightarrow \text{FROM HOBBY KING } W = 1916 \text{ g}$$

$$\Rightarrow m = 1.916 \text{ kg}$$

$$= 4.224 \text{ lbm}$$

$$L = 72 \text{ in}$$

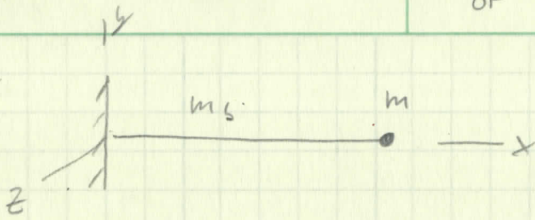
$$\omega_n = \sqrt{\frac{3(13.4 \times 10^6 \text{ lbf/in}^2)(0.4239 \text{ in}^4)}{3(4.224 \text{ lbm})(72 \text{ in})^3 \left[\frac{1 \text{ lbf}}{32.174 \text{ lbm} \cdot \text{ft/s}^2} \right] \left[\frac{\text{ft}}{12 \text{ in}} \right]}}$$

$$\# \text{ MOTORS} = 37.3 \text{ rad/s}, \quad f_n = \omega_n / 2\pi$$

$$f_n = 5.94 \text{ Hz}$$

$$\text{RPM} = (37.3 \frac{\text{rad}}{\text{s}}) \left[\frac{1 \text{ rev}}{2\pi \text{ rad}} \right] \left[\frac{60 \text{ s}}{\text{min}} \right]$$

$$= 356 \text{ rev/min}$$



$$\omega_n = \sqrt{\frac{3EI}{(m + 0.23m_b)L^3}}$$

EVERYTHING IS THE SAME BUT m_b

$$m_b = L \cdot \rho \quad \rho = 1.6 \text{ lbm/ft} \quad (\text{COMBO 7})$$

$$= (72 \text{ in}) (0.36 \text{ lbm/ft}) \left[\frac{1 \text{ ft}}{12 \text{ in}} \right]$$

$$= 2.16 \text{ lbm}$$

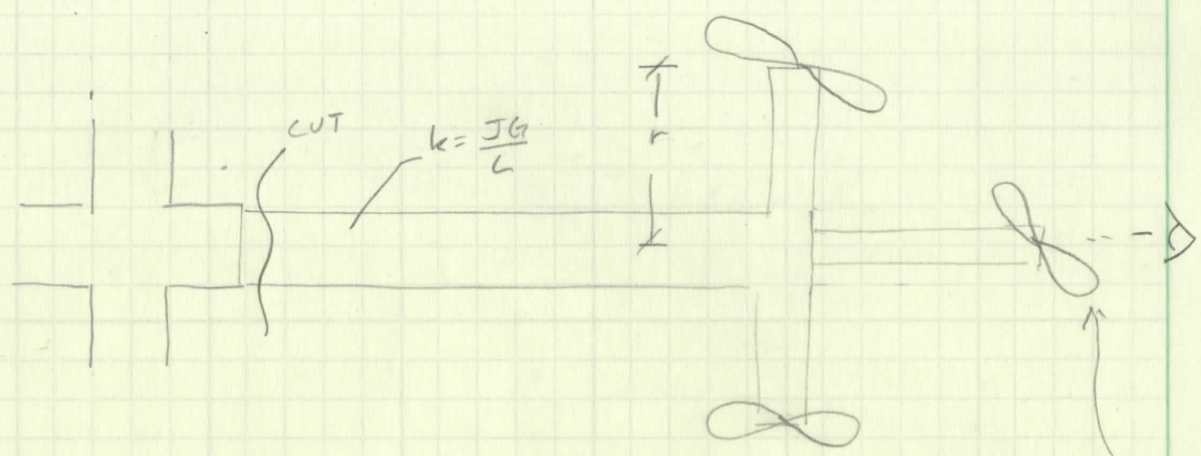
$$\Rightarrow \omega_n = \sqrt{\frac{3(13.4 \times 10^6 \text{ lb}^2/\text{in}^2)(0.4239 \text{ lbm})}{(3)(4.224 \text{ lbm}) + (0.23)(2.16 \text{ lbm})} \left[\frac{1 \text{ lb} \cdot \text{ft}}{32.174 \text{ lbm} \cdot \text{ft/s}^2} \right] \left[\frac{1 \text{ ft}}{12 \text{ in}} \right]}$$

$$= 36.59 \text{ rad/s}$$

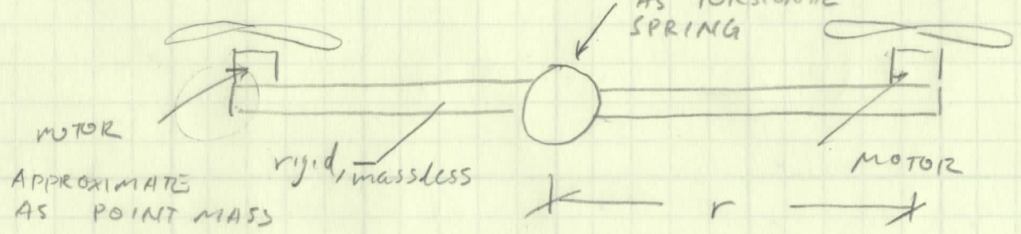
$$f_n = 5.82 \text{ Hz}$$

$$\text{RPM} = 349 \text{ rev/min}$$

TORSIONAL NATURAL FREQUENCY

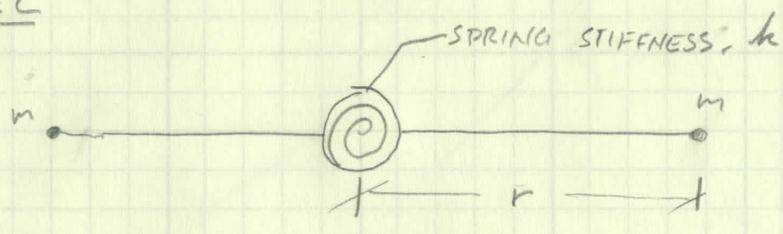


LOOKING DOWN THE TUBE



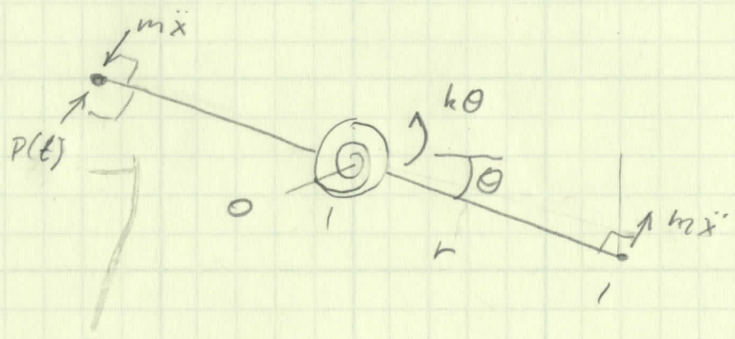
ASSUME MOTOR DOES NOT CONTRIBUTE TO TORSION

NEW MODEL



PERTURB SYSTEM TO FIND ITS RESPONSE + NATURAL FREQ.

FBD



NOTE TORSION STIFFNESS:

$$k = \frac{GJ}{L} \quad \frac{N \cdot m}{rad}$$

$$\frac{[N/m^2][m^4]}{m} \quad \frac{kg \cdot m}{s^2}$$

EOM

$$\sum M_o \quad -P(t)r + mx'' + m\ddot{x}r + k\theta = 0$$

$$-P(t)r + 2mr(r\ddot{\theta}) + k\theta = 0$$

$$2mr^2\ddot{\theta} + k\theta = P(t)r$$

← arc length

$$x = r\theta$$

$$\dot{x} = r\dot{\theta}$$

$$\ddot{x} = r\ddot{\theta}$$

NORMALIZING THE EOM GIVES US

$$\ddot{\theta} + \frac{k}{2mr^2} \theta = \frac{P(t)}{2mr}$$

, Note that

$$\frac{k}{2mr^2} = \omega_n^2 \implies \omega_n = \sqrt{\frac{k}{2mr^2}}$$

SUBSTITUTING FOR $k = GJ/L$

$$\omega_n = \sqrt{\frac{GJ/L}{2mr^2}}$$

TAKE G FROM "PERFORMANCE COMPOSITES"
 \implies IN-PLANE SHEAR MODULUS FOR
STANDARD CARBON FIBER

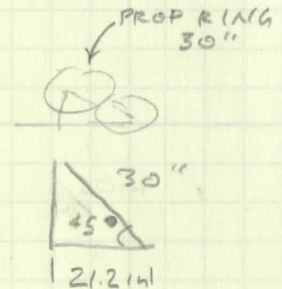
$$= 33 \text{ GPa} = 2,786,245 \text{ PSI}$$

$$= 4.78 \times 10^6 \text{ PSI}$$

$$J = \frac{\pi}{2} (r_o^4 - r_i^4)$$

$$= \frac{\pi}{2} \left[\left(\frac{2.628 \text{ in}}{2} \right)^4 - \left(\frac{2.5 \text{ in}}{2} \right)^4 \right]$$

$$= 0.8478 \text{ in}^4$$



$$L = 72 \text{ in}, \quad m = 4.22 \text{ lbm}, \quad r = ? \text{ ASSUME } = 21.2 \text{ in}$$

$$\omega_n = \sqrt{\frac{(4.78 \times 10^6 \text{ lbf/in}^2)(0.8478 \text{ in}^4)}{2(4.22 \text{ lbm})(21.2 \text{ in})^2(72 \text{ in}) \left[\frac{1 \text{ lbf}}{32.174 \text{ lbm} \cdot \text{ft/s}^2} \right] \left[\frac{1 \text{ ft}}{12 \text{ in}} \right]}}$$

$$= 75.7 \text{ rad/s}$$

$$f_n = 12.04 \text{ Hz}$$

$$\text{RPM} = 722 \text{ rev/min}$$

FOR A FIXED CANTILEVER BEAM WITH INITIAL CONDITIONS

$$\eta \Big|_{x=0} = 0, \quad \frac{d\eta}{dx} \Big|_{x=0} = 0, \quad M \Big|_{x=L} = EI \frac{d^2\eta}{dx^2} = 0,$$

$$V \Big|_{x=L} = EI \frac{d^3\eta}{dx^3}$$

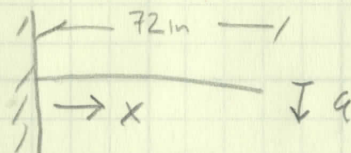
FOR THE GENERAL SOLUTION OF THE HOMOGENEOUS EQN

$$\eta(x) = C_1 \sinh(\lambda x) + C_2 \cosh(\lambda x) + C_3 \sin(\lambda x) + C_4 \cos(\lambda x)$$

REFERENCE

INTRO TO STRUCTURAL DYNAMICS: THEORY + APPLICATIONS - KASPER + HALL

WHERE $\eta(x)$ IS DISPLACEMENT ALONG THE BEAM



$$E = 18.2 \times 10^6 \text{ psi}$$

$$I = 0.9309 \text{ m}^4$$

$$m = 0.39 + \frac{29.92}{72 \text{ in}} \left[\frac{1 \text{ ft}}{12 \text{ in}} \right] = 5 \frac{\text{lbm}}{\text{ft}}$$

YIELDS THE NONTRIVIAL SOLUTIONS FOR ω .

$$\Rightarrow \omega_i = \frac{(\lambda_i L)^2}{L^2} \sqrt{EI/m}$$

$$\lambda_{1L} = 1.875104069$$

$$\lambda_{2L} = 4.694091133$$

$$\lambda_{3L} = 7.854757438$$

$$\Rightarrow \omega_1 = \frac{3.5106015270}{L^2} \sqrt{EI/m}$$

$$= \frac{3.5106}{(72 \text{ in})^2} \sqrt{(18.2 \times 10^6 \text{ lb/ft}^2)(0.9309 \text{ m}^4)} \left(\frac{5 \text{ lbm/ft}}{32.174 \text{ ft/s}^2} \right)^{1/2} \left[\frac{1 \text{ ft}}{12 \text{ in}} \right]^2$$

$$= 84.8 \text{ rad/s}$$

$$= 810 \text{ RPM}$$

AND FORM HIGHER MODES

$$\omega_2 = 5085 \text{ RPM} \quad \leftarrow$$

$$\omega_3 = 14240 \text{ RPM}$$

ASSUME $L = 52 \text{ in}$ (ENDS AT LENGTH OF ONLY ARM)

$$\rightarrow \omega_1 = 1555 \text{ RPM}$$

$$\omega_2 = 9750 \text{ RPM}$$

$$\omega_3 = 27301 \text{ RPM}$$

NEED NUMERICAL RESULTS.

NOTE MASS PLACED AT END OF BEAM WILL DECREASE NATURAL FREQUENCY, WHICH WILL BE A BETTER ESTIMATE OF THIS SYSTEM.

PROPULSION SYSTEMS

APPENDIX B16

12/5/2014

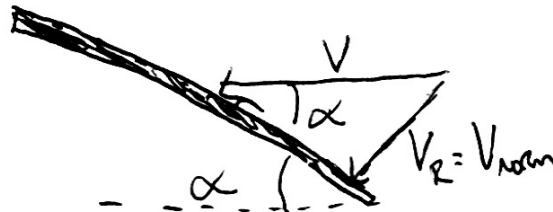
AIRCRAFT PERFORMANCE PROGRAM

1) CREATE PROPELLOR FUNCTION
function $[C_T, C_P, \text{eta}_p, D] = \text{prop}(J)$

2) CREATE MOTORPROP FUNCTION
function $[\text{throttle}, \text{RPM}] = \text{motorprop}(V, h, \text{THRUST}, \text{PROP})$

- $V = V \sin \alpha$

$[0-15 \text{ mph}]$



- THRUST = $[250 \text{ to } 200 \text{ lbs} \rightarrow 2 \times \dots]$

- $h = 10 \text{ FT}$

THRUST STARTS @ 1, RPM STAYS @ RPM MAX

$J = V \sin \alpha / \text{RPM} D$

$[C_T, C_P, \text{eta}_p, D] = \text{prop}(J)$

THRUSTMATCH = $C_T \rho \Omega^2 D^4$

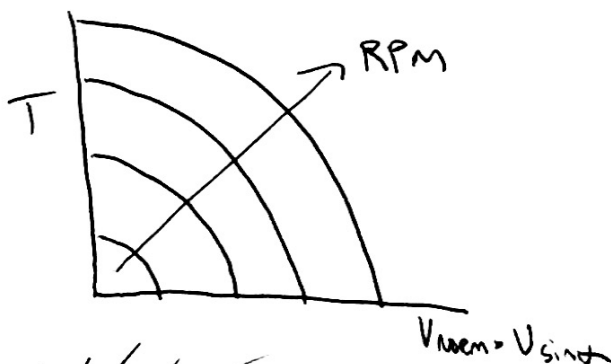
MATCH: $T - \text{THRUSTMATCH} > \text{diff}$

- ITERATE!

OUTPUT THROTTLE + RPM WHEN MATCHED

NOW I HAVE RPM + THROTTLE @ EVERY:
 $V + T$

PLOT



3. *[Signature]*

3) function $[\eta] = \text{rubbermodel}[\text{motor}, \omega, Q]$

APPENDIX B16

NEED: MOTOR PARAMETERS \rightarrow

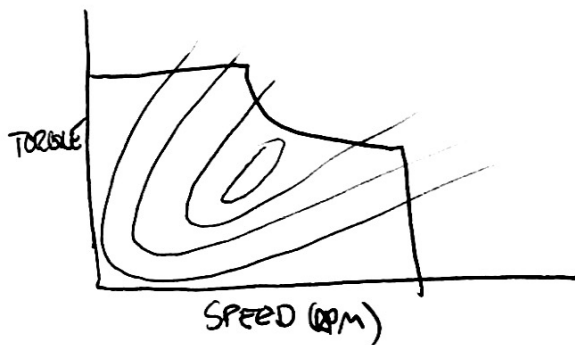
ω [RPM] $[0 \rightarrow \text{RPM MAX (BLADE)}]$

Q [TORQUE (NM)] $[0 \rightarrow \text{MAX TORQUE DELIVERABLE}]$

MOTOR PARAM: $\text{motor}.\omega_{\text{opt}} = \text{optimum } \omega$
 $\text{motor}.Q_{\text{opt}} = \text{optimum torque}$
 $\text{motor}.\eta_{\text{opt}} = \text{OPTIMUM EFFICIENCY}$
 $\text{motor}.K_0 = ?$
 $\text{motor}.K_q = ?$
 $\text{motor}.K_p = ?$
 $\text{motor}.K_{\omega} = ?$

FIND MOTOR MODEL (SPEED (RPM) VS TORQUE)

2 (3 4) kW



* MODEL OBTAIN MOTOR MANUF.
MODEL w/ rubbermotor

* SPECIAL THANKS TO PROFESSOR ROBERT A. McDONALD

4) PICK MAX EFFICIENCY POINT AND GET

- (LAB TORQUE, RPM (SPEED))

USE THRUST VS VELOCITY (2)

- FWD RPM

- T FROM V OR

- V FROM T

5) POWER EQUATIONS

... POWER REQUIRED

* FOR REFERENCE ONLY

AIRCRAFT PERFORMANCE FWAC PROJECTPARAMETERS

$$C_{D_{BOS}} = 1.0 \text{ [AIRCRAFT BODY DRAG]}$$

$$T_{THRUST} = [254 \text{ lbs} + 200 \text{ lbs} \times 2]$$

$$VELOCITY = [0 - 20 \text{ FT/S}]$$

$$C_{D_0} = 0.1 \sim \text{ASSUMPTION}$$

$$\text{PITCH, } \alpha = 30^\circ$$

$$\text{CLIMB, } \theta = 0^\circ$$

$$\text{WEIGHT, } W = 254 + 200 \text{ lbs}$$

$$\text{AREA, } A = \pi(R)^2$$

$$\text{RADIUS, } R$$

$$\text{DENSITY, } \rho = \text{STD ATM}$$

$$\Omega = \text{RPM} \times (2\pi/\omega)$$

$$\text{NUMBER OF PROPS, } N$$

$$K_1 = 1.15 \sim \text{CORRECTION}$$

$$K_2 = 4.65 \sim \text{HUB } V/\omega$$

$$K_3 = 4.5 \sim \text{HUB } H$$

$$\text{HEIGHT, } H \text{ [FT]}$$

$$\text{LENGTH, } L \text{ [FT]}$$

$$\text{WIDTH, } \omega \text{ [FT]}$$

$$\text{NUMBER BLADES/PROP, } N_b$$

$$\text{CHORD, } C \text{ [FT]}$$

EQUATIONSBLADE THEORY

$$P = P_m + P_0 + P_p + P_c$$

INDUCED PROFILE PARASITE CLIMB

$$P_m = K_1 \gamma_i C_T (\rho A \Omega^3 R^5)$$

$$\gamma_i = \gamma - M \tan \alpha$$

$$\gamma_i = \frac{C_T}{2\sqrt{M^2 + \gamma^2}}, \quad u = \frac{V \cos \alpha}{\Omega R}$$

* INFLUX RATIO + HELICOPTER ADVANCE RATIO

∴ SOLVE ITERATIVELY

$$P_0 = \frac{1}{2} \left(\frac{F}{A}\right) M^3 (\rho A \Omega^3 R^5)$$

$$- F = C_{D_{BOS}} \cdot [H \cdot W + \left[\frac{L}{\omega} - 1\right] H \cdot W \sin \theta]$$

• SELF-GENERATED DRAG AREA CALCULATION

$$P_c = W V \sin \theta$$

$$C_T = \frac{T}{\rho A \Omega^2 R^2}$$

ACTUATOR DISK THEORY

$$P_{\text{TOTAL}} = V_i T$$
$$= \frac{\left(\frac{T}{\eta}\right)^{3/2}}{\sqrt{2 \rho A}}$$

6) ACTUATOR DISK THEORY FUNCTION

$$\text{Function } [k_w] = \text{ADT}(\eta, T_{\text{HESTMAX}}, R)$$

$$- A = (\pi) * R^2$$

FIND: BEARING STRESS OF EACH PROPELLOR MOUNT BOLT ON THE PROPELLOR, FACTOR OF SAFETY, AND IF IT FAILS FOR...

- CONTINUOUS TORQUE
- PEAK TORQUE

GIVEN:

BOLT PATTERN DIAMETER = 44mm
CONTINUOUS TORQUE = 13 N-m
PEAK TORQUE = 20 N-m

HOLE DIAMETER = 5mm
HUB THICKNESS = 30.48mm

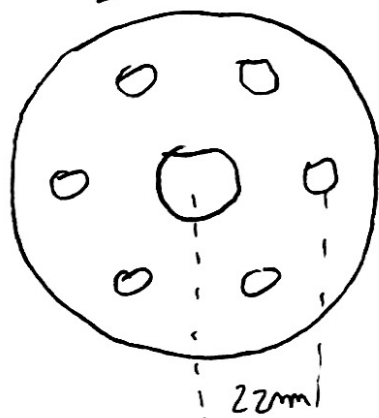
ASSUMPTIONS:

FAILURE IN SHEAR

SHEAR STRENGTH: BEACHWOOD = 2100 PSI

NUMBER OF BOLTS, $n = 6$

SOLUTION



SCHEMATIC

CONTINUOUS TORQUE

$$F = \frac{T}{r}$$

$$F = \frac{13 \text{ N-m}}{(22 \text{ mm}/1000)}$$

$$F = 590 \text{ N}$$

$$F_{\text{BOLT}} = F/n$$

$$F_{\text{BOLT}} = 590 \text{ N} / 6$$

$$F_{\text{BOLT}} = 98 \text{ N}$$

$$\sigma = \frac{P}{A}$$

$$\sigma = \frac{98 \text{ N}}{(5/1000) \times (30.48/1000)}$$

$$\sigma = 643.05 \text{ KN/m}^2$$

∴ CONVERT TO PSI

$$\sigma = 93.27 \text{ psi}$$

$$FS = 2100 \text{ psi} / 93.27 \text{ psi}$$

$$FS = 2251 \rightarrow \text{SAFE}$$

PEAK TORQUE

$$F = \frac{T}{r}$$

$$F = \frac{20 \text{ N}\cdot\text{m}}{(22 \text{ mm}/1000)}$$

$$F = 909.1 \text{ N}$$

$$F/\text{BOLT} = F/n$$

$$F/\text{BOLT} = 909.1 \text{ N}/6$$

$$\underline{F/\text{BOLT} = 151.5 \text{ N}}$$

$$\sigma = \frac{P}{A}$$

$$\sigma = \frac{151.5 \text{ N}}{(5 \text{ mm}/1000)(30.48 \text{ mm}/1000)}$$

$$\sigma = 994.1 \text{ N}/\text{m}^2$$

∴ CONVERT TO PSI

$$\sigma = 144.2 \text{ psi}$$

$$FS = 2160 \text{ psi} / 144.2 \text{ psi}$$

$$\underline{FS = 14.6 \rightarrow \text{SAFE}}$$

Appendix C

Electric Commuter Multicopter

General References and Tables

Controls Test Procedures

Test A: Motor drive test

1. Assemble full structural dodeca-copter frame
2. Attach all motors to structure
3. Connect one motor to ESC and ESC to servo tester
4. Verify servo tester is at zero state (full CCW position)
5. Connect battery to ESC, motors should beep to indicate they are armed
6. Slowly and steadily turn servo tester from zero-state to full throttle and back--motor should go from zero to full speed to zero.
7. Disconnect battery
8. Repeat steps 3 through 7 for six and twelve motors
9. Disconnect ESC's from servo tester
10. To proceed, the user must calibrate the transmitter and receiver through Mission Planner's Radio Calibration.
11. Connect all ESC's to flight controller
12. Connect receiver to flight controller
13. Turn on flight controller through the battery eliminator circuit (BEC)
14. Bind transmitter to receiver
15. Disconnect battery and remove bind plug
16. Reconnect batteries
17. Arm flight controller by holding the red button on the PixHawk until it is solid. Then hold the left stick of the transmitter down and to the right--flight controller will change from blinking blue to solid blue when armed
18. The craft is now armed and ready to be tested
19. Steadily and slowly throttle up from zero to full speed to zero
20. Disarm flight controller

21. Disconnect batteries

Test B: Fixed Arm Cluster Test

1. Attach four loaded motors to craft
2. Place scale on level surface and then a cinder block on top of the scale
3. Place the craft face up on top of the scale
4. Firmly tie down craft to cinderblock
5. Place video recording device in a location that can see the scale
6. Open Mission Planner and connect to the Saitek controller
7. Open the Radio tab to see the radio-thrust values--values should range from about 1100 to 1900. Record the maximum and minimum of these values as they was used to find thrust percentages
8. Arm the flight controller and connect batteries and ESC's
9. Begin recording with video recorder
10. Throttle up to about 40% throttle, and stay there for several second. Record the radio-thrust value. Repeat for 50% and 60% throttle
11. Throttle down and disarm flight controller
12. Stop recording device
13. Repeat steps 8-12 for eight then twelve propellers
14. Disconnect batteries

15. Clean up

Test C: Floating Tether Test

1. Lay down mats into 30ft square
 2. Place cinder blocks at two opposite corners of the square
 3. Tie rope to one arm of the craft and to the cinderblocks
 4. Repeat for opposite arm
 5. Energize the multicopter
 6. Clear the safety circle
 7. Increase power until the multicopter is in hover 5 ft off the ground
 8. Increase the hover height of the multicopter to 8ft, and decrease the hover height back to 5ft
 9. Move the multicopter forward and then back to the original position
 10. Move the multicopter left and then right to return to the original position
 11. Yaw the multicopter a full 360 degrees, slowly increasing the yaw rate until the maximum rate is achieved
 12. Move the multicopter forward and perform a 90 degree turn left and then right while in forward flight
 13. Fly the multicopter for 2 to 3 more minutes performing the previously attempted maneuvers in succession
 14. Land the multicopter
15. Enter the safety circle and depower the system

Test D: Redundancy Test

1. Remove marked motor by unplugging motor from its ESC
2. Energize the multicopter
3. Clear the safety circle
4. Take the vehicle to 5 ft hover
5. Operate the vehicle under standard conditions
6. Visually inspect response and measure time for multicopter to correct itself
7. Decrease power back to hover at 5 ft off the ground
8. If controller is successful power down
9. Land the multicopter
10. Enter the safety circle and depower the system

Test F: Disturbance Test

1. Attach tether to the multicopter, and mark the safety circle
2. Energize the multicopter
3. Clear the safety circle
4. Increase power until the multicopter is in hover 5 ft off the ground
5. Fly the multicopter to the opposite end of its tether, until tether becomes taut
6. Use stopwatch to measure time to correct itself (if measureable)
7. If controller is successful power down
8. Land the multicopter
9. Enter the safety circle and depower the system

Test G: User Interface Test

1. Set-up multicopter on flat table
 2. Remove propellers to unload system
 3. Attach the telemetry module to the Pixhawk's TELEM port
 4. Open Mission Planner on laptop
 5. Plug in and install second telemetry module into the laptop
 6. Set-up Saitek X52 on table and plug into the laptop
 7. Download all necessary drivers
8. Toggle on Joystick in Mission Planner and configure controller
9. Enable Joystick controls
10. Set connection channel and connect the telemetry modules via Mission Planner

11. Arm vehicle and Saitek control system
12. Test throttle up and down via the Saitek controller
13. Test roll, pitch, and yaw
14. Clean up and disassemble

Determining the Flexural Modulus of a Unidirectional Carbon Fiber Tube

ME 410 Term Project

For Professor Birdsong

By Marley Miller and Grant Pocklington

Introduction

As part of the Electric Commuter Multicopter senior project at Cal Poly, a 3 point bend test was done on a custom-made piece of unidirectional carbon fiber tubing in order to validate its structural properties and clear it for use in the full scale design of a manned electric multicopter. The experiment done by the senior project team highlighted a possible concern in the stiffness of the carbon fiber tubing which could be disastrous if not corrected for; unfortunately, the testing method was not sophisticated enough to allow them to confidently isolate the source of the issue. Below in Figure 1 is a photo of the team's experimental apparatus for the test.



Figure 1. Previous testing run by the Electric Commuter Multicopter senior project team which estimated the flexural modulus of a carbon fiber tube.

The testing performed by the senior project team made use of dial indicators poised under the carbon fiber tube to determine the tube's deflection under a given load. However, this testing method meant that the dial indicators also measured the deflection of the test setup, resulting in some additional strain being calculated for a given load and a lower overall modulus being calculated for the tube. In addition, the tube often rotated about in the automotive jacks between the application of additional weights, resulting in a loss of zero for the trial and lower overall accuracy for the test. As such, we propose to run another 3 point bend test on the same section of tubing in order to experimentally determine the effective flexural modulus of the tubing through the use of strain gages. This would allow us to determine with a much higher degree of confidence if the carbon tubing will perform as intended or if it needs to be redesigned, as this method is not affected by the deflection of the

testing apparatus and should be much more precise and repeatable. than the test performed earlier. However, we also decided to explore dynamic options for testing the modulus, so we ran two different vibration tests in order to compare those results with the ones found from the static testing. We decided upon testing the stiffness properties of the tube with a cantilever (fixed-free) vibration test as well as a free-free vibration test. This would give us two different data sets that we can then use vibration theory with to solve for the flexural modulus. With the results we gather we hope to be able to confirm that the tube is in fact stiff enough, or definitively prove that the tube needs to be redesigned in order to move forward with the senior project. The analysis we are doing will also allow for the comparison between the static and dynamic testing methods for finding the flexural modulus of the tube.

Background and Research

In a paper titled “Short-Beam and Three-Point-Bending Tests for the Study of Shear and Flexural Properties in Unidirectional-Fiber-Reinforced Epoxy Composites,” the ratio of the length to thickness of composite tubes and beams were considered and tested. The researchers developed a relationship between the shear stress and the flexure stress to failure based on the thickness and length of the member tested in a three point bend test. The results found that if the length-to-thickness ratio is small (5 as they tested), the normal stress values will be much lower than the shear stress values. This means that with a thinner and longer member, the normal stresses in the specimen is going to be much higher than the shear stress, which means that the thin and long member we have, the shear stress is going to be negligible. It is also notable that the shear stress will be seen in the resin acts as the matrix to the fibers of the composite, and the composite itself will not be seeing any shear stress. For us, this means that the behavior of a longer tube will be dictated more by normal stresses in beam bending than by the shear in the beam; this is desirable for our tests so long as the beam does not reach a critical normal stress value during testing.

In another technical paper titled “Cantilever Beam Static and Dynamic Response Comparison with Mid-Point Bending for Thin MDF Composite Panels,” a study was undertaken that compared the estimated elastic moduli for a given samples using both classical static beam bending analysis and dynamic frequency response on the sample. For a collection of MDF composite samples, static and dynamic tests were run on each sample the statically obtained modulus of elasticity was compared to the results of the frequency test. In all reported cases, the dynamically obtained value for the modulus for a sample was slightly but measurably higher than its statically obtained value. The paper concluded by noting that the static modulus values obtained using a cantilever beam setup and a three-point bending setup correlated well with the values obtained using vibrational techniques. This highlights the potential for using vibrational analysis of our carbon fiber tubes to reinforce the estimates obtained using traditional bend test techniques.

Predictions

In preparation for the original senior project test in April, the structural group for the senior project team predicted that the flexural modulus of the carbon fiber tubes would be about 11.0 Msi based on simple volume-fraction calculations for the composite layup schedule of the tubes. This estimate was based on the conservative assumption that, of the 36 plies making up the tube, only 22 of those plies (the plies in the longitudinal direction of the tube) actually added to the stiffness of the tube. Previous testing of the tube yielded an estimated flexural modulus of 8.5 Msi, a value which was 34% lower than expected. With the test using strain gauges, we were expecting to see a value of between 11 Msi (based on our conservative estimates) and 13 Msi (an optimistic estimate that accounts for the 14 off-axis plies) based on volume fraction based calculations done for the tube.

Using the value from the conservative calculation, we expected to observe an oscillation frequency of around 57 Hz, ideally somewhat higher in order to be closer to the high end of the estimated 11-13 Msi. The value calculated is the value of the ideal natural frequency, which will have to be found using the observed frequency and adjusting for damping effects of the carbon tube. The raw value that is read will therefore be very slightly lower than 57 Hz, but well within the ballpark for the conservative estimate. The equation used assumes first mode of vibration, as that is the only mode we expect to be visible and readable. It also assumes that the tube inner and outer diameters are consistent throughout the entire length of the tube, as we took the average of the difference in order to solve for the moment of inertia. When we solved the equation for the modulus, we also went ahead and found the statistical error based on the precision of our measurements which resulted in a value of +/- 0.17 Msi.

Once again using the value from the conservative calculation, we are expecting to observe an oscillation frequency of around 11.5 Hz. The value calculated for this test is assuming the natural frequency, so we will had to be mindful of damping in order to get the natural frequency from the observed frequency. The equation used also assumes the first mode of vibration, so we had to avoid noisy sections of the data that could be indicative of multiple modes of vibration. The equation also required us to assume that the tube properties and geometry are constant across the length of the tube.

Methods

Shown below in Figure 2 is a photo of our set up for the three point bend test. For this test, we planned to use two roller ends for the boundary conditions in order to ensure that the tube will not be strained in the incorrect directions giving us inaccurate results. This was accomplished by taking the ends of the tube and laying them on top of two jack stands and wrapping them with paracord to ensure that they wouldn't slip off, but still had the ability to slide axially if they needed to. In order to gather the strain data, we used the Vishay P3 box in

conjunction with two strain gauges mounted across the tube from one another. This allows us to take static measurements with a half bridge configuration, doubling the sensitivity of the measurement to increase resolution and reducing any axial effects that might have been present. We then used a gym bag located exactly in between the two end conditions hung by paracord to hold the weights we had on hand, which were a combination of 20lb and 25lb weights. The gym bag seemed to hold over 225 pounds comfortably, so we loaded the bag carefully with the weights and measured the strain straight from the P3 box for each total weight.

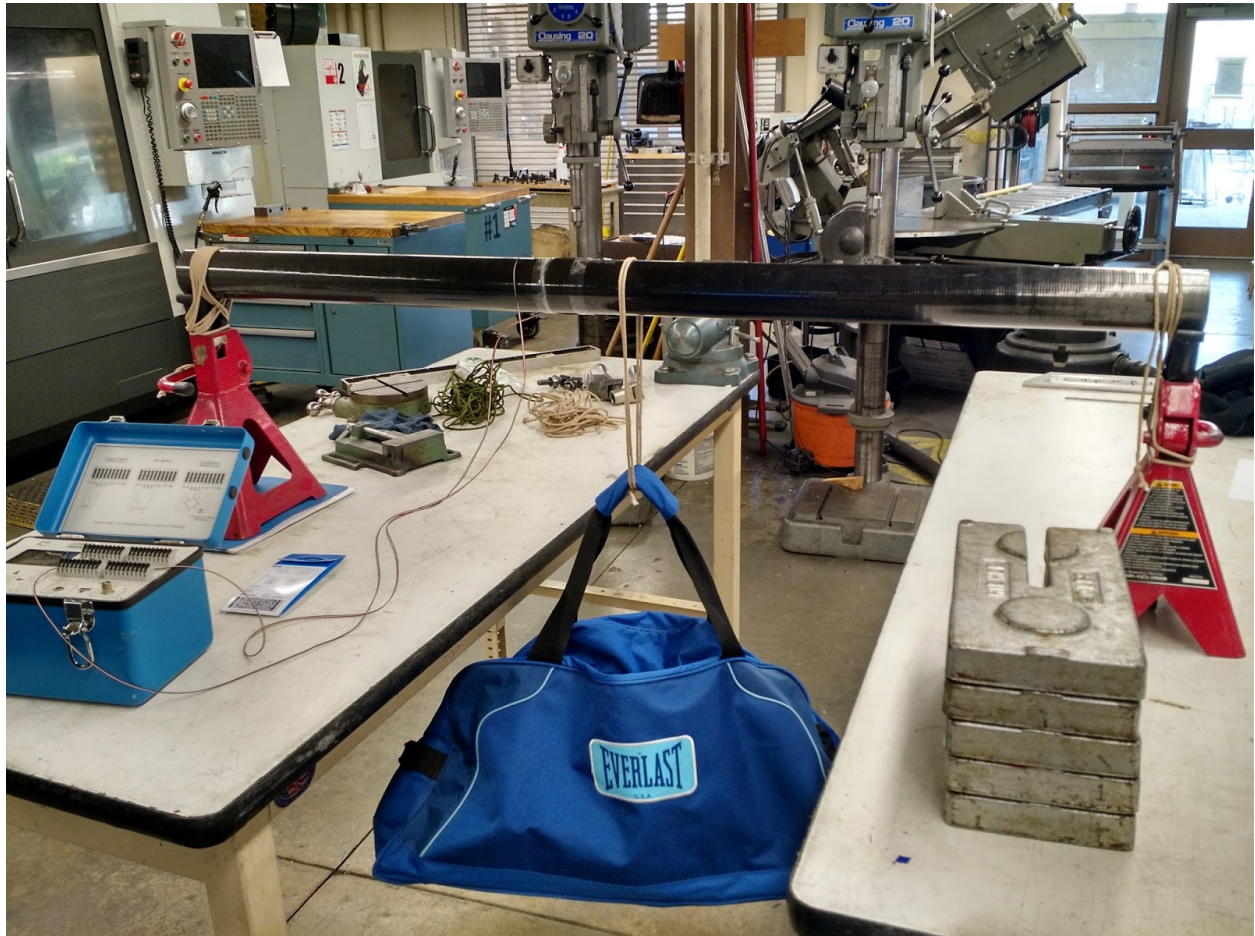


Figure 2. Our test setup for the three point bend test of the carbon fiber tube.

For the test, we did loading and unloading to check hysteresis, as well as prove that our setup would go back to zero. It also proved to be a safer method of deloading the tube plate by plate rather than trying to unload all 225+ pounds at once. In order to obtain flexural modulus from this method, we plotted strain vs. load applied and then found the stress on the beam where the strain gauges are located using Equation 1 below

$$\sigma = \frac{Pxh}{4I_x} \quad (1)$$

where σ is the stress at the strain gauges due to bending on the tube, P is the applied load, x is the distance from the nearest support to the strain gauges, and I_x is the second moment of area of the tube.

The stresses and strains for each load from our test were used to estimate the flexural modulus of the beam using the fundamental relationship shown below in Equation 2

$$E = \frac{\sigma}{\epsilon} \quad (2)$$

where E is the flexural modulus, σ is the stress at the strain gauges due to bending on the tube, and ϵ is the bending strain recorded with the strain gauges.

For the fixed-free vibration test, we used a 3-jaw rotary chuck to hold the tube in place. This allowed for a very secure grip on the tube and acted as a heavy test platform which would resist moving during the test. When gripping the tube, we opted to use a plug on the interior of the tube to make sure that the tube wouldn't crush under the force applied by the chuck to hold it securely. The test setup can be seen below in Figure 3.



Figure 3. Depiction of the cantilever vibration test performed on the carbon fiber tube.

In order to complete this vibration test, we also had to switch from the P3 box to the Poly DAQ in order to get a higher sampling rate for the accelerometer sensor that we needed to use. We bonded the accelerometer to the side of the free end of the tube with tape in order to make sure that we wouldn't strike it with the hammer for the testing. We discovered that the hammer caused the tube to move in the fixture, so we decided to use a finger to flick the tube to induce vibration without applying too much force to move the tube in the rotary chuck. The direct output from the external analog accelerometer was measured in millivolts, which we plotted against time to be able to see the oscillations caused by the flicking.

To obtain our estimates for the flexural modulus, we first went through our data and found the damped frequency of oscillation by measuring the time difference between two adjacent wave peaks of each trial. The equation used here can be found below in Equation 3

$$f_d = \frac{1}{T} \quad (3)$$

where T is the time between adjacent peaks and f_d is the damped natural frequency which was measured with the accelerometer for each trial. This damped natural frequency was used to calculate the natural frequency of the beam with Equation 4 below

$$f_d = f_n \sqrt{1 - \zeta^2} \quad (4)$$

where ζ is the damping ratio exhibited by the tube in our tests, f_d is the damped natural frequency of the tube, and f_n is the natural frequency of the tube. This damping ratio was calculated with the use of the log decrement method, shown below in Equations 5 and 6,

$$\delta = \frac{1}{n} \ln \frac{y(t)}{y(t+nT)} \quad (5)$$

$$\zeta = \frac{1}{\sqrt{1 + \left(\frac{\delta}{\pi}\right)^2}} \quad (6)$$

where δ is the log decrement for each trial, $y(t)$ is the amplitude for the initial peak being measured in each trial, $y(t+nT)$ is the amplitude of the next peak being measured in the same trial, n is the number of oscillations away the next measured peak is from the initial peak, and ζ is the damping ratio of the tube. In our trials we obtained an average damping ratio of 0.07; this damping ratio was the average of the damping ratios found during all of our test trials and was obtained using log decrement theory.

With the natural frequency of the tube calculated for each trial, we then used vibration theory to solve for the flexural modulus based on the frequency, material properties, and tube dimensions. Using Equation 7 below

$$f_n = \frac{\beta^2}{2\pi} \sqrt{\frac{EI_x}{mL^3}} \quad (7)$$

where E is the flexural modulus, I_x is the second moment of area of the tube, m is the mass of the tube, L is the length of the tube, f_n is the calculated natural frequency of the tube, and β is a constant that equals 1.8751 for a beam in the first mode of vibration, we were able to back out the flexural modulus of the tube for each trial in our testing.

For the free-free vibration test, we suspended the tube in air with a string of paracord running through the length of the tube. The experimental apparatus for this test can be found below in Figure 4.



Figure 4. Free-free test apparatus used for vibration testing the carbon fiber tube.

This allowed for the tube to not be constrained on either end to fulfill the free-free end conditions. In order to gather the data, we used both the external accelerometer in conjunction with the Poly DAQ and the Poly DAQ onboard accelerometer in different trials to compare them. In order to induce the vibration, we used a ball peen hammer and struck the tube at different parts of the tube. The location of the striking of the tube didn't seem to have any effect on the magnitude or frequency of the vibration at the location of the accelerometer.

For each trial, the accelerometer outputs were plotted against time in order to see the oscillations, and similarly to the previous test, we went through the data and found the damped frequency of oscillation by taking the inverse of the time difference between the peaks (see Equation 3 above). Using Equation 4 above, this damped frequency was converted to the beam's natural frequency with the damping ratio of 0.07 obtained using the log decrement relationship above in Equations 5 and 6. Finally, the experimental flexural modulus for each trial could be obtained with the use of Equation 7 above and a value of 4.733 for β to account for the change in end conditions for the tube.

Analysis and Results

Shown below in Table 1 are the results of our testing done on the carbon fiber tube.

Table 1. Estimates of flexural modulus for our tube in static and dynamic testing.

Test Method	Flexural Modulus [Msi]
Three point bend test	12.1 ± 0.05
Fixed-free (cantilever) vibration test	8.9 ± 0.8
Free-free vibration test	N/A

From the three point bend test, we were able to gather very repeatable data. We did a total of three trials, with the latter two trials including checks for hysteresis by unloading the weights and comparing the strain readings to those obtained during the loading sequence. The superposition of all data points from all three tests can be seen below in Figure 5.

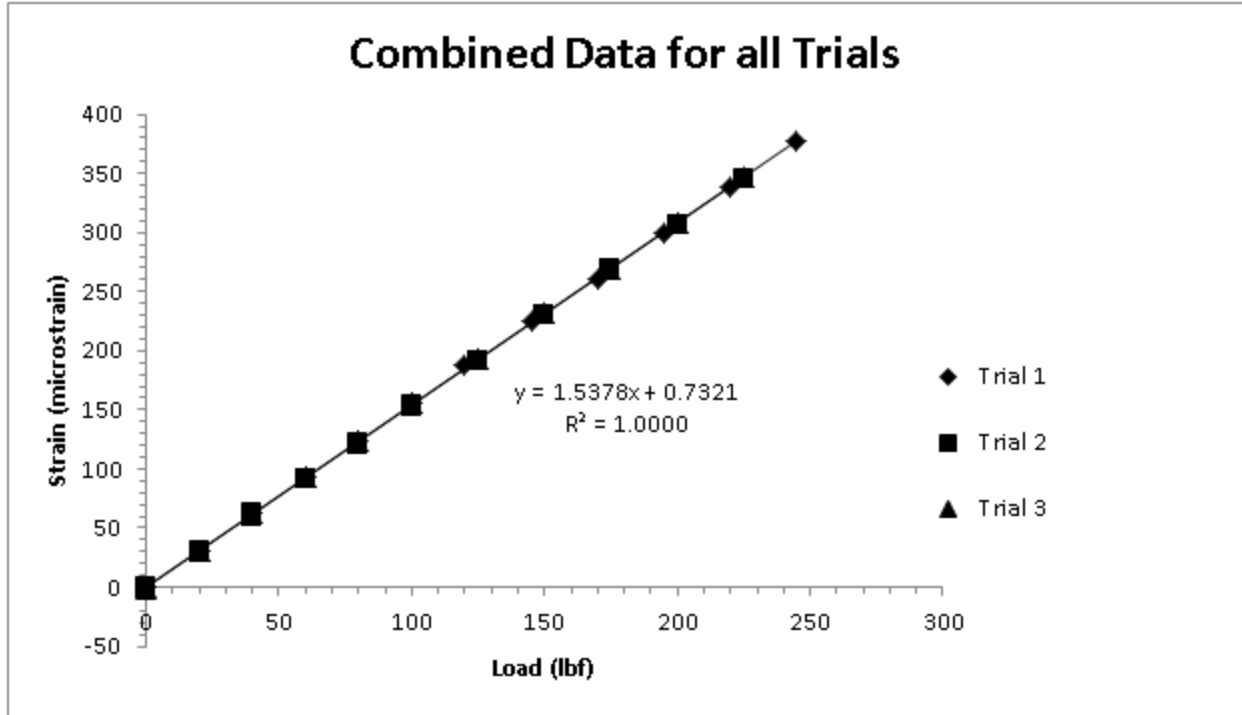


Figure 5. All test data from the three trials of the 3-point bend test on the same plot.

We were consistently within 2 microstrain for every single weight tested on both hysteresis checks, meaning that there was no observable hysteresis during the tests. Shown below in Figure 6 is a closer look at the second trial in the test where the strains measured during the loading and unloading of the tube were compared; the differences between the two data sets are imperceptible and the regression models for each are very close to one another. We ended up with a slight discrepancy at the zero point, with one trial ending at two microstrain lower than at the start and with another trial ending at one microstrain lower than the start point. This was assumed to be insignificant in light of how the strain measurements ranged from zero to nearly 400 microstrain.

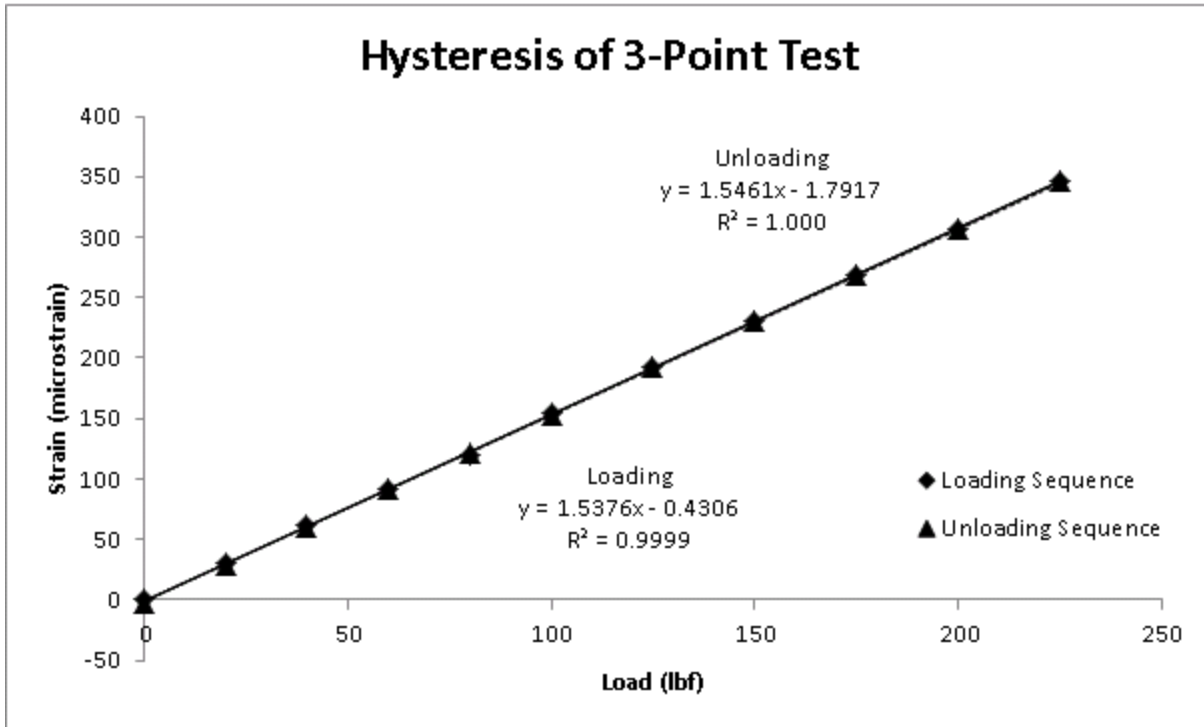


Figure 6. An examination of the loading and unloading of the tube to show negligible effects of hysteresis.

After backing out the applied stress on the tube for each applied weight in each trial, we were able to solve for the experimental flexural modulus by dividing the stress applied by the measured strain. Doing the relevant statistical work for a single sample, we estimate that the true modulus exists in the range between 12.03 and 12.14 Msi with 95% confidence, or that its estimated value is about 12.1 ± 0.05 Msi.

Plotting the stress vs. strain of the tube for the three trials, we obtain a similar estimate for the flexural modulus of 12.00 Msi; this value is slightly different because it is based on a regression model that includes the zero point of each trial. This zero point was neglected in the averaging method because including a modulus value of zero would artificially drive the modulus estimate down. Our official estimate for the flexural modulus is based on the earlier work described above which yields a value of 12.1 Msi; we feel as though this value is more accurate because, by neglecting the inconsistent loading step for each of our trials where a small weight is first applied to the tube, the data becomes slightly more consistent. The stress-strain curve for our tube can be found below in Figure 7.

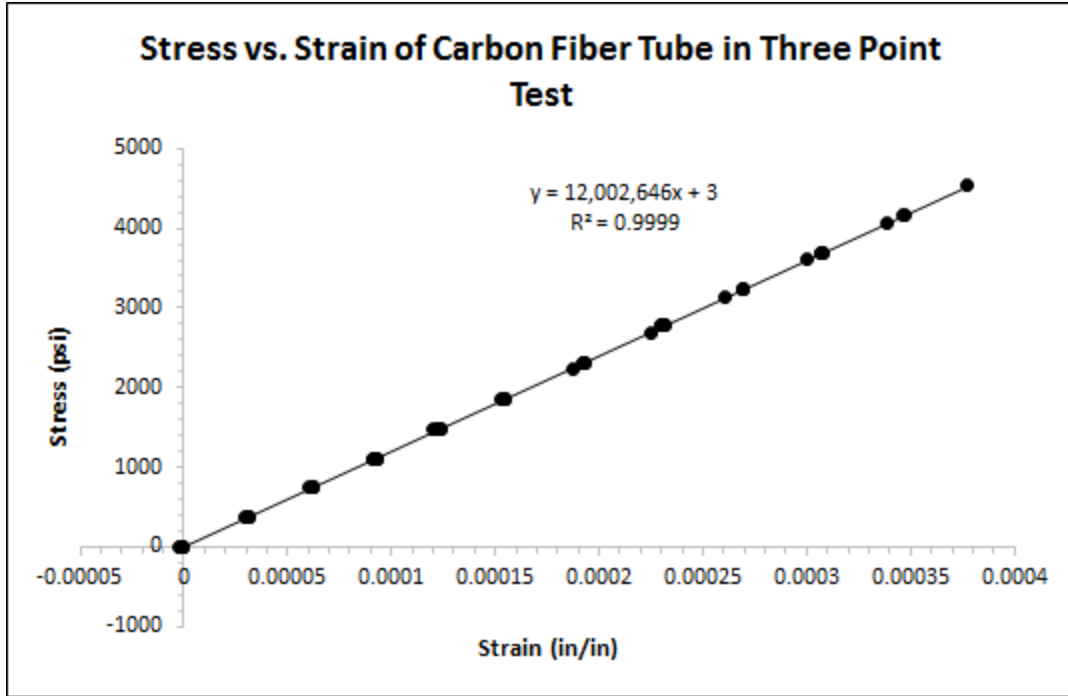


Figure 7. Stress-strain plot for the tube during the three point bend test.

Using a 2 sample t-test to compare this data to that obtained during the previous test done by the senior project team, we obtained a t-statistic of 56 for the test, resulting in an extraordinarily low alpha value which can be assumed to be zero for our purposes. This shows without any doubt that our estimate for the flexural modulus was different than the value obtained with the previous testing. Considering the methods used for our test, we can also determine that the testing with strain gauges is much more accurate. This value is also well within the spec of the tube that was designed and ordered, leading us to believe that the model we used was accurate and that our method of testing was reliable. To see our raw test data, the calculations that yielded our modulus estimates, and the load-deflection curves for each trial, please see Appendix A.

The fixed-free vibration test data gave us somewhat consistent modulus estimates once we neglected the first few noisy oscillations in each trial that was most likely caused by multiple higher order vibration modes manifesting themselves immediately after the excitation of the tube; a representative plot of our free-free vibration trials can be found below in Figure 8. The noisy signal at the very beginning of the impulse can be seen as well as the more consistent vibrations that follow the initial excitation.

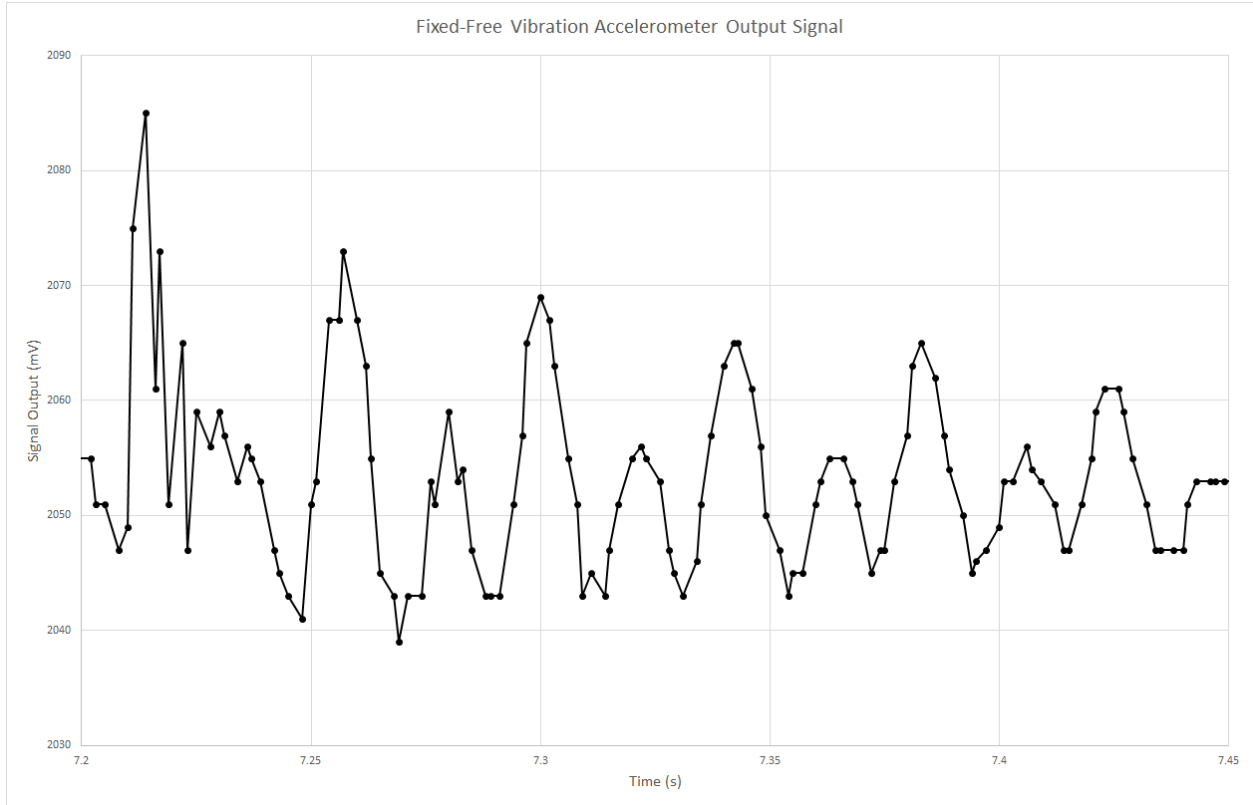


Figure 8. Representative sample of the vibration data we collected during the free-free test.

We were able to use the oscillations measured after the noise disappeared on each trial in order to find the frequency of oscillation for the first mode equation that we used in our model. We also proceeded to find the damping constant (estimated to be about 0.07) from the log decrement method in order to convert the damped frequency we measured into the natural frequency. This then allowed us to use the first mode equation effectively to solve for the flexural modulus. The predicted range of the true flexural modulus based on the fixed-free test was 8.1 to 9.7 Msi with 95% confidence, which on average is 70% lower than the expected value based on the static testing done. This could be caused by a number of factors, including the possibly insecure attachment of the accelerometer to the tube with clear tape, viscoelastic effects of the tube under high frequency vibration, or general operator error during the testing that may have resulted in the misreading of the vibration or in accidentally interfering with the vibration of the tube. The Nyquist frequency of the accelerometer sensor and PolyDAQ combination was far higher than the expected frequency that would be encountered in this experiment, so we did not run into any aliasing issues.

The free-free vibration test that was performed gave us data which we initially thought was usable, miraculously yielding a flexural modulus of 12.5 Msi to match our static testing and expectations for the measured natural frequency of about 8 Hz. However, we later realized that the data we had gathered was significantly aliased and was therefore useless for

our purposes. Shown in Figure 9 is an example of the data gathered with the aliased frequency.

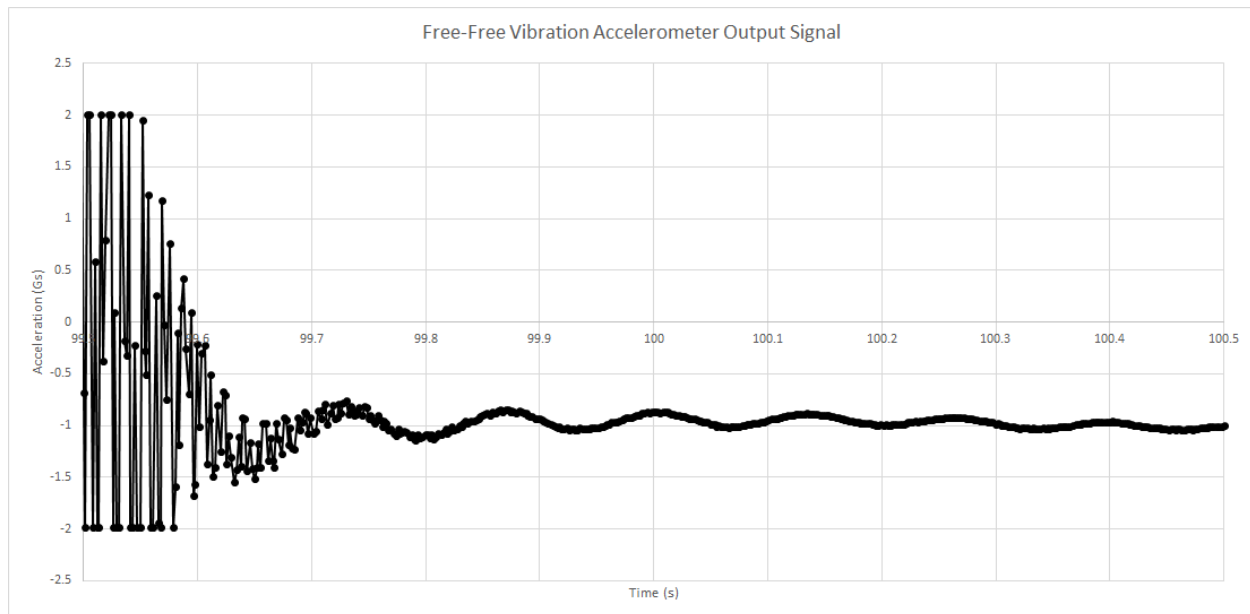


Figure 9. Representative sample of the aliased data from free-free vibration testing

We used the onboard accelerometer to gather the data as it gave us what seemed to be a good oscillation, and our calculations seemed to agree that the frequency should be much lower than that of the fixed-free test. However, we later realized that we had dropped a factor of 10^6 in our calculation, meaning that the actual frequency we should have expected to see several orders of magnitude higher. This meant we were not sampling at nearly a high enough frequency and that, instead of observing a natural frequency of about 8 Hz, we were instead seeing the results of heavy aliasing effects since we were recording data at a rate much lower than the minimum frequency needed to sample the data. This ultimately resulted in our data being entirely useless for the purposes of flexural modulus estimation. We recalculated the oscillation frequency from the model equation in order to find the correct necessary frequency of oscillation to have about 11.5-12 Msi flexural modulus and got a value of 363 Hz. This means that in order to properly be able to acquire the data for this test, we would have needed to have had an accelerometer and DAQ with a 750-800Hz sampling rate at the very least to sample fast enough to see the high frequency of oscillation of the tube.

Conclusion

From the data we gathered, we can confidently conclude that the three point bend test is an accurate test. We obtained an estimated flexural modulus of 12.1 ± 0.05 Msi with 95% confidence. This means that the tube almost certainly has a flexural modulus that is high enough for the purposes of the senior project without running the risk of the tube flexing too much, causing the onboard systems to malfunction and cause a crash with a human

passenger onboard. The data generated from the fixed-free vibration test was less than ideal, resulting in a calculated modulus of 8.9 Msi. This value is about 30% lower than the value obtained from the 3 point bend test which had very consistent, repeatable data and no observable hysteresis. There was also no usable data gathered from the free-free vibration test, as we underestimated the necessary frequency and used an accelerometer and DAQ that were not up to spec for the actual required frequency. In conclusion, we believe that the three point bend test yielded accurate results, and the estimates obtained from that test will be passed on to the senior project team. The dynamic testing results ranged from poor to miserable with the cantilever and free-free vibration tests, highlighting the difficulties in obtaining useful and accurate data with dynamic testing.

Appendices

- A. Three point bend test Excel spreadsheet and plots
- B. Cantilever vibration test Excel spreadsheet and plots
- C. Free-free vibration test Excel spreadsheet and plots
- D. Hand calculations
- E. Proposal and Progress Report

References

Sideridis, E., and G. A. Papadopoulos. Short-Beam and Three-Point-Bending Tests for the Study of Shear and Flexural Properties in Unidirectional-Fiber-Reinforced Epoxy Composites. Tech. Wiley InterScience, 19 Dec. 2003. Web. 18 May 2015.

Hunt, John F. "Cantilever Beam Static and Dynamic Response Comparison with Mid-Point Bending for Thin MDF Composite Panels." Bioresources. Com (2013): n. pag. Bioresources.com. 12 Nov. 2012. Web. 18 May 2015.
<https://www.ncsu.edu/bioresources/BioRes_08/BioRes_08_1_115_Hunt_ZGF_Cantilever_Beam_Bending_MDF_3244.pdf>.

Project Requirements

The customer requires the vehicle must:

- Be safe to operate
- Be free of electrical hazards
- Be Propeller Safe
- Have VTOL capability
- Be capable of sustained flight
- Be capable of unmanned flight
- Comply with all FAA regulations listed under FAR Part 103
- Facilitate a single passenger payload
- Be able to hover in a steady fashion
- Have a simple control interface
- Have a minimal footprint
- Be durable in regular and gentle operation
- Maximize usage of COTS parts
- Have an emergency shutdown

We have decided upon the following minimal technical specifications:

- Ingress protection rating of IP23W or better
- No exposed electrical connections
- Prop sides 100% shrouded
- Fully loaded weight-to-thrust ratio of 1 : 1.2
- Minimum of 10 minutes sustained flight
- Minimum range of remote operation of 100 feet
- Maximum weight of 254 pounds (including batteries/fuel)
- Must have a payload capacity of 200 pounds
- Max hovering angular deviation: 20° from horizontal
- Maximum of 6 Degrees of freedom in the control system
- Maximum footprint of 18 feet x 18 feet
- Minimum design factor of safety of 1.20
- Minimum of 50% of parts must be COTS

Quality Function Deployment

QFD: House of Quality
 Project: Electric Commuter Multicopter
 Revision: -
 Date: 16OCT14

Correlations	
Positive	+
Negative	-
No Correlation	
Relationships	
Strong	●
Moderate	○
Weak	▽
Direction of Improvement	
Maximize	▲
Target	◇
Minimize	▼

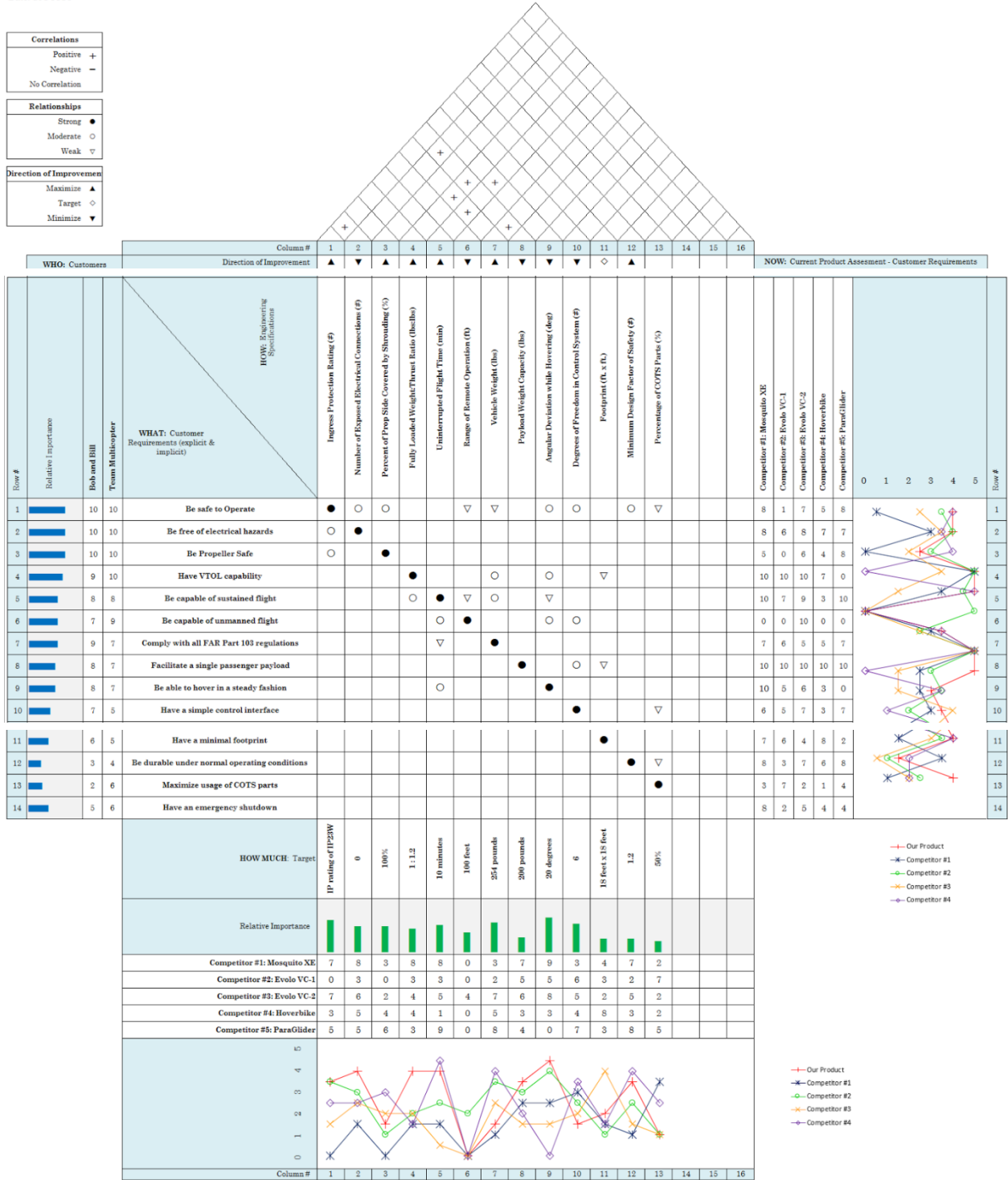


Figure 1. Quality Function Deployment (QFD).

Fuel Energy Density Chart

Table 1: Energy density of commonly used fuels. [54]

Fuels	Lower Heating Value (LHV) [1]			Higher Heating Value (HHV) [1]			Density
	Btu/ft ³ [2]	Btu/lb [3]	MJ/kg [4]	Btu/ft ³ [2]	Btu/lb [3]	MJ/kg [4]	grams/ft ³
Gaseous Fuels @ 32 F and 1 atm							
Natural gas	983	20,267	47.141	1089	22,453	52.225	22.0
Hydrogen	290	51,682	120.21	343	61,127	142.18	2.55
Still gas (in refineries)	1458	20,163	46.898	1,584	21,905	50.951	32.8
Liquid Fuels							
Crude oil	129,670	18,352	42.686	138,350	19,580	45.543	3,205
Conventional gasoline	116,090	18,679	43.448	124,340	20,007	46.536	2,819
Reformulated or low-sulfur gasoline	113,602	18,211	42.358	121,848	19,533	45.433	2,830
CA reformulated gasoline	113,927	18,272	42.500	122,174	19,595	45.577	2,828
U.S. conventional diesel	128,450	18,397	42.791	137,380	19,676	45.766	3,167
Low-sulfur diesel	129,488	18,320	42.612	138,490	19,594	45.575	3,206
Petroleum naphtha	116,920	19,320	44.938	125,080	20,669	48.075	2,745
NG-based FT naphtha	111,520	19,081	44.383	119,740	20,488	47.654	2,651
Residual oil	140,353	16,968	39.466	150,110	18,147	42.210	3,752
Methanol	57,250	8,639	20.094	65,200	9,838	22.884	3,006
Ethanol	76,330	11,587	26.952	84,530	12,832	29.847	2,988
Butanol	99,837	14,775	34.366	108,458	16,051	37.334	3,065
Acetone	83,127	12,721	29.589	89,511	13,698	31.862	2,964
E-Diesel Additives	116,090	18,679	43.448	124,340	20,007	46.536	2,819
Liquefied petroleum gas (LPG)	84,950	20,038	46.607	91,410	21,561	50.152	1,923
Liquefied natural gas (LNG)	74,720	20,908	48.632	84,820	23,734	55.206	1,621
Dimethyl ether (DME)	68,930	12,417	28.882	75,610	13,620	31.681	2,518
Dimethoxy methane (DMM)	72,200	10,061	23.402	79,197	11,036	25.670	3,255
Methyl ester (biodiesel, BD)	119,550	16,134	37.528	127,960	17,269	40.168	3,361
Fischer-Tropsch diesel (FTD)	123,670	18,593	43.247	130,030	19,549	45.471	3,017
Renewable Diesel I (SuperCetane)	117,059	18,729	43.563	125,294	20,047	46.628	2,835
Renewable Diesel II (UOP-HDO)	122,887	18,908	43.979	130,817	20,128	46.817	2,948
Renewable Gasoline	115,983	18,590	43.239	124,230	19,911	46.314	2,830
Liquid Hydrogen	30,500	51,621	120.07	36,020	60,964	141.80	268
Methyl tertiary butyl ether (MTBE)	93,540	15,094	35.108	101,130	16,319	37.957	2,811
Ethyl tertiary butyl ether (ETBE)	96,720	15,613	36.315	104,530	16,873	39.247	2,810
Tertiary amyl methyl ether (TAME)	100,480	15,646	36.392	108,570	16,906	39.322	2,913
Butane	94,970	19,466	45.277	103,220	21,157	49.210	2,213
Isobutane	90,060	19,287	44.862	98,560	21,108	49.096	2,118
Isobutylene	95,720	19,271	44.824	103,010	20,739	48.238	2,253
Propane	84,250	19,904	46.296	91,420	21,597	50.235	1,920

Decision Matrices

Table 2: Original Decision Matrix

Considerations	Safety		VTOL	Sustain Cruise	UAV	Weight (103)	Payload	Midflight Hover	Control System	Footprint	Durability	COTS	Flight Ability		Aesthetics	Novelty	Interest*	Cost	Total
	Prop	Flight											Speed	Maneuver ability					
Scaling Factor	6	2	6	4	3	6	3	2	2	4	1	2	2	2	1	1	3	4	54
X-copter																			
Design #1 - Under Body Prop Vehicle	2	3	6	4	4	3	3	5	4	3	3	4	2	5	3	3	5	4	201
Design #2 - Over Head Prop Vehicle Standing	4	3	5	4	4	2	3	5	4	3	3	4	2	5	5	3	5	4	203
Design #3 - Over Head Prop Vehicle Sitting	4	3	5	4	4	2	3	5	4	3	3	4	2	5	4	3	5	4	202
Design #4 - In line Props	2	3	5	4	4	3	3	5	4	4	3	4	2	5	5	3	5	3	197
Design #5 - Quad Flaps	4	3	5	4	4	2	3	5	3	3	3	3	4	5	5	3	5	3	199
Fixed Wing																			
Design #1 - N-Plane	3	4	0	5	4	2	4	0	5	3	5	5	5	3	4	2	2	5	167
Design #3 - Folding Wings	3	4	0	5	4	2	4	0	5	4	5	3	5	3	4	2	2	5	167
Auto-Gyro																			
Design #1 - N-Gyro	3	4	1	4	2	4	3	0	3	4	4	4	4	4	2	4	3	5	172
Design #2 - With Power	3	4	4	4	2	3	3	1	2	4	4	3	4	4	2	4	3	4	178
Design #3 - Ducted Fan Under	2	4	4	4	2	3	3	1	2	4	4	3	4	4	2	4	3	4	172
Lighter-Than-Air																			
Design #1 - Blimp	4	5	5	4	4	1	1	5	4	1	5	4	1	1	2	3	1	1	152
Design #2 - N-Blimp	4	5	5	4	4	1	1	5	4	1	5	4	1	1	2	3	1	1	152
Parachute																			
Design #1 - Paramotor	4	4	1	3	0	5	2	0	4	3	4	5	3	4	2	2	2	5	164
Design #2 - N-Paraglider	4	4	1	3	0	5	2	0	4	3	4	5	3	4	2	2	2	4	160
Combinations																			
Design #1 - Raft/N-Copter	3	3	5	4	4	3	2	5	4	4	3	3	1	4	3	5	3	3	188
Design #2 - MultiGyro/Copter	3	4	5	4	4	3	3	4	3	4	3	2	4	4	3	5	4	3	196
Design #3 - Blimp/MultiCopter	3	4	5	4	4	3	2	5	4	2	3	3	1	4	2	2	2	2	171
Design #4 - In Wing Props	3	3	4	5	4	3	3	2	2	3	4	1	5	3	4	5	3	3	179
Design #5 - Rotating Props/Osprey	2	2	4	5	4	3	3	2	2	3	3	1	5	3	5	4	3	2	166
Competitors																			
VC1	0	3	5	4	4	3	3	5	4	3	2	4	2	4	2	5	2	4	172

Table 3: Reduced decision matrix of top five design concepts

Considerations	Safety		VTOL	Cruise	UAV	Weight	d	r	s	t	y	COTS	Flight Ability		Aesthetics	y	*	Cost	l
	p	t											d	ty					
Scaling Factor	6	2	6	4	3	6	3	2	2	4	1	2	2	2	2	2	2	3	4
Design #1 - Multicopter (under body props)	2	3	6	4	4	3	3	5	4	3	3	4	2	5	3	4	5	4	209
Design #2 - Multicopter (overhead props)	4	3	5	4	4	2	3	5	4	3	3	4	2	5	5	4	5	4	213
Design #3 - Hoverbike/Hoverboard	2	3	5	4	4	3	3	5	4	4	3	4	2	5	5	4	5	3	207
Design #4 - Powered VTOL Gyrocopter	3	4	4	4	2	3	3	1	2	4	4	3	4	4	2	4	3	4	184
Design #5 - Multi-Gyrocopter	3	4	3	4	4	2	3	4	3	4	3	2	4	4	3	5	4	3	186

Schedule / Gantt Chart

Table 4: Team Multicopter Schedule

ID	Name	Duration	Start	Finish	Predecessors
1	Testing	8,33d?	01/27/2015	03/02/2015	
2	Structure	8d?	01/27/2015	03/02/2015	
3	Order all parts by	3d?	01/27/2015	02/06/2015	
4	Arm, tubing, weld, adhesive combined testing	1,67d?	02/09/2015	02/13/2015	3
5	Drop Test	1,67d?	02/16/2015	02/23/2015	4
6	Evaluation of results	1,67d?	02/23/2015	03/02/2015	4,5
7	Motor	6d?	01/28/2015	02/20/2015	
8	Order all parts by	1d?	01/28/2015	01/30/2015	
9	Electrical safety	1d?	02/02/2015	02/04/2015	
10	Motor test plan approval	1d?	02/02/2015	02/04/2015	
11	Circuitry assembly	1d?	02/02/2015	02/04/2015	8
12	Test jig assembly	1d?	02/04/2015	02/06/2015	8
13	Test assembly	1d?	02/09/2015	02/11/2015	12
14	Thrust, power, heat test	1d?	02/12/2015	02/16/2015	13
15	Evaluation of results	1d?	02/16/2015	02/22/2015	9,10,14
16	Controls	8,33d?	02/04/2015	03/02/2015	
17	Flight controller/motor layout selection	1d?	02/04/2015	02/06/2015	
18	Scale model design completed	1d?	02/09/2015	02/11/2015	17
19	Order all parts by	1d?	02/12/2015	02/16/2015	18
20	Assembly of structure, controls, power	1d?	02/16/2015	02/22/2015	18
21	Test of flight stability/control	1d?	02/23/2015	02/25/2015	20
22	Evaluation of results	1d?	02/26/2015	03/02/2015	21
23	Critical Design Review	3d?	01/27/2015	02/06/2015	
24	Completed report	1d?	01/27/2015	01/29/2015	
25	Class presentation	1d?	01/30/2015	02/03/2015	24
26	Sponsor presentation	1d?	02/04/2015	02/06/2015	25
27	Adjust/finance Design	1,67d?	02/09/2015	02/13/2015	26
28	Manufacturing	17,33d?	02/27/2015	05/11/2015	27
29	All parts ordered by	1d?	02/27/2015	03/03/2015	
30	Structure	15d?	03/02/2015	05/01/2015	
31	Fixture/mount fabrication	10d?	03/02/2015	04/10/2015	
32	Carbon tube sizing/fitting	10d?	03/02/2015	04/10/2015	
33	Prop rings	10d?	03/02/2015	04/10/2015	
34	Suspension adjustments	10d?	03/02/2015	04/10/2015	
35	Assembly	6d?	04/01/2015	04/24/2015	31,32,33,34
36	Testing/safety verification	1d?	04/29/2015	05/01/2015	35
37	Power/Motor	3d?	03/11/2015	03/23/2015	
38	Circuitry to place batteries in parallel/series modules	1d?	03/11/2015	03/13/2015	
39	Battery mounts	1d?	03/11/2015	03/13/2015	
40	Motor mounts	1d?	03/11/2015	03/13/2015	
41	Drill prop hole patterns	1d?	03/11/2015	03/13/2015	
42	Testing (similar to first motor test)/safety verification	2d?	03/16/2015	03/23/2015	38,39,40,41
43	Controls	2,67d?	03/11/2015	03/20/2015	
44	Vibration isolation unit	1d?	03/11/2015	03/13/2015	
45	Electrical/heat shielding	1d?	03/11/2015	03/13/2015	
46	Motor configuration settings in software	1d?	03/11/2015	03/13/2015	
47	Wireless data transfer to record flight conditions	1d?	03/18/2015	03/20/2015	46
48	Assembly	9,67d?	04/01/2015	05/11/2015	
49	Combine power circuitry with controls	1d?	04/01/2015	04/03/2015	42,47
50	Combine power circuitry with structure	1d?	04/06/2015	04/08/2015	49
51	Final assembly	1d?	05/04/2015	05/06/2015	36,50
52	Safety verification	1d?	05/07/2015	05/11/2015	51
53	Testing	4d?	05/13/2015	05/28/2015	27
54	Tethered thrust	1d?	05/13/2015	05/15/2015	51
55	Stability	1d?	05/18/2015	05/20/2015	54
56	Hover	2d?	05/21/2015	05/28/2015	55
57	Expo	0,33d?	05/29/2015	05/29/2015	
58	Final Project Report	0,33d?	06/05/2015	06/05/2015	

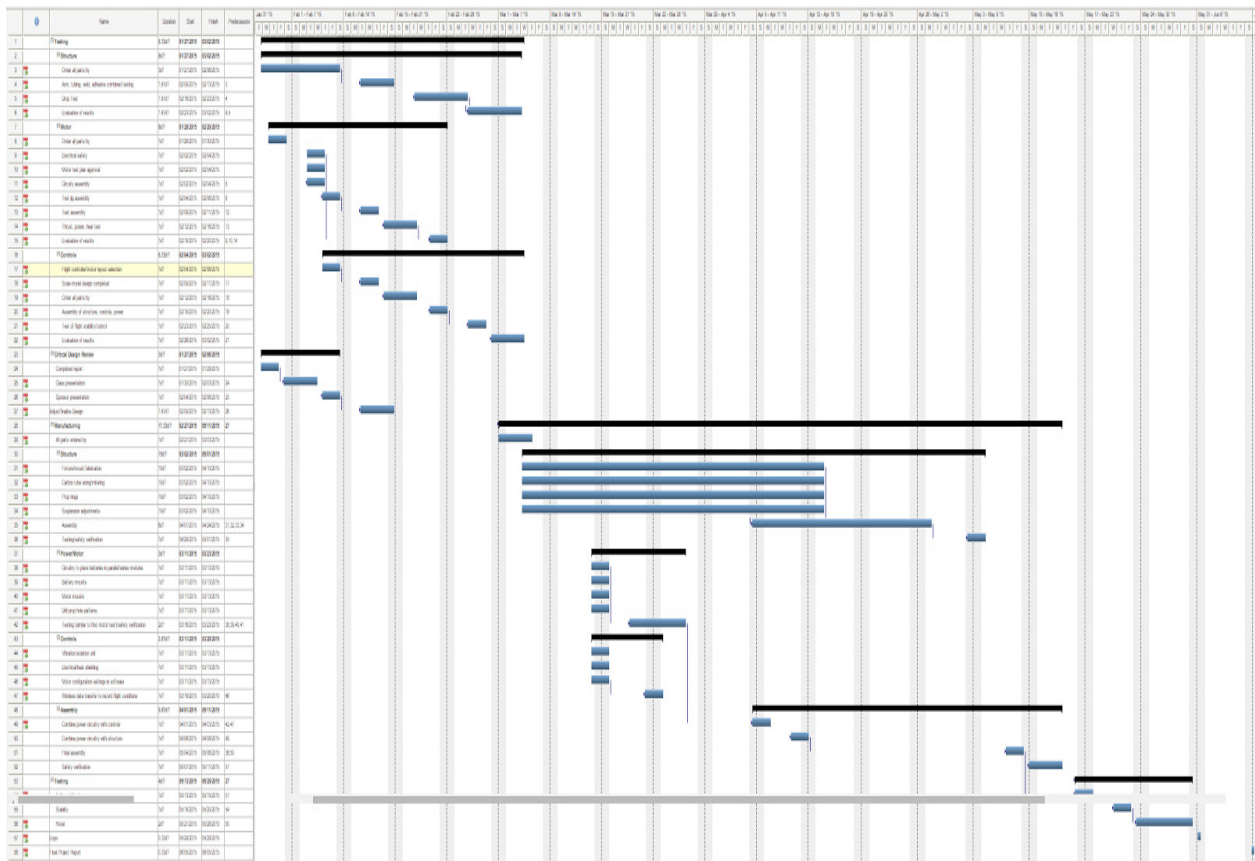


Figure 2: Gantt Chart Layout

Table 4: Revised FMEA for Critical Design Review

Item / Function	Potential Failure Mode	Potential Effect(s) of Failure	Severity (1-10)	Potential Cause(s) / Mechanism(s) of Failure	Occurrence	Criticality	Recommended Action(s)	Actions Implented into Critical Design
Structure	Bracket joints debond	Frame comes apart, crash, pilot dies	10	Impacts, fatigue, not enough bond length, severe bending or torsion, improper assembly	7	70	High Safety Factor, clean/prep surfaces before bonding	Calculated necessary bonding surface area. High Safety Factor
	Carbon frame cracks	Loss of strength, frame breaks, crash, pilot dies	8	Brackets crush arms, UV exposure, high/low temperature exposure, moisture exposure, impacts, defective manufacturing	9	72	Limit outdoor exposure, Inspect tubes	Limit outdoor exposure, Inspect tubes. Safety Factor above 1.2. Designed to prevent impacts
	Structure gives user splinters or cuts user	User has splinters or a cut	2	Structure has cracks or exposed spikes	2	4	Visual check of structure	Visual check of structure. Frequent maintenance
	Structure flexes too much	Sensors misread, crash, pilot dies	7	Hits vibrational mode, weather occurences, tubes not stiff enough	7	49	Shorter and stiffer arms	Calculated deflection at tip ends to not exceed 8 degrees
	Fasteners loosen	Structure falls apart, projectile components, crash, pilot dies	5	Broken fasteners, vibration, improper manufacturing	8	40	Use Loctite®, nyloc, or cotterpins to keep fasteners in place	Using Loctite® thread locker
	Structure twists in air	Structure breaks, motors become unaligned, crash, pilot dies	7	Motors thrust in opposite directions, structure hits vibrational mode, impact on spar	4	28	Layup schedule designed to resist some torsion	Layup schedule includes enough 45 degree plies to counteract the small torsion on main carbon arms
	Structure twists on ground	Pilot injury, structure breaks, motors become unaligned	5	Impact on spar, thermal expansion, warping	7	35	Layup schedule designed to resist some torsion	Layup schedule includes enough 45 degree plies to counteract the small torsion on main carbon arms
	Structure catches fire	Severe user injury or death, loss of structure	7	Batteries combust or wires short to structure, external flame sources	4	28	Ensure electrical insulation, separate batteries from frame	Seperating the batteries from the frame by fiberglass, an inert material
Motors	Mismatched torque on the spar arms	Excess stress on structure	3	Motor is mounted at the wrong angle or is connected improperly	7	21	Double-check construction	Proper control analysis, Ensure proper visual inspection
	Improper thrust direction	Instability, loss of control, crash, pilot dies	7	Motor is mounted at the wrong angle or is connected improperly	4	28	Double-check construction	Proper alignment of structural equipment with accurate manufacturing techniques
	Electric connection failure	Loss of power, loss of user control, instability, crash, pilot dies	7	Corrosion in electrical wiring, improper installation	4	28	Use crimps for connections, check connections	Proper electrical hard wiring. Crimps, connectors, and check for no exposed wire
	Motor overheats	Loss of power/potential motor burnout	4	Running motor too hard for extended periods of time	7	28	Add heat sinks to motors, include speed governor in control system	Inrunner motors have heat sinks on the outer diameter to increase heat transfer convection.

Table 4: Revised FMEA for Critical Design Review

	Mechanical failure	Loss of power/ considerable reduction of power	7	Running motor too hard, corrosions damage, fatigue	4	28	Properly size motors, do routine maintenance, protect motor during storage	Motors are able to dissamble and be assessed for maintenance. In addition, control system account for redundancies incase one motor fails during flight. Motors are powerful enough and oriented in such a way that they are capable of redundancy
	Electrical failure	Loss of power/ considerable reduction of power	7	Drawing too much power, corrosion, short circuit	4	28	Properly size electrical components, insulate/protect components well	Proper wire and wiring components. Use electrical tape or fiber glass insulation on every part that has the potential of abrasion.
Propellers	Propeller cracks or breaks	Severe injury or death, loss of thrust	8	Debris, fatigue, impact, interference with prop rings	7	56	Tolerance between prop and ring, shrouding the prop	The propellers are made out of carbon fiber (high strength material, compared to wood which is not). The tolerance between prop and ring is 1.5" so interference is mitigated.
	Propeller disengages from motor	Severe injury or death, loss of thrust	10	Debris, hub failure, assembly error, manufacturing defect	2	20	Ensure prop fastener is tightened thoroughly	The propellers will be rigidly attached to the Joby motors by 6 screws. Visual inspection and frequent maintanence is required
	Vibrating Propellers	Vibrations/pote ntial motor damage and decreased performance	5	Prop imbalance	8	40	Operate at low speeds to determine imbalance	Test #1 of propulsion is to spin propellers at low speeds to observe any structural imbalance in the props.
	Propeller hub loosens	Vibration, non uniform thrust, loss of thrust	7	Improper installation, loose fasteners	4	28	Ensure prop fastener is tightened thoroughly	The propellers will be rigidly attached to the Joby motors by 6 screws. Visual inspection and frequent maintanence is required
	Propellor hub cracks or breaks	Severe injury or death, loss of thrust	9	Vibration, fatigue, impacts	4	36	Protect hub from outside objects	The entire propeller will be surrounded by a concentric carbon fiber ring and in addition a metal mesh grating will be wrapped around the ring to restrict large objects coming into contact with the propellers
Controls	Signal interpretation failure	Loss of control (catastropic failure), confuse current state, state-lock, motor shut-off	8	Picks up wrong signal, noise sensitivity, reversed connections, instability, lack of sensitivy, hardware failure, out of range of coms, attenuation	7	56	Mount control system on vibration isolator	Proper electrical hard wiring. Crimps, connectors, and check for no exposed wire. The proper control system will also be implemented
	Signal failure	Catastrophic failure, motor shut-off, state- lock	10	Software, hardware, or control loop malfunction, unable to reset, out of range of coms., system reset/shut-off, attenuation	5	50	Redundant hardware and system checks	System analysis before hand. Check control boards for proper data analysis. Proper electrical hard wiring. Crimps, connectors, and check for no exposed wire.

Table 4: Revised FMEA for Critical Design Review

	Reset failure	In-flight shut off, crash, death or serious injury	8	Power surge, static shock, electrical short, unable to reset	4	32	Redundant hardware and system checks	System analysis before hand. Check control boards for proper data analysis. Proper electrical hard wiring. Crimps, connectors, and check for no exposed wire.
	Software/compiling failure	Unable to update software or device drivers	4	Improper software/hardware interface	4	16	Selection of compatible software, firmware, hardware	System analysis before hand. Check control boards for proper data analysis. Proper electrical hard wiring. Crimps, connectors, and check for no exposed wire.
	Navigation failure	Crash, death or serious injury	4	Throttle, pitch, and/or yaw "stick" in place, loss of GPS signal, out of range of coms., attenuation	6	24	Establish communication towers, and multiple modes of communication	GPS onboard. System analysis before hand. Check control boards for proper data analysis. Proper electrical hard wiring. Crimps, connectors, and check for no exposed wire.
Electronics	Battery Deterioration	System failure	5	Low temperature exposure, high temperature exposure, moisture exposure	7	35	Battery charge schedule and chart/Battery storage plan	Battery charge schedule and chart. Battery storage plan. After each flight the batteries will be charged.
	Battery nonstart	System failure	3	Low temperature exposure, incorrect wiring, moisture exposure	7	21	Battery storage plan	Proper electrical hard wiring. Crimps, connectors, and check for no exposed wire. The proper control system will also be implemented. Battery charge schedule and chart/Battery storage plan
	Overvoltage	Motor failure, combustion	5	Incorrect battery configuration, incorrect circuitry, carbon conductivity	7	35	Circuitry review	System analysis before hand. Check control boards for proper data analysis. Proper electrical hard wiring. Crimps, connectors, and check for no exposed wire.
	Undervoltage	System failure	7	Forgot to charge, power draw too high, parasitic discharge	7	49	Circuitry review	System analysis before hand. Check control boards for proper data analysis. Proper electrical hard wiring. Crimps, connectors, and check for no exposed wire.
	Overcurrent	Undervoltage, battery deterioration, combustion	5	Short circuit, incorrect circuitry, carbon conductivity, moisture exposure	6	30	Circuitry review	System analysis before hand. Check control boards for proper data analysis. Proper electrical hard wiring. Crimps, connectors, and check for no exposed wire.
	Battery puncture	Power failure, explosion	8	Impact, structure failure	4	32	Battery protection box or relocation of batteries	Fiber glass will be implemented between the batteries and the structure
	Battery charge failure	Uneven discharge, loss of power, battery deterioration	5	User error, incorrect circuitry, incorrect battery configuration, parasitic discharge	7	35	Battery charge schedule and chart	Battery charge schedule and chart. Battery storage plan. After each flight the batteries will be charged.

Table 4: Revised FMEA for Critical Design Review

	Reverse voltage	Electronics failure	5	Incorrect battery configuration, incorrect circuitry	4	20	Circuitry review	Proper battery configuration. System analysis before hand. Check control boards for proper data analysis. Proper electrical hard wiring. Crimps, connectors, and check for no exposed wire.
	Sensor or control system failure	System failure	7	Interference with control system, magnetic instruments, and radio frequency instruments	7	49	Shield control system	The flight controller will be attached directly under the seat of the user in a well insulated metal box.
	Electronics overheats	System failure, combustion, battery deterioration, electronics deterioration	8	Incorrect circuitry, incorrect wiring, overcurrent, short circuit, high temperature exposure	7	56	Heatsink components	Additional heatsinks will not be considered due to weight restrictions.
User	Loss of consciousness	Loss of control, serious death or injury	10	G Forces, sickness, impact, vertigo, intoxication, drug impariment	1	10	Limit G-Forces, user warnings	This is a design for 1.2G. Control system will be intuitive so user can mitigate the likely hood of human error, therefore less likely to crash
	Over response	Crash, serious death or injury	8	Distractions, muscle spasms	7	56	Control compensation	Control system should respond intuitively to the human sensors
	Under response	Crash, serious death or injury	8	Distractions, muscle spasms	5	40	Control compensation	Control system should respond intuitively to the human sensors
	Misread instruments	Structure failure, possible death or injury	6	Visual impairment, use misunderstanding	4	24	Clear and visible instrument panel (lighted), accesibility options	Control system will be intuitive, with a throttle on the side of the user and a toggle in the middle.
	Smoke Impairment	Serious burns, injury or death	10	Motor and/or electrical fire	3	30	Fire extinguisher. Orientation of user with respect to props	propellers are oriented off-center from the user, it is less likely the trajectory of the smoke will come in contact with the user than if he or she were directly behind the propellers

Electric Commuter Multicopter Motor and Propeller Test Plan and Safety Document

January 26, 2015

Team Members:

Alex O'Hearn

Art Norwood

Blake Sperry

Ike Sheppard

Jarrell Washington

Kyle Kruse

Marley Miller

Oliver Kunz

Sam Juday

Propeller Test Plan

Purpose

The Electric Multicopter senior project intends to perform a motor test. The purpose of the motor test will be to analyze the performance of an 80CC Turnigy Rotomax hobby motor spinning an Xoar 30x10 propeller, and compare its performance to the performance of an industrial motor, the JM1S motor from JobyMotors, using the same propeller. The test will be an attempt to measure; the thrust provided by the motor, power consumption of the motor, and the ability of the motor to accelerate the propeller.

Equipment

The equipment required for this test is:

- 80CC Turnigy Rotomax motor
- Xoar 30x10 propeller
- Electronic Speed Controller (ESC)
- Throttle controller
- 2 7S batteries
- 100ft of 2 gauge wire
- Emergency Disconnect Switch
- Wire connectors
- 20ft of wooden 2x6s
- Hinge
- Screws
- Thermocouples
- Non-contact Tachometer
- Scale
- Protection wall
- Voltmeter
- Clamp ammeter
- Table or alternative solid test base

Propeller Test Plan

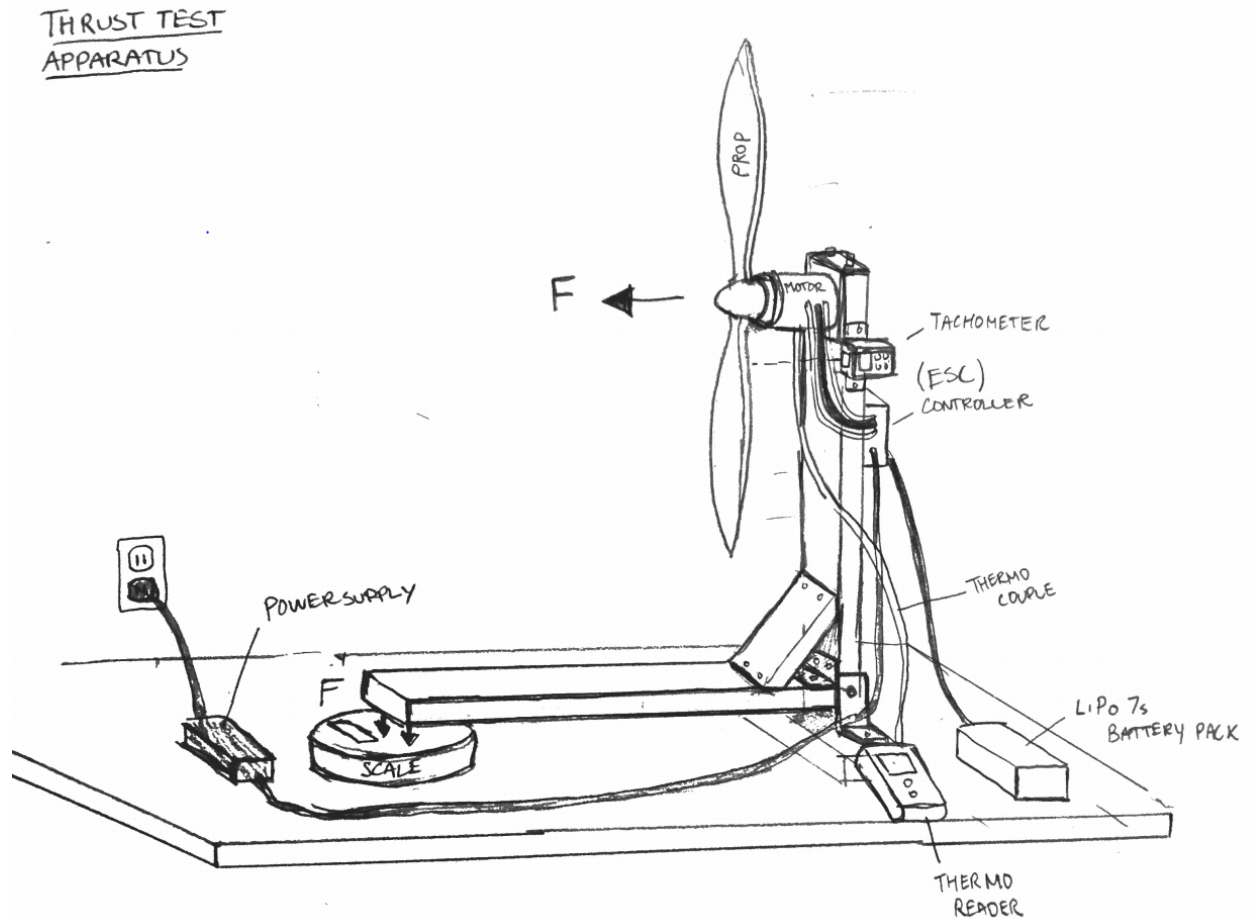


Figure 1. Test Setup Conceptual Sketch

Setup and Procedure

The test setup is shown in figure 1. The thrust of the propeller will create a moment around the hinge. The scale will provide the reaction force offsetting the moment created by the propeller, and will then be able to record the thrust of the propeller. Thermocouples will be mounted on the motor base near the coils to measure the coil temperature. A non-contact tachometer will be used to measure the rotation speed of the propeller. The scale will measure the force produced by the propeller. Both the scale, thermocouple reader, and the tachometer will be filmed so that the data can be analyzed later.

The following are general procedures for each of the three tests we wish to run. A more detailed step-by-step procedure for each test can be found in appendix 1.

The first test will be a general performance and system calibration test. In order to perform the first motor test the motor speed will be slowly throttled through its power range. Using this curve the desired setting which leads to 50lbs of thrust can be determined. This test will also serve as the initial balancing test to ensure that catastrophic vibrations do not occur since the speed will be increased slowly and if vibrations are noticed the motor can be quickly shut off via a kill switch.

Propeller Test Plan

The second test will be the propeller acceleration test. This test will be performed by setting the throttle about 20% below the 50lbs thrust operating point, and then increasing the throttle to the 50lbs thrust operating point and measuring the response time. The throttle will then be increased another 20 percent and the response time will be recorded.

The third test will be the steady state test at the 50lbs thrust operating point. We will run the motor for the remainder of the battery life (we expect only a few minutes) to test if the motor can sustain the load for a sustain time. The final temperature of the motor will be measured to make sure the motor does not overheat. The power draw of the motor will also be recorded to ensure that the motor performance is not decreasing over time.

Data Acquisition

The instruments used to measure the data for this test are a non-contact thermometer, thermocouples, a bathroom scale, voltmeter, and clamp ammeter. These instruments will be recorded by video cameras (phone cameras) to allow for the data to be analyzed later and for the test operators to remain safely behind a protective wall during the test.

The reporting rate of the instruments will need to be fast enough to record the propeller acceleration during the response time test for the motor. The JM1S motor was able to accelerate the propeller at a rate of 250 RPM/s, and a 20% increase in thrust corresponded to approximately a 400 RPM increase in speed so the acceleration should take approximately 1.5 to 2 seconds.

The most important measurement to record during the acceleration is the thrust. The RPM, temperature, voltage, and current are most important for the steady state tests, and to confirm that our acceleration started and stopped at the correct points so a slow reporting rate can be acceptable. The thrust measurement will need to report values a couple times per second in order for the acceleration tests to be worthwhile. In order to get the reporting speed a bathroom scale with a needle will be used, so the reporting rate will be equal to the frame per second rate of the camera filming the scale.

For all other tests the changes in the values being measured will be small and over a long time period so the report rate of the instruments will not be an issue.

Expected Results

We expect the results of the test, will show that the propeller will produce 50lbs of thrust at about 4500 RPM with a power draw of between 5.5 and 6kW. We do not expect that the performance of the motor will decrease over time since we should be operating below the max continuous operating conditions for the motor. For the acceleration test we expect that the motor will accelerate around 250 RPM/s. If the 80CC Turnigy Rotomax motor is able to closely match these performance criteria it will show that the motor is a suitable substitute for the industrial JM1S JobyMotor product in the final design.

Safety Concerns and Solutions

There are various safety risks involved during the test. The safety risks can be grouped into mechanical risks and electrical risks. The mechanical risks are; propeller breaking, critical vibrations, and flying debris strikes. The electrical risks; are overheating/overpowering, short circuits, electrocution risks.

Propeller Test Plan

If the propeller were to break the immediate result would be a large rapidly moving flying object. The broken piece of the propeller could cause serious harm to anyone it strikes. In addition the propeller would become very imbalanced, and would quickly cause the destruction of the test setup.

In order to mitigate the risks of the propeller breaking, first the propeller will be inspected before use for any defects or signs of weakness. An emergency shutoff switch will be installed so that power can quickly be removed from the motor to hopefully prevent damage to the test structure and components in case of a broken propeller. To reduce the risk of harm to the test operators the operators will stand out of the plane of rotation of the propeller. In addition the controls for the motor will be lead at least 50ft away from the test stand to allow for the operators to stand behind either a temporary wall or building for protection.

The risk of damage due to vibrations developing will be reduced though an initial balance test for the propeller. Also the speed of the motor will be increased slowly during the first test. If vibrations are detected the motor will be stopped, and additional stiffening will be added to the test structure and the propeller will be checked again for imbalance.

Flying debris are likely to pose the biggest risk during testing. If some sort of flying debris were to strike the propeller, damage could occur that leads to the propeller breaking and or critical vibrations. In addition flying debris could be shot through the propeller, or deflected off the propeller at very high speeds posing a significant safety hazards. The first step to reduce the risk from flying debris is to ensure the test setup is done in an area clear of lose debris. The area should be cleared of lightweight objects, such as sticks leaves and small rocks, which could easily be blown by the propeller. To protect against injury from the flying debris the operators will be standing behind a temporary wall or building for protection. The operators will also not be positioned behind the propeller, where most of the flying debris would be expected to fly.

To protect against overheating or overpowering any device in the test system we will carefully monitor the voltage and current. The systems that are at risk of overheating or overpowering are the motor, ESC, wires, and batteries. The limiting capacities of each device is listed in Table 1. Through careful monitoring and clearly known limits the risk of overheating or overpowering should be very low.

Table 1. Limiting capacities for devices used in test.

	Max Voltage	Minimum Voltage	Max Current	Max Power
Motor	51.8V	NA	150 A	6600 W
ESC	60 V	22.2 V	250 A	15000 W
Wires	NA	NA	158 A	NA
Battery*	29.4 V	24.5 V	325 A	7960 W

*Values listed are per pack, test will consist of 2 packs in series.

** Highlighted values are the critical value for the category

Given the voltages we are working with electrocution is a safety concern for the test. Any exposed wire or connection will be a possible source for electrocution. To solve this problem we will use wire connectors with insulation that protects users whenever possible. Any additional connection that we are unable to insulate via commercially available products will be located in such a spot that direct contact is unlikely, and will be insulated via other methods (electrical tape).

Propeller Test Plan

Safety Equipment

A protection wall will be made if a location with preexisting protection cannot be found. The plate will be made of half inch plywood covered on one side by 16 gauge steel. A diagram of the plate can be found in appendix 3. The plate will be 4 feet tall and 6 feet wide and will allow for four to five people to safely hide behind.

A circuit breaker will be included in the electrical circuit that will function to protect against short circuits, and as an emergency kill switch. The circuit breaker will be behind the wall with the test operators. If deemed necessary the test operators can flip the circuit breaker removing all power from the system stopping the motor quickly. The circuit breaker will also allow the motor to be completely depowered whenever the test operators are near the propeller.

A fire extinguisher will be on hand in case of fire. However, a normal ABC fire extinguisher will not be able to extinguish our LiPo batteries should they catch fire. To extinguish a battery fire a bucket of sand, or a shovel should be nearby to allow for the fire to be suffocated.

Conclusion

The purpose of this test will be to determine if the 80CC Turnigy Rotomax motor can serve as a cheaper substitute for the JM1S motor from JobyMotors. Due to the nature of the test there are several safety concerns that need to be addressed. The main safety concern is some sort of flying projectile and overloading the electrical system. Both safety concerns have been identified above and solutions to protect against both have been proposed. Using these safety guidelines the motor test will be able to be carried out in a safe manner and produce valuable test data.

Propeller Test Plan

Appendix 1

System Calibration test

1. Set up the test stand as shown in figure 1
2. Start all cameras recording
3. All test operators leave test area and go behind protective wall
4. Energize the system by closing the kill switch
5. Slowly increase the motor throttle from 0 to 90% at a steady rate over the course of approximately 1 to 1.5 minutes
6. Return throttle to 0% and allow for propeller to quit spinning
7. De-energize the system by opening the kill switch
8. Stop cameras and save the videos for future analysis

Acceleration test

1. Set up the test stand as shown in figure 1
2. Start all cameras recording
3. All test operators leave test area and go behind protective wall
4. Energize the system by closing the kill switch
5. Turn the throttle to 80% of the required setting for 50lbs of thrust and allow propeller speed to settle
6. Suddenly increase the throttle to the setting which produces 50lbs of thrust, and allow propeller speed to settle
7. Suddenly increase the throttle to 120% of the required setting for 50lbs of thrust and allow propeller speed to settle
8. Return the throttle to 80% of the 50lbs thrust setting, and repeat steps 6 and 7 two more times
9. Return throttle to 0% and allow for propeller to quit spinning
10. De-energize the system by opening the kill switch
11. Stop cameras and save the videos for future analysis

Steady state test

1. Set up the test stand as shown in figure 1
2. Start all cameras recording
3. All test operators leave test area and go behind protective wall
4. Energize the system by closing the kill switch
5. Set throttle to the 50lbs of thrust setting, allow the motor to run until the battery voltage is 24.8V (.3V above minimum safe operating voltage)
6. Return throttle to 0% and allow for propeller to quit spinning
7. De-energize the system by opening the kill switch
8. Stop cameras and save the videos for future analysis

Propeller Test Plan

Appendix 2

BOM and Cost Analysis

Table A2.1. Bill of materials and cost

Item	Quantity	Price	Total cost	Purchased (yes/no)
Rotomax Turnigy 80CC Motor	1	282.3	282.32	Yes
Infrared Thermometer	1	27.65	27.65	Yes
QO 200 Amp AIR QOM2 Frame Size Main Circuit Breaker	1	38.99	38.99	No
2x6 8ft board	3	4.53	13.59	No
#10 3 in. Phillips Square Flat-Head Multi-Material Screws	1	7.98	7.98	No
Xoar 30x10 propeller	1	57.25	57.25	Yes
non-contact tachometer	1	11.93	11.93	Yes
3-1/2 in. Satin Nickel 5/8 in. Radius Door Hinge	1	2.78	2.78	No
500ft. 2-Gaugre Stranded XHHW Wire	1	144	144	No
7s LiPo Battery	2	131	261.92	Yes
Turnigy Dlux 250A 14s 60V ESC	1	206.9	206.91	Yes
HoMedics® Analog Scale	1	19.99	19.99	No
Steel Bracket	4	4.46	17.84	No
36x48 16 Gauge Sheet Metal	2	46.76	93.52	No
1/4X20-1.25 Cap Screws	8	.30	2.4	No
1/4 washers	16	.30	4.8	No
1/4X20 hex nuts	8	.30	2.4	No
4x8 1/2 plywood sheet	1	17.58	17.58	No
Total			1213.85	

Appendix 3

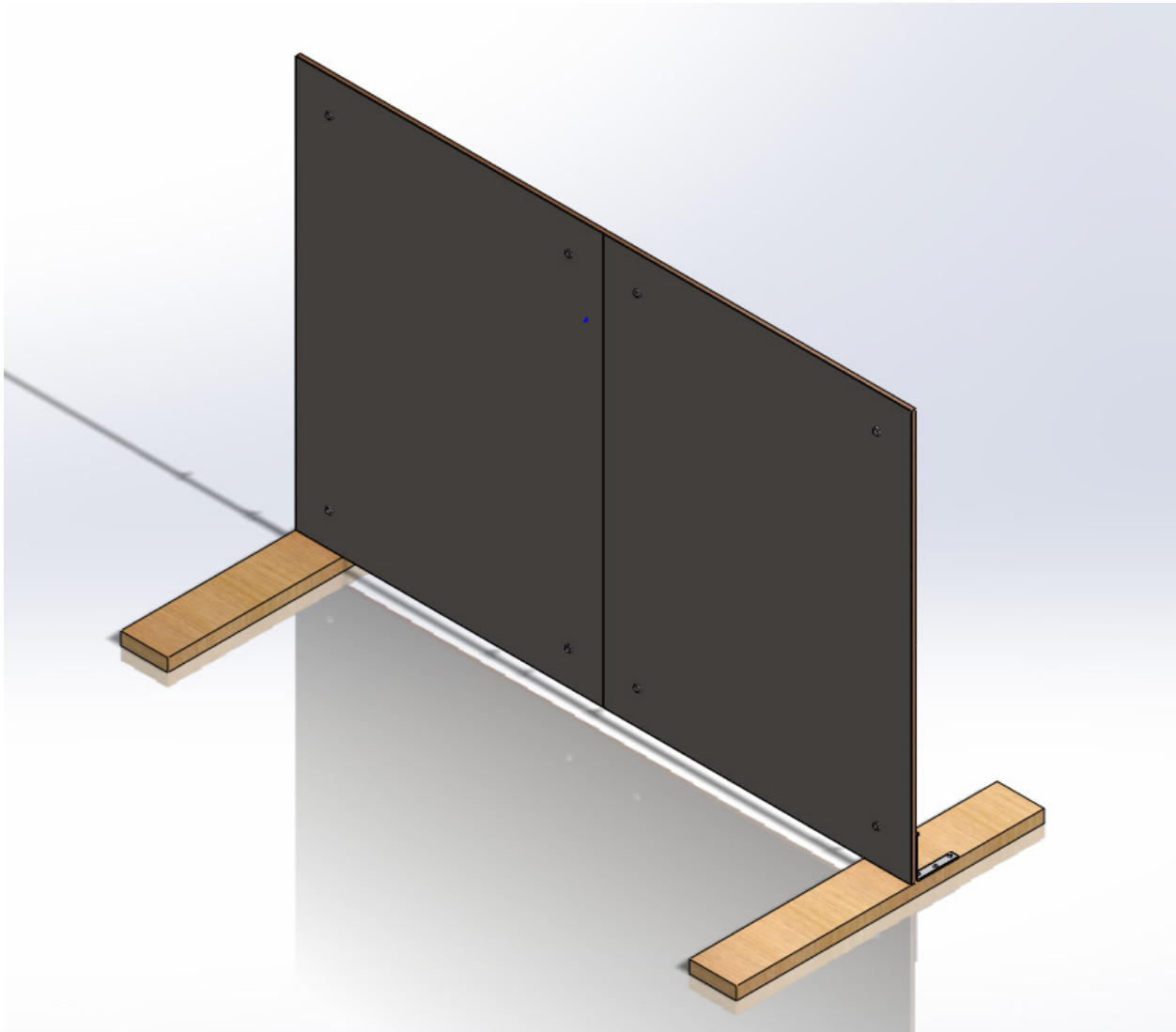


Figure A3.1. Protection Wall

Propeller Test Plan

Appendix 4

Test Setup Drawings

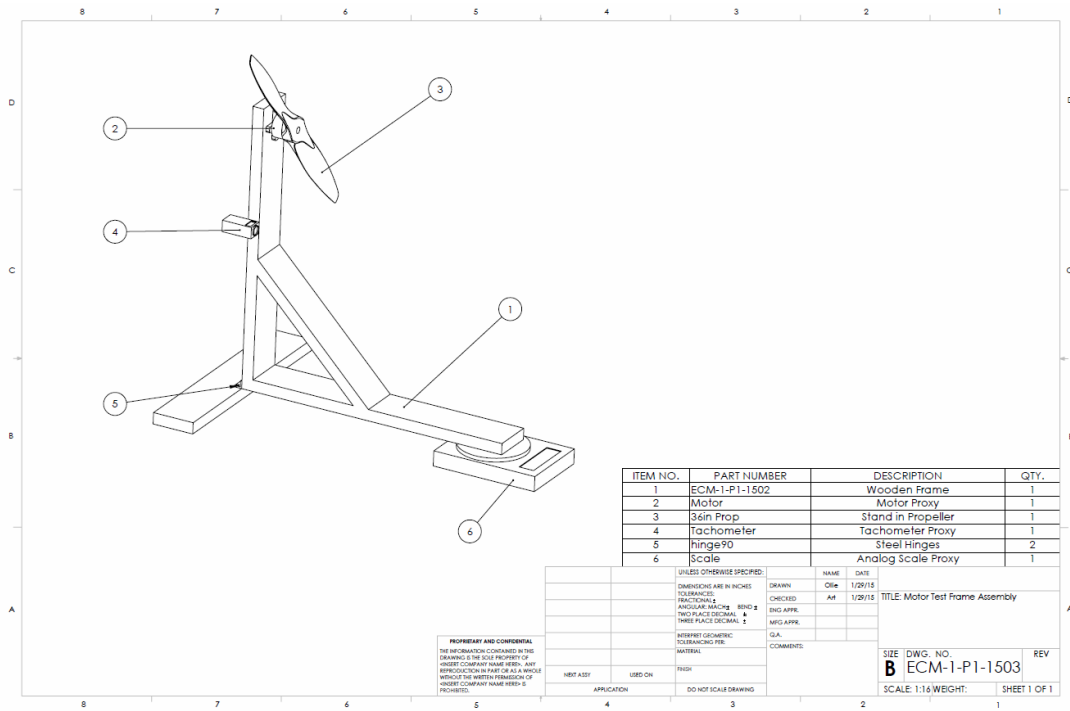


Figure A4.1. Test Setup

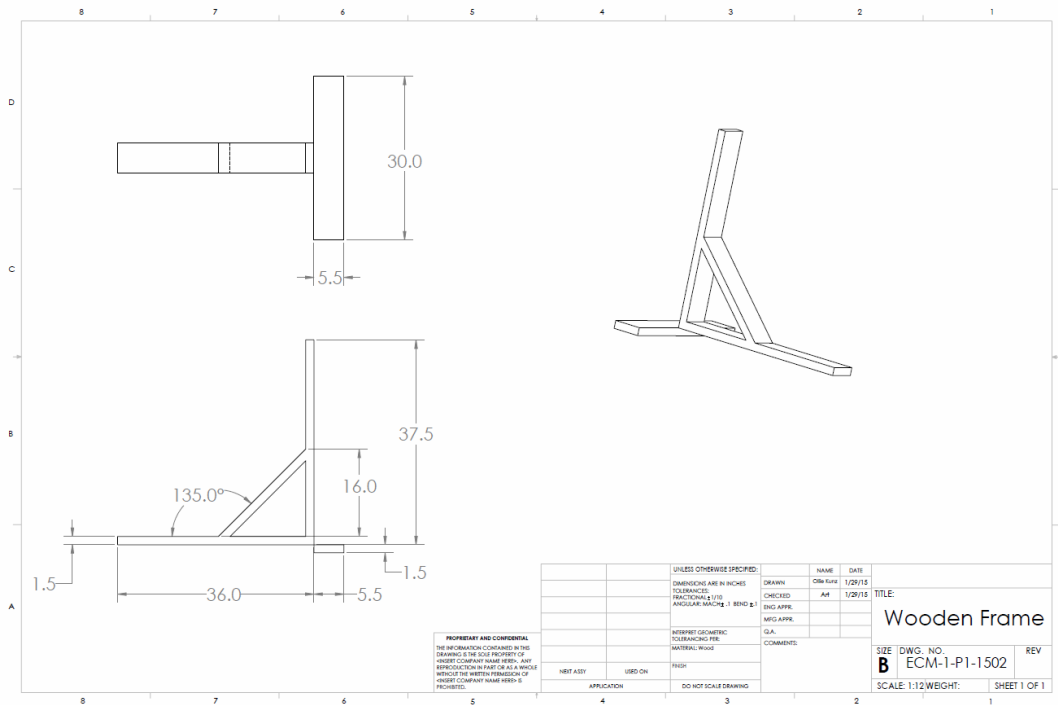


Figure A4.2. Frame Detail drawing

Propeller Test Plan

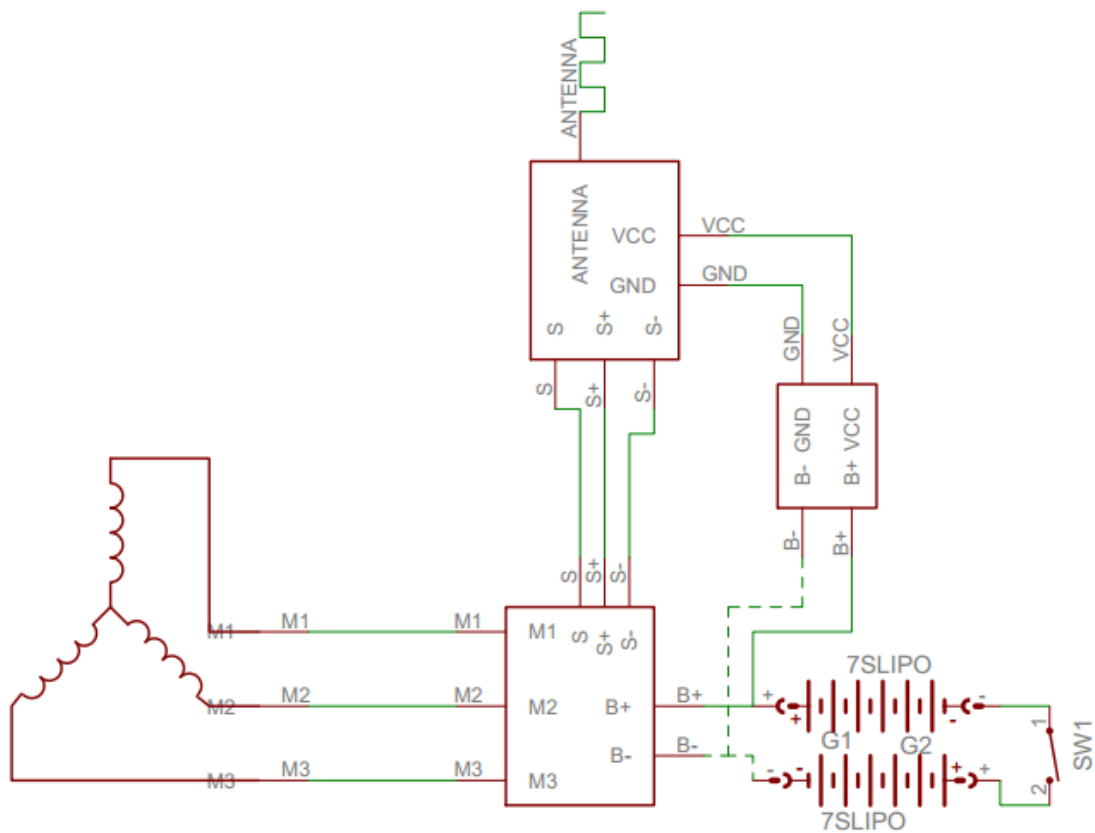


Figure A4.3. Wiring Diagram

Appendix D

Electric Commuter Multicopter

Product Literature and Technical Specifications

3M

Scotch-Weld™

Epoxy Adhesive

2216 B/A

Technical Data

December, 2009

Product Description

3M™ Scotch-Weld™ Epoxy Adhesive 2216 B/A is a flexible, two-part, room temperature curing epoxy with high peel and shear strength. Scotch-Weld epoxy adhesive 2216 B/A is identical to 3M™ Scotch-Weld™ Epoxy Adhesive EC-2216 B/A in chemical composition. Scotch-Weld epoxy adhesive EC-2216 B/A has been labeled, packaged, tested, and certified for aircraft and aerospace applications. Scotch-Weld epoxy adhesive 2216 B/A may be used for aircraft and aerospace applications if proper Certificates of Test have been issued and material meets all aircraft manufacturer's specification requirements.

Typical Uncured Physical Properties

Note: The following technical information and data should be considered representative or typical only and should not be used for specification purposes.

Product	3M™ Scotch-Weld™ Epoxy Adhesive					
	2216 B/A Gray		2216 B/A Tan NS		2216 B/A Translucent	
	Base	Accelerator	Base	Accelerator	Base	Accelerator
Color:	White	Gray	White	Tan	Translucent	Amber
Base:	Modified Epoxy	Modified Amine	Modified Epoxy	Modified Amine	Modified Epoxy	Modified Amine
Net Wt.: (lb/gal)	11.1-11.6	10.5-11.0	11.1-11.6	10.5-11.0	9.4-9.8	8.0-8.5
Viscosity: (cps) (Approx.) Brookfield RVF #7 sp. @ 20 rpm	75,000 - 150,000	40,000 - 80,000	75,000 - 150,000	550,000 - 900,000	11,000 - 15,000	5,000 - 9,000
Mix Ratio: (by weight)	5 parts	7 parts	5 parts	7 parts	1 part	1 part
Mix Ratio: (by volume)	2 parts	3 parts	2 parts	3 parts	1 part	1 part
Work Life: 100 g Mass @ 75°F (24°C)	90 minutes	90 minutes	120 minutes	120 minutes	120 minutes	120 minutes

Features

- Excellent for bonding many metals, woods, plastics, rubbers, and masonry products.
- Base and Accelerator are contrasting colors.
- Good retention of strength after environmental aging.
- Resistant to extreme shock, vibration, and flexing.
- Excellent for cryogenic bonding applications.
- The tan NS Adhesive is non-sag for greater bondline control.
- The translucent can be injected.
- Meets DOD-A-82720.

3M™ Scotch-Weld™ Epoxy Adhesive 2216 B/A

Typical Cured Physical Properties

Product	3M™ Scotch-Weld™ Epoxy Adhesive		
	2216 Gray	2216 Tan NS	2216 Translucent
Color	Gray	Tan	Translucent
Shore D Hardness ASTM D 2240	50-65	65-70	35-50
Time to Handling Strength	8-12 hrs.	8-12 hrs.	12-16 hrs.

Typical Cured Electrical Properties

Product	3M™ Scotch-Weld™ Epoxy Adhesive	
	2216 Gray	2216 Translucent
Arc Resistance	130 seconds	
Dielectric Strength	408 volts/mil	630 volts/mil
Dielectric Constant @ 73°F (23°C)	5.51–Measured @ 1.00 KHz	6.3 @ 1 KHz
Dielectric Constant @ 140°F (60°C)	14.17–Measured @ 1.00 KHz	—
Dissipation Factor 73°F (23°C)	0.112 Measured @ 1.00 KHz	0.119 @ 1 KHz
Dissipation Factor 140°F (60°C)	0.422–Measured @ 1.00 KHz	—
Surface Resistivity @ 73°F (23°C)	5.5 x 10 ¹⁶ ohm–@ 500 volts DC	—
Volume Resistivity @ 73°F (23°C)	1.9 x 10 ¹² ohm-cm–@ 500 volts DC	3.0 x 10 ¹² ohm-cm @ 500 volts DC

Typical Cured Thermal Properties

Product	3M™ Scotch-Weld™ Epoxy Adhesive	
	2216 Gray	2216 Translucent
Thermal Conductivity	0.228 Btu-ft/ft ² h °F	0.114 Btu-ft/ft ² h °F
Coefficient of Thermal Expansion	102 x 10 ⁻⁶ in/in/°C between 0-40°C 134 x 10 ⁻⁶ in/in/°C between 40-80°C	81 x 10 ⁻⁶ in/in/°C between -50-0°C 207 x 10 ⁻⁶ in/in/°C between 60-150°C

Typical Cured Outgassing Properties

Outgassing Data
NASA 1124 Revision 4

	% TML	% CVCM	% Wtr
3M™ Scotch-Weld™ Epoxy Adhesive 2216 Gray	.77	.04	.23

Cured in air for 7 days @ 77°F (25°C).

Handling/Curing Information

Directions for Use

1. For high strength structural bonds, paint, oxide films, oils, dust, mold release agents and all other surface contaminants must be completely removed. However, the amount of surface preparation directly depends on the required bond strength and the environmental aging resistance desired by user. For suggested surface preparations of common substrates, see the following section on surface preparation.
2. These products consist of two parts. Mix thoroughly by weight or volume in the proportions specified on the product label and in the uncured properties section. Mix approximately 15 seconds after a uniform color is obtained.

3M™ Scotch-Weld™ Epoxy Adhesive 2216 B/A

Handling/Curing Information (continued)

3. For maximum bond strength, apply product evenly to both surfaces to be joined.
4. Application to the substrates should be made within 90 minutes. Larger quantities and/or higher temperatures will reduce this working time.
5. Join the adhesive coated surfaces and allow to cure at 60°F (16°C) or above until firm. Heat, up to 200°F (93°C), will speed curing.
6. The following times and temperatures will result in a full cure:

Product	3M™ Scotch-Weld™ Epoxy Adhesive		
	2216 Gray	2216 Tan NS	2216 Translucent
Cure Temperature	Time	Time	Time
75°F (24°C)	7 days	7 days	30 days
150°F (66°C)	120 minutes	120 minutes	240 minutes
200°F (93°C)	30 minutes	30 minutes	60 minutes

7. Keep parts from moving until handling strength is reached. Contact pressure is necessary. Maximum shear strength is obtained with a 3-5 mil bond line. Maximum peel strength is obtained with a 17-25 mil bond line.
8. Excess uncured adhesive can be cleaned up with ketone type solvents.*

Adhesive Coverage: A 0.005 in. thick bondline will typically yield a coverage of 320 sq. ft/gallon

Application and Equipment Suggestions

These products may be applied by spatula, trowel or flow equipment. Two-part mixing/proportioning/dispensing equipment is available for intermittent or production line use. These systems are ideal because of their variable shot size and flow rate characteristics and are adaptable to many applications.

Surface Preparation

For high strength structural bonds, paint, oxide films, oils, dust, mold release agents and all other surface contaminants must be completely removed. However, the amount of surface preparation directly depends on the required bond strength and the environmental aging resistance desired by user.

The following cleaning methods are suggested for common surfaces.

Steel or Aluminum (Mechanical Abrasion)

1. Wipe free of dust with oil-free solvent such as acetone or alcohol solvents.*
2. Sandblast or abrade using clean fine grit abrasives (180 grit or finer).
3. Wipe again with solvents to remove loose particles.
4. If a primer is used, it should be applied within 4 hours after surface preparation.

*When using solvents, extinguish all ignition sources, including pilot lights, and follow the manufacturer's precautions and directions for use. Use solvents in accordance with local regulations.

3M™ Scotch-Weld™ Epoxy Adhesive 2216 B/A

Surface Preparation (continued)

Aluminum (Chemical Etch)

Aluminum alloys may be chemically cleaned and etched as per ASTM D 2651. This procedure states to:

1. Alkaline Degrease – Oakite 164 solution (9-11 oz/gal of water) at 190°F ± 10°F (88°C ± 5°C) for 10-20 minutes. Rinse immediately in large quantities of cold running water.

2. **Optimized FPL Etch Solution (1 liter):**

Material	Amount
Distilled Water	700 ml plus balance of liter (see below)
Sodium Dichromate	28 to 67.3 grams
Sulfuric Acid	287.9 to 310.0 grams
Aluminum Chips	1.5 grams/liter of mixed solution

To prepare 1 liter of this solution, dissolve sodium dichromate in 700 ml of distilled water. Add sulfuric acid and mix well. Add additional distilled water to fill to 1 liter. Heat mixed solution to 66 to 71°C (150 to 160°F). Dissolve 1.5 grams of 2024 bare aluminum chips per liter of mixed solution. Gentle agitation will help aluminum dissolve in about 24 hours.

To etch aluminum panels, place them in FPL etch solution heated to 66 to 71°C (150 to 160°F). Panels should soak for 12 to 15 minutes.

3. Rinse: Rinse panels in clear running tap water.
4. Dry: Air dry 15 minutes; force dry 10 minutes (minimum) at 140°F (60°C) maximum.
5. If primer is to be used, it should be applied within 4 hours after surface preparation.

Plastics/Rubber

1. Wipe with isopropyl alcohol.*
2. Abrade using fine grit abrasives (180 grit or finer).
3. Wipe with isopropyl alcohol.*

Glass

1. Solvent wipe surface using acetone or MEK.*
2. Apply a thin coating (0.0001 in. or less) of 3M™ Scotch-Weld™ Structural Adhesive Primer EC-3901 to the glass surfaces to be bonded and allow the primer to dry a minimum of 30 minutes @ 75°F (24°C) before bonding.

*When using solvents, extinguish all ignition sources, including pilot lights, and follow the manufacturer's precautions and directions for use. Use solvents in accordance with local regulations.

3M™ Scotch-Weld™
Epoxy Adhesive
 2216 B/A

**Typical Adhesive
 Performance
 Characteristics**

A. Typical Shear Properties on Etched Aluminum

ASTM D 1002

Cure: 2 hours @ 150 ± 5°F (66°C ± 2°C), 2 psi pressure

Test Temperature	Overlap Shear (psi)		
	3M™ Scotch-Weld™ Epoxy Adhesive		
	2216 B/A Gray Adhesive	2216 B/A Tan NS Adhesive	2216 B/A Trans. Adhesive
-423°F (-253°C)	2440	—	—
-320°F (-196°C)	2740	—	—
-100°F (-73°C)	3000	—	—
-67°F (-53°C)	3000	2000	3000
75°F (24°C)	3200	2500	1700
180°F (82°C)	400	400	140

Test Temperature	Shear Modulus (Torsion Pendulum Method)
-148°F (-100°C)	398,000 psi (2745 MPa)
-76°F (-60°C)	318,855 psi (2199 MPa)
-40°F (-40°C)	282,315 psi (1947 MPa)
32°F (0°C)	218,805 psi (1500 MPa)
75°F (24°C)	49,580 psi (342 MPa)

B. Typical T-Peel Strength

ASTM D 1876

Test Temperature	T-Peel Strength (piw) @ 75°F (24°C)		
	3M™ Scotch-Weld™ Epoxy Adhesive		
	2216 B/A Gray Adhesive	2216 B/A Tan NS Adhesive	2216 B/A Trans. Adhesive
75°F (24°C)	25	25	25

3M™ Scotch-Weld™
Epoxy Adhesive
 2216 B/A

**Typical Adhesive
 Performance
 Characteristics**
(continued)

C. Overlap Shear Strength After Environmental Aging-Etched Aluminum

Environment	Time	Overlap Shear (psi) 75°F (24°C)		
		3M™ Scotch-Weld™ Epoxy Adhesive		
		2216 B/A Gray Adhesive	2216 B/A Tan NS Adhesive	2216 B/A Trans. Adhesive
100% Relative Humidity @ 120°F (49°C)	14 days 30 days 90 days	2950 psi 1985 psi 1505 psi	3400 psi 2650 psi	1390 psi
*Salt Spray @ 75°F (24°C)	14 days 30 days 60 days	2300 psi 500 psi 300 psi	3900 psi 3300 psi	1260 psi
Tap Water @ 75°F (24°C)	14 days 30 days 90 days	3120 psi 2942 psi 2075 psi	3250 psi 2700 psi	1950 psi
Air @ 160°F (71°C)	35 days	4650 psi	4425 psi	
Air @ 300°F (149°C)	40 days	4930 psi	4450 psi	3500 psi
Anti-icing Fluid @ 75°F (24°C)	7 days	3300 psi	3050 psi	2500 psi
Hydraulic Oil @ 75°F (24°C)	30 days	2500 psi	3500 psi	2500 psi
JP-4 Fuel	30 days	2500 psi	2750 psi	2500 psi
Hydrocarbon Fluid	7 days	3300 psi	3100 psi	3000 psi

*Substrate corrosion resulted in adhesive failure.

D. Heat Aging of 3M™ Scotch-Weld™ Epoxy Adhesive 2216 B/A Gray
 (Cured for 7 days @ 75°F [24°C])

Overlap Shear (psi)	Time aged @ 300°F (149°C)			
	0 days	12 days	40 days	51 days
-67°F (-53°C)	2200	3310	3120	2860
75°F (24°C)	3100	5150	4930	4740
180°F (82°C)	500	1000	760	1120
350°F (177°C)	420	440	560	—

3M™ Scotch-Weld™
Epoxy Adhesive
 2216 B/A

Typical Adhesive Performance Characteristics
(continued)

E. Overlap Shear Strength on Abraded Metals, Plastics, and Rubbers.

Overlap shear strengths were measured on 1" x 1/2" overlap specimens. These bonds were made individually using 1" by 4" pieces of substrate (Tested per ASTM D 1002).

The thickness of the substrates were: cold rolled, galvanized and stainless steel – 0.056-0.062", copper – 0.032", brass – 0.036", rubbers – 0.125", plastics – 0.125". All surfaces were prepared by solvent wiping/abrading/ solvent wiping.

The jaw separation rate used for testing was 0.1 in/min for metals, 2 in/min for plastics, and 20 in/min for rubbers.

Substrate	Overlap Shear (psi) @ 75°F (24°C)	
	3M™ Scotch-Weld™ Epoxy Adhesive	
	2216 B/A Gray Adhesive	2216 B/A Tan NS Adhesive
Aluminum/Aluminum	1850	2350
Cold Rolled Steel/Cold Rolled Steel	1700	3100
Stainless Steel/Stainless Steel	1900	
Galvanized Steel/Galvanized Steel	1800	
Copper/Copper	1050	
Brass/Brass	850	
Styrene Butadiene Rubber/Steel	200*	
Neoprene Rubber/Steel	220*	
ABS/ABS Plastic	990*	1140*
PVC/PVC, Rigid	940*	
Polycarbonate/Polycarbonate	1170*	1730*
Acrylic/Acrylic	1100*	1110*
Fiber Reinforced Polyester/ Reinforced Polyester	1660*	1650*
Polyphenylene Oxide/PPO	610	610
PC/ABS Alloy / PC/ABS Alloy	1290	1290

*The substrate failed during the test.

Storage

Store products at 60-80°F (16-27°C) for maximum storage life.

Shelf Life

When stored at the recommended temperatures in the original, unopened containers, the shelf life is two years from date of shipment from 3M.

3M™ Scotch-Weld™ Epoxy Adhesive 2216 B/A

Precautionary Information

Refer to Product Label and Material Safety Data Sheet for health and safety information before using this product. For additional health and safety information, call 1-800-364-3577 or (651) 737-6501.

Technical Information

The technical information, recommendations and other statements contained in this document are based upon tests or experience that 3M believes are reliable, but the accuracy or completeness of such information is not guaranteed.

Product Use

Many factors beyond 3M's control and uniquely within user's knowledge and control can affect the use and performance of a 3M product in a particular application. Given the variety of factors that can affect the use and performance of a 3M product, user is solely responsible for evaluating the 3M product and determining whether it is fit for a particular purpose and suitable for user's method of application.

Warranty, Limited Remedy, and Disclaimer

Unless an additional warranty is specifically stated on the applicable 3M product packaging or product literature, 3M warrants that each 3M product meets the applicable 3M product specification at the time 3M ships the product. 3M MAKES NO OTHER WARRANTIES OR CONDITIONS, EXPRESS OR IMPLIED, INCLUDING, BUT NOT LIMITED TO, ANY IMPLIED WARRANTY OR CONDITION OF MERCHANTABILITY OR FITNESS FOR A PARTICULAR PURPOSE OR ANY IMPLIED WARRANTY OR CONDITION ARISING OUT OF A COURSE OF DEALING, CUSTOM OR USAGE OF TRADE. If the 3M product does not conform to this warranty, then the sole and exclusive remedy is, at 3M's option, replacement of the 3M product or refund of the purchase price.

Limitation of Liability

Except where prohibited by law, 3M will not be liable for any loss or damage arising from the 3M product, whether direct, indirect, special, incidental or consequential, regardless of the legal theory asserted, including warranty, contract, negligence or strict liability.

ISO 9001:2000

This Industrial Adhesives and Tapes Division product was manufactured under a 3M quality system registered to ISO 9001:2000 standards.



Industrial Adhesives and Tapes Division

3M Center, Building 225-3S-06
St. Paul, MN 55144-1000
800-362-3550 • 877-369-2923 (Fax)
www.3M.com/industrial



*Recycled Paper
40% pre-consumer
10% post-consumer*

3M and Scotch-Weld are trademarks of 3M Company.
Printed in U.S.A.
©3M 2009 78-6900-9583-7 (12/09)



105 Epoxy Resin® / 206 Slow Hardener®

Technical Data Sheet

105 System 105/206

General description

105/206 Epoxy is used for general coating and bonding applications when extended working and cure time are needed or to provide adequate working time at higher temperatures.

105/206 forms a high-strength, moisture-resistant solid with excellent bonding and barrier coating properties. It will wet out and bond to wood fiber, fiberglass, reinforcing fabrics, foam and other composite materials, and a variety of metals.

105/206 Epoxy can be thickened with WEST SYSTEM fillers to bridge gaps and fill voids and can be sanded and shaped when cured. With roller applications, it has excellent thin-film characteristics, allowing it to flow out and self-level without “fish-eyeing.” Multiple coats of 105/206 Epoxy create a superior moisture barrier and a tough, stable base for paints and varnishes. It is formulated without volatile solvents resulting in a very low VOC content. It has a relatively high flash point, no strong solvent odor and does not shrink after curing. It is not intended for clear coating natural finished wood.

Handling characteristics

Mix ratio by volume (300 Mini Pump ratio)	· · ·	5 parts resin : 1 part hardener
by weight	· · · · ·	5.36 : 1
Acceptable ratio range by weight	· · · · ·	4.83 : 1 to 6.01 : 1
Mix viscosity (at 72°F) ASTM D-2393	· · · · ·	725 cps
Pot life (100g at 72°F)	· · · · ·	20 to 25 minutes
Working time, thin film*	· · · · ·	90 to 110 minutes
Cure to a solid, thin film*	· · · · ·	10 to 15 hours
Cure to working strength	· · · · ·	1 to 4 days
Minimum recommended temperature	· · · · ·	60°F (16°C)

**Epoxy cures faster at higher temperatures and in thicker applications.*

Physical properties of cured epoxy

Specific gravity	· · · · ·	1.18
Hardness (Shore D) ASTM D-2240	· · · · ·	82
Compression yield ASTM D-695	· · · · ·	11,500 psi
Tensile strength ASTM D638	· · · · ·	7,300 psi
Tensile elongation ASTM D-638	· · · · ·	4.5%
Tensile modulus ASTM D-638	· · · · ·	4.60E+05
Flexural strength ASTM D-790	· · · · ·	11,800 psi
Flexural modulus ASTM D-790	· · · · ·	4.50E+05
Heat deflection temperature ASTM D-648	· · · · ·	123°F
Onset of Tg by DSC	· · · · ·	126°F
Ultimate Tg	· · · · ·	139°F
Annular shear fatigue @ 100,000 cycles	· · · · ·	10,100 lb

Storage/Shelf life

Store at room temperature. Keep containers closed to prevent contamination. With proper storage, resin and hardeners should remain usable for many years. After a long storage, verify the metering accuracy of the pumps. Mix a small test batch to assure proper curing.

Over time, 105 Resin will thicken slightly and will therefore require extra care when mixing. Repeated freeze/thaw cycles during storage may cause crystallization of 105 Resin. Warm resin to 125°F and stir to dissolve crystals. Hardener may darken with age, but physical properties are not affected by color. Be aware of a possible color shift if very old and new hardener are used on the same project.

Manufactured for
WEST SYSTEM by:



Gougeon Brothers Inc.
P.O. Box 908
Bay City, MI 48707

866-937-8797

www.westsystem.com

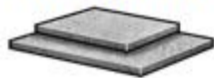
March, 2013

Easy-to-Weld 4130 Alloy Steel

Its carbon content is low enough for good weldability but high enough to give this steel abrasion and impact resistance. 4130 is often used for gears, fasteners, and structural applications.

Warning: Physical, mechanical, and chemical properties are not guaranteed and are intended only as a basis for comparison.

Sheets with Material Certification—Unpolished



- Yield Strength: 50,000 psi
- Hardness: Medium (up to Rockwell B85)
- Can be hardened up to Rockwell C60

Meet AMS 6350-6351. Each sheet comes with a traceable lot number and material test report. All sheets are annealed. 0.025" to 0.125" thick sheets are cold rolled. 0.160" and thicker are hot rolled. Width and length tolerances are $\pm 1/16"$.

Easy-to-Weld 4130 Alloy Steel

Its carbon content is low enough for good weldability but high enough to give this steel abrasion and impact resistance. 4130 is often used for gears, fasteners, and structural applications.

Warning: Physical, mechanical, and chemical properties are not guaranteed and are intended only as a basis for comparison.

Round Tubes—Unpolished (Cold Drawn)



- Yield Strength: 70,000 psi
- Hardness: Hard (Rockwell C19)
- Can be hardened up to Rockwell C49

Meet AMS-T-6736 and MIL-T-6736B. Straightness tolerance is 0.030" per 3 feet. Length tolerance is $\pm 1"$.

BLACK MAX COMFORTLITE SEAT

Part # 13-05554

In Stock

★★★★★ (0) [review this](#)

Quantity:

\$218.95

Current Sub-total: \$218.95

[Add to Wishlist](#)

[Add To Cart](#)



(Click image for a larger view)



[Email](#)

[Print](#)

[Like](#) 0

[Tweet](#) 0

[Pin it](#)

Overview

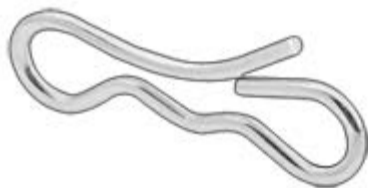
Reviews

Q+A

- 18" Wide X 19" Deep x 26" High
- 6061-T6 Aluminum Base and tubing.
- Assembled with AN Hardware.
- Material made from durable cordura nylon
- Includes a large storage pocket in the back
- Additional storage between pan and seat
- Pivots down to make it easier to get in behind the seat on a tandem

Bow Tie Cotter Pin

Zinc-Plated Steel, 3/16"-1/4" Pin Diameter, 3/64" Wire Diameter



Packs of 50

In stock

\$7.77 per pack of 50

ADD TO ORDER

92418A221

Fits Clevis Pin Diameter	3/16" to 1/4"
--------------------------	---------------

Wire Diameter	3/64"
---------------	-------

Length	1"
--------	----

Additional Specifications	Zinc-Plated Steel
---------------------------	-------------------

Their double-head design lets you push or pull these pins from either side of the hole. Once in place there's little chance they will be vibrated out or knocked off. Zinc-plated steel pins are rust resistant.

Newport 301

Description:

Newport 301 is a 250°F (121°C) to 300°F (149°C) cure, toughened, controlled flow epoxy resin system. Versatile processing, excellent mechanical properties, and long out time make Newport 301 suitable for a variety of applications, including large scale structures where layup requirements can take days or weeks.

Application:

Newport 301 is well suited for structural applications in sporting goods, marine, medical, and industrial manufacturing.

Newport 301 can be supplied with most commercially available fibers in both woven form (designated as NB) as well as unidirectional tape (designated as NCT), including:

- Carbon
- Quartz
- Aramid
- S-glass
- E-glass
- Other specialty fibers and fabrics

Woven fabrics are available in standard commercial widths up to 60 inches (1.5 M). Unitape widths up to 39 inches (1M) are available in standard fiber weights ranging from 90 to 300 gsm.

Benefits/Features:

- Excellent mechanical properties
- Moderate tack
- Good toughness
- Controlled flow
- >30 days out time at 70°F (21°C)
- Available on a wide range of unidirectional fibers and fabrics

Recommended Processing Conditions:

Newport 301 can be cured at temperatures from 250°F (121°C) to 300°F (149°C) depending on part size and complexity. Large scale structures can be cured as low as 180°F-200°F (82°C- 93°C) (with extended cure times). Low, medium, and high pressure molding techniques may be used to cure 301 products. Recommended cure cycle is 50 psi (345 kPa); 3°F (1.7°C)/min ramp to 275°F (135°C); hold for 60 minutes, cool to <140°F (60°C).

Physical Properties:

Gel Time 275°F (135°C):	3 - 5 minutes
Specific Gravity:	1.22
Tg (DMA, E'):	120°C (248°F)
CTE (ppm/°C)	60 ± 10 (below Tg)

Mechanical Properties:**Neat resin properties*:**

Tensile strength, ksi	8.3
Tensile modulus, Msi	0.46
Flexural strength, ksi	14.6
Flexural modulus, Msi	0.50

* Values are average and do not constitute a specification

7781 E-Glass Reinforcement

The mechanical properties listed in the following table are average values obtained from NB 301 with style 7781 woven fiberglass. All values are based using an "in-hot out-hot" press cure at 275° F 135°C) for 45 minutes and 25 psi (172 kPa). Results are as tested, not normalized.

Property	Test Method	RT*	160°F*
0° Tensile strength, ksi	ASTM D-638 Type I	54	45
0° Tensile modulus, Msi		3.5	3.6
0° Compressive strength, ksi	SACMA 1R-94	61	51
0° Compressive modulus, Msi		3.6	3.7
0° Flexural strength, ksi	ASTM D-790	68	54
0° Flexural modulus, Msi		3.5	3.3
0° Short Beam Shear strength, ksi	SACMA 8R-94	9.8	7.5

* Values are average and do not constitute a specification

Standard Modulus Unidirectional Carbon Fiber Reinforcement

The mechanical properties listed in the following table are average values obtained from NB 301 with 34-700 carbon fiber at 35% RC. All values are based using a press cure at 275°F (135°C) for 60 minutes and 25 psi (172 kPa) pressure. Results are normalized to 60% fiber volume, except for 0° SBS strength and all 90° properties.

Property	Test Method	RT*
0° Tensile strength, ksi	ASTM D- 3039	295
0° Tensile modulus, Msi		19
Strain, μ in/in		14,700
Poisson's ratio		0.304
0° Compressive strength, ksi	SACMA 1R-94	180
0° Compressive modulus, Msi		18.6
0° Flexural strength, ksi	ASTM D-790	280
0° Flexural modulus, Msi		18.2
0° Short Beam Shear strength, ksi	SACMA 8R-94	13.2

Property	Test Method	RT*
90° Tensile strength, ksi	ASTM D- 3039	8.7
90° Tensile modulus, Msi		1.3
Strain, μ in/in		6,100
Poisson's ratio		0.017
90° Compressive strength, ksi	SACMA 1R-94	28.8
90° Compressive modulus, Msi		1.2
90° Flexural strength, ksi	ASTM D-790	16.7
90° Flexural modulus, Msi		1.2
90° Short Beam Shear strength, ksi	SACMA 8R-94	1.3

* Values are average and do not constitute a specification

3K Plain Weave Carbon Fabric Reinforcement

The mechanical properties listed in the following table are average values obtained from NB 301 with 3K PW carbon fabric, press cured at 250°F (121°C) for 60 minutes with 25 psi (172 kPa) pressure. Results are normalized to 55% fiber volume, except for 0° SBS strength.

Property	Test Method	RT*
0° Tensile strength, ksi	ASTM D-638 Type I	81
0° Tensile modulus, Msi		9.1
0° Compressive strength, ksi	SACMA 1R-94	78
0° Compressive modulus, Msi		7.9
0° Flexural strength, ksi	ASTM D-790	129
0° Flexural modulus, Msi		7.7
0° Short Beam Shear strength, ksi	SACMA 8R-94	9.2

* Values are average and do not constitute a specification



Typical NCT 301 Carbon Unitape Mechanical Property Values

(Results are as tested, not normalized).

NCT301 (AS4 fiber)	Test Method	RT*
0° Tensile strength, ksi	ASTM D-3039	300
0° Tensile modulus, Msi		18.5
0° Compressive strength, ksi	SACMA 1R-94	200
0° Compressive modulus, Msi		17.9
0° Flexural strength, ksi	ASTM D-790	230
0° Flexural modulus, Msi		18.6
0° Short Beam Shear strength, ksi	SACMA 8R-94	13.7

*Values are average and do not constitute a specification

NCT301 (T700 fiber)	Test Method	RT*
0° Tensile strength, ksi	ASTM D-3039	360
0° Tensile modulus, Msi		18.9
0° Compressive strength, ksi	SACMA 1R-94	186
0° Compressive modulus, Msi		18.1
0° Flexural strength, ksi	ASTM D-790	240
0° Flexural modulus, Msi		18.5
0° Short Beam Shear strength, ksi	SACMA 8R-94	14.1

*Values are average and do not constitute a specification

NCT301 (TRH50 fiber)	Test Method	RT*
0° Tensile strength, ksi	ASTM D-3039	344
0° Tensile modulus, Msi		21.8
0° Compressive strength, ksi	SACMA 1R-94	210
0° Compressive modulus, Msi		-
0° Flexural strength, ksi	ASTM D-790	235
0° Flexural modulus, Msi		20.0
0° Short Beam Shear strength, ksi	SACMA 8R-94	11.0

*Values are average and do not constitute a specification

NCT301 (MR60H fiber)	Test Method	RT*
0° Tensile strength, ksi	ASTM D-3039	395
0° Tensile modulus, Msi		22.9
0° Compressive strength, ksi	SACMA 1R-94	205
0° Compressive modulus, Msi		20.4
0° Flexural strength, ksi	ASTM D-790	239
0° Flexural modulus, Msi		21.2
0° Short Beam Shear strength, ksi	SACMA 8R-94	13.6

*Values are average and do not constitute a specification

NCT301 (MR40 fiber)	Test Method	RT*
0° Tensile strength, ksi	ASTM D-3039	285
0° Tensile modulus, Msi		23.2
0° Compressive strength, ksi	SACMA 1R-94	183
0° Compressive modulus, Msi		20.6
0° Flexural strength, ksi	ASTM D-790	220
0° Flexural modulus, Msi		20.9
0° Short Beam Shear strength, ksi	SACMA 8R-94	13.4

* Values are average and do not constitute a specification

NCT301 (HR40 fiber)	Test Method	RT*
0° Tensile strength, ksi	ASTM D-3039	340
0° Tensile modulus, Msi		31.4
0° Compressive strength, ksi	SACMA 1R-94	175
0° Compressive modulus, Msi		28.9
0° Flexural strength, ksi	ASTM D-790	224
0° Flexural modulus, Msi		28.4
0° Short Beam Shear strength, ksi	SACMA 8R-94	13.8

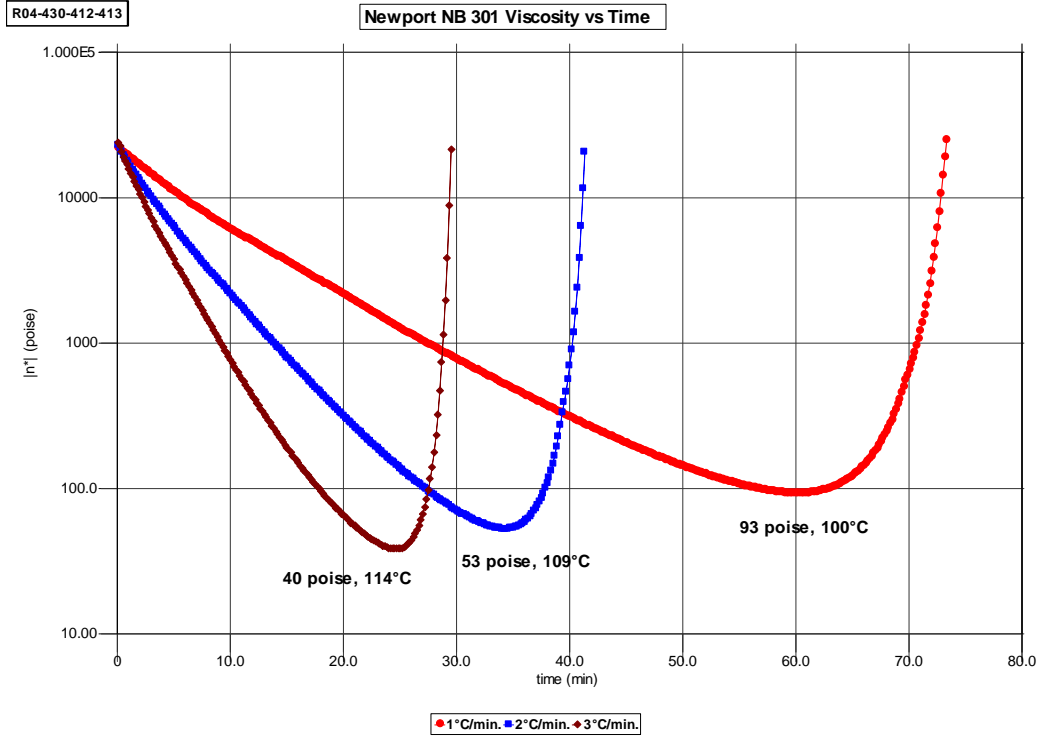
* Values are average and do not constitute a specification

NCT301 (HS40 fiber)	Test Method	RT*
0° Tensile strength, ksi	ASTM D-3039	322
0° Tensile modulus, Msi		35.2
0° Compressive strength, ksi	SACMA 1R-94	148
0° Compressive modulus, Msi		31.6
0° Flexural strength, ksi	ASTM D-790	179
0° Flexural modulus, Msi		30.5
0° Short Beam Shear strength, ksi	SACMA 8R-94	14.2

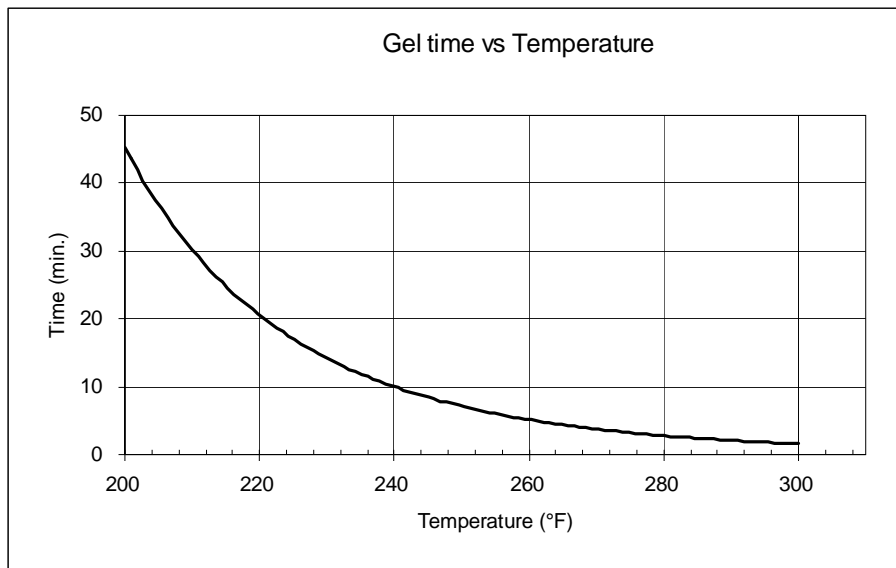
* Values are average and do not constitute a specification

Melt Viscosity Profile of Newport 301

A TA (model AR2000) parallel plate rheometer was used to determine the melt viscosity profile of the neat resin system.



Gel Curve Profile of Newport 301



Prepreg Storage:

Material can be stored at 40°F (4°C) for 3 months, or 0°F (-18°C) for 6 months. Out time is more than 30 days at room temperature 70°F (21°C).

Availability:

Newport 301 is available on a wide variety of woven fabrics and unidirectional tapes including aramid, E-glass, S-glass, carbon, and other fibers. Some product characteristics such as areal weight, resin content, gel time can be tailored within reason to meet specific requirements. Contact Newport about any specialty fibers or requirements.

Standard prepreg fabric widths:

E-glass 38, 50 inches

Carbon 42, 50 inches

Kevlar® 38, 50 inches

Standard unidirectional tape widths: 12, 24, 36 inches; 0.5, 1 meter

For orders, pricing, availability, technical assistance or other inquiries please contact:

CORPORATE OFFICES

Newport Adhesives and Composites

1822 Reynolds Ave,

Irvine, CA 92614

Tel: (949) 253-5680

Fax: (949) 253-5692

Sales@newportad.com

<http://www.newportad.com>

(Kevlar® is a trademark of the DuPont Company)

Disclaimer: The information contained herein has been obtained under controlled laboratory conditions and are typical or average values and do not constitute a specification, guarantee, or warranty. Results may vary under different processing conditions or in combination with other materials. The data is believed to be reliable but all suggestions or recommendations for use are made without guarantee. You should thoroughly and independently evaluate materials for your planned application and determine suitability under your own processing conditions before commercialization. Furthermore, no suggestion for use or material supplied shall be considered a recommendation or inducement to violate any law or infringe any patent.



Spring-Tempered Steel Jumbo Compression Spring

8" Length, 2.187" OD, .25" Wire Diameter



Packs of 1

In stock

\$12.53 per pack of 1

96485K164

Spring OD	2.187"
Wire Diameter	0.250"
Compressed Length	3.63"
Maximum Load	274.00 lbs.
Rate	61.80 lbs./inch
Additional Specifications	Spring-Tempered Steel—Closed and Ground Flat Ends 8" Overall Length

Choose steel music wire for strength; spring-tempered steel for heat resistance; brass for durability and heat resistance; or phosphor bronze for strength, heat resistance, and corrosion resistance.



Material Safety Data Sheet

Copyright, 2008, 3M Company. All rights reserved. Copying and/or downloading of this information for the purpose of properly utilizing 3M products is allowed provided that: (1) the information is copied in full with no changes unless prior written agreement is obtained from 3M, and (2) neither the copy nor the original is resold or otherwise distributed with the intention of earning a profit thereon.

PRODUCT NAME: Scotch-Weld(TM) Epoxy Adhesive 2216 B/A, Gray
MANUFACTURER: 3M
DIVISION: Industrial Adhesives and Tapes Division

ADDRESS: 3M Center
St. Paul, MN 55144-1000

EMERGENCY PHONE: 1-800-364-3577 or (651) 737-6501 (24 hours)

Issue Date: 08/05/2008
Supersedes Date: 07/10/2003

Document Group: 11-3168-9

ID Number(s):

62-2216-0530-6, 62-2216-0535-5, 62-2216-1430-8, 62-2216-1435-7, 62-2216-5430-4, 62-2216-6430-3, 62-2216-7430-2, 62-2216-7431-0

This product is a kit or a multipart product which consists of multiple, independently packaged components. An MSDS for each of these components is included. Please do not separate the component MSDSs from this cover page. The document numbers of the MSDSs for components of this product are:

10-3167-3, 10-3174-9

Revision Changes:

Copyright was modified.
Kit: Component document group number(s) was modified.
Kit: Division name was modified.
Kit: ID Number Heading was added.
Kit: ID Number(s) was added.

DISCLAIMER: The information in this Material Safety Data Sheet (MSDS) is believed to be correct as of the date issued. 3M MAKES NO WARRANTIES, EXPRESSED OR IMPLIED, INCLUDING, BUT NOT LIMITED TO, ANY IMPLIED WARRANTY OF MERCHANTABILITY OR FITNESS FOR A PARTICULAR PURPOSE OR COURSE OF PERFORMANCE OR USAGE OF TRADE. User is responsible for determining whether the 3M product is fit for a particular purpose and suitable for user's method of use or application. Given the variety of factors that can affect the use and application of a 3M product, some of which are uniquely

within the user's knowledge and control, it is essential that the user evaluate the 3M product to determine whether it is fit for a particular purpose and suitable for user's method of use or application.

3M provides information in electronic form as a service to its customers. Due to the remote possibility that electronic transfer may have resulted in errors, omissions or alterations in this information, 3M makes no representations as to its completeness or accuracy. In addition, information obtained from a database may not be as current as the information in the MSDS available directly from 3M.



Material Safety Data Sheet

Copyright, 2013, 3M Company All rights reserved. Copying and/or downloading of this information for the purpose of properly utilizing 3M products is allowed provided that: (1) the information is copied in full with no changes unless prior written agreement is obtained from 3M, and (2) neither the copy nor the original is resold or otherwise distributed with the intention of earning a profit thereon.

SECTION 1: PRODUCT AND COMPANY IDENTIFICATION

PRODUCT NAME: Scotch-Weld™ Epoxy Adhesive 2216, Gray (Part B)
MANUFACTURER: 3M
DIVISION: Industrial Adhesives and Tapes Division
ADDRESS: 3M Center, St. Paul, MN 55144-1000

EMERGENCY PHONE: 1-800-364-3577 or (651) 737-6501 (24 hours)

Issue Date: 03/19/13
Supersedes Date: 02/17/12

Document Group: 10-3167-3

Product Use:

Intended Use: Structural adhesive

SECTION 2: INGREDIENTS

<u>Ingredient</u>	<u>C.A.S. No.</u>	<u>% by Wt</u>
EPOXY RESIN	25068-38-6	70 - 80
KAOLIN	1332-58-7	20 - 30

SECTION 3: HAZARDS IDENTIFICATION

3.1 EMERGENCY OVERVIEW

Specific Physical Form: Viscous Liquid

Odor, Color, Grade: Gray very slight epoxy odor.

General Physical Form: Liquid

Immediate health, physical, and environmental hazards: May cause allergic skin reaction.

3.2 POTENTIAL HEALTH EFFECTS

Eye Contact:

Moderate Eye Irritation: Signs/symptoms may include redness, swelling, pain, tearing, and blurred or hazy vision.

Skin Contact:

Moderate Skin Irritation: Signs/symptoms may include localized redness, swelling, itching, and dryness.

Allergic Skin Reaction (non-photo induced): Signs/symptoms may include redness, swelling, blistering, and itching.

Inhalation:

Respiratory Tract Irritation: Signs/symptoms may include cough, sneezing, nasal discharge, headache, hoarseness, and nose and throat pain.

Prolonged or repeated exposure may cause:

Pneumoconiosis: Sign/symptoms may include persistent cough, breathlessness, chest pain, increased amounts of sputum, and changes in lung function tests.

Ingestion:

Gastrointestinal Irritation: Signs/symptoms may include abdominal pain, stomach upset, nausea, vomiting and diarrhea.

SECTION 4: FIRST AID MEASURES

4.1 FIRST AID PROCEDURES

The following first aid recommendations are based on an assumption that appropriate personal and industrial hygiene practices are followed.

Eye Contact: Flush eyes with large amounts of water. If signs/symptoms persist, get medical attention.

Skin Contact: Remove contaminated clothing and shoes. Immediately flush skin with large amounts of water. Get medical attention. Wash contaminated clothing and clean shoes before reuse.

Inhalation: Remove person to fresh air. If signs/symptoms develop, get medical attention.

If Swallowed: Do not induce vomiting unless instructed to do so by medical personnel. Give victim two glasses of water. Never give anything by mouth to an unconscious person. Get medical attention.

SECTION 5: FIRE FIGHTING MEASURES

5.1 FLAMMABLE PROPERTIES

Autoignition temperature

No Data Available

Flash Point

248 °C [*Test Method:* Pensky-Martens Closed Cup]

Flammable Limits(LEL)

Not Applicable

Flammable Limits(UEL)

Not Applicable

5.2 EXTINGUISHING MEDIA

Non-combustible. Choose material suitable for surrounding fire.

5.3 PROTECTION OF FIRE FIGHTERS

Special Fire Fighting Procedures: Water may be used to blanket the fire. Wear full protective equipment (Bunker Gear) and a self-contained breathing apparatus (SCBA).

Unusual Fire and Explosion Hazards: No unusual fire or explosion hazards are anticipated.

Note: See STABILITY AND REACTIVITY (SECTION 10) for hazardous combustion and thermal decomposition information.

SECTION 6: ACCIDENTAL RELEASE MEASURES

6.1. Personal precautions, protective equipment and emergency procedures

Evacuate unprotected and untrained personnel from hazard area. The spill should be cleaned up by qualified personnel. Ventilate the area with fresh air.

6.2. Environmental precautions

For larger spills, cover drains and build dikes to prevent entry into sewer systems or bodies of water. Place in a closed container approved for transportation by appropriate authorities.

Clean-up methods

Observe precautions from other sections. Call 3M- HELPS line (1-800-364-3577) for more information on handling and managing the spill. Contain spill. Working from around the edges of the spill inward, cover with bentonite, vermiculite, or commercially available inorganic absorbent material. Mix in sufficient absorbent until it appears dry. Collect as much of the spilled material as possible.

In the event of a release of this material, the user should determine if the release qualifies as reportable according to local, state, and federal regulations.

SECTION 7: HANDLING AND STORAGE

7.1 HANDLING

Avoid eye contact. Do not eat, drink or smoke when using this product. Wash exposed areas thoroughly with soap and water. Avoid skin contact. Avoid breathing of vapors. Keep container closed when not in use. Avoid breathing of dust created by cutting, sanding, grinding or machining. For industrial or professional use only. Avoid contact with oxidizing agents. Use general dilution ventilation and/or local exhaust ventilation to control airborne exposures to below Occupational Exposure Limits. If ventilation is not adequate, use respiratory protection equipment.

7.2 STORAGE

Store away from acids. Store away from heat. Store away from oxidizing agents.

SECTION 8: EXPOSURE CONTROLS/PERSONAL PROTECTION

8.1 ENGINEERING CONTROLS

Provide appropriate local exhaust for cutting, grinding, sanding or machining. Use in a well-ventilated area. Provide ventilated enclosure for heat curing. Curing enclosures must be exhausted to outdoors or to a suitable emission control device.

8.2 PERSONAL PROTECTIVE EQUIPMENT (PPE)

8.2.1 Eye/Face Protection

Avoid eye contact.

The following eye protection(s) are recommended: Safety Glasses with side shields
Indirect Vented Goggles

8.2.2 Skin Protection

Avoid skin contact.

Select and use gloves and/or protective clothing to prevent skin contact based on the results of an exposure assessment. Consult with your glove and/or protective clothing manufacturer for selection of appropriate compatible materials.

Gloves made from the following material(s) are recommended: Polymer laminate

8.2.3 Respiratory Protection

Avoid breathing of vapors. Avoid breathing of dust created by cutting, sanding, grinding or machining.

An exposure assessment may be needed to decide if a respirator is required. If a respirator is needed, use respirators as part of a full respiratory protection program. Based on the results of the exposure assessment, select from the following respirator type(s) to reduce inhalation exposure:

Half facepiece or full facepiece air-purifying respirator suitable for particulates

For questions about suitability for a specific application, consult with your respirator manufacturer.

8.2.4 Prevention of Swallowing

Do not eat, drink or smoke when using this product. Wash exposed areas thoroughly with soap and water.

8.3 EXPOSURE GUIDELINES

<u>Ingredient</u>	<u>Authority</u>	<u>Type</u>	<u>Limit</u>	<u>Additional Information</u>
KAOLIN	ACGIH	TWA, respirable fraction	2 mg/m ³	

SOURCE OF EXPOSURE LIMIT DATA:

ACGIH: American Conference of Governmental Industrial Hygienists

CMRG: Chemical Manufacturer Recommended Guideline

OSHA: Occupational Safety and Health Administration

AIHA: American Industrial Hygiene Association Workplace Environmental Exposure Level (WEEL)

SECTION 9: PHYSICAL AND CHEMICAL PROPERTIES

Specific Physical Form:	Viscous Liquid
Odor, Color, Grade:	Gray very slight epoxy odor.
General Physical Form:	Liquid
Autoignition temperature	<i>No Data Available</i>
Flash Point	248 °C [<i>Test Method:</i> Pensky-Martens Closed Cup]
Flammable Limits(LEL)	<i>Not Applicable</i>
Flammable Limits(UEL)	<i>Not Applicable</i>
Boiling Point	<i>Not Applicable</i>
Density	1.33 g/ml [@ 20 °C]
Vapor Density	<i>Not Applicable</i>
Vapor Pressure	<=0.1 mmHg [@ 25 °C]
Specific Gravity	1.33 [@ 20 °C] [<i>Ref Std:</i> WATER=1]
pH	<i>Not Applicable</i>
Melting point	<i>Not Applicable</i>
Solubility in Water	Nil
Evaporation rate	<i>Not Applicable</i>
Hazardous Air Pollutants	0 % weight [<i>Test Method:</i> Calculated]
Volatile Organic Compounds	1 g/l [<i>Test Method:</i> tested per EPA method 24]
Volatile Organic Compounds	1 g/l [<i>Test Method:</i> tested per EPA method 24] [<i>Details:</i> EU VOC content]
Kow - Oct/Water partition coef	<i>No Data Available</i>
Percent volatile	0.06 % weight [<i>Test Method:</i> ASTM METHOD]
VOC Less H2O & Exempt Solvents	1 g/l [<i>Test Method:</i> tested per EPA method 24]

VOC Less H2O & Exempt Solvents

12 g/l [Test Method: tested per EPA method 24] [Details: when used as intended with Part A]

Viscosity

75,000 - 150,000 centipoise [Test Method: Brookfield]

SECTION 10: STABILITY AND REACTIVITY

Stability: Stable.

Materials and Conditions to Avoid:

10.1 Conditions to avoid

Heat is generated during cure. Do not cure a mass larger than 50 grams in a confined space to prevent a premature reaction (exotherm) with production of intense heat and smoke.

10.2 Materials to avoid

Strong acids

Strong oxidizing agents

Hazardous Polymerization: Hazardous polymerization will not occur.

Hazardous Decomposition or By-Products

<u>Substance</u>	<u>Condition</u>
Aldehydes	During Combustion
Carbon monoxide	During Combustion
Carbon dioxide	During Combustion
Ketones	During Combustion

SECTION 11: TOXICOLOGICAL INFORMATION

Please contact the address listed on the first page of the MSDS for Toxicological Information on this material and/or its components.

SECTION 12: ECOLOGICAL INFORMATION

ECOTOXICOLOGICAL INFORMATION

Not determined.

CHEMICAL FATE INFORMATION

Not determined.

SECTION 13: DISPOSAL CONSIDERATIONS

Waste Disposal Method: Dispose of completely cured (or polymerized) wastes in a sanitary landfill.

As a disposal alternative, incinerate uncured product in an industrial or commercial incinerator in the presence of a combustible material.

EPA Hazardous Waste Number (RCRA): Not regulated

Since regulations vary, consult applicable regulations or authorities before disposal.

SECTION 14: TRANSPORT INFORMATION

ID Number(s):

62-2216-4130-1, 62-2216-5930-3, 62-2216-6830-4, 62-2216-8530-8, 62-2216-8535-7, 62-2216-9530-7

Not regulated per U.S. DOT, IATA or IMO.

*These transportation classifications are provided as a customer service. As the shipper YOU remain responsible for complying with all applicable laws and regulations, including proper transportation classification and packaging. 3M transportation classifications are based on product formulation, packaging, 3M policies and 3M understanding of applicable current regulations. 3M does not guarantee the accuracy of this classification information. This information applies only to transportation classification and **not the packaging, labeling, or marking requirements**. The original 3M package is certified for U.S. ground shipment only. If you are shipping by air or ocean, the package may not meet applicable regulatory requirements.*

SECTION 15: REGULATORY INFORMATION

US FEDERAL REGULATIONS

Contact 3M for more information.

311/312 Hazard Categories:

Fire Hazard - No Pressure Hazard - No Reactivity Hazard - No Immediate Hazard - Yes Delayed Hazard - Yes

STATE REGULATIONS

Contact 3M for more information.

CHEMICAL INVENTORIES

The components of this product are in compliance with the chemical notification requirements of TSCA.

All applicable chemical ingredients in this material are listed on the European Inventory of Existing Chemical Substances (EINECS), or are exempt polymers whose monomers are listed on EINECS. Contact 3M for more information.

INTERNATIONAL REGULATIONS

Contact 3M for more information.

This MSDS has been prepared to meet the U.S. OSHA Hazard Communication Standard, 29 CFR 1910.1200.

SECTION 16: OTHER INFORMATION

NFPA Hazard Classification

Health: 2 Flammability: 1 Reactivity: 1 Special Hazards: None

National Fire Protection Association (NFPA) hazard ratings are designed for use by emergency response personnel to address the hazards that are presented by short-term, acute exposure to a material under conditions of fire, spill, or similar emergencies. Hazard ratings are primarily based on the inherent physical and toxic properties of the material but also include the toxic properties of combustion or decomposition products that are known to be generated in significant quantities.

Revision Changes:

Section 1: Product use information was modified.

Section 8: Respiratory protection - recommended respirators information was modified.

Section 8: Respiratory protection - recommended respirators was modified.

Sections 3 and 9: Odor, color, grade information was modified.

Section 8: Respiratory protection - recommended respirators guide was modified.

Copyright was modified.

Section 8: Respiratory protection - recommended respirators punctuation was deleted.

DISCLAIMER: The information in this Material Safety Data Sheet (MSDS) is believed to be correct as of the date issued. 3M MAKES NO WARRANTIES, EXPRESSED OR IMPLIED, INCLUDING, BUT NOT LIMITED TO, ANY IMPLIED WARRANTY OF MERCHANTABILITY OR FITNESS FOR A PARTICULAR PURPOSE OR COURSE OF PERFORMANCE OR USAGE OF TRADE. User is responsible for determining whether the 3M product is fit for a particular purpose and suitable for user's method of use or application. Given the variety of factors that can affect the use and application of a 3M product, some of which are uniquely within the user's knowledge and control, it is essential that the user evaluate the 3M product to determine whether it is fit for a particular purpose and suitable for user's method of use or application.

3M provides information in electronic form as a service to its customers. Due to the remote possibility that electronic transfer may have resulted in errors, omissions or alterations in this information, 3M makes no representations as to its completeness or accuracy. In addition, information obtained from a database may not be as current as the information in the MSDS available directly from 3M

3M USA MSDSs are available at www.3M.com



Material Safety Data Sheet

Copyright, 2012, 3M Company All rights reserved. Copying and/or downloading of this information for the purpose of properly utilizing 3M products is allowed provided that: (1) the information is copied in full with no changes unless prior written agreement is obtained from 3M, and (2) neither the copy nor the original is resold or otherwise distributed with the intention of earning a profit thereon.

SECTION 1: PRODUCT AND COMPANY IDENTIFICATION

PRODUCT NAME: 3M™ Scotch-Weld™ Epoxy Adhesive 2216, Gray (Part A)
MANUFACTURER: 3M
DIVISION: Industrial Adhesives and Tapes Division
ADDRESS: 3M Center, St. Paul, MN 55144-1000

EMERGENCY PHONE: 1-800-364-3577 or (651) 737-6501 (24 hours)

Issue Date: 02/17/12
Supersedes Date: 01/04/12

Document Group: 10-3174-9

Product Use:

Specific Use: Accelerator for 2-Part Epoxy Adhesive
Intended Use: Structural adhesive

SECTION 2: INGREDIENTS

<u>Ingredient</u>	<u>C.A.S. No.</u>	<u>% by Wt</u>
ALIPHATIC POLYMER DIAMINE	68911-25-1	40 - 70
KAOLIN	1332-58-7	30 - 60
BIS(3-AMINOPROPYL) ETHER OF DIETHYLENE GLYCOL	4246-51-9	7 - 13
TOLUENE	108-88-3	0.1 - 1.0
TITANIUM DIOXIDE	13463-67-7	0 - 0.5

SECTION 3: HAZARDS IDENTIFICATION

3.1 EMERGENCY OVERVIEW

Specific Physical Form: Viscous

Odor, Color, Grade: pungent odor, gray.

General Physical Form: Liquid

Immediate health, physical, and environmental hazards: May cause chemical eye burns. May cause severe skin irritation. May cause allergic skin reaction. Contains a chemical or chemicals which can cause birth defects or other reproductive harm.

3.2 POTENTIAL HEALTH EFFECTS

Eye Contact:

Corrosive (Eye Burns): Signs/symptoms may include cloudy appearance of the cornea, chemical burns, severe pain, tearing, ulcerations, significantly impaired vision or complete loss of vision.

Skin Contact:

Severe Skin Irritation: Signs/symptoms may include localized redness, swelling, itching, dryness, cracking, blistering, and pain.

Allergic Skin Reaction (non-photo induced): Signs/symptoms may include redness, swelling, blistering, and itching.

Inhalation:

Respiratory Tract Irritation: Signs/symptoms may include cough, sneezing, nasal discharge, headache, hoarseness, and nose and throat pain.

Prolonged or repeated exposure may cause:

Pneumoconiosis: Sign/symptoms may include persistent cough, breathlessness, chest pain, increased amounts of sputum, and changes in lung function tests.

May be absorbed following inhalation and cause target organ effects.

Ingestion:

Gastrointestinal Irritation: Signs/symptoms may include abdominal pain, stomach upset, nausea, vomiting and diarrhea.

May be absorbed following ingestion and cause target organ effects.

Target Organ Effects:

Contains a chemical or chemicals which can cause birth defects or other reproductive harm.

SECTION 4: FIRST AID MEASURES

4.1 FIRST AID PROCEDURES

The following first aid recommendations are based on an assumption that appropriate personal and industrial hygiene practices are followed.

Eye Contact: Immediately flush eyes with large amounts of water for at least 15 minutes. Get immediate medical attention.

Skin Contact: Remove contaminated clothing and shoes. Immediately flush skin with large amounts of water. Get medical attention. Wash contaminated clothing and clean shoes before reuse.

Inhalation: Remove person to fresh air. If signs/symptoms develop, get medical attention.

If Swallowed: Do not induce vomiting unless instructed to do so by medical personnel. Give victim two glasses of water. Never give anything by mouth to an unconscious person. Get medical attention.

SECTION 5: FIRE FIGHTING MEASURES

5.1 FLAMMABLE PROPERTIES

Autoignition temperature

No Data Available

Flash Point

≥ 201 °F [*Test Method: Closed Cup*]

Flammable Limits(LEL)

Not Applicable

Flammable Limits(UEL)

Not Applicable

5.2 EXTINGUISHING MEDIA

Non-combustible. Choose material suitable for surrounding fire.

5.3 PROTECTION OF FIRE FIGHTERS

Special Fire Fighting Procedures: Water may be used to blanket the fire. Wear full protective equipment (Bunker Gear) and a self-contained breathing apparatus (SCBA).

Unusual Fire and Explosion Hazards: No unusual fire or explosion hazards are anticipated.

Note: See STABILITY AND REACTIVITY (SECTION 10) for hazardous combustion and thermal decomposition information.

SECTION 6: ACCIDENTAL RELEASE MEASURES

6.1. Personal precautions, protective equipment and emergency procedures

Evacuate unprotected and untrained personnel from hazard area. The spill should be cleaned up by qualified personnel. Ventilate the area with fresh air.

6.2. Environmental precautions

For larger spills, cover drains and build dikes to prevent entry into sewer systems or bodies of water. Collect the resulting residue containing solution. Place in a closed container approved for transportation by appropriate authorities. Dispose of collected material as soon as possible.

Clean-up methods

Observe precautions from other sections. Call 3M- HELPS line (1-800-364-3577) for more information on handling and managing the spill. Contain spill. Collect as much of the spilled material as possible. Clean up residue with an appropriate solvent selected by a qualified and authorized person. Ventilate the area with fresh air. Read and follow safety precautions on the solvent label and MSDS.

In the event of a release of this material, the user should determine if the release qualifies as reportable according to local, state, and federal regulations.

SECTION 7: HANDLING AND STORAGE

7.1 HANDLING

Avoid eye contact. Do not eat, drink or smoke when using this product. Wash exposed areas thoroughly with soap and water. Avoid skin contact. Avoid breathing of vapors. Keep out of the reach of children. Keep container closed when not in use. Avoid breathing of dust created by cutting, sanding, grinding or machining. For industrial or professional use only. Use general dilution ventilation and/or local exhaust ventilation to control airborne exposures to below Occupational Exposure Limits. If ventilation is not adequate, use respiratory protection equipment.

7.2 STORAGE

Store away from heat.

SECTION 8: EXPOSURE CONTROLS/PERSONAL PROTECTION

8.1 ENGINEERING CONTROLS

Provide appropriate local exhaust for cutting, grinding, sanding or machining. Use in a well-ventilated area. Provide ventilated enclosure for heat curing. Curing enclosures must be exhausted to outdoors or to a suitable emission control device.

8.2 PERSONAL PROTECTIVE EQUIPMENT (PPE)

8.2.1 Eye/Face Protection

Avoid eye contact.

The following eye protection(s) are recommended: Safety Glasses with side shields
Indirect Vented Goggles

8.2.2 Skin Protection

Avoid skin contact.

Select and use gloves and/or protective clothing to prevent skin contact based on the results of an exposure assessment. Consult with your glove and/or protective clothing manufacturer for selection of appropriate compatible materials.

Gloves made from the following material(s) are recommended: Polymer laminate

8.2.3 Respiratory Protection

Avoid breathing of vapors. Avoid breathing of dust created by cutting, sanding, grinding or machining.

Select one of the following NIOSH approved respirators based on airborne concentration of contaminants and in accordance with OSHA regulations: Half facepiece or fullface air-purifying respirator with N95 particulate filters

Select and use respiratory protection to prevent an inhalation exposure based on the results of an exposure assessment. Consult with your respirator manufacturer for selection of appropriate types of respirators.

8.2.4 Prevention of Swallowing

Do not eat, drink or smoke when using this product. Wash exposed areas thoroughly with soap and water.

8.3 EXPOSURE GUIDELINES

<u>Ingredient</u>	<u>Authority</u>	<u>Type</u>	<u>Limit</u>	<u>Additional Information</u>
KAOLIN	ACGIH	TWA, respirable fraction	2 mg/m ³	
TITANIUM DIOXIDE	ACGIH	TWA	10 mg/m ³	
TITANIUM DIOXIDE	CMRG	TWA, as respirable dust	5 mg/m ³	
TITANIUM DIOXIDE	OSHA	TWA, as total dust	15 mg/m ³	
TOLUENE	ACGIH	TWA	20 ppm	
TOLUENE	CMRG	STEL	75 ppm	Skin Notation*
TOLUENE	OSHA	TWA	200 ppm	
TOLUENE	OSHA	CEIL	300 ppm	

* Substance(s) refer to the potential contribution to the overall exposure by the cutaneous route including mucous membrane and eye, either by airborne or, more particularly, by direct contact with the substance. Vehicles can alter skin absorption.

SOURCE OF EXPOSURE LIMIT DATA:

ACGIH: American Conference of Governmental Industrial Hygienists

CMRG: Chemical Manufacturer Recommended Guideline

OSHA: Occupational Safety and Health Administration

AIHA: American Industrial Hygiene Association Workplace Environmental Exposure Level (WEEL)

SECTION 9: PHYSICAL AND CHEMICAL PROPERTIES

Specific Physical Form:

Viscous

Odor, Color, Grade:

pungent odor, gray.

General Physical Form:	Liquid
Autoignition temperature	<i>No Data Available</i>
Flash Point	>=201 °F [<i>Test Method:</i> Closed Cup]
Flammable Limits(LEL)	<i>Not Applicable</i>
Flammable Limits(UEL)	<i>Not Applicable</i>
Boiling Point	<i>No Data Available</i>
Density	1.26 g/ml [@ 20 °C]
Vapor Density	<i>Not Applicable</i>
Vapor Pressure	<=0.1 mmHg [@ 25 °C]
Specific Gravity	1.26 [@ 20 °C] [<i>Ref Std:</i> WATER=1]
pH	<i>Not Applicable</i>
Melting point	<i>Not Applicable</i>
Solubility in Water	Nil
Evaporation rate	<i>Not Applicable</i>
Hazardous Air Pollutants	< 1 % weight [<i>Test Method:</i> Calculated]
Volatile Organic Compounds	43 g/l [<i>Test Method:</i> tested per EPA method 24]
Volatile Organic Compounds	43 g/l [<i>Test Method:</i> tested per EPA method 24] [<i>Details:</i> EU VOC content]
Kow - Oct/Water partition coef	<i>No Data Available</i>
Percent volatile	3.4 % weight [@ 110 °C] [<i>Test Method:</i> ASTM METHOD] [<i>Details:</i> ASTM D2369]
VOC Less H2O & Exempt Solvents	43 g/l [<i>Test Method:</i> tested per EPA method 24]
VOC Less H2O & Exempt Solvents	12 g/l [<i>Test Method:</i> tested per EPA method 24] [<i>Details:</i> when used as intended with Part B]
Viscosity	40,000 - 80,000 centipoise [@ 20 °C] [<i>Test Method:</i> Brookfield]

SECTION 10: STABILITY AND REACTIVITY

Stability: Stable.

Materials and Conditions to Avoid:

10.1 Conditions to avoid

Heat is generated during cure. Do not cure a mass larger than 50 grams in a confined space to prevent a premature reaction (exotherm) with production of intense heat and smoke.

10.2 Materials to avoid

None known

Hazardous Polymerization: Hazardous polymerization will not occur.

Hazardous Decomposition or By-Products

<u>Substance</u>	<u>Condition</u>
Amine Compounds	During Combustion
Carbon monoxide	During Combustion
Carbon dioxide	During Combustion
Oxides of Nitrogen	During Combustion

SECTION 11: TOXICOLOGICAL INFORMATION

Please contact the address listed on the first page of the MSDS for Toxicological Information on this material and/or its components.

SECTION 12: ECOLOGICAL INFORMATION

ECOTOXICOLOGICAL INFORMATION

Not determined.

CHEMICAL FATE INFORMATION

Not determined.

SECTION 13: DISPOSAL CONSIDERATIONS

Waste Disposal Method: Cure (harden, set, or react) the product according to product instructions. Dispose of completely cured (or polymerized) wastes in a sanitary landfill. As a disposal alternative, incinerate uncured product in an industrial or commercial incinerator.

Since regulations vary, consult applicable regulations or authorities before disposal.

SECTION 14: TRANSPORT INFORMATION

ID Number(s):

62-2217-8530-6, 62-2217-8535-5, 62-2217-9530-5

Not regulated per U.S. DOT, IATA or IMO.

*These transportation classifications are provided as a customer service. As the shipper YOU remain responsible for complying with all applicable laws and regulations, including proper transportation classification and packaging. 3M transportation classifications are based on product formulation, packaging, 3M policies and 3M understanding of applicable current regulations. 3M does not guarantee the accuracy of this classification information. This information applies only to transportation classification and **not the packaging, labeling, or marking requirements**. The original 3M package is certified for U.S. ground shipment only. If you are shipping by air or ocean, the package may not meet applicable regulatory requirements.*

SECTION 15: REGULATORY INFORMATION

US FEDERAL REGULATIONS

Contact 3M for more information.

311/312 Hazard Categories:

Fire Hazard - No Pressure Hazard - No Reactivity Hazard - No Immediate Hazard - Yes Delayed Hazard - Yes

STATE REGULATIONS

Contact 3M for more information.

CALIFORNIA PROPOSITION 65

<u>Ingredient</u>	<u>C.A.S. No.</u>	<u>Classification</u>
TOLUENE	108-88-3	*Female reproductive toxin
TOLUENE	108-88-3	*Developmental Toxin

* WARNING: contains a chemical or chemicals which can cause birth defects or other reproductive harm.

CHEMICAL INVENTORIES

The components of this product are in compliance with the chemical notification requirements of TSCA.

All applicable chemical ingredients in this material are listed on the European Inventory of Existing Chemical Substances (EINECS), or are exempt polymers whose monomers are listed on EINECS. Contact 3M for more information.

INTERNATIONAL REGULATIONS

Contact 3M for more information.

This MSDS has been prepared to meet the U.S. OSHA Hazard Communication Standard, 29 CFR 1910.1200.

SECTION 16: OTHER INFORMATION

NFPA Hazard Classification

Health: 3 Flammability: 1 Reactivity: 1 Special Hazards: None

National Fire Protection Association (NFPA) hazard ratings are designed for use by emergency response personnel to address the hazards that are presented by short-term, acute exposure to a material under conditions of fire, spill, or similar emergencies. Hazard ratings are primarily based on the inherent physical and toxic properties of the material but also include the toxic properties of combustion or decomposition products that are known to be generated in significant quantities.

Revision Changes:

- Section 3: Immediate skin hazard(s) was modified.
- Section 3: Potential effects from eye contact was modified.
- Section 3: Potential effects from skin contact information was modified.
- Section 3: Potential effects from inhalation information was modified.
- Section 5: Extinguishing media information was modified.
- Section 5: Unusual fire and explosion hazard information was modified.
- Section 8: Prevention of swallowing information was modified.
- Section 9: Property description for optional properties was modified.
- Section 15: Ingredient comment heading was deleted.
- Section 15: Inventories comment was deleted.

DISCLAIMER: The information in this Material Safety Data Sheet (MSDS) is believed to be correct as of the date issued. 3M MAKES NO WARRANTIES, EXPRESSED OR IMPLIED, INCLUDING, BUT NOT LIMITED TO, ANY IMPLIED WARRANTY OF MERCHANTABILITY OR FITNESS FOR A PARTICULAR PURPOSE OR COURSE OF PERFORMANCE OR USAGE OF TRADE. User is responsible for determining whether the 3M product is fit for a particular purpose and suitable for user's method of use or application. Given the variety of factors that can affect the use and application of a 3M product, some of which are uniquely within the user's knowledge and control, it is essential that the user evaluate the 3M product to determine whether it is fit for a particular purpose and suitable for user's method of use or application.

3M provides information in electronic form as a service to its customers. Due to the remote possibility that electronic transfer may have resulted in errors, omissions or alterations in this information, 3M makes no representations as to its completeness or accuracy. In addition, information obtained from a database may not be as current as the information in the MSDS available directly from 3M

3M USA MSDSs are available at www.3M.com

MATERIAL SAFETY DATA SHEET

West System Inc.

1. CHEMICAL PRODUCT AND COMPANY IDENTIFICATION

PRODUCT NAME:..... WEST SYSTEM® 105 Epoxy Resin®.
PRODUCT CODE:..... 105
CHEMICAL FAMILY:..... Epoxy Resin.
CHEMICAL NAME:..... Bisphenol A based epoxy resin.
FORMULA:..... Not applicable.

MANUFACTURER:
West System Inc.
102 Patterson Ave.
Bay City, MI 48706, U.S.A.
Phone: 866-937-8797 or 989-684-7286
www.westsystem.com

EMERGENCY TELEPHONE NUMBERS:
Transportation
CHEMTREC:..... 800-424-9300 (U.S.)
703-527-3887 (International)
Non-transportation
Poison Hotline: 800-222-1222

2. HAZARDS IDENTIFICATION

EMERGENCY OVERVIEW

HMIS Hazard Rating: **Health - 2** **Flammability - 1** **Physical Hazards - 0**

WARNING! May cause allergic skin response in certain individuals. May cause moderate irritation to the skin. Clear to light yellow liquid with mild odor.

PRIMARY ROUTE(S) OF ENTRY:..... Skin contact.

POTENTIAL HEALTH EFFECTS:

ACUTE INHALATION:..... Not likely to cause acute effects unless heated to high temperatures. If product is heated, vapors generated can cause headache, nausea, dizziness and possible respiratory irritation if inhaled in high concentrations.

CHRONIC INHALATION:..... Not likely to cause chronic effects. Repeated exposure to high vapor concentrations may cause irritation of pre-existing lung allergies and increase the chance of developing allergy symptoms to this product.

ACUTE SKIN CONTACT:..... May cause allergic skin response in certain individuals. May cause moderate irritation to the skin such as redness and itching.

CHRONIC SKIN CONTACT:..... May cause sensitization in susceptible individuals. May cause moderate irritation to the skin.

EYE CONTACT:..... May cause irritation.

INGESTION:..... Low acute oral toxicity.

SYMPTOMS OF OVEREXPOSURE:..... Possible sensitization and subsequent allergic reactions usually seen as redness and rashes. Repeated exposure is not likely to cause other adverse health effects.

MEDICAL CONDITIONS AGGRAVATED BY EXPOSURE:..... Pre-existing skin and respiratory disorders may be aggravated by exposure to this product. Pre-existing lung and skin allergies may increase the chance of developing allergic symptoms to this product.

3. COMPOSITION/INFORMATION ON HAZARDOUS INGREDIENTS

<u>INGREDIENT NAME</u>	<u>CAS #</u>	<u>CONCENTRATION</u>
Bisphenol-A type epoxy resin	25085-99-8	> 50%
Benzyl alcohol	100-51-6	< 20%
Bisphenol-F type epoxy resin	28064-14-4	< 20%

4. FIRST AID MEASURES

FIRST AID FOR EYES:..... Flush immediately with water for at least 15 minutes. Consult a physician.

FIRST AID FOR SKIN:..... Remove contaminated clothing. Wipe excess from skin. Remove with waterless skin cleaner and then wash with soap and water. Consult a physician if effects occur.

FIRST AID FOR INHALATION:..... Remove to fresh air if effects occur.

FIRST AID FOR INGESTION No adverse health effects expected from amounts ingested under normal conditions of use. Seek medical attention if a significant amount is ingested.

5. FIRE FIGHTING MEASURES

FLASH POINT: >200°F (Tag Closed Cup)

EXTINGUISHING MEDIA: Foam, carbon dioxide (CO₂), dry chemical.

SPECIAL FIRE FIGHTING PROCEDURES: Wear a self-contained breathing apparatus and complete full-body personal protective equipment. Closed containers may rupture (due to buildup of pressure) when exposed to extreme heat.

FIRE AND EXPLOSION HAZARDS: During a fire, smoke may contain the original materials in addition to combustion products of varying composition which may be toxic and/or irritating. Combustion products may include, but are not limited to: phenolics, carbon monoxide, carbon dioxide.

6. ACCIDENTAL RELEASE MEASURES

SPILL OR LEAK PROCEDURES: Stop leak without additional risk. Dike and absorb with inert material (e.g., sand) and collect in a suitable, closed container. Warm, soapy water or non-flammable, safe solvent may be used to clean residual.

7. HANDLING AND STORAGE

STORAGE TEMPERATURE (min./max.): 40°F (4°C) / 120°F (49°C)

STORAGE: Store in cool, dry place. Store in tightly sealed containers to prevent moisture absorption and loss of volatiles. Excessive heat over long periods of time will degrade the resin.

HANDLING PRECAUTIONS: Avoid prolonged or repeated skin contact. Wash thoroughly after handling. Launder contaminated clothing before reuse. Avoid inhalation of vapors from heated product. Precautionary steps should be taken when curing product in large quantities. When mixed with epoxy curing agents this product causes an exothermic, which in large masses, can produce enough heat to damage or ignite surrounding materials and emit fumes and vapors that vary widely in composition and toxicity.

8. EXPOSURE CONTROLS/PERSONAL PROTECTION

EYE PROTECTION GUIDELINES: Safety glasses with side shields or chemical splash goggles.

SKIN PROTECTION GUIDELINES: Wear liquid-proof, chemical resistant gloves (nitrile-butyl rubber, neoprene, butyl rubber or natural rubber) and full body-covering clothing.

RESPIRATORY/VENTILATION GUIDELINES: Good room ventilation is usually adequate for most operations. Wear a NIOSH/MSHA approved respirator with an organic vapor cartridge whenever exposure to vapor in concentrations above applicable limits is likely.

Note: West System, Inc. has conducted an air sampling study using this product or similarly formulated products. The results indicate that the components sampled for (epichlorohydrin, benzyl alcohol) were either so low that they were not detected at all or they were significantly below OSHA's permissible exposure levels.

ADDITIONAL PROTECTIVE MEASURES: Practice good caution and personal cleanliness to avoid skin and eye contact. Avoid skin contact when removing gloves and other protective equipment. Wash thoroughly after handling. Generally speaking, working cleanly and following basic precautionary measures will greatly minimize the potential for harmful exposure to this product under normal use conditions.

OCCUPATIONAL EXPOSURE LIMITS: Not established for product as whole. Refer to OSHA's Permissible Exposure Level (PEL) or the ACGIH Guidelines for information on specific ingredients.

9. PHYSICAL AND CHEMICAL PROPERTIES

PHYSICAL FORM: Liquid.

COLOR: Clear to pale yellow.

ODOR: Mild.

BOILING POINT: > 400°F.

MELTING POINT/FREEZE POINT: No data.

VISCOSITY: 1,000 cPs.

pH: No data.

SOLUBILITY IN WATER: Slight.

SPECIFIC GRAVITY: 1.15

BULK DENSITY: 9.6 pounds/gallon.

VAPOR PRESSURE: < 1 mmHg @ 20°C.

VAPOR DENSITY: Heavier than air.

% VOLATILE BY WEIGHT: ASTM D 2369-07 was used to determine the Volatile Content of mixed epoxy resin and hardener. Refer to the hardener's MSDS for information about the total volatile content of the resin/hardener system.

10. STABILITY AND REACTIVITY

STABILITY: Stable.

HAZARDOUS POLYMERIZATION: Will not occur by itself, but a mass of more than one pound of product plus an aliphatic amine will cause irreversible polymerization with significant heat buildup.

INCOMPATIBILITIES: Strong acids, bases, amines and mercaptans can cause polymerization.

DECOMPOSITION PRODUCTS: Carbon monoxide, carbon dioxide and phenolics may be produced during uncontrolled exothermic reactions or when otherwise heated to decomposition.

11. TOXICOLOGICAL INFORMATION

No specific oral, inhalation or dermal toxicology data is known for this product. Specific toxicology information for a bisphenol-A based epoxy resin present in this product is indicated below:

Oral: LD₅₀ >5000 mg/kg (rats)

Inhalation: No Data.

Dermal: LD₅₀ = 20,000 mg/kg (skin absorption in rabbits)

TERATOLOGY: Diglycidyl ether bisphenol-A (DGEBA) did not cause birth defects or other adverse effects on the fetus when pregnant rabbits were exposed by skin contact, the most likely route of exposure, or when pregnant rats or rabbits were exposed orally.

REPRODUCTIVE EFFECTS: DGEBA, in animal studies, has been shown not to interfere with reproduction.

MUTAGENICITY: DGEBA in animal mutagenicity studies were negative. In vitro mutagenicity tests were negative in some cases and positive in others.

CARCINOGENICITY:

NTP Product not listed.

IARC Product not listed.

OSHA Product not listed.

No ingredient of this product present at levels greater than or equal to 0.1% is identified as a carcinogen or potential carcinogen by OSHA, NTP or IARC.

Ethylbenzene, present in this product < 0.1%, is not identified by OSHA or NTP as a carcinogen, but is identified by NTP as a Group 2B substance possibly carcinogenic to humans.

Many studies have been conducted to assess the potential carcinogenicity of diglycidyl ether of bisphenol-A. Although some weak evidence of carcinogenicity has been reported in animals, when all of the data are considered, the weight of evidence does not show that DGEBA is carcinogenic. Indeed, the most recent review of the available data by the International Agency for Research on Cancer (IARC) has concluded that DGEBA is not classified as a carcinogen.

Epichlorohydrin, an impurity in this product (<5 ppm) has been reported to produce cancer in laboratory animals and to produce mutagenic changes in bacteria and cultured human cells. It has been established by the International Agency for Research on Cancer (IARC) as a probable human carcinogen (Group 2A) based on the following conclusions: human evidence – inadequate; animal evidence – sufficient. It has been classified as an anticipated human carcinogen by the National Toxicology Program (NTP). Note: It is unlikely that normal use of this product would result in measurable exposure concentrations to this substance.

12. ECOLOGICAL INFORMATION

Prevent entry into sewers and natural waters. May cause localized fish kill.

Movement and Partitioning:

Bioconcentration potential is moderate (BCF between 100 and 3000 or Log Kow between 3 and 5).

Degradation and Transformation:

Theoretical oxygen demand is calculated to be 2.35 p/p. 20-day biochemical oxygen demand is <2.5%.

Ecotoxicology:

Material is moderately toxic to aquatic organisms on an acute basis. LC50/EC50 between 1 and 10 mg/L in most sensitive species.

13. DISPOSAL CONSIDERATIONS

WASTE DISPOSAL METHOD: Evaluation of this product using RCRA criteria shows that it is not a hazardous waste, either by listing or characteristics, in its purchased form. It is the responsibility of the user to determine proper disposal methods.

Incinerate, recycle (fuel blending) or reclaim may be preferred methods when conducted in accordance with federal, state and local regulations.

14. TRANSPORTATION INFORMATION

DOT
 SHIPPING NAME:..... Not regulated.
 TECHNICAL SHIPPING NAME:..... Not applicable.
 D.O.T. HAZARD CLASS:..... Not applicable.
 U.N./N.A. NUMBER:..... Not applicable.
 PACKING GROUP:..... Not applicable.

IATA
 SHIPPING NAME:..... Not regulated.
 TECHNICAL SHIPPING NAME:..... Not applicable.
 HAZARD CLASS:..... Not applicable.
 U.N. NUMBER:..... Not applicable.
 PACKING GROUP:..... Not applicable.

15. REGULATORY INFORMATION

OSHA STATUS:..... Slight irritant; possible sensitizer.
TSCA STATUS:..... All components are listed on TSCA inventory or otherwise comply with TSCA requirements.

Canada WHIMIS Classification:..... D2B

SARA TITLE III:
SECTION 313 TOXIC CHEMICALS None (de minimus).

STATE REGULATORY INFORMATION:
 The following chemicals are specifically listed or otherwise regulated by individual states. For details on your regulatory requirements you should contact the appropriate agency in your state.

<u>COMPONENT NAME</u> <u>/CAS NUMBER</u>	<u>CONCENTRATION</u>	<u>STATE CODE</u>
Epichlorohydrin 106-89-8	< 5ppm	¹ CA
Phenyl glycidyl ether 122-60-1	<5ppm	¹ CA
Ethylbenzene 100-41-4	< 0.1%	¹ CA, NJ, PA
Benzyl alcohol 100-51-6	< 20%	MA, PA, NJ

¹: These substances are known to the state of California to cause cancer or reproductive harm, or both.

16. OTHER INFORMATION

REASON FOR ISSUE:..... Changes made in Sections 10, 11, 14 & 15.
PREPARED BY:..... G. M. House
APPROVED BY:..... G. M. House
TITLE:..... Health, Safety & Environmental Manager
APPROVAL DATE:..... June 22, 2011
SUPERSEDES DATE:..... February 6, 2011
MSDS NUMBER:..... 105-11b

Note: The Hazardous Material Indexing System (HMIS), cited in the Emergency Overview of Section 3, uses the following index to assess hazard rating: 0 = Minimal; 1 = Slight; 2 = Moderate; 3 = Serious; and 4 = Severe.

This information is furnished without warranty, expressed or implied, except that it is accurate to the best knowledge of West System Inc. The data on this sheet is related only to the specific material designated herein. West System Inc. assumes no legal responsibility for use or reliance upon these data.

MATERIAL SAFETY DATA SHEET

West System Inc.

1. CHEMICAL PRODUCT AND COMPANY IDENTIFICATION

PRODUCT NAME:..... WEST SYSTEM® 206 Slow Hardener
PRODUCT CODE:..... 206
CHEMICAL FAMILY:..... Amine.
CHEMICAL NAME:..... Modified aliphatic polyamine.
FORMULA:..... Not applicable.

MANUFACTURER:
West System Inc.
102 Patterson Ave.
Bay City, MI 48706, U.S.A.
Phone: 866-937-8797 or 989-684-7286
www.westsystem.com

EMERGENCY TELEPHONE NUMBERS:
Transportation
CHEMTREC:..... 800-424-9300 (U.S.)
703-527-3887 (International)
Non-transportation
Poison Hotline:..... 800-222-1222

2. HAZARDS IDENTIFICATION

EMERGENCY OVERVIEW

DANGER Causes burns to eyes and skin. Harmful if swallowed. Harmful if absorbed through the skin. May be harmful if inhaled. Can cause allergic reaction. Aspiration hazard. Clear liquid with ammonia odor.

PRIMARY ROUTE(S) OF ENTRY:..... Skin and eye contact, inhalation.

POTENTIAL HEALTH EFFECTS:

ACUTE INHALATION:..... Excessive exposure to vapor or mist is irritating to the upper respiratory tract, causing nasal discharge, coughing, and discomfort in eyes, nose, throat and chest. Severe cases may cause difficult breathing and lung damage.

CHRONIC INHALATION:..... May cause lung damage. May cause respiratory sensitization in susceptible individuals. Repeated exposures may cause internal organ damage.

ACUTE SKIN CONTACT:..... Corrosive. Prolonged contact may cause skin damage with burns and blistering. Wide spread contact may result in material being absorbed in harmful amounts.

CHRONIC SKIN CONTACT:..... May cause persistent irritation or dermatitis. Repeated contact may cause allergic reaction/sensitization and possible tissue destruction. Can be absorbed through the skin in amounts that can cause internal organ damage.

EYE CONTACT:..... Corrosive. May cause blurred vision. May cause irritation with corneal injury resulting in permanent vision impairment or even blindness.

INGESTION:..... Moderately toxic. May cause gastrointestinal irritation or ulceration. May cause burns of the mouth and throat. Aspiration hazard.

SYMPTOMS OF OVEREXPOSURE:..... Skin irritation, burns and blistering. Irritation of the nose and throat, possible headache. Eye irritation and blurred vision.

MEDICAL CONDITIONS AGGRAVATED BY EXPOSURE:..... Existing respiratory conditions, such as asthma and bronchitis. Existing skin conditions.

3. COMPOSITION/INFORMATION ON HAZARDOUS INGREDIENTS

<u>INGREDIENT NAME</u>	<u>CAS #</u>	<u>CONCENTRATION (%)</u>
Polyoxypropylenediamine	9046-10-0	30-50
Polymer of epichlorohydrin, bisphenol-A, and diethylenetriamine	31326-29-1	10-30
Tetraethylenepentamine	112-57-2	10-30
Diethylenetriamine	111-40-0	5-20
Reaction products of triethylenetetramine and propylene oxide	26950-63-0	5-20
Triethylenetetramine	112-24-3	1-10

4. FIRST AID MEASURES

FIRST AID FOR EYES: Immediately flush with water for at least 15 minutes. Get prompt medical attention.

FIRST AID FOR SKIN: Remove contaminated clothing. Immediately wash skin with soap and water. Do not apply greases or ointments. Get medical attention if severe exposure.

FIRST AID FOR INHALATION: Move to fresh air and consult physician if effects occur.

FIRST AID FOR INGESTION: Give conscious person at least 2 glasses of water. Do not induce vomiting. Aspiration hazard. If vomiting should occur spontaneously, keep airway clear. Get medical attention.

5. FIRE FIGHTING MEASURES

FLASH POINT: > 200°F (Open Cup)

EXTINGUISHING MEDIA: Dry chemical, alcohol foam, carbon dioxide (CO₂), dry sand, limestone powder.

FIRE AND EXPLOSION HAZARDS: Burning can generate toxic fumes. Products of combustion may include, but not limited to: oxides of nitrogen, volatile amines, ammonia, nitric acid, nitrosamines. When mixed with sawdust, wood chips, or other cellulosic material, spontaneous combustion can occur under certain conditions. If hardener is spilled into or mixed with sawdust, heat is generated as the air oxidizes the amine. If the heat is not dissipated quickly enough, it can ignite the sawdust.

SPECIAL FIRE FIGHTING PROCEDURES: Use full-body protective gear and a self-contained breathing apparatus. Use of water may generate toxic aqueous solutions. Do not allow water run-off from fighting fire to enter drains or other water courses.

6. ACCIDENTAL RELEASE MEASURES

SPILL OR LEAK PROCEDURES: Stop leak without additional risk. Wear proper personal protective equipment. Dike and contain spill. Ventilate area. Large spill - dike and pump into appropriate container for recovery. Small spill - recover or use inert, non-combustible absorbent material (e.g., sand, clay) and shovel into suitable container. Do not use sawdust, wood chips or other cellulosic materials to absorb the spill, as the possibility for spontaneous combustion exists. Wash spill residue with warm, soapy water if necessary.

7. HANDLING AND STORAGE

STORAGE TEMPERATURE (min./max.): 40°F (4°C) / 90°F (32°C).

STORAGE: Store in cool, dry place with adequate ventilation.

HANDLING PRECAUTIONS: Use only with adequate ventilation. Do not breath vapors or mists from heated material. Avoid contact with skin and eyes. Wash thoroughly after handling. When mixed with epoxy resin this product causes an exothermic reaction, which in large masses, can produce enough heat to damage or ignite surrounding materials and emit fumes and vapors that vary widely in composition and toxicity.

8. EXPOSURE CONTROLS/PERSONAL PROTECTION

EYE PROTECTION GUIDELINES: Chemical splash goggles, full-face shield or full-face respirator.

SKIN PROTECTION GUIDELINES: Wear liquid-proof, chemical resistant gloves (nitrile-butyl rubber, neoprene, butyl rubber or natural rubber) and full body-covering clothing.

RESPIRATORY/VENTILATION GUIDELINES: General mechanical or local exhaust ventilation. With inadequate ventilation, use a NIOSH/MSHA approved air purifying respirator with an organic vapor cartridge.

Note: West System, Inc. has conducted an air sampling study using this product or similarly formulated products. The results indicate that the components sampled for (amines) were either so low that they were not detected at all or they were well below OSHA's permissible exposure levels.

ADDITIONAL PROTECTIVE MEASURES: Use where there is immediate access to safety shower and emergency eye wash. Provide proper wash/cleanup facilities for proper hygiene. Contact lens should not be worn when working with this material. Generally speaking, working cleanly and following basic precautionary measures will greatly minimize the potential for harmful exposure to this product under normal use conditions.

OCCUPATIONAL EXPOSURE LIMITS: Not established for product as whole. Refer to OSHA's Permissible Exposure Level (PEL) or the ACGIH Guidelines for information on specific ingredients.

9. PHYSICAL AND CHEMICAL PROPERTIES

PHYSICAL FORM Liquid.

COLOR Light-yellow.
ODOR Ammonia-like.
BOILING POINT > 480°F.
MELTING POINT/FREEZE POINT No data.
pH 11.4
SOLUBILITY IN WATER Appreciable.
SPECIFIC GRAVITY 1.01
BULK DENSITY 8.45 pounds/gallon.
VAPOR PRESSURE < 1 mmHg @ 20°C.
VAPOR DENSITY Heavier than air.
VISCOSITY 200 cPs
% VOLATILE BY WEIGHT ASTM 2369-07 was used to determine the Volatile Matter Content of mixed epoxy resin and hardener. 105 Resin and 206 Hardener, mixed together at 5:1 by weight, has a density of 1176 g/L (9.81 lbs/gal). The combined VOC content for 105/206 is 9.59 g/L (0.08 lbs/gal).

10. STABILITY AND REACTIVITY

STABILITY: Stable.

HAZARDOUS POLYMERIZATION: Will not occur.

INCOMPATIBILITIES: May react violently when in contact with oxidizing materials, acids or halogenated compounds such as methylene chloride. Reactions may be slow initially, then may rapidly generate heat and vapor pressure.

DECOMPOSITION PRODUCTS: Very toxic fumes and gases when burned. Decomposition products may include, but not limited to: oxides of nitrogen, volatile amines, ammonia, nitric acid, nitrosamines.

11. TOXICOLOGICAL INFORMATION

No specific oral, inhalation or dermal toxicology data is known for this product.

Oral: Expected to be moderately toxic.

Inhalation: Expected to be moderately toxic.

Dermal: Expected to be moderately toxic.

CARCINOGENICITY:

NTP No.

IARC No.

OSHA No.

No ingredient of this product present at levels greater than or equal to 0.1% is identified as a carcinogen or potential carcinogen by OSHA, NTP or IARC.

12. ECOLOGICAL INFORMATION

In the non-cured liquid form this product may be harmful if released to the environment. Do not allow into sewers, on the ground or in any body of water.

13. DISPOSAL CONSIDERATIONS

WASTE DISPOSAL METHOD: Evaluation of this product using RCRA criteria shows that it is not a hazardous waste, either by listing or characteristics, in its purchased form. It is the responsibility of the user to determine proper disposal methods.

Incinerate, recycle (fuel blending) or reclaim may be preferred methods when conducted in accordance with federal, state and local regulations.

14. TRANSPORTATION INFORMATION

DOT Non-Bulk

SHIPPING NAME: Polyamines, liquid, corrosive, n.o.s.

TECHNICAL SHIPPING NAME: Polyoxypropylenediamine.

HAZARD CLASS: Class 8

U.N./N.A. NUMBER: UN 2735

PACKING GROUP: PG II

ICAO/IATA

SHIPPING NAME: Polyamines, liquid, corrosive, n.o.s.

TECHNICAL SHIPPING NAME: Polyoxypropylenediamine

HAZARD CLASS: Class 8

U.N. NUMBER: UN 2735

PACKING GROUP: PG II

MARINE POLLUTANT: No

IMDG

SHIPPING NAME: Polyamines, liquid, corrosive, n.o.s.
 TECHNICAL SHIPPING NAME: Polyoxypropylenediamine
 HAZARD CLASS: Class 8
 U.N. NUMBER: UN 2735
 PACKING GROUP: PG II
 EmS: F-A, S-B
 MARINE POLLUTANT: No

15. REGULATORY INFORMATION

OSHA STATUS: Corrosive; possible sensitizer.
TSCA STATUS: All components are listed on TSCA inventory or otherwise comply with TSCA requirements.

CANADA WHMIS CLASSIFICATION: D2A – Very toxic material causing other toxic effects. E – Corrosive.
CEPA Chemical Inventory Status: All components are listed or are otherwise compliant with CEPA requirements.

SARA TITLE III:
SECTION 313 TOXIC CHEMICALS: None.

STATE REGULATORY INFORMATION:

The following chemicals are specifically listed or otherwise regulated by individual states. For details on your regulatory requirements you should contact the appropriate agency in your state.

<u>COMPONENT NAME</u>	<u>STATE CODE</u>
Tetraethylenepentamine 112-57-2	RI, MA, NJ, PA
Tetraethylenetriamine 112-24-3	RI, MA, NJ, PA
Diethylenetriamine 111-40-0	RI, MA, NJ, PA

16. OTHER INFORMATION

REASON FOR ISSUE: Changes made in Section 2, 3 and 14.
PREPARED BY: G. M. House
APPROVED BY: G. M. House
TITLE: Health, Safety & Environmental Manager
APPROVAL DATE: April 3, 2013
SUPERSEDES DATE: February 10, 2011
MSDS NUMBER: 206-13a

This information is furnished without warranty, expressed or implied, except that it is accurate to the best knowledge of West System Inc. The data on this sheet is related only to the specific material designated herein. West System Inc. assumes no legal responsibility for use or reliance upon these data.

18-8 Stainless Steel Pan Head Slotted Machine Screw

12-24 Thread, 3/4" Length



Packs of 50

In stock

\$8.06 per pack of 50

91792A294

ADD TO ORDER

Thread Size	12-24
Length	3/4"
Additional Specifications	18-8 Stainless Steel
RoHS	Compliant

Screws up to 2" long are fully threaded; those longer than 2" have at least 1 1/2" of thread. Length is measured from under the head.

Type 316 Stainless Steel Hex Nut

5/16"-24 Thread Size, 1/2" Wide, 17/64" High



Packs of 50

In stock

\$7.92 per pack of 50

94804A315

[ADD TO ORDER](#)

Material	Type 316 Stainless Steel
----------	--------------------------

Thread Size	5/16"-24
-------------	----------

Width	1/2"
-------	------

Height	17/64"
--------	--------

Additional Specifications	Plain
---------------------------	-------

RoHS	Compliant
------	-----------

Also known as full or finished nuts, these common nuts are also our most popular. They typically come in sizes 1/4" and larger and have a Class 2B thread fit. Sizes 1 1/2" and smaller have dimensions that meet ANSI/ASME B18.2.2.



GRAFIL 34-700

Grafil 34-700 carbon fiber is a continuous, high strength, PAN based fiber. It is available in 12K and 24K filament count tows. They can be supplied in either round tow or flat tow formats. The flat tow (designated by 'WD') is the ideal fiber to use in applications where spreading is required, e.g., tape production. The round tow is used in applications where spreading is not necessarily required, e.g., braiding and weaving.

Typical Fiber Properties

Tow Tensile	Strength	700 ksi 4830 MPa	SRM 16
	Modulus	34 msi 234 GPa	
Typical Density		0.065 lb.in ³ 1.80 g/cm ³	SRM 15
Typical Yield	12K	620 yds/lb 800 mg/m	SRM 13
	24K	310 yds/lb 1600 mg/m	SRM 13

Typical Mechanical Properties

Tensile Properties	0°	Strength	373 ksi 2572 MPa	ASTM D3039 / 0°8ply
		Modulus	19.9 msi 137 GPa	ASTM D3039 / 0°8ply
	90°	Strength	11.17 ksi 81 MPa	ASTM D3039 / 0°16ply
		Modulus	1.34 msi 9.2 GPa	ASTM D3039 / 0°16ply
Compressive Properties	0°	Strength	198 ksi 1365 MPa	ASTM D3410 / 0°16ply
		Modulus	18.5 msi 127 GPa	ASTM D3410 / 0°16ply
	90°	Strength	30.5 ksi 210 MPa	ASTM D3410 / 0°20ply
		Modulus	1.49 msi 10.2 GPa	ASTM D3410 / 0°20ply
Flexural Properties	0°	Strength	253 ksi 1745 MPa	ASTM D790 / 0°16ply, L/D=32, Vf=61%
		Modulus	19.1 msi 132 GPa	ASTM D790 / 0°16ply, L/D=32, Vf=61%
	90°	Strength	14.9 ksi 102 MPa	ASTM D790 / 0°16ply, L/D=16, Vf=61%
		Modulus	1.28 msi 8.8 GPa	ASTM D790 / 0°16ply, L/D=16, Vf=61%
ILSS	Strength	14.1 ksi 97 GPa	ASTM D2344 / 0°16ply, L/D=4, Vf=59%	

- 250F Epoxy Prepregs
- Resin: Mitsubishi Rayon #340 resin system
- Tensile and compressive properties are normalized to 60% fiber volume

5900 88th Street
 Sacramento, CA
 95828, USA
 Tel: 916.386.1733
 Fax: 916.383.7668
 Web: www.grafil.com



ISO 9001:2000
 FM 56416

High-Strength Grade 8 Steel Cap Screw

1/4"-20 Fully Threaded, 3/4" Long, Zinc-Plated

Packs of 100

In stock

\$12.01 per pack of 100

92620A540

ADD TO ORDER

Material	Steel
Grade	8
Finish	Zinc Yellow-Chromate Plated
Thread Size	1/4"-20
Head Width	7/16"
Head Height	11/64"
Screw Size	1/4" (0.250")
Length	3/4"
Thread Length	Full
RoHS	Not Compliant

The standard for high-strength cap screws, these are made from alloy steel and have a minimum tensile strength of 150,000 psi. Length is measured from under the head.

Inch screws are marked on the head with six radial lines to indicate Grade 8. Screws have a minimum Rockwell hardness of C33 and a Class 2A thread fit. They also meet ASME B18.2.1 and SAE J429.

Zinc Yellow-Chromate Plated—Screws are rust resistant.

Zinc Aluminum Coated Steel Hex Nut

Grade 8, 1/4"-20 Thread Size, 7/16" Wide, 7/32" High



Packs of 100

In stock

\$6.74 per pack of 100

93827A211

ADD TO ORDER

Material	Grade 8 Steel
----------	---------------

Thread Size	1/4"-20
-------------	---------

Width	7/16"
-------	-------

Height	7/32"
--------	-------

Additional Specifications	Ultra Coated
---------------------------	--------------

RoHS	Compliant
------	-----------

Also known as full or finished nuts, these common nuts are also our most popular. They typically come in sizes 1/4" and larger and have a Class 2B thread fit. Sizes 1 1/2" and smaller have dimensions that meet ANSI/ASME B18.2.2.

Xoar Prop

Note: Data is only provided for a 28" prop. The props for this project will be custom 30", so no technical data is immediately available.

Link:<http://www.xoarintl.com/rc-propellers/precision-pair/PJP-T-28-Precision-Pair-Carbon-Fiber-Propeller/>

SPECIFICATIONS				^ Back To Top
Diameter	Pitch	Average Net Weight/Prop*	Shaft Size+	
28"	8	73 ± 1 g	8 mm	
<p>*Suggested Average Net Weight per size is for Reference Only. Actual weight varies among the specification of the prop (diameter x pitch) and other external factors. Please Note: Measuring equipment and method will greatly affect the result.</p> <p>+Suggested shaft diameters are manufacture standard. Custom shaft sizes available in 4, 6, 8, 10mm upon request. Please contact us before placing orders.</p>				

Joby Motor

Note: This project will be using the JM1S motor

Link: <http://www.jobymotors.com/public/views/pages/products.php>

High and Low Voltage Motors Available



Construction	inrunner	inrunner	inrunner	inrunner	
Nominal Voltage	40-500	35-700	50 - 700	100 - 600	V
Poles	22	22	46	46	
Nominal RPM	6000	6000	2500	2500	
Maximum RPM	9000	9000	3500	3500	
Diameter	154	154	200	200	mm
Mass	1800	2750	3350	4000	g
Length	53.1	65	65	75	mm
Continuous Torque	13	21	40	53	N-m
Continuous Shaft Power at Nominal RPM	8.2	13.2	10.5	14	kW
Peak Torque	20	32	60	80	N-m
Peak Shaft Power at Nominal RPM (15s)	12.6	20.1	15.7	20.9	kW
Price	\$1,200	\$1,800	\$2,400	\$3,200	USD

Standard Available Windings

JM1S	—	JM1	—	JM2S	—	JM2	—
Kv	Bus Voltage	Kv	Bus Voltage	Kv	Bus Voltage	Kv	Bus Voltage
175	45 V	200	40 V	—	—	—	—
160	50 V	145	55 V	—	—	—	—
120	65 V	105	75 V	—	—	—	—
100	80 V	90	90 V	50	50 V	—	—
75	110 V	75	110 V	33	75 V	—	—
50	160 V	65	125 V	25	100 V	30	100 V
25	325 V	45	180 V	12	250 V	19	150 V
18	450 V	30	270 V	6	500 V	9.5	300 V
16	500 V	16	500 V	4	700 V	5	600 V

Windings shown indicate most popular winding choices. Custom windings available upon request.

Joby Motor JM1S

Winding Info

Winding	Kv	Bus Voltage
3T Delta	175	40-50
2T Wya	160	45-55
4T Delta	120	60-70
3T Wya	100	70-90
4T Wya	75	100-120
13T Wya	25	300-350
18T Wya	18	400-500

rpm/V at nominal load and rpm will be about 80% of listed kv

Test Data:

Winding	Propeller	Voltage	Lipo Cells (equiv.)	Power In (kW)	RPM	Thrust (kg)
3T Delta	JC 26x12	50	14s	10.9	7000	34
2T Wya	JC 26x12	50	14s	8.0	6500	30
2T Wya	HK 27x10	50	14s	8.0	6500	30
2T Wya	Xoar 30x10	50	14s	10.5	6100	42
4T Delta	Xoar 32x12	50	14s	8.6	5100	34



Upgrade your 80cc size gas engine model with the Turnigy RotoMax 80cc Brushless [outrunner](#) motor. This motor will provide clean and efficient power for your large scale aircraft without the mess and hassle of fuel.

When combined with a 14s [Lipoly](#) battery and a 200Amp [ESC](#) the RotoMax motor will supply punchy, responsive power that only an electric setup can provide.

This motor is specifically suited for carbon fiber & wooden propellers and features an IC style 6 bolt hole design. The shaft has also been tapped to suit a 5mm bolt to make fitting a spinner of your choice easy.

Spec.

Battery: 12 Cell ~ 14 Cell / 44.4V ~ 51.8V

RPM: 195kv

Max current: 150A

Watts: 6600w

No load current: 44V/4.8A

Internal resistance: 0.013 ohm

Weight: 1916g

Diameter of shaft: 10mm

Winding: 8T

Stator Pole: 24

Motor Pole: 20

Stator Diameter: 101

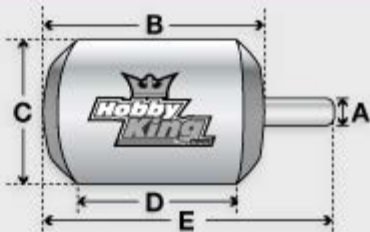
Lamination Thickness: 0.2mm

Suggested [ESC](#): 200A 14S Compatible

Product Config Table

Kv(rpm/v)	195
Weight (g)	1916
Max Current(A)	150
Resistance(mh)	0
Max Voltage(V)	52
Power(W)	6600
Shaft A (mm)	10
Length B (mm)	110
Diameter C (mm)	108
Can Length (mm)	48
Total Length E (mm)	142

[Update/Add my own data](#)
[Customer Data](#)



COMPARE

OpenPilot Revolution Hardware Set

Link: <http://store.openpilot.org/home/21-revolution-hardware-kit.html>

- OpenPilot Revolution STM32F4 Flight Controller with In-built OPLink Modem, right angle headers
- OpenPilot V9 GPS
- OpenPilot OPLink Mini 433Mhz 100mw Modem
- 2 x OpenPilot Serial Cables
- Revolution RC cable
- Revolution 433Mhz antenna
- Rubber Duck 433Mhz antenna
- MMCX to SMA Pigtail

Electronic Speed Controller

Link:http://www.hobbyking.com/hobbyking/store/_57873_Turnigy_dlux_250A_HV_14s_60v_ESC_AR_Warehouse_.html?strSearch=Turnigy%20dlux%20250

Turnigy® dlux ESCs have set a new bench mark in quality and performance.

Each ESC uses a twin PCB design separating the motor power supply & MCU. This design allows for optimum component layout on each PCB and provides the ideal configuration for heat dissipation and thermal efficiency. Both PCBs are enclosed in an aluminum heat sink casing to ensure maximum heat dispersion. The switching Fet's in this ESC are genuine top quality International Rectifier HEXFET's.

All Turnigy dlux ESCs can be programmed via a programing card or by transmitter.

Note: This in an OPTO ESC you will require an external BEC or Receiver battery.

Specs:

Max Cont Current: **250A**
Max Burst Current: **275A**
BEC: **N/A (OPTO)**
LiPo: **6~14S**
NiMH: **18~42cells**
Weight: **456grams**
Max RPM (2-pole): **200,000rpm**
Size: **135 x 77 x 50mm**
Motor Plug: **Female 6mm bullet Connector**
Battery Plug: **Nil**

Features:

Low Internal Resistance
Low Operating Temperature
Over Temperature Protection
Spark Eliminator
High Quality Hexfets (Mosfets)

Programming Options:

Battery Type: Lixx / Nimh
Forward/Reverse
Soft Start
LV Cut off Type (Ignore, Reduce Power, Stop Motor)
LV Cut off setting
Timing
Switching (8,16kHz)
Factory Restore

Default factory settings:

Brake: off
Battery: LiPo Auto Detect
Low Voltage Cut: 3.2v (power down motor)
Timing: Auto
Frequency: 8KHz

8AWG Power Cable

Link: <http://www.progressiverc.com/prc-silicone-wire-by-the-foot-8-awg.html>

- **Wire Type:** 8 AWG Silicone
- **Outside Diameter:** 5mm
- **Current Rating:** 200A

Power Cable Connectors

Link: http://www.activepowersports.com/castle-creations-ccb6-5x3-6-5mm-bullet-conn-13g-8g-200a-3-cc-bullet-6-5mm/?gclid=Cj0KEQiA0aemBRC8p87zv_mc5qYBEiQAIeEMQU-wFRG-q10AdUaYiYc4n_t8ZX31nPpv2liJnwywqSsaAhsL8P8HAQ

Castle Creations - CCBUL6.5X3 6.5mm Bullet Conn 13G/8G 200A (3) - CC BULLET 6.5MM

Turnigy 7s LiPo

Link: http://www.hobbyking.com/hobbyking/store/uh_viewItem.asp?idProduct=59238

Product Config Table

Capacity(mAh)	5000
Config (s)	7
Discharge (c)	65
Weight (g)	978
Max Charge Rate (C)	8
Length-A(mm)	155
Height-B(mm)	49
Width-C(mm)	64

[Update/Add my own data](#)
[Customer Data](#)



COMPARE

USA EAST WAREHOUSE

THIS ITEM IS ONLY AVAILABLE TO USA CUSTOMERS. YOU WILL BE ABLE TO FIND THE SAME ITEM UNDER A DIFFERENT LISTING IN OUR WEBSITE FOR INTERNATIONAL PURCHASES.

[International Warehouse](#)

150W Soldering Iron

Link:<http://www.amazon.com/Watt-Volt-Soldering-Chisel-Style/dp/B008MG9H3A#productDetails>

Brand new soldering Iron
Chisel tip (3/8" at tip, 1/2" at widest point)
Voltage: 120V
Power: 150 watts
Lightweight with a wood handle
Tool length: 11 inches(28cm)
Cable Length: 53.5 inches(136cm), US plug
Smooth melted solder flow and ideally lustrous finish
Ideal for general Home and Shop use

Turnigy Battery Eliminator Circuit (BEC)

Link:http://www.hobbyking.com/hobbyking/store/_24753_Turnigy_dlux_10A_10_60V_HV_SBEC.html

Features:

- Stable, reliable power supply for your servos/receiver
- 10~60V input allowing for use with 3~14S lipoly batteries
- 10A continuous/15A peak servo current capability
- Dual power output leads
- Selectable servo output voltage 5.2V/6V/6.8V/7.4V/8.4V
- Optional adjustable low voltage alarm/LED
- Thermal and current overload protection

Specs:

Input Voltage: **3~14S Lipoly (10~60V)**
Output Voltage: **5.2V/6.0V/6.8V/7.4V/8.4V selectable**
Output Current: **10A @ 6V continuous (15A @ 6V peak)**
Adjustable Low Voltage Alarm: **10~60V**
Switch Type: **Fail Safe (fail safe on) pin-flag contactless type**
Power Connector: **Input: bare leads / Output: JR style plug x 2**
Dimensions: **15.7 x 31 x 54mm**
Weight: **45g**

USB to PPM Converter

Link:

Features:

Channel resolution v2.0: 2048 (11bit)

Channel resolution v1.0: 1024 (10bit) **Old version**

Max Channel Count: 10 channel

PPM Mode: Positive/Negative PPM selectable

Cable Length: 120cm

Software: GNU licensed OpenSource Software for everyone

Transmitter and Receiver

Link:http://hobbywireless.com/scherrer-uhf-long-range-rc-c-98_100/scherrer-uhf-tx-rx-700-lite-p-1538.html

External firmware upgrade port
Running LED
Completely new software
Selectable PPM/PWM (S-Bus planned to come soon) upon boot.
9 servo channels
PPM output (also called SUM signal)
Rssi output 0.5 to 3.3V from min to mix
Supply voltage 4-10 Volts
Supply current RX alone 18mA at 5V
Possible to upgrade to MCX connector
Wideband frequency hopping system
Uses 433 to 440 MHz ISM licence free band
User firmware upgradeable
Wide user temperature range -40C to +70C ambient
Weight 8 Grams
The receiver board is 26 x 53mm.
Tx Specifications

It comes packed with all the well known features and a lot of new such as

Support Fixed/Variable PPM input
Futaba input, all up to 12 channels
Head tracker input
AUX input (for option boards)
Option board port
Output power switch
Firmware update port
Status Led
Military standard input plugs with screw protection
The TX700 comes in a new design that reduces the height dramatically.

Joby JM1S Test Data

Time	Current	Voltage	Thrust	Torque	Input Power	Output Power	Efficiency	RPM
1	1.582	53.869	-0.345	0.004	85.223	0.030	0.03	72.7
2	7.143	53.760	-0.305	0.630	384.006	113.810	29.64	1725.6
3	6.736	53.763	1.366	1.472	362.165	309.176	85.37	2005.2
4	8.109	53.756	2.356	0.988	435.906	222.789	51.11	2152.3
5	9.826	53.749	2.830	1.172	528.147	289.233	54.76	2355.8
6	10.285	53.748	3.478	1.377	552.776	357.434	64.66	2478.6
7	10.277	53.747	3.887	1.382	552.344	360.834	65.33	2493.5
8	10.288	53.746	3.953	1.377	552.931	360.970	65.28	2503.7
9	10.287	53.746	3.896	1.382	552.897	363.308	65.71	2509.7
10	10.276	53.746	3.925	1.384	552.271	365.207	66.13	2520.5
11	10.290	53.746	3.920	1.377	553.044	364.876	65.98	2531.2
12	10.274	53.746	3.987	1.373	552.205	364.088	65.93	2532.5
13	10.267	53.746	3.961	1.384	551.817	367.498	66.60	2535.7
14	10.274	53.746	3.921	1.393	552.188	368.751	66.78	2528.6
15	10.281	53.746	4.076	1.404	552.535	369.819	66.93	2516.1
16	10.273	53.746	4.176	1.410	552.131	373.207	67.59	2526.9
17	10.268	53.744	4.119	1.404	551.842	373.056	67.60	2537.0
18	10.207	53.745	4.053	1.391	548.564	371.130	67.65	2547.4
19	10.243	53.745	4.022	1.382	550.525	367.027	66.67	2536.7
20	10.249	53.745	4.050	1.399	550.843	371.834	67.50	2538.8
21	10.239	53.745	3.959	1.396	550.281	370.868	67.40	2537.7
22	10.258	53.745	4.006	1.395	551.332	369.939	67.10	2532.0
23	14.003	53.726	4.134	1.407	752.351	374.359	49.76	2541.5
24	46.099	52.195	4.509	1.934	2406.129	744.589	30.95	3677.0
25	53.337	51.870	10.920	4.709	2766.590	2247.447	81.24	4557.3
26	52.764	51.870	14.837	4.785	2736.882	2288.985	83.63	4567.7
27	52.433	51.871	14.561	4.714	2719.727	2258.783	83.05	4576.1
28	52.811	51.871	14.474	4.670	2739.356	2232.621	81.50	4565.5
29	53.037	51.869	14.745	4.762	2750.984	2274.639	82.68	4561.4
30	52.804	51.871	14.697	4.783	2738.961	2287.718	83.53	4567.0
31	52.144	51.871	14.781	4.741	2704.773	2274.049	84.08	4580.1
32	52.365	51.871	14.785	4.685	2716.224	2243.686	82.60	4573.6
33	52.475	51.870	14.729	4.712	2721.885	2255.752	82.87	4572.0
34	52.757	51.871	14.670	4.729	2736.543	2263.269	82.71	4570.6
35	52.959	51.870	14.819	4.744	2746.978	2286.353	83.23	4602.7
36	54.514	51.868	14.355	4.712	2827.526	2284.323	80.79	4629.7
37	55.229	51.866	15.202	4.879	2864.527	2364.300	82.54	4627.3
38	56.112	51.866	15.426	4.953	2910.278	2417.395	83.06	4660.5
39	73.939	51.842	15.247	4.984	3833.118	2542.502	66.33	4871.7
40	89.139	51.825	17.841	6.226	4619.632	3533.525	76.49	5419.5
41	89.706	51.828	21.676	6.996	4649.255	3979.813	85.60	5432.2
42	88.521	51.825	22.164	7.072	4587.628	4031.026	87.87	5443.3
43	88.703	51.826	21.638	6.919	4597.079	3943.909	85.79	5443.3
44	88.915	51.826	21.938	6.973	4608.117	3973.411	86.23	5441.3
45	89.355	51.825	21.811	6.982	4630.817	3970.190	85.73	5430.4
46	88.285	51.826	21.957	6.988	4575.487	3983.259	87.06	5443.3
47	88.294	51.828	21.717	6.922	4576.117	3945.927	86.23	5443.3
48	88.921	51.825	21.700	6.909	4608.398	3954.776	85.82	5466.2
49	90.678	51.825	21.798	6.945	4699.443	3963.716	84.34	5450.1
50	104.732	51.811	22.218	7.123	5426.253	4149.725	76.47	5563.3
51	146.367	51.767	23.187	7.939	7576.906	5222.483	68.93	6282.2
52	153.856	51.759	29.087	10.003	7963.480	6828.064	85.74	6518.2
53	154.008	51.759	30.854	10.275	7971.329	7003.942	87.86	6509.0
54	156.335	51.757	30.929	10.296	8091.458	7002.660	86.54	6495.0
55	155.712	51.758	31.497	10.477	8059.398	7129.886	88.47	6498.6
56	156.176	51.757	31.013	10.412	8083.151	7077.103	87.55	6491.0
57	155.243	51.759	30.754	10.469	8035.194	7124.391	88.66	6498.6
58	155.751	51.759	31.285	10.403	8061.552	7076.939	87.79	6496.1
59	155.985	51.757	31.361	10.447	8073.372	7099.493	87.94	6489.7
60	154.685	51.760	31.080	10.427	8006.432	7094.665	88.61	6497.3
61	151.655	51.762	30.671	10.338	7849.959	7066.036	90.01	6526.8
62	155.230	51.759	30.042	10.102	8034.467	6877.176	85.60	6500.8
63	155.933	51.757	31.254	10.408	8070.663	7077.459	87.69	6493.3
64	138.399	51.776	31.772	10.479	7165.777	7120.394	99.37	6488.6
65	54.241	51.876	30.497	9.421	2813.820	4779.708	169.87	4844.6

Motor: Joby JM1S 1109M1S
3-phase 2TY
ESC: Jeti Spin Pro 220
Prop: HK 27x10

31-Jan-14

highlighted values are full power

Joby JM1S Test Data

66	30.163	52.647	18.050	4.435	1587.982	1818.009	114.49	3914.9
67	19.455	53.703	11.193	3.058	1044.781	1109.408	106.19	3464.9
68	7.790	53.765	8.607	2.227	418.805	640.069	152.83	2744.7
69	0.610	53.911	5.447	0.938	32.859	145.925	444.09	1484.9
70	0.586	53.914	2.126	-0.031	31.574	-3.057	-9.68	945.8
71	0.592	53.913	0.839	-0.030	31.905	-2.035	-6.38	647.0
72	0.590	53.912	0.527	-0.023	31.825	-1.125	-3.53	463.5
73	0.589	53.912	0.401	-0.029	31.745	-0.988	-3.11	323.9
74	0.590	53.911	0.338	-0.024	31.808	-0.557	-1.75	225.0
75	0.593	53.910	0.312	-0.023	31.953	-0.342	-1.07	142.7
76	0.595	53.909	0.300	-0.015	32.081	-0.123	-0.38	80.7
77	0.591	53.909	0.305	-0.004	31.883	-0.030	-0.09	75.0

Average Full Power Values

Current	Voltage	Thrust	Torque	Input Power	Output Power	Efficiency	RPM
155.171	51.758	30.892	10.286	8031.393	7003.301	87.204	6502.003

Experiment Step By Step Procedures

System Calibration test

1. Set up the test stand as shown in figure 1
2. Start all cameras recording
3. All test operators leave test area and go behind protective wall
4. Energize the system by closing the kill switch
5. Slowly increase the motor throttle from 0 to 90% at a steady rate over the course of approximately 1 to 1.5 minutes
6. Return throttle to 0% and allow for propeller to quit spinning
7. De-energize the system by opening the kill switch
8. Stop cameras and save the videos for future analysis

Acceleration test

1. Set up the test stand as shown in figure 1
2. Start all cameras recording
3. All test operators leave test area and go behind protective wall
4. Energize the system by closing the kill switch
5. Turn the throttle to 80% of the required setting for 50lbs of thrust and allow propeller speed to settle
6. Suddenly increase the throttle to the setting which produces 50lbs of thrust, and allow propeller speed to settle
7. Suddenly increase the throttle to 120% of the required setting for 50lbs of thrust and allow propeller speed to settle
8. Return the throttle to 80% of the 50lbs thrust setting, and repeat steps 6 and 7 two more times
9. Return throttle to 0% and allow for propeller to quit spinning
10. De-energize the system by opening the kill switch
11. Stop cameras and save the videos for future analysis

Steady state test

1. Set up the test stand as shown in figure 1
2. Start all cameras recording
3. All test operators leave test area and go behind protective wall
4. Energize the system by closing the kill switch
5. Set throttle to the 50lbs of thrust setting, allow the motor to run until the battery voltage is 24.8V (.3V above minimum safe operating voltage)
6. Return throttle to 0% and allow for propeller to quit spinning
7. De-energize the system by opening the kill switch
8. Stop cameras and save the videos for future analysis

Propulsion Appendices

Raw Test Data

	Time	RPM	Voltage (V)	Current (A)	Thrust (lbf)
1 st Throttle Up	1.00	0	59.88	3.5	14
	2.00	1740	54.67	4	23
	3.00	3450	54.12	3.8	17
	4.00	4050	53.53	16.8	19
	5.00	4560	51.99	16	18
	6.00	5070	51	5.9	45
	7.00	5490	49.94		50
	8.00	5640	53.7	70.8	4
	9.00	3540	54.05	0.5	2
	10.00	930	54.26	0	2
2 nd Throttle Up	0.00	0	54.79	0	2
	1.00	270	54.73	1.6	3
	2.00	1230	54.49	1.5	10
	3.00	2130	54.94	0.6	12
	4.00	2880	54.14	1.9	18
	5.00	3300	53.91	5.6	24
	6.00	3630	53.31	4.8	15
	7.00	4230	52.75	5.7	20
	8.00	4680	52.13	3.7	17
	9.00	4980	51.44	5.6	18
	10.00	5190	50.64	5	24
	11.00	5370	50.12	4.8	35
	12.00	5460	49.43	4.1	40
	13.00	5550	48.92	4.2	45
	14.00	5700	47.37	12.7	50
	15.00	4440	52.37	54.1	2
	16.00	720	51.73	4.8	6
	17.00	1530	53.11	3.1	2
	18.00	210	53.38	0.5	2
19.00	0	53.55	0.2	2	
3 rd Throttle Up	0.00	0	54.15	0.1	2
	1.00	120	53.96	6.8	6
	2.00	1590	53.88	13	13
	3.00	2640	53.33	40.6	24
	4.00	3660	52.99	46.7	25
	5.00	4170	52.06	83.9	21

Propulsion Appendices

	6.00	4800	51.3	109.2	20
	7.00	5070	50.15	130.4	34
	8.00	5400	49.77	166.3	42
	9.00	5520	48.89	187	45
	10.00	5670	47.91	220.6	52
	11.00	5790	46.59	257.4	50
	12.00	5820	45.86	267.5	51
	13.00	5850	46.48	253.9	43
	14.00	5730	46.35	222.4	45
	15.00	5670	46.23	225.9	43
	16.00	5640	46.19	226.5	45
	17.00	5670	46.3	219.4	40
	18.00	5670	47.27	175.3	27
	19.00	5400	47.3	182.2	31
	20.00	5430	47.65	178.6	23
	21.00	5020	47.75	139.8	48
	22.00	5460	46.17	236.9	45
	23.00	5640	45.89	241.3	46
	24.00	5670	45.88	230.5	44
	25.00	5730	45.92	224.2	44
	26.00	5670	47.39	175.5	18
	27.00	5170	46.31	185.8	45
	28.00	5610	45.66	240.1	46
	29.00	5790	45.33	242	45
Failure	30.00	5610	50.03	120.1	5
	31.00	2970	50.79	53.8	2
	32.00	900	51.15	0.1	2
	33.00	120	51.37	5.7	2
	34.00	0	51.65	0.2	2

Table A2.1. Turnigy Rotomax 80cc raw data

Propulsion Appendices

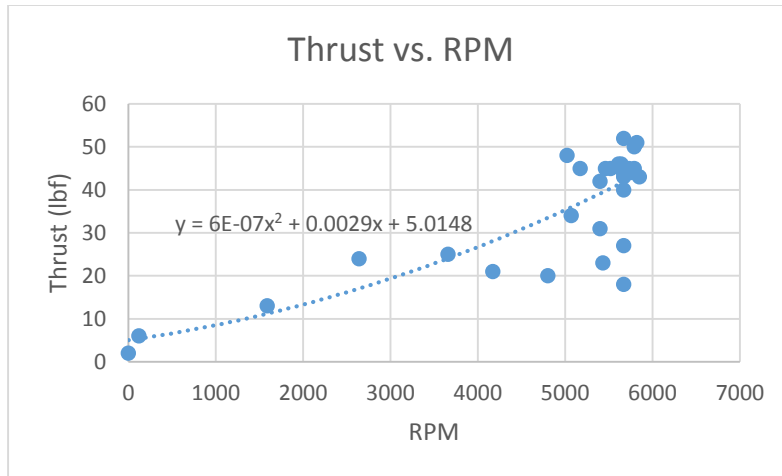


Figure A2.1. Thrust vs RPM for the Turnigy Rotomax 80cc motor

JM1S Data

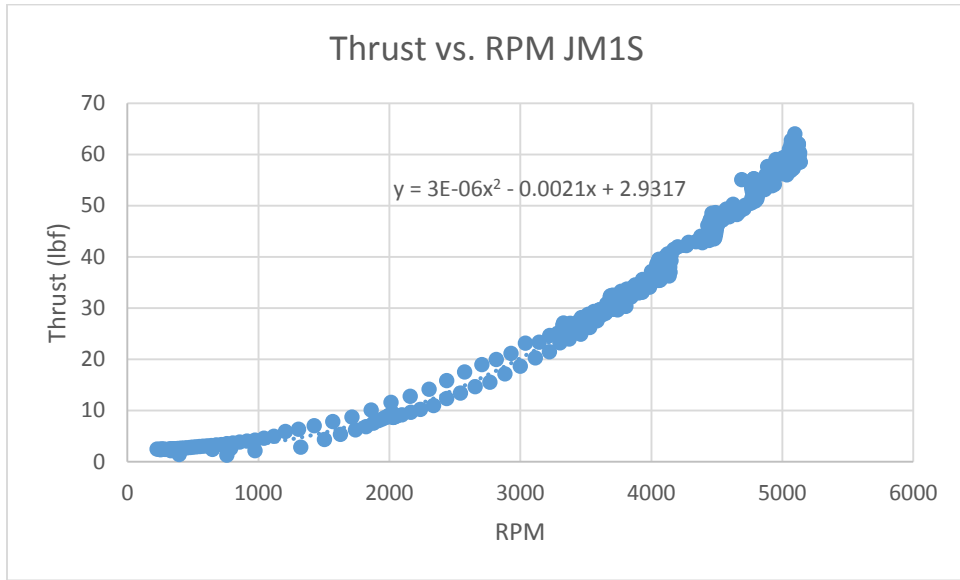


Figure A3.1. Thrust vs RPM for the JM1S motor

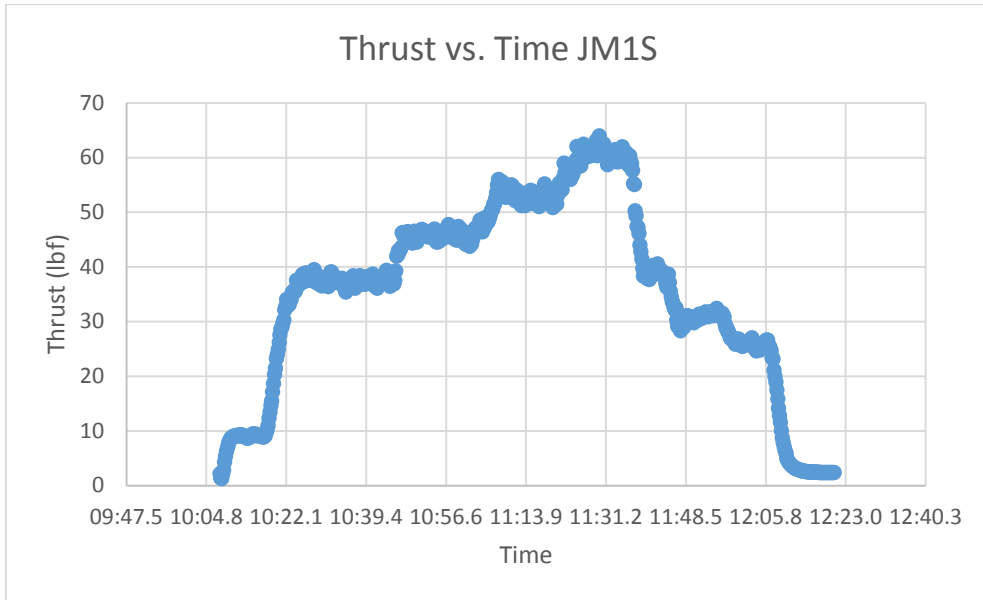


Figure A3.2. Thrust vs time for the JM1S motor

Future Test Improvements and Other Notes

Improvements for future tests

The first improvement would be to use a more finely controlled throttle. During the test the thrust of the propeller could not be finely adjusted. Due to this we are lacking data for much of the operating range. Also the lack of throttle control made a slow ramp up nearly impossible, so if there was vibrations occurring we would not have been able to slowly increase speed to detect them. For this test we used the joystick of a remote control. The reason for using the joystick is that the integration of the control into the system was very simple. However, the joystick did not allow for easy and accurate control of the throttle percentage. For future tests a knob throttle is recommended for use. The knob would allow for more movement over the throttle range which would allow for finer adjustment. The knob would also allow for greater repeatability since the position of the throttle could be marked and repeated for future tests.

An improvement for test safety would be to check the amperage rating of the circuit breaker. The circuit breaker used for this test was a 200A circuit breaker. However, the precise trip is not clear. Upon further research the trip current appears to be 300A. If it were possible a circuit breaker with a lower trip current would allow for greater protection against burning another. We did not trip the circuit breaker during this test so we cannot comment on its current interrupting abilities, but we are still confident that it would work for short circuits.

If possible future tests should use a DAQ. While our test results were adequate to verify the performance of the motor, the specific performance data of the motor will contain large uncertainties. As a result we cannot for sure predict the performance of the motor, just approximate magnitudes. Also extracting the data from our tests will prove quite difficult since each value will need to be read at specific times from the videos. A DAQ would allow us to get much more accurate results, however, would require considerably more work during setup and much more expensive equipment, and should only be used if highly accurate data is needed.

The general construction of the test setup should be improved, in both materials and construction techniques. The video shot from the side of the propeller shows that the structure was bending during the test. The bending is likely what caused the large fluctuations in thrust indicated by the scale.

A more expensive tachometer should be used for further tests. The tachometer we used appeared to be very inaccurate and slow to change. Comparing the thrust vs RPM of our test and the JM1S test data shows very little similarity. Since the thrust vs RPM should be independent of motors, and the thrust measurement is reasonably accurate the RPM measurements must have significant errors.

Other Notes

- Very little vibration was noticed during the test. Based on this observation the risk of vibration is significantly less than expected for the full multicopter assembly.

Propulsion Appendices

- The propeller produced a significant amount of noise. During testing of the full assembly ear protection will be required.
- The test confirmed why the overhead prop configuration was not practical. The propeller was blowing debris on the ground up to 20ft away, and would have almost certainly blow something into the pilot at high velocity during flight causing injury

Additional Photos of Test Setup



Figure A5.1

Propulsion Appendices



Figure A5.2



Figure A5.3



Figure A5.4

Electric Commuter Multicopter Motor and Propeller Test Plan and Safety Document

January 26, 2015

Team Members:

Alex O'Hearn

Art Norwood

Blake Sperry

Ike Sheppard

Jarrell Washington

Kyle Kruse

Marley Miller

Oliver Kunz

Sam Juday

Propeller Test Plan and Safety Document

Purpose

The Electric Multicopter senior project intends to perform a motor test. The purpose of the motor test will be to analyze the performance of an 80CC Turnigy Rotomax hobby motor spinning an Xoar 30x10 propeller, and compare its performance to the performance of an industrial motor, the JM1S motor from JobyMotors, using the same propeller. The test will be an attempt to measure; the thrust provided by the motor, power consumption of the motor, and the ability of the motor to accelerate the propeller.

Equipment

The equipment required for this test is:

- 80CC Turnigy Rotomax motor
- Xoar 30x10 propeller
- Electronic Speed Controller (ESC)
- Throttle controller
- 2 7S batteries
- 100ft of 2 gauge wire
- Emergency Disconnect Switch
- Wire connectors
- 20ft of wooden 2x6s
- Hinge
- Screws
- Thermocouples
- Non-contact Tachometer
- Scale
- Protection wall
- Voltmeter
- Clamp ammeter
- Table or alternative solid test base

Propeller Test Plan

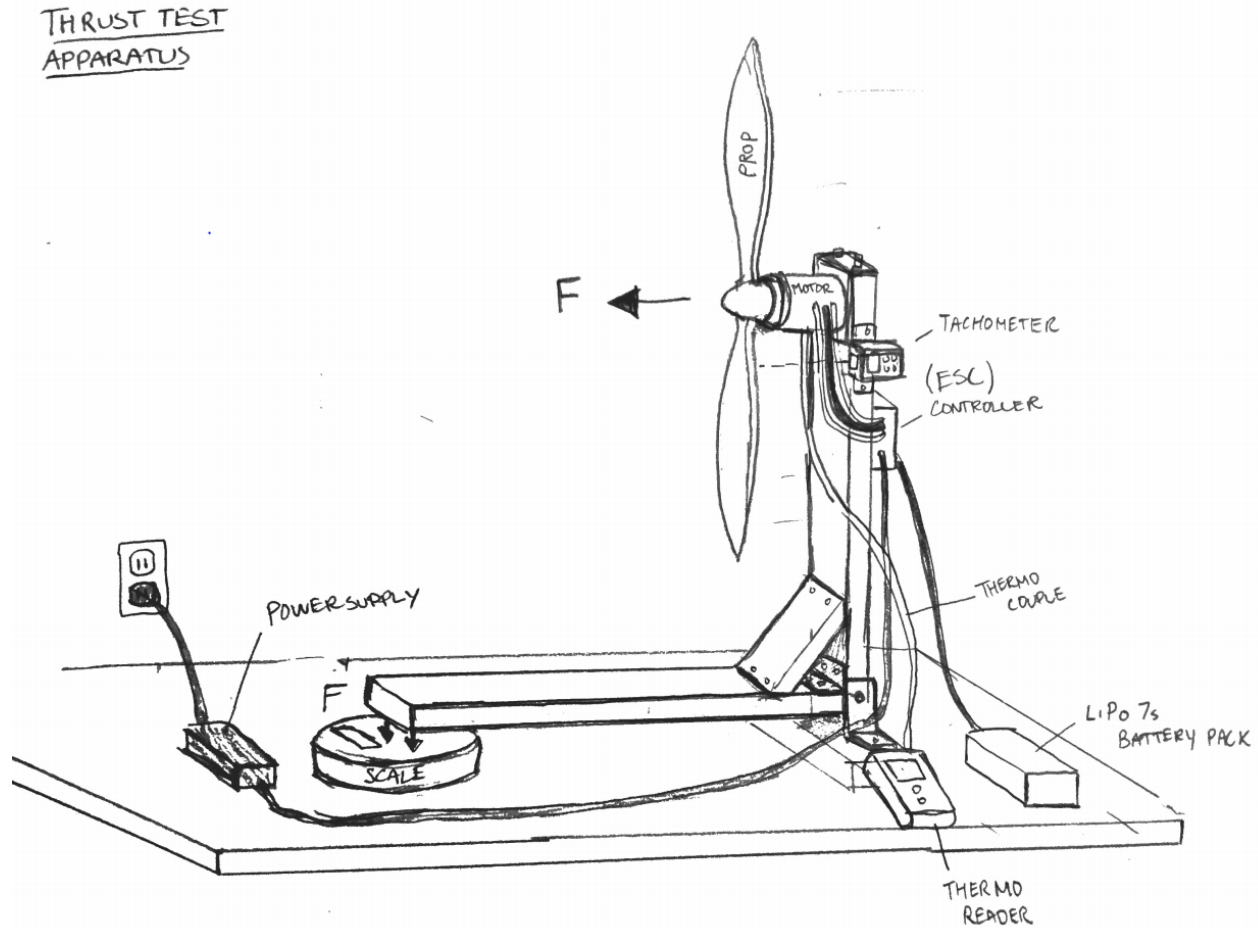


Figure 1. Test Setup Conceptual Sketch

Setup and Procedure

The test setup is shown in figure 1. The thrust of the propeller will create a moment around the hinge. The scale will provide the reaction force offsetting the moment created by the propeller, and will then be able to record the thrust of the propeller. Thermocouples will be mounted on the motor base near the coils to measure the coil temperature. A non-contact tachometer will be used to measure the rotation speed of the propeller. The scale will measure the force produced by the propeller. Both the scale, thermocouple reader, and the tachometer will be filmed so that the data can be analyzed later.

The following are general procedures for each of the three tests we wish to run. A more detailed step-by-step procedure for each test can be found in appendix 1.

The first test will be a general performance and system calibration test. In order to perform the first motor test the motor speed will be slowly throttled through its power range. Using this curve the desired setting which leads to 50lbs of thrust can be determined. This test will also serve as the initial balancing test to ensure that catastrophic vibrations do not occur since the speed will be increased slowly and if vibrations are noticed the motor can be quickly shut off via a kill switch.

Propeller Test Plan

The second test will be the propeller acceleration test. This test will be performed by setting the throttle about 20% below the 50lbs thrust operating point, and then increasing the throttle to the 50lbs thrust operating point and measuring the response time. The throttle will then be increased another 20 percent and the response time will be recorded.

The third test will be the steady state test at the 50lbs thrust operating point. We will run the motor for the remainder of the battery life (we expect only a few minutes) to test if the motor can sustain the load for a sustain time. The final temperature of the motor will be measured to make sure the motor does not overheat. The power draw of the motor will also be recorded to ensure that the motor performance is not decreasing over time.

Data Acquisition

The instruments used to measure the data for this test are a non-contact thermometer, thermocouples, a bathroom scale, voltmeter, and clamp ammeter. These instruments will be recorded by video cameras (phone cameras) to allow for the data to be analyzed later and for the test operators to remain safely behind a protective wall during the test.

The reporting rate of the instruments will need to be fast enough to record the propeller acceleration during the response time test for the motor. The JM1S motor was able to accelerate the propeller at a rate of 250 RPM/s, and a 20% increase in thrust corresponded to approximately a 400 RPM increase in speed so the acceleration should take approximately 1.5 to 2 seconds.

The most important measurement to record during the acceleration is the thrust. The RPM, temperature, voltage, and current are most important for the steady state tests, and to confirm that our acceleration started and stopped at the correct points so a slow reporting rate can be acceptable. The thrust measurement will need to report values a couple times per second in order for the acceleration tests to be worthwhile. In order to get the reporting speed a bathroom scale with a needle will be used, so the reporting rate will be equal to the frame per second rate of the camera filming the scale.

For all other tests the changes in the values being measured will be small and over a long time period so the report rate of the instruments will not be an issue.

Expected Results

We expect the results of the test, will show that the propeller will produce 50lbs of thrust at about 4500 RPM with a power draw of between 5.5 and 6kW. We do not expect that the performance of the motor will decrease over time since we should be operating below the max continuous operating conditions for the motor. For the acceleration test we expect that the motor will accelerate around 250 RPM/s. If the 80CC Turnigy Rotomax motor is able to closely match these performance criteria it will show that the motor is a suitable substitute for the industrial JM1S JobyMotor product in the final design.

Safety Concerns and Solutions

There are various safety risks involved during the test. The safety risks can be grouped into mechanical risks and electrical risks. The mechanical risks are; propeller breaking, critical vibrations, and flying debris strikes. The electrical risks; are overheating/overpowering, short circuits, electrocution risks.

Propeller Test Plan

If the propeller were to break the immediate result would be a large rapidly moving flying object. The broken piece of the propeller could cause serious harm to anyone it strikes. In addition the propeller would become very imbalanced, and would quickly cause the destruction of the test setup.

In order to mitigate the risks of the propeller breaking, first the propeller will be inspected before use for any defects or signs of weakness. An emergency shutoff switch will be installed so that power can quickly be removed from the motor to hopefully prevent damage to the test structure and components in case of a broken propeller. To reduce the risk of harm to the test operators the operators will stand out of the plane of rotation of the propeller. In addition the controls for the motor will be lead at least 50ft away from the test stand to allow for the operators to stand behind either a temporary wall or building for protection.

The risk of damage due to vibrations developing will be reduced though an initial balance test for the propeller. Also the speed of the motor will be increased slowly during the first test. If vibrations are detected the motor will be stopped, and additional stiffening will be added to the test structure and the propeller will be checked again for imbalance.

Flying debris are likely to pose the biggest risk during testing. If some sort of flying debris were to strike the propeller, damage could occur that leads to the propeller breaking and or critical vibrations. In addition flying debris could be shot through the propeller, or deflected off the propeller at very high speeds posing a significant safety hazards. The first step to reduce the risk from flying debris is to ensure the test setup is done in an area clear of lose debris. The area should be cleared of lightweight objects, such as sticks leaves and small rocks, which could easily be blown by the propeller. To protect against injury from the flying debris the operators will be standing behind a temporary wall or building for protection. The operators will also not be positioned behind the propeller, where most of the flying debris would be expected to fly.

To protect against overheating or overpowering any device in the test system we will carefully monitor the voltage and current. The systems that are at risk of overheating or overpowering are the motor, ESC, wires, and batteries. The limiting capacities of each device is listed in Table 1. Through careful monitoring and clearly known limits the risk of overheating or overpowering should be very low.

Table 1. Limiting capacities for devices used in test.

	Max Voltage	Minimum Voltage	Max Current	Max Power
Motor	51.8V	NA	150 A	6600 W
ESC	60 V	22.2 V	250 A	15000 W
Wires	NA	NA	181 A	NA
Battery*	29.4 V	24.5 V	325 A	7960 W

*Values listed are per pack, test will consist of 2 packs in series.

** Highlighted values are the critical value for the category

Given the voltages we are working with electrocution is a safety concern for the test. Any exposed wire or connection will be a possible source for electrocution. To solve this problem we will use wire connectors with insulation that protects users whenever possible. Any additional connection that we are unable to insulate via commercially available products will be located in such a spot that direct contact is unlikely, and will be insulated via other methods (electrical tape).

Propeller Test Plan

Safety Equipment

A protection wall will be made if a location with preexisting protection cannot be found. The plate will be made of half inch plywood covered on one side by 16 gauge steel. A diagram of the plate can be found in appendix 3. The plate will be 4 feet tall and 6 feet wide and will allow for four to five people to safely hide behind.

A circuit breaker will be included in the electrical circuit that will function to protect against short circuits, and as an emergency kill switch. The circuit breaker will be behind the wall with the test operators. If deemed necessary the test operators can flip the circuit breaker removing all power from the system stopping the motor quickly. The circuit breaker will also allow the motor to be completely depowered whenever the test operators are near the propeller.

A fire extinguisher will be on hand in case of fire. However, a normal ABC fire extinguisher will not be able to extinguish our LiPo batteries should they catch fire. To extinguish a battery fire a bucket of sand, or a shovel should be nearby to allow for the fire to be suffocated.

Conclusion

The purpose of this test will be to determine if the 80CC Turnigy Rotomax motor can serve as a cheaper substitute for the JM1S motor from JobyMotors. Due to the nature of the test there are several safety concerns that need to be addressed. The main safety concern is some sort of flying projectile and overloading the electrical system. Both safety concerns have been identified above and solutions to protect against both have been proposed. Using these safety guidelines the motor test will be able to be carried out in a safe manner and produce valuable test data.

Propeller Test Plan

Appendix 1

System Calibration test

1. Set up the test stand as shown in figure 1
2. Start all cameras recording
3. All test operators leave test area and go behind protective wall
4. Energize the system by closing the kill switch
5. Slowly increase the motor throttle from 0 to 90% at a steady rate over the course of approximately 1 to 1.5 minutes
6. Return throttle to 0% and allow for propeller to quit spinning
7. De-energize the system by opening the kill switch
8. Stop cameras and save the videos for future analysis

Acceleration test

1. Set up the test stand as shown in figure 1
2. Start all cameras recording
3. All test operators leave test area and go behind protective wall
4. Energize the system by closing the kill switch
5. Turn the throttle to 80% of the required setting for 50lbs of thrust and allow propeller speed to settle
6. Suddenly increase the throttle to the setting which produces 50lbs of thrust, and allow propeller speed to settle
7. Suddenly increase the throttle to 120% of the required setting for 50lbs of thrust and allow propeller speed to settle
8. Return the throttle to 80% of the 50lbs thrust setting, and repeat steps 6 and 7 two more times
9. Return throttle to 0% and allow for propeller to quit spinning
10. De-energize the system by opening the kill switch
11. Stop cameras and save the videos for future analysis

Steady state test

1. Set up the test stand as shown in figure 1
2. Start all cameras recording
3. All test operators leave test area and go behind protective wall
4. Energize the system by closing the kill switch
5. Set throttle to the 50lbs of thrust setting, allow the motor to run until the battery voltage is 24.8V (.3V above minimum safe operating voltage)
6. Return throttle to 0% and allow for propeller to quit spinning
7. De-energize the system by opening the kill switch
8. Stop cameras and save the videos for future analysis

Propeller Test Plan

Appendix 2

BOM and Cost Analysis

Table A2.1. Bill of materials and cost

Item	Quantity	Price	Total cost	Purchased (yes/no)
Rotomax Turnigy 80CC Motor	1	282.3	282.32	Yes
Infrared Thermometer	1	27.65	27.65	Yes
QO 200 Amp AIR QOM2 Frame Size Main Circuit Breaker	1	38.99	38.99	No
2x6 8ft board	3	4.53	13.59	No
#10 3 in. Phillips Square Flat-Head Multi-Material Screws	1	7.98	7.98	No
Xoar 30x10 propeller	1	57.25	57.25	Yes
non-contact tachometer	1	11.93	11.93	Yes
3-1/2 in. Satin Nickel 5/8 in. Radius Door Hinge	1	2.78	2.78	No
500ft. 2-Gaugre Stranded XHHW Wire	1	144	144	No
7s LiPo Battery	2	131	261.92	Yes
Turnigy Dlux 250A 14s 60V ESC	1	206.9	206.91	Yes
HoMedics® Analog Scale	1	19.99	19.99	No
Steel Bracket	4	4.46	17.84	No
36x48 16 Gauge Sheet Metal	2	46.76	93.52	No
1/4X20-1.25 Cap Screws	8	.30	2.4	No
1/4 washers	16	.30	4.8	No
1/4X20 hex nuts	8	.30	2.4	No
4x8 1/2 plywood sheet	1	17.58	17.58	No
Total			1213.85	

Appendix 3

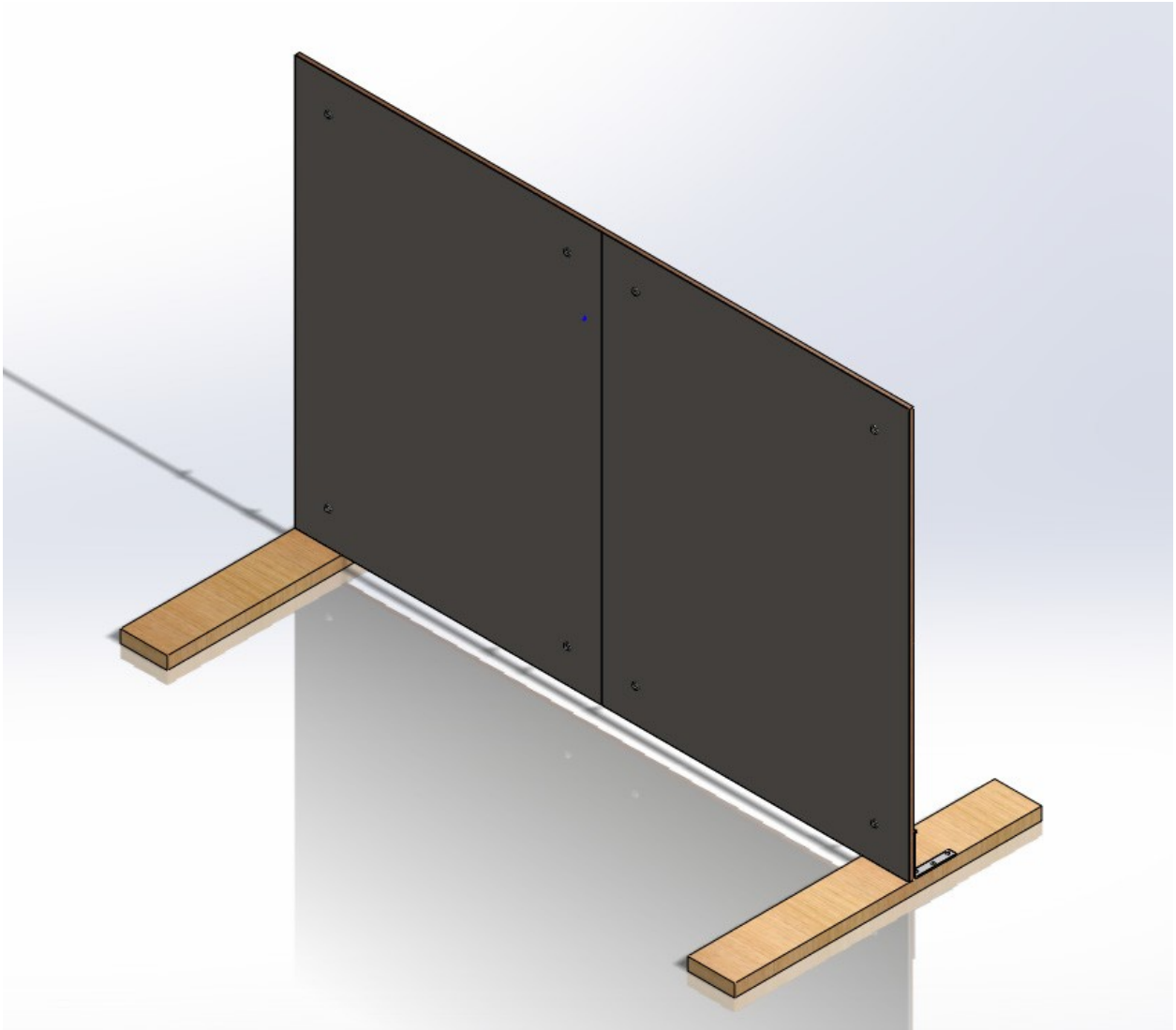


Figure A3.1. Protection Wall

Propeller Test Plan

Appendix 4

Test Setup Drawings

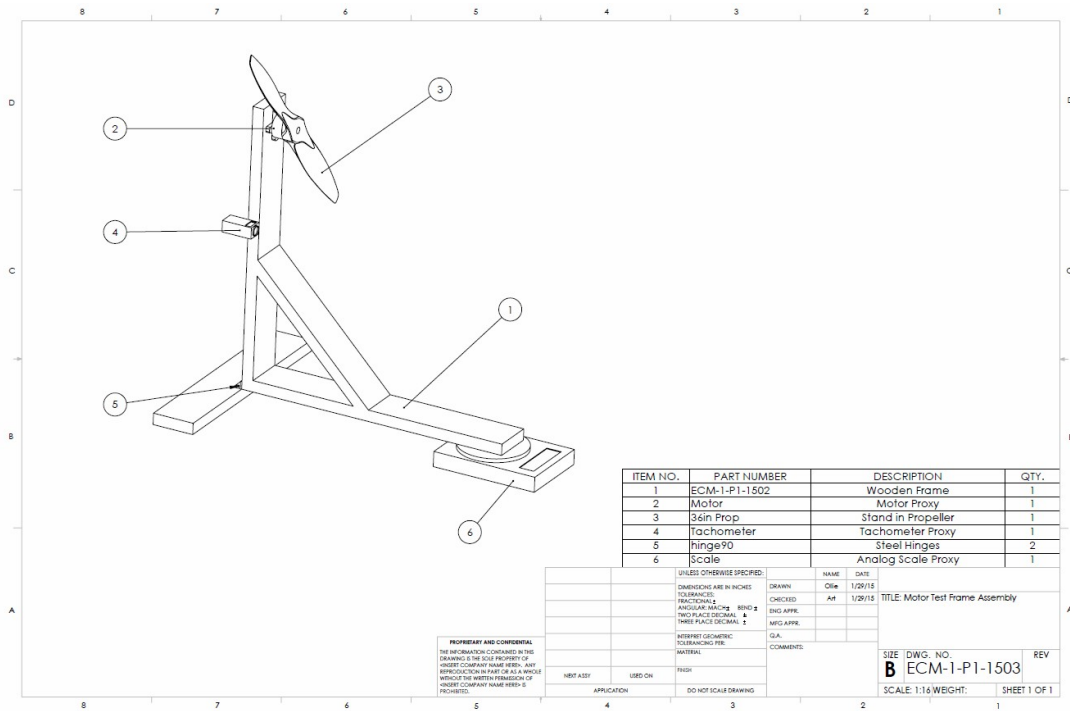


Figure A4.1. Test Setup

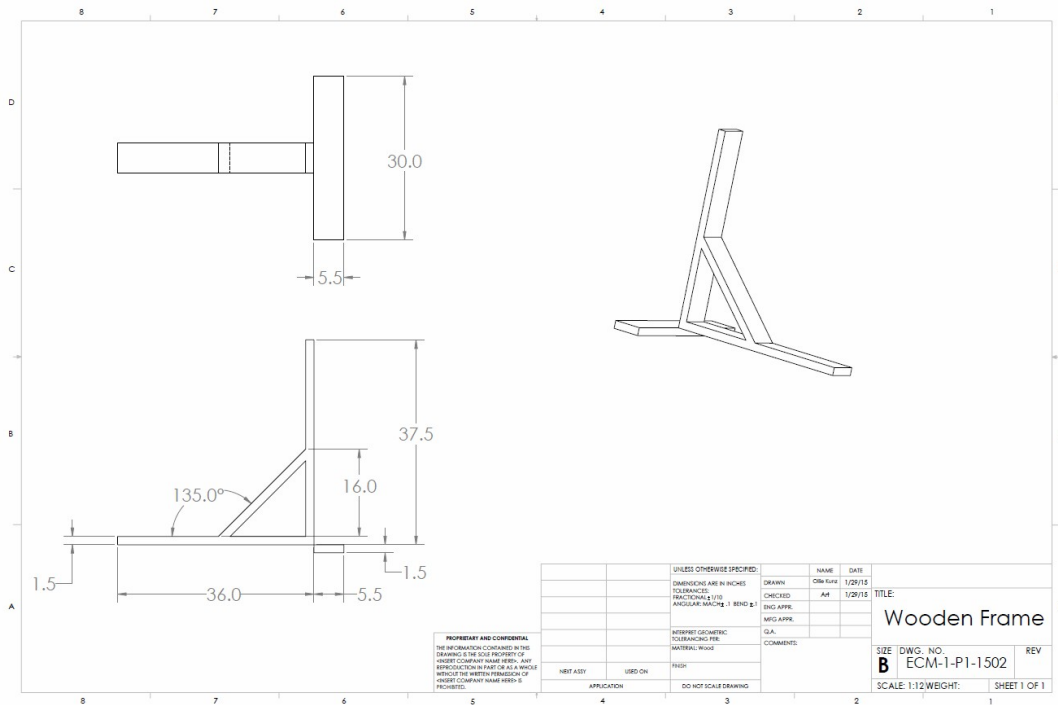


Figure A4.2. Frame Detail drawing

Propeller Test Plan

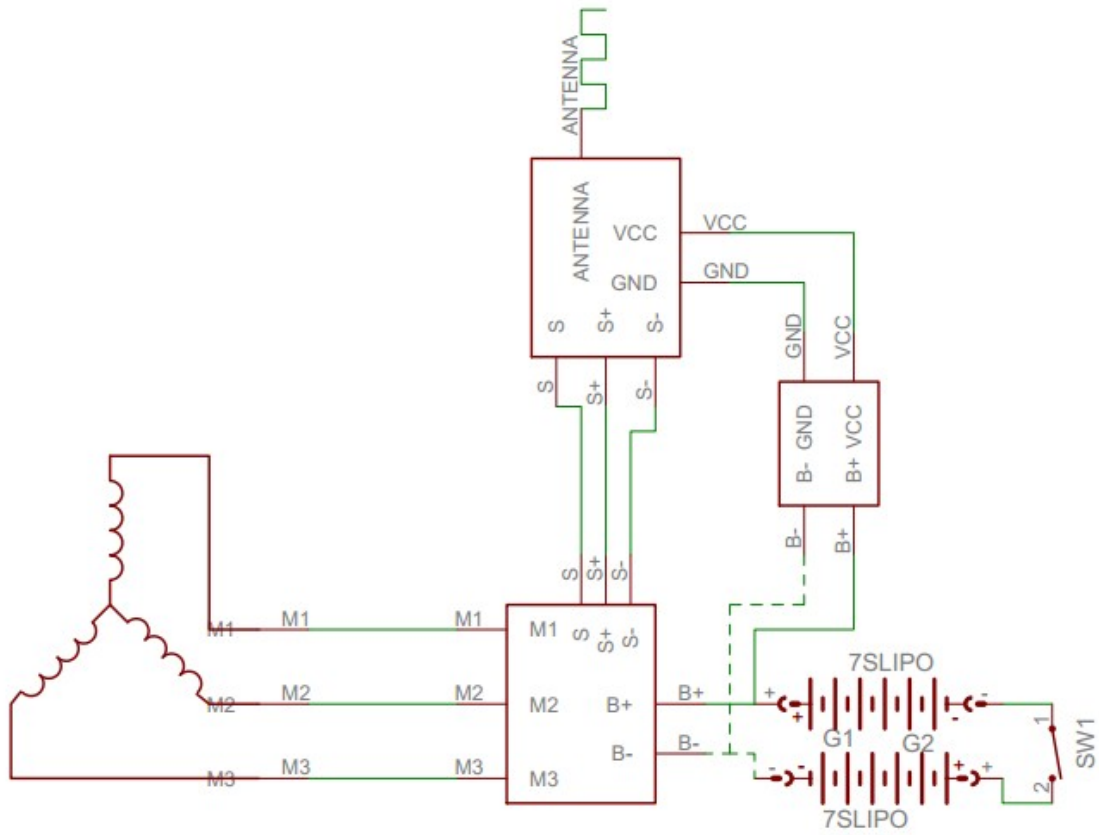


Figure A4.3. Wiring Diagram

Propeller Test Plan

Appendix 5

Emergency Information and Procedures

Local emergency numbers

Hospital:

Sierra Vista Regional Medical Center
1010 Murray Avenue
San Luis Obispo, CA 93405
Ph: 805-546-7600

Fire:

2160 Santa Barbara Ave
San Luis Obispo, CA 93401
Ph: (805) 781-7380

Directions to test location (from Cal Poly Campus):

Head west on Highland Dr.

Turn right onto N Santa Rosa St.

Continue on N Santa Rosa St. (Hwy 101) for 1.1 miles

Turn right at the white mailbox (423 N Santa Rosa St.) on to a gravel road

Continue on dirt road for ¼ mile

Test location will appear on right, approximately 150 feet from the road.

Safety Protocols

During testing if the test supervisor feels that a situation is unsafe, they have the authority to stop the test at any time and take the appropriate actions necessary to ensure that it is safe to continue testing.

If any individual is injured the test supervisor will have the authority to summon medical attention or send the person to receive medical attention. If it is determined that medical attention is required, the test supervisor will be responsible for calling 911 or the appropriate emergency number. If the injured person is the test supervisor the secondary test supervisor will assume the authority of the test supervisor.

In the case of a fire, the local fire department will be called immediately, no matter how small the fire is.

If any portion of the test setup breaks, further testing will be abandoned until the cause of the failure can be identified and the test setup is adequately fixed to prevent future failures.

Propeller Test Plan

Appendix 6

Test operator verification of safety training

Test Date: _____

By signing this for I verify that I have read and understand **the Electric Commuter Multicopter Motor and Propeller Test Plan and Safety Document**, and will follow to the test supervisors' directions.

Test Supervisor:

Name: _____ Signature: _____ Date: _____

Secondary Test Supervisor:

Name: _____ Signature: _____ Date: _____

Other Test Operators:

Name: _____ Signature: _____ Date: _____

Name: _____ Signature: _____ Date: _____

Name: _____ Signature: _____ Date: _____

Name: _____ Signature: _____ Date: _____

Name: _____ Signature: _____ Date: _____

Name: _____ Signature: _____ Date: _____

Name: _____ Signature: _____ Date: _____

Name: _____ Signature: _____ Date: _____

Name: _____ Signature: _____ Date: _____

Appendix E: Bibliography

- [1] United States. US Department of Transportation. Federal Aviation Administration. *103-7 The Ultralight Vehicle*. N.p.: Federal Aviation Administration, 1984. Web. 5 Oct. 2014. <[http://rgl.faa.gov/Regulatory_and_Guidance_Library/rgAdvisoryCircular.nsf/list/AC%20103-7/\\$FILE/Signature.pdf](http://rgl.faa.gov/Regulatory_and_Guidance_Library/rgAdvisoryCircular.nsf/list/AC%20103-7/$FILE/Signature.pdf)>.
- [2] "Federal Aircraft Regulations, Part 103:." *FAR Part 103*. The Ultralight Home Page, n.d. Web. 5 Oct. 2014. <<http://www.ultralighthomepage.com/FAR.part103.html>>.
- [3] "Chapter 14: Airspace." *Pilot's Handbook of Aeronautical Knowledge*. N.p.: Federal Aviation Administration, 2008. 14-1-4-10. *Pilot's Handbook of Aeronautical Knowledge*. Federal Aviation Administration, 2008. Web. 12 Oct. 2014. <http://www.faa.gov/regulations_policies/handbooks_manuals/aviation/pilot_handbook/media/PHAK%20-%20Chapter%2014.pdf>.
- [4] "Background of Ultralight Historical." *Human'Air*. Human'Air, n.d. Web. 19 Oct. 2014. <<http://www.human-air.net/en/ulmhistoric>>.
- [5] "E-volo | Aviation Pioneering – Aviation Future." *Evolo* RSS. N.p., n.d. Web. 20 Oct. 2014. <<http://www.e-volo.com/information>>.
- [6] "E-volo | VC1 – Proof of Concept." *Evolo* RSS. N.p., n.d. Web. 20 Oct. 2014. <<http://www.e-volo.com/information/vc1-proof-of-concept>>.
- [7] "E-volo | VC200 – the First Volocopter to Carry Two People." *Evolo* RSS. N.p., n.d. Web. 20 Oct. 2014. <<http://www.e-volo.com/ongoing-development/vc-200>>.
- [8] "E-volo | How Long Can The Volocopter Fly?" *Evolo* RSS. N.p., n.d. Web. 20 Oct. 2014. <<http://www.e-volo.com/information/how-long-can-you-fly>>.
- [9] Malloy, Chris. "THE HOVERBIKE." – *MA Hoverbike*. N.p., n.d. Web. 17 Oct. 2014. <<http://www.hover-bike.com/MA/the-hoverbike/how-you-can-own-it/>>.
- [10] DeRoche, Mark. "The Aero-X - Aerofex." *Aerofex The AeroX Comments*. Aerofex Corp, n.d. Web. 17 Oct. 2014. <<http://aerofex.com/theaerox/>>.
- [11] Lewis, Jeff. "Autogyro History and Theory." *Autogyro History and Theory*. N.p., 4 Jan. 2002. Web. 16 Nov. 2014.
- [12] "The Butterfly LLC - The Ultralight Butterfly Specifications." *The Butterfly LLC - The Ultralight Butterfly Specifications*. N.p., n.d. Web. 17 Nov. 2014.
- [13] Cartier, Kerry. "Popular Rotorcraft Association :: Gyroplane FAQs." *Popular Rotorcraft Association :: Gyroplane FAQs*. N.p., n.d. Web. 16 Nov. 2014.
- [14] Dodson, Brian. "Redesigned Martin Jetpack Deliveries Expected to Start in 2014." *Redesigned Martin Jetpack Deliveries Expected to Start in 2014*. Gizmag, 28 Sept. 2013. Web. 20 Oct. 2014. <www.gizmag.com/martin-jetpack-p12/29215>
- [15] "The Martin Jetpack – Fly the Dream." *The Martin Jetpack*. N.p., 2013. Web. 20 Oct. 2014. <www.martinjetpack.com>
- [16] "BlackHawk Kestrel Paramotor Frame." BlackHawk Paramotor, 2011. Web. 16 Oct. 2014. <<http://www.blackhawkparamotor.com/cages/blackhawk-kestrel-paramotor>>.
- [17] "Paramotor FAQ." *Flying High Paramotors*. N.p., n.d. Web. 16 Oct. 2014. <<http://flyhighparamotors.com/paramotor-f-a-q/>>.

- [18] "Scout Paramotors Innovative Features - Scout Paramotors USA." *Scout Paramotors USA*. Team Fly Halo, 2014. Web. 16 Oct. 2014. <<http://scoutparamotorsusa.com/scout-paramotors-innovative-features/>>.
- [19] "Learn to Fly." *Bhpa.co.uk*. British Hang Gliding & Paragliding Association, n.d. Web. 16 Oct. 2014. <http://www.bhpa.co.uk/sport/bhpa/learn_to_fly/>.
- [20] "Frequently Asked Questions." *Paramotor FAQ : Adventure Replies to All Questions*. N.p., n.d. Web. 16 Oct. 2014. <<http://www.paramoteur.com/faq>>.
- [21] "Heavy Lift Nylon Blimps | Blimps." *Heavy Lift Nylon Blimps | Blimps*. N.p., n.d. Web. 17 Nov. 2014.
- [22] "Mosquito Aviation - Home of the Ultimate Ultralight Helicopter : New ! Carbon Fibre Tailrotors." *Mosquito Aviation - Home of the Ultimate Ultralight Helicopter : New ! Carbon Fibre Tailrotors*. N.p., n.d. Web. 21 Oct. 2014. <<http://www.innovator.mosquito.net.nz/mbbs2/cfr.asp>>.
- [23] "Kolb FireFly, Kolb FireFly Part 103 Legal Ultralight Aircraft, Kolb FireFly Ultra Lite Plane, Ultralight News Newsmagazine." *Kolb FireFly Ultralight, Kolb FireFly Part 103 Legal Ultralight Aircraft, Kolb FireFly Ultra Lite Plane, Ultralight News Newsmagazine*. Ultralight News, n.d. Web. 20 Oct. 2014. <<http://www.ultralightnews.com/ssulbg/firefly-thenewkolbaircraft.html>>
- [24] "Kolb Aircraft Firefly 103 Legal Ultralight." *Kolb Aircraft Firefly 103 Legal Ultralight*. N.p., Sept. 2011. Web. 20 Oct. 2014.<www.kolbaircraft.com/firefly.htm>
- [25] Page, Lewis. "'Personal Air Vehicle' VTOL Jump-copter in Key Flight Test." • *The Register*. N.p., 24 Jan. 2011. Web. 16 Nov. 2014.
- [26] "Carter Aviation Technologies, An Aerospace Research & Development Company." *Carter Aviation Technologies*. Carter Aviation Technologies, 2014. Web. 16 Nov. 2014.
- [27] "Patent WO2013174751A3 - Method for Controlling an Aircraft in the Form of a Multicopter and Corresponding Control System." *Google Books*. N.p., n.d. Web. 17 Nov. 2014.
- [28] "Patent US20060266881 - Vertical Takeoff and Landing Aircraft Using a Redundant Array of Independent Rotors." *Google Books*. N.p., n.d. Web. 17 Nov. 2014.
- [29] "Patent DE102012202698A1 - Vertical Take-off and Landing Aircraft for Transporting People or Loads, Has Signal Processing Unit Performing Position Control Such That Aircraft Is Horizontally Located in Space without Pilot's Control Inputs or Remote Control." *Google Books*. N.p., n.d. Web. 17 Nov. 2014.
- [30] Brain, Marshall, and William Harris. "How Helicopters Work." *HowStuffWorks*. HowStuffWorks.com, n.d. Web. 19 Oct. 2014. <<http://science.howstuffworks.com/transport/flight/modern/helicopter.htm>>.
- [31] Norris, Donald. "Flight Basics." *Build Your Own Quadcopter: Power up Your Designs with the Parallax Elev-8*. N.p.: McGraw-Hill/TAB Electronics, 2014. N. pag. *Safari Tech Books Online*. Web. 18 Oct. 2014. <http://proquest.safaribooksonline.com/book/hardware-and-gadgets/9780071822282/2-quadcopter-flight-dynamics/ch02lev1sec1_html>.
- [32] Norris, Donald. "Quadcopter Controls." *Build Your Own Quadcopter: Power up Your Designs with the Parallax Elev-8*. N.p.: McGraw-Hill/TAB Electronics, 2014. N. pag. *Safari Tech Books Online*. Web. 18 Oct. 2014. <http://proquest.safaribooksonline.com/book/hardware-and-gadgets/9780071822282/2-quadcopter-flight-dynamics/ch02lev1sec2_html>.
- [33] Krasner, Helen. "How Do Helicopters Fly? Lift, Drag, and Thrust." *Decoded Science*. N.p., 21 Nov. 2012. Web. 20 Oct. 2014. <<http://www.decodedscience.com/how-do-helicopters-fly/20418>>.

- [34] Gibiansky, Andrew. "Quadcopter Dynamics, Simulation, and Control Introduction." (n.d.): n. pag. *Andrew Gibiansky*. Andrew Gibiansky, 23 Nov. 2012. Web. 2 Oct. 2014. <<http://andrew.gibiansky.com/downloads/pdf/Quadcopter%20Dynamics,%20Simulation,%20and%20Control.pdf>>.
- [35] "APM Copter." *ArduCopter*. 3D Robotics, n.d. Web. 20 Oct. 2014. <<http://copter.ardupilot.com/>>.
- [36] "AeroQuad - The Open Source Quadcopter / MultiCopter." *AeroQuad*. AeroQuad Open Source Project, n.d. Web. 20 Oct. 2014. <<http://aeroquad.com/content.php>>.
- [37] "OpenPilot.org – The Next Generation Open Source UAV Autopilot." *OpenPilot*. Open Pilot Foundation, 2013. Web. 20 Oct. 2014. <<http://www.openpilot.org/>>.
- [38] Cantrell, Paul. "Ground Effect." *Helicopter Aviation*. Paul Cantrell, n.d. Web. 18 Nov. 2014.
- [39] "Chapter 4: Aerodynamics of flight." *Pilot's Handbook of Aeronautical Knowledge*. N.p.: Federal Aviation Administration, 2008. 14-1-4-10. *Pilot's Handbook of Aeronautical Knowledge*. Federal Aviation Administration, 2008. Web. 17 Nov. 2014. <http://www.faa.gov/regulations_policies/handbooks_manuals/aviation/pilot_handbook/media/PHAK%20-%20Chapter%2014.pdf>.
- [40] Cascio, Jamais. "Open the Future: Record Battery Energy Density in Context [Updated]." *Open the Future: Record Battery Energy Density in Context [Updated]*. N.p., 27 Feb. 2012. Web. 20 Oct. 2014. <http://www.openthefuture.com/2012/02/record_battery_energy_density.html>
- [41] "All About Batteries." *Ni-MH Batteries (Nickel Metal Hydride)*. N.p., 16 Feb. 2013. Web. 18 Nov. 2014.
- [42] "What's the Best Battery?" *Advantages and Limitations of the Different Types of Batteries*. Battery University, n.d. Web. 19 Oct. 2014. <http://batteryuniversity.com/learn/article/whats_the_best_battery>
- [43] Nugent, Tom. *Laser Power for UAVs*. Tech. N.p.: LaserMotive LLC, 2010. Print. <<http://lasermotive.com/wp-content/uploads/2010/04/Wireless-Power-for-UAVs-March2010.pdf>>
- [44] Akturk, Ali, and Cengiz Camci. "ASME DC | Journal of Turbomachinery | Tip Clearance Investigation of a Ducted Fan Used in VTOL Unmanned Aerial Vehicles-Part I: Baseline Experiments and Computational Validation." *ASME DC | Journal of Turbomachinery | Tip Clearance Investigation of a Ducted Fan Used in VTOL Unmanned Aerial Vehicles-Part I: Baseline Experiments and Computational Validation*. N.p., 26 Sept. 2013. Web. 18 Nov. 2014.
- [45] www.esotec.org/hbird/HTML/DuctMyths_F.html
- [46] "Average Annual Miles per Driver by Age Group." *Average Annual Miles per Driver by Age Group*. United States Department of Transportation - Federal Highway Administration, 26 Sept. 2014. Web. 17 Oct. 2014. <<https://www.fhwa.dot.gov/ohim/onh00/bar8.htm>>.
- [47] Schrank, David, Bill Eisele, and Tom Lomax. "Urban Mobility Report." (n.d.): n. pag. INRIX Traffic Data, Dec. 2012. Web. 17 Oct. 2014.
- [48] "Compare Side-by-Side." *Fueleconomy.gov*. US Department of Energy, 2014. Web. 17 Oct. 2014. <<http://www.fueleconomy.gov/feg/Find.do?action=sbs&id=34489>>.
- [49] "F-150 STX." Ford, 2014. Web. 17 Oct. 2014. <<http://www.ford.com/trucks/f150/trim/stx/>>.
- [50] *Pilot's Operating Handbook*. N.p.: PiperSport Distribution Inc., 03 Oct. 31. PDF.

- [51] "R22 BETA II Helicopter." *Robinson Helicopter Co.* N.p., n.d. Web. 17 Oct. 2014. <http://www.robinsonheli.com/rhc_r22_beta_ii.html>.
- [52] Department of Mechanical Engineering. *ME 428-429-430 Senior Design Project Lecture #1 Budget, Travel, Research.* San Luis Obispo: California Polytechnic State University, n.d. PPT.
- [53] Maekawa, Shoji, Kouichi Shibasaki, Toyotoshi Kurose, Toshiyuki Maeda, Yoshitaka Sasaki, and Tatsuya Yoshino. "Tear Propagation of a High-Performance Airship Envelope Material." *Journal of Aircraft* 45.5 (2008): 1546-553. Web.
- [54] Boundy, Bob, Susan W. Diegel, Lynn Wright, and Stacy C. Davis. *Biomass Energy Data Book.* Appendix A. N.p.: US Department of Energy, 2011. Print.<http://cta.ornl.gov/bedb/appendix_a/Lower_and_Higher_Heating_Values_of_Gas_Liquid_and_Solid_Fuels.pdf>
- [55] Steiger, Jon N. "The Ultralight Home Page." *The Ultralight Home Page.* N.p., n.d. Web. 20 Oct. 2014. <<http://www.ultralighthomepage.com>>
- [56] Department of Mechanical Engineering. *ME428/ME429/ME430 Senior Project Reference Book and Success Guide.* San Luis Obispo: n.p., 2014. Department of Mechanical Engineering, Sept. 2014. Web. 14 Oct. 2014.
- [57] *Renewable Energies.* By Art MacCarley. Germany, Munich. July-Aug. 2014. Performance.
- [58] "Commercial / Business Aerospace Testing Services." *Aerospace Testing.* Dayton T. Brown Inc., 2014. Web. 17 Nov. 2014.
- [59] Budynas, Richard G., and Keith J. Nisbett. *Shigley's Mechanical Engineering Design with Additional Materials.* 9th ed. N.p.: McGraw-Hill Companies, 2011. Print. California Polytechnic State University.

Appendix F: Mini Multicopter Operator's Guide

The following summarizes the steps to safely operate the Mini, a 42inx42 twelve-rotor multicopter used to verify the controls scheme that is to be implemented onto the full-scale craft. The description has been broken into the following sections:

1. Propulsion
2. Electronics
3. Controls and Mission Planner
4. Flight

Shown below in Figure 1 is a top view of the Mini

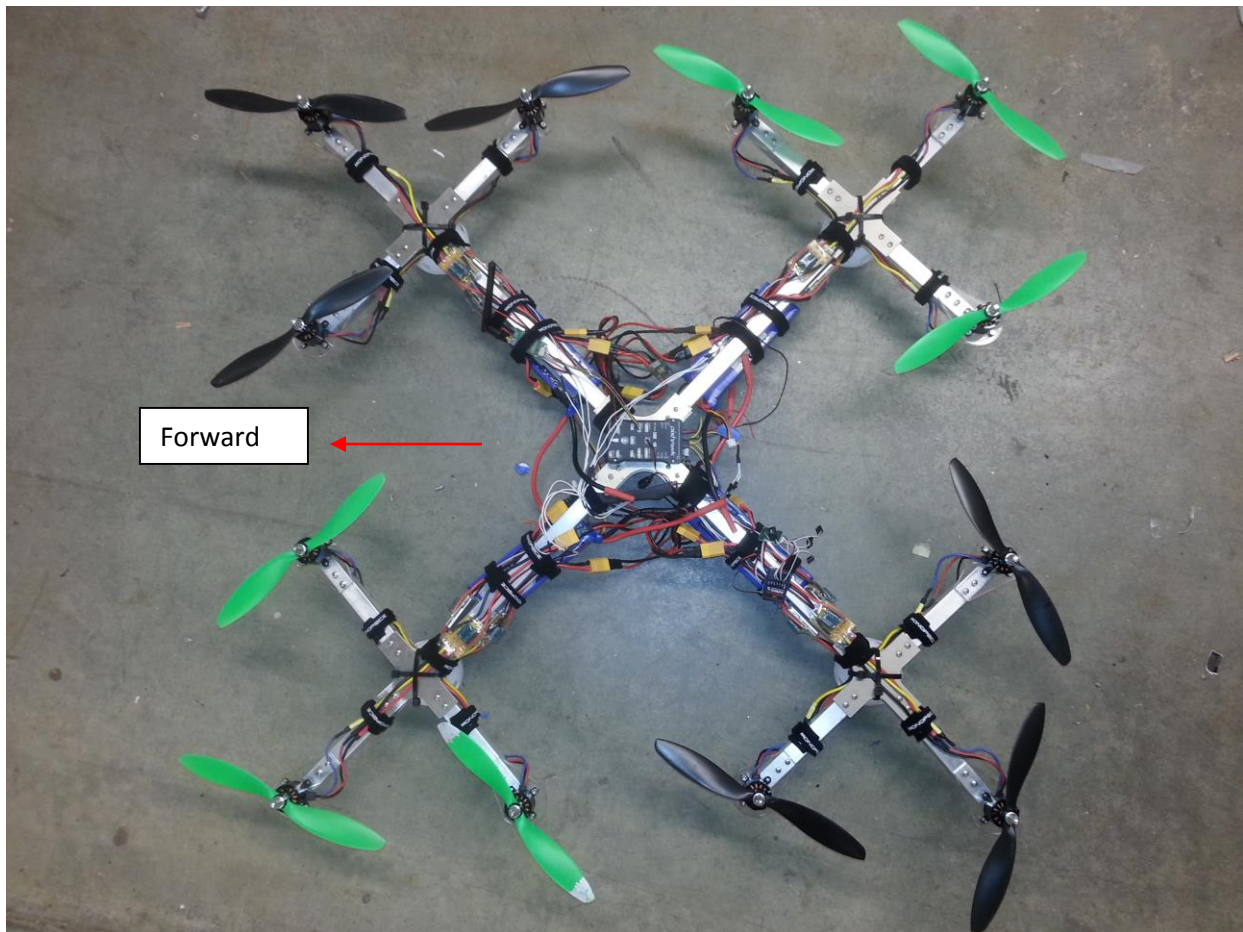


Figure 1. Top-view of the Mini showing its forward direction with respect to the Pixhawk flight controller.

Propulsion

The components of the propulsion are the following:

- 6 Clockwise (CW) Propellers

- 6 Counterclockwise (CCW) Propellers
- 12 Motors

The setup of the propulsion system is relatively simple and the attachment of the propeller to the motor is straightforward and will not be described. The main concern is to have the CCW and CW propellers configured properly. In this project an X-configuration was employed where the green propellers are CCW and the black are CW. In addition, the motors of the CW must spin in the opposite direction of the CCW propeller. This can be achieved by switching one of the servo-to-motor cables. This difference in wiring is shown below in Figures 2a and 2b.

ESC to motor wiring for the black CW-spinning motor

- Yellow to Blue
- Red to Red
- Black to Back

ESC to motor wiring for the green CCW-spinning motor

- Yellow to Blue
- Red to Black
- Black to Red

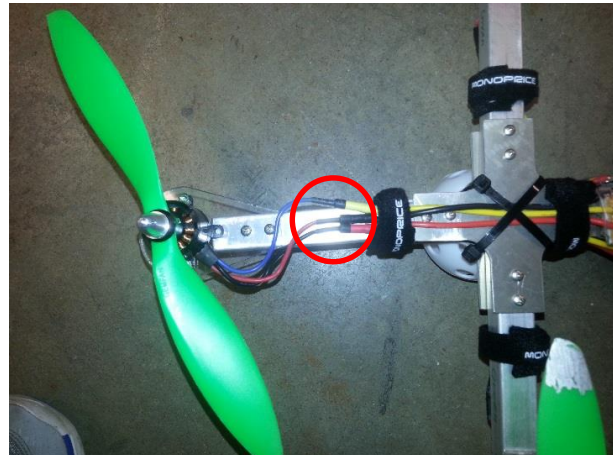


Figure 2a(Left) Black, CW-rotating motor wiring configuration

Figure 2b(Right) Green, CCW-rotating motor wiring configuration

As a safety precaution, before motors are ever turned on, verify that the motors are securely fixed to the frame of the craft and that the propellers are securely mounted to the motors.

Electronics

The components of the electronics include the following:

- 4 LiPo 5000mAh Batteries
- 12 Electronic Speed Controllers (ESC)
- DC Battery Charger

- Power Supply
- Power Distribution Board (PDB)
- XT60 connectors

Now the charging of the batteries and their connection to the craft will be described. To charge the LiPo batteries, a battery charger is required. The team had only a DC charger available to them but AC chargers can be used as a substitute. Additionally, the team was able to use a 5A, 30V DC power supply from the Cal Poly Robotics Club. It worked for charging purposes but because of its power limit, it took extensive amounts of time to charge the batteries. For a complete charge from a complete discharge, the total time was one and a half to two hours! It was found that the four LiPo's could be charged concurrently in order to minimize the amount of time spent in the charging process.

Additionally, care must be taken to prevent overcharge or overdischarge of the LiPos. Maximum voltage per cell for a LiPo is 4.2V. In the battery configuration used in this project, two two-cell Lipos are placed in series; this is a total of four cells in series and a total voltage of 16.8V (4.2x4). The minimum voltage per cell for a LiPo is 3.0V, that is a total voltage of 12V (3.0x4). Cell voltages can be checked with a multimeter on the LiPo's balancing leads. The following steps were taken to charge the batteries.

1. Disconnect all ESCs from their respective XT60 connections to the power distribution board
2. Connect batteries in their standard layout to the power distribution board. The standard layout consists of two sets of two LiPos in series and these two sets connected in parallel. The power and ground connectors of the parallel connection connect to the PDB.
3. Plug in the DC power supply to wall-outlet
4. Turn on power supply and set voltage limit to 17.6V, the proper voltage for the charger
5. Turn off the power supply
6. Connect the battery-balancing leads to the balancing ports of the charger. This will allow the total voltage of each battery to be observed during the charging process. The following three figures depict the connections used for the batteries.

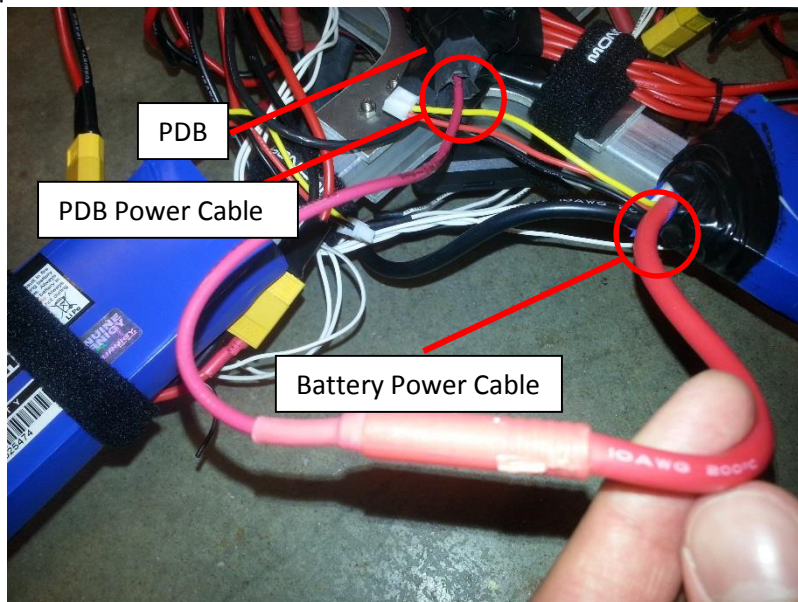


Figure 3. One of the two connections used to connect a battery power cable to the PDB

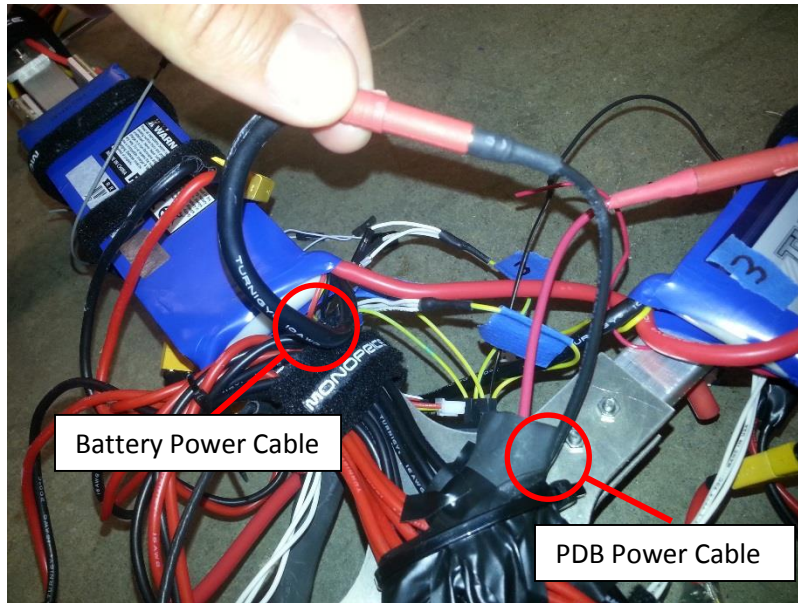


Figure 4. One of the two connections used to connect a battery ground cable to the PDB

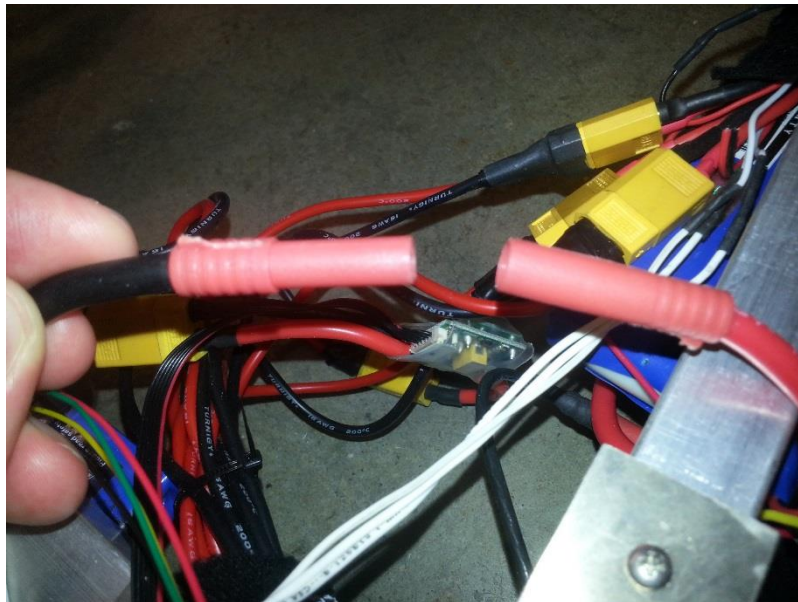


Figure 5. One of the two connections connecting the batteries in series

7. Connect the power-out cable of the battery charger to one of the XT60 connections. This is where the batteries will draw power from the battery charger.

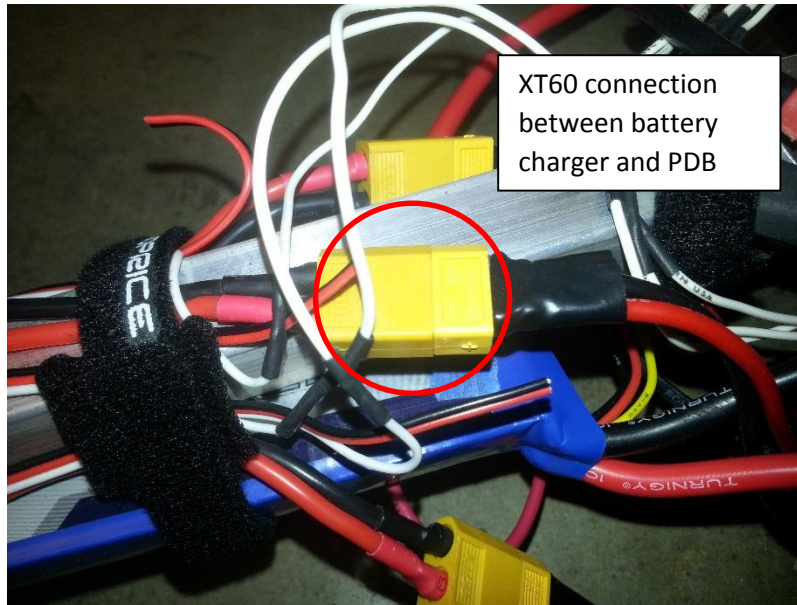


Figure 6. XT60 connection between the battery charger and PDB

8. Connect the charger to the power supply, turn the power supply back on and then increase current from the power supply until the charger turns on
9. Once on, the user can alter a range of settings on the charger's user-interface
 - a. Set Battery Type to LiPo
 - b. Set Charge Voltage to 16.8
 - c. Set Charge Rate to 1C (max charge rate is limited by the DC power supply and battery)
10. Begin charging by holding the "Start/Stop" button on the battery charger.
11. The battery charger will then begin charging, showing the time elapsed, the number of milliamp hours charged, and the current voltage. Do a check to make sure all the current readings are reasonable and that nothing is smoking. **If anything seems wrong**, cut power by turning the power supply off, unplugging the power supply, or by holding the "Start/Stop" button on the battery charge to stop the charge.
12. Charging will take one and half to two hours if started at a full discharge. This is a significant amount of time but DO NOT leave the batteries unattended EVER. Always check on the batteries and make sure they are not heating up or overcharging.
13. Once charged, the total voltage on the batteries should be 16.8V and each battery cell should be about 4.2V. If voltages between batteries and cells varies significantly—about 0.3V for the cells—then the batteries should be balanced. This can also be done with the battery charger.

The method to power the craft will be now be described.

1. Connect the twelve male XT60 ESC connections to the twelve female XT60 connections on the PDB
2. Connect the power module to the power port on the PixHawk. The location of the power port on the Pixhawk is shown below in Figure 7.

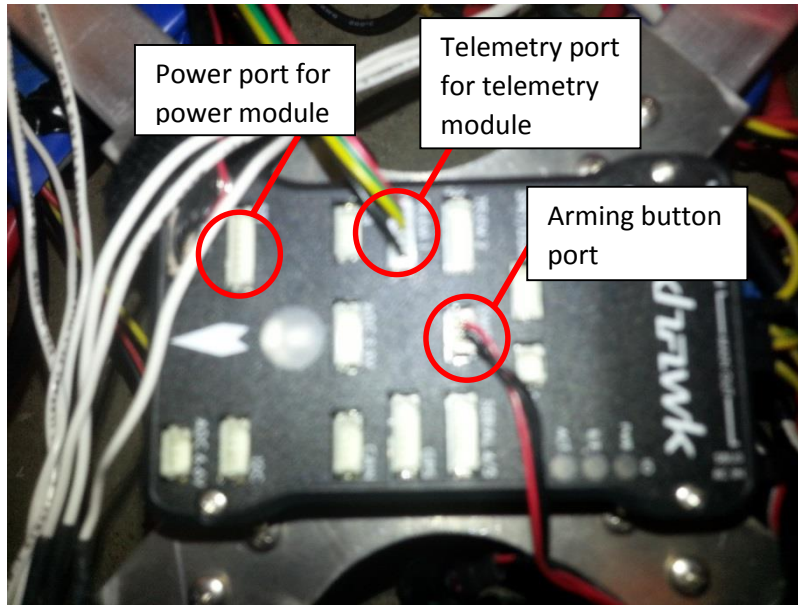


Figure 7. Power, telemetry, and arming switch port locations on the Pixhawk

3. Connect the four servo signal cables to the Pixhawk's output ports, one through four. These cables have been labeled one through four to avoid mistakes as plugging in the wrong cable to the wrong port will yield an uncontrollable craft. A picture of this port layout is shown below in Figure 8. Note that only one ground connection needs to be made.

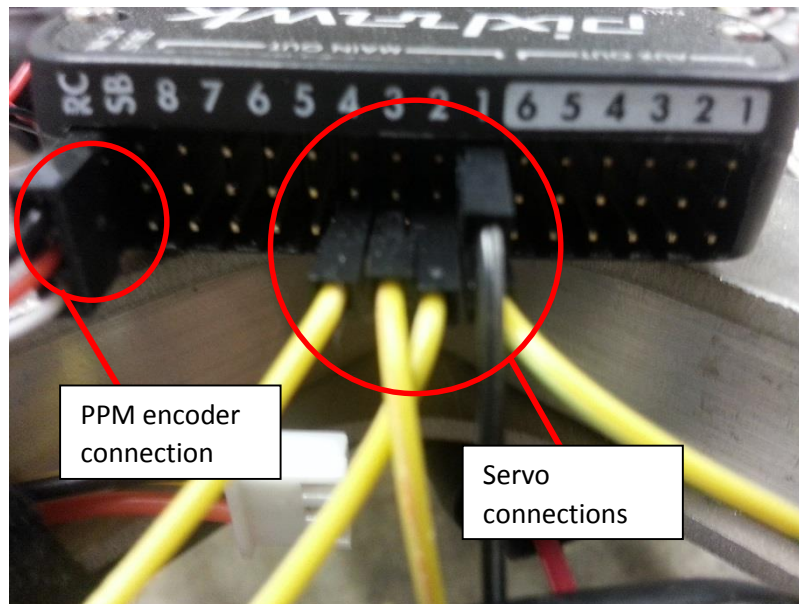


Figure 8. Connections of the ESC's servo-signal cables to the "Main Out" ports of the Pixhawk. The left of the figure shows the connection for the PPM Encoder.

4. Connect the batteries to the PDB in the same manner as that described in the charging section
 - a. Note, that unplugging the parallel connection exposes conductive metal. To avoid shorting components, disconnect the series connections when it is desired to turn the craft off.

5. Once the batteries have been turned on, the motors should beep, indicating that they are armed. Additionally, the main LED on the Pixhawk should begin blinking blue. If the Pixhawk is blinking a different color consult the Pixhawk forum.

Controls and Mission Planner

The components of the controls include the following:

1. Pixhawk
2. PPM Encoder
3. Receiver and Transmitter
4. Telemetry Module
5. Saitek x52
6. Mission Planner software

When first setting up and calibrating the Pixhawk, the operator must first connect to Mission Planner, or some similar software. Mission Planner is free and relatively easy to use. The following steps should be taken when calibrating the Pixhawk and setting up the control scheme to be used in the craft. Note, that this does not need to be done more than once. If properly calibrated with the right control scheme (Ex: x vs + for a quadcopter), the operator need not return to this part of the operations guide.

1. Download and install Mission Planner onto your working machine, most likely a laptop
2. Open Mission Planner
3. Use a USB mini B cable to connect the laptop to the Pixhawk
4. In Mission Planner select "Connect" in the top right of the window
 - a. This is a relatively inconsistent process and may need to be repeated if it initially fails. This is most likely a bug present in the Mission Planner software.
 - b. Once successfully connected, the "Connect" button will now provide you with the option to disconnect, as shown below in Figure 9.

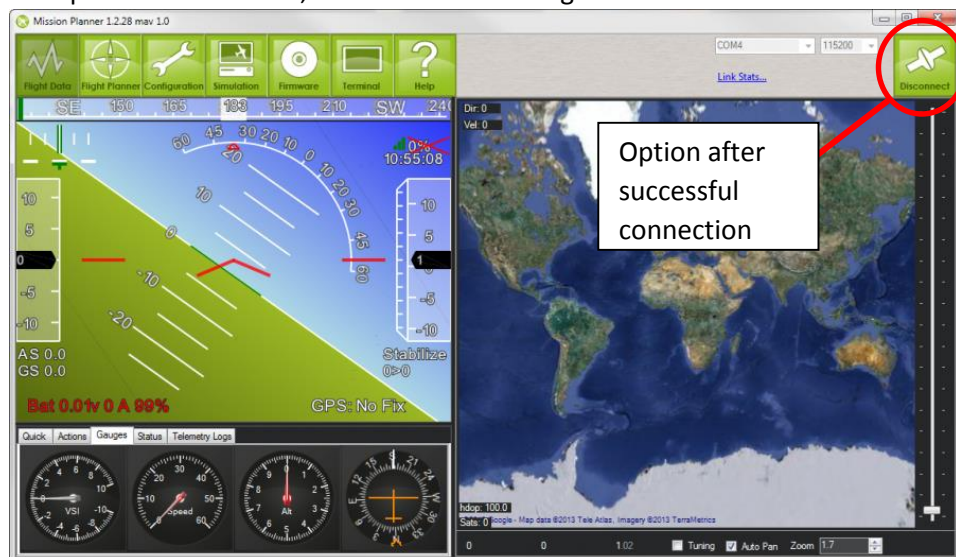


Figure 9. Mission Planner window showing successful connection to Pixhawk.

- Now navigate to the configuration and set up. You will be presented with a window shown below to select the type of configuration you wish. This project used the x configuration shown below in Figure 10. Feel free to choose a different configuration but all of the ports on the Pixhawk and subsequent controls have been set up for the x-configuration.

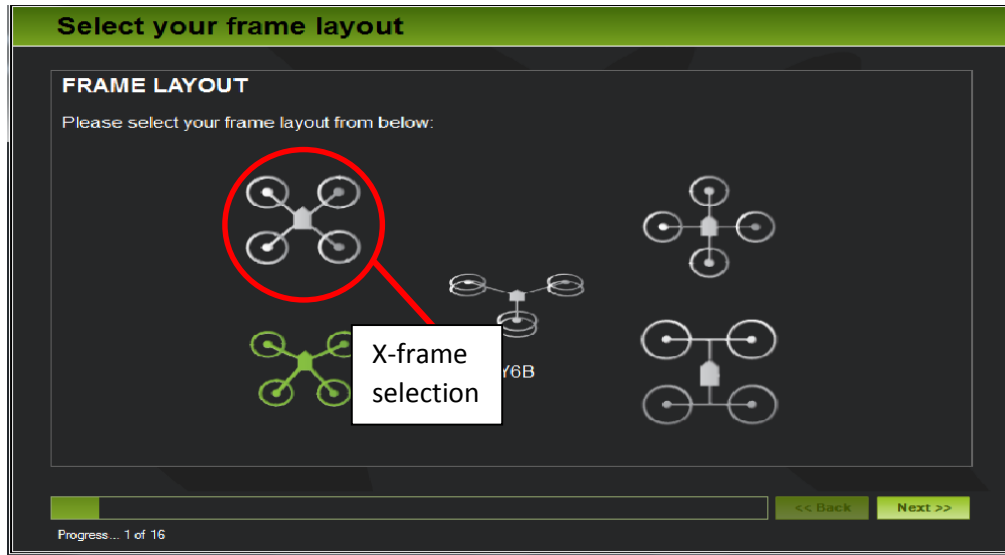


Figure 10. Frame layout selection for the Mini.

- You will then need to go through the calibration of the Pixhawk's gyroscopes/accelerometers and its on-board compass in the "Initial Setup."
- Next, you will need to calibrate the Radio, which involves the transmitter and receiver. However, before this can be done, the receiver and transmitter must be bound. The binding procedure will not be described here as plenty of information is available online.
- Once the receiver and transmitter have been bound, the receiver can then be connected to the PPM Encoder. Note that the PPM Encoder has 8 input connectors but only four are used to control the Mini. Each Encoder connector is labeled one through eight and connects to one of the four used pins on the receiver. The pins used on the receiver are throttle (Thro), aileron (Aile), elevator (Elev), and rudder (Rudd). In order to control the craft properly, the following connection configuration must be used. If these connections are not utilized then, for example, throttle input from the user will be interpreted as yaw by the receiver. Below, Figure 11 shows the PPM connectors connected to the receiver.
 - PPM (3) to Receiver (Thro)
 - PPM (1) to Receiver (Aile)
 - PPM(2) to Receiver (Elev)
 - PPM(4) to Receiver (Rudd)

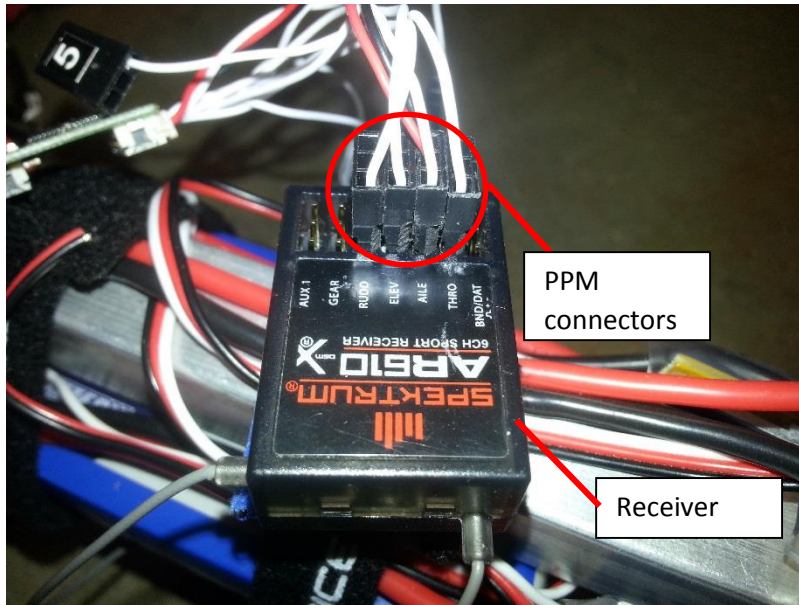


Figure 11. Receiver connected to respected PPM encoder connectors

9. Once successfully connected, you may now enter into the Radio Calibration of the Mission Planner where you can check that all of user inputs are being interpreted correctly by the flight controller. If they are not, some of the PPM to receiver connections may have to be changed. Figure 12 shows the window used for the radio calibration.



Figure 12. Radio calibration window in Mission Planner

10. If the operator wants to set up the Saitek x52, the following steps should be taken.
11. Download the drivers for the selected telemetry module
12. Connect the USB telemetry module to the laptop and the connector telemetry module to the Pixhawk as show in Figure 7.
13. For completion of the setup follow the resources found online by searching for Pixhawk telemetry module setup.

Flight

The procedure for flying the craft is as follows:

1. Double check the wiring described in the previous section and keep in mind that once the batteries and ESCs are both plugged in the motors are powered and they have the possibility of moving.
2. Make sure either the Saitek or the Spektrum are connected/bound correctly.
3. Pressing the arm switch on the Saitek or moving the left stick on the Spektrum to the bottom right corner will arm the craft and the propellers will spin at idle speed.
4. The craft can take off if the throttle is moved up slowly. The craft will stabilize itself once it is off the ground based on the calibration it has received.
5. If you want to roll, pitch or yaw the craft you must do so while the throttle is in a non-zero position keeping in mind any nearby objects or persons. The control scheme is shown in Figure 13 below where rudder is yaw, aileron is roll, and elevator is pitch.
6. If at any point the craft gets out of hand you can turn throttle back to zero and the motors will go to idle and stop spinning after 15 seconds or you can hit the disarm button the Saitek and the motors will stop immediately. This can happen at any point during flight, so thought should be given to where it will land from that point.

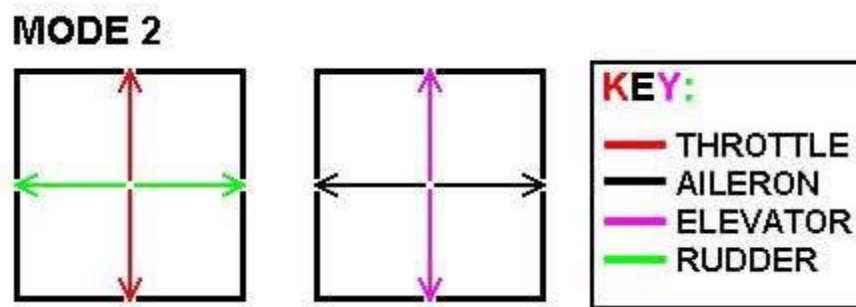


Figure 13. Control scheme for a mode 2 transmitter.